

U.S. NAVAL
RESEARCH
LABORATORY

2017 NRL REVIEW

WASHINGTON, DC • STENNIS SPACE CENTER, MS • MONTEREY, CA



We are advancing research
further than
you can imagine.®

We provide the advanced scientific capabilities required to bolster our country's position of global naval leadership. Here, in an environment where the Nation's best scientists and engineers are inspired to pursue their passion, everyone is focused on research that yields immediate and long-range applications in the defense of the United States.



NRL REVIEW STAFF

EDITOR

Gary Kuhlmann

COORDINATOR

Jonna Atkinson

CONSULTANT

Kathy Parrish

DESIGN, LAYOUT, AND GRAPHIC SUPPORT

Jonna Atkinson

PHOTOGRAPHIC PRODUCTION

Gayle Fullerton

Jamie Hartman

James Marshall



COMMANDING OFFICER

CAPT Scott D. Moran, USN



DIRECTOR OF RESEARCH

Dr. Bruce G. Danly

REVIEWED AND APPROVED

NRL/PU/3430--18-631

RN: 18-1231-2268

August 2018

Scott D. Moran, Captain, USN

Commanding Officer

FOREWORD



Since 1923, consistent excellence across a range of scientific fields at the Naval Research Laboratory (NRL) — the Navy’s only full-spectrum corporate laboratory — has brought new capabilities into existence and matured technologies critical to U.S. naval forces and the nation. With this 2017 NRL Review, we offer a glimpse into the groundbreaking research performed by over 2,500 government professionals last year.

NRL’s 2017 achievements continue the laboratory’s long record of high-impact research. In these pages, you will meet some of our staff and gain insight into their efforts and expertise. We’ve included examples of the recognition they received from organizations inside and outside of government, because our entire organization takes pride in their achievements. Discovery is a team sport at NRL, and at an institutional level we also recognize the supporting work that makes every science and engineering gain possible.

NRL employees are **explorers**. They design and operate specialized scientific equipment to examine phenomena of every kind and size, from atomic-scale microscopy to galactic-scale radio astronomy. Hundreds of exploratory research programs within and across a portfolio of basic and applied research make NRL a truly unique work environment that fosters creative energy throughout a diverse and vibrant workforce.

NRL employees are **futurists**. They develop and implement new generations of capabilities relevant to the military. As you will see in the following pages, these efforts take many forms, including revolutionary advances being made in semiconductors, batteries, robotic devices, fuel cells, quantum devices, and much more.

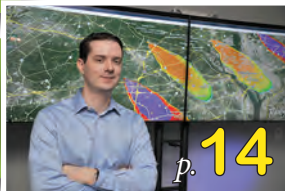
NRL employees are **protectors**. It’s critical to note that they are proud of their contributions to naval forces and the nation. Navy operational forecasts for weather, space, oceans and sea ice continue to improve, thanks to the models developed by NRL meteorologists, oceanographers, physicists and computer scientists. Many examples of this work follow in the pages ahead, such as the use of NRL software tools for the 2017 Presidential Inauguration and emerging research into poorly-understood occurrences, such as fire-triggered thunderstorms.

A remarkable combination of personnel, equipment, organization and culture make NRL the performer of choice for a broad sponsor base. We are humbled to have the opportunity to introduce the lab’s far-reaching — and often astonishing — capabilities. Due to space limitations, these examples represent only some of the compelling and important work performed by NRL’s dedicated and highly effective staff; for a more complete picture, please visit us on the web at www.nrl.navy.mil.

Dr. Bruce G. Danly
Director of Research

CAPT Scott D. Moran
Commanding Officer

We are advancing **further than you can imagine.**[®]



NRL'S INVOLVED!

- 2 Our People Make a Big Difference
- 7 The Great Years of Rath — Materials Science and Component Technology Head Concludes 41-Year Career at NRL
- 11 NRL Celebrates 50 Years of Fellowship During Annual Children's Holiday Party
- 14 NRL's CT-Analyst Supports Presidential Inauguration
- 16 NRL Develops Lighter, Field-Repairable Transparent Armor
- 18 VXS-1 Warlocks Assist NASA in Snow Pack Research Campaign
- 20 HBCU/MI Program at NRL Celebrates 25th Anniversary

THE NAVAL RESEARCH LABORATORY

- 24 NRL — Our Heritage
- 27 NRL Today

FEATURED RESEARCH

- 78 Looking Inside a Big Onion
Safely Measuring Tor
- 84 Cold Atoms Hold the Key to Long-Lived Quantum Memory
Quantum Memories Based on Optically Trapped Neutral Atoms
- 91 A New Era for the Vacuum Tube
Three-Dimensional Printing and Electroforming for Millimeter-Wave Vacuum Electronics
- 99 A MIGHTI Flight for Ionospheric Insight
From Sensor Idea to Satellite Instrument

RESEARCH ARTICLES

acoustics

- 108 Impulsive Noise Mitigation of Fire Suppression Systems
- 110 Understanding the Influence of Disorder in Atomically Thin Materials
- 113 A Mixture Theory Based Approach to Poroacoustics

atmospheric science and technology

- 116 Understanding Intense Pyroconvection and Its Impacts
- 118 Seeding the Wave Guide
- 120 Aerosol and Cloud Research in the South China Sea

chemical/biochemical research

- 124 From the Depths of Marine Dark Biosphere
- 125 Shark Antibodies Make a Splash

electronics and electromagnetics

- 130 Reshaping Antenna Patterns Using Metasurface Radomes
- 132 NRL Participates in NATO Electronic Warfare Trial
- 134 Magnetolectric Microbeam Resonators for Magnetic Field Sensing
- 137 Intense Laser-Driven Ion Accelerator
- 139 Normally-Off AlGaIn/GaN MOS-HEMTs with Record Performance
- 141 NexGen High Frequency Surface Wave Radar

information technology and communications

- 146 Goal Reasoning for AUV Control
- 147 The Application of Complex Network Analytics to Dynamic Wireless Network Systems
- 149 Navy Malware Catalog
- 151 Predicting Academic Attrition in Naval Air Traffic Control Training

materials science and technology

- 156 Modular Hydrogen Fuel Cells
- 157 Microstructures and Properties of As-Cast AlCrFeMnV, AlCrFeTiV, and AlCrMnTiV High Entropy Alloys
- 160 Non-Thermal X-ray Production from an Array of Non-Interacting, Magnetically-Imploded Wires

nanoscience technology

- 164 Novel Active Tuning for Infrared Photonics
- 166 Opening a New Window into Nanoparticle Toxicity

ocean science and technology

- 170 Parameterization of Whitecap Fraction Based on Satellite Observations
- 173 Successful Self-Embedment of a Large Benthic Microbial Fuel Cell Anode
- 175 What Is the Impact of Light on Ocean Primary Production and Hypoxia?

optical sciences

- 180 Waveguides for Non-Mechanical Beam Steering in the Mid-Wave Infrared
- 182 Optical System Protection Using Pupil-Plane Phase Masks
- 183 Simultaneous Optical Beamforming for Phased-Array Applications

remote sensing

- 188 Automatic Target Recognition of Small Crafts Using Multichannel Imaging Radar
- 190 Dust-Infused Baroclinic Cyclone Storm Clouds
- 192 A Mutli-Channel Testbed for Next-Generation Maritime SAR Systems

simulation, computing, and modeling

- 198 Advances in Simulation Technologies to Reduce Noise from Supersonic Military Aircraft Jets
- 201 Kr Plasmas on the Z and the National Ignition Facilities
- 203 Supporting Weather Forecasters in Predicting and Monitoring Saharan Air Layer Dust Events that Impact the Greater Caribbean
- 205 Reactive Flow Modeling for Hypersonic Flight

space research and satellite technology

- 210 Mitigation of Spacecraft Communications Blackout via Microparticle Injection
- 211 LASCO: Pioneer of Space Weather
- 213 Slim-Edged Silicon Detectors: Advanced Nano-Fabrication Technology
- 215 Solar Coronal Power Spectra Modeling

SPECIAL AWARDS AND RECOGNITION

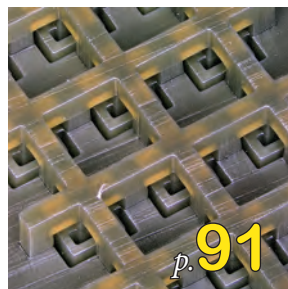
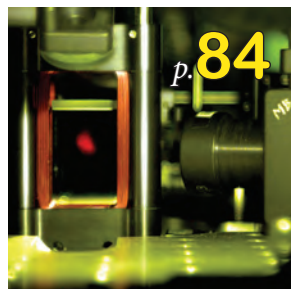
- 220 Special Awards and Recognition
- 229 Alan Berman Research Publication and NRL Edison (Patent) Awards
- 233 NRC/ASEE Postdoctoral Research Publication Awards

PROGRAMS FOR PROFESSIONAL DEVELOPMENT

- 236 Programs for NRL Employees — Graduate Programs, Continuing Education, Professional Development, Equal Employment Opportunity (EEO) Programs, and Other Activities
- 238 Programs for Non-NRL Employees — Postdoctoral Research Associateships, Faculty Member Programs, Professional Appointments, and Student Programs
- 241 NRL Employment Opportunities

GENERAL INFORMATION

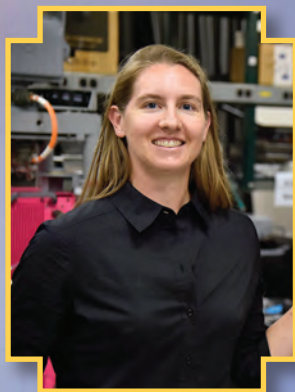
- 244 Technical Output
- 245 Key Personnel
- 246 Contributions by Divisions, Laboratories, and Departments
- 249 Subject Index
- 251 Author Index
- 252 Map/Quick Reference Telephone Numbers



- 2** Our People Make a Big Difference
- 7** The Great Years of Rath — Materials Science and Component Technology Head Concludes 41-Year Career at NRL
- 11** NRL Celebrates 50 Years of Fellowship During Annual Children's Holiday Party
- 14** NRL's CT-Analyst Supports Presidential Inauguration
- 16** NRL Develops Lighter, Field-Repairable Transparent Armor
- 18** VXS-1 Warlocks Assist NASA in Snow Pack Research Campaign
- 20** HBCU/MI Program at NRL Celebrates 25th Anniversary

Our People Make a **BIG** Difference

The *NRL Review* dramatically illustrates the range of **research capabilities and innovative technologies** that make the U.S. Naval Research Laboratory a leader in so many fields. Driving all of NRL's innovations and successes are the **highly motivated people** who work here. It is these people who provide the talent, creativity, and sustained effort to **turn ideas into realities** in support of the Navy mission. In this section, we proudly highlight some of these special people.



We are **explorers** • We are **futurists** • We are **protectors**



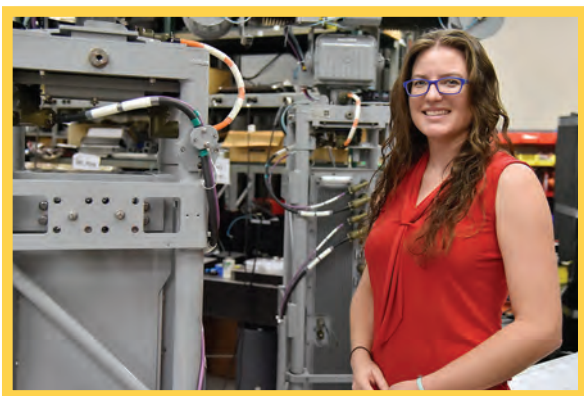
MS. KENAN COLE is a mechanical engineer in the Tactical Electronic Warfare Division. She received a B.S. degree and an M.S. degree in mechanical engineering from The George Washington University (GWU). She is currently pursuing a Ph.D. at GWU in multi-vehicle formation control. Ms. Cole has worked at NRL since 2009 as a mechanical engineer on maritime electronic warfare (EW) systems. She was the mechanical design lead on a highly successful quick reaction capability program. This program involved development of a special variant of the Transportable Electronic Warfare Module (TEWM) system. Ms. Cole has continued to work on TEWM design and capability improvements, demonstrating many of the improvements during at-sea Fleet experiments such as RIMPAC and Northern

Edge. Ms. Cole also has performed research in coordinated micro-jammer EW concepts. She is scheduled in FY18 to lead a new base research program focused on cooperative beamforming for micro-jammers. “The variety of projects that I have had the opportunity to work on and field test, coupled with the people I have had the pleasure of working alongside, has made NRL a remarkable place to continue to learn.”



DR. VIRGINIA DEGIORGI is head of the Multifunctional Materials Branch in the Materials Science and Technology Division. After receiving a bachelor of science degree and a master of engineering degree from the University of Louisville, she joined the Breeder Reactor Components Project at Westinghouse Electric Corporation, where she worked on advanced steam generator designs, including prototype testing. She became the first — and at the time, youngest — woman to win the prestigious B.G. Lamme corporate scholarship available only to Westinghouse employees. This enabled her to complete her Ph.D. in engineering mechanics at Southern Methodist University, where she focused her research on the 3D aspects of metallic fracture, using both computational and experimental techniques. Since

joining NRL in 1986, Dr. DeGiorgi has applied her computational, mathematical, and engineering skills to a variety of Navy-relevant problems. She also has studied fracture of metals, including computational modeling techniques for electrochemical corrosion, groundbreaking work on piezoelectric and shape memory alloy-based smart materials, incorporating corrosion into integrated computational materials engineering, electromagnetic rail gun performance, and the interaction between structural response and coatings failure for Navy ship components. She is an established leader in the international naval community on computational modeling of electrochemical corrosion and defense-related impressed current cathodic protection systems. In 2001, she started what turned into a long-term relationship with ONR, providing program management and technical support for TechSolutions, SwampWorks, and disruptive technology programs and support for Future Naval Capabilities Programs. Dr. DeGiorgi enjoys interaction with her colleagues, and welcomes the back-and-forth brainstorming sessions so critical to advanced research projects. She is passionate about supporting the next generation of researchers, especially those who have made the commitment to join NRL. She is a role model for women considering a career in this field, and her career highlights the opportunities available at NRL. “NRL is an exciting and challenging place to do science. NRL provides unique opportunities to make a difference to the Naval enterprise, both as a researcher and as a technical expert for the decision makers. The ability to investigate new problems, crossing organization lines to tap into the expertise of my fellow NRLers, allows us to identify the foundational science and create the technological breakthroughs required by the future Navy.”



MS. SUZANNE MCDONALD is an electrical engineer in the Electronic Warfare Modeling and Simulation Branch's Special Project Section. She graduated from Texas Tech University in 2008 and began working at NRL in 2009. Ms. McDonald has worked on a variety of projects, including self-stabilizing buoys, unmanned aircraft vehicles, communication devices, and maritime electronic warfare (EW) systems. She currently leads installation, maintenance, and training of the AN/SLQ-62 EW system, an NRL-developed ship-based active electronic attack system. In addition, Ms. McDonald is a key contributor to the team focused on AN/SLQ-62 system design and capability improvements. She and the AN/SLQ-62 NRL team received a letter of recognition from RADM Klunder, Chief of Naval Research,

for their outstanding efforts completing and delivering the system. In addition, Ms. McDonald has participated in multiple Navy at-sea exercises, including Northern Edge 2017. "One of my favorite things about working at NRL is participating in all phases of a project. In a large company, an engineer would typically only be involved in one or two phases. Here we start with a concept, design a prototype, build it, test it, evaluate the results, redesign if needed, and assist in transitioning the equipment to the Navy."



MR. KRIS RAMSEY is a Contracting Officer/Specialist in the Contracting Division. He started with NRL in November 2009, and has supported many areas of NRL, including the Chemistry Division, the Technical Electronic Warfare Division, the Information Technology Division (ITD), and the Human Resources Office. Over the past two years, he has been the lead specialist on one of the largest contracts at NRL for the ITD. This contract, a \$250-million Multiple Award Contract (MAC), provides support for almost all of ITD. The contract is designed to provide ITD with the best solutions for their specific requirement and save money through competitive task orders. He hopes methods similar to the ITD-MAC can be used to provide efficient and timely solutions to other divisions. "The most important part

of the acquisition process is communication and teamwork between the divisions and the Contracting Division. My goal at NRL is to support the Divisions by providing sound guidance and effective tools to those involved in the acquisition process. The end goal is to develop and process quality and timely contract actions to support the needs of all the Divisions."

We are advancing research **further than you can imagine.**[®]



DR. SIGNE REDFIELD is a roboticist in the Control Systems Branch of the Spacecraft Engineering Department in the Naval Center for Space Technology. She has been working for the Navy since 2002, and at NRL since 2014. Her research interests include fault tolerance and verification of autonomous systems, the development of task representations for autonomous robots, and autonomy architectures for environments with limited communications. Dr. Redfield received a bachelor's degree in electrical engineering and music from Johns Hopkins University and both a master's degree and a doctorate degree in electrical engineering from the University of Florida. After completing her doctorate, she spent eight years at the Naval Surface Warfare Center in Panama City, Florida, working on the development of autonomy

architectures and behaviors to support multi-robot mine countermeasures operations. In 2010, she joined the London office of ONR Global as the Associate Director for Autonomy and Unmanned Systems, providing the Navy with insight into ongoing research across the various domains of robotics in the international community and securing funding for international researchers to do work of interest to the Navy. On her return to the United States, she joined NRL to support the Robotic Servicing of Geostationary Satellites program, research funded by the Defense Advanced Research Projects Agency (DARPA). Her role on this program is to design a servicing robot autonomy architecture that supports autonomous mission operations and fault management in space. She also supports ONR participation in a NATO research task group on autonomy in communication-limited environments. She is co-chair of the IEEE Robotics and Automation Society's Technical Committee on Performance Evaluation and Benchmarking of Robotic and Automated Systems, and is active in the development of IEEE standards for robots. "NRL is giving me the opportunity to focus on a fascinating and underserved area of robotics — the development of tools and techniques to better understand our domain and to smooth our robots' transition from the laboratory to the real world."



MR. STEVE SOUZA has been working for NRL since March 2004 as the Finance and Administrative Management Specialist for the Marine Meteorology Division in Monterey, California. Before joining NRL, Mr. Souza served on active duty with the U.S. Air Force for six years. He then pursued graduate studies at the Monterey Institute of International Studies, from which he holds an M.B.A. degree in international management and a B.A. degree in international policy studies. After several years at NRL, Steve had a brief stint with a partner Naval activity, and upon his return to NRL, he became the Marine Meteorology Division's first Certified Defense Financial Manager. Mr. Souza plays a key role in payroll and contract management of 120 people, and in the implementation and daily management

of funding and maintenance of 350 job orders, on average, annually. During his time at NRL, without hesitation, he has covered every desk in the support group when vacancies and absences have occurred. Mr. Souza has long been an MS Excel enthusiast and routinely accepts any spreadsheet challenge presented. Over the years, his VBA for Excel programming skills and Oracle database proficiency have served the Division management well with reliable efficiencies in the financial management environment. He describes NRL financial management as an exciting, dynamic experience. "Naval financial management is like flying. In an appropriated activity, the most difficult times are at the beginning and ending of the fiscal year. You take off, set the autopilot of your 737, and land at the end of the year with relative predictability. Whereas in the Working Capital fiscal model, you are in a fire-bomber, take off at the beginning of the fiscal year, blindly hug the cloudy terrain, go through turbulence and then at the end of the fiscal year, you need to land on an aircraft carrier — at night!"



MR. RYAN TAYLOR is head of the Material Control Branch in the Supply and Information Services Division. He joined NRL in 2003 as an office automation clerk under the Student Temporary Employment Program. He became a full-time NRL employee in 2004 as a property disposal technician, and in this position, he played a pivotal role in the modernization of NRL's asset management system, assisting in the design, testing, and implementation of applications and reports that made the system more functional for NRL users and helped NRL better meet property accountability standards. He became head of the Property Disposal Section in 2011, and focused on reducing the administrative burden of the property disposal process for all divisions by eliminating the collection of unnecessary and

redundant documentation, and by streamlining business processes. He currently leads the Shipping, Receiving, Supply Store, and Disposal sections, where he oversees critical material control functions in support of the NRL community, helping to ensure that NRL receives the material, supplies, and equipment needed to meet its core mission of scientific research and technical development for the DoD.



DR. KATHRYN WAHL is a research materials engineer, and heads the Molecular Interfaces and Tribology Section in the Surface Chemistry Branch of the Chemistry Division. She has worked at NRL since 1992, starting as a National Research Council postdoctoral researcher after receiving a Ph.D. in materials science and engineering from Northwestern University. During her NRL career, she has worked on a broad range of materials problems in adhesion, friction, and wear. She specializes in developing a fundamental understanding of slip and adhesion through creating instrumentation and experiments that probe the contacts in real time. She has applied this work to solving problems in nanometer-scale slip and adhesion as well as solid lubrication and barnacle adhesion in macroscopic contacts.

Currently, she leads basic research efforts in a barnacle adhesion program with colleagues across NRL from both the Center for Biomolecular Science and Engineering and the Materials Science and Technology Division. She also leads a program in tribo-corrosion research with scientists from the Center for Corrosion Science in the Chemistry Division. Both programs focus on world-class research in Navy-relevant subject matter, and on enabling personnel to develop superb technical skills and connections to both the DoD and global science and technology communities. "The best things about working at NRL have been the opportunity to work with, mentor, and be mentored by, fantastic people, as well as reinvent myself. I've been everything from a marine biologist working on barnacle adhesive one day to an engineer in a hard hat analyzing and inspecting water lubricated propulsor bearings the next."



The Great Years of Rath

Materials Science and Component Technology Head Concludes 41-Year Career at NRL

Walk into Dr. Bhakta B. Rath's office on a mid-August morning, and he welcomes you with a warm hello and handshake before settling in behind a desk piled unreasonably high with countless stacks of folders, documents, DoD correspondence, and other paperwork requiring the attention of a man who leads more than 750 researchers and manages a \$260 million budget.

Dressed casually in tan slacks, white oxford dress shirt, and loosened tie, Rath, the Associate Director of Research for Materials Science and Component Technology at the U.S. Naval Research Laboratory (NRL), looks just like what he is and has been – a highly regarded professor, scientist, researcher, patent developer, and expert in the field of materials science and engineering.

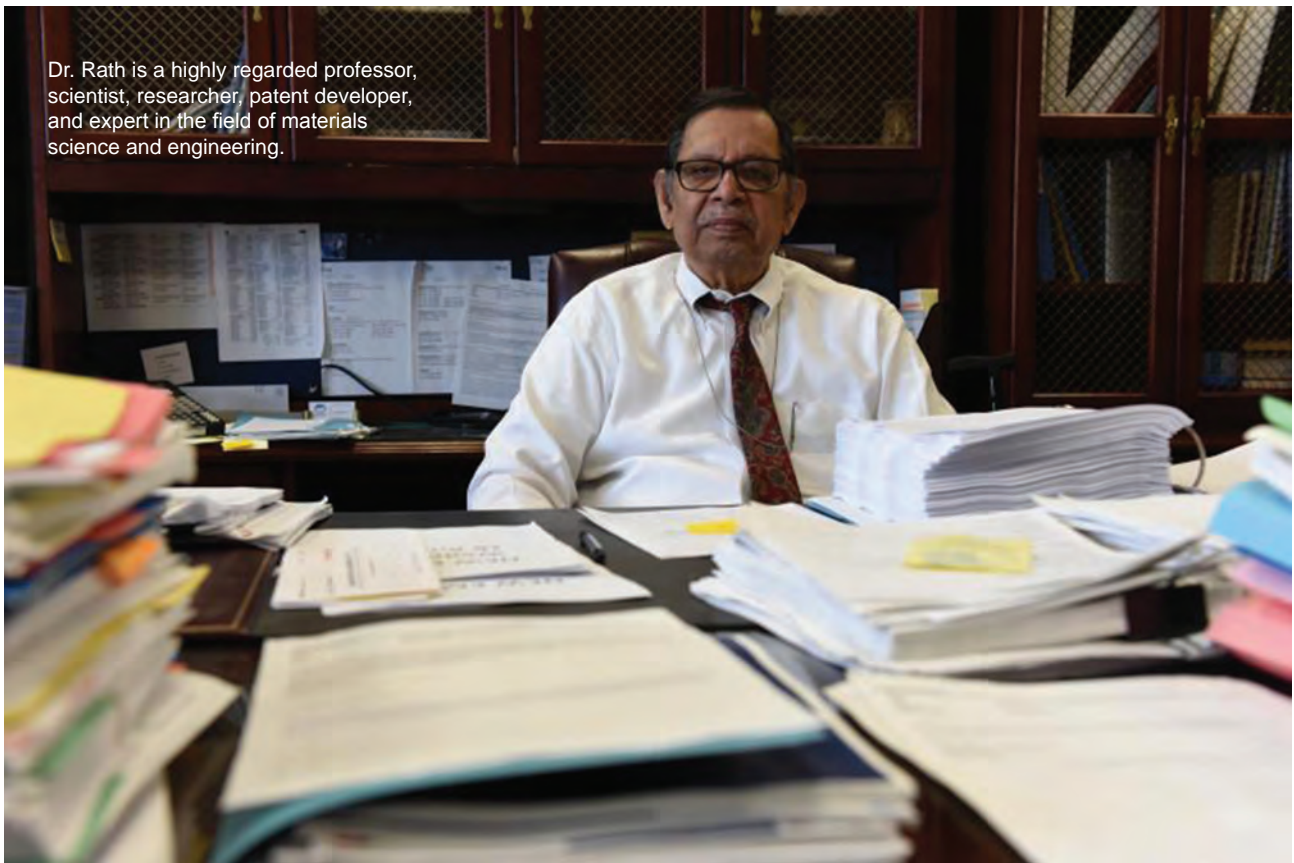
The walls of his office are literally covered with mementos of a rich career that has taken him to every continent on the planet except Antarctica. Look around, and you'll see diplomas from the

Illinois Institute of Technology, Michigan Tech University, countless honorary degrees, photos with secretaries of defense and state, photos with other science and research luminaries, and a photo with President George W. Bush. Look further, and there's even a certificate acknowledging a knighthood (equivalent honor) bestowed upon him by the president of India.

A wall-to-wall bookshelf behind his desk, overflowing with books, papers, and other research material, looms behind the doctor like a tidal wave ready to engulf a surfer. You can't help but think it'd be a treasure trove for eager Ph.D. candidates to peruse. Reminding himself of an international phone call he must take later that morning, this is not the picture of a man preparing to retire.

With slightly graying hair, an animated and lively conversational style, and a face that belies his 82 years, one can't help but imagine him leading researchers in his department for another decade. But as late summer eases into fall, Rath is in the last

Dr. Rath is a highly regarded professor, scientist, researcher, patent developer, and expert in the field of materials science and engineering.



few days of what can best be described as a brilliant career.

Dr. Rath retired September 2, 2017. A ceremony celebrating his four decades of research at NRL took place September 12.

On this summer morning in August, though, he took a few minutes to reminisce about his life and a career in which he led nearly 1,000 researchers at NRL in various capacities, had more than 300 papers published, edited or co-edited nearly 30 books and proceedings, and became a member or leader in over 10 professional or scientific societies ... the list goes on.

A Small Village in India

The second youngest of five, Rath grew up in Cuttack, India, the second largest city in the state of Odisha, where his parents made education a high priority.

“Education was always emphasized,” said Rath. “My parents believed it was the most important thing a young man can do.”

His three brothers and sister are all “highly educated,” according to Rath. Each of them are retired now from practicing law or the engineering field, after studying and working mostly in India.

Remaining in India, though, would not be in Rath’s future. A circuitous set of circumstances landed him in the United States.

He graduated in 1955 from Ravenshaw College (now a university) in Cuttack with a degree in math, physics, and chemistry. Then it was off to Germany to earn a master’s degree in metallurgy. Now a father of three – twin sons and a daughter – Rath was a “maverick” back in those days. “I was very brash and restless back then,” he said. “I wanted to see the world.”

Germany and Adam

A German company was building a huge steel plant in India and wanted to send only the brightest students to Germany to study, according to Rath. He applied, and was one of two selected for a full scholarship. Now was the time for work – before the work.

“I didn’t know German from Adam, so I decided I needed to learn German,” Rath explained. After three months of intensive tutoring, all he could say in German was “Where is the bathroom?” and “Where is the restaurant?”

“I said, ‘This is where I am going to study metallurgy? In the German language, with German professors?’”

Moving on.

Welcome to the USA

After forfeiting his scholarship to Germany, Rath researched several schools in the United States specializing in metallurgical studies. His mother gave

him two years to earn his master's degree before returning home to begin his career.

It came down to four schools: Columbia University ("not a good fit"), University of Montana ("too far"), University of Missouri ("okay"), and Michigan Technological University ("the best choice").

After arriving at Michigan Tech in Houghton, Michigan, Rath found that working with students from the United States and other countries around the world was not a problem. In fact, he enjoyed it. He was outgoing and eager to absorb his studies inside and outside the classroom. But the weather? That was another story.

Growing up in India, warm weather wasn't an issue, of course, but the coldest temperatures the future member of the *Who's Who in Science* had ever experienced before arriving in Michigan was only 60 degrees.

"I had never even seen snow before, and the winters in Michigan reach minus-20 degrees," Rath remembered, seemingly bristling at the thought nearly 60 years later. "I had no idea how cold it would be."

Needless to say, the double-breasted suits and light overcoat he purchased en route to the States would not be enough to fend off the numbing Michigan winters. "I learned they would be hopelessly useless," Rath remembered with a chuckle.

A Simple Solution

Weather, however, would only be the beginning of his worries at Michigan Tech.

During Rath's initial meeting with his department head (DH), he learned there would be a little more classwork required than what he had planned.

"He looked at my transcripts from Ravenshaw and realized I didn't have any courses in metallurgy," said Rath. Then came the peppering of questions concerning metallurgy courses.

DH: "Do you have electro metallurgy?"

Rath: "No."

DH: "Pyro metallurgy?"

Rath: "No."

DH: "How about ..."

Rath: "No."

DH: "Perhaps you have ..."

Rath: "No."

You get the picture.

The DH realized Rath didn't have any courses or background in metallurgy, but he offered a simple solution. Rath's DH broke the news that he would have to earn a bachelor's in metallurgical engineering before working on his master's. He was looking at a six- to seven-year prospect. This, of course, was not an ideal situation.

"I told him I promised my mother I would return to India in two years," Rath said. That's how she agreed to his forfeiting the scholarship to Germany in the first place.

So Rath and his new DH made a deal. He allowed Rath to work on his bachelor's and master's requirements simultaneously, and he could take the bachelor's courses in any order that was offered by the department which would fit his schedule.

"He said, 'If you think you can finish in two years, that's your choice.'

"I decided I would take the challenge," Rath said. "I was a young man – healthy, strong, and stupid."

And so it went – 35-plus courses per year, classes year 'round. "I did it all in two years," said Rath. "The bachelor's requirements, master's research, and thesis. I didn't sleep much four nights a week."

After Michigan Tech, it was on to a fellowship at the Illinois Institute of Technology, in Chicago. That promise to return to India in two years?

"After finishing my master's and bachelor's, I was not very happy about it," Rath admitted. "All of the teachings were like a cookbook. I wanted to know the fundamentals of how matter behaves, from the atomic and electronic level up."

He decided the only way to do this was to pursue his doctorate. His mother gave her blessing. Rath earned his Ph.D. in 1961, and was still missing something. After several discussions and some back and forth with his mother, off he went to teach at Washington State University and pursue research projects during the summers.

Early on at Washington State, Rath traveled home a few times to meet, court, and marry his wife, Sushama (Panigrahi) Rath. A widower now, he was married to Sushama for 50 years, raising twin sons and a daughter with her. Both of the boys are attorneys. His daughter is in business administration. Rath spent five years at Washington State, followed by seven years at a highly renowned lab in Pittsburgh called the Edgar C. Bain Laboratory for Fundamental Research of the U.S. Steel company, and another five years at McDonnell Douglas in St. Louis.

Welcome to NRL

NRL reached out for his services sometime in early 1976. The NRL letter inviting him for an interview mistakenly went unanswered for weeks, until he came across it one afternoon while clearing off his desk. He finally responded and got that interview. Things obviously went well, and after wrapping things up in St. Louis, Dr. Rath arrived at NRL in October

"Education was always emphasized," said Rath. "My parents believed it was the most important thing a young man can do."

1976 as head of the physical metallurgy branch, leading five sections.

“After being here, I fell in love with the lab, fell in love with the work we are doing here,” he said. “There are high-caliber, world-class scientists here,” he beamed. “I was delighted to be able to guide 15 to 17 scientists in the branch and build it up,” he said about his early days at NRL. “We got a lot of funding and started many new research activities.”

Ironically, he wasn’t really looking for the division head position when it opened. He submitted his resume only as a “benchmark” for selecting the new hire. “He or she should be better than this,” he said when submitting his qualifications. Nobody was, so he was hired.

Rath spent 41 years here at the lab – six as a branch head and another four as a division head, with the last 31 years as an Associate Director of Research (ADOR) in the Materials Science and Component Technology Research Directorate. He leads more than 750 scientists and engineers, managing a \$260 million-plus budget.

During his three decades as the ADOR, there have been countless papers, conferences, collaborations, and research projects, and there has been an immense impact in his field. His research impact on improved and advanced materials could be felt for decades.

“Our mission is to solve problems of the intricacies and behavior of matter,” Rath said. “We want to understand how nature has perfected matter over billions of years and what we can do to improve and make new matter. That is our job.”

He said it’s a job he has dedicated his life to pursuing, hopefully leaving scientific progress and talented researchers in his wake. He mentored five scientists who were inducted into the National Academy.

And those mementos on the office walls? “I will leave my collectibles here at NRL for some young researchers to see,” he mused. He hopes there will be a room reflecting his contributions to the Navy, DoD, and the Nation.

“I want them to say, ‘If Dr. Rath can do all of this, I can do it too,’” Rath added. “I want them to be inspired, to be creative thinkers.”

With a vision for the future, he has established endowments at three universities in Michigan, Colorado, and Illinois to recognize with a cash prize the best Ph.D. thesis, endorsed by U.S. industries of its value.

As Rath leans back slightly in his chair, he gives a final thought on the legacy he leaves behind. “I want young researchers to make grand contributions,” he said, “for our nation.”



The walls and much of Dr. Rath’s office are filled with mementos of a rich career that has taken him to every continent except Antarctica. “I will leave my collectibles here at NRL for some young researchers to see. I want them to say, ‘If Dr. Rath can do all of this, I can do it too.’”



NRL Celebrates 50 Years of Fellowship During Annual Children's Holiday Party



A light rain fell under gray skies during a 40-degree morning the day of December 12, 2016, as four buses full of school-aged children — pre-kindergarten to 7th grade — arrived at Building 222 on the U.S. Naval Research Laboratory. Braking gently at the curb, the bus opened its doors with a familiar hiss, and one by one, 90 boys and girls came pouring onto the sidewalk, eager, excited, and ready for a great day.

They were visiting NRL for the 50th Annual Children's Holiday Party, an event which food, fun, friendship, joy and laughter rule the day.

As the children moved down a hallway toward the auditorium to meet Santa, one little fella, barely 3 feet tall, seemed more than ready to jumpstart the day's festivities. "Where's Santa?" he asked, head peering around each corner. "I'm looking for Santa."

The kindergartener, along with his fellow students, got what he was looking for, as the jolly elf and Mrs. Claus were the first event on the day's agenda.

Each student met the globe-trotting couple for a photo and good wishes before settling in for a day



The Naval Research Laboratory celebrated 50 years of hosting neighboring students for a children's holiday party Dec. 12, 2016. During the annual event, young schoolchildren visit the lab to enjoy games, music, food, and entertainment before receiving gifts.

full of Christmas caroling, a dance contest, a Q&A session with the lab's commanding officer CAPT Mark Bruington ("Do you work or play on the lab?" "Have you been around the world?" and "How'd you get your ribbons?" were just a few of the questions asked), a visit by Ronald McDonald, and a performance by ventriloquist Willie Brown.

CAPT Bruington explained some of his ribbons to the curious students and confirmed that he has traveled around the globe a few times. Between jokes, Brown and his "dummy" Woody, encouraged the kids to "treat others with respect, always do your best, and continue to work hard for good grades."

The day would not have been complete without a lunch of hamburgers, hot dogs, chips, cookies, and drinks.

"I'm having a great time," said 1st grader Valencia Millner, while munching a handful of potato chips. "The dance contest was a lot fun."

The 6-year-old wasn't the only one having a good time. NRL has hosted the holiday party every year since 1966 for neighboring students from the District's Ward 8 community. The students selected to visit the lab may not have any Christmas otherwise, according to NRL volunteers, who are more than eager to help their neighbors.

"I love the concept of giving back and helping the community," said Cindy Allen, who works in NRL's Supply Division and has been volunteering for 30 years. Allen, along with co-workers Judy Hope and Linda Brown, are the event's main organizers. "It feels good to help provide a Christmas for children who might need it," Allen said.



According to Allen, the NRL community funds the annual event through donations and fund-raisers such as cookouts and bake sales.

Josh Caldwell, a researcher at the lab, is one of numerous donators for this year's party. "I feel strongly that we need to do as much as we can to offer opportunities to all," he said, "especially those who might not get those opportunities otherwise."

"This is an ideal opportunity to give back," Caldwell said.

There are nine elementary schools in Ward 8 that participate in the holiday partnership with the lab – Garfield, Hendley, Leckie, Malcolm X, Martin Luther King Jr., Patterson, Savoy, Simon, and Turner. Lab volunteers usually host 120 students from four of the nine schools each year. Because this is holiday party's 50-year anniversary, NRL leadership and volunteers decided months ago that 10 hand-selected students from all nine schools would help celebrate the big event.



Local schoolchildren enjoyed snacks and entertainment, sang Christmas carols, and visited with Santa Claus and Ronald McDonald.

"It's important to be active in the local community," said Bruington. Famous for participating in the dance contest with the students, Bruington said the significance for him is "seeing so many kids ... their enthusiasm, excitement, and participation" in the day's events. "It's infectious," he said. "It's better to give than to receive," he continued. "Who better to give to than your neighbors."

"This is a good thing the lab is doing," said Donald Ross, a school psychologist at Leckie, first-time attendee and one of several chaperones. "I can see this brings a lot of cheer to the kids," he continued. "I hope the lab keeps this going."

Smiles and laughter were the theme throughout the day as students were encouraged to treat others

with respect, continue to work hard in school and at home, and remembers that the main purpose of the holiday season is giving.

“This has always been a heartwarming event,” said Roz Williams, a social worker at Garfield. This was Williams’ fifth holiday event. “This is a good thing,” she said. “It’s a great opportunity for the kids.”

As the afternoon came to a close, there was still a buzz in the air as students grabbed their coats before making their way back to the buses. One last thing — there was still the matter of receiving a Santa-sized bundle of gifts to top off the day.

There were smiles all around as students grabbed their Christmas goodies of toys, games, books, educational materials, hats and gloves, holiday candy, and personal care items before loading up. Some of the sacks weighed as much as the child. “What’s in here?” a little boy asked, tussling with his bag, looking like one of Santa’s helpers trying to load a sleigh.

A little girl grabbed her holiday bag on the way out, and with a warm smile on her face, simply said, “Thank you.”



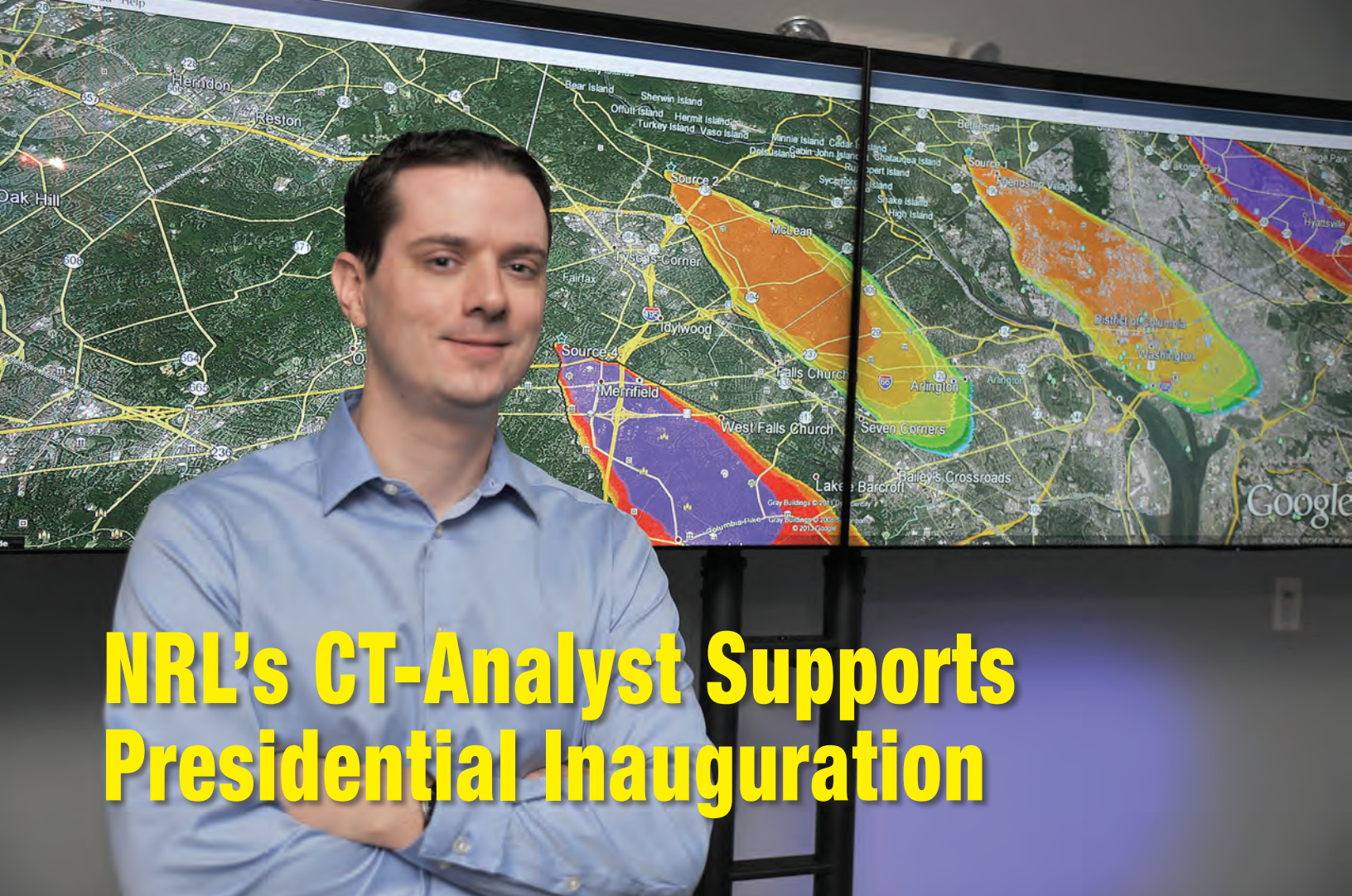
A local student is all smiles as he receives his Santa-sized bag full of gifts at the end of the day.

As volunteers, students, and chaperones said their goodbyes, you couldn’t help but notice the dreary skies had given way to sunshine and an unseasonable 50-plus degrees.

It was a great day.



**U.S. NAVAL
RESEARCH
LABORATORY**



NRL's CT-Analyst Supports Presidential Inauguration

Adam Moses, a computer scientist at the Naval Research Laboratory, displays CT-Analyst software simulation of a potential hazard zone of a chemical, biological, or radiological threat.

The U.S. Naval Research Laboratory (NRL) supported the 2017 inauguration of the President of the United States with CT-Analyst, software developed by researchers in the Laboratories for Computational Physics and Fluid Dynamics.

CT-Analyst software provides first-responders with the capability to produce fast and accurate hazard area predictions for the intentional or accidental release of airborne chemical, biological, and radiological (CBR) agents in urban settings.

The software's basic operation involves placing a source, a potential contaminant of unknown type and origin, and enabling its footprint, which defines the hazard area. Based on the wind condition, CT-Analyst will display a highlighted area to indicate all areas downwind from the source that could possibly be affected.

"Our tool doesn't just isolate the hazard zone it provides a worst-case scenario," said Adam Moses, a computer scientist at NRL. "Because in a real-life,

real-time scenario you are not worried about precise plume coverage down to the inches, you want to know roughly where it is and isn't safe to deploy resources and where to begin looking for victims."

Moses says that, when compared to other plume modeling applications, the CT-Analyst software does not require a full recalculation, and a new result can be produced just as quickly when the input conditions are changed. Another key difference is its ease of use — the CT-Analyst software can be given to a first responder and learned in a matter of 10-20 minutes, as opposed to most other CBR modeling software, which often requires extensive training.

"We actually model in its entirety all the buildings from ground to height... the initial calculation is based on a full 3D model, and then reduced into complexity to a generalized wind field table, and this is actually a really big deal (referring to its ability to drag the plume prediction in real-time instead of delayed response) and really only our tool can do it. Most of the other tools can model the similar things

but the problem is that they need all this information and then they would start the model which may take ten minutes or even an hour or more depending on the complexity. Our results are available in milliseconds.”



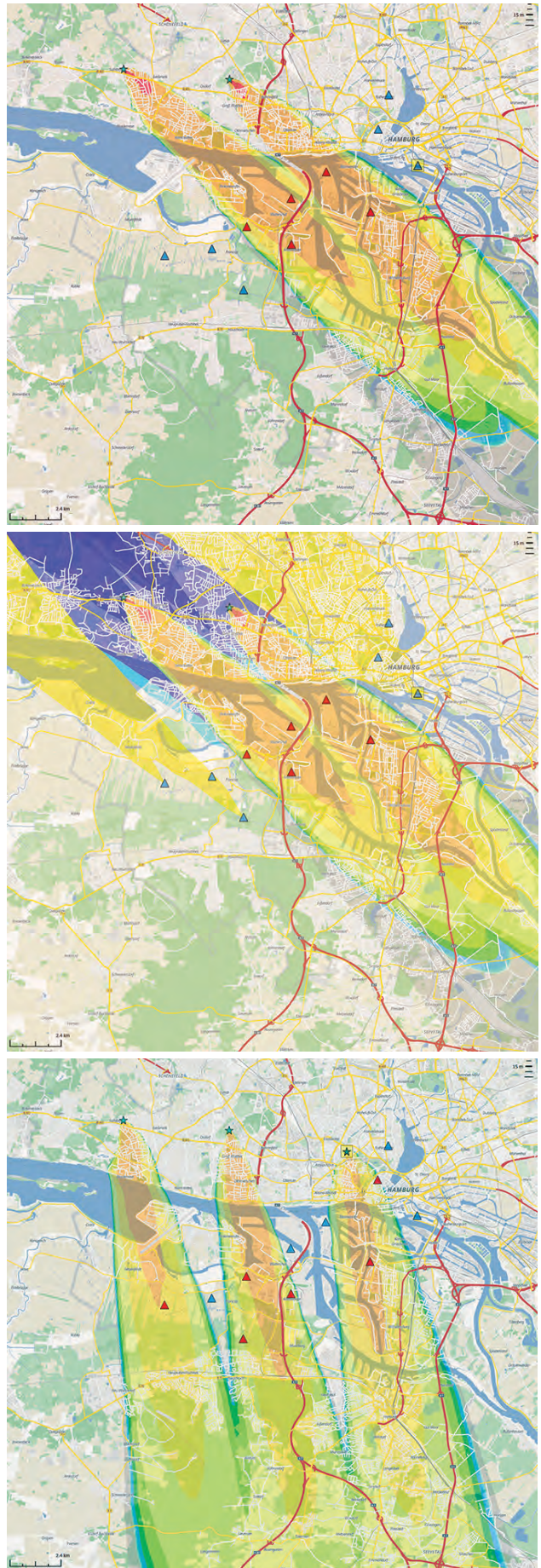
Adam Moses uses CT-Analyst software to showcase a simulated affected area by a chemical, biological or radiological threat.

Moses explains that he and the NRL CT-Analyst team pre-compute the wind field by using the urban geometry, the terrain, and the water, computing for a week on a supercomputer, and then they create a simplified model with all the different scenarios for a given area. “So that when it comes down to using this tool, we’ve distilled every case into this much smaller database and then we just do lookups. So, we can just drag the location of the source from one spot on the map to another, and in real time, it makes adjustments, whereas other software of this type might take minutes or hours.”

This year’s U.S. presidential inauguration, as in previous years, concluded without any actual CBR threats. Moses and the rest of the CT-Analyst team were able to run their software and provide real-time feedback to the Inauguration emergency command. As reports of suspicious packages or unattended bags came in, the CT-Analyst team rapidly produced reports, providing decision-makers instant access to “what-if” scenarios based on only a little information.

“It’s reassuring to know the team was available as a resource if needed,” said Capt. Thomas Chenworth, of the District of Columbia Fire and Emergency Medical Service Department, Hazardous Materials Unit. “I look forward to training on and utilizing the CT-Analyst software in the coming months for our daily responses within the city and region.”

NRL’s CT-Analyst software was also used in support of Super Bowl LI in Houston.





The NRL-developed transparent polymer armor consists of alternating layers of elastomeric polymer and a harder material substrate. Very small crystalline domains, which also provide rigidity, give the polymer its transparency.

NRL Develops Lighter, Field Repairable Transparent Armor

Research chemists at the U.S. Naval Research Laboratory (NRL) have developed and patented a transparent thermoplastic elastomer armor to reduce weight, inherent in most bullet-resistant glass, while maintaining superior ballistic properties.

Thermoplastic elastomers are soft, rubbery polymers converted by physical means, rather than a chemical process, to a solid. Consequently, the solidification is reversible, and enables damaged armor surfaces to be repaired on the fly in the field.

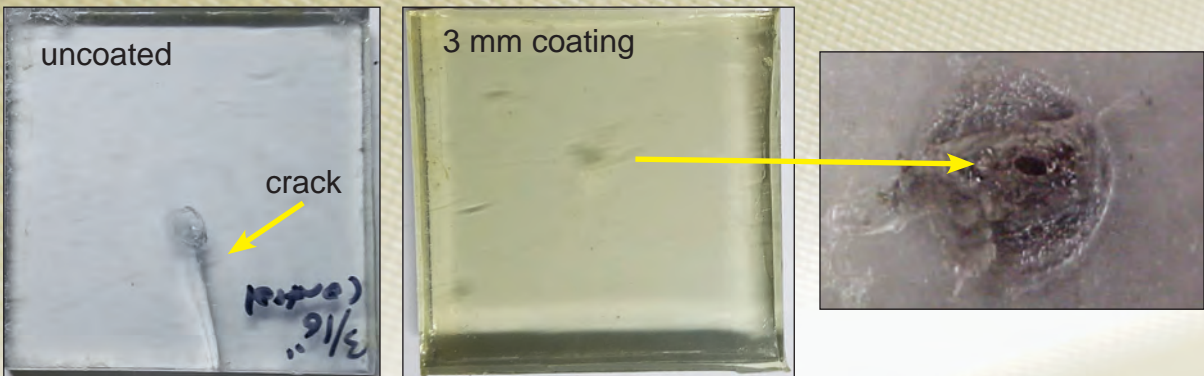
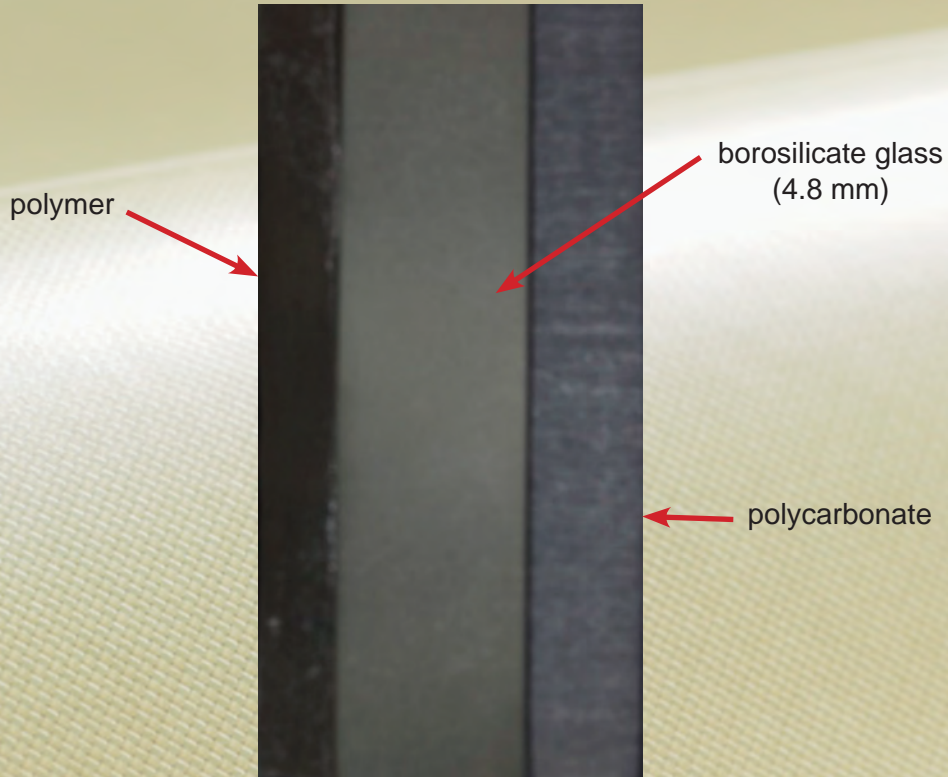
“Heating the material above the softening point, around 100 °C, melts the small crystallites, enabling

the fracture surfaces to meld together and reform via diffusion,” said Mike Roland, a senior scientist, in Soft Matter Physics in the NRL Chemistry Division. “This can be accomplished with a hot plate, akin to an iron, that molds the newly forming surface into a smooth, flat sheet with negligible effect on integrity.”

Up to now, NRL scientists have tested the use of polymeric materials as a coating to achieve improved impact resistance of hard substrates. Applying polyurea and polyisobutylene layers enhance the ballistic performance of armor and helmets, and achieve greater ballistic effectiveness and mitigation of blast waves.

By using a variation of employing thermoplastic elastomers, Roland and Daniel Fragiadakis, a research physicist in the Materials Chemistry Branch of the Chemistry Division, have been able to recreate superior ballistic properties of polyurea and polyisobutylene coatings, with the added benefit of the material being transparent, lighter than conventional bullet-resistant glass, and repairable.

“Because of the dissipative properties of the elastomer, the damage due to a projectile strike is limited to the impact locus. This means that the affect on visibility is almost inconsequential, and multi-hit protection is achieved,” Roland said. ✦



Ballistic testing.

An in-flight technician assigned to Scientific Development Squadron ONE (VXS-1) visually inspects an NP-3C Orion before a research mission in support of SnowEx.



VXS-1 Warlocks Assist NASA in Snow Pack Research Campaign

The Scientific Development Squadron ONE (VXS-1) “Warlocks,” part of the U.S. Naval Research Laboratory, located at Naval Air Station, Patuxent River, Maryland, participated in SnowEx, a NASA-sponsored campaign, Feb. 16–26, 2017, in Colorado.

The exercise is a multi-year campaign to test a variety of sensors and techniques to improve water measurements in snow over different terrains, a key factor in calculating water supplies in many parts of the world, according to NASA scientists and U.S. Forest Service officials. NASA provided the test equipment, a variety of sophisticated sensors, scanners, and radar, which was used aboard VXS-1’s NP-3C Orion.

SnowEx took place primarily in the Rocky Mountains of Grand Mesa, Colorado, with other operations at Senator Beck Basin, near Silverton, Colorado. The squadron operated out of Peterson Air Force Base in Colorado Springs.

“This was a unique opportunity for us,” said CMDR David Neall, VXS-1’s executive officer. NASA has its own P-3 aircraft, but they were not available for this mission, according to Neall. “They (NASA) asked for our assistance, and it turned out to be great timing that we were able to support them,” he said. The P-3 aircraft is perfect for a mission like this, said LT Denise Miller, one of the pilots for SnowEx. “It has long endurance and long range — up to 10 hours,” said Miller. “We can fly it anywhere on the planet.”

During the two-week campaign, scientists and forestry experts collected a variety of airborne and ground-based measurements of the snow-packed mountains. The SnowEx team included more than 100 scientists from universities and agencies across the United States, Europe, and Canada. SnowEx is sponsored by the Terrestrial Hydrology Program in NASA’s Earth Science Division, Washington, D.C., and managed by Goddard Space Flight Center, Greenbelt,



The SnowEx exercise is a multi-year campaign to test a variety of sensors and techniques to improve water measurements in snow over different terrains. NASA provided the test equipment, a variety of sophisticated sensors, scanners, and radar, used aboard VXS-1's NP-3C Orion.

Maryland. The U.S. Forest Service led the ground campaign in Grand Mesa and Senator Beck Basin.

Working with the Forest Service's ground experts and NASA scientists had Miller viewing this mission as a career milestone. "This mission was an exciting surprise for me, for all of us," she said. "We helped gather important information, how water affects farming and people's quality of life."



LT Denise Miller was a SnowEx campaign NP-3C Orion pilot. The P-3 aircraft is perfect for the mission, due to its long-range and endurance capabilities, she said. NASA provided the test equipment, a variety of sophisticated sensors, scanners, and radar, used aboard VXS-1's NP-3C Orion.

For decades, satellites have measured snowfall and the area covered by snow, but they cannot consistently measure how much water is contained in the snow over all terrains, Dr. Edward Kim, NASA's SnowEx project scientist, explained. That's why information gathered from the overhead flights, combined with data from the ground team – scientists working in shifts in frigid, well-below-freezing temperatures and 60 mph winds — is vitally important "to get a global picture," he said.

This research is important for many reasons, Kim continued. "Snow is critical to society," he said. According to Kim, snow's ability to provide water, its potential as a natural hazard, problems stemming from snow droughts, water security (i.e., who has snow, and therefore, water) as well as the powdery substance's affect on weather and climate are of high interest to scientists.

More than one-sixth of the world's population relies on seasonal snow and glaciers for water. As much as three-quarters of the water used in the western United States comes from snow.

"Nearly 80 percent of the water used in the western part of the country to sustain human life and crop irrigation starts as mountain snowfall," said Frank McCormick, a research program manager with the U.S. Forest Service.

"Our knowledge of snow becomes increasingly important as the population of the West and the world increases," said Karl Wetlaufer, a hydrologist with the U.S. Department of Agriculture.

Better measurements of snow are of significant interest for managers of fresh water availability, natural hazards, winter-dependent industries, and ecosystem impacts. The measurements made in campaigns such as SnowEx could ultimately lead to a snow-observing satellite mission, Kim said.

VXS-1 crew members are excited about the opportunity to assist in a far-reaching endeavor. "It's incredible working with NASA on a large, scientific project," said Naval Aircrewman (Avionics) 1st Class Rodney Hynes. Hynes is an inflight technician with the squadron. "I'm going to go home and tell my kids all about it."

As the SnowEx campaign progresses through 2022, VXS-1 will continue to play a critical role in NASA's research, said Neall. "This is a once-in-a-lifetime opportunity. To play a part in testing this equipment and helping gather data that could probably guide life-changing decisions for how we operate and plan for water resources. Participating in this project is unprecedented. It's amazing to be a part of that."

NRL VXS-1's aircraft operate worldwide on extended detachments and annually log more than 600 flight hours. These aircraft are the sole airborne platforms for numerous projects such as bathymetry, electronic countermeasures, gravity mapping, and radar development research. The squadron has a flawless safety record, having amassed more than 74,000 hours of accident-free flying over a 54-year period.



Mr. Paul Charles, Program Director
NRL HBCU/MI Internship Program

HBCU/MI Program at NRL Celebrates 25th Anniversary

The U.S. Naval Research Laboratory's Historically Black College and Universities/Minority Institutions (HBCU/MI) internship program was conceived as a small program with a desired goal of encouraging greater participation in science and technology by underrepresented minority students.

In 1992, this concept was brought to light under the direction of Dr. Joel Schnur (former Director of the Center for Bio/Molecular Science and Engineering) and Dr. Bruce Gaber (former Deputy Director), and with financial support from Dr. Robert Wellek of the National Science Foundation. Their vision was to provide "hands-on" research experiences that would energize each student's interest in science, technology, engineering, and mathematics (STEM). The interns would be mentored by NRL scientists

and advised on the ideals of establishing goals and focusing on ways of achieving them. As Drs. Schnur, Gaber, and Wellek conversed, each realized the benefits and impact this vision would have on NRL and the Department of Defense. It would (1) increase minority representation at the master's and doctoral levels in the science and technology (S&T) field, which remains staggeringly low; (2) increase diversity in S&T at NRL; and (3) aid in strengthening NRL's future S&T workforce.

Through a cooperative agreement with Clark Atlanta University (CAU) to jointly administer the program and with the assistance of Dr. Melvin Webb (CAU biology professor, Director of PRISM-D, and MARC-U-STAR honors program) and Ms. Jacqui Jackson (Assistant Program Manager), an initial

candidate pool was brought forth. Designed as a 10-week summer internship program, the program gave five talented undergraduate interns the opportunity to participate in a research experience that would mold their future.

Over the years, program leadership transitioned from Dr. David Turner to Dr. Mark Spector (now Program Manager at the Office of Naval Research – Code 331), who would incorporate a few new elements into the program, such as an oral presentation and a written technical report to sharpen the interns speaking and technical skills.

In the early 1990s, Paul Charles joined the Center for Bio/Molecular Science and Engineering as a research scientist and earnestly became involved in the program. In 2005, Mr. Charles took the helm and began to lead the program. With the support of co-directors, mentors, and administrative support staff, the program has blossomed into a comprehensive, multi-component, interdisciplinary program with sustainable growth each year. Research topics include chemical and biological sensor design and engineering, organic/inorganic molecular imprinting, three-dimensional analysis of materials, biofuels and alternative energy materials, laser fabrication of living tissue for sensing applications, nanocrystalline magnetic materials for power electronics applications, robotics and aerospace engineering, synthesis for high strength materials, systems biology, and many more. Mr. Charles and his co-directors believe that “educating the youth in the STEM disciplines is critical for the Navy and all the branches of the military in order to remain at the forefront in science and technology. As a nation, we have proven ourselves worldwide to be leaders in the S&T field, however, we must continue to strengthen our workforce by mentoring our youth.” In addition to conducting scientific research and the written and oral report elements, a professional development component was incorporated into the program schedule. The components include (1) resume writing/interviewing skills workshop; (2) laboratory safety and ethics in science and engineering seminars; (3) graduate school site visits; and (4) an oral presentation workshop. It was

the belief that these additional components would provide the intern with a fundamental base that would benefit them long-term upon completion of their 10-week research experience.

To promote student-to-student team building and networking, program leaders organized BBQ picnics, pizza socials, Washington Nationals baseball games, outings to Baltimore’s Inner Harbor, and physical fitness trips to the recreation center. Mr. Charles believes in promoting a “family atmosphere that will help create a higher level of performance. Engaging and helping each other will always provide a path to success.”

Through continued funding by the Office of Naval Research (Anthony Smith, Sr., Director, Department of the Navy HBCU/MI Program Manager), the program has dramatically increased in applicants and participants. To date, the program has had 326 intern participants, of whom 57 percent have been women. Minority participation in the program is 99 percent, with African-Americans making up 74 percent of participants and Hispanics 24 percent. The program has expanded to include more than 40 HBCU/MI universities, with a continued effort to increase the number of participating college and universities. From this internship program, 40 articles with interns as co-authors have been published in top-tiered journals (e.g., *Nature*, *Journal of the American Chemical Society*, *Journal of Applied Physics*, *Biosensors and Bioelectronics*, and *Metallurgical Materials Transactions A*). As a result of mentoring and tireless efforts, many of the past participants have benefited from the program and continued on to graduate school to achieve their highest academic goals by obtaining a master’s degree, a Ph.D., or an MD/Ph.D.

As the NRL HBCU/MI Internship program enters its 25th anniversary year, it recognizes global diversity and inclusion, and continues to promote diversity in the STEM disciplines. Encouraging our youth to strive for excellence with the belief that “ideas are limitless with no boundaries of race, gender or color” will help position our nation as a leader at the forefront of science and technology.



The U.S. Naval Research Laboratory's Historically Black College and University and Minority Institution (HBCU/MI) internship program celebrated its 25th anniversary on July 27, 2017, with an engaging science, technology, engineering, and math (STEM) forum. The well attended event included past HBCU/MI interns, Department of Defense (DoD) personnel, and NRL leadership as guest speakers, and closed with an awards ceremony.

Mr. Anthony C. Smith, Sr., the Department of the Navy's HBCU/MI program director recognizes the NRL's HBCU/MI program as a model that should be followed by other DoD agencies in its implementation and performance. "NRL's HBCU/MI internship program has done a phenomenal job for the last 25 years," said Smith. "Many of the program's past participants have gone on to complete competitive doctorate programs." Past participants, who went on to earn their doctorate degrees, spoke of their experience during the ceremony.

DISTINGUISHED GUEST SPEAKERS



Mr. Anthony C. Smith, Sr.
Program Director
DON HBCU/MI Program



Dr. George Spanos
Technical Director
The Minerals, Metals & Materials
Society



Dr. Bradley Ringeisen
Deputy Director
Biological Technology Office
Defense Advanced Research
Program Agency



Dr. Alexis Lewis
Program Director
The National Science Foundation



Dr. Jonathan Madison
Research Scientist
Org. 1851 – Materials Mechanics
Sandia National Laboratories



Dr. Cherise Bernard
Senior Manager of Global
Strategic Networks
Elsevier



Dr. Oscar Morales-Collazo
Research Scientist
University of Notre Dame
Department of Chemical and
Biomolecular Engineering



Dr. Michael Rawlings
AAAS S&T Policy Fellow
Division of Civil, Mechanical,
and Manufacturing Innovation
National Science Foundation



- 24** NRL – Our Heritage
- 27** NRL Today
- 28** NRL Research Divisions
- 68** Research Support Facilities
- 71** Other Research Sites

NRL — OUR HERITAGE

The early 20th century founders of the Naval Research Laboratory (NRL) knew the importance of science and technology in building naval power and protecting national security. They knew that success depended on taking the long view, focusing on the long-term needs of the Navy through fundamental research. NRL began operations on July 2, 1923, as the United States Navy's first modern research institution, and it continues today as one of the Navy's premier research and development centers.

Thomas Edison's Vision: The first step came in May 1915, a time when Americans were deeply worried about the great European war. Thomas Edison, when asked by a *New York Times* correspondent to comment on the conflict, argued that the Nation should look to science. "The Government," he proposed in a published interview, "should maintain a great research laboratory....In this could be developed...all the technique of military and naval progression without any vast expense." Secretary of the Navy Josephus Daniels seized the opportunity created by Edison's public comments to enlist Edison's support. He agreed to serve as the head of a new body of civilian experts — the Naval Consulting Board — to advise the Navy on science and technology. The Board's most ambitious plan was the creation of a modern research facility for the Navy. Congress allocated \$1.5 million for the institution in 1916, but wartime delays and disagreements within the Naval Consulting Board postponed construction until 1920.

The Laboratory's two original divisions — Radio and Sound — pioneered in the fields of high-frequency radio and underwater sound propagation. They produced communications equipment, direction-finding devices, sonar sets, and perhaps most significant of all, the first practical radar equipment built in this country. They also performed basic research, participating, for example, in the discovery and early exploration of the ionosphere. Moreover, the Laboratory was able to work gradually toward its goal of becoming a broadly based research facility. By the beginning of World War II, five new divisions had been added: Physical Optics, Chemistry, Metallurgy, Mechanics and Electricity, and Internal Communications.

World War II Years and Growth: Total employment at the Laboratory jumped from 396 in 1941 to 4400 in 1946, expenditures from \$1.7 million to \$13.7 million, the number of buildings from 23 to 67, and the number of projects from 200 to about 900. During WWII, scientific activities necessarily were concentrated almost entirely on applied research. New electronics equipment — radio, radar, sonar — was developed. Countermeasures were devised. New lubricants were produced, as were antifouling paints, luminous identification tapes, and a sea marker to help save survivors of disasters at sea. A thermal diffusion process was conceived and used to supply some of the ^{235}U isotope needed for one of the first atomic bombs. Also, many new devices that developed from booming wartime industry were type tested and then certified as reliable for the Fleet.



The Naval Research Laboratory was conceived in 1915 during a correspondence between the Secretary of the Navy, Josephus Daniels (seated at his desk on the right), and Thomas Edison, who is shown here standing at his desk.



The Naval Consulting Board and Navy Department officials surround Thomas Edison and Josephus Daniels, who are seated behind the desk.



Secretary Daniels breaks ground for Building 1 in 1920.

Post-WWII Reorganization: The United States emerged into the postwar era determined to consolidate its significant wartime gains in science and technology and to preserve the working relationship between its armed forces and the scientific community. While the Navy was establishing its Office of Naval Research (ONR) as a liaison with and supporter of basic and applied scientific research, it was also encouraging NRL to broaden its scope and become, in effect, its corporate research laboratory. There was a transfer of NRL to the administrative oversight of ONR and a parallel shift of the Laboratory's research emphasis to one of long-range basic and applied investigation in a broad range of the physical sciences.

However, rapid expansion during WWII had left NRL improperly structured to address long-term Navy requirements. One major task — neither easily nor

rapidly accomplished — was that of reshaping and coordinating research. This was achieved by transforming a group of largely autonomous scientific divisions into a unified institution with a clear mission and a fully coordinated research program. The first attempt at reorganization vested power in an executive committee composed of all the division superintendents. This committee was impracticably large, so in 1949, a civilian director of research was named and given full authority over the program. Positions for associate directors were added in 1954, and the laboratory's 13 divisions were grouped into three directorates: Electronics, Materials, and Nucleonics.

The Breadth of NRL: During the years since World War II, the Laboratory has conducted basic and applied research pertaining to the Navy's environments



NRL in its first year, 1923. Building 1, which housed the Laboratory's first research spaces, stands by itself on the left. Starting from the bank of the Potomac River and forming a line opposite Building 1 is the coal-fired power station, pattern shop, foundry, and machine shop.



NRL in the 21st century. In its more than 90 years, NRL has evolved into a large research and development campus with some 100 buildings and nearly 2500 full-time employees, more than half of which hold master's or doctoral degrees.

of earth, sea, sky, space, and cyberspace. Investigations have ranged widely — from monitoring the Sun's behavior, to analyzing marine atmospheric conditions, to measuring parameters of the deep oceans. Detection and communication capabilities have benefited by research that has exploited new portions of the electromagnetic spectrum, extended ranges to outer space, and provided a means of transferring information reliably and securely, even through massive jamming. Submarine habitability, lubricants, shipbuilding materials, firefighting, and the study of sound in the sea have remained steadfast concerns, to which have been added recent explorations within the fields of virtual reality, superconductivity, biomolecular science and engineering, and nanotechnology.

The Laboratory has pioneered naval research into space — from atmospheric probes with captured V-2 rockets, through direction of the Vanguard project (America's first satellite program), to inventing and developing the first satellite prototypes of the Global Positioning System (GPS). Today, NRL is the Navy's lead laboratory in space systems research, as well as in fire research, tactical electronic warfare, microelectronic devices, and artificial intelligence.

The consolidation of NRL and the Naval Oceanographic and Atmospheric Research Laboratory, with

centers at Bay St. Louis, Mississippi, and Monterey, California, added critical new strengths to the Laboratory. NRL now is additionally the lead Navy center for research in ocean and atmospheric sciences, with special strengths in physical oceanography, marine geosciences, ocean acoustics, marine meteorology, and remote oceanic and atmospheric sensing.

The Twenty-First Century: The Laboratory is focusing its research efforts on new Navy strategic interests in the 21st century, a period marked by global terrorism, shifting power balances, and irregular and asymmetric warfare. NRL scientists and engineers are working to give the Navy the special knowledge, capabilities, and flexibility to succeed in this dynamic environment. While continuing its programs of basic research that help the Navy anticipate and meet future needs, NRL also moves technology rapidly from concept to operational use when high-priority, short-term needs arise — for pathogen detection, lightweight body armor, contaminant transport modeling, and communications interoperability, for example. The interdisciplinary and wide-ranging nature of NRL's work keeps this "great research laboratory" at the forefront of discovery and innovation, solving naval challenges and benefiting the nation as a whole.

NRL TODAY

Organization and Administration

The Naval Research Laboratory is a field command under the Chief of Naval Research, who reports to the Secretary of the Navy via the Assistant Secretary of the Navy for Research, Development and Acquisition.

Heading the Laboratory with joint responsibilities are CAPT Scott D. Moran, USN, Commanding Officer, and Dr. Bruce G. Danly, Director of Research. Line authority passes from the Commanding Officer and the Director of Research to three Associate Directors of Research, the Director of the Naval Center for Space Technology, and the Associate Director for Business Operations. Research divisions are organized under the following functional directorates:

- Systems
- Materials Science and Component Technology
- Ocean and Atmospheric Science and Technology
- Naval Center for Space Technology

The *NRL Fact Book*, published every two years, contains information on the structure and functions of the directorates and divisions.

NRL operates as a Navy Working Capital Fund (NWCF) Activity. All costs, including overhead, are charged to various research projects. Funding in FY16 came from the Chief of Naval Research, the Naval Systems Commands, and other Navy sources; government agencies such as the U.S. Air Force, the Defense Advanced Research Projects Agency, the Department of Energy, and the National Aeronautics and Space Administration; and several nongovernment activities.

Personnel Development

At the end of FY16, NRL employed 2601 persons — 36 officers, 60 enlisted, and 2505 civilians. In the research staff, there are 895 employees with doctorate degrees, 392 with master's degrees, and 463 with bachelor's degrees. The support staff assists the research staff by providing administrative support, computer-aided design, machining, fabrication, electronic construction, publication and imaging, personnel development, information retrieval, large mainframe computer support, and contracting and supply management services.

Opportunities for higher education and other professional training for NRL employees are available through several programs offered by the Employee Relations Branch. These programs provide for graduate work leading to advanced degrees, advanced training, college course work, short courses, continuing education, and career counseling. Graduate students, in certain cases, may use their NRL research for thesis material.

For non-NRL employees, several postdoctoral research programs exist. There are also agreements with several universities for student opportunities, as well as summer and part-time employment programs. Summer and interchange programs for college faculty members, professional consultants, and employees of other government agencies are also available. These programs are described in the *NRL Review* chapter “Programs for Professional Development.”

NRL has active chapters of Women in Science and Engineering (WISE), Sigma Xi, Toastmasters International, and the Federal Executive and Professional Association. An amateur radio club, a drama group, and several sports clubs are also active. NRL has a Recreation Club that provides gymnasium and weight-room facilities. NRL also has an award-winning Community Outreach Program. See “Programs for Professional Development” for details on all these programs and activities.

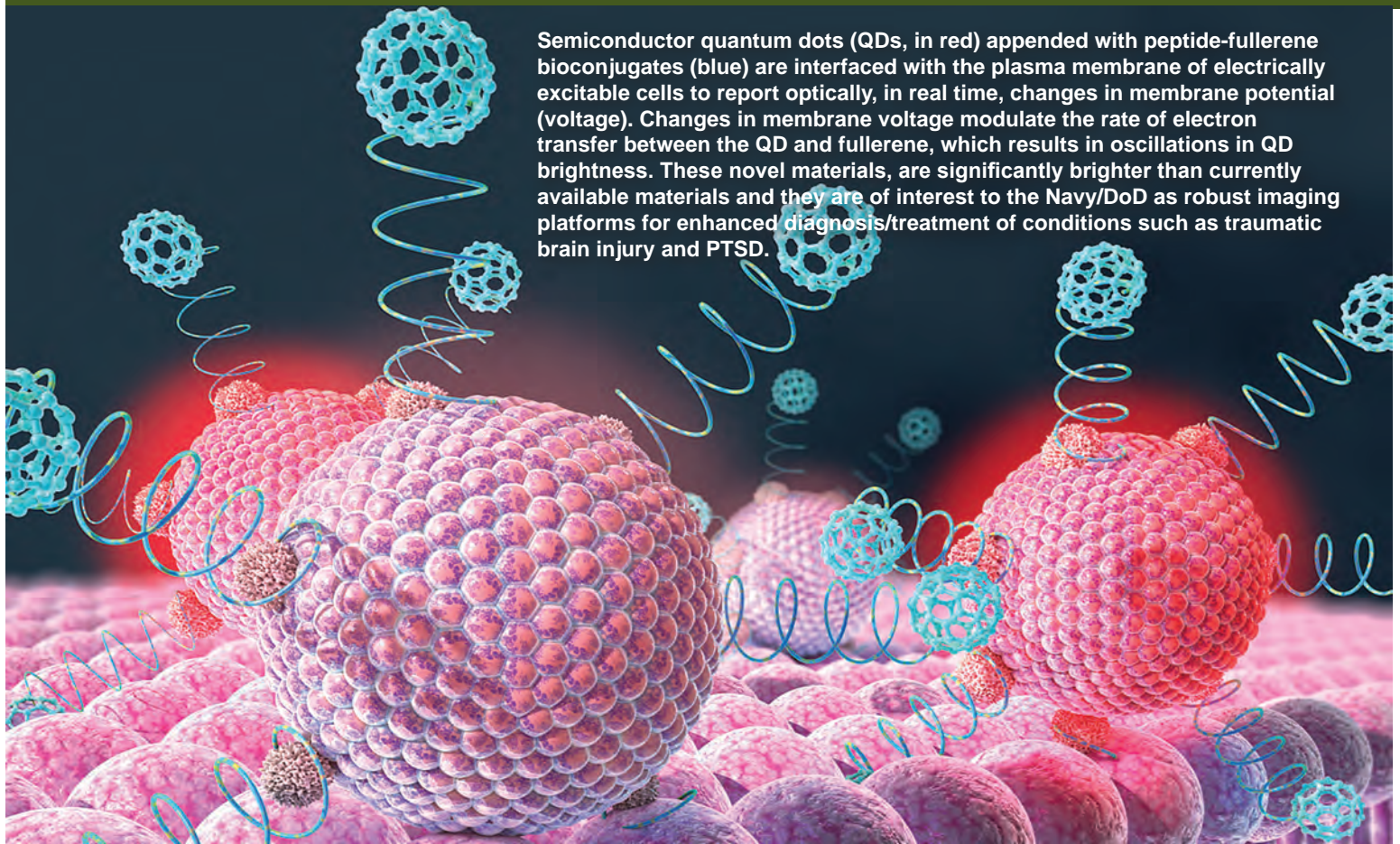
NRL has its very own credit union. Established in 1946, NRL Federal Credit Union (NRLFCU) is a sound financial institution that serves over 22,000 members including NRL employees, contractors, select employee groups and their families as well as consumers via the American Consumer Council. Focusing on its mission of Trusted Partners for Life, NRLFCU provides many free and low-cost products and services including free checking with free bill pay, Visa Check-Card, and mobile banking with remote deposit, auto and personal loans, credit cards, mortgages, and more. NRLFCU offers direct deposit, online access, and local branches (including one in Building 222, one in Waldorf, Maryland, and one in Alexandria, Virginia). Additionally, NRLFCU has relationships with several ATM networks to provide you with access to tens of thousands of surcharge-free ATMs. NRLFCU also offers personalized full-service investment and brokerage services. For more information, call 301-839-8400 or visit nrlfcu.org.

Public transportation to NRL is provided by Metrobus. Metrorail service is three miles away.

Sites and Facilities

NRL's main campus in Washington, D.C., consists of 90 main buildings on about 131 acres. NRL also maintains 15 other research sites, including a vessel for fire research and a Flight Support Detachment. The many diverse scientific and technological research and support facilities are described here. More details can be found in the *NRL Major Facilities* publication at www.nrl.navy.mil.

Institute for Nanoscience



Semiconductor quantum dots (QDs, in red) appended with peptide-fullerene bioconjugates (blue) are interfaced with the plasma membrane of electrically excitable cells to report optically, in real time, changes in membrane potential (voltage). Changes in membrane voltage modulate the rate of electron transfer between the QD and fullerene, which results in oscillations in QD brightness. These novel materials, are significantly brighter than currently available materials and they are of interest to the Navy/DoD as robust imaging platforms for enhanced diagnosis/treatment of conditions such as traumatic brain injury and PTSD.

The revolutionary opportunities available in nanoscience and nanotechnology led to a National Nanotechnology Initiative in 2001. In that same year, the U.S. Naval Research Laboratory (NRL) Institute for Nanoscience was established. The prospect for nanoscience to provide a dramatic change in the performance of materials and devices was the rationale for identifying this emerging field as one of the Department of Defense strategic research areas for basic research funding on a long-term basis.

The mission of the NRL Institute for Nanoscience is to conduct highly innovative, interdisciplinary research at the intersections of the fields of materials, electronics, chemistry, and biology in the nanometer size domain. The Institute exploits the broad multidisciplinary character of the Naval Research Laboratory to bring together scientists with disparate training and backgrounds to pursue common goals at the intersection of their respective fields in systems at this length scale. The Institute provides the Navy and DoD with scientific leadership in this complex, emerging area and identifies opportunities for advances in future defense technology. NRL's

nanoscience research programs and accomplishments directly impact nearly all Naval S&T focus areas.

The Institute's research program emphasizes multidisciplinary efforts across a wide range of DoD-centric science and technology, such as:

- Neuromorphic computing for intelligent autonomy
- Quantum information process for secure communication, enhanced sensing and solving complex battlefield optimization problems
- Bio/inorganic interfaces for monitoring/treating warfighter health and improved prosthetics
- Nanostructured materials for energy storage/conversion, improved armor, etc.

The Institute for Nanoscience building, opened in October 2003, provides NRL scientists access to state-of-the-art laboratory space and fabrication facilities. The building has 5000 ft² of Class 100 clean room space for device fabrication, 4000 ft² of "quiet" lab space with temperature controlled to ± 0.5 °C, acoustic isolation at the NC35 standard (35 dB at 1 kHz), floor vibration

isolation to $<150 \mu\text{m/s rms}$ at 10 to 100 Hz and $<0.3 \text{ mOe}$ magnetic noise at 60 Hz, and 1000 ft^2 of “ultra-quiet” laboratory space with temperature controlled to $\pm 0.1 \text{ }^\circ\text{C}$ and acoustic isolation at the NC25 standard (25 dB at 1 kHz). Equipment includes a complete suite of fabrication tools including deposition and etch systems, optical mask aligners, two electron beam

writers, a three-dimensional nanolithography tool, a focused ion beam writer, an optical pattern generator for mask making, a plasma-enhanced atomic layer deposition system, a laser machining tool, and a wide variety of characterization tools including an aberration-corrected transmission electron microscope.



Institute for Nanoscience clean room.



The Institute for Nanoscience research building.

Laboratory for Autonomous Systems Research



The Laboratory for Autonomous Systems Research

The Laboratory for Autonomous Systems Research contains a number of specialized high bays and laboratories to support our multidisciplinary research and development. The high bays recreate important environments and allow us to reduce the cost of research and development. The environments help to bridge the gap between bench science, where real-world conditions cannot be duplicated, and fielded experiments, which provide realism, but can be very expensive. A collaborative area allows teams of researchers to work together. In addition to modular furniture designed to enhance collaboration, project offices are available for team leads to manage their projects. In addition, a meeting room with projection equipment can be reserved.

The *prototyping high bay* allows for the development and evaluation of autonomous systems. The high bay is approximately 150 × 75 ft, with a height of 30 ft, and includes a number of unique features and systems to support experimentation with a combination of ground and air vehicles, as well as people that are interacting with the systems.

The *tropical high bay* simulates a southeastern Asian rainforest. This greenhouse is about 40 × 60 ft, with a height of 46 ft, and has live growth, a stream, pond, and appropriate terrain. A variety of tropical plants, native to southeast Asian rain forests, are maintained in the greenhouse, with an appropriate density of plants and foliage, and a three-level canopy. The temperature is held constant at 80 °F with 80% humidity. The terrain in the high bay is accurate and provides a realistic environment for autonomous ground vehicles. Development of ground, air and climbing vehicles is supported by this high bay, as well as sensor research.

The littoral zone is that part of a sea, lake or river that is close to the shore. The *littoral high bay* includes various tanks and pools to support the evaluation of autonomous systems, power and energy systems, and sensor systems that need to work in water environments and along the shore. The high bay is 54 × 76 ft, with a height of 28 ft, and includes an overhead crane. A wide range of research is performed in this high bay, including integration of component technologies into working prototypes.



The prototyping high bay.

The *desert high bay* provides sand and rock for evaluating autonomous systems designed for these challenging environments. The 2.5 ft deep sand pit allows evaluation of vehicles designed for desert environments. The facility also supports research in the development of passive and active sensors.

An outdoor *upland forest* research area is a laboratory for testing equipment and activities in environmental conditions that approximate those of a upland forest. The goal is to replicate a broadleaf evergreen forest that is approximate to human settlement and has experienced disturbance due to human cultivation and harvesting of vegetation and other uses. The forest includes a waterfall, ponds and a large collection of boulders arranged into box canyons. The boulders are arranged to offer varying degrees of navigational difficulty.

Four 20 × 40 ft *human-systems interaction labs* support development of novel autonomous system interfaces, and research and testing of advanced human-system interaction techniques. These labs overlook the prototyping high bay. Two of the interactions labs are adjacent on the first floor and two are adjacent on the second floor. Each pair may be combined into a single 20 × 80 ft lab by opening a partition between the adjacent rooms.

The *power and energy lab* provides a safe, controlled environment for the evaluation of new power and energy sources from the component level to integrated systems. The lab has the following features: dry room for custom battery assembly and experimentation, particularly for lithium-based battery technology; glovebox containing argon for safe handling of lithium; solar simulators for photovoltaic research; environmental chambers for temperature and atmosphere stress testing; gas manifolds dedicated to fuels and oxidizers; and isolation room for safe evaluation of systems.

The *sensor lab* is available to test and calibrate a variety of individual chemical and biological sensors or complete sensor systems. This fully equipped laboratory is designed to serve as a test platform for sensor prototypes prior to full-scale field demonstrations and has some unique features. The Ambient Air Test Facility provides continuous exposure of developmental sensors to outside air through an insulated duct with continuously variable flow velocities from 1 to 34 mph (0.5 to 17 m/s). Sections of the flow tube can be configured for isokinetic sample access. The large walk-in environmental chamber (11 × 10 × 10 ft) can be used to evaluate sensors and autonomous systems for temperature and humidity effects while simultaneously exposing them to test analytes at varying concentrations. This chamber can be controlled from -30 to +185 °F and from 10% to 95% relative humidity. The small environmental and altitude chamber (approximately 64 cubic feet) can be used to evaluate sensors for effects of temperature, humidity and pressure. It can be controlled from -50 to +350 °F, from 10% to 95% relative humidity, and the barometric pressure can be controlled from -9000 ft to +100,000 ft of altitude. It includes a flange that provides electrical, gas and liquid feedthroughs. An automated gas chromatography system allows for characterization and quantification of samples. Trace detection limits of vapor and liquid samples is possible by implementing a variety of different detectors and sample introduction techniques. Several different vapor generation systems are provided that can be implemented to create mixtures of analytes. Vapors can be prepared in both zero and humidified air for sensor and instrumental analysis. Verification and quantification of analytes being introduced to sensors can be simultaneously quantified by an online gas chromatography system. Also housed in the sensor lab is a 100 ft² anechoic chamber with an antenna characterization system, used to evaluate small communications systems for autonomous systems. The laboratory contains a full complement of instruments and equipment necessary for work with chemicals and biological materials at Biosafety Level 2 (BSL-2), including walk-in and bench top fume hoods and biosafety cabinets.

The *machine shop* provides the machines and tools for both metal and woodworking to support the Laboratory's research and engineering staff. The electronics shop provides hooded soldering stations and test equipment to support the development of electronic components for prototypes. In addition, the electronics shop contains multiple types of 3D prototyping machines, 3D printers, high resolution scanners and CAD/CAM software to support the rapid design and production of parts for vehicles, sensors and power and energy systems.



Electromagnetic Maneuver Warfare Testbed

NRL has gained worldwide renown as the “birthplace of U.S. radar” and, for nearly a century has maintained its reputation as a leading center for radar-related research and development. A number of facilities managed by NRL’s Radar Division continue to add to this reputation.

A major Division asset is the Antenna and Radar Cross Section (RCS) Measurement Facility capable of characterizing the radiation and impedance properties of antenna systems, performing RCS measurements, and measuring the s -parameters of radiofrequency (RF)-system components. This facility consists of two separate measurement resources, a compact range and an anechoic chamber, each providing multiple measurement options for frequencies in the range of 2 to 110 GHz. The compact range reflector simulates far-field conditions in a cylindrical quiet zone (phase error $<10^\circ$) with an 8 ft diameter and 8 ft length for RCS measurements and also has a near-field scanner capable of planar, cylindrical, or spherical nearfield antenna characterizations. The anechoic chamber provides far-field antenna patterns and s -parameter measurements of RF system components

and has a second smaller near-field scanner for antenna characterizations.

Another significant Division asset is the Computational Electromagnetics (CEM) Facility, which supports complex, high-fidelity electromagnetic modeling of naval platforms, targets, and antennas. The facility produces detailed estimates of the radar cross section of ships. The Radar Division developed the Radar Target Signature (RTS) model specifically for calculating the radar signature of ships in a sea multipath environment. RTS calculates the radar signatures of large objects using computer models that describe the geometry and material properties of the objects. The radar signature of smaller objects, such as phased array antennas, can be accurately calculated using any of several low frequency computational electromagnetic software packages available within the facility. The facility contains a Linux cluster of 75 Apple Mac Pro computers with a total of 840 processors and 3.4 TB of physical memory. The CEM Facility also has multiple-CPU supercomputers used to design phased array antennas. This provides for tremendous synergism between the CEM group and the Antenna and Radar

Cross Section Measurement Facility. Innovative and novel designs generated in the CEM environment transition immediately for assessment in the compact range. This rapid feedback between theoretical and experimental development shortens the development cycle for new and novel antenna designs using new materials. The Division has a revitalized radar imaging and signal processing facility utilizing multicore PCs running both Linux and Windows operating systems. The Division supports operational systems by developing algorithms for synthetic aperture radar (SAR) and inverse SAR (ISAR) imaging and detection of difficult targets in harsh clutter environments. Software is available for real-time playback of ISAR data and offline processing of SAR data stored on RAID systems with a current online capacity of 96 TB. The systems are connected by a high-speed network. Data is obtained from sponsors or collected using a number of fleet assets, to include the AN/APS-153(V)5.

In support of ship-based radar applications, the Division operates the Radar Test Facility at the Chesapeake Bay Detachment (CBD) near Chesapeake Beach, Maryland. The site has the AN/SPS-49A(V)1 long-range air search radar that is used to support R&D as well as fleet initiatives. The radar has been instrumented with a “sidecar” signal processor that supports the development and evaluation of new signal processing concepts. A new asset is the S-Band Waveform Development Testbed. This system operates with up to a 400 MHz instantaneous bandwidth using arbitrary waveforms and can be used for investigating advanced waveforms and signal processing for clutter and interference mitigation. With a 43 dB gain monopulse antenna, the system can collect data from representative targets at operationally relevant ranges.

The Electromagnetic Maneuver Warfare (EMW) test bed at CBD is a Systems Directorate installation operated by the Radar Division, with extensive collaboration and contributions from other NRL divisions and industry partners. The facility was originally established as the test bed for the Advanced Multifunction Radio Frequency Concept (AMRFC) prototype. It was subsequently modified to add the Multifunction Electronic Warfare (MFEW) Advanced Development Model (ADM), and most recently expanded to incorporate several Integrated Topside (InTop) and Electromagnetic Maneuver Warfare Command & Control (EMC2) prototypes now in development. The goal of these Office of Naval Research (ONR) sponsored programs is to demonstrate the integration of multiple shipboard RF functions, including radar, electronic warfare (EW), information operations (IO), communications (Comms), and other legacy and

newly developed RF capabilities by utilizing a common pool of resources including broadband array antennas, signal and data processing, and signal generation and display hardware controlled by standardized resource allocation management software. The test bed operates over a very wide range of frequencies. The MRF facility consists of interconnected shipping containers modified to house the various multifunction systems and support their associated arrays; a central operator control space; dedicated power and cooling facilities; cabling and system interconnect infrastructure; and administrative, maintenance, and security spaces. The array faces are mounted on pallets at a 15° tilt-back to emulate shipboard installation, and overlook the Chesapeake Bay, facing east in the direction of the Tilghman Island test range on the Maryland Eastern Shore. Presently installed systems include the original AMRFC test bed, and the MFEW and InTop EW/IO/Comm ADMs. New InTop prototypes in development include the Flexible Distributed Array Radar (FlexDAR), the Submarine Satellite Communications ADM, and the Low-Band RF Intelligent Distribution Resource (LowRIDR) multifunction/multiband prototype. Space, power, and cooling have been designed and reserved for these systems along with additional capacity for future EMC2 developments.

The Division originated the concept of high frequency over-the-horizon radar and continues to make significant contributions to the field today. It has access to the Navy’s AN/TPS-71 Relocatable Over-the-Horizon Radar (ROTHR) and in addition to providing direct technical support for the program, data collected by the radar is used to support improvements to the systems as well as to evaluate new and innovative HF radar concepts. The Division recently developed a relocatable high frequency surface wave radar that is being used to explore phased array antenna geometries and associated beamforming concepts.



S-Band Waveform Development Testbed.

Information Technology



The Dynamic Spectrum Access Laboratory utilizes a Universal Software Radio Peripheral environment, allowing scientists to conduct communications-based spectrum utilization and efficiency simulations prior to field testing.

NRL's Information Technology Division (ITD) conducts basic research, exploratory development, and advanced technology demonstrations in the collection, transmission, processing, dissemination, and presentation of information. ITD's research program spans the areas of artificial intelligence (AI), autonomous systems, high assurance systems, tactical and strategic computer networks, large data systems, modeling and simulation, virtual and augmented reality, visual analytics, human/computer interaction, communication systems, transmission technology, and high performance computing.

NRL's RF Communications Laboratory conducts research in satellite communications systems and modulation techniques, develops advanced systems for line-of-sight communications links, and conducts designs for the next generation of airborne relays. A Voice Communication Laboratory supports the research and development of tactical voice technology, adaptive digital signal processing, embedded systems design, and software defined radios; a Mobile Network

Modeling Laboratory supports modeling, emulation, development, and scenario-based performance evaluation of both tactical network and Mobile Ad Hoc Networking (MANET) capabilities; and a Dynamic Spectrum Allocation/Cognitive Radio Technology Test Lab provides the capability to analyze, test, and develop dynamic, cognitive, networked tactical wireless communications capabilities that efficiently share and exploit the spectrum.

The Center for Computational Science (CCS) hosts the high performance computing (HPC) and communications efforts at NRL. CCS participates in the DoD HPC Affiliated Research Center (ARC) program providing supercomputer research access to NRL and DoD customers. For high-performance networking, the Center runs the Advanced Technology Demonstration Network (ATDnet) in the Washington, D.C., metro area that provides dark fiber access to research partners. Other research supports high-speed connections (tens to hundreds of Gbps). Current efforts range from mapping traditional large shared memory (SHMEM)

problems onto scalar computing systems to emerging cloud architectures to extremely large storage (petabytes and beyond).

CCS provides a full range of IT infrastructure to support NRL-wide needs, including web application development and system support along with equipment that supports a cable TV plant, SIPRNet, backbone fiber based network, services and external connectivity to the Defense Research and Engineering Network (DREN). DREN is a high-bandwidth wide area network that provides the communications path within the HPC community, to DoD networks and to the Internet. A current research effort includes Openflow between multiple DREN sites, including NRL.

The Autonomous Systems and Robotics Laboratory provides the ability to develop and evaluate intelligent software, hardware, sensors, and interfaces for human interaction with autonomous systems. The lab includes a number of ground and air platforms as well as equipment for evaluating interfaces, including eye trackers. A variety of passive and active sensors support research in perception for autonomous systems. The Audio Laboratory combines a state-of-the-art 3D sound environment and multitask test bed for basic and applied human performance studies and Navy information display research. The core of the new Visual Analytics Laboratory is a display wall composed of LCD tiles, which enable teams of analysts to explore massive, diverse streams of data, supporting research into the science of analytical reasoning facilitated by visual interfaces. The Service Oriented Architecture Laboratory is used to investigate, prototype, and evaluate flexible, loosely coupled web services that can be rapidly combined to meet dynamically changing warfighter needs. The Behavioral Detection Laboratory features a 50-node Cloud cluster to support the develop-



Octavia, one of three anthropomorphic robots at the Navy Center for Applied Research in Artificial Intelligence, uses and understands gestures in order to communicate in high noise environments.

ment of algorithms, processes, and sensor suites associated with behavioral indicators of deception.

The Configurable Synthetic Merged Environments (CSME, or Sesame) Laboratory enables the assessment of Naval systems, individuals, and teams using virtual prototyping techniques to simulate future warfighting scenarios within surface, undersea, land (including man-portable wearable gear), and air domains. Individuals and teams are able to interact with each other and synthetic entities in a realistic manner to improve training effectiveness. The CSME Laboratory is a complement to the Department of Navy's warfighter performance portfolio.

The Navy Cyber Defense Research Laboratory (NCDRL) provides a valuable resource for research and development (R&D) into the broad spectrum of Cyber, including Information Assurance (IA) and Computer Network Defense (CND). R&D activities include network security systems engineering, malicious code analysis, penetration testing, and reverse engineering. Collectively, NCDRL aims to equip the cyber-warrior at



The Navy Cyber Defense Research Laboratory reconfigurable infrastructure.

the front lines of defending the network with the tools and capabilities needed to accomplish their mission, while augmenting the information security posture of the Navy and DoD.

NCDRL provides researchers access to a full range of computing infrastructure, which includes general purpose reconfigurable hardware, virtualization technologies, traffic generation and emulation test beds, deep packet inspection platforms, network intrusion detection/prevention systems, continuous monitoring, and sandbox instrumentation platforms. The environment is robust enough to support testing of a wide array of developmental security technologies as well as USN/DoD IA initiatives (COTS/GOTS) which are vigorously assessed prior to production deployments.

Optical Sciences



Advanced Thin Films Laboratory

The Optical Sciences Division has a broad program of basic and applied research in optics and electro-optics. Areas of concentration include fiber-optic sensing, development of optical materials and sensors for the visible and infrared (IR) spectral regions, integrated optical devices, signal processing, optical communications, panchromatic and hyperspectral imaging for surveillance and reconnaissance, and laser development. Collectively, these technologies form the core of advanced data gathering and communications equipment, designed to aid both the Fleet and the larger Department of Defense community.

To maintain its technical edge in these areas, Optical Sciences maintains a variety of advanced facilities and equipment for manufacturing, testing, and characterizing optical devices and systems.

The Advanced Thin Films Laboratory is a world-class facility for the growth and characterization of optical thin films. The primary deposition system is a cluster tool consisting of interconnected high vacuum chambers, allowing complex, heterogeneous, multilayer films to be deposited without breaking vacuum during processing. The system includes a glove box, sample

distribution robot, sputtering chambers for chalcogenide materials and oxides, evaporators for metals and dielectrics, an ultrahigh vacuum optical characterization chamber, an atomic layer deposition chamber with oxide and sulfide capability, and a mask changing module to enable layers to be patterned in situ, eliminating interfacial defects that result from exposure to air.

Other deposition tools within the Advanced Thin Films Laboratory include a stand-alone thermal evaporator for the deposition of IR-transparent chalcogenide glasses, a stand-alone sputterer, and a custom system for deposition on optical fiber. The laboratory also contains a suite of optical, electronic, and thin film characterization equipment. Upgrades are currently under way to install a plasma-enhanced metal-organic chemical vapor deposition system and expanded wet synthesis capability.

The Ultrashort Laser Facility permits experiments to measure the optical nonlinear response of different materials to ultrashort laser pulses. The information learned from such experiments helps in the development of materials that can be used for optical telecom-

munications, for the protection of sensors and human eyes from hostile laser irradiation, and for the development of new active laser sources.

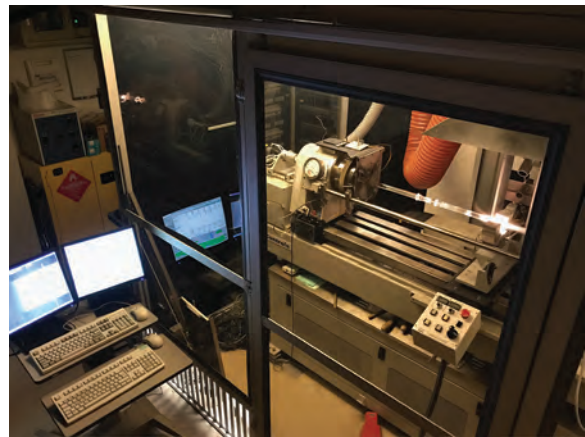
Other recently added facilities include the Optical Fiber Preform Fabrication Facility for making doped and undoped, multimode, single-mode, multicore, and photonic crystal glass preforms at temperatures as high as 2300 °C; the Surface Characterization Facility for ultraviolet and X-ray photoemission spectroscopy, atomic force and scanning tunneling microscopy (STM), and STM-induced light emission measurements; and the molecular beam epitaxial growth system dedicated to infrared lasers and detectors based on GaSb/InAs/AlSb quantum well and superlattice structures.

In addition, an extensive set of laboratories exists to develop and test new laser and nonlinear frequency conversion concepts and to evaluate nondestructive test and evaluation techniques. Fiber-optic sensor testing stations include acoustic test cells and a three-axis magnetic sensor test cell. There is also an Ultralow-loss Infrared Fiber-Optic Waveguide Facility using high-temperature IR glass technology. The facilities for ceramic optical materials include powder preparation, vacuum presses, and a 50-ton hot press for sintering.

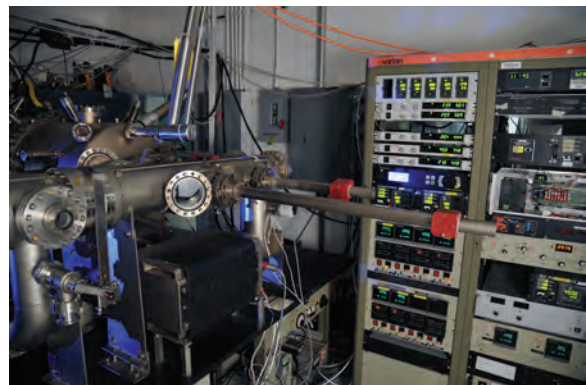
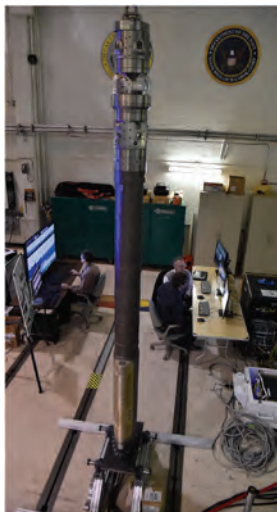
The Focal Plane Array Evaluation Facility allows measurement of the optical and electrical characteristics of infrared focal plane arrays being developed for advanced Navy sensors. The IR Missile-Seeker Evaluation Facility performs open-loop measurements of the susceptibilities of IR tracking sensors to optical countermeasures. An ultra-high-vacuum multichamber deposition apparatus is used for fabrication of electro-optical devices and can be interlocked with the Surface Characterization Facility.



The bio-aerosol containment chamber allows NRL scientists to test the limits of new optical detection strategies aimed at providing warning in the event of a chemical or biological attack.



The optical sciences advanced materials group maintains unique glass processing capability. The MCVD Lathe (shown here) allows scientists to create Silica fiber preforms in which the chemical composition of the glass is tailored to achieve specific optical properties. Applications include high-power fiber lasers operating in eye safer regimes and optical fibers operating in radiation-rich environments.



Molecular beam epitaxy (MBE) system dedicated to quantum confined GaSb/InAs/AlSb structures for midwave infrared laser development.

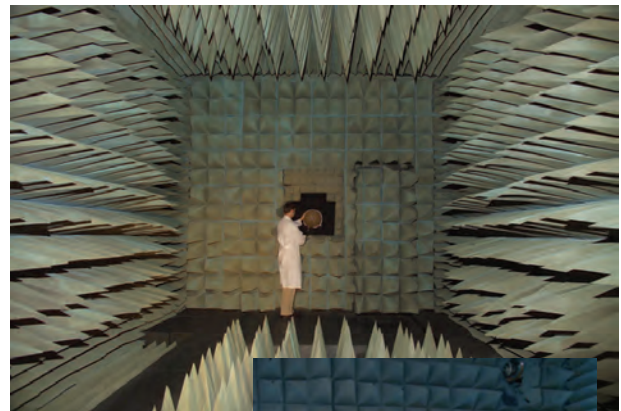
Optical sciences develops and fields numerous electro-optical/infrared systems. Clockwise from left: 360° panoramic periscope for Va. Class submarines, Distributed Aperture Infrared Countermeasure (DAIRCM) system, compact hyperspectral imager, and Common Airborne Situational Awareness (CASA) imaging pod.

Tactical Electronic Warfare

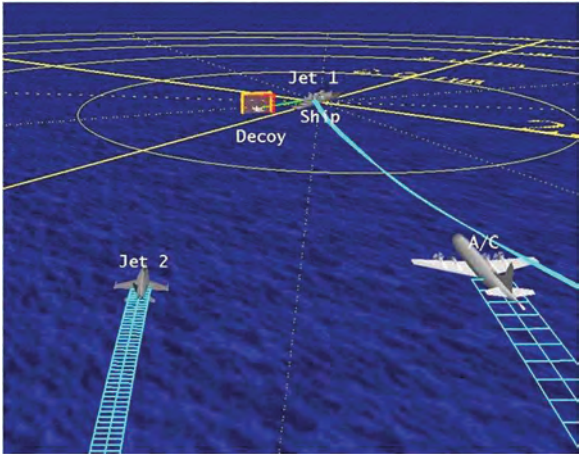


Learjets with simulators during fleet exercises.

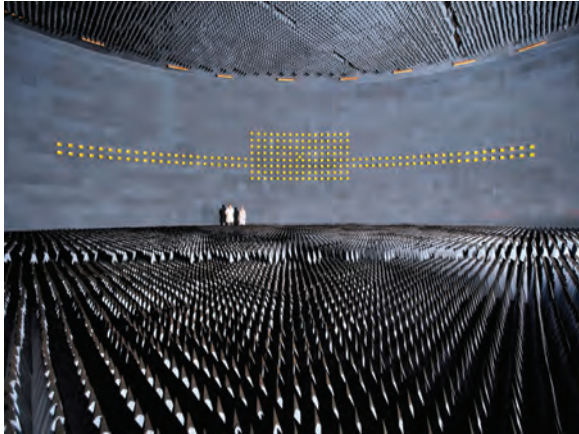
The Tactical Electronic Warfare (TEW) Division's program for electronic warfare (EW) research and development covers the entire electromagnetic spectrum. The program includes technology research and advanced developments and their applicability to producing EW products for the Fleet. The range of ongoing activities includes components, techniques, and subsystems development as well as system conceptualization, design, and EW effectiveness evaluation. The focus of the research activities extends across the entire breadth of the battlespace. These activities emphasize providing the methods and means to detect and counter enemy hostile actions via threat neutralization — from the beginning, when enemy forces are being mobilized for an attack, to final stages of the engagement. In conducting this program, the TEW Division employs an extensive array of special research and development laboratories, anechoic chambers, and modern computer systems for modeling and simulation. Dedicated field sites and airborne platforms allow for the conduct of field experiments and operational trials. This combination of scientists, engineers, and specialized facilities also supports the innovative use of all Fleet defensive and offensive EW assets currently available to operational forces.



Radio Frequency Countermeasures anechoic chamber for EW testing.



The Tactical Electronic Warfare Division (TEWD) develops and implements advanced visualization tools to support electronic warfare (EW) systems development and analysis.



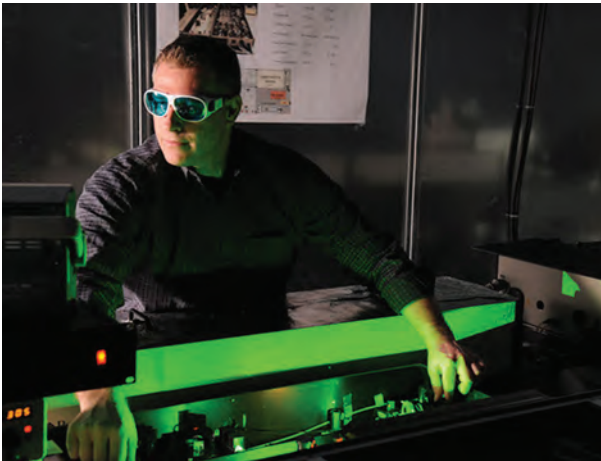
The Central Target Simulation Facility is a high-performance, hardware-in-the-loop simulator for real-time closed-loop testing and evaluation of electronic warfare systems and techniques to counter the antiship missile threats.



EATES — Electronic Attack Technique Evaluation System, a stand-alone portable electronic attack testing system.



TEWD engineers prepare for dynamic testing of the 4000 lb Roll-Pitch Stabilized Antenna System mounted on NRL's Ship Motion Simulator located at the Chesapeake Bay Detachment facility.

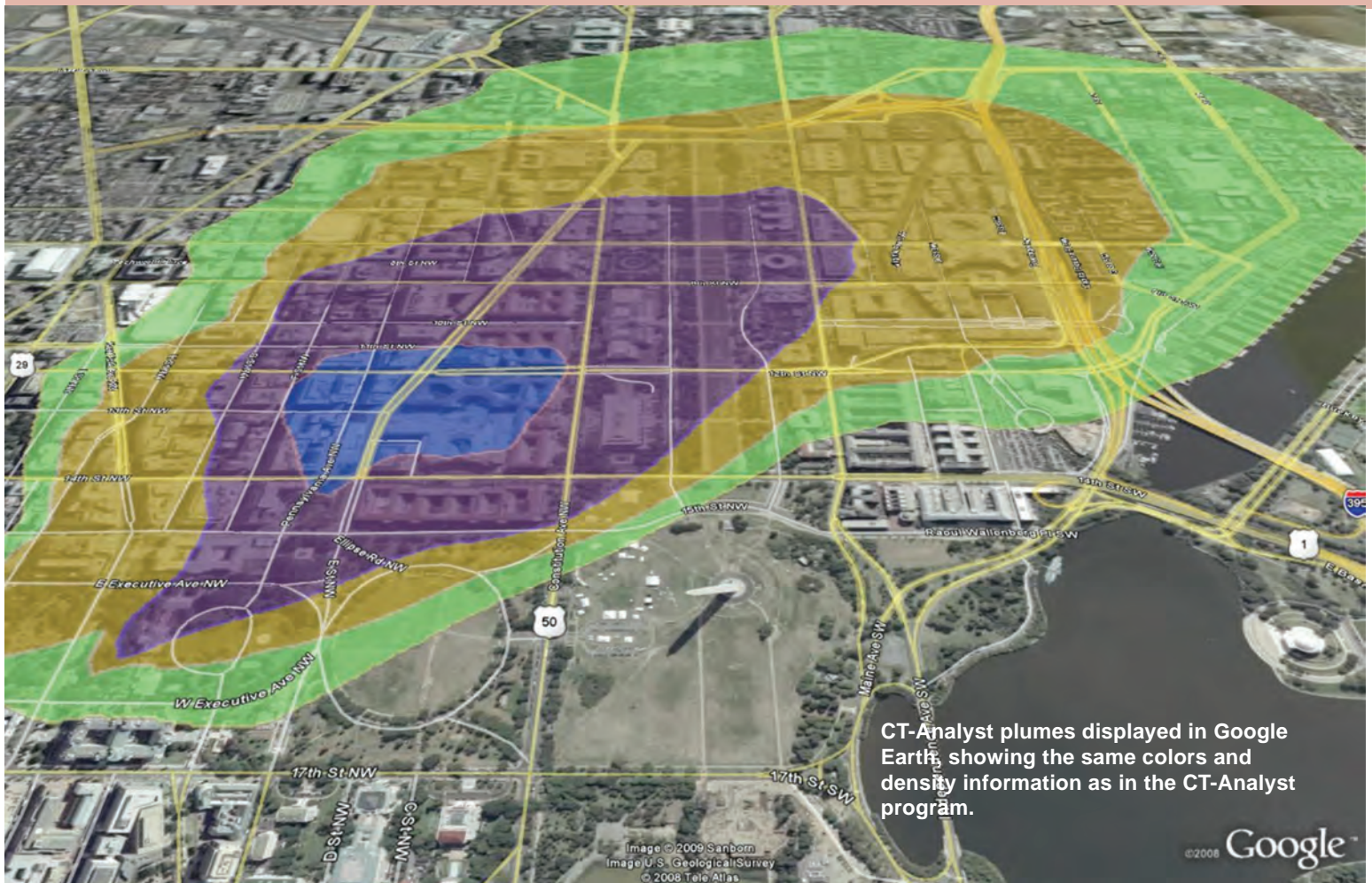


NRL research physicist aligning the TEWD 30 TW Ti:Sapphire laser system.



XFC prototype in flight under fuel cell power.

Laboratories for Computational Physics and Fluid Dynamics



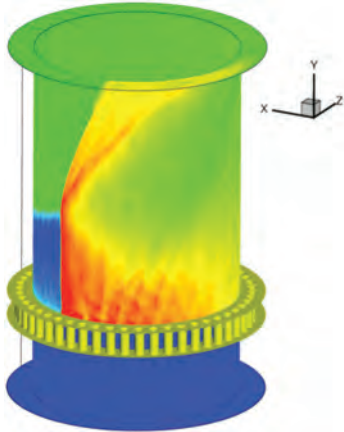
The Laboratories for Computational Physics and Fluid Dynamics (LCP&FD) is staffed by physicists, engineers, and computer scientists who develop software and use high-performance computers to solve priority problems for the Navy, the Department of Defense, and the Nation when existing capabilities and available commercial software prove inadequate to the application. For example, the LCP&FD developed the CT-Analyst crisis management software (figure above) so that first responders can have instant predictions of an airborne contaminant spread in an urban environment.

The LCP&FD maintains a very powerful collection of computer systems applied to a broad collection of work. There are currently 3296 clustered x86_64 cores and their associated support systems. In addition, there are over 40 Apple workstations in the group, most of which are capable of large calculations both independently and in parallel ad hoc clusters.

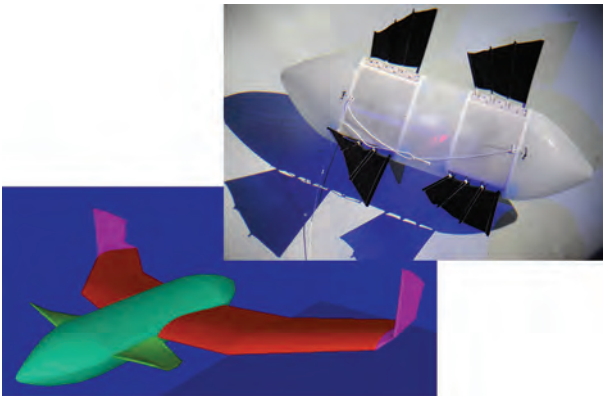
There are five 64-bit x86 multicore distributed memory clusters, each well coupled with Infiniband

high-speed switched interconnect. Three of the clusters contain manycore coprocessors. The newest system consists of 136 Intel Xeon Phi coprocessors. The second consists of 16 NVIDIA Maxwell class GPUs and 70 Intel Xeon Phi coprocessors. The third system comprises 88 NVIDIA Fermi class GPUs. All of the many-core processors are tightly coupled to their associated x86_64 multicore processor nodes. A Scale MP based shared memory machine is available for large memory processing.

All systems share 250 terabytes of storage for use during a simulation and at least one gigabyte of memory per processor core. All unclassified systems share a common disk space for home directories as well as 3 terabytes of AFS space.

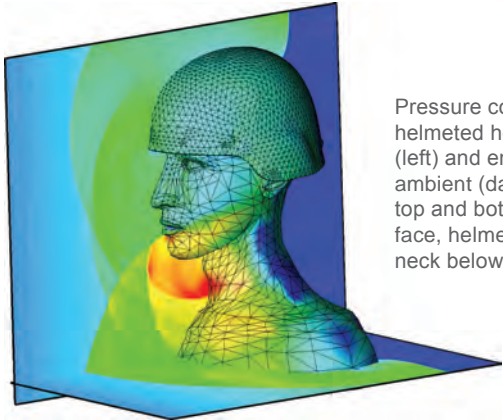
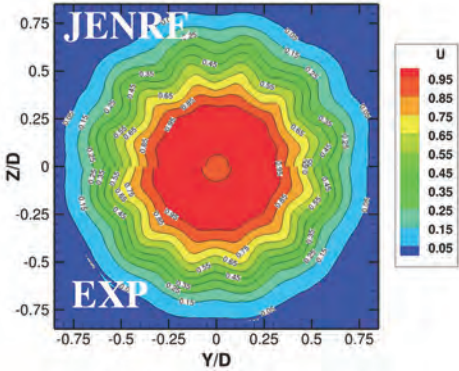


The computed flow field inside a rotating detonation engine with mixture plenum (bottom), injector plate and injectors (center), and combustion chamber (top). This new class of engines has been investigated computationally and shown to have the potential to reduce fuel consumption by 25% while providing the same performance as current gas-turbine engines.



Development of bio-inspired unmanned underwater vehicle propulsion and control mechanisms is accomplished using unsteady three-dimensional computational fluid dynamics tools. These designs and the subsequent construction of the bio-robotic mechanisms are expanding the envelope of unmanned air and sea vehicle performance.

Simulations using the NRL developed JENRE code show that it predicts supersonic jet flow features and noise very accurately. Here the computed (top half of picture) cross-sectional jet velocity is compared to the experimentally measured data (bottom half).



Pressure contours resulting from blast interaction with a helmeted head. The shock wave approaches from the front (left) and envelopes the geometry; the boundary between ambient (dark blue) and post-shock (green) air is seen at the top and bottom right. Interacting shock reflections from the face, helmet, and torso generate high pressures (red) on the neck below the chin.

Chemistry



The Haas VM-3 Vertical Machining Center with a 5-axis trunnion table for in-house, rapid prototyping of devices ranging from simple components to complete instrumentation systems for technology demonstrations.

NRL has been a major center for chemical research in support of naval operational requirements since the late 1920s. The Chemistry Division continues this tradition. The Chemistry Division conducts basic research, applied research, and development studies in the broad fields of diagnostics, dynamics, synthesis, materials, surface/interfaces, environment, corrosion, combustion, and fuels. Specialized programs currently within these fields include the synthesis and characterization of organic and inorganic materials, coatings, composites, nondestructive evaluation, surface/interface modification and characterization, nanometer structure science/technology, chemical vapor processing, tribology, solution and electrochemistry, mechanisms and kinetics of chemical processes, analytical chemistry, theoretical chemistry, decoy materials, radar-absorbing materials/radar-absorbing structures (RAM/RAS) technology, chemical/biological warfare defense, atmosphere analysis and control, environmental remediation and protection, corrosion science and engineering, marine coatings, personnel

protection, and safety and survivability. The Division has several research facilities.

Chemical analysis facilities include a wide range of modern photonic, phononic, magnetic, electronic, and ionic-based spectroscopic/microscopic techniques for bulk and surface analysis.

The Magnetic Resonance Facility includes advanced high-resolution solid-state nuclear magnetic resonance (NMR) spectroscopy techniques to observe nuclei across much of the periodic table and provides detailed structural and dynamical information.

The Nanometer Characterization/Manipulation Facility includes fabrication and characterization capability based on scanning tunneling microscopy/spectroscopy, atomic force microscopy, and related techniques.

The Materials Synthesis/Property Measurement Facility has special emphasis on polymers, surface-film processing, and directed self-assembly.

The Chemical Vapor and Plasma Deposition Facility is designed to study and fabricate materials, such as

diamond, using in situ diagnostics, laser machining, and plasma deposition reactors.

The Navy Fuel Research Facility performs basic and applied research to understand the underlying chemistry that impacts the use, handling, and storage of current and future Navy mobility fuels.

The Combustion Science and Fire research facilities include an intermediate and full-scale facility at the Chesapeake Bay Detachment (CBD) and the Joint Maritime Test Facility (JMTF) to conduct basic to advanced research. The facilities support current and future fire suppression systems relevant to large-scale fire, provide resources for technology development/transition, and fire hazard assessment analysis/ Live Fire Test & Evaluation (LFT&E) surrogate testing in support of the Congressional Title 10 mandate. The CBD site has custom test rigs and test chambers to evaluate specific Navy damage control concerns on surface ships and submarines. The combustion research is supported by a large spray combustion test building and a range of optical diagnostic equipment for high-speed velocimetry, spray measurement, acoustics, thermometry, chemical species measurement, and imaging in ultraviolet, visible, and infrared.

The Marine Corrosion and Coatings Facility located on Fleming Key at Key West, Florida, offers a “blue” ocean environment and unpolluted, flowing seawater for studies of environmental effects on materials. Equipment is available for experiments involving accelerated corrosion and weathering, general corro-

sion, long-term immersion and alternate immersion, fouling, electrochemical phenomena, coatings application and characterization, cathodic protection design, ballast water treatment, marine biology, and corrosion monitoring.

The Chemistry Division has focused on force protection/homeland defense (FP/HD) since September 11, 2001, especially on the development of improved detection techniques for chemical, biological, and explosive threats, and for narcotics. This work includes the development of the Trace Explosives Sensor Testbed and the Trace Vapor Generator for Explosives and Narcotics (TV-Gen) to assess materials, sensors or systems for chemical hazards, explosives and narcotics detection in support of counter-IED, border security, and airport security. Bio-safety level II laboratories are used to test prototype biodetection schemes. In support of these efforts, the Division recently commissioned a Haas VM-3 Vertical Machining Center with a 5-axis trunnion table for in-house, rapid prototyping of devices ranging from simple components, completing instrumentation systems for technology demonstrations.

The Surface Characterization Facility includes a suite of instrumentation, including an X-ray photoelectron spectroscopy system and a glancing angle surface X-ray diffractometer. Optical and spectroscopic microscopy systems enable topographic imaging and chemical analysis and mapping, with submicron spatial resolution.



The Trace Explosives Sensor Testbed (TESTbed) has dedicated computer control of a standardized vapor delivery system with an automated data collection system suitable for obtaining high-quality data for sensor validation.



The Trace Vapor Generator for Explosives and Narcotics (TV-Gen) is a portable, compact vapor generation system capable of reproducibly and accurately generating trace vapors (parts per quadrillion to parts per million) of troublesome, low vapor pressure compounds such as explosives and narcotics for delivery to sensors and materials undergoing testing or calibration.

Materials Science and Technology



The Cameca atom probe provides 3D information on the composition and structure of alloys and devices at the atomic scale.

The Materials Science and Technology Division (MSTD) at the U.S. Naval Research Laboratory (NRL) provides expertise and facilities to foster a broad range of materials innovation. The Division houses many specialized and unique facilities for carrying out basic and applied materials modeling, synthesis, and characterization research.

Electronic structure and multiphysics modeling is performed in The Center for Computational Materials Science, which operates several high performance computing clusters that complement the resources of the DoD Supercomputing Resource Centers. These hardware resources are used to run in-house custom-developed and externally custom-developed codes (VASP, LAMMPS, ALE3D, CUBIT, AERO-suite) and commercial codes (COMSOL, ANSYS, ABAQUS, etc.) for understanding fundamental materials properties.

In 2015, MSTD added a new 3D X-ray Computed Microtomography facility built on a Zeiss Xradia 520 Versa X-ray microscope. This system allows for in situ measurement of component geometry and material microstructure under different loading conditions of strain and temperature. This system is unique in its capability for diffraction contrast tomography (DCT) that has

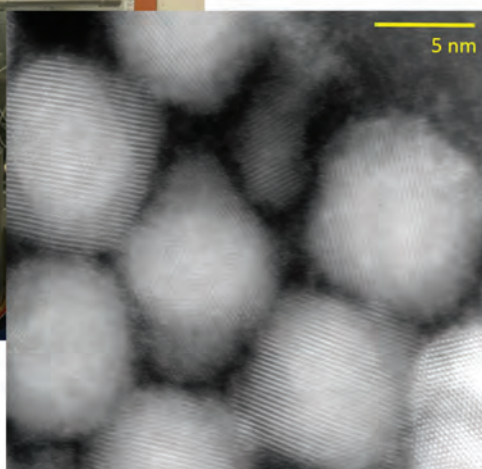
only been previously available on synchrotron beamlines. DCT provides nondestructive, high-resolution grain maps for polycrystalline samples. The system is useful for characterization of a wide range of materials, including additive-manufactured materials, batteries, fuel cells, joined materials, composites, and corrosion products as well as hard and soft biological materials and imaging of subcellular to cellular features with submicron resolution.

The Electrical, Magnetic, and Optical Measurement Facility contains instruments for fundamental studies of the magnetic, electrical, optical, and thermal properties of materials and devices. Magnetometry and magnetotransport measurements are performed within a Quantum Design MPMS SQUID magnetometer (± 5 T; 1.7–400 K) and PPMS system (± 9 T; 1.7–400 K) and a Microsense LLC vibrating sample magnetometer (± 2 T; 90–800 K). MSTD has added new capabilities in the measurement and characterization of artificial multi-ferroic materials.

The Bulk Materials Fabrication Facility provides equipment for fabrication and processing, including arc-melting and furnace casting for conventional metallic alloys, a single crystal growth furnace, and rapid solidification by splat quenching or melt spinning. Ceramic and ceramic-matrix composites processing facilities include



Dark field scanning transmission electron microscopy image revealing the atomic-scale core-shell structure of PbTe/PbS nanoparticles.



conventional, controlled atmospheric furnaces, hot presses, milling facilities, tape casting, particle, and sol-gel and organometallic coating processing capabilities.

The Thin-Film Materials Synthesis and Processing Facility provides users a variety of techniques for growth and processing of thin films (thickness 1 μm or less). Sputter deposition is a versatile method of depositing metallic and dielectric films, and several tools are available for growth on samples up to 8 inches



The Materials Science and Technology Division's Accelerator Mass Spectrometry Facility provides positive ion analysis of materials for trace chemical and isotope composition.

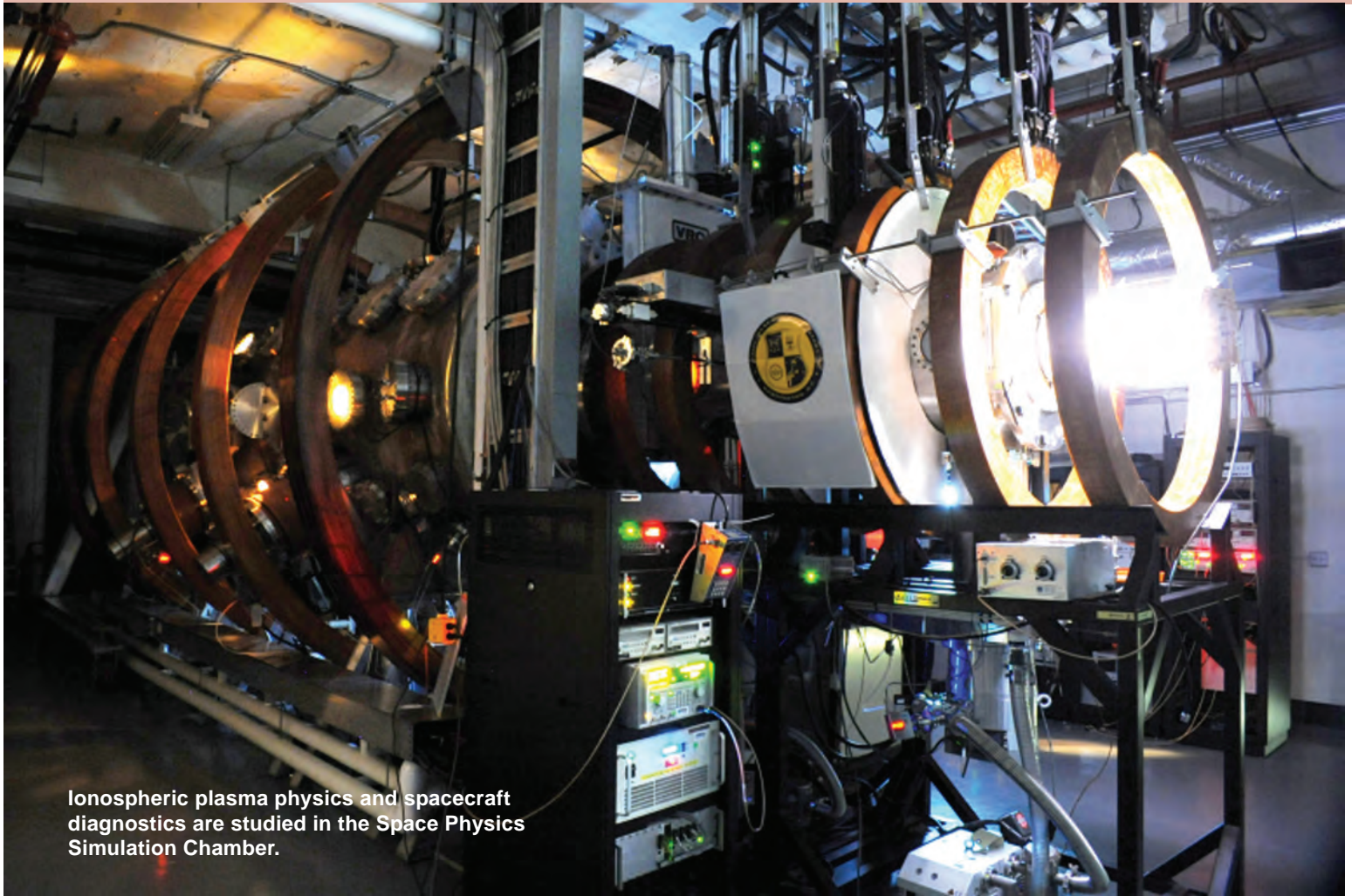
in diameter and at room and elevated temperature, or growth in magnetic field. Thermal evaporation of metals is implemented in both high-vacuum and ultra-high-vacuum systems with surface science tools for analysis. Pulsed laser deposition with variable stage temperature and controlled atmosphere is the preferred method for growth of oxides. Laser direct-write ablation and deposition processes provide unique methods for imposing CAD-defined features to a substrate.

The Micro/Nanostructure Characterization Facility contains equipment for imaging of materials from the macro-scale down to the atomic scale. This facility includes a JSM-7001F variable pressure scanning electron microscope (SEM), an FEI Tecnai G2 30 analytical scanning transmission electron microscope (STEM), a JEOL 2200FS field-emission analytical STEM, and a new Nion aberration-corrected STEM with 80 picometer resolution. These electron microscopes have capabilities for energy dispersive X-ray spectroscopy, electron energy loss

spectroscopy, Z-contrast imaging, spectral compositional mapping, and electron backscatter diffraction. This facility also includes a new robotic serial sectioning system (RS3D) for automatically removing small amounts of material and then imaging the structure, crystallography, or chemistry of the exposed surface in an SEM for 3D reconstruction of materials. NRL has also acquired a state-of-the-art Cameca 4000X Si LEAP (local electrode atom probe) to analyze the true 3D structure of materials at atomic resolution with chemical sensitivity approaching 10 atomic parts per million.

The Accelerator Mass Spectrometry Facility at NRL is currently equipped with a single stage accelerator mass spectrometer (SSAMS) capable of analyzing positive ions, making the NRL SSAMS facility globally unique, because all other AMS facilities accept only negative ions. The capability opens the possibility of analysis of positive ions of nearly the entire periodic table. At NRL, the SSAMS is currently coupled to a secondary ion mass spectrometer. The marriage of these two instruments allows for trace isotopic and elemental analyses of solid materials, particles, and films, and facilitates spatially resolved analysis of complex materials spanning the range from semiconductors and engineered materials to nuclear and geochemically interesting samples.

Plasma Physics



Ionospheric plasma physics and spacecraft diagnostics are studied in the Space Physics Simulation Chamber.

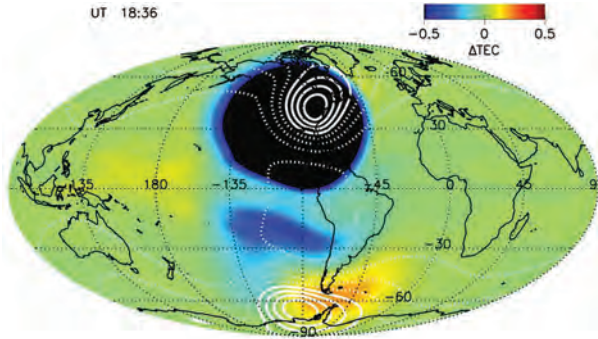
The Plasma Physics Division conducts basic and applied research in space plasmas, inertial confinement fusion (ICF), ultra-short-pulse laser interactions, directed energy, railguns, pulsed-power and intense particle beams, nuclear weapons effects and radiography, materials processing, advanced diagnostics, radiation-atomic physics, and nonlinear dynamics.

The Space Physics Simulation Chamber generates near-Earth plasma environments for studying space plasma phenomena and spacecraft diagnostic development and testing. Nike is a major KrF laser facility for studying ICF target physics. The Ultrashort-Pulse Laser (USPL) facility has both a 10 Hz (15 TW) and kilohertz (0.45 TW) Ti:Sapphire laser to investigate laser-driven acceleration and nonlinear laser-plasma interactions, and a smaller mobile Ti:sapphire system. Directed energy research is performed in the High Energy Laser Lab, which has four multikilowatt fiber lasers to study laser propagation, incoherent beam combining, and

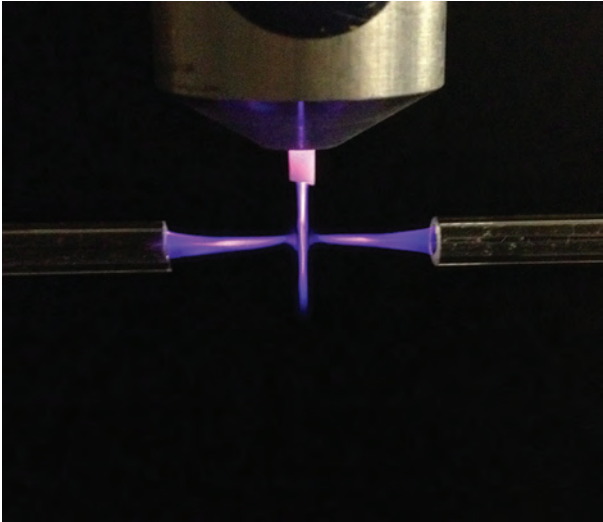
power beaming. The Materials Testing Facility houses a new medium caliber launcher (MCL) railgun used to study the materials issues of electromagnetic launch and a small

caliber, battery-powered railgun that will fire repetitively and expand our knowledge of materials, pulsed power, and energy storage. The Division has two large, high-voltage, pulsed-power devices, Gamble II and Mercury, which are used to produce intense electron and ion beams, flash X-ray sources, and high-density plasmas for application to nuclear weapons effects testing and radiography. The Division uses both microwaves and plasmas for materials processing applications. The microwave materials processing laboratory includes a 20 kW, CW, 83 GHz gyrotron. The Large Area Plasma Processing System (LAPPS) generates ultralow-temperature plasmas for studying the modification of energy sensitive materials such as polymers, graphene, and biologicals. Atmospheric plasma systems

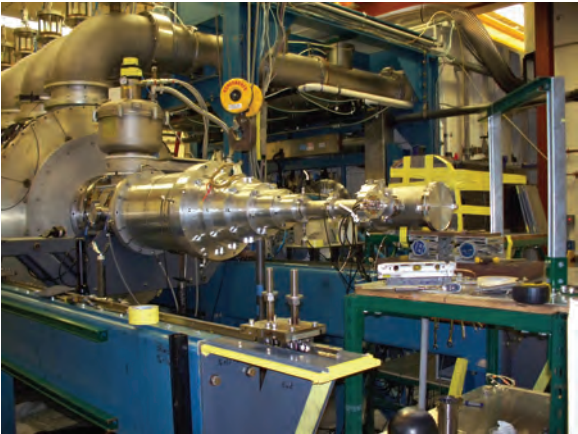
using plasma jets or pulsed discharges are being developed for materials processing and plasma biology applications.



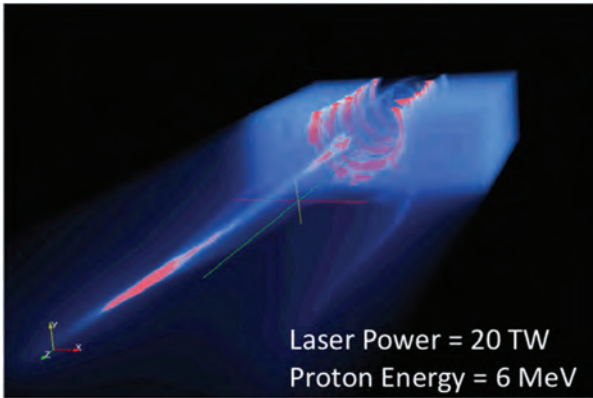
Predicted change in total electron content (TEC) in the ionosphere during the Aug. 21, 2017, eclipse. Calculations are from the SAMI-3 ionospheric plasma simulation code.



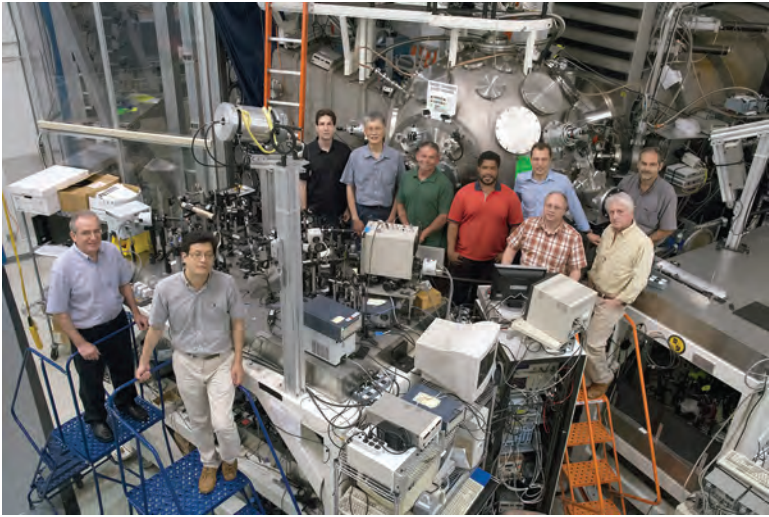
Atmospheric pressure plasma jet operating in the presence of opposing noble gas jets. The noble gas flow, which is orthogonal to the plasma jet's axis (vertical), serves to lengthen and redirect the discharge propagation.



Tapered front-end of Mercury accelerator (6 MV, 360 kA, 50 ns) for dual-axis down-hole radiography.

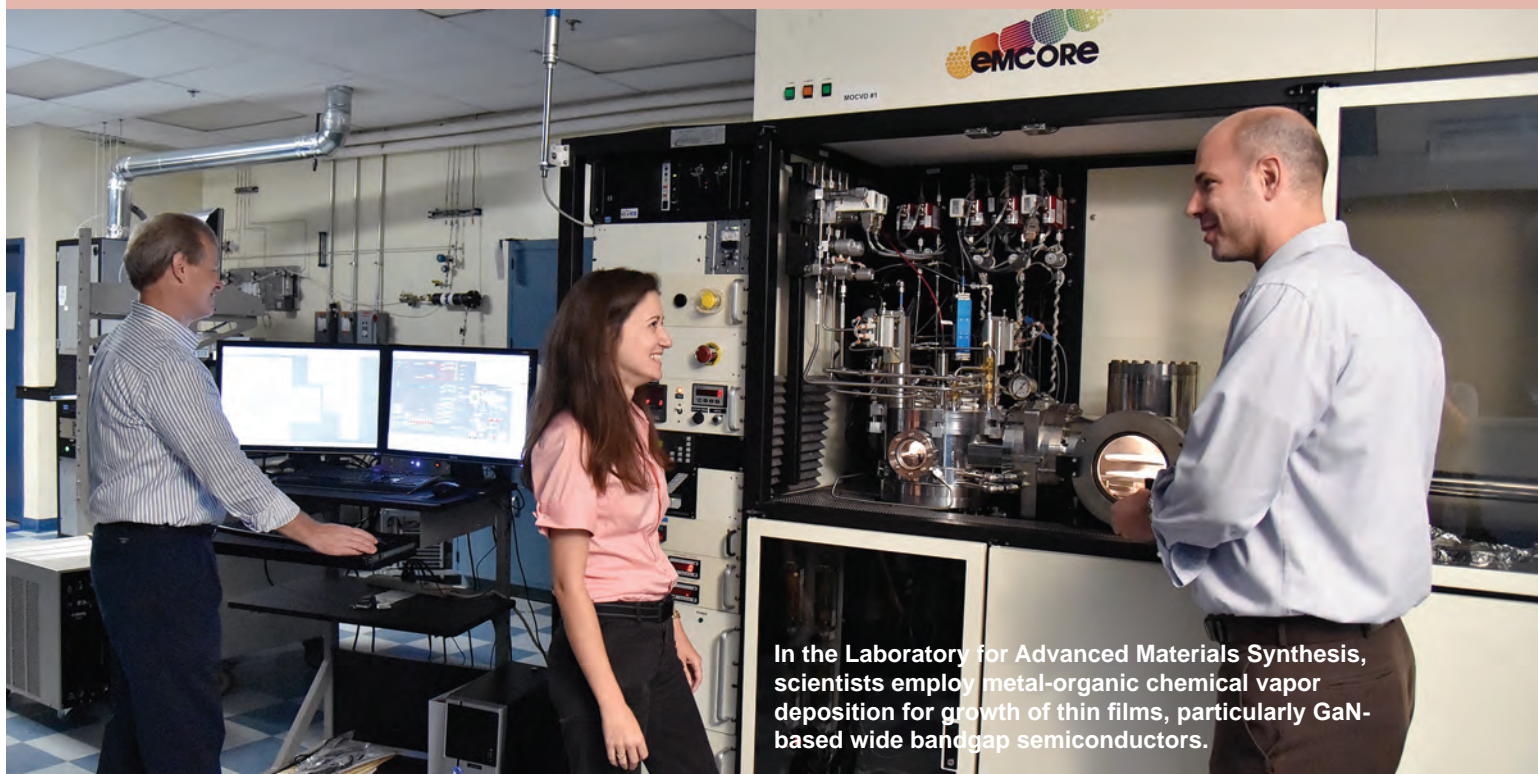


TURBOWAVE simulation of proton acceleration from a hydrogen gas target driven by an ultrashort-pulse laser.



Nike target chamber area and members of the Nike team. The Nike laser is used to study target physics for inertial confinement fusion and various defense applications.

Electronics Science and Technology



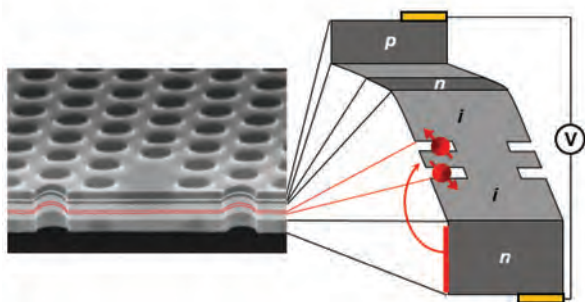
In the Laboratory for Advanced Materials Synthesis, scientists employ metal-organic chemical vapor deposition for growth of thin films, particularly GaN-based wide bandgap semiconductors.

The Electronics Science and Technology Division (ESTD) performs a multidisciplinary, broadly based research program that is both world class and highly relevant. Our mission is to invent, develop, and transition revolutionary capabilities to the Navy and Marine Corps as well as anticipate and counter technological surprise. Our technically diverse staff of experimental, theoretical, and computational physicists; surface and materials scientists; chemists; electrical, electronic, chemical, and mechanical engineers reflects the multidisciplinary nature of the Division's research. The synergy that results from the collaboration between these experts ensures the development of world-class electronics science and technology. Our well-equipped laboratories and unique fabrication facilities provide the research tools needed to move rapidly from a flash of inspiration to real-world demonstration.

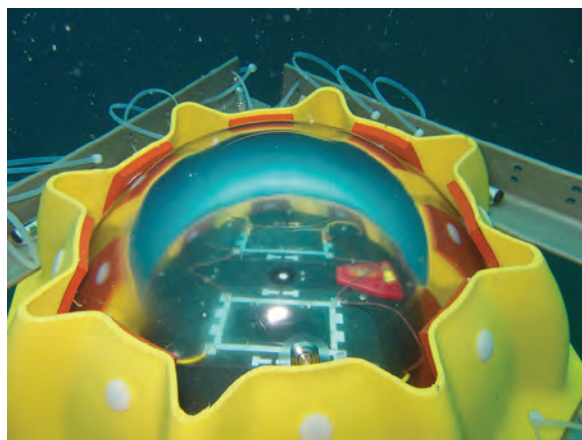
The Division operates 16 major facilities: Compound Semiconductor Processing Facility (CSPF), Laboratory for Advanced Materials Synthesis (LAMS), Center for Advanced Materials Epitaxial Growth and Characterization (Epicenter), Electronic Transport Laboratory (ETL), Advanced Silicon Carbide Epitaxial Research Laboratory (ASCERL), Solar Cell Characterization Laboratory (SCCL), Ultrafast Laser Facility (ULF), Ultra-Violet Photolithography Laboratory for Submillimeter-Wave Devices (UV-PL), Millimeter-Wave Vacuum Electronics Fabrication Facility (MWVEFF), Solid-State

Qubit Coherent Spectroscopy Laboratory (SSQCSL), 3D Laser Lithography Laboratory (3DLLL), Optoelectronic Scanning Electron Characterization Facility (OSECF), Infrared Materials and Detectors Characterization Laboratory (IR Characterization Lab), Atomic Layer Deposition System (ALD), Atomic Layer Epitaxy System (ALE), and High Pressure Multi-Anvil System (HPMAS).

The CSPF processes compound semiconductor structures on a service basis, especially if advanced fabrication equipment is required. However, most fabrication can be hands-on by NRL scientists to assure personal process control and history. The LAMS uses metal-organic chemical vapor deposition to synthesize a wide range of thin films, particularly wide band gap semiconductors such as gallium nitride (GaN) and related alloys with indium nitride (InN) and aluminum nitride (AlN), enabling the realization of unipolar and bipolar device structures. The Epicenter (a joint activity of ESTD, Materials Science and Technology, Optical Sciences, and Chemistry Divisions) is dedicated to the growth of multilayer nanostructures by molecular beam epitaxy (MBE). Current research involves the growth and etching of conventional III-V semiconductors, ferromagnetic semiconductor materials, 6.1 Å III-V semiconductors, and II-VI semiconductors. The ETL enables comprehensive DC and RF electronic characterization of materials and devices down to cryogenic temperatures and under a variety of magnetic and optical field condi-

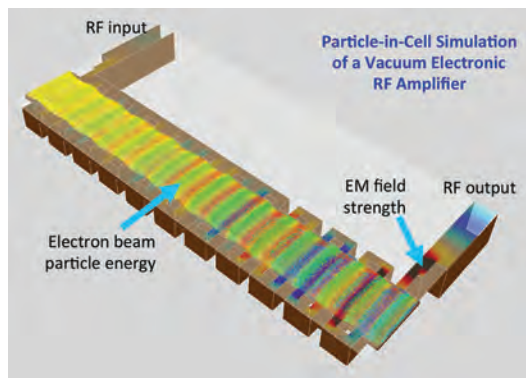


Scanning electron micrograph of a photonic crystal membrane, showing an array of holes with the missing holes forming a cavity. The band structure of the diode with two coupled quantum dots is displayed to the right.

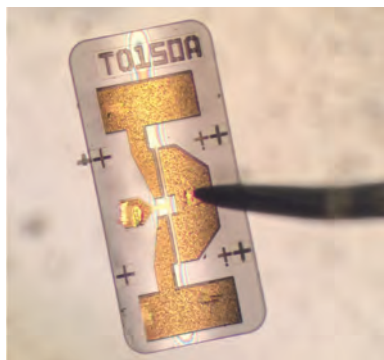


To validate performance models of underwater energy harvesting, measurements of the solar spectrum filtered through seawater as well as solar cell performance underwater are measured. In this photograph, solar cells and a spectral radiometer are housed inside a glass sphere, and measurements are made at various depths.

tions. The ASCERL develops thin-film heterostructure materials needed for high-voltage, high-power silicon carbide (SiC) power electronic components. ASCERL uses an EPIGRESS reactor capable of growing thick, low-defect, ultra-high-purity SiC epitaxial layers. The SCCL studies new and emerging solar cell technologies for tactical applications including terrestrial and space environments. The ULF is optimized for the characterization of photophysical and photochemical processes on a timescale of tens of femtoseconds. It includes a synchronously pumped dye laser system for simulating the effects of charge deposited in semiconductors characteristic of space radiation. The UV-PL and MWVEFF are key laboratories for developing precision, all-metal structures for electron optics, electron beam-wave interaction, and passive electromagnetic devices. The UV-PL uses lithographic techniques and chemical electroform-



NRL's GPU-accelerated 3D particle-in-cell code, Neptune, simulates non-linear beam-wave interactions that produce millimeter-wave amplification in vacuum electronic devices. This cut-away visualization illustrates energy and density modulation of an electron beam traveling through a coupled-cavity structure, as electron energy is transferred coherently to the electromagnetic wave.



A free-standing gallium nitride radiofrequency transistor released from silicon carbide and transferred to a silicon substrate using a patent-pending epitaxial lift-off process based on transition metal nitride materials developed at NRL.

ing to create feature sizes as small as 5 μm , compatible with devices that can produce coherent electromagnetic radiation at submillimeter wavelengths. The MWVEFF contains computer numerically controlled milling machines, lathes, and wire electric discharge machining (EDM) tools for fabrication of millimeter-wave and submillimeter-wave components. The SSQCSL consists of several cryogenic optical microscopy systems, including one with high magnetic fields, and many lasers, detectors, and spectrometers for optically controlling and probing semiconductor quantum systems. The 3DLLL writes 0.1 μm diameter volume elements in photoresist. By moving the focal spot through a viscous puddle of the photoresist, it is possible to create complex and highly detailed sub-micron scale structures in three dimensions for applications in optics, photonics, biofluidics, and many other areas.

Center for Bio/Molecular Science and Engineering



Center bioengineers and summer students are developing flexible electronics on biomaterials.

The Center for Bio/Molecular Science and Engineering conducts cross-disciplinary, bio-inspired research and development to address problems relevant to the Navy and Department of Defense by exploiting biology's well-known ability for developing effective materials and sensing systems. The primary goal is to translate cutting-edge, bio-based discoveries into useful materials, sensors, and prototypes that can be scaled up, are robust, and lead to enhanced capabilities in the field. The challenges include identifying biological approaches with the greatest potential to solve Navy problems and that provide new capabilities while focusing on bio-inspired solutions to problems that have not otherwise been solved by conventional means.

Studies involve biomaterial development for chemical/biological warfare defense, structural and functional

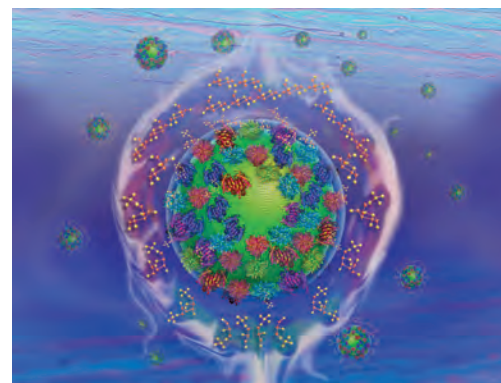
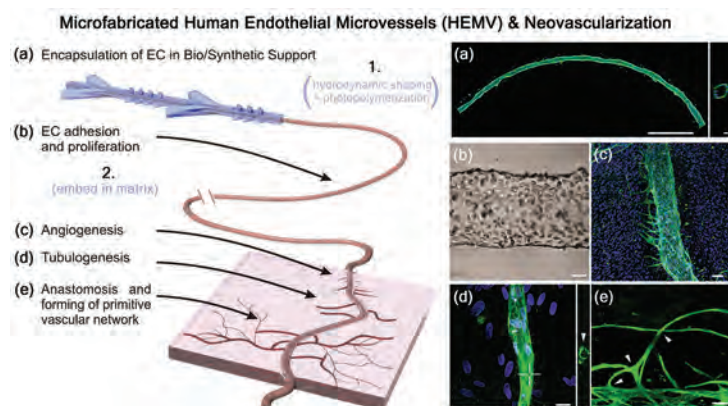
applications, and environmental quality/cleanup. Program areas include optical biosensors, nanoscale manipulations, genomics and proteomics, bio/molecular and cellular arrays, surface modification, energy harvesting, systems and synthetic biology, tissue engineering, and bio-organic materials from self-assembly.

The staff of the Center is an interdisciplinary team with expertise in biochemistry, surface chemistry, biophysics, molecular and cell biology, organic synthesis, materials science, and engineering. The Center also collaborates throughout the U.S. Naval Research Laboratory and with other government laboratories, universities, and industry.

The Center's modern facilities include laboratories for research in chemistry, biochemistry, systems biology, and physics. Specialized areas include con-

trolled-access laboratories for cell culture and molecular biology, an electron microscope facility, a scanning probe microscope laboratory, instrument rooms with access to a variety of spectrophotometers, a multichannel surface plasmon resonance (SPR) sensor, and an optical microscope facility that includes polarization, fluorescence, and confocal microscopes. Additional laboratories accommodate nuclear magnetic resonance (NMR) spectroscopy, liquid chromatography–mass spectrometry (LCMS), and fabrication of microfluidic and micro-optical systems in polymers. The Center maintains a state-of-the-art X-ray diffraction system that includes a MicroSTAR-H X-ray generator. In combination with new detectors and components, the system is ideal for data collection on proteins or very

small single crystals of organic compounds and also capable of collecting data on films and powders. Core facilities have been established for fluorescence activated cell sorting (FACS), micro-array analysis, next-generation sequencing, circular dichroism spectroscopy, and 3D printing and rapid prototyping. The Center has recently installed an analytical ultracentrifuge to facilitate separation and characterization of proteins and protein complexes. The mass spectrometry (MS) facility was also enlarged to enable small molecule and proteomic analyses of biological, environmental, and clinical samples by offering state-of-the-art instrumentation and proteomics expertise in preparation, analysis, and bioinformatic interpretation of experimental data and manual interpretation of MS/MS spectra.

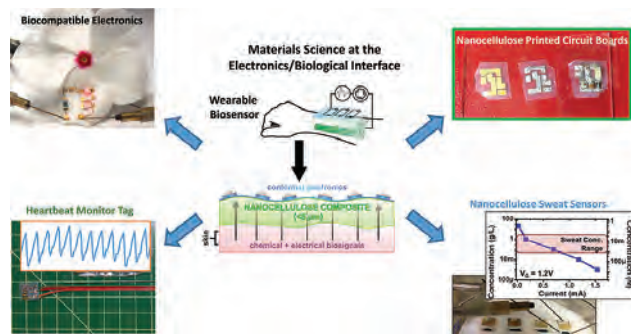


Neovascularization Strategy and Implementation. Primary human endothelial cells encapsulated in a bio-macromolecular tubule using a hydrodynamic shaping device. The resultant human endothelial microvessel (HEMV) matures with a coherent endothelium and is then characterized by fluorescence and bright-field microscopy.

Schematic of a nanoparticle displaying multiple enzymes that collectively engage in multistep biocatalysis. These systems are used to understand the mechanisms involved in altering enzyme activity and assembling a totally artificial enzyme biosynthetic pathway on nanoparticles.



Microbe-powered ocean sensor undergoing testing in coastal Maine. Oceanographic moorings equipped with benthic microbial fuel cells (BMFCs) are being developed to persistently power oceanographic sensors. BMFCs use marine sediment organic matter as the fuel.



Nanocellulose electronics research explores materials science at the interface of biology and electronics, resulting in biocompatible electronics which can be used as wearable biosensors. Examples in this picture include printed circuit boards, heartbeat monitor tags, and sweat-sensing decals.

Acoustics

NRL's "Reliant" unmanned undersea vehicle with towed acoustic array being deployed during a long range active acoustics experiment.



The Acoustics Division's research program spans the domains of quantum and classical physics. It addresses spatial scales from nanometers to hundreds of kilometers and temporal scales from less than microseconds to the seasonal and long-term variability of the oceans. The Division's research topics include the following:

(1) The study of the impact of riverine, ocean, and atmospheric fluid dynamics on the phase coherent properties of acoustic signals with the objective of predicting the performance variability of acoustic systems, including autonomous unmanned underwater systems and their underwater acoustic communications networks;

(2) The prediction and measurement of the spatial-spectral scattered and radiated acoustics fields by complex three-dimensional structures with application to advanced mine countermeasures, counter unmanned systems, antisubmarine warfare (ASW) detection concepts, and advanced stealth for underwater vehicles;

(3) The continued development, expansion, and adaptation of full physics underwater acoustic propagation and scattering theories that can be used to simulate the propagation of scattered and radiated fields;

(4) The measurement and theoretical description of the spatial/temporal variability of the deterministic/statistical properties of acoustic signals scattered from marine organisms, the near-surface ocean volume, the air-sea interface, and the sea bottom/subbottom, with the objective of reducing the impact of non-target acoustic signal clutter on naval mine countermeasures and anti-submarine warfare system performance;

(5) Creation of novel methods of the assimilation of acoustic data into ocean and atmospheric models that extend their respective temporal prediction capabilities and lower residual uncertainties in the environment;

(6) The application of data science and machine-learning to acoustics for improved computational speeds and the spatial-temporal understanding of vari-

ability; air–sea interface, and the sea bottom/subbottom, with the objective of reducing the impact of non-target acoustic signal clutter on naval mine countermeasures and ASW system performance;

(7) The design from first principles of thin-film micro and nano-structures (e.g., new thermo-electric, signal processing, thermal transport control, metal materials, and sensors) that have unique phonon and macroscale sound transmission, reflection, and transduction properties;

(8) The development of micro and mesoscale structures and materials that result in novel metamaterials exhibiting exhibit extreme wave propagation and phononic behavior.

The experimental and computational component of the Division's research program requires the utilization of high-performance computers, the NRL Institute for Nanoscience experimental facilities, the University National Oceanographic Laboratory System's ships and measurement systems, and the design and use of state-of-the-art laboratory, underwater, and atmospheric research instrumentation.

At-Sea Research: The Division uses autonomous unmanned vehicles, distributed autonomous sensors, autonomous moorings, and measurement systems attached to ships. Undersea acoustic propagation and ambient noise measurements are made with a fully autonomous moored acoustic data acquisition suite.

Ship-attached instruments are used to investigate the four-dimensional properties of acoustic signals scattered from the ocean's surface, bottom, and volume.

A 53-cm diameter Bluefin and three Ocean Server IVer2 autonomous underwater vehicles are used to test autonomous underwater vehicle countermeasures, counter unmanned underwater vehicles, ASW concepts, and autonomous vehicle control algorithms designed to function in environments with unanticipated events.

Laboratory Facilities: The Acoustics Division has several nationally unique laboratory facilities. The Laboratory for Structural Acoustics supports experimental research in which acoustic radiation, scattering, and surface vibration measurements of fluid-loaded and non-fluid-loaded structures are performed. This 1 million gallon in-ground pool facility (55 ft diameter, 50 ft depth) has vibration and temperature control, anechoic interior walls, and automated three-dimensional scattering cross section measurement capabilities.

A large acoustically treated in-air measurement facility (50 × 40 ft, with a height of 38 ft) is used for structural acoustic and vibration measurements on satellite payload fairings, active and passive material systems for sound control, and new transducer and sensor systems.

The Shallow Water Acoustics Laboratory is a large acoustic tank (25 ft × 35 ft, with a depth of 25 ft) with a marine sediment bottom to study the impact of sediment burial on the structural response of mines or improvised explosive devices.

The Salt Water Tank Facility (6 m × 6 m × 3.5 m) is designed to study a variety of physical phenomena under both saline and non-saline conditions at temperatures from 0 °C to 40 °C, including acoustics in bubbly media, and serves as the main test facility for larger scale elasto-acoustic metamaterials.

An ultrasonic measurements laboratory is used for small-scale acoustics experiments designed to measure the effectiveness of small scale acoustic metamaterials in saline and non-saline environments.

A microfluidics laboratory that has as a central component a PIV system to track the flow of liquids and emulsions under the influence of acoustic fields.

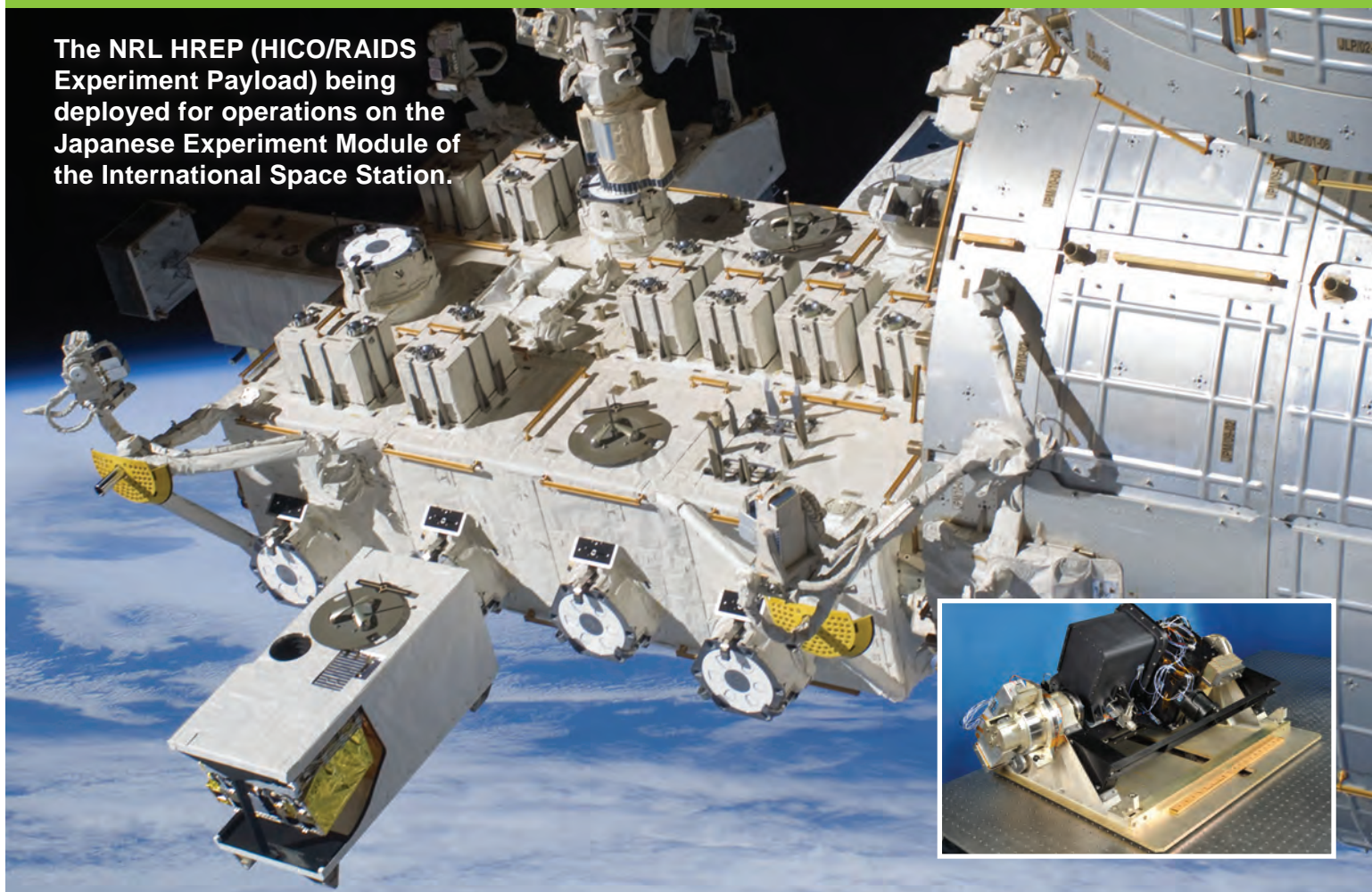
Center for Additive Manufacturing Research: The Acoustics Division also maintains and runs NRL's Center for Additive Manufacturing. This includes an ExOne Binder Jet, a Concept Laser M2, and a Hybrid Technology Additive/Subtractive System. There are also several smaller additive manufacturing machines and two Polymer Stratasys system printers. These offer the maximum amount of variety in additive manufacturing with an open process space to facilitate the performance of both basic/applied research and bespoke part fabrication in virtually any printing medium. Also in the Center are dedicated geometrical, mechanical, and acoustic testing facilities; their co-location facilitates precise and full understanding of as-built parts and structured materials.



The Acoustic Division is working with the Proteus Large Displacement Unmanned Underwater vehicle from Huntington Ingalls. The division is currently applying the Low Frequency Broadband technology to detect and classify this class of vehicle, which is an emerging threat.

Remote Sensing

The NRL HREP (HICO/RAIDS Experiment Payload) being deployed for operations on the Japanese Experiment Module of the International Space Station.



The Remote Sensing Division is the Navy's center of excellence for remote sensing research and development, conducting a broad program of basic and applied research across the full electromagnetic spectrum using active and passive techniques from ground-, air-, and space-based platforms. Current applications include earth, ocean, atmospheric, astronomy, astrometry, and astrophysical science, and surveillance/reconnaissance activities, including maritime domain awareness, antisubmarine warfare, and mine warfare. Special emphasis is given to developing space-based platforms and exploiting existing space systems.

A major Division research focus is environmental remote sensing of the littoral environment. Specific research areas include maritime hyperspectral imaging for in-water environmental remote sensing and land-based trafficability studies, radar measurements of the ocean surface for the remote sensing of waves and currents, and model- and laboratory-based hydrodynamics.

Airborne sensors used for characterization of the littoral environment include visible/near-infrared (VNIR)

and shortwave infrared (IR) hyperspectral imagers; a VNIR multichannel and hyperspectral polarimetric imager; a nonimaging VNIR polarimetric spectrometer; longwave and midwave IR thermal cameras; an X-band, 2-channel interferometric synthetic aperture radar (SAR); and the NRL Focused Phased Array Imaging Radar (NRL FOPAIR), an X-band, high-frame-rate, polarimetric, multi-phase center SAR system.

As an outgrowth of our airborne littoral sensing program, the Division developed the Hyperspectral Imager for the Coastal Ocean (HICO), the world's first spaceborne VNIR hyperspectral sensor specifically designed for coastal maritime environmental observations. HICO was launched to the International Space Station in September 2009, and operated until September 2014; it has provided scientific imagery of varied coastal types worldwide. After a 3-year Navy mission, HICO was supported by NASA in 2013 and 2014.

New littoral research areas include the exploitation of polarized hyperspectral imaging, active (lidar-based) sensing of the water column, and laboratory and field-

based research on the relationship between in-water particle aggregates and turbulence.

For radiometric and spectral calibration of the visible and IR imaging sensors, the Division operates a calibration facility that includes a NIST-traceable integrating sphere and a set of gas emission standards for wavelength calibration.

The Division's Free Surface Hydrodynamics Laboratory (FSHL) supports ocean remote sensing research. The lab consists of a 10 m wave tank equipped with a computer-controlled wave generator and a comprehensive set of diagnostic tools. Recent work focuses on the physics of breaking waves, their infrared signature, and their role in producing aerosols. Experiments conducted in the FSHL are also used to test and validate numerical results and analytical theories dealing with the physics of the ocean's free surface.

Non-littoral environmental research areas include the remote sensing of sea ice and soil moisture, the measurement of ocean surface winds, and middle atmospheric research. NRL (in a collaboration between the Naval Center for Space Technology and the Remote Sensing Division) developed the first spaceborne polarimetric microwave radiometer, WindSat, launched in January 2003 and still operational. Its primary mission was to demonstrate the capability to remotely sense the ocean surface wind vector with a passive system. WindSat provides major risk reduction for development of the microwave imager for the next-generation Department of Defense operational environmental satellite program. WindSat data are processed at the Navy Fleet Numerical Meteorology and Oceanography Center (FNMOC), and operationally assimilated into the Navy's global weather model, as well as that of several civilian weather agencies worldwide. In addition, the Remote Sensing Division is exploiting WindSat's unique data set for the remote sensing of other environmental parameters, including sea surface temperature, soil moisture, and sea ice concentration.

The Division also carries out a vigorous research program in the remote sensing of middle atmospheric constituents by ground-based millimeter-wave spectroscopy. The centerpiece of that program is the Microwave Atmospheric Spectroscopy Laboratory (MASL) for remote sensing of the middle atmosphere (20-80 km, encompassing the stratosphere and mesosphere). This is the only project of its kind in the United States and the largest and most successful ground-based atmospheric microwave spectroscopy project in the world. MASL now includes multiple copies of three sensors: (1) Water Vapor Millimeter-wave Spectrometer (WVMS); (2) Microwave Ozone Profiling Instrument (MOPI); and (3) the Chlorine Monoxide Experiment (ChLOE). These

instruments are deployed at five sites: Table Mountain, California; Mauna Loa, Hawaii; Mauna Kea, Hawaii; Lauder, New Zealand; and Scott Base, Antarctica. The MASL instruments are part of the international Network for the Detection of Atmospheric Composition Change. The MASL program is a collaboration with the University of Massachusetts and the State University of New York Stony Brook.

The Division has research programs in astronomy and astrophysics ranging in wavelength from the optical to longwave radio (HF), with an emphasis on interferometric imaging. Facilities include the Navy Precision Optical Interferometer (NPOI), located near Flagstaff, Arizona, a joint project between the U.S. Naval Observatory and the NRL Remote Sensing Division. When completed, NPOI will be the highest-resolution ground-based optical telescope in the world. Current applications include optical astrometry, unfilled aperture imaging technologies research, astrophysical research, and (most recently) research into the imaging of deep space satellites.

As an outgrowth of this imaging research, the Division has established an adaptive/active polymer lens laboratory, consisting of a clean room environment and specialized equipment for conducting research and development, fabrication, characterization, and metrology related to adaptive polymer lenses and other types of custom polymer optics.

The Division is also at the forefront of research in low-frequency (<100 MHz) radio astronomy and associated instrumentation and interferometric imaging techniques. The Division developed and installed VHF receivers on the National Radio Astronomy Observatory's Very Large Array (VLA), designed the next-generation HF receiver system for the EVLA (Expanded VLA), and developed imaging techniques necessary to correct for ionospheric phase disturbances, important at HF frequencies. The newly completed (November 2014) NRL VLA Low Band Ionospheric and Transient Experiment (VLITE) provides continuous imaging observations at 352 MHz with 64 MHz bandwidth. VLITE, which originally included 10 VLA antennas but was recently upgraded to a 16 antennas system, is a unique facility for astrophysical transient detection and ionospheric remote sensing.

The Division is also collaborating with the University of New Mexico on the Long Wavelength Array, a prototype, next-generation, HF imaging array ultimately with 200 to 300 km baselines.

Finally, the Division operates the NRL SEALAB (Scene Exploitation and Analysis Laboratory), which is the primary conduit of Division imaging research to the operational community.

Oceanography



NRL scientists prepare to deploy a bottom-mounted SEPTR mooring in the Gulf of Mexico.

The Oceanography Division is the major center for in-house Navy research and development in oceanography. It is known nationally and internationally for its unique combination of theoretical, numerical, experimental, and remotely sensed approaches to oceanographic problems. The Division's modeling focus is on a truly integrated global to coastal strategy, from deep water, including arctic regions, to the coast, including straits, harbors, bays, inlets, and rivers. This focus requires emphasis on both ocean circulation and wave/surf prediction, with additional focus on coupling the ocean models to atmospheric, ice, biological, optical, and sediment models. This work includes processing and analysis of satellite and in-water observations, development of numerical model systems, and using advanced data assimilation techniques for predicting the ocean environment. This modeling is conducted on the Navy's and Department of Defense's most powerful vector and parallel process-

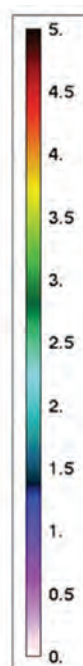
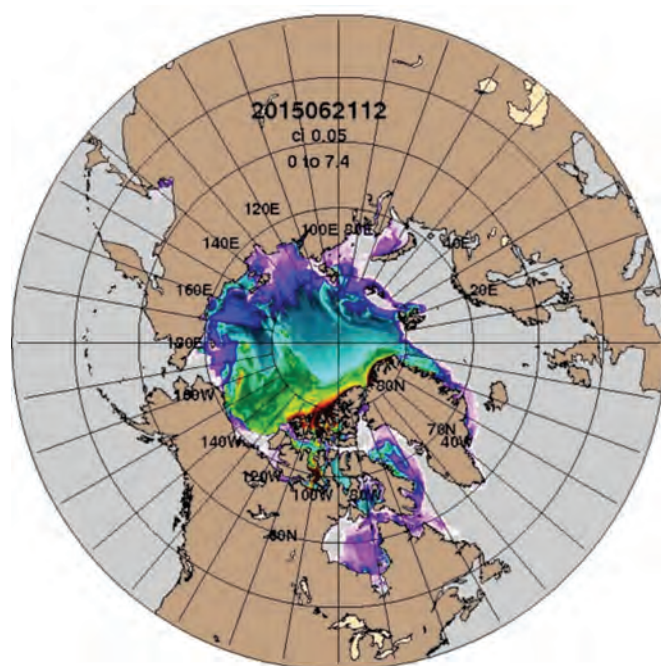
ing machines. The Division's in-house Ocean Dynamics and Prediction Computational Network Facility provides computer services to scientists for program development, graphics, data processing, and storage as well as network connectivity to other Navy and DoD sites, including the High Performance Computing centers. The computational system enables leading-edge oceanographic numerical prediction research applicable to Navy operations affected by environmental variations at scales of meters to hundreds of kilometers and time scales of seconds to weeks. To study the results of this intense modeling effort, the Division operates a number of highly sophisticated graphic systems that help researchers visualize ocean and coastal dynamic processes. Problems addressed cover a wide scope of physics including parameterization of oceanic processes; construction and analysis of ocean models and forecast systems; and basic and applied research of ocean dynamics, surface waves, thermoha-

line circulation, nearshore circulation, estuarine and riverine modeling, arctic ice modeling, internal waves, and ocean/atmosphere/wave/ice coupling. Additional emphasis is on optimization of underwater, airborne, and satellite observing systems; representation of ocean processes affecting temperature, salinity, and mixed-layer depth; uncertainty analysis in coupled systems; ensemble and probabilistic ocean forecasting; targeting ocean observations; representing probability in ocean/acoustic systems; and satellite-observed surface heat fluxes. The goal is to build cutting-edge technology systems that transition to operational forecast centers.

The Division's Ocean Sciences Branch conducts basic and applied research in ocean physics, air-sea interaction, ocean optics, coupled physical bio-optical modeling, and marine microbially influenced corrosion. Emphasis of this research is on understanding the oceans' physical processes and their interactions with the atmosphere and biological/chemical systems at scales ranging from basin-scale to microscale. Numerical and analytical models are developed and tested in laboratory and field experiments. The results of this research support the Navy's operational capability for predictions of oceanic atmospheric exchanges, acoustic propagation/detection, light transmission/emission, and influences of microbes on marine corrosion. The seagoing experimental programs of the Division range worldwide. Unique measurement systems include a wave measurement system to acquire in situ spatial properties of water waves; a

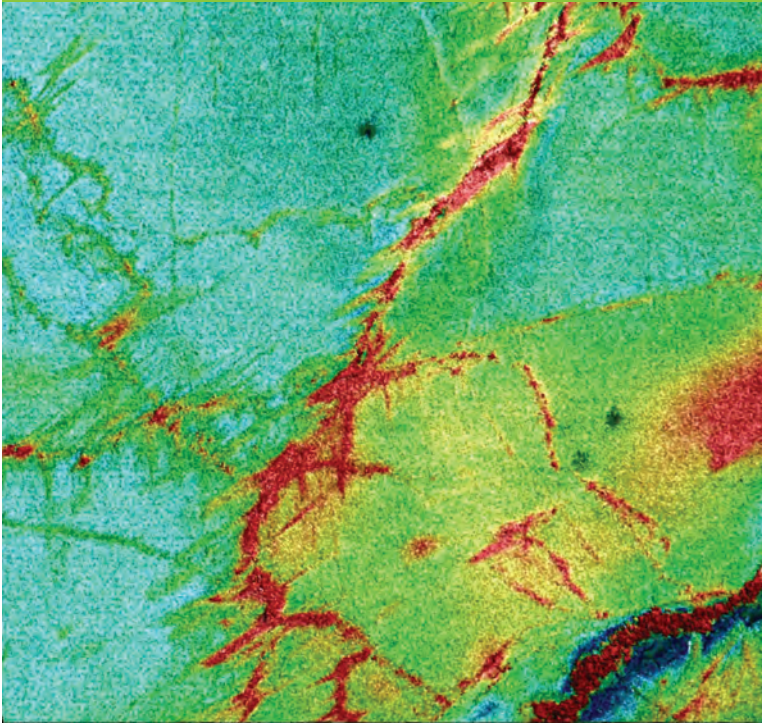
salinity mapper that acquires images of spatial and temporal sea surface salinity variabilities in littoral regions; an integrated absorption cavity and optical profiler system; a towed optical hyperspectral array and a Shipboard Lidar Optical Profiler (SLOP) for studying ocean optical characteristics; self-contained, bottom-mounted, upward-looking acoustic Doppler current profilers (ADCPs) for measuring ocean variability; and a Shallow water Environmental Profiler in Trawl-safe, Real-time configuration (SEPTR). A newly acquired Rayleigh-Bénard convective tank and a hybrid underwater camera support the Division's ocean optics programs, providing object detection and identification in extremely turbid underwater environments. Instruments for sensing the littoral environment include a Vertical Microstructure Profiler (VMP), a Scanfish, and four Slocum Gliders equipped with a microstructure (turbulence) package.

The Division's remote sensing research focuses on radiative transfer theory, optical ocean instrumentation, lasers and underwater imaging and vision, satellite and aircraft remote sensing, and remote sensing of bio-optical signatures. The research includes applying aircraft and satellite ocean color and thermal infrared signatures for understanding the biogeochemical cycles in the surface ocean. Additional emphasis is on algorithm and model development using satellite and aircraft data (SeaWifs, MODIS, MERIS, AVHRR, VIIRS, OCM, GOCI, HICO, and CASI) to address the spatial and temporal variability of coastal optical properties.

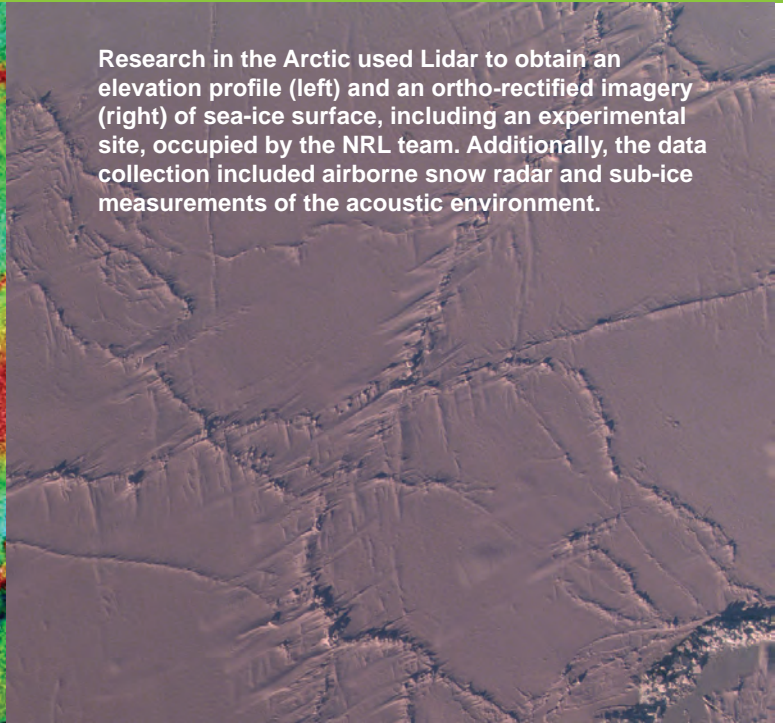


Arctic ice thickness (meters) from the Coupled HYCOM/CICE System for June 21, 2015.

Marine Geosciences



Research in the Arctic used Lidar to obtain an elevation profile (left) and an ortho-rectified imagery (right) of sea-ice surface, including an experimental site, occupied by the NRL team. Additionally, the data collection included airborne snow radar and sub-ice measurements of the acoustic environment.



The Marine Geosciences Division is the major Navy in-house center for research and development in marine geology, geophysics, sediment dynamics, geodesy, geoacoustics, geotechnology, and geospatial information and systems. Research is focused on three primary thrust areas: (1) Characterization and Prediction in Seafloor and Terrestrial Regions, (2) Dynamic Littoral and Riverine Processes, (3) Geospatial Sciences and Technology.

Characterization and Prediction in Seafloor and Terrestrial Regions. Research subthrusts include: (1) Terrain Trafficability. Division scientist collaborate with the Remote Sensing Division and ERDC (Vicksburg, Mississippi) scientists to exploit remotely sensed hyperspectral, LIDAR, and low-frequency Synthetic Aperture Radar (SAR). Data from these systems provide information about the surface and sub-surface properties and structure to estimate trafficability parameters for complex and heterogeneous soils. This research also includes work on real-time spectral and LIDAR terrain sensing ahead of a vehicle for dynamic inputs into the vehicles' adaptive controls. (2) Polarimetric SAR Applications. Division researchers have deployed overseas to conduct field test and evaluation of a low-frequency, ultra-wideband, polarimetric SAR for detecting a wide range of objects of military interest. The SAR instrument was flown by NRL's VXS-1 aircraft and proved to be extremely effective. Division scientist are expanding the SAR utility for this portion of the electromagnetic

spectrum with new military applications. (3) Machine Learning to Predict Seafloor Properties. As part of a carbon flux research project, machine-learning techniques are being applied to predict seafloor properties where the properties cannot be directly measured. The ocean is far too vast for complete, direct sampling of seafloor parameters. However, machine learning techniques find correlations between the desired quantity, in this case seafloor porosity, and other, well-known quantities, (e.g., distance from the coast, bathymetry, etc.). A new global model initiative will focus on extending these techniques in concert with a deterministic model of sediment physics to predict acoustic properties everywhere on the seafloor. (4) Sediment Characterization to Improve Sea Mine Detection. As part of a complex sediment characterization initiative to improve acoustic and seismic detection of sea mine deployments, NRL has conducted sea trials deploying various synthetic targets and collected data on various deployment signatures, relative to the in-water and bottom conditions. From this environmental preparation, acoustic classifiers can be built with high probability of detection and low probability of false alarm for detecting sea mine deployments.

Dynamic Littoral and Riverine Processes. Research subthrusts include: (1) Modeling Sediment Transport. The Division continues to expand its modeling of sediment transport phenomena across many orders of magnitude, from the discrete particle scale (where the motions of individual sand grains are simulated) to the

continuum scale (where sand ripples and bathymetric changes are predicted). (2) Prediction of Seafloor Roughness Evolution. The Division recently completed the development of the new Naval Seafloor Evolution Archetype (NSEA) model. This spectral ripple model, NSEA, predicts variations in seafloor roughness given measured or forecasted wave conditions in sandy environments. The new model allows researchers to predict the evolution of spectral ripple wavelengths on the seafloor, and is in good agreement with observations. (3) Prediction of Riverine Parameters. Division scientists developed a new parametric method for estimating depth and discharge in open channel flow hydraulics using observations of surface currents and water surface elevation. The parametric inverse process was validated on a small grid using remotely sensed surface velocity measurements and water surface elevation on the Kootenai River in Idaho. (4) Using AUVs to Characterize Estuary Hydrodynamics. One of the Division research initiatives is aimed at using autonomous underwater vehicles to resolve the spatial structure of oceanographic fronts and other hydrodynamic features. Characterizing the “soundscape” in these complex geoacoustic regions where fresh water from rivers enter the brackish waters of estuaries poses a significant operational challenge for the Navy. Initial analysis has focused on estimating sound speed in the sampled surficial sediments, while future analysis will include quantifying the details of the sedimentology to inform acoustic propagation models for transmission loss. (5) Seafloor Properties. Geoacoustic characterization of well-rounded to highly angular sands has established a positive correlation between shear strength of sand and a nonlinear coefficient describing the propagation of an interface wave on the seafloor. This research has important implications for characterizing seafloor properties remotely. (6) Unexploded Ordinance Remediation. A series of ambitious field experiments by Division scientists have demonstrated that munitions density is the most important parameter for predicting burial and mobility of unexploded ordnance in the underwater environment. These novel findings will significantly impact future cost and methods for remediation and management of over 10 million acres of DoD contaminated underwater sites.

Geospatial Sciences and Technology. Research subthrusters include: (1) Navigation Chart Modernization. Division scientist are modernizing the production processes for navigation

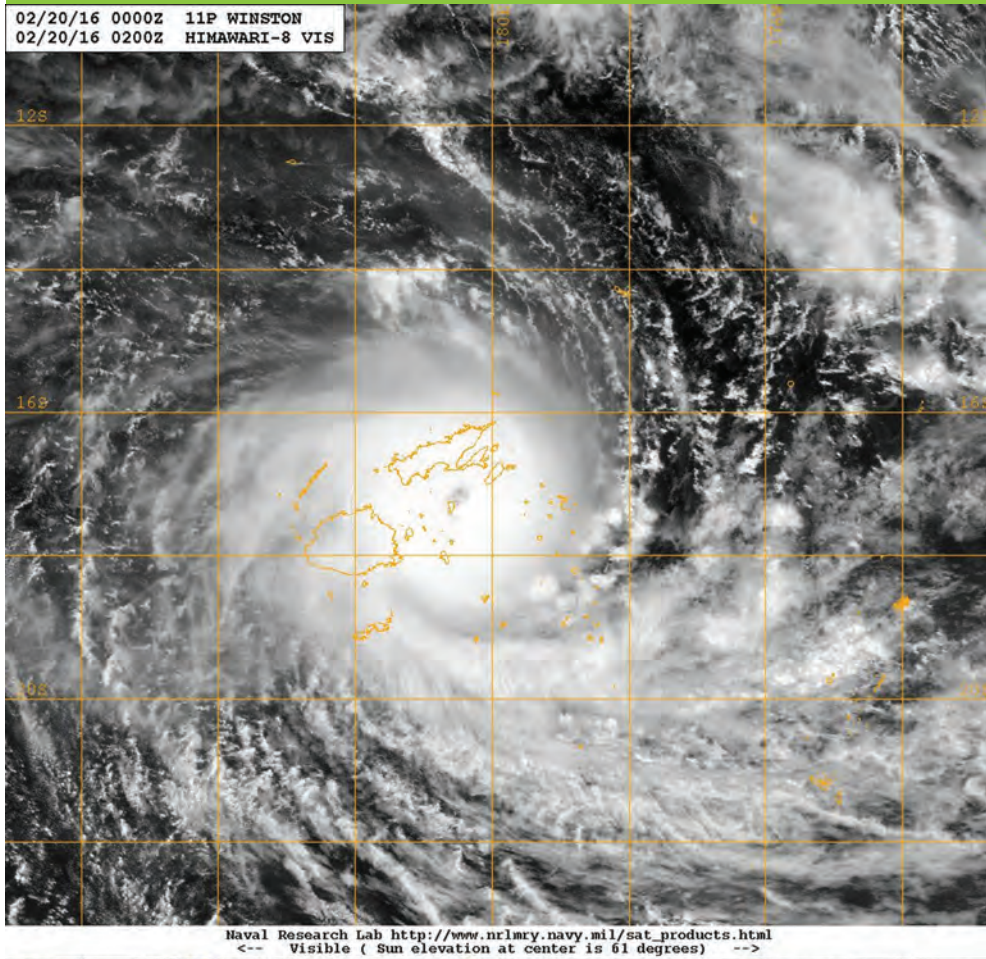
and planning charts with the National Geospatial-Intelligence Agency’s (NGA) Maritime and Aeronautical production offices. New versions of the Digital Nautical Chart verification software and Seamless Enroute Chart production system were developed and included a dynamic, full-color compressed raster chart production system. (2) High Performance Mapping Services. The Marine Geosciences Division is a key performer for NGA’s Innovative GEOINT App Provider Program. NRL provides all high performance data services for this effort using the NRL created Tile Server system that incorporates technology from over 10 NRL Patents to deliver map products for DoD. (3) Environmental Mine Warfare Products. Scientists in the Division developed the Environmental Post Mission Analysis software as a component of the Net-Centric Sensor Analysis for Mine Warfare system for use in the Littoral Combat Ship. These environmental preparation capabilities utilize on-scene data to update environmental databases and reduce mine warfare timelines for detecting mine-like changes on the seabed. (4) Mine Warfare Mapping Products. NRL developed Geospatial Area Folders to provide the ability for rapidly creating geospatially enabled intelligence products from multisource intelligence data. This product is reducing production timelines by 80% in regional headquarters to deliver actionable intelligence to the warfighter. (5) Geospatial Human-Computer Interaction Research. The Division has expanded its human factors research to improve Navy warfighter performance using geospatial applications and further automate Navy processes. This research has included extensive user trials for the creation of a prototype watchfloor for Command Task Group 80.7 Physical Battlespace Awareness Maritime Operations Center. (6) Advanced Hybrid Computer Architecture. Division scientists started a new hybrid computer architecture research program to investigate advanced hardware configurations for improved performance of

Navy processing algorithms. Early results indicate process speedups of over 1000 times using innovative new memory architectures and updated algorithms.



This figure shows a portion of a Nevada test range where Division researchers are studying vehicle and human trafficability. Slopes calculated from the airborne LIDAR (1 m grid) are overlaid on the airborne photogrammetry.

Marine Meteorology



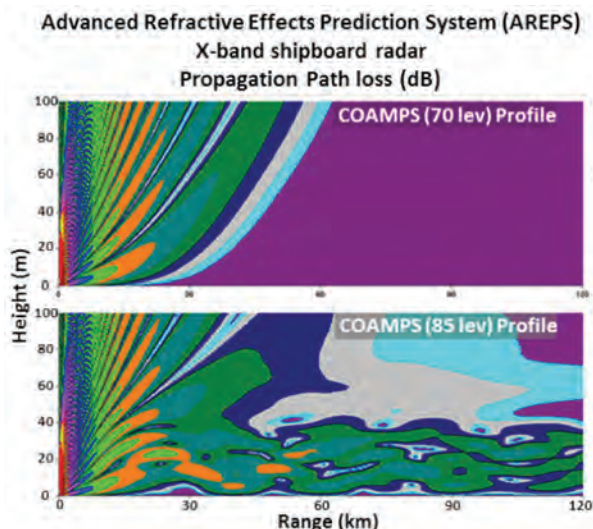
Cyclone Winston over the Fiji Islands as seen in visible imagery produced at NRL Monterey from Himawari-8 Advanced Himawari Imager (AHI) data.

The Marine Meteorology Division, located in Monterey, California, conducts cutting-edge basic and applied research in the atmospheric sciences. The Division develops high resolution meteorological analysis and prediction systems and other decision support products to support Navy, Department of Defense (DoD), and other customers operating at theater, operational, and tactical levels. The Division is collocated with the Fleet Numerical Meteorology and Oceanography Center (FNMOC), the Navy's operational production center for numerical weather prediction (NWP) and satellite imagery interpretation.

The Division's Atmospheric Dynamics and Prediction Branch studies atmospheric processes such as air-sea-ice interaction, tropical cyclone intensification, atmospheric dynamics, and cloud/aerosol physics. The Branch develops numerical weather analysis and prediction systems and coupled air/land/ocean/ice systems for operational use using local high-performance computing resources and offsite DoD Supercomputing

Resource Centers as well as FNMOC assets. Leveraging these theoretical studies and field data collected from around the world, the Division's Meteorological Applications Development Branch develops, improves, and transitions satellite imagery products, decision aids, and probabilistic prediction tools that provide unique and tailored guidance used by Fleet and Marine forces around the globe.

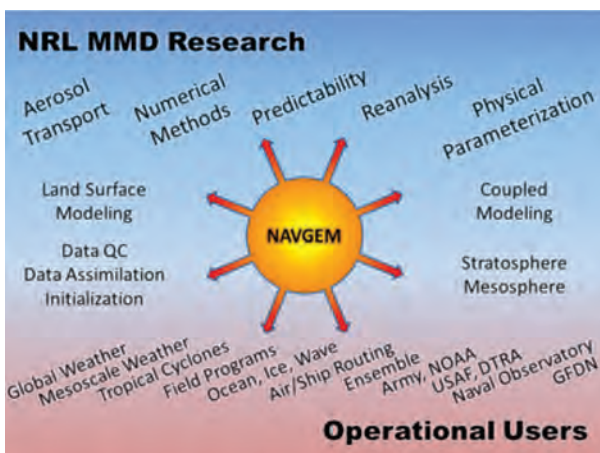
The heart of the Division's research program into atmospheric processes is the Navy Global Environmental Model (NAVGEN), which ties together R&D in regional and tactical scale NWP models, systems to assimilate millions of weather observations per day in which to produce highly accurate long-range predictions to support Navy planning and operations. The NRL Advanced Variational Data Assimilation System-Advanced Representer (NAVDAS-AR) merges millions of observations separated by time and distance from which NAVGEN produces a coherent picture of the atmosphere and long-range predictions. The coupled



Comparison of AREPS predictions using high-resolution COAMPS in the lower atmosphere.

Ocean-Atmosphere Mesoscale Prediction System (COAMPS) then uses NAVGEM's initial output to provide higher resolution tactical scale forecasts.

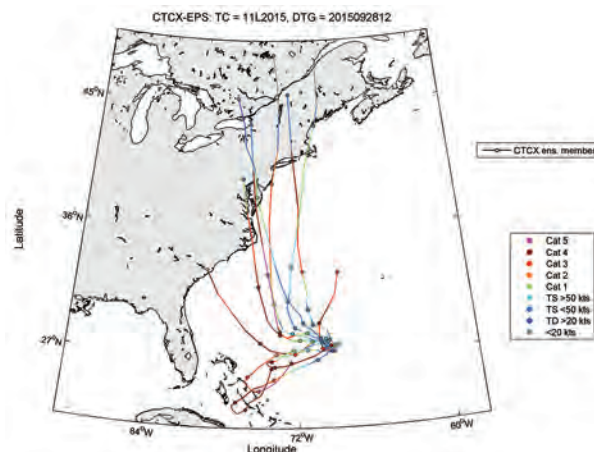
The Division's regional-scale NWP prowess is provided operationally via the COAMPS-On Scene system (COAMPS-OS) which allows users to easily set up complex NWP models via "reach-back," create tailored operational forecasts, and post-process model output into tactically relevant advanced decision support applications. Other applications further exploit meteorological information for decision superiority using cornerstone operational applications, including the Joint METOC Viewer (JMV), Automated Tropical Cyclone Forecasting (ATCF) system, automated ship routing, Atmospheric Acoustic Propagation (AAP) for



Relationship between NAVGEM and other NRL Marine Meteorology Division R&D programs.

helicopters, and the Advanced Refractive Effects Prediction System (AREPS) for electromagnetic propagation predictions.

The Division advances the state of the art of satellite-derived environmental characterization and tropical cyclone structure and intensity analysis. Next-generation satellite data provides enhanced spectral coverage, increased spatial resolution, and quicker temporal refresh of these products. Exploitation of these high volume data sets is accomplished through the NRL MMD-developed Geo-located Information Processing System (GeoIPS). GeoIPS is a portable data ingest and processing system for R&D, near real-time demonstrations, and efficient transitions to operations.



Real-time ensemble forecasts of Hurricane Joaquin for 1200 GMT, Sept. 28, 2015, from COAMPS showing large uncertainty in predicted track and intensity.

The Division performs end-to-end studies of electro-optical (EO) performance predictions ranging from studies of basic aerosol, cloud, and radiation processes to projects that integrate theory, field research, remote sensing, and numerical aerosol and EO prediction at global to mesoscales. The Division is unique in the community in its depth of capabilities to develop and support systems that can globally characterize the EO environment, as well as support of Navy and DoD tactical decision support products.

Space Science



Michelson Interferometer for Global High-resolution Thermospheric Imaging (MIGHTI) spaceflight instrument in an NRL Space Science Division cleanroom. On orbit, MIGHTI will measure neutral winds and temperature in the thermosphere to assess the dramatic variability of the Earth's ionosphere.

The Space Science Division conducts a broad-spectrum RDT&E program in solar-terrestrial physics, astrophysics, upper/middle atmospheric science, and astronomy. Division researchers conceive, plan, and execute scientific research and development programs and transition the results to operational use. They develop instruments to be flown on satellites, sounding rockets, and balloons; and ground-based facilities and mathematical models. The Division's focus is to discover, develop, and demonstrate innovative technologies, methods, and products needed to ensure Navy and Marine Corps robust access to space-associated capabilities of critical importance.

The Division's Vacuum Ultraviolet Solar Instrument Test (SIT) facility is an ultra-clean solar instrument test facility designed to satisfy the rigorous contamination requirements of state-of-the-art solar spaceflight instruments. The facility has a 400 ft² Class 10 clean room and a large Solar Coronagraph Optical Test Chamber (SCOTCH). The SIT clean room is ideally suited for assembly and test of contamination-

sensitive spaceflight instrumentation. It contains a large vibration-isolated optical bench and a 1-ton capacity overhead crane. The SCOTCH consists of a large vacuum tank and a precision instrument-pointing table. The Division also maintains extensive facilities for supporting ultraviolet (UV) spectroscopy sounding rocket programs. These facilities include a dedicated Class 1000 instrument clean room and a gray room area for assembling and testing the rocket payloads; the gray room incorporates all the fixtures required for safe handling of payloads. Further, the Division rocket facilities include a large UV optical test chamber that is additionally equipped with a large vibration- and thermal-isolated optical bench for telescope testing, which allows the laboratory area to be turned into a schlieren facility.

The Division has a wide range of new satellite, rocket, balloon, and ground-based instruments under development. These include the Wide-Field Imager (WISPR) aboard the Parker Solar Probe mission that will periodically enter the solar corona and acquire

detailed time-lapse imagery of small scale solar wind structures; the SoloHI imager aboard the Solar Orbiter mission that will obtain long duration time-lapse imagery of the quasi-steady flow and transient disturbances in the solar wind above specific solar disk features; the Ultraviolet Spectro-Coronagraph (UVSC) Pathfinder that will, from geosynchronous orbit, make the first detection of suprathermal seed particles in the solar corona and lead to a capability to predict the onset of Solar Energetic Particle (SEP) storms at Earth; the Compact CORonagraph (CCOR), a low-complexity and low-cost single-stage coronagraph that enables early assessment of the terrestrial solar coronal mass ejection threat; the Helium Resonance Scattering in the Corona and HELiosphere (HERSCHEL) suborbital payload that investigates the origin and acceleration of the fast and slow solar wind; and the NRL-led SuperMISTI detection system, intended to demonstrate standoff detection, identification, and imaging of radiological/nuclear weapons of mass destruction in maritime environments.

Advanced space-based research is performed in a number of areas. Division experiments are measuring the Earth's thermosphere and ionosphere to improve space weather forecasting for these near-space atmospheric regions that significantly influence the performance of important operational systems such as GPS navigation, communication, and space debris tracking. In August 2016, the Fermi Gamma-ray Space Telescope, major portions of which were developed and tested by NRL's Space Science Division and Spacecraft Engineering Department, completed eight years of successful operation on orbit. Division scientists have had lead roles in several key scientific discoveries using Fermi, including confirmation of the long-standing belief that shocks formed from exploding stars are the source of the high-energy cosmic rays seen at Earth; creation of a highly efficient means of discovering new pulsars, the rapidly rotating cores of dead stars that serve as precise astrophysical clocks; and discovery that our Sun accelerates particles to extreme energies even in relatively weak flares, and does so for hours after the impulsive event. Two Space Science Division-led heliophysics space instrument capabilities, the Large Angle Spectrometric and Coronagraphic Telescope (LASCO) on the SOHO mission and the Sun-Earth Connection Coronal Heliospheric Investigation (SECCHI) on the STEREO mission, are continuing to advance understanding of the solar corona and the importance of coronal mass ejections in determining space weather at Earth.

Division scientists, using the Division network of computers and workstations and other connected high performance computing assets, develop and maintain

physical models in support of their research. These include research to extend the operational Navy Global Environmental Model (NAVGENM) from its current upper boundary to altitudes of ~100 km; and SoftWare for Optimization of Radiation Detectors (SWORD), a vertically integrated radiation transport software tool for graphically setting up, running, and analyzing results from numerical simulation of high energy radiation detection systems and other systems that operate in a high energy radiation environment.



NRL's major role in the Fermi mission (launch 2008, upper left) has enabled broadly based astrophysical investigations, including the gamma-ray sky map (upper right) identifying over 3000 point sources and new insight into particle acceleration and radiations from pulsars, supernova remnants, active galactic nuclei, and many other topics. Space science research in detector design enabled by NRL's Institute for Nanoscience (NSI) has resulted in three pending patents relating to "slim edge" detectors (middle left) and charge control using atomic layer deposition, and three patents on deep reactive ion etching of detectors (lower left). Other division work at the NSI has resulted in patents for a fabrication method for nanometer-scale level structures and for detecting chemical or radiological agents using electrophoretic displays. The J-PEX extreme-ultraviolet sounding rocket experiment (lower center) provided unprecedented spectral resolution on white dwarf stars. Division research in radiological/nuclear weapons of mass destruction (WMD) detection resulted in the dual container SuperMISTI detection system (middle right, in transport to Norfolk maritime testing) providing standoff detection and imaging of WMD. Image (lower right) shows SuperMISTI image of radiation source (blue block) hidden in the hold of USS *Cape Chalmers*.

Space Systems Development Department

Space Systems Development Department Optical Test Facility transmits laser light at both 1064 nm and 1550 nm for both satellite laser ranging and free space optical communication signals.



The Space Systems Development Department (SSDD) at the U.S. Naval Research Laboratory is responsible for the end-to-end definition, design, development, integration, test, and operation of space systems that satisfy naval and national defense requirements.

The total system engineering philosophy employed by the SSDD enables seamless sensor-to-shooter capabilities to be deployed that optimize the interfaces between command and control, on-orbit satellite collection, and onboard and ground processing functions; the dissemination of data to tactical and national users; and the design of tools that provide for the automated correlation and fusion of collected information with other sources.

Research and development is conducted in the areas of space system architectures; advanced mission data processing and data analysis techniques; advanced information systems concepts, including enterprise and cloud computing and networking of space, air, ground, and subsurface sensors; and mission simula-

tion techniques. Intelligence collection, advanced radiofrequency (RF), optical, and laser communication, satellite laser ranging, digital signal processing, data management, and space navigation systems are constantly improved upon to satisfy evolving requirements. These systems are engineered for maximum reuse and interoperability.

Having conceived of and developed the payload for the first Global Positioning System (GPS) satellite, the SSDD continues to be a center of excellence in the research and development of advanced GPS technology. Advanced theoretical and experimental investigations are applied to expanding the design and interoperability of systems used for a wide range of military, space, geodetic, and time dissemination applications. These investigations involve critical precise time generation and measurement technology for passive and active ranging techniques incorporating advanced data transmission and signal design. Precise time and time interval research involves theoretical and experimental development of atomic time/frequency standards,

instrumentation, and timekeeping to support highly precise and accurate timescale systems in scientific and military use. Net-centric systems are critically dependent on highly accurate and stable time/frequency standards coordinated to a common timescale through the diverse dissemination comparison techniques developed within the SSDD.

The Precision Clock Evaluation Facility (PCEF) is one of the major facilities within NRL's Naval Center for Space Technology. The PCEF was developed to support development of high-precision clocks for GPS spacecraft and ground applications, primarily atomic standards. Space atomic clocks are evaluated, qualified, and acceptance-tested for space flight using the assets of this facility. Testing includes long- and short-term performance evaluation and environmental testing (including shock and vibration). Investigations of on-orbit anomalies are performed within the PCEF to attempt to duplicate similar effects in space-qualified hardware under controlled conditions. The facility was originally developed to evaluate developments in the GPS concept development program (Block I) and expanded for the dedicated space clock development conducted during operational system development and deployment. The ability to evaluate and test highly precise atomic clocks, especially in a space environment, requires unique facilities, precise time and frequency references, and precise instrumentation. The primary time and frequency reference for the PCEF is a specially designed environmental chamber housing a number of hydrogen masers combined with measurement equipment permitting a realization of Coordinated Universal Time (UTC) to be maintained as UTC (NRL) in cooperation with the International Bureau of Weights and Measures (BIPM) for reference and research purposes.

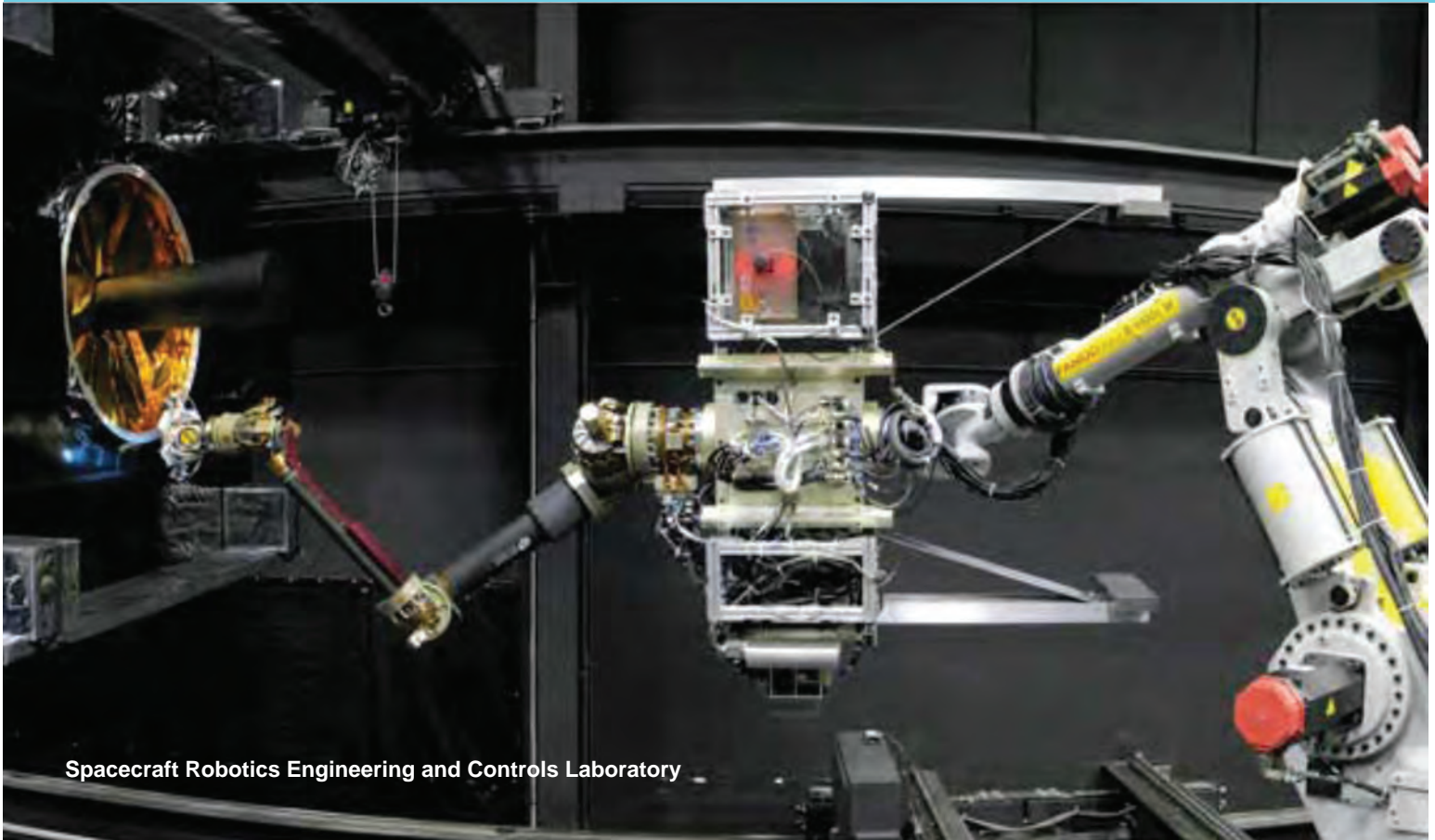
In addition to a wide array of test tools and facilities, the Department operates several field sites, including the Midway Research Center facility in Stafford, Virginia; the Blossom Point Tracking Facility in Welcome, Maryland; and the Chesapeake Bay Detachment Radar Range in Chesapeake Beach, Maryland.

To support transition partners and deliver improved capability, NRL requires its own R&D transportable ground station to serve as a Tasking, Collection, Processing, Exploitation and Dissemination (TCPED) Test Bed for various satellite constellations. The transportable antenna, shown in the picture, provides the communications link for the Test Bed, which allows NRL to perform R&D by incorporating new satellites, hardware, processing and exploitation algorithms, and National to Commercial orchestration

strategies desired by sponsors. After full integration and test, successful product and process improvements can transition to operational systems. In addition, the X-band antenna can receive RF signals from other sources transmitting within the proper frequency band and, given commercial satellite vendor intentions, migrate to include transmit capability for direct tasking of such vendor satellites as Pleiades and WorldView already on orbit and offered through satellite direct access programs. This transportable antenna allows NRL to seek research opportunities that require these communications at either the NRL main laboratory or remote locations.

The NRL Chesapeake Bay Detachment (NRL-CBD) LaserComm Test Facility (LCTF) is the longest operating maritime free space optical (FSO) test facility (currently over 15 years). It includes facilities at NRL-CBD, NRL-Tilghman Island and the 10-mile test range over the Chesapeake Bay between the two locations. It has evolved over its 15 year lifetime from a basic research facility for studying the effects of the atmosphere on laser propagation in the maritime environment, to the premiere test facility for maritime testing and evaluation of internally and externally developed lasercomm systems. The current LCTF operates 24/7 and includes atmospheric sensors at NRL-CBD and NRL-Tilghman Island and a probe laser propagating between the two sites to fully diagnose and understand lasercomm propagation in the maritime environment. These diagnostics operate simultaneously with lasercomm systems under test, enabling quantifiable evaluations of system performance. This enables identification of problem areas in systems and gives guidance to improve hardware and software to obtain optimal lasercomm system performance. The testing and optimization of systems at the LCTF has led to the successful demonstration of multiple lasercomm systems for land, sea, and air platforms — with development currently under way for a space based platform. A major success story for the LCTF is the spiral development (primarily at the LCTF) of the TALON FSO terminal for the U.S. Marine Corps; the terminal completed significant amounts of iterative test at the LCTF, which allowed the Government to reduce significant risk before demonstrating the system at operational training ranges. The TALON FSO and related projects have leveraged the extensive atmospheric and scintillation collection capability to develop FSO availability models based on real field data. It is expected that lasercomm propagation studies and developmental testing at the LCTF will continue for many years to come.

Spacecraft Engineering Department



Spacecraft Robotics Engineering and Controls Laboratory

The Spacecraft Engineering Department (SED) and the Space Systems Development Department, together comprising NRL's Naval Center for Space Technology (NCST), cooperatively develop space systems to respond to Navy, Department of Defense, and national mission requirements with improved performance, capacity, reliability, efficiency, and life cycle cost.

The SED facilities that support this work include integration and test highbays, large and small anechoic radio frequency chambers, varying levels of clean rooms, shock and vibration tables, an acoustic reverberation chamber, battery laboratory, large and small thermal/vacuum test chambers, a thermal systems integration and test laboratory, two-phase heat transfer facility, a spin test facility, a static loads test facility, and a spacecraft robotics engineering and control system interaction laboratory.

Integration and Test Facilities: The department maintains a wide range of specialized RF chambers for test of antennas, receivers, transmitters, electronics, and other flight systems. Two main anechoic chambers are used for the test and verification of antennas and flight systems. The tapered chamber is 31 × 31 × 125 ft,

with a 100 ft measurement distance; it is instrumented from 100 MHz to 18 GHz for radiation patterns, and is regularly used for electromagnetic interference (EMI) measurements as well. The rectangular chamber is 10 × 12 × 20 ft, with a 14 ft measurement distance, and is instrumented from 1 to 400 GHz. There is also a 3 × 3 ft millimeter-wave near-field scanner that is also instrumented up to 400 GHz, but capable of measurements up to at least 600 GHz. All the measurement facilities are computer-controlled and fully automated, allowing multiple antennas and polarizations to be measured at the same time. A third RF chamber is dedicated to electromagnetic interference/radio frequency interference (EMI/RFI) testing. This welded steel chamber measures 23 × 23 × 20 ft and provides as much as 120 dB shielding effectiveness up to 18 GHz and 100 dB from 18 to 50 GHz. The chamber uses a hybrid anechoic material consisting of wideband pyramidal absorbers and ferrite tiles for performance from 20 MHz to 50 GHz. The EMI chamber is equipped with instrumentation to perform the full range of MIL-STD-461 EMI qualification testing. A 10 ft high × 11 ft wide sliding bladder door allows easy access of large test items to the main chamber.

The Laminar Flow Clean Room provides an ISO 5 (Class 100) ultraclean environment for the cleaning, assembly, and acceptance testing of contamination-sensitive spacecraft components, as well as integration of complete spacecraft subsystems. The facility is used primarily to support spacecraft propulsion systems but has been used to support all spacecraft electrical, electronic, and mechanical subsystems.

The Vibration Test Facility simulates the various vibration-loading environments present during flight operations and demonstrates compliance to design specifications. It consists of the following shakers: Unholtz-Dickie T5000 50K lbf random 2-in. double amplitude (DA) stroke, Ling 4022 30K lbf random 2-in. DA stroke, Ling 2022 16K lbf random 2-in. DA stroke, and a Ling 335 16K lbf random 1-in. DA stroke.

The Acoustic Reverberation Simulation Facility is a 10,000 ft³ reverberation chamber that simulates the acoustic environment that spacecraft experience during launch. The maximum capable sound pressure level is approximately 152 dB.

The Battery Laboratory supports design, development, and testing for space and terrestrial battery hardware. The lab consists of a MACCOR battery test system, which is a fully automated computerized test system that can cycle multiple batteries/cells simultaneously; and a Thermotron thermal chamber to support testing at temperature extremes.

The Thermal Fabrication and Test Facility supports the design, fabrication, installation, and verification of spacecraft thermal control systems. It also provides for the analytical thermal design and analysis of any spacecraft.

The Advanced Two Phase Heat Transfer Facility provides for concept development, performance verification, and basic research of all manner of high performance heat pipes; capillary and mechanically pumped fluid loops; and advanced modeling methods comprised of both commercially available and internally developed analytical codes, to include computational fluid dynamics techniques.

The Thermal Vacuum Test Facility consists of one large, two medium, and several small chambers. The large chamber is a 16 ft diameter by 30 ft long horizontal end loading cylinder; the medium chambers are 7 ft diameter by 8 ft tall vertical bottom loading cylinders. One of the medium chambers and the large chamber are cryogenic pumped, providing an oil-free vacuum environment. The other medium chamber has a diffusion pump system capable of evacuation rates similar to the rates that occur during launch ascent. All three chambers are equipped with gaseous nitrogen

conditioned thermal shrouds capable of temperatures between -150°C and $+125^{\circ}\text{C}$. The large chamber and both medium chambers are enclosed within a 2100 ft² clean room specified at ISO 7 (Class 10,000) and certified to ISO 5 (Class 100).

The Spin Test Facility contains a Space Electronics model Product of Inertia-3500 Spin Balance Instrument, a self-contained and fully automatic system for the measurement of dynamic balance, product of inertia, moment of inertia, and center of gravity offset (dynamic) in a single setup.

The Static Loads Test Facility provides the capability to perform modal survey testing on a wide variety of spacecraft and structures. It consists of two 6 ft \times 12 ft \times 6 in. thick, \sim 15,500 lb steel plates (attachable) with floating base, six 75 lbf stinger shakers (1/2-in. DA stroke), two 250 lbf stinger shakers (4-in. DA stroke), and a \sim 300-channel data acquisition system (expandable).

Spacecraft Robotics Engineering and Controls Laboratory: This facility contains the Proximity Operations Testbed (POT), the largest dual-platform motion simulator of its kind, and the Gravity Offset Table (GOT). The POT allows engineers to simulate the rendezvous and proximity operations of spacecraft docking and robotic grappling of target satellites. The test bed encompasses the entire 45 ft \times 100 ft Space Robotics Laboratory, providing a large area to perform spacecraft maneuvers on two motion simulation platforms. The Gravity Offset Table is a 77,000 lb solid slab of granite measuring 20 ft \times 15 ft and 1.5 ft thick. It is ground to a precision flatness within 0.0018 inches across its surface. The GOT is used to simulate satellite rendezvous and contact dynamics under conditions in which the hardware is able to float freely on a cushion of air across the flat surface, nearly negating the effects of gravity and friction on the overall body mass. This is thought to be the largest single slab precision granite table in the country. Its large size allows engineers to simulate servicing of very large objects with significant structural flexibility to a degree of accuracy unmatched by any other space robotics facility. The robotics laboratory supports research in the emerging field of space robotics, including autonomous rendezvous and capture, remote assembly operations, and machine learning. It allows full-scale, hardware-in-the-loop testing of flight mechanisms, sensors, and logic of space robotic systems.

RESEARCH SUPPORT FACILITIES

Technology Transfer Office

The NRL Office of Technology Transfer (TTO) is responsible for facilitating partnerships between NRL and industry and academia to support the transfer of NRL's innovative technologies for public benefit. TTO utilizes authorized agreements to provide NRL expertise and non-exclusive and exclusive rights to NRL inventions, and leverages Government Purpose Licenses (GPLs) to transition NRL technologies for manufacture and sale solely for Navy and other U.S. Government purposes.

TTO markets NRL technology through its website, by participating in exhibitions at trade shows and scientific conferences; by posting content NRL's social media sites and other public affairs channels, in coordination with the efforts of NRL scientists; and through DoD-contracted Partnership Intermediaries such as TechLink. It also works with state and local economic development offices to identify local partnership and commercialization opportunities. In addition to GPLs and other agreements for the management of NRL's patent portfolio, the two primary agreement types utilized by TTO are Cooperative Research and Development Agreements (CRADAs) (15 USC 3710a) and commercial patent license agreements (PLAs) (35 USC 209).

CRADAs provide a vehicle for NRL scientists and engineers to collaborate with their counterparts in industry, academia, and state and local governments. Under a CRADA, a partner may provide funding to NRL for collaborative work, and is granted an exclusive option to license technologies developed during the performance of the CRADA. TTO works with the NRL scientist to sufficiently define the project's scope and work statement and negotiates the terms of the agreement with the CRADA partner.

Through PLAs, a company is granted the right to make, use, and sell NRL technologies commercially in exchange for equitable licensing fees and royalties. Revenue is distributed among inventors and additionally used for awards for the scientific community and in support of activities that further promote technology transfer and transition. PLAs most commonly are partially exclusive (exclusive for a particular field of use or geographic area) or non-exclusive. TTO reviews the commercialization plan submitted by the potential licensee in support of its application for a license, negotiates agreement terms, and monitors the licensee for timely payments and diligence in commercializing the licensed invention.

Technical Information Services

The Technical Information Services (TIS) Branch combines publication, printing and duplication, graphics, photographic and photo-archiving services, video production, and exhibit support into an integrated organization. Publication services include writing, editing, composition, publications consultation and production, and printing management. The Service Desk provides quick turnaround digital black-and-white and color copying/printing, CD/DVD duplication, and passport and ISOPREP photos. Graphic support includes technical and scientific illustrations, computer graphics, design services, display and conference posters, and framing. Large format printers offer exceptional color print quality up to 1200 dpi and produce indoor posters and signs up to 56 inches. Lamination and mounting are available. Photographic services include digital still camera coverage for data documentation, both at NRL and in the field. Photographic images are captured with state-of-the-art digital cameras and can be output to a variety of archival media. Photofinishing services provide custom printing and quick service color prints from digital files. Video services include producing video reports and technical videos and capturing presentations of scientific and technical programs. TIS digital video editing equipment allows in-studio and on-location editing. TIS' photoarchivist is digitizing and ingesting all of NRL's historical and recent photos/negatives into an integrated database. The TIS Exhibits Program works with NRL's scientists and engineers to develop exhibits that best represent a broad spectrum of NRL's technologies and promote these technologies to scientific and non-scientific communities at conferences throughout the United States.

Contracting Division

The Contracting Division is responsible for the acquisition of major research and development materials, services, and facilities where the value is in excess of \$150,000. It also maintains liaison with the ONR Procurement Directorate on NRL procurement matters. Specific functions include providing consultant and advisory services to NRL division personnel on acquisition strategy, contractual adequacy of specifications, and potential sources; reviewing procurement requests for accuracy and completeness; initiating and processing solicitations for procurement; awarding contracts; performing contract administration and post-award monitoring of contract terms and conditions, delivery,

contract changes, patents, etc., and taking corrective actions as required; providing acquisition-related training to division personnel; and interpreting and implementing acquisition-related U.S. Government, DoD, and Navy regulations.

Financial Management Division

The Financial Management Division develops, coordinates, and maintains an integrated system of financial management that provides the Commanding Officer, Director of Research, Associate Director of Research for Business Operations, and other NRL officials with the information and support needed to fulfill the financial and resource management aspects of their responsibilities.

The Division translates NRL program requirements into the financial plan, formulates the NRL budget, monitors and evaluates performance with the budget plan, and provides recommendations and advice to NRL management for corrective actions or strategic program adjustments. The Division maintains accounting records of NRL's financial and related resources transactions, and prepares reports, financial statements, and other documents in support of both NRL management needs and compliance with external reporting requirements. The Division provides financial management guidance, policies, advice, and documented procedures to ensure that NRL operates in compliance with Navy and DoD regulations and with economy and efficiency.

The Division also coordinates efforts with the Defense Finance and Accounting Service to complete payment transactions related to NRL business, e.g., the payment of NRL personnel for payroll and travel expenses and the payment to NRL contractors and vendors for goods and services purchased by NRL.

Additionally, the Division provides administrative support to NRL's Management Information Systems Office.

Research and Development Services Division

The Research and Development Services Division is responsible for the physical plant of NRL and subordinated field sites. Responsibilities include military construction, engineering, and coordination of construction; facility support services and planning as well as maintenance, repair, and operation of all infrastructure systems; transportation; and occupational safety, health and industrial hygiene, and environmental safety. The Division provides engineering and technical assistance to NRL research divisions in the installation and operation of equipment critical in support of the research mission.

Administrative Services

The Administrative Services Branch is responsible for collecting and preserving the documents that comprise NRL's corporate memory. Archival documents include personal papers and correspondence, laboratory notebooks, and work project files — documents that are appraised for their historical or informational value and considered to be permanently valuable. The Branch provides records management services, training, and support for the maintenance of active records, including electronic records, as an important information resource. The Branch is responsible for processing NRL's incoming and outgoing correspondence, and provides training and support on correct correspondence formats and practices. The Branch is responsible for NRL's Forms and Reports Management Programs (including designing electronic forms and maintaining a web site for lab-wide use of electronic forms), and for providing NRL postal mail services for first class and accountable mail as well as mail pickup and delivery throughout NRL. The Branch also provides NRL Locator Service.

Ruth H. Hooker Research Library

NRL's Ruth H. Hooker Research Library to supports NRL and ONR scientists in conducting their research by making a comprehensive collection of the most relevant scholarly information available and useable; by providing direct reference and research support; by capturing and organizing the NRL research portfolio; and by creating, customizing, and deploying a state-of-the-art digital library.

Print and digital library resources include extensive technical report, book, and journal collections dating back to the 1800s housed in a centrally located research facility staffed by subject specialists and information professionals. The collections include 50,000 books; 54,000 digital books; 115,000 bound historical journal volumes; more than 3500 current journal subscriptions; and approximately 2 million technical reports in paper, microfiche, or digital format (classified and unclassified). Research Library staff members provide advanced information consulting; literature searches against all major online databases including classified databases; circulation of materials from the collection including classified literature up to the SECRET level; and retrieval of articles, reports, proceedings, or documents from almost any source around the world. Staff members provide scheduled and on-demand training to help researchers improve productivity through effective use of the library's resources and services.

The Research Library staff has developed and is continuing to expand the NRL Digital Library. The Digital Library currently provides desktop access to

thousands of journals, books, and reference sources to NRL-DC, NRL-Stennis, NRL-Monterey, and the Office of Naval Research.

Library systems provide immediate access to scholarly information, including current and archival journals, trade magazines, and conference proceedings that are fully searchable at the researcher's desktop (more than 15,400 titles). Extensive journal archives from all the major scientific publishers and scholarly societies are now available online. The breadth and depth of content available through TORPEDO, NRL's locally loaded digital repository, continues to grow and provides a single point of access to scholarly information by providing full text search against journals, books, conference proceedings, and technical reports from 20 publishers (15.7 million items by May 1, 2016). The NRL Online Bibliography, a web-based publications information system, is ensuring that the entire research portfolio of written knowledge from all NRL scientists and engineers since the 1920s will be captured, retained, measured, and shared with current and future generations.

OTHER RESEARCH SITES

NRRL has acquired or made arrangements over the years to use a number of major sites and facilities outside of Washington, D.C., for research. The largest facility is located at Stennis Space Center (NRL-SSC) near Bay St. Louis, Mississippi. Others include a facility near the Naval Postgraduate School in Monterey, California (NRL-MRY), and the Chesapeake Bay Detachment (CBD) and Scientific Development Squadron ONE (VXS-1) in Maryland. Additional sites are located in Virginia, Alabama, and Florida.

Stennis Space Center (NRL-SSC)

The U.S. Naval Research Laboratory field site located at John C. Stennis Space Center, Mississippi (NRL-SSC) is located in the southwest corner of Mississippi about 40 miles northeast of New Orleans, Louisiana, and 20 miles from the Mississippi Gulf Coast. NRL-SSC consists of the Marine Geosciences Division; Oceanography Division; a branch of the Acoustic Division; the Office of Research Support Services; and branches of Contracts, Security, and Legal Offices. These codes occupy more than 155,000 ft² of research, computation, laboratory, administrative, and warehouse space. Facilities include the sediment core laboratory, moving-map composer facility, real-time ocean observations and forecast facility, ocean color data receipt and processing facility, environmental microscopy facility, maintenance and calibration systems, Ocean Dynamics and Prediction Computational Network Facility, Command Center Prototype and numerous laboratories for acoustic, geosciences, and oceanographic computation, data analysis, instrumentation calibration and testing. Additional areas are available for instrumentation and training associated with unmanned vehicles as well as space for constructing, staging, refurbishing, and storing seagoing equipment.

NRL-SSC personnel have been located at SSC since the early 1970s, when they were part of the Naval Ocean Research and Development Activity and, later, the Naval Oceanographic and Atmospheric Research Laboratory before consolidating with NRL in 1992. Other Navy tenants at SSC include Commander, Naval Meteorology and Oceanography Command (CNMOC); the Naval Oceanographic Office (NAVOCEANO); Naval Oceanography Operations Command (NOOC); Naval Small Craft Instruction and Technical Training School (NAVSCIATTS); Special Boat Team Twenty-Two (SBT-22); the Department of Navy Human Resource Center, SE; and numerous other Navy commands. Other Federal and state agencies at SSC involved in marine-

related science and technology include NASA, elements of the National Oceanic and Atmospheric Administration, the U.S. Geological Survey, the Environmental Protection Agency, the Center for Higher Learning, the University of Southern Mississippi School of Ocean Science and Technology, and a Mississippi State University Geospatial Center.

NRL-SSC's collocation with such a diverse range of Federal, state, and private organizations allows for excellent collaborative partnerships.

NRL-SSC especially benefits from the company of CNMOC and NAVOCEANO, which are major operational users of the oceanographic, acoustic, and geosciences technology developed by NRL-SSC researchers. NAVOCEANO operates the Navy DoD Supercomputing Resource Center (Navy DSRC) also located at SSC. One of the Nation's High Performance Supercomputing Centers, the Navy DSRC provides operational support to the warfighter and access to NRL for ocean and atmospheric prediction efforts. NAVOCEANO also operates the Maury Library, which holds the largest oceanographic collection of its kind in the world.



John C. Stennis Space Center, Mississippi (NRL-SSC).

Monterey (NRL-MRY)

The NRL Monterey detachment (NRL-MRY) is located in Monterey, California, on a 5-acre Annex about one mile from the Naval Support Activity, Monterey (NSAM) main base and the Naval Postgraduate School (NPS) campus. The Marine Meteorology Division has occupied this site since the early 1970s, when the U.S. Navy collocated its meteorological research facility with the operational center, Fleet Numerical Meteorology and Oceanography Center (FNMOC). This collocation of research, education, and operations continues to be a winning formula. FNMOC remains the primary customer for the numerical weather prediction and satellite product systems developed by NRL-MRY. NRL-MRY scientists have direct access to FNMOC's supercomputers, allowing advanced development using the real-time, on-site, global atmospheric and oceanographic databases, in the same computational environment as operations. Such access offers unique advantages for successfully implement-

ing new systems and system upgrades, and allows for rapid integration of new research results into the operational systems. NRL-MRY occupies two out of the five primary buildings on the Annex with a total floor space of approximately 40,000 ft². One of the buildings, the Marine Meteorology Center, was completed and dedicated in October 2012, and houses the atmospheric aerosol laboratory, computer facility, the Meteorology Applications Development Branch, and the Division's front office suite. A configurable, cutting-edge aerosol and radiation measuring and observation platform is situated on the roof of the building for long-term monitoring of the air quality in Monterey, complementing the standard meteorological observation suite of the National Weather Service Forecast Office for San Francisco/Monterey Bay, collocated in the Annex.



NRL Monterey's 15,000 ft² Marine Meteorology Center. The building was dedicated in October 2012.

NRL-MRY acquires approximately 3 TB of global satellite data daily and, using state-of-the-art processing software, produces approximately 100,000 imagery products per day in near real-time for distribution on its public and classified web pages. A new generation of geostationary satellite sensors will allow end users to see weather events on a spatial and temporal scale not previously available. NRL-MRY has added a ground station on site for collection of data from the new generation of GOES (U.S.) geostationary satellites, allowing real-time data processing of these sensor data and providing imagery for improved observational analysis and weather forecasts.

Chesapeake Bay Detachment (CBD)

NRL's Chesapeake Bay Detachment (CBD) occupies a 168-acre site near Chesapeake Beach, Maryland, and provides facilities and support services for research in radar, electronic warfare, optical devices, materials, communications, and fire research.

Because of its location high above the western shore of the Chesapeake Bay, unique experiments can be performed in conjunction with the Tilghman Island site, 16 km across the bay from CBD. Some of these experiments include low-clutter and generally low-background radar measurements. Using CBD's support vessels, experiments are performed that involve

dispensing chaff over water and characterizing aircraft and ship radar targets. Basic research is also conducted in radar antenna properties, testing of radar remote sensing concepts, use of radar to sense ocean waves, and laser

propagation. A ship motion simulator (SMS) that can handle up to 12,000 lb of electronic systems is used to test and evaluate radar, satellite



CBD's LCM-8 providing test support for electronic warfare research.

communications, and line-of-sight RF communications systems under dynamic conditions (various sea states).

CBD also hosts facilities of the Navy Technology Center for Safety and Survivability that are primarily dedicated to conducting experimental studies related to all aspects of shipboard safety, particularly related to flight decks, submarines, and interior ship conflagrations. Additional research areas include conventional and novel oil spill remediation technology and gas turbine combustor development. The Center has a variety of specialized facilities including two fully instrumented real-scale fire research chambers for testing small (28 m³) and large (300 m³) volume machinery spaces, a gas turbine engine enclosure and flammable liquid storeroom fire suppression systems; three test chambers (0.3, 5, and 324 m³) for conducting experiments up to 6 atmospheres of pressure; a 50 ft × 50 ft fire test chamber fitted with a large-scale calorimeter hood rated up to 3 MW; a 10,000 ft² mini-deck that affords capabilities for studying characteristics and suppression of flight deck fires and suppression techniques; and an LCAC gas turbine engine module. The 5 m³ chamber has instrumentation and equipment to study cell-to-cell failure propagation in lithium-ion batteries. These instruments include high-speed visible and infrared cameras, a Fourier transform infrared (FTIR) spectrometer for in situ, real-time chemical species identification, temperature, pressure, and heat flux measurements, and remote, real-time nondispersive infrared (NDIR) monitoring of selected chemical species. Two 125 CFM air compressors support gas turbine component and oil spill remediation research. An actively-cooled, instrumented 1 m² pan is used to examine crude oil in situ ignition and burn behavior. Scheduled additions to the facility include a large-scale spray combustion building for studying oil well blowout behavior; multi-compartment burn test structure to examine shipboard fire propagation and containment;

and an International Maritime Organization-approved machine space structure to examine fire behavior in ship engine compartments.

The Radar Range facility at CBD, together with the Maritime Navigation Radar (MNR) Test Range at Tilghman Island, provide the emitters and analysis tools for developing comprehensive maritime domain awareness capabilities. The MNR consists of dozens of radars that represent a precise cross section of today's actual MNR environment. An integrated suite of advanced sensors has been developed for data collection and processing to identify and classify vessels. A suite of similar sensors and processors has been integrated into a transportable shelter, the Modular Sensor System, that can be rapidly deployed to ports or other sites for enhanced maritime awareness reporting.

The Laser Communication Test Facility (LCTF) at CBD includes facilities at NRL-CBD, NRL-Tilghman Island and the ten mile test range over the Chesapeake Bay between the two locations. It is the premiere test facility for maritime testing and evaluation of internally and externally developed lasercomm systems. The LCTF operates 24/7 and includes atmospheric sensors at NRL-CBD and NRL-Tilghman Island and a probe laser propagating between the two sites to fully diagnose and understand lasercomm propagation in the maritime environment. These diagnostics operate simultaneously with lasercomm systems under test, enabling quantifiable evaluations of system performance. This enables identification of problem areas in systems and gives guidance to improve hardware and/or software to obtain optimal lasercomm system performance. The testing and optimization of systems at the LCTF has led to the successful demonstration of multiple lasercomm systems for land, sea, and air platforms - with development currently underway for a space based platform.

Scientific Development Squadron ONE (VXS-1)

Scientific Development Squadron ONE (VXS-1), located at Naval Air Station (NAS) Patuxent River, Maryland, is manned by 11 Naval officers, 54 enlisted sailors, and three Government civilians. VXS-1 provides airborne science and technology (S&T) research platforms to support Naval Research Laboratory (NRL) and Office of Naval Research (ONR) projects. VXS-1 is the sole airborne S&T squadron in the U.S. Navy, and conducts scientific research and advanced technological development for the Department of Defense, the Department of the Navy, Naval Air Systems Command (NAVAIR), and many other governmental and non-governmental agencies. VXS-1 operates and maintains three NP-3 and one RC-12 research aircraft. In addi-



NP-3C Orion.

tion, the squadron serves as the Aircraft Reporting Custodian (ARC) for nine ScanEagle Unmanned Aircraft Systems (UAS) and the U.S. Navy's only manned airship, the MZ-3A. VXS-1 routinely conducts a wide variety of S&T missions from remote detachment sites around the globe. In 2015, the squadron completed research detachments to U.S. Air Force Forward Operating Location, Curacao; Marine Corps Air Station Kaneohe Bay, Hawaii; Cooperative Security Location Comalapa, El Salvador; NAS North Island, California; NAS Point Mugu, California; and Barrow, Alaska. The squadron has provided flight support for numerous diverse research programs: ONR Code 31's ROUGH WIDOW system, focused on systems integration, sensor fusion, and performance testing of systems in operational maritime patrol environments; ONR's PMR-51 GAMERA sensor development and testing; NAVAIR Code 4.6's UAS Operator Spatial/Situational Awareness Project testing; NAVAIR's Project MORGAN testing; NAVAIR's Advanced Project Division's OCEAN HARVEST testing; NRL's Common Airborne Situational Awareness (CASA) system development and testing, vital to providing U.S. Navy Seventh Fleet with an electro-optic system to monitor intercepting aircraft maneuvers; and Multiple-Link Common Data Link System (MLCS) testing for NRL's Information Technology Division. The squadron's ongoing contributions to the Naval Research Enterprise now total over 73,000 flight hours spanning 54 years of Class "A" mishap-free operations.

Midway Research Center

The Midway Research Center (MRC) is a worldwide test range that provides accurate, known signals as standards for performance verification, validation, calibration, and anomaly resolution. In this role, the MRC ensures the availability of responsive and coordinated scheduling, transmission, measurement, and reporting of accurate and repeatable signals. The MRC, under the auspices of NRL's Naval Center for Space Technology, provides NRL with state-of-the-art facilities dedicated to Naval communications, navigation, and basic research. The headquarters and primary site is located on 162 acres in Stafford County, Virginia. The main site consists of three 18.2 m, radome-enclosed, precision tracking antennas and a variety of smaller

antennas. The MRC has the capability to transmit precision test signals with multiple modulation types. Its normal configuration is transmit but can be configured to receive as required. The MRC also provides cross-mission and cross-platform services from worldwide locations using a combination of fixed and transportable resources and a quick-reaction, unique signals capability. Assets include Pulsar Systems (several worldwide locations), a 45 m tracking antenna in Palo



Midway Research Center facility in Stafford, Virginia.

Alto, California, and a 25 m tracking antenna system on Guam. The MRC instrumentation suite includes nanosecond-level time reference to the U.S. Naval Observatory, precision frequency standards, accurate RF and microwave power measurement instrumentation, and precision tracking methodologies. The MRC also contains an Optical Test Facility with two specialized suites of equipment: a multipurpose Transportable Research Telescope (TRTEL) used for air-to-ground optical communications and for passive satellite tracking operations, and a satellite laser ranging system built around a 1 m telescope as a tool for improving customer ephemeris validation processes.

Pomonkey Facility

The Naval Research Laboratory's Pomonkey Facility is a field laboratory with a variety of ground-based antenna systems designed to support research and development of space-based platforms. Located 25 miles south of Washington, D.C., the facility sits on approxi-



The NRL Pomonkey Facility.

mately 140 acres of NRL-owned land, which protect its systems from encroaching ground-based interferers. Among its various precision tracking antennas, the facility hosts the largest high-speed tracking antenna in the United States. Boasting a diameter of 30 m, its range of trackable platforms includes those in low Earth orbit through those designed for deep space

missions. The facility's antenna systems are capable of supporting missions at radio frequencies from 50 MHz through 20 GHz and can be easily configured to meet a variety of mission requirements. The ease of system configuration is due to the facility's stock of multiple antenna feeds, amplifiers, and downconverters. Other facility assets include an in-house ability to design, fabricate, test, and implement a variety of radio frequency components and systems. The facility also hosts a suite of spectrum analysis instrumentation that, when coupled to its antenna systems, provides a unique platform for a variety of research and development missions.

Blossom Point Tracking Facility

The Blossom Point Tracking Facility (BPTF) provides engineering and operational support to several complex space systems for the Navy and other sponsors. BPTF is the nation's first satellite command and control facility, established in 1956. The station is situated on the Potomac River shore, approximately 40 miles south of Washington, D.C. A 600 meter buffer zone surrounds the facility's occupied 42 acres of land used by NRL through a land use agreement with the U.S. Army. The site consists of 10 antennas capable of providing simultaneous tracking and data acquisition, health and status monitoring, and command and control in UHF, L, S, C, X, USB, and SGLS bands. Blossom Point Tracking Facility is a highly automated facility able to support both operational and experimental spacecraft. The facility fully supports all spacecraft from concept definition and design to flight operations within the orbits of LEO, MEO, HEO, and GEO. In addition, BPTF is dedicated as a Mission Operations Center (MOC)/Satellite Operations Center (SOC) supporting interfaces to the Air Force Satellite Control Network (AFSCN). An experienced team of industry and government members provides the expertise to oversee space system operations for the life of the spacecraft. The shared and autonomous infrastructures reduce mission operational and management



Blossom Point Tracking Facility.

costs, providing value to a wide array of potential customers. As a key member of the NRL Space Systems Development Department, Blossom Point Tracking Facility provides prelaunch, launch, and post-launch support, flight operations, and mission data processing.

Marine Corrosion Facility

The Chemistry Division's Marine Corrosion Facility (MCF) located in Key West, Florida, is a tenant command to the Naval Air Station, Key West, on its Trumbo Point Annex. The site offers a "blue" ocean environment with natural seawater characterized by historically small compositional variation and a stable biomass. This continuous source of stable, natural seawater provides a site ideally suited for studies of marine environmental effects on materials, including accelerated and long-term exposure testing and materials evaluation.



NRL's Marine Corrosion Facility in Key West, FL.

The MCF began as a small field exposure site for NRL in the late 1960s, encompassing only a small office and outdoor laboratory on shared facilities. The MCF was staffed full time by NRL researchers starting in 1986 and has experienced significant growth since; today, the MCF includes several buildings on a 4-acre site. The major facilities include a Marine Coatings Application and Test Facility, a high temperature corrosion laboratory, a corrosion fatigue laboratory, a Full-Scale Shaft Bearing Test Facility, a Ballast Water Treatment System Evaluation Facility and associated marine biology laboratory, a 20,000 ft² atmospheric test site, once-through natural seawater exposure troughs, and the Navy's only Cathodic Protection Physical Scale Modeling (CP-PSM) Design Facility. The CP-PSM provides a highly accurate capability to physically model the electrochemical behavior of ship hulls and outboard structures to understand both the characteristics and adequacy of corrosion control systems and their relation to underwater electromagnetic fields. The CP-PSM has been the cornerstone to Navy impressed current cathodic protection systems, providing new construc-

tion design requirements for NAVSEA Program Executive Offices and Allied navies. The MCF's newest capability coming online in 2017 is the Center for Corrosion and Atmospheric Structural Testing (C-COAST). The C-COAST facility is a DoD unique test capability that enables atmospheric corrosion testing in a tropical marine environment with the ability to apply static and dynamic structural loads to the articles in test. The C-COAST will have the capacity to test at the coupon level, subsystems, and all the way up to full systems.

The MCF maintains extensive capabilities for RDT&E of marine engineering and coatings technologies and supports a wide array of Navy and industrial sponsors. Equipment is available for experiments involving accelerated corrosion and weathering, general corrosion, long-term immersion and alternate immersion, fouling, electrochemical phenomena, coatings application and characterization, ballast water treatment, marine biology, and corrosion monitoring. In 2009, the facility received a comprehensive refurbishment due to hurricane damage.

Joint Maritime Test Facility (JMTF)

The Joint Maritime Test Facility (JMTF) located at Little Sand Island, Mobile, Alabama, is under the auspices of NRL and the USCG Research Development Center (RDC). The JMTF oversees the operation of a large In Situ Burn tank, which includes a wave generator to test various technologies related to oil spill containment and remediation strategies. The JMTF also has five small boats: an LCM-8, LCM-3, a 35-ft personnel boat, and two 24-ft motor launches. The small boats are available to transport both personnel and equipment to Little Sand Island and to conduct sea trials for various marine radar, 3D sonar imaging, and communication technology RDT&E studies related to the marine environment.



The Joint Maritime Test Facility in Little Sand Island, Mobile, AL.

- 78** **Looking Inside a Big Onion**
Safely Measuring Tor
- 84** **Cold Atoms Hold the Key to Long-Lived Quantum Memory**
Quantum Memories Based on Optically Trapped Neutral Atoms
- 91** **A New Era for the Vacuum Tube**
Three-Dimensional Printing and Electroforming for Millimeter-Wave Vacuum Electronics
- 99** **A MIGHTI Flight for Ionospheric Insight**
From Sensor Idea to Satellite Instrument

Looking Inside a Big Onion

Onion routing refers to the practice of encasing data and its routing instructions in multiple layers of encryption, making it more difficult to trace a user's Internet activity. Researchers who might cut into that onion, so to speak, for data analysis could risk the confidentiality of sensitive data and endanger the privacy of millions of Web users. Building on recent advancements in privacy-preserving aggregation, the U.S. Naval Research Laboratory has developed a way to provide high-level measurement studies of Web-privacy onion-routing networks while also incorporating rigorous security and privacy safeguards.





Safely Measuring Tor

R. Jansen and A. Johnson
Information Technology Division

Tor software (The Tor Project, Inc., Seattle, Washington) is the most popular network in the world for Internet communications security. The usage and operation of Tor is not well understood, however, because its privacy goals make common measurement approaches ineffective or risky. Our research group in the Center for High Assurance Computer Systems, a branch of the Information Technology Division at the U.S. Naval Research Laboratory, has developed a system called PrivCount that aggregates measurements across Tor relays and over time to produce outputs with provable security guarantees. We used PrivCount to perform a measurement study of Tor of sufficient breadth and depth to inform accurate models of Tor users and traffic. Our results indicate that Tor has 710,000 users connected but only 550,000 active at a given time, that Web traffic now constitutes 91 percent of data bytes on Tor, and that the strictness of relays' connection policies significantly affects the type of application data they forward.

INTRODUCTION

About 15 years ago, the U.S. Naval Research Laboratory initiated the Onion Routing project—now commonly known as Tor—to develop software for preserving one's privacy while use the Web. (Privacy-promoting nonprofit The Tor Project [Seattle, Washington] took over stewardship of the work in 2006.) Today the Tor network¹ is among the most popular tools for online privacy. Many important communities, including intelligence and law enforcement, use its onion-routing protocol to keep their Web, media, and email activity private. The statistics illustrate Tor's widespread use and extensive impact. As of this writing in July 2017, the Tor network consists of around 7,000 volunteer-run relays that forward user traffic to its destination, the network collectively forwards nearly 100 Gbps of traffic, and an estimated 2 million users connect every day. Moreover, Tor's user population has doubled since 2014, and its traffic has quadrupled in that time.

Typical methods for network monitoring cannot be applied directly to Tor because of its strong privacy goals. For example, measuring the number of users is difficult because Tor is designed to keep users anonymous, and, in any case, to protect against legal or technical compromise of data, information about users' identities should not be collected. Tor itself currently gathers few measurements (not even on its number of users), mainly from heuristic techniques of unknown accuracy. Therefore, much information about Tor remains unknown, e.g., how many users actively use the network at a given time, how much data is Web traffic, and how many connections are made using Tor.

Our research group in the Center for High Assurance Computer Systems at the U.S. Naval Research Lab-

oratory (NRL) has developed PrivCount, an efficient and flexible system for privacy-preserving measurement on Tor.² PrivCount extends the PrivEx system of Elahi et al. (2014),³ designed specifically for private Tor measurement, by making it suitable for the kinds of exploratory measurements used during research. PrivCount can safely and accurately collect a wide range of useful statistics about Tor by incorporating both secure aggregation and differential privacy;⁴ the PrivCount technology ensures that only network-wide statistics are revealed and that such statistics do not reveal much about any individual activity. PrivCount also provides forward privacy, which guarantees that even the local state of a node on the Tor network contains no sensitive data. We developed an open-source tool implementing PrivCount that is robust, secure, and particularly convenient to use for research on Tor.

Due to privacy concerns, there have been few published studies measuring Tor network traffic characteristics. Although we also measured Tor, user privacy was a primary motivation of our work: PrivCount provides formal guarantees about security and privacy, and the only outputs from the measurement process were the aggregated counts that are safe to share publicly. Further, to the best of our knowledge, previous studies did not use a non-default exit policy, while we found that a non-trivial shift in traffic type occurs when switching from the default exit policy to one that allows common file-sharing ports (as described below in the Measurements section, under Exit Policy Analysis).

Our research deployment of PrivCount involved six independent contributors in four countries, of which all would need to be compromised in order to violate the security properties of the system. We performed aggregation of measurements across seven Tor relays,

which prevents identification of any of the relays as the source of a particular traffic characteristic.

We collected client and destination statistics with the goal of informing future models of Tor traffic and network improvement. Our results on exit traffic indicate that traffic to Web ports now constitutes 91 percent of data bytes on Tor, up from 42 percent in 2010. We also provide a first estimate of the number of Tor users outside of Tor's own measurement and using an entirely different method. Our data indicate that, in any given 10 minutes, an average of 710,000 users are connected to Tor, of which just over 550,000 (77 percent) are active. We also looked at the effect of exit policies, which relays use to limit which network addresses they will connect to, and found evidence that exit policies significantly affect the type of traffic exiting a relay. Results show that many of the Tor measurements of most interest can be taken privately and practically. Low-cost research efforts can productively use PrivCount, while the Tor Project itself could benefit from its security and privacy properties that exceed in many ways the security of Tor's own measurement methods.

TOR BACKGROUND

The Tor network consists of a set of relays run by volunteers. Tor clients use these relays to anonymize their Internet traffic by executing the onion-routing protocol. In onion routing, a client sends traffic over a Tor circuit (Fig. 1), which typically consists of three nodes. To construct a circuit, the client repeatedly adds another node to the end of a partial circuit (initially consisting of the client only) by sending encrypted

commands through the partial circuit. Messages from the client are encrypted once for each node on the circuit; each node decrypts and forwards the messages. Messages to the client from the destination are encrypted and forwarded by each node and then iteratively decrypted by the client. This onion encryption prevents each relay from learning more than the node behind it or ahead of it, as it were, on the circuit, and in particular, averts the identification by any relay or local network observer of both the source and destination.

The final node in a circuit sends messages unencrypted to the destination (application-layer encryption may be present, however). Tor circuits can carry multiple streams, each of which corresponds to a Transmission Control Protocol connection (commonly called a TCP connection) between the final node and the destination. The last node on the circuit is known as the exit, which must be chosen from among those relays configured with an exit policy that allows connecting to the Internet address of the desired destination. The first node in a circuit is a guard, and each client chooses a small set of relays (one by default) that can appear in this position. Without guards, every client would eventually choose a malicious relay for the sensitive position next to a client.

PRIVCOUNT DESIGN

Private Counting. To safely gather statistics from the Tor network, we designed and implemented a privacy-preserving data collection and aggregation system called PrivCount that expands upon the secret-sharing variant of PrivEx,³ i.e., PrivEx-S2. PrivCount is a dis-

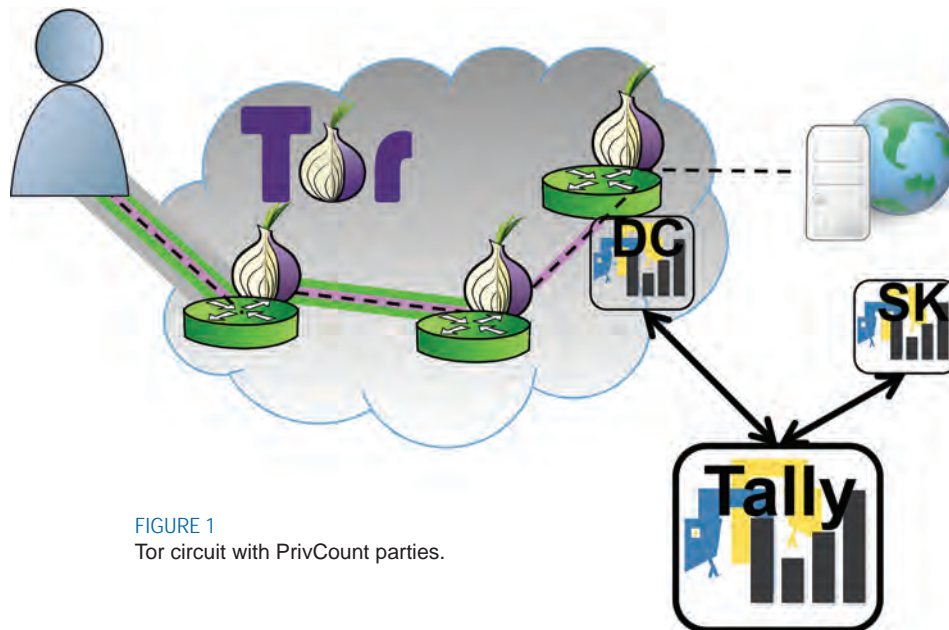


FIGURE 1
Tor circuit with PrivCount parties.

tributed counting system that relies on multiple nodes and entities to ensure privacy and security. It counts a series of events over time and computes various statistics from those events. For example, PrivCount can count the data transferred over the measuring relays or the users connecting to the measuring relays. PrivCount incorporates elements of secure multi-party computation and differential privacy to secure the measurement process and guarantee privacy of the final aggregated output.

Roles and Architecture. A PrivCount deployment contains a tally server (TS), one or more data collector (DC) nodes, and one or more share keeper (SK) nodes. Our implementation of these entities consists of a patch to the Tor C source and a Python program for each new entity (see Fig. 1).

Tally Server. The PrivCount TS is the central point of the system. The TS authenticates and tracks the DC and SK nodes before admitting them, tracks their availability and status, and synchronizes systems operations. To minimize the attack surface of a PrivCount deployment, the TS acts as a central proxy for all communication between the other nodes. The TS server port is the only port required to be open and Internet-accessible in the entire PrivCount system; the DCs and SKs only make outgoing connections to the TS. However, despite its central position, the TS is still untrusted, and all communication between DCs and SKs is encrypted and authenticated.

Data Collectors. PrivCount DC nodes are the main nodes for processing measurements. Each DC is co-resident with a Tor process in the same server and responsible for maintaining statistics from events in that Tor process. The DC maintains a set of counters for each statistic. Each counter is initialized with the sum of normally-distributed random noise and uniformly-random shared values. The noise serves to provide differential privacy of the final, aggregated value. The shared values serve to blind the counter; one such number is chosen for each SK, and then each is sent to the corresponding SKs before being securely erased at the DC. This process ensures forward privacy: any compromise of a DC will not leak past local counter values (the counters will appear random). The DCs increment the counters during the collection period and then send the final values to the TS during aggregation.

Share Keepers. PrivCount SK nodes are responsible for storing the shared values assigned to it by the DC nodes; for each counter, each SK will have received one shared value from each DC. During aggregation, each SK for each counter sums the shared values they received from the DCs and sends the sum to the TS. Once the TS receives all counts from the DCs and all summed shared values from the SKs, the TS sums the counts from all DCs for each counter and then “de-blinds” each counter by subtracting the summed shared

values. As long as at least one SK acts honestly in summing the secret numbers, the TS cannot learn individual DC counts, and nothing is revealed but the final aggregated count, which is protected under differential privacy.

Details about the PrivCount protocol and proofs of its security are available in our full technical paper.² Our implementation of PrivCount is available in its open-source code repository.⁵

MEASUREMENTS

Because the privacy of Tor users was a primary concern, we practiced data minimization during the measurement process: we focused our collection of statistics on only those that aid Tor traffic modeling efforts. We considered measurements from both entry and exit relay positions, because both positions provide useful information for modeling purposes.

Deployment. We deployed PrivCount on the live Tor network with seven relays (three guards and four exits), seven DC nodes, six SK nodes, and a tally server; the nodes were run by six operators in four countries. We executed several collection periods, focusing on different sets of statistics across them, from April through August 2016.

Exit Policy Analysis. We conducted an analysis of the exit policies used by Tor exit relays. Measurements included the number of circuits, streams, and bytes observed at our relays. (Figure 2 shows some results.) The x-axis shows the following exit policies:

- Default: the default exit policy, which blocks common file-sharing ports;
- Open: a policy that allows all ports; and
- Strict: a stricter-than-default policy that blocks Web ports (80 and 443).

The legend shows different categories of traffic:

- Web: traffic with ports 80 and 443;
- Interactive: SSH port 22 and those used for Internet Relay Chat; and
- Other: the remaining ports.

When moving from Default to Open (meaning file sharing ports are allowed), the number of Other circuits and streams increased as more file-sharing traffic was observed on our nodes, but the number of Web circuits and streams did not change by much. However, Other bytes took up a much larger proportion of the traffic than Web bytes, indicating that file-sharing traffic may be drowning out browser traffic. We also found that Interactive traffic is a very small part of the overall traffic observed at our relays.

Inferring Network Totals. We extrapolated our measurements to infer total network-wide statistics by taking into account the fraction of the network comprised by our relays. We compared our network estimates to those taken in 2008 by McCoy et al. (2008)⁶ and in

2010 by Chaabane et al. (2010),⁷ which were limited studies undertaken without the privacy protections of PrivCount. Figure 3 shows results from the two studies.

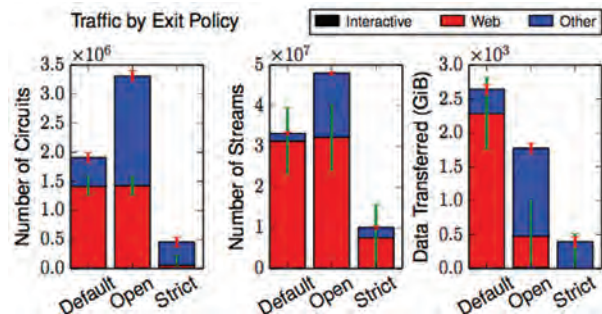


FIGURE 2 PrivCount measurements by exit policy and traffic type.

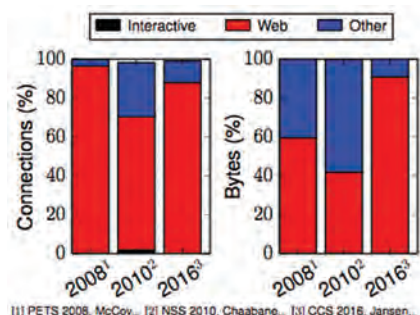


FIGURE 3 Tor traffic type distribution by year.

We observed an increase in the percentage of Web connections since 2010 and a large increase in the amount of Web traffic since both 2008 and 2010. The increases may be due to less file-sharing traffic on Tor, or to more file-sharing traffic on the ports typically used for Web traffic.

User Statistics. Finally, we measured the average number of unique users connecting to our relays over 10-minute periods and the number of those users who were active (i.e., those who sent data on their circuits). We again used our measurements to infer the total number of active users across the entire Tor network during an average 10 minutes. Figure 4 shows results from this part of our study.

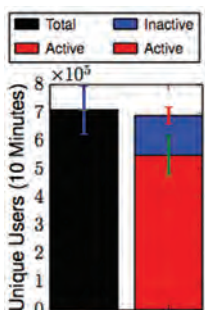


FIGURE 4 Estimated number of concurrent Tor users.

Based on our observations, we estimate that Tor had about 710,000 unique users connecting to the network in an average 10 minutes during our measurement, and, of those, about 550,000 (77 percent) were active. We compared our results to Tor’s user estimates. Based on Tor Browser update ping data (update pings happen twice per day), we can roughly estimate between 800,000 and 1.6 million concurrent Tor users during the same period we took our PrivCount measurements. The lower end of this estimated range is within our own 95-percent confidence interval (itself a result of both sampling error and the added noise). Also, based on downloads of Tor consensus documents, Tor estimates about 1.75 million daily users during our measurement period. These estimates of concurrent and daily users suggest that Tor users turn over about 2.5 times per day.

SUMMARY AND CONCLUSION

In this research, we demonstrated a robust and convenient system for better understanding Tor network activities. Building on recent advancements in privacy-preserving aggregation, we developed a Tor measurement system that incorporates rigorous security and privacy properties. Our high-level measurement study, using PrivCount, has given us a set of data well-suited to advance Tor research, especially in the area of traffic modeling and simulation.

ACKNOWLEDGMENTS

This work has been partially supported by the Defense Advanced Research Projects Agency (DARPA); the National Science Foundation (NSF) under grant number CNS-1527401; and the Department of Homeland Security (DHS) Science and Technology Directorate, Homeland Security Advanced Research Projects Agency, Cyber Security Division, under agreement number FTCY1500057. The views expressed in this work are strictly those of the authors, and do not necessarily reflect the official policy or position of DARPA, NSF, DHS, or NRL.

[Sponsored by DARPA and Department of Homeland Security]

References

- R. Dingleline, N. Mathewson, and P. Syverson, “Tor: The Second-Generation Onion Router,” *Proceedings of the 13th Conference on USENIX Security Symposium*, Aug. 9–13, 2004. USENIX Association, Berkeley, Calif., 21 (2004).
- R. Jansen and A. Johnson, “Safely Measuring Tor,” *Proceedings of the 2016 ACM SIGSAC Conference on Computer and Communications Security*, Oct. 24–28, 2016, Vienna, Austria. Association for Computing Machinery, New York, 1553–1567 (2016).
- T. Elahi, G. Danezis, and I. Goldberg, “PrivEx: Private Collection of Traffic Statistics for Anonymous Communication Networks,” *Proceedings of the 2014 ACM SIGSAC Conference*

on *Computer and Communications Security*, Nov. 3–7, 2014, Scottsdale, Ariz. Association for Computing Machinery, New York, 1068–1079 (2014).

⁴ C. Dwork and A. Roth, “The Algorithmic Foundations of Differential Privacy,” *Foundations and Trends in Theoretical Computer Science* 9(3–4), 211–407 (2014).

⁵ “privcount/privcount: Privacy-preserving Tor statistics aggregation tool that implements the secret-sharing variant of the PrivEx algorithm” <<https://github.com/privcount/privcount>>.

⁶ D. McCoy, K. Bauer, D. Grunwald, T. Kohno, and D. Sicker, “Shining Light in Dark Places: Understanding the Tor Network,” *Proceedings of the Eighth International Symposium on Privacy Enhancing Technologies*, N. Borisov and I. Goldberg, eds., July 23–25, 2008, Leuven, Belgium. Springer-Verlag Berlin Heidelberg, 63–76 (2008).

⁷ A. Chaabane, P. Manils, and M.A. Kaafar, “Digging into Anonymous Traffic: A Deep Analysis of the Tor Anonymizing Network,” *Proceedings of the 2010 Fourth International Conference on Network and System Security*, Y. Xiang, P. Samarati, J. Hu, W. Zhou, and A-R. Sadeghi, eds., Sept. 1–3, 2010, Melbourne, Australia. The Institute of Electrical and Electronics Engineers, 167–174 (2010).



THE AUTHORS



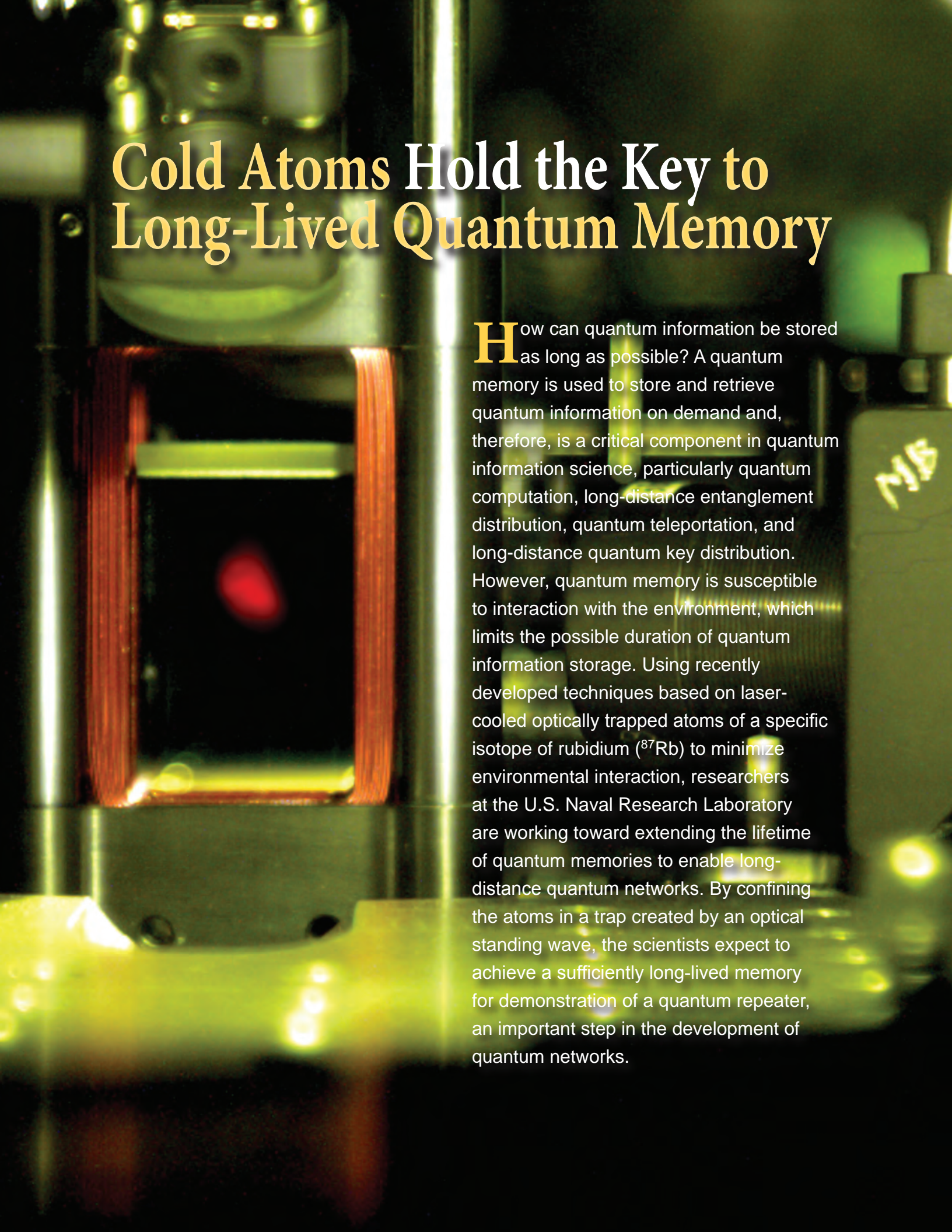
ROB JANSEN is a computer scientist in the Center for High Assurance Computer Systems at NRL. His research interests include security and privacy of distributed systems; anonymous communication; and parallel and distributed simulation. He focuses on designing and building practical and useful systems and software, and, therefore, exploring tradeoffs between performance and security is often central to his work. Jansen developed a tool called Shadow that is used by research institutions around the world to simulate and analyze the popular Tor Anonymity and Bitcoin Cryptocurrency Networks. Shadow has revolutionized the research and development of these systems by making it possible not only to easily explore performance enhancements and speed improvements but also to understand how adversarial threats affect these systems; all of this work can be done safely inside the Shadow application running on a standard computer.

On the basis of Jansen’s research, Shadow already is in use to find and fix security vulnerabilities in Tor, and has aided in making Tor faster for its users, who include journalists, human rights activists, diplomats, and millions of other people. Jansen received a Ph.D. from the computer science department at the University of Minnesota.



AARON JOHNSON is a computer scientist in the Center for High Assurance Computer Systems at NRL. His research interests include private communication and privacy-preserving data analysis. He has performed foundational mathematical research in the area of anonymous communication by modeling and analyzing the security of onion routing. He has also applied mathematically rigorous privacy-preserving methods to publishing sensitive genetic and network data. Much of his work has been focused on the Tor network, an onion-routing network used by over 2 million users daily to secure their communications. He designed several improvements to Tor, including denial-of-service defenses, faster onion services, privacy-preserving network monitoring, and refinements to Tor’s path selection. Many of these results have been incorporated into the Tor network, and provide enhanced security, performance, and utility to its many

users. Johnson received a Ph.D. from the computer science department at Yale University and completed postdoctoral training at the University of Texas at Austin.



Cold Atoms Hold the Key to Long-Lived Quantum Memory

How can quantum information be stored as long as possible? A quantum memory is used to store and retrieve quantum information on demand and, therefore, is a critical component in quantum information science, particularly quantum computation, long-distance entanglement distribution, quantum teleportation, and long-distance quantum key distribution. However, quantum memory is susceptible to interaction with the environment, which limits the possible duration of quantum information storage. Using recently developed techniques based on laser-cooled optically trapped atoms of a specific isotope of rubidium (^{87}Rb) to minimize environmental interaction, researchers at the U.S. Naval Research Laboratory are working toward extending the lifetime of quantum memories to enable long-distance quantum networks. By confining the atoms in a trap created by an optical standing wave, the scientists expect to achieve a sufficiently long-lived memory for demonstration of a quantum repeater, an important step in the development of quantum networks.

Quantum Memories Based on Optically Trapped Neutral Atoms

M. Bashkansky,¹ A. Black,¹ T. Akin,² M. Piotrowicz,³ A. Kuzmich,⁴ and J. Reintjes³

¹*Optical Sciences Division*

²*National Research Council Postdoctoral Research Associate*

³*Sotera Defense Solutions, Inc.*

⁴*Department of Physics, University of Michigan*

A quantum memory uses matter to store and retrieve quantum information, typically via an interface with an optical channel that transmits single photons. Quantum memories are key components of secure quantum communication and quantum information processing schemes. Our research group in the Optical Sciences Division of the U.S. Naval Research Laboratory is interested in the development of a quantum memory in ensembles of laser-cooled rubidium atoms. We have made progress toward the creation of a quantum repeater based on four such memories. To demonstrate the storage of quantum information, we have operated a single quantum memory as a source of heralded single photons via collectively enhanced spontaneous Raman emission. We have demonstrated optical lattice trapping of 10^6 atoms that can dramatically increase the possible storage time. Non-classical operation of the heralded photon source is indicated by a measured value of the normalized cross-correlation coefficient, $g^{(2)}$, of 150. The memory operates at the $1/e$ coherence time of 3 ms.

BACKGROUND

The beginning of research into quantum information science can be traced to Richard Feynman's 1982 proposal¹ that computers that take advantage of quantum mechanical principles may have certain advantages over classical computers. Since then, researchers have proposed or demonstrated various methods of using quantum information to achieve results that cannot be obtained with classical physics. One of the most striking proposals is the quantum computer itself. Using Peter Shor's algorithm² to find prime factors of large numbers, quantum computers can, in principle, defeat current cryptography techniques. Although practical quantum computers do not exist as of this writing, work is under way in many countries to create such a computer. Furthermore, current classically encrypted information can be stored for now and kept until decryption by quantum computers someday becomes possible.

Threats to conventional cryptography have fueled research into fundamentally unbreakable cryptographic techniques. Here, quantum information science again comes to the rescue with a technique called quantum key distribution, or QKD. Using QKD, the communicating parties use unique aspects of quantum mechanics (QM) to construct a cryptographic key for encrypting communication. QM allows the parties to ensure the secrecy of their information by detecting with absolute certainty if someone is trying to eavesdrop on

their key construction. It is now possible to buy commercial QKD systems, but these systems are limited to an effective distance of about 100 kilometers because of photon loss in their optical fibers. Optical losses in a fiber occur in classical communication as well, but here the problem is solved by using larger numbers of photons and classical repeaters that amplify and clean up the signal before it becomes too weak. This solution is not viable in QKD because QKD relies on single photons and QM does not allow noiseless amplification or cloning of photons. That principle underscores the fundamental security of QKD, i.e., QKD is secure because QM prohibits the photon cloning that otherwise would allow an intruder to steal information without detection.

Researchers have proposed "quantum repeater" protocols that allow joining of multiple shorter QM entangled segments into a longer one by performing certain measurement on portions of the segments. Quantum repeaters extend techniques such as QKD and quantum teleportation to longer distances. Quantum memories are a critical component of such quantum repeater-based protocols.

Quantum memory research has been an active field in recent years.³ Quantum memories have been demonstrated in single trapped atoms and ions, warm and cold atomic ensembles, quantum dots, rare-earth ions in solids, and nitrogen vacancy centers in diamond. The different approaches have distinct advantages and disadvantages, with respective tradeoffs between memory

storage time, photon emission rates, photon frequency width, and environmental sensitivity. Our research in the Optical Sciences Division of the U.S. Naval Research Laboratory focused first on warm, and later on cold, trapped atomic ensembles.

COLD ATOM QUANTUM MEMORY

Figure 1 illustrates our quantum memory implementation in rubidium (Rb) atoms. The quantum memory relies on a “ Λ ” (Lambda) level configuration in the Rb atom, with two long-lived ground states “g1” and “g2” and an excited state “e”. Initially, the entire ensemble of 10^7 atoms is prepared in the “g1” ground state. A near-resonant, classical laser beam generates a spontaneous Stokes photon via a Raman process, creating a single excitation in the atomic ensemble, as shown in Fig. 1(a). Classically, one would say that one of the atoms has made a transition to the other “g2” ground state. However, quantum mechanics tells us that this single excitation is distributed over all the atoms in the ensemble, and, therefore, is relatively insensitive to some atomic losses. Furthermore, ground states are long-lived, and we can prepare atoms in atomic states with minimal sensitivity to the environment, such as those used in atomic clocks.

Detection of the Stokes photon signifies creation of the unit excitation in the form of atomic coherence between the two ground states (Fig. 1(a)). The quantum information is now stored in the form of this long-lived coherence. One can also say that the Stokes photon is entangled with the quantum state stored in the memory. To access the quantum information, we read it out from the atomic ensemble memory as an anti-Stokes photon using a classical read laser beam, as depicted in Fig. 1(b). Now, the initial Stokes photon and the anti-Stokes photons are entangled.

The non-classical nature of this entanglement is measured by the second-order normalized cross-correlation function $g^{(2)}$ between the Stokes and anti-Stokes photons. $g^{(2)}$ is simply the ratio of the measured rate

of photon coincidences (between Stokes and anti-Stokes photons) to the rate of coincidences that would be expected with uncorrelated photon production. Under stable experimental conditions, a value of $g^{(2)} > 2$ indicates that the photon production, and hence the excitation stored in memory is not described by classical statistics.

The storage time of the quantum memory depends on environmental factors such as magnetic and electric fields, and on collisions as well as coherence-destroying atomic motion. In our previous work using a warm atomic vapor as a quantum memory,⁴ we were limited to 4 μ s quantum memory time due to atomic motion, even with the shielding of the external fields. This atomic motion is greatly reduced in laser-cooled, trapped atomic ensembles such as those produced in a magneto optic trap (MOT), where temperatures of 20 μ K are readily achieved. Figure 2 shows an image of fluorescence from such a cloud of cold, trapped atoms in our laboratory.

In principle, since the MOT trapping beams and fields have to be turned off during the quantum memory operation, the memory storage time can be limited by the gravitational falling of the atoms to a few milliseconds. In practice, a small angle between the Write/Read beams and the detected Stokes/anti-Stokes photons is used to reduce optical backgrounds. This angle increases susceptibility to motional dephasing. Together with the Larmor precession in the residual magnetic field, this limits the storage time in the MOT to a few microseconds.

In our MOT-based quantum memory setup, we measured $g^{(2)}$ at $t = 0$ to be 40.1 ± 3.2 . The 1/e decay time of the coherence was measured to be $\sim 30 \mu$ s, and the memory storage time (the time it takes the value of $g^{(2)}$ to drop to 2) to be $\sim 90 \mu$ s.

OPTICAL LATTICE

Additional techniques have been developed to reduce the effect of the magnetic field by using opti-

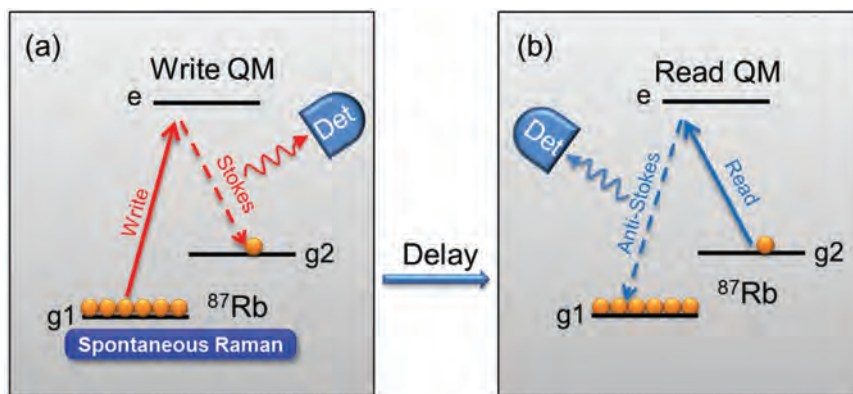


FIGURE 1 Writing and reading quantum memory based on ^{87}Rb atoms.

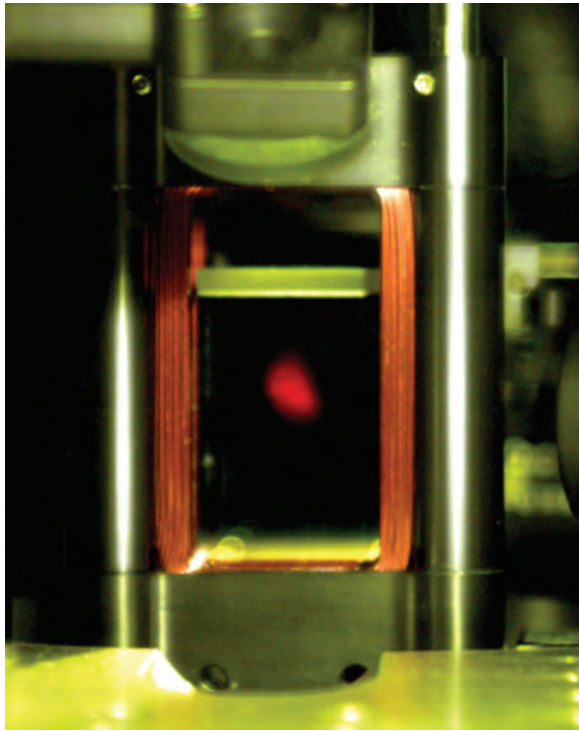


FIGURE 2
Fluorescence image of a cloud of ^{87}Rb atoms confined in a magneto optical trap.

cal pumping and first-order magnetic field insensitive atomic states (clock states). Other techniques permit completely overcoming motional decoherence in cold atoms; in one technique, far red-detuned interfering optical beams can trap atoms in sub-micron regions of high intensity by forming what is known as an optical lattice.

Figure 3 shows a schematic of the optical lattice setup and the fluorescent image of the optical lattice. Because of the in-plane geometry of the incident and emitted optical fields, we only need the optical lattice to confine the atoms tightly in one dimension to arrest atomic motion. Motion along the beam direction or in the vertical plane does not affect the memory time. The lifetime of atoms in our optical lattice is limited by collisions with the background gas in the imperfect vacuum, and is about 20 s. This lifetime can be increased with a better vacuum. The memory time is determined now only by the coherence between the two ground states, which depends on external fields and also on the inhomogeneous dephasing of the atomic spins due to energy shifts caused by the intense lattice laser beams (so-called AC Stark shifts). With magnetic field compensation, our memory time increased to over 600 μs . Using optical pumping to magnetic field insensitive atomic sublevels, the $1/e$ memory time in our setup was increased to about 3 ms. It is possible to use uniform magnetic fields and circularly polarized lattice beams to compensate for the differential AC Stark shift. Us-

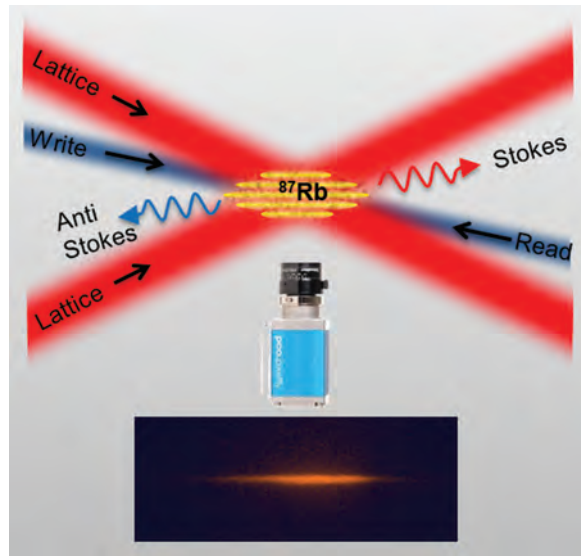


FIGURE 3
Setup for ^{87}Rb quantum memory in an optical lattice and a fluorescence image of a cloud of ^{87}Rb atoms confined in an optical lattice.

ing this approach, memory time was demonstrated to increase to hundreds of ms.⁵ More sophisticated techniques⁶ are available to increase the cold atom memory time to over 10 s.

QUANTUM REPEATER

The overarching goal of the present work is to implement four quantum memories to create a quantum repeater. To securely transmit an encryption key, two remote quantum memories QM1 and QM2 must be entangled. This entanglement is produced non-deterministically, by detecting a single Stokes photon from two quantum memories simultaneously, as shown in Fig. 4(a). When such a photon is detected, a single quantum excitation is shared between the two remote quantum memories, and the two quantum memories can be used as an entanglement resource. To create a quantum repeater, we need one quantum excitation shared between quantum memories QM1 and QM2 and a second quantum excitation shared between QM3 and QM4, as shown in Fig. 4(b). We then read out any stored excitations in QM2 and QM3 at the same time. When a single anti-Stokes photon is detected from QM2 and QM3, the quantum excitation in QM2 and QM3 is destroyed, while the remaining single quantum excitation is shared over a longer distance between QM1 and QM4. This “entanglement swapping” process can, in principle, be extended over many quantum repeater nodes to produce entanglement over very long distances. These measurements are probabilistic: sometimes they fail, and sometimes they succeed. When an internal measurement succeeds, the result has to be stored in quantum memory, while the failed ones are

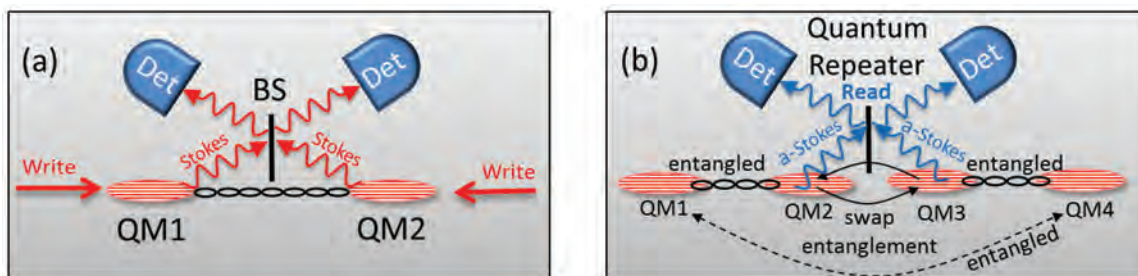


FIGURE 4

(a) Entangling two quantum memories by detecting a single Stokes photon generated from both memories. (b) Quantum repeater is implemented by reading out a single anti-Stokes photon from the adjacent memories.

repeated and all links are successfully created from one end of the communication channel to the other.

CONCLUSION

This article discusses the application of cold trapped atoms to quantum memories and illustrated techniques that can be used to improve memory storage time. Improvements in single-photon detectors and various optical components are still needed to achieve long distance quantum networks. We are developing newer techniques to improve scalability, such as internal conversion to telecommunication wavelengths and combining cold atom memories with Rydberg atom interactions. We are also developing passive stabilization schemes to reduce requirements on interferometric stability, which is normally required for the quantum repeater operation.

ACKNOWLEDGMENTS

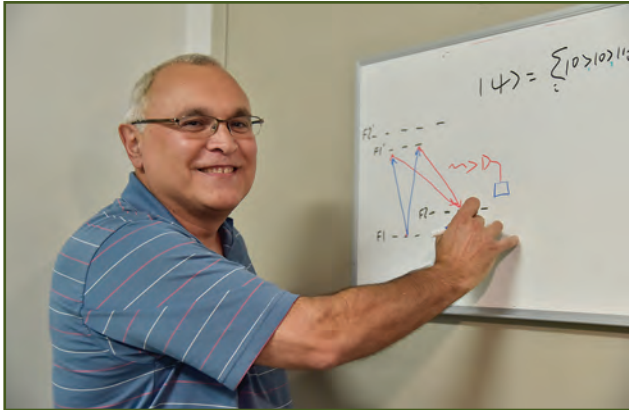
This work is supported by the Office of the Assistant Secretary of Defense for Research and Engineering.
[Sponsored by OASD/R&E]

References

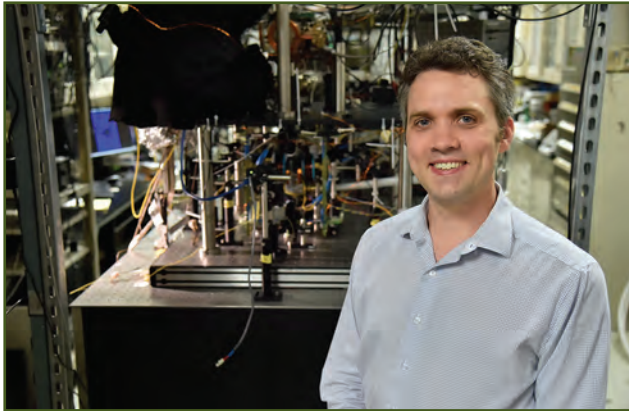
- ¹ R. Feynman, "Simulating Physics with Computers," *Int. J. Theo. Phys.* **21**(6/7), 467–488 (1982).
- ² P.W. Shor, "Algorithms for Quantum Computation: Discrete Logarithms and Factoring," *Proceedings of the 35th Annual Symposium on Foundations of Computer Science*, IEEE Computer Society Press, 124–134 (1994).
- ³ C. Simon, M. Afzelius, J. Appel, Al Boyer de la Giroday, S.J. Dewhurst, N. Gisin, C.Y. Hu, F. Jelezko, S. Kroll, J.H. Müller, J. Nunn, E.S. Polzik, J.G. Rarity, H. De Riedmatten, W. Rosenfield, A.J. Shields, N. Sköld, R.M. Stevenson, R. Thew, I.A. Walmsley, M.C. Weber, H. Weinfurter, J. Wrachtrup, and R.J. Young, "Quantum Memories," *Eur. Phys. J. D* **58**, 1–22 (2010).
- ⁴ M. Bashkansky, F.K. Fatemi, and I. Vurgaftman, "Quantum Memory in Warm Rubidium Vapor with Buffer Gas," *Opt. Lett.* **37**(2), 142 (2012).
- ⁵ Y.O. Dudin, T.A.B. Kennedy, and A. Kuzmich, "Light Storage in a Magnetically Dressed Optical Lattice," *Phys. Rev. A* **81**, 041805(R) (2010).
- ⁶ Y.O. Dudin, L. Li, and A. Kuzmich, "Light Storage on the Time Scale of a Minute," *Phys. Rev. A* **87**, 031801(R) (2013).



THE AUTHORS

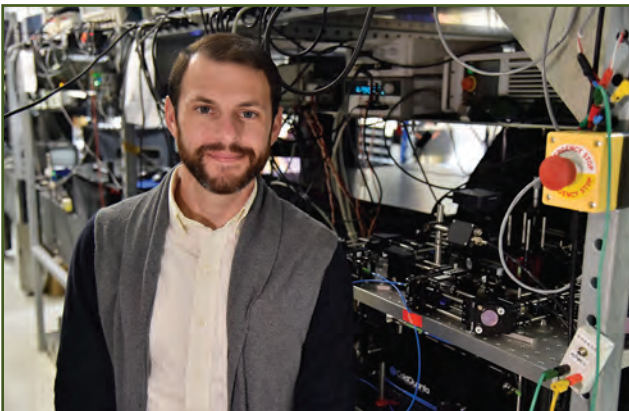


MARK BASHKANSKY received a Ph.D. in physics in 1988 from the Columbia University Graduate School of Arts and Sciences. He has been employed as a research physicist at NRL since 1988. He specializes in basic and applied research in theory and experiment in nonlinear optics, quantum optics, and atomic physics. He has an extensive publishing record in archival journals. He is also the author of eight patents, an NRL Review article, and three book chapters (one each in *OSA Handbook of Optics Volume IV: Optical Properties of Materials, Nonlinear Optics, Quantum Optics, Encyclopedia of Modern Optics*; and *Slow Light: Science and Applications*). He is a member of the Optical Society of America and the American Physical Society. He is the recipient of two Alan Berman Research Publication Awards. He participated in three programs of research funded by the Defense Advanced Research Projects Agency (on Synthetic Aperture Ladar for Tactical Imaging [SALTI], Precision Inertial Navigation Systems [PINS], and Slow Light).

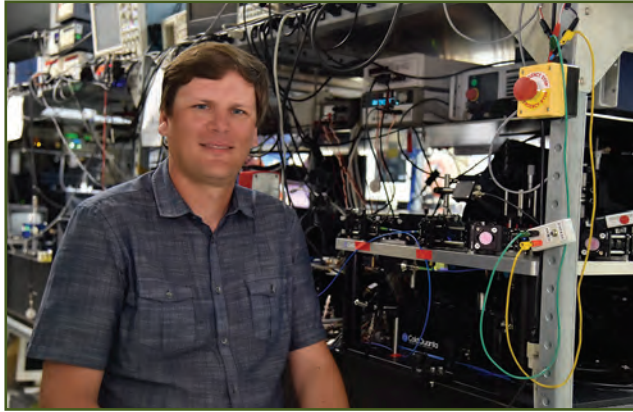


ADAM BLACK joined NRL in 2016 to study the applications of laser-cooled atomic ensembles in quantum information and sensing. He is currently investigating chip-based interfaces between cold atoms and nanophotonic optical waveguides as a way to achieve strong coupling between matter and photonic channels. He is also developing novel sources of cold atoms to improve stability in quantum sensors. From 2007 to 2016, as director of Space Systems at AOSense, Inc., in Sunnyvale, California, he developed atom interferometric inertial sensors. At AOSense, he designed a gravity gradiometer for geodesy, demonstrated the first cold atom interferometer to eliminate dead time from its measurement cycle, and co-authored five patents (granted and pending). As National Research Council postdoctoral fellow at the National Institute of Standards and Technology (2005–07), he led research on spinor dynamics and

photoassociation spectroscopy in an optically trapped antiferromagnetic Bose Einstein condensate. He holds a B.A. in physics from Harvard University and a Ph.D. in physics from Stanford University; at Stanford, he studied the collective interactions of cold atoms with resonator-enhanced optical modes.



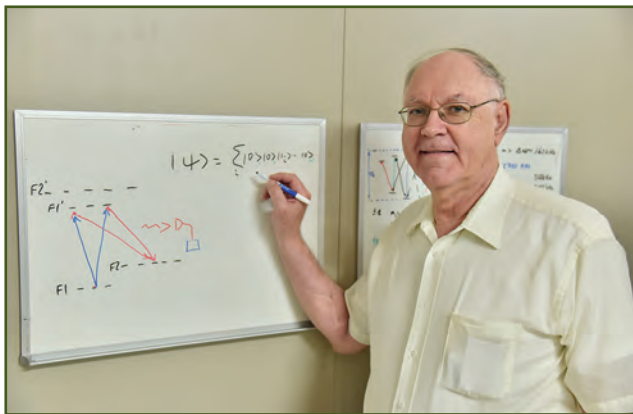
THOMAS AKIN is a National Research Council postdoctoral research associate in the Optical Sciences Division at NRL, where he works with Mark Bashkansky in the Quantum Electro-Optics Section (Code 5613). He received a B.S. in physics from the University of Arkansas, where he used dynamic light scattering techniques to study the properties of protein deflagration. He received an M.S. and a Ph.D., both in physics, from the University of Oklahoma, where he studied electromagnetically induced transparency in an ultracold rubidium gas using laser fields with orbital angular momentum. At NRL, he is working toward the demonstration of a full quantum repeater with nodes comprised of four optically trapped ultracold rubidium ensembles.



MICHAL PIOTROWICZ is an atomic physicist contractor in the Optical Sciences Division at NRL. He received a master's degree from Gdansk University of Technology in Poland in 2004 and a Ph.D. from The Open University (Milton Keynes, England) in 2010. Before he joined the NRL team in 2016, his work involved electromagnetically induced transparency with Rydberg atoms and quantum gates-based on neutral atoms. He is currently working on quantum memories and quantum repeaters with single photons in atomic ensembles.



ALEX KUZMICH is the Martin L. Perl Professor of Physics at the University of Michigan. His research has been in quantum optics and atomic physics. Among his notable achievements are the first experimental demonstration of the quantum state transfer between matter and light, the first experiments on quantum light generation using strongly interacting Rydberg atomic states, and the first demonstration of cooling and trapping of a multiply-charged ion (triple-charged thorium). He received a Ph.D. from the University of Rochester in 2000 under the guidance of Leonard Mandel.



JOHN F. REINTJES received a B.S. in physics from the Massachusetts Institute of Technology in 1966 and a Ph.D. in applied physics from Harvard University in 1972. He held a postdoctoral appointment at the IBM Thomas J. Watson Research Center and then joined the research staff at NRL in 1973. At NRL, he served as section head in the Optical Physics Branch of the Optical Sciences Division from 1982 to 1995. He held the position of Senior Scientist for Quantum Electronics from 1995 until he retired in 2007 from federal service. He joined Sotera Defense Solutions, Inc., in 2007 as a senior research scientist and also began serving as a support contractor at NRL, a role he maintains as of this writing. He has published many articles in archival journals, handbooks, and encyclopedias, including *OSA Handbook of Optics*; *CRC Handbook of Laser Science and Technology, Supplement 2*; and *McGraw-Hill Encyclopedia of Science and Technology*.

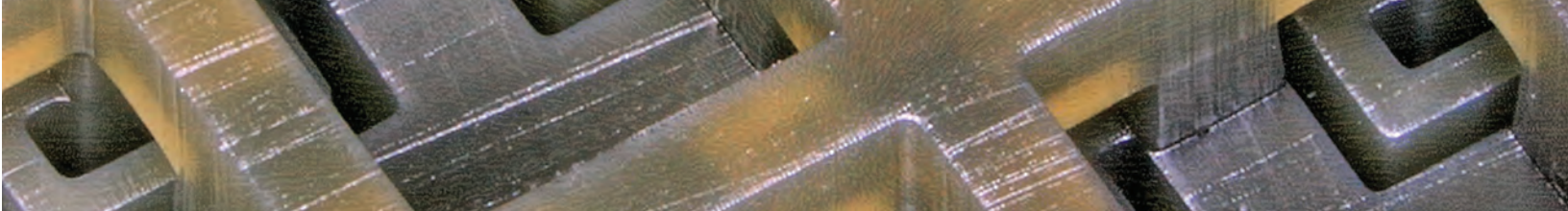
He is the author of the book *Nonlinear Optical Parametric Processes in Liquids and Gases* (Academic Press, 1984). He is a fellow of the Optical Society of America and the Washington Academy of Science, and a member of the American Physical Society and of Sigma Xi. He is the recipient of eight Alan Berman Research Publication Awards at NRL, the NRL-Sigma Xi Award in Pure Science in 1984, the Navy Meritorious Civilian Service Medal in 1985, a Technology Transfer Award from the Federal Laboratory Consortium for his work in optical particle analysis in 2001, and a Presidential Rank Award for Meritorious Senior Scientist in 2003.

A New Era for the Vacuum Tube

Peek inside an antique radio and you'll find what look like small light bulbs. They're vacuum tubes—the predecessors of the silicon transistor. Vacuum tubes in most consumer electronics went the way of the dinosaurs in the 1960s, but they have remained vital for certain applications via a specialized version known as a traveling-wave tube that's more powerful, more efficient, and hardier than the transistor. The ability of the traveling-wave tube to boost electromagnetic wave signals with high power and bandwidth makes it indispensable for modern commercial and military applications, such as wireless communications and radar. This is especially true at the high-frequency millimeter-wave end of the spectrum, well beyond the operating frequencies of conventional radiofrequency systems.

The traveling-wave tube's potential for very high frequencies is great, but making the device isn't all that easy. The device requires extremely small internal circuits that can operate at millimeter-wave frequencies. The U.S. Naval Research Laboratory is developing innovative ways to fabricate the tiny circuits with three-dimensional additive printing and electroforming technologies.

So the vacuum tube may be poised for a comeback. NRL scientists are combining all they know about circuit technology and the best of manufacturing processes to help make it happen.



Three-Dimensional Printing and Electroforming for Millimeter-Wave Vacuum Electronics

A.M. Cook, C.D. Joye, J.P. Calame, and F.K. Perkins
Electronics Science and Technology Division

Researchers in the Electromagnetics Technology Branch of the Electronics Science and Technology Division of the U.S. Naval Research Laboratory (NRL) are actively engaged in study and development of key technologies for vacuum electronic amplifier devices operating at frequencies ranging from 30 GHz to 300 GHz, the millimeter-wave range. Possible Naval applications include high-data-rate wireless communications, imaging, radar, and electronic warfare. Of all coherent source technology in the millimeter-wave range, the vacuum electronic amplifier offers the highest output power, the greatest efficiency, and the best power per weight ratio. Our research focuses on fabrication of the millimeter-wave circuit at the heart of the device; the circuit, which must withstand high electromagnetic power density, has features far smaller than a millimeter, and must be fabricated to micron precision. While advanced lithographic and micro-machining techniques developed at NRL have been successful, further improvements are restricted by their fundamental physical limitations, i.e., the techniques are inherently planar and two-dimensional in form. To overcome these limitations, our research team in the Electromagnetics Technology Branch is combining three-dimensional (3D) printing technology and electroforming techniques to fabricate fully 3D millimeter-wave circuits and components. Using our innovative fabrication technique, which begins with a plastic mold built on a commercial 3D printer, we can produce monolithic circuits in solid electrical-grade copper that are suitable for high-power operation. The 3D-printed mold electroforming process can leverage a variety of 3D printing technologies and materials.

INTRODUCTION

Millimeter-wave (mmW) amplifier devices are of increasing importance for a variety of applications — from car radar guidance systems to 5G high-speed data networks, and from high-resolution security imaging to electromagnetic protection of Naval vessels on the open sea. Some of these applications require substantial increases in power, bandwidth, and efficiency. The vacuum electronic amplifier — a type of vacuum tube — can boost the transmit power of operational signals by 100 to 1,000 times, and, as a result, project radio-frequency (RF) waves far and wide, even in uncertain atmospheric conditions. Vacuum electron (VE) devices offer ultimate power and efficiency because the electron current powering the millimeter waves streams through empty space in the device core, unimpeded by a semiconductor crystal lattice.

The idea of a modern vacuum tube might call to mind the sort of small glass tube that once powered radios and audio amplifiers. But VE devices have kept pace with engineering advancements and materials research and development, becoming a complex assembly of materials such as engineered composites, nanofabricated arrays, copper, steel, gold, sapphire, and diamond, and they can generate up to thousands of watts of mmW power in a single device that measures

a few inches across. The internal circuits that transport this amount of RF power are extremely small at mmW frequencies — well below the millimeter size range in many critical features. Fabrication of the circuits requires the precision necessary for maintaining correct RF synchronism and resonance for operation. It also requires pure copper, the ideal electrical material because it is highly conductive and because it has the high thermal conductivity needed for effective cooling. Pure copper is also compatible with the electron emitter material in vacuum. Thus, for device operating bands in the high frequency spectrum, two major obstacles must be overcome to achieve the full potential of mmW amplifiers: (1) the design and fabrication of suitable circuits with extremely small critical features and (2) the creation of these features within stringent limitations of suitable materials. To address these problems, our research team is studying how to apply three-dimensional (3D) printing and micron-scale additive manufacturing to fully 3D fabrication. Our research should open unprecedented freedom and innovation in the design of mmW devices.

In previous work with ultraviolet lithography and copper electroforming (UV-LIGA), which is an extended two-dimensional (2D) form of additive manufacturing, we showed that an electroformed copper circuit made from a polymer photoresist mold can

function as a viable amplification circuit in a mmW traveling-wave tube amplifier.¹ Ours was the first demonstrated VE amplifier ever to use an additively manufactured RF circuit, and set records in power and bandwidth performance at an operating frequency of 220 GHz while satisfying uncertainties about whether circuits produced with electroplated copper by this process would perform under vacuum. However, the inherently 2D nature of lithography precludes fabrication of 3D circuit features that could enhance amplifier performance, and makes difficult the fabrication of the embedded channel for the electron beam current. We have recently developed a fabrication process that uses the highest-resolution plastic 3D printing technologies to create mmW circuits in 3D geometries from pure copper.

3D-PRINTED MOLD ELECTROFORMING

Commercial technology exists to 3D-print parts directly from metal, including copper, by locally sintering metal powder with a laser, but the process is generally unsuitable for mmW components. The build resolution of a direct metal printing process is substantially coarser than what is achievable with plastic printing, which limits the precision of fabricated parts. Another concern is material purity. Because small voids are left between metal powder particles during sintering, a second alloy is usually introduced to fill in the metal matrix and achieve full density of the final metal part, which would diminish the electrical performance of a VE circuit and potentially render it unusable in vacuum. In addition, the raw metal nanoparticles oxidize easily, which degrades the electrical properties of the final printed metal.

We developed a hybrid process that we term 3D-printed mold electroforming (3D-PriME).² The process takes advantage of the extremely high resolution achievable by optically-based polymer plastic 3D printing technologies, while retaining the ideal material properties of pure copper. Figure 1 illustrates the process steps. First, a mold of the desired mmW circuit is created on a plastic 3D printer in an inverse geometry, i.e., the empty space of the circuit is printed rather than the actual form (Fig. 1(a)). We show a mold of a prototypical serpentine waveguide circuit, a workhorse of mmW power amplifiers (Fig. 1(d)). This circuit type is characterized by a relatively tall periodically folding waveguide structure and a round tunnel through the center to pass the electron beam current. In the second step, we electrochemically plate (electroform) pure electrical-grade copper onto and through the plastic mold, covering it in bulk copper and filling all empty spaces (Fig. 1(b)). (Electroforming is distinct from surface plating only in that the copper is built up into a bulk, rigid structure rather than just a thin layer.)

Finally, we use downstream chemical etching to remove the 3D-printed plastic material completely from the copper, leaving a solid copper circuit (Fig. 1(c)). In this downstream chemical etching process, the polymer is etched away by a gas of reactive oxygen and fluorine radicals that are inert to the copper surface and do not damage the circuit.³ The etch is isotropic, able to remove polymer from “hidden” 3D features, such as the electron beam current tunnel, and from the entire 3D circuit volume.

The commercial 3D printing technology we use to create mmW circuit forms in polymer material is an optical process known as stereolithography. Using a high-resolution digital video projector with effective pixel sizes as small as 10–15 μm , the stereolithography machine projects images of 2D slices of the desired 3D geometry into a tray of liquid photosensitive polymer resin. The visible and UV light comprising the 2D image cures the liquid it touches into a layer of solid plastic, 15–25 μm thick, and the machine continues to stack thin layers of varying 2D images until the entire 3D object is formed. The minimum volume pixel (voxel) size is thus approximately 10 μm \times 10 μm \times 15 μm , depending on the light absorption and curing properties of the specific resin, which dictates the ultimate build resolution of the 3D-printed parts. This resolution is suitable for making mmW circuits, operating in the 100 GHz range, that have geometric features, such as holes, slots, and cavities, ranging in size from 100 μm to 2 mm.

Figure 1(d) shows a 3D-printed inverse mold of a prototypical mmW amplifier circuit designed for operation near 100 GHz. Some artifacts of the finite printer resolution are apparent, such as the layering visible in the vertical direction and the conical curvature of the bridge-like cylindrical beam tunnel where it meets each vertical wall structure. These effects can be taken into account in the theoretical design of the amplifier device, and may be minimized further by using different polymer build materials or adjusting optical exposure settings in the 3D printer. Most important, we observe good accuracy and precision of specific dimensions critical to the amplifier operation, such as the length of the repeating structure period and the total structure height. These dimensions affect the operating frequency and the synchronism between the millimeter waves and the electron beam, and are finely tuned in the design to produce the desired performance. By making repeated measurements at each period of the structure, we observed the as-fabricated critical dimensions to vary approximately 0.5% from the design values across the entire circuit. This variance is close to, though somewhat less precise than, what we achieve by current state-of-the-art techniques such as high-speed micromachining and UV-LIGA.

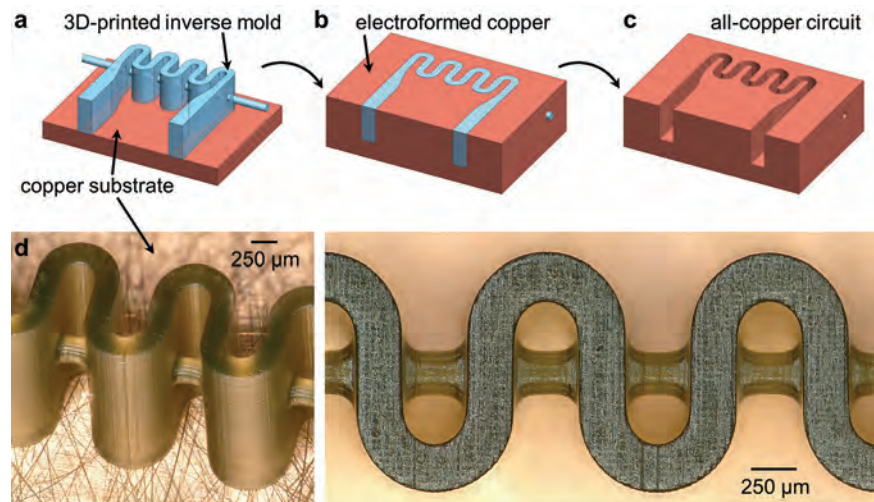


FIGURE 1

3D-printed mold electroforming process sequence. (a) A plastic inverse mold of a millimeter-wave circuit is 3D-printed onto a substrate. (b) Copper is electroformed to cover the entire mold and fill empty volume. (c) The 3D-printed mold is completely etched away by isotropic downstream chemical etching, leaving a solid copper circuit. The circuit top is left open to allow etching, and will be covered by a flat copper plate. (d) Microscope photos of a serpentine waveguide circuit mold 3D-printed onto copper substrate.

The 3D-printed mold is either bonded to a copper substrate, printed onto the substrate directly, or coated with a thin metal layer to provide a conducting surface for electroforming. It is then immersed in a liquid electroplating solution and connected to a voltage supply, and copper crystals begin to grow onto the mold atom by atom. When enough copper is built up to cover the polymer mold, the circuit is removed from the plating liquid. We then machine or polish the top surface of the electroformed part to remove extraneous raw copper formations and obtain a flat surface, and place it in a downstream chemical etching chamber. It is necessary to leave some of the 3D-printed mold exposed after electroforming, so that it can be etched away. To accomplish this, the circuit geometry is designed to have an open top that is eventually covered by a flat copper plate, or otherwise having relief channels or small openings for the etchant to reach the 3D-printed plastic.

Figure 2 shows an electroformed copper circuit after the mold has been completely removed. This particular sample was electroformed by starting with a gold layer, 200 nm thick, covering the entire mold on a plastic substrate. Visible are the top plane of the circuit as well as parts of the inner waveguide walls and bottom floor. A remarkable feature seen in this sample is that the copper forms close to the plastic surface, even into tiny layer corrugations and micron-scale surface texture. While this formation leads to excellent replication of the plastic mold by the copper in striking detail, it can also create undesired roughness on the electrical surfaces, because the inherent surface texture and layering of the 3D-printed material is imprinted into the

electroformed copper. These effects are visible in the zoomed-in photos of Figs. 2(b) and 2(c). Another key issue is areas of missing copper that did not properly electroform (indicated by black arrows in Fig. 2(c)). This issue was a result of the gold plating allowing copper to form from the high points of the mold at the same time as the floor, eventually blocking off fluid flow in between and leading to pockets of trapped electroforming solution, where the plating reaction stagnated. This problem can be solved by printing the circuit mold directly onto a copper substrate, as shown in Fig. 1(d), which serves as the bottom plane for copper to build upward in only one direction. Fluid is thus allowed to flow upward out of the mold, avoiding trapped fluid pockets. This method is used successfully for mmW circuits in the analogous UV-LIGA electroforming process developed at NRL.¹

TERAHERTZ CIRCUITS WITH 3D NANO-PRINTING

A key advantage of the 3D-PriME fabrication technique is that the 3D-printed material is ultimately removed and not incorporated as part of the final copper part. Thus, the mmW circuits produced by this method are not beholden to particulars or undesirable properties of unique, often proprietary 3D printer materials or machinery. In addition, new advances in commercial additive manufacturing technology can always be folded into the 3D-PriME process without changing the ideal material properties of the final copper circuit. For example, the build resolution of the optical stereolithography technology we have used is limited to a 10

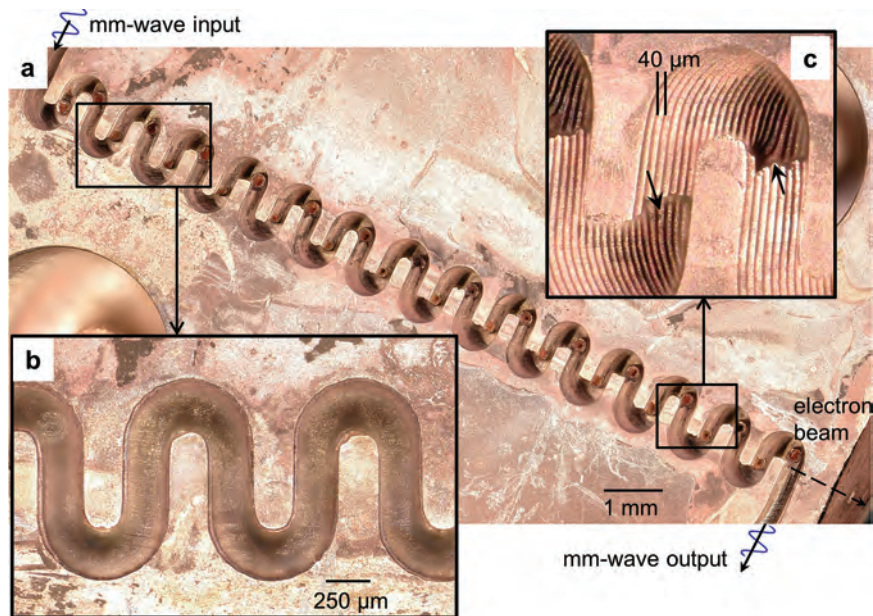


FIGURE 2
 (a) Tilted top view of electroformed copper circuit after 3D-printed material is completely etched away. The waveguide ports where millimeter waves would enter and exit the amplifier are indicated in the upper left-hand and lower right-hand portions of the image, respectively. The electron beam current trajectory and tunnel exit hole are visible in the lower right-hand part of the image. (b) Detail of copper circuit top view, showing top and bottom surfaces of the waveguide channel in focus simultaneously. The imprinted texture of the 3D-printed plastic is evident on the bottom surface. (c) Detail of wall inside waveguide. Ridges from 40 μm thick printed layers are visible. Black arrows indicate areas of missing copper.

μm voxel size, but that size is not an absolute limit for 3D-PriME fabrication. Using a commercial direct-laser-writing 3D nanofabrication system based on a multi-photon nonlinear optical process, which has an ultimate voxel resolution of less than 100 nm, we were able to 3D-print circuit molds more than 10 times smaller than that shown in Fig. 1(d). Figure 3 shows circuit molds designed for traveling-wave tube circuits operating in the terahertz frequency range at 1,350 GHz. These molds will subsequently be electroformed and etched using the same process described above.

METAMATERIALS

Another class of electromagnetic structures that seem a natural fit for 3D fabrication are metamaterials, which are designed to have artificial bulk electromagnetic material properties by arranging miniature resonant RF structures in large arrays. Because metamaterials are massively periodic and microfeatured, they are difficult to fabricate in anything other than sheet-like lithographic or similar processes, which are not typically amenable to 3D features or out-of-plane extrusions. Our goal is to create metamaterials from 3D-printed molds, thereby facilitating the robust formation of metals, ceramics, and engineered composites together into tailored 3D

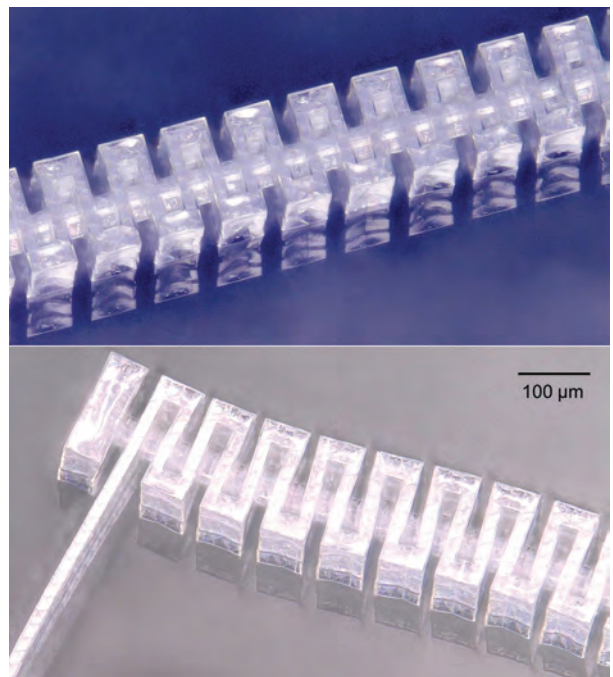


FIGURE 3
 Circuit mold for a 1,350 GHz traveling-wave tube made using multi-photon direct laser writing 3D printer. A reflection from the glass substrate is visible at the base of the structure in each photo.

geometries. This fabrication technique could produce metamaterials that would withstand high temperature and high power, and that, thus, would overcome a common weakness of today's delicate microfabricated prototypes, especially at mmW frequencies. Figure 4 shows a 3D-printed mold for an array of split-ring resonant structures that we made for a scaled-model test at an operating frequency near 10 GHz. The structure provides the electromagnetic design shape as well as structural rigidity and fixturing for the forming of functional materials into the mold, which will ultimately be etched away.

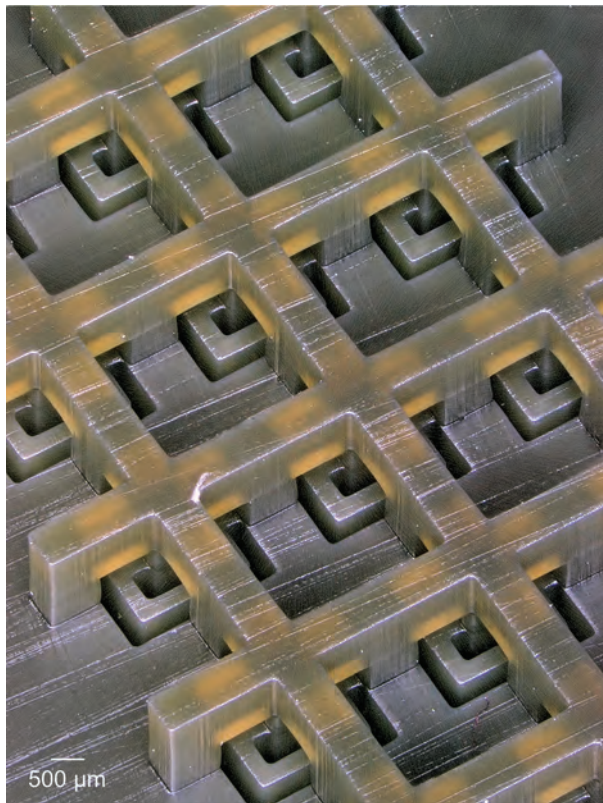


FIGURE 4
3D-printed mold for split-ring resonator type metamaterial.

SUMMARY

In this research, we developed a new 3D additive fabrication method for creating mmW amplifier circuits in pure electrical-grade copper. We demonstrated the use of a commercial high-resolution polymer 3D printing process for molding pure bulk copper 3D geometries in precise detail. We demonstrated the creation of a copper traveling-wave tube amplifier circuit designed for 100 GHz operating frequency by our 3D-PriME process, and showed the use of a 3D nano-printing technology to create amplifier circuit molds for operation at over 1,000 GHz. In addition to

amplifier circuits, we showed the use of 3D printing for exotic structures with engineered electromagnetic properties (metamaterials). This research establishes the utility of our new method across a variety of commercial 3D printing technologies and electromagnetic structure types, and over a range of at least a decade in RF frequency spectrum, spanning the mmW and terahertz ranges.

[Sponsored by the Base Program (CNR funded)]

References

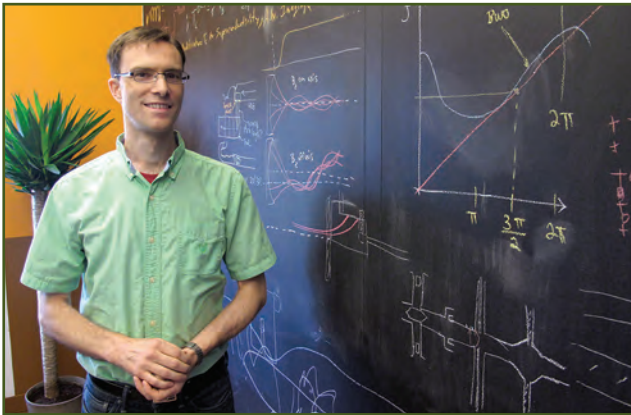
- ¹ C.D. Joye, A.M. Cook, J.P. Calame, D.K. Abe, A.N. Vlasov, I.A. Chernyavskiy, K.T. Nguyen, E.L. Wright, D.E. Pershing, T. Kimura, M. Hyttinen, and B. Levush, "Demonstration of a High Power, Wideband 220-GHz Traveling Wave Amplifier Fabricated by UV-LIGA," *IEEE Trans. Electron Devices* **61**, 1672–1678 (2014).
- ² A.M. Cook, C.D. Joye, J.P. Calame, and D.K. Abe, "3D-Printed Mold Electroforming for Microfabrication of W-band TWT Circuits," *Proceedings of IEEE 18th International Vacuum Electronics Conference*, London, UK (2017).
- ³ R. Engelke, J. Mathuni, G. Ahrens, G. Gruetzner, M. Bednarzik, D. Schondelmaier, and B. Loechel, "Investigations of SU-8 Removal from Metallic High Aspect Ratio Microstructures with a Novel Plasma Technique," *Microsyst. Technol.* **14**, 1607–1612 (2008).



THE AUTHORS



ALAN M. COOK received a B.S. in physics from Arizona State University in 2003 and an M.S. and a Ph.D., both in physics, from the University of California, Los Angeles, in 2005 and 2009, respectively. His graduate research demonstrated a method of generating powerful sub-millimeter-wave radiation from a strongly-focused electron beam in a linear accelerator. In 2009, he joined the Plasma Science and Fusion Center at the Massachusetts Institute of Technology, where his postdoctoral research focused on nanosecond millimeter-wave plasma dynamics and frequency-selective photonic crystal electron accelerators. In 2011, he joined NRL as a research physicist. His current work focuses on microfabrication methods and materials for high-power vacuum electronic amplifiers in the upper-millimeter-wave frequency range. He is the recipient of a 2012 Dr. Delores M. Etter Top Scientists and Engineers of the Year Award, an NRL Technology Transfer Award, and an Alan Berman Research Publication Award.



COLIN D. JOYE received a B.S. in electrical engineering and computer science from Villanova University in 2002 and an M.S. and a Ph.D., both in electrical engineering, from the Massachusetts Institute of Technology (MIT) in 2004 and 2008, respectively. He was a research assistant and visiting scientist in the Waves and Beams Division at the MIT Plasma Science and Fusion Center from 2002 to 2008. In 2008, he joined the former Vacuum Electronics Branch at NRL as a Karle Fellow. His research interests include millimeter-wave vacuum electron amplifiers and novel microfabrication techniques. In 2016, he received the Presidential Early Career Award for Scientists and Engineers. He is also the recipient of a 2012 Dr. Delores M. Etter Top Scientists and Engineers of the Year Award, an NRL Technology Transfer Award, and two Alan Berman Research Publication Awards.



JEFFREY P. CALAME received three degrees in electrical engineering from the University of Maryland, College Park: a B.S. in 1985, an M.S. in 1986, and a Ph.D. in 1991. His graduate research from 1985 to 1991 involved the development of a high peak power gyrokystron, a type of multi-megawatt microwave amplifier. From 1992 to 1997, he performed postdoctoral research at the University of Maryland on microwave amplifiers, the microwave processing of materials, and the dielectric properties of ceramics. In 1997, he joined NRL as an electronics engineer in the Vacuum Electronics Branch, and from 1997 to 2003, he developed high average power, wideband millimeter-wave amplifiers for radar applications. He is presently Section Head in the Electromagnetics Technology Branch, where he performs and supervises research on millimeter-wave amplifiers for electronic warfare, communications, and radar applications.

He also performs research on related advanced materials and microfabrication technologies, including microwave absorbing materials, high heat flux cooling, additive manufacturing, and high-peak-power energy storage.



F. KEITH PERKINS received an S.B. in physics from the Massachusetts Institute of Technology in 1982 and an M.S. and a Ph.D., both in materials science, from the University of Wisconsin-Madison in 1988 and 1992, respectively. He worked at the University of Wisconsin Synchrotron Radiation Center from 1983 to 1988. He held a National Research Council postdoctoral fellowship tenured at NRL from 1992 to 1995, at the end of which he was converted to a permanent staff member in Electronics Science and Technology Division. Since then, his work has included high resolution lithography, chemical vapor sensors from nanophase materials, and growth and applications of carbon nanotubes, and he says that he is now surprised to find himself back to working on high resolution lithography. He received a Top Navy Scientists and Engineers of the Year Award in 2007.

A MIGHTI Flight for Ionospheric Insight

Say you're flying from Africa to South America and you want to use geopositioning along the way. What's the likelihood that you're going to face an outage during, say, a nighttime flight? Right now, it's anyone's guess.

The U.S. Naval Research Laboratory (NRL) aims to help remove the guesswork. NRL scientists have sent into space an instrument designed to study the Earth's thermosphere. The Michelson Interferometer for Global High-resolution Thermospheric Imaging (MIGHTI) instrument will help researchers better understand space variations that contribute to disruptions in communications equipment, radar, and global positioning systems on Earth.

NRL's MIGHTI instrument was scheduled to launch in December 2017 onboard NASA's Ionospheric Connection Explorer mission. NRL is one of the few places in the country that supports the development of satellite sensors completely, from concept to execution — from the first spark of an idea to the reality of a satellite payload, including operational data analysis algorithms. The MIGHTI instrument is a recent example.



From Sensor Idea to Satellite Instrument

C.R. Englert,¹ C.M. Brown,¹ K.D. Marr,¹ and J.M. Harlander²

¹Space Science Division

²Space Systems Research Corporation (Alexandria, Virginia)

Motivated by the need to measure altitude profiles of atmospheric wind in the thermosphere/ionosphere region from space, the Space Science Division has led the development of an innovative optical technique with advantages over previously deployed instrumentation. Within about a decade (from 2005 to 2016), the new concept, patented by the Navy and named the Doppler Asymmetric Spatial Heterodyne (DASH) technique, was matured from an idea to a space-qualified payload. The NRL-developed Michelson Interferometer for Global High-resolution Thermospheric Imaging (MIGHTI) satellite instrument, the first space-based DASH instrument, is part of the NASA Ionospheric Connection (ICON) Explorer mission.

The idea of this new type of space-based, high-altitude wind sensor was first demonstrated at NRL with a simple bench setup in 2005 and published in 2006. The first monolithic interferometers, which are the “heart” of the sensor, were designed and built in the following years. Data analysis techniques were developed, and several ground-based thermospheric wind measurements were conducted in 2010 and 2011 to demonstrate and validate the approach. On the strength of these results, the new technique was selected for the wind sensor of the NASA ICON mission. This article describes the optical technique and the major milestones of its development.

INTRODUCTION

Developed by the NRL Space Science Division, the Michelson Interferometer for Global High-resolution Thermospheric Imaging (MIGHTI) satellite instrument is part of NASA’s Ionospheric Connection (ICON) Explorer mission. The ICON mission, led by Thomas Immel at the University of California, Berkeley, flies a suite of instruments designed to explore the mechanisms controlling the environmental conditions in space and how they are modified by weather in the lower atmosphere. In studying this region where Earth’s weather and space weather meet, researchers hope to find answers to their questions about how Earth’s upper atmosphere behaves, because this part of the atmosphere is essential for the performance of many systems that use long-distance radio wave propagation.

NRL’s MIGHTI instrument aboard the ICON satellite contributes to reaching the mission goals by measuring the neutral winds and temperatures in the Earth’s low-latitude thermosphere. The MIGHTI instrument uses the Doppler Asymmetric Spatial Heterodyne (DASH) spectroscopy technique, which was co-invented and pioneered by NRL. The payload consists of two identical units that observe the Earth’s thermosphere with perpendicular viewing directions. As the ICON satellite travels eastward and continuously images the thermosphere and ionosphere, MIGHTI measures the vector components of the vertical wind profile.

NRL’s MIGHTI is named for Albert Michelson, a physicist known for his research on the measurement of the speed of light using a related interferometer type. More directly, MIGHTI builds on technology previously used in NRL’s SHIMMER (Spatial Heterodyne Imager for Mesospheric Radicals), a payload aboard STPSat-1. The NRL MIGHTI team is led by Christoph Englert, head of the Geospace Science and Technology Branch in the Space Science Division.

The MIGHTI instrument has origins in NRL research that reaches back to early 2005. In early 2005, our small team at NRL worked with research partners at the University of Wisconsin, Madison, and St. Cloud State University on the first satellite instrument to use a monolithic Spatial Heterodyne Spectrometer (SHS) interferometer to measure the mesospheric trace gas hydroxyl, or OH, a highly reactive radical and an important player in atmospheric chemistry. This measurement uses the diffuse fluorescence of OH as seen from space on the Earth’s horizon and requires very high spectral resolution in a narrow wavelength interval in the near ultraviolet, making SHS a good technique for this problem.¹

Much as it does in a Fourier Transform Spectrometer (FTS), light coming into an SHS is split into two interferometer arms. After being reflected at the ends of the arms, the beams are recombined at a beamsplitter, where they interfere constructively or destructively (to varying degrees, one way or the other), depending on the optical path difference (OPD) introduced by the

two arms and the signal wavelength. Measuring the resulting intensity for different OPDs allows us to create an interferogram, which is equivalent to the Fourier transform of the incident spectrum. In a conventional FTS, the different OPDs are created by moving mirrors in one or both arms, and the interferogram is recorded as a function of OPD using a single element detector. In SHS, the arms are terminated by tilted diffraction gratings, and each grating groove can be considered as a separate mirror at different OPD. Thus, by projecting the gratings onto an imaging detector, an SHS instrument can record many hundred interferogram samples simultaneously. The discrete steps between the grating grooves also result in a heterodyning effect, which allows for low spatial frequencies of the interferogram features on the detector while achieving high spectral resolution without moving interferometer parts.

SHS is particularly suitable for applications that require high resolution over a limited wavelength region and diffuse sources. In addition, the “multiplex noise” disadvantage, which any FTS must accept, is minimized if the source is limited to the signal of interest, without a large background signal.

DOPPLER ASYMMETRIC SPATIAL HETERODYNE SPECTROSCOPY

The above properties of SHS make it suitable for measuring the faint signal of naturally occurring air-glow from oxygen atoms in the Earth’s upper atmosphere. This measurement helps researchers determine the local wind speed from the Doppler shift of these almost monochromatic emissions. For this problem, very small wavelength shifts, on the order of one part in 50 million, must be determined from the measured interferogram.

The thin line in Fig. 1 illustrates the typical interferogram of a temperature-broadened emission line. The interferogram consists of a cosine-shaped signal with a bell-shaped envelope due to the fact that the oxygen emission line is not monochromatic. The difference between this interferogram and an interferogram from a slightly Doppler-shifted emission line, which has a slightly different cosine fringe frequency, is shown as the thick black line. The difference maximizes at a particular OPD away from the center ($OPD=0$) location. Thus, to measure the wind in the upper atmosphere, it is most efficient to build an interferometer that only measures an OPD interval in which the measured signal is most sensitive to the Doppler shift. The resulting interferometer is “asymmetric,” with one arm longer than the other, giving rise to the name Doppler Asymmetric Spatial Heterodyne Spectroscopy, or DASH, as it is known.²

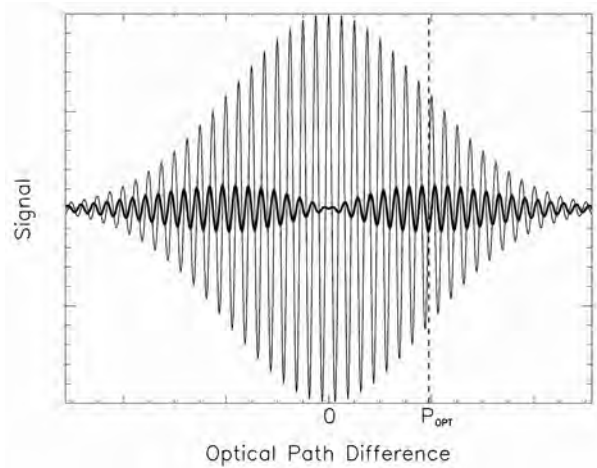


FIGURE 1
Thin line: Interferogram of a temperature broadened emission line. Thick line: difference between this interferogram and one for a slightly Doppler shifted line with a slightly different fringe frequency. The signal difference is largest around P_{OPT} , for which the measurement will be most sensitive.

FIRST BREADBOARD, BRASSBOARD, AND MONOLITHIC DASH INTERFEROMETERS

We performed our first demonstration of a DASH interferometer in 2005. We modified a breadboard SHS interferometer built for a different project but that allowed us to easily configure asymmetric arm lengths. In this first experiment, shown in Fig. 2, we measured the small wavelength changes of laser diodes, and we published the concept in 2006.³

A year later, using NASA support, we started constructing a brassboard experiment to measure actual Doppler shifts in the near infrared, using laser light

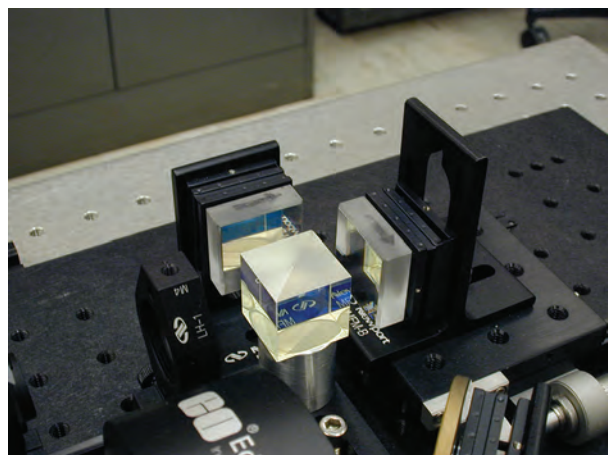


FIGURE 2
Breadboard setup of a Spatial Heterodyne Spectrometer (SHS) interferometer with a cubic beamsplitter and two adjustable gratings. The grating on the right was translated away from the beamsplitter to demonstrate the Doppler Asymmetric Spatial Heterodyne (DASH) concept by simultaneously measuring small wavelength shifts of two laser diodes.

bounced off a spinning, reflective wheel. Furthermore, this effort resulted in the first thermally compensated, monolithic DASH interferometer (Fig. 3).⁴ Monolithic designs are particularly beneficial for spaceflight instrumentation, because they are robust and, therefore, at low risk of misalignment from vibrations during launch. Also, because its design eliminates all moving interferometer parts, DASH offers greatly increased reliability of spaceflight instrumentation.

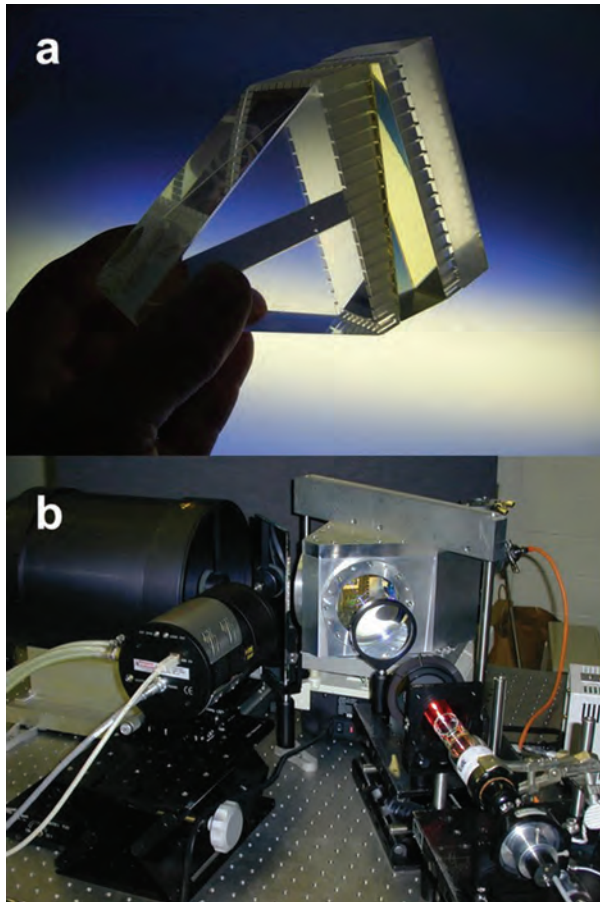


FIGURE 3
 (a) First monolithic DASH interferometer. This interferometer used a triangular Kösters prism as the beamsplitter, allowing the use of only one grating in the parallel interferometer arms. (b) Breadboard setup for testing of the monolithic interferometer using a neon hollow cathode lamp as the signal source.

MEASURING REAL WINDS FROM THE GROUND

After successfully demonstrating the DASH technique in the laboratory, we shifted our focus to another milestone: the first measurement of real atmospheric winds using the DASH technique. Upper atmospheric winds can be measured from the ground using the same airglow lines that are observed from space, provided that there are no clouds blocking the signal from

the upper atmosphere. In 2009, we began building a portable DASH instrument from mainly commercial off-the-shelf components (Fig. 4). We performed our first ground-based measurements from the rooftop of the NRL Space Science Division building, in Washington, DC, in 2010. The patent for the DASH technique was also awarded to the Navy that year. We repeated the wind measurements from a much less light-polluted site in North Carolina in 2011.⁵ These observations were conducted simultaneously with a Fabry-Perot instrument (the gold standard in devices for ground-based upper atmospheric wind measurements).



FIGURE 4
 The portable DASH ground-based instrument positioned on a concrete column inside an observation hut with removable roof at the Pisgah Astronomical Research Institute in North Carolina.

THE PATH TO SPACE

In 2011, concurrent with running our ground-based DASH measurements, we joined researchers at the University of California, Berkeley, in soliciting NASA with a proposed ICON mission that would incorporate the MIGHTI instrument. In spring 2013, NASA selected the proposed ICON mission for spaceflight. As part of the ICON proposal activities, and specifically to optimize the MIGHTI sensor design, we continued to study key instrument parameters, such as the thermal behav-

ior of DASH interferometers.⁶ The finished MIGHTI payload was delivered to the ICON project in February 2016. The complete instrument consists of a calibration lamp unit, an electronics unit, and two identical optical sensors (Fig. 5(a)) that observe the atmosphere with two perpendicular viewing directions. This configuration allows researchers to determine the wind speed and direction as a function of altitude, because the Doppler shift contains only information on the wind velocity component along the viewing direction.

Figure 5(b) shows the optical bench of one of the sensor units during assembly. The optical bench holds all of the optical elements, including the interferometer in its holder, on the left, and the imaging detector, shown in the yellow enclosure on the right. Figure 6 shows the MIGHTI interferometers⁷ as they look before their integration into the instrument (the photo shows two used for flight and a third that is a spare). The figure depicts the cubic beamsplitters with the long and short interferometer arms attached to the front-left and back-left cube sides, respectively.

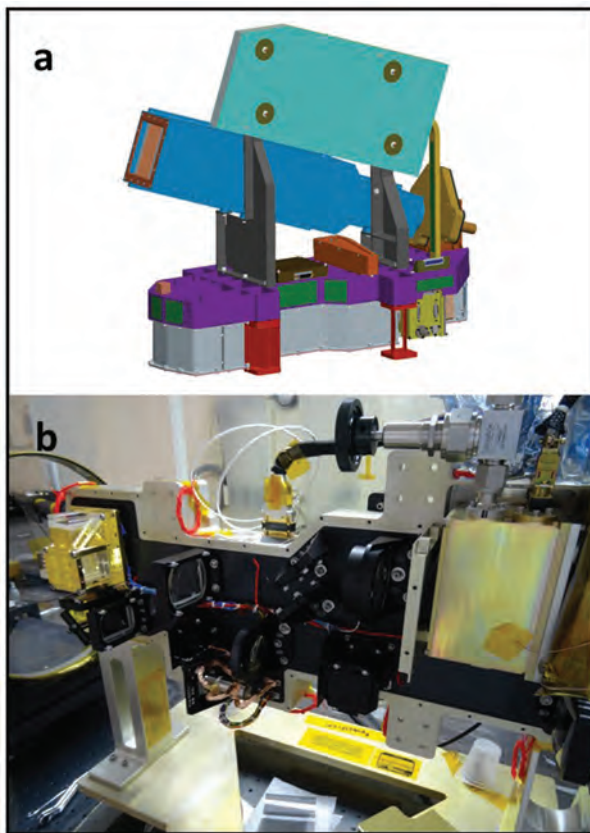


FIGURE 5
(a) Solid model of a single optical sensor for the Michelson Interferometer for Global High-resolution Thermospheric Imaging (MIGHTI) satellite instrument. The optical bench is the purple structure. It holds all optical elements of the sensor. Light is accepted via the blue baffle. The cyan surface is a radiator, which rejects heat generated by cooling the detector. (b) Optical bench of one of the MIGHTI sensors during assembly.

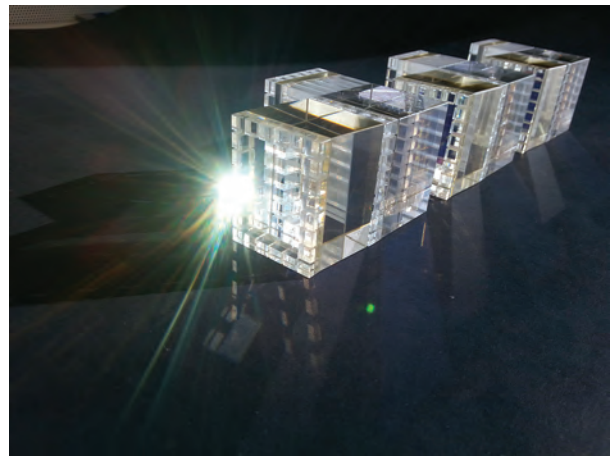


FIGURE 6
Monolithic, temperature-compensated interferometers for MIGHTI, two for flight and one spare.

CONCLUSION

In July 2017, MIGHTI was fully integrated and tested onboard the ICON satellite.⁸ Figure 7 shows the complete spacecraft with the solar panels in the deployed position. The two arrows indicate the locations of the two MIGHTI optical sensors. The ICON mission was launched in December 2017 from the Reagan Test Site at the Kwajalein Atoll, about 2,500 miles west of Hawai'i; the launch placed the satellite in a low-inclination, low-Earth orbit (Fig. 8). ICON is an Explorer-class mission, led by the University of California, Berkeley, and managed at NASA's Goddard Space Flight Center in Greenbelt, Maryland. ICON is slated for a nominal two-year mission but, if all goes well, conceivably could be extended to accomplish additional science. The data that ICON provides will give atmospheric scientists reliable and continuous insight into thermospheric and ionospheric processes. NRL's MIGHTI instrument onboard the ICON satellite will contribute to the mis-



FIGURE 7
Fully integrated NASA Ionospheric Connection (ICON) Explorer satellite with deployed solar panels. The locations of the two MIGHTI optical sensors are indicated by the arrows.

sion's goal of better understanding what causes the large variability of the upper atmosphere. The analysis of the mission data will bring us a significant step closer to reliable predictions of the upper atmospheric state and its potential impacts on Earth-based systems.



FIGURE 8
Artist's conception of ICON on orbit.

ACKNOWLEDGMENTS

This work was sponsored by the NRL Base Program (CNR funded), the NRL Capital Purchase Program, NASA's Planetary Instrument Definition and Development Program, and NASA's Explorers Program through contracts NNG12FA45C and NNG12FA42I. The authors thank the MIGHTI team for their dedication and invaluable contributions to this effort.

[Sponsored by the NRL Base Program (CNR funded) and NASA]

References

- ¹ C.R. Englert, M.H. Stevens, D.E. Siskind, J.M. Harlander, and F.L. Roesler, "Spatial Heterodyne Imager for Mesospheric Radicals on STPSat-1," *J. Geophys. Res.* **115**(D20), (2010). doi:10.1029/2010JD014398
- ² C.R. Englert, D.D. Babcock, and J.M. Harlander, "Doppler Asymmetric Spatial Heterodyne Spectroscopy (DASH): Concept and Experimental Demonstration," *Appl. Opt.* **46**(29), 7297–7307 (2007).
- ³ C.R. Englert, J.M. Harlander, D.D. Babcock, M.H. Stevens, and D.E. Siskind, "Doppler Asymmetric Spatial Heterodyne Spectroscopy (DASH): An Innovative Concept for Measuring Winds in Planetary Atmospheres," *Proc. SPIE* **6303**, S.M. Hammel and A. Kohnle, eds., SPIE Optics and Photonics, Aug. 13–17, 2006, San Diego, Calif., 63030T-1 (2006).
- ⁴ J.M. Harlander, C.R. Englert, D.D. Babcock, and F.L. Roesler, "Design and Laboratory Tests of a Doppler Asymmetric Spatial Heterodyne (DASH) Interferometer for Upper Atmospheric Wind and Temperature Observations," *Opt. Express* **18**(25), 26430–26440 (2010).
- ⁵ C.R. Englert C.R., J.M. Harlander, C.M. Brown, J.W. Meriwether, J.J. Makela, M. Castelaz, J.T. Emmert, D.P. Drob, and K.D. Marr, "Coincident Thermospheric Wind Measurements Using Ground-Based Doppler Asymmetric Spatial Heterodyne (DASH) and Fabry-Perot Interferometer (FPI) Instruments," *J. Atmos. Sol.-Terr. Phys.* **86**, 92–98, (2012). doi:10.1016/j.jastp.2012.07.002.

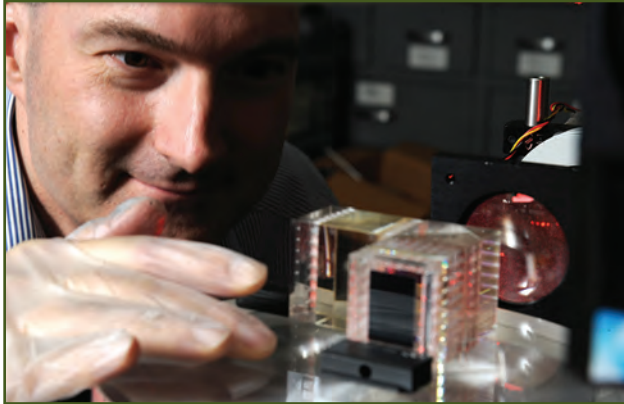
⁶ K.D. Marr, C.R. Englert, J.M. Harlander, and K. Miller, "Thermal Sensitivity of DASH Interferometers: The Role of Thermal Effects during the Calibration of an Echelle DASH Interferometer," *Appl. Opt.* **52**(33), 8082–8088 (2013). doi: 10.1364/AO.52.008082.

⁷ J.M. Harlander, C.R. Englert, C.M. Brown, K.D. Marr, I.J. Miller, V. Zastera, B.W. Bach, and S.B. Mende, "Michelson Interferometer for Global High-resolution Thermospheric Imaging (MIGHTI): Monolithic Interferometer Design and Test," *Space Science Reviews* (2017). doi:10.1007/s11214-017-0374-4.

⁸ C.R. Englert, J.M. Harlander, C.M. Brown, K.D. Marr, I. Miller, J.E. Stump, J. Hancock, J. Peterson, J. Kumler, W. Morrow, T. Mooney, S. Ellis, S.B. Mende, S.E. Harris, M.H. Stevens, J.J. Makela, B.J. Harding, and T.J. Immel, "Michelson Interferometer for Global High-resolution Thermospheric Imaging (MIGHTI): Instrument Design and Calibration," *Space Science Reviews* (2017). doi 10.1007/s11214-017-0358-4.



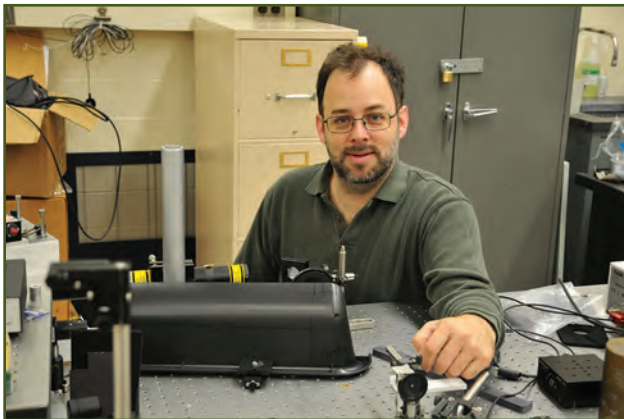
THE AUTHORS



CHRISTOPH R. ENGLERT received a graduate degree in physics from the Technical University of Munich in 1996 and a doctorate degree in physics from the University of Bremen in 1999. He accepted a National Research Council postdoctoral associateship at the NRL Space Science Division (SSD) in 1999. He joined the NRL staff in 2001. Today, he is head of the SSD Geospace Science and Technology Branch. Since 1999, Dr. Englert has worked on spatial heterodyne spectroscopy instrumentation and spectral data analysis in several wavelength regions from the near ultraviolet (UV) to the thermal infrared. His roles in spaceborne sensor projects have included instrument scientist of a near UV spectrometer on the STS-112 space shuttle mission, principal investigator of the Spatial Heterodyne Imager for Mesospheric Radicals (SHIMMER) on STPSat-1, and the instrument lead for the MIGHTI instrument on the NASA ICON mission. His main interests range from space-based optical sensors to upper atmospheric research of importance to the Navy and the wider DoD.

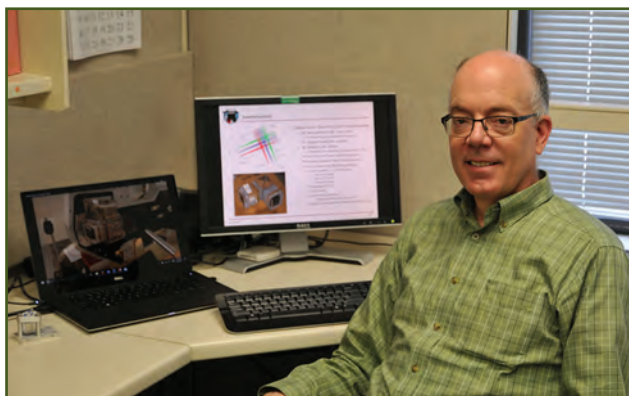


CHARLES M. BROWN earned a Ph.D. in chemical physics from the University of Maryland in 1971. He started working at NRL in September 1971 as a postdoctoral associate through the Research Associateship Programs of the National Academy of Sciences. He has been a physicist in the Space Science Division since 1971. His research interests are in spectroscopy, ranging from the X-ray region to the near infrared, with application to subjects like solar and laser heated plasmas as well as geophysical measurements. Much of his recent work has been in optical design and construction of new spaceflight instruments for solar and geophysical research. He has helped build space instruments that include the Bent Crystal Spectrometer (BCS) for the Yohkoh mission, the Extreme Ultraviolet Imaging Spectrometer (EIS) for the Hinode mission, the Middle Atmosphere High Resolution Spectrometer Investigation (MAHRSI) for two space shuttle missions, and the Michelson Interferometer for Global High-resolution Thermospheric Imaging (MIGHTI) for the NASA ICON mission.



KENNETH D. MARR received a B.S. in physics from Principia College in 1999 and a Ph.D. in plasma physics from the Massachusetts Institute of Technology (MIT) in 2010. While at MIT, he worked at the Plasma Science and Fusion Center under the supervision of B. Lipschultz, using spectroscopy to study plasma rotation in the Alcator C-Mod tokamak. In 2011, Dr. Marr was awarded a grant from the National Research Council to join Christoph Englert at NRL for several projects, including characterization of the Doppler Asymmetric Spatially Heterodyned (DASH) interferometer used on the Michelson Interferometer for Global High-resolution Thermospheric Imaging (MIGHTI) experiment on the NASA ICON mission. Dr. Marr is now a research physicist on the staff of NRL, and works on the MIGHTI project.

THE AUTHORS



JOHN M. HARLANDER graduated from the University of Wisconsin-Madison with a Ph.D. in physics in 1991 and then joined the Department of Physics at St. Cloud State University (Minnesota). In 2015, he retired from teaching to focus on long-term research interests in interference spectroscopy with applications in atmospheric science and astrophysics. A pioneer in spatial heterodyne spectroscopy (SHS), Dr. Harlander is a co-developer of Doppler Asymmetric SHS (DASH). He has been collaborating with the NRL Space Science Division on SHS and DASH instrumentation since 1991. He is a co-investigator on the NASA ICON mission, serving as the optical designer, and has been a key player in the alignment, testing, and calibration of the Michelson Interferometer for Global High-resolution Thermospheric Imaging (MIGHTI) instrument on ICON. Dr. Harlander is currently an emeritus professor of physics at St. Cloud State University and a senior scientist at Space Systems Research Corporation in Alexandria, Virginia.

- 108** Impulsive Noise Mitigation of Fire Suppression Systems
- 110** Understanding the Influence of Disorder in Atomically Thin Materials
- 113** A Mixture Theory Based Approach to Poroacoustics

Impulsive Noise Mitigation of Fire Suppression Systems

P.C. Herdic,¹ W.G. Szymczak,¹ B.H. Houston,¹ and J. Vignola²

¹Acoustics Division

²Catholic University of America

Introduction: The Medium Tactical Vehicle Replacement (MTVR), a truck designed for the U.S. Navy and Marine Corps, is equipped with an Automatic Fire Extinguishing System (AFES) that generates impulsive acoustic levels in the range of 160 dBp (peak). Because these acoustic levels are considered hazardous to hearing, personnel are required to wear double layer ear protection in the MTVR's cabin. However, wearing the protective gear can impair awareness of the battlefield environment. In our study, we identified two significant noise sources (as illustrated in field measurements; see Fig. 1): (1) the tank squib valve noise (~160 dBp) that releases the fire suppressant and (2) the supersonic discharge flow noise (~154 dBp) generated at the nozzle exit. We developed mitigation strategies to reduce the noise levels, using an AFES laboratory simulator to make the evaluation measurements and flow models to guide the prototype piping/manifold design.

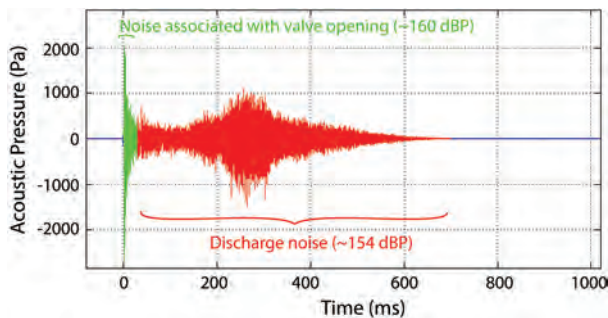


FIGURE 1

Typical noise response of the Automatic Fire Extinguishing System (AFES) (driver location) from field measurement (U.S. Army Aberdeen Test Center, Christopher J. Czech).

AFES Laboratory Simulator: The AFES system on the MTVR includes a pressurized tank (900 psi) containing nitrogen, HFC-227 refrigerant, and sodium bicarbonate. The contents are released by an electronically controlled explosive valve, referred to as a squib valve, through piping terminated by a discharge nozzle. We designed an AFES simulator that incorporated the actual AFES piping and a pressurized nitrogen tank having the same volume as the tank of the “real” AFES. With our AFES simulator, we could develop and evaluate mitigation approaches to AFES noise levels. We refilled the pressurized tank easily with a large nitrogen storage bottle (Fig. 2). We replaced the single usage squib valve with a solenoidal valve for repeated

evaluation testing. We implemented an aluminum valve enclosure with detailed Sorbothane sealing to mitigate the valve noise (Fig. 3). For flow noise mitigation, we replaced the end nozzle with a prototype manifold consisting of a volume expansion chamber, perforated screens to slow gas flow, and multiple exit nozzles (Fig. 3). The prototype manifold could be equipped with different perforated screens, allowing us to evaluate the fractional hole openings and closing off subsets of the multiple exit tubes.

Flow Models: A simple analysis of compressible gas flow released from a high pressure reservoir through the original AFES piping section reveals that the flow at the nozzle will be “choked” at the exit, causing the flow to move at the speed of sound. Such flows are a significant noise source,¹ and, therefore, reducing the exit velocity to subsonic levels will lead to significant reduction of flow noise. We used a simplified flow model, derived from mass and momentum conservation laws, to predict flow quantities at five places in the AFES simulator: (1) the pressurized tank, (2) the piping, (3) the volume expansion chamber, (4) the perforated sheets, and (5) the exit openings. In particular, the model yielded predictions of both the discharge Mach number (exit speed divided by sound speed) and total discharge time (an important measurement because an extended discharge time would reduce the effectiveness of the system). Using the open area ratio (OAR) of the perforated sheets and the total discharge area as design parameters, we computed a response surface based on evaluating the sum of the peak discharge Mach number and the discharge time, as shown in the two-dimensional contour display in Fig. 4. Lower values on the color bar (green and below) in the figure are desirable for design considerations. The model suggests that larger discharge areas, together with perforation OARs between 0.1 and 0.5, will produce subsonic exit flow with a sufficiently short discharge time.

Simulator Results: We measured valve noise performance with the aluminum enclosure sealed with Sorbothane. The measurements demonstrate a 17.3 dBp reduction in solenoidal valve noise (Fig. 5). The peak noise of the unsealed solenoid valve of the simulator is significantly lower (14 dBp) than that of the squib valve shown in Fig. 1. The acoustics are assumed to be linear with reduction levels being independent of source level. We measured flow noise performance with different numbers of open exit tubes and two different OAR screens (59% and 25%). We found only a slight (0.8 dB) noise reduction resulting from the prototype manifold by itself with no screens and all tubes open. The most significant reductions came from using the 25% OAR screen, whereby we attained noise reduction

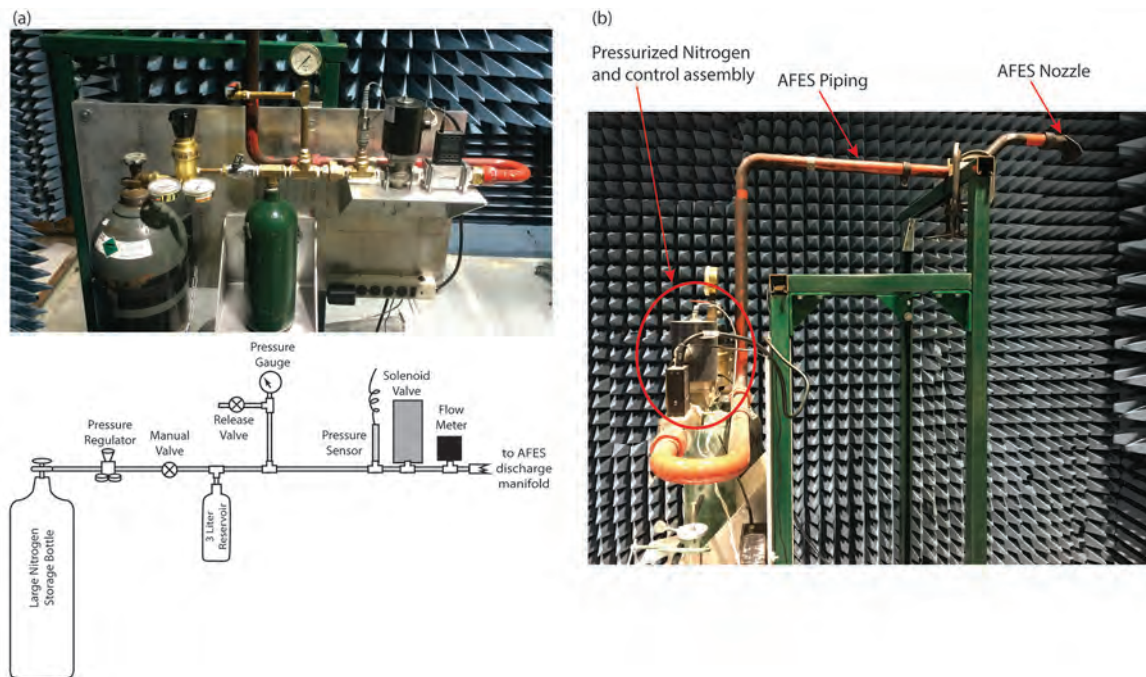


FIGURE 2 AFES laboratory simulator showing (a) nitrogen storage tanks with control assembly and (b) AFES piping with nozzle (same as that of an AFES installed in a Medium Tactical Vehicle Replacement (MTVR) truck).

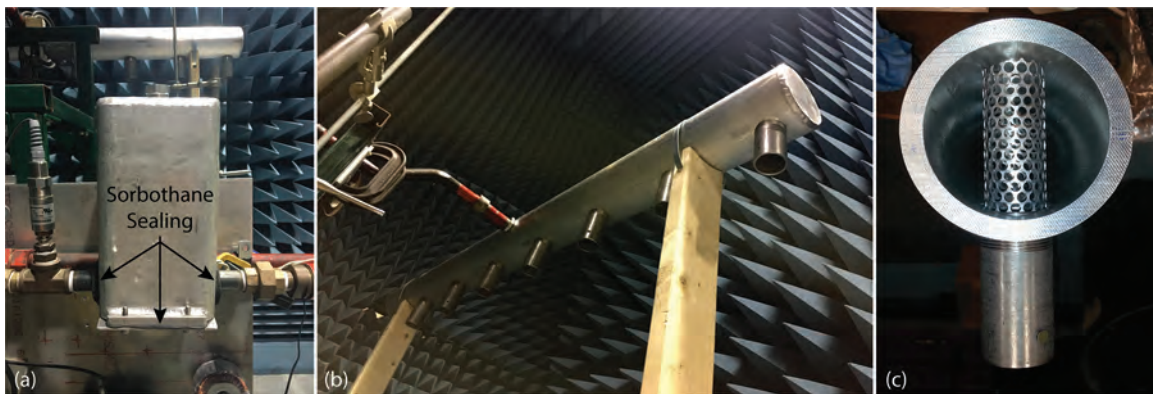


FIGURE 3 Detail on mitigation approaches: (a) valve enclosure, (b) prototype manifold with expansion volume, and (c) perforated sheets in prototype manifold (prior to welding end) and multiple exit nozzles.

of 11.5 dBP (Fig 5). The number of open exit tubes had relatively little effect on the peak noise measured, a result that does not match well with the model predictions. However, in evaluating the data, we have not yet completely considered distance attenuation effects associated with the location of open exit tube(s) and microphones.

Conclusions: Significant noise reductions in the AFES are achievable through combination of a carefully sealed valve enclosure and an increase in the flow resistance through the use of perforated sheets. The reduced noise levels fall within a decibel range considered to be

relatively safe, and setting the AFES noise threshold at this quieter decibel level could relieve concerns about hearing loss and eliminate the requirement for wearing hearing protection in the MTVR cabin. While the volume of our prototype manifold expansion is larger than practical due to the size constraints of the MTVR cabin, both experimentation and modeling suggest a relatively low dependence of the expansion volume on noise suppression, and, therefore, smaller volumetric systems will not significantly affect the noise reduction properties.

[Sponsored by PEO Land Systems, U.S. Marine Corps, through Giang (James) Pham]

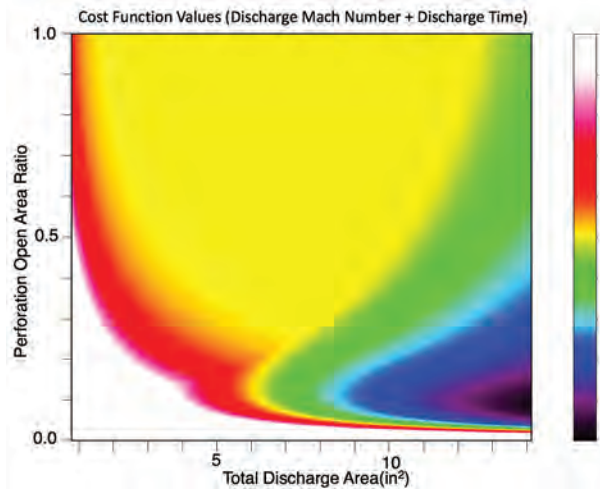


FIGURE 4 Model response function as a cost function for the prototype manifold design. Lower values (green and below) are desirable for design consideration.

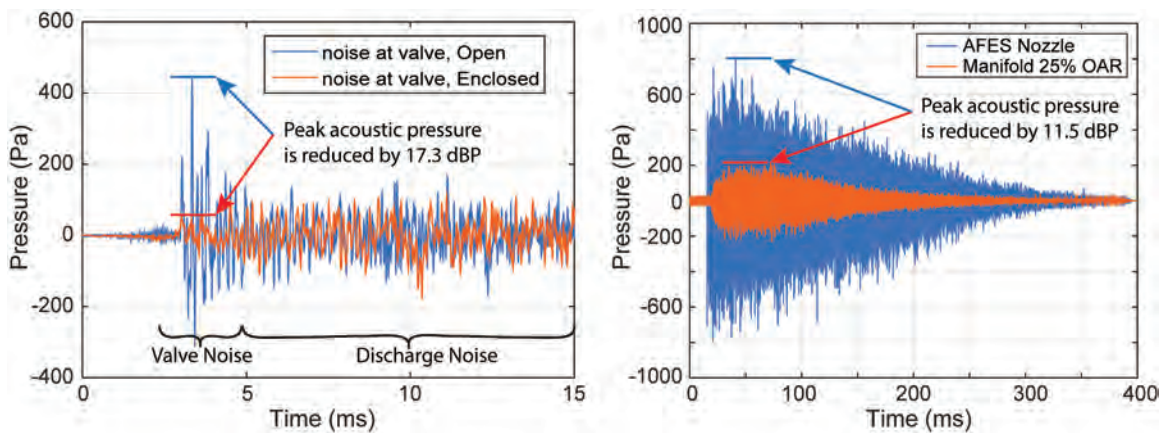


FIGURE 5 Performance results showing the reduction in acoustic peak levels of (a) valve noise using the enclosure (17.3 dBP reduction) as measured near the solenoid location and (b) flow noise using prototype manifold (11.5 dBP reduction) near the nozzle exit.

Reference

¹ A. Powell, "On the Mechanism of Choked Jet Noise," *Proc. Phys. Soc. B.* (1953).



Understanding the Influence of Disorder in Atomically Thin Materials

B.R. Matis, B.H. Houston, and J.W. Baldwin
Acoustics Division

Introduction: Disorder in atomically thin materials can originate from intrinsic and extrinsic sources and significantly affect fundamental material properties as well as limit overall device functionality. Controlling the disorder, therefore, offers the capability of systematically modifying material properties and enhancing device performance, a capability with clear advantages

to the development of technology. Here, we exemplify how controlled disorder influences the electronic and magnetotransport in three atomically thin materials: graphene, hydrogenated graphene, and molybdenum disulphide. Results of our study include modified expressions for the magnetoresistivity in spatially inhomogeneous materials, emergent spin glass formation in chemically modified materials, and favorably modified resonant tunneling device characteristics in materials with inhomogeneous charge distributions. The results have implications for advancing basic understanding of disorder in such materials and of two-dimensional magnetic materials, spintronics, resonant tunneling diodes, and high-frequency electronics.

Disorder Through Spatial Inhomogeneity: Prior to performing chemical modification, we study the transport properties of spatially inhomogeneous graphene (Fig. 6(a)), measuring a sample much longer (>1000 times) than the average crystallographic grain size.¹ We find that the magnetotransport is largely dependent on

charge disorder, similar to the case of single-crystal graphene. Figure 6(b) shows the percent change in the magnetoresistivity $\Delta\rho_{xx}/\rho_0$ as a function of magnetic field B for increasing electron carrier concentration n_e along with fittings to Eq. (1), where α and A are fitting parameters and μ represents carrier mobility.

$$\rho_{xx}(B) = \rho_{xx}(0) \left(1 - \alpha + \left[\frac{\alpha}{\sqrt{1 + 2A(\mu B)^2/\alpha}} \right] \right)^{-1} \quad (1)$$

Results of the fittings in Fig. 6(b) provide an expression for the dimensionless coefficient A , which is plotted in Fig. 6(c) versus n/n_{rms} where n_{rms} is the density fluctuations. The fit shown in Fig. 6(c) is expressed by Eq. (2), which represents a modified expression for the charge carrier density dependence of the magnetoresistivity with respect to the case of single-crystal graphene.

$$A = \left[\beta \left(\frac{n_0}{n_{rms}} \right) - \gamma \right]^\eta \quad (2)$$

Deviations in the functional form of A with respect to single-crystal graphene (where $\beta = 1/2$, $\gamma = 0$ and $\eta = -2$) is a result of the spatial disorder generated by the grain boundaries throughout the film, with β , γ and η determined by the extent of the spatial disorder.

Disorder Through Chemical Functionalization:

Hydrogenation of devices similar to the one shown in Fig. 6(a) results in magnetic moment formation as the hydrogen atoms covalently bond to the carbon atoms in graphene. For certain hydrogen concentrations, we find that the magnetic moments exhibit spin glass ordering, resulting in a new atomically thin fundamental magnetic system in which the random competition between ferromagnetic and antiferromagnetic exchange interactions gives way to a frustrated state with no long-range magnetic order.² In hydrogenated graphene, we observe two characteristic properties of canonical spin glasses: (1) logarithmic time-dependent relaxations in the remnant magnetoresistance following magnetic field sweeps (Fig. 7(a), observed in resistivity measurements as a function of time) and (2) strong variances in the remnant magnetoresistance following field-cooled and zero-field-cooled scenarios (Fig. 7(b), observed in resistivity measurements while cooling to cryogenic temperatures with and without magnetic fields). Measurements as a function of hydrogen concentration (Fig. 7(c)) reveal that the critical magnetic dopant density required to observe spin glass formation in two-dimensions via magnetotransport is the density that results in $\rho(B=0) \sim h/2e^2$, which is the quantum unit of resistivity where h is Planck's constant and e the fundamental unit of electric charge, corresponding to the point at which the system undergoes a transition from weak to strong localization.

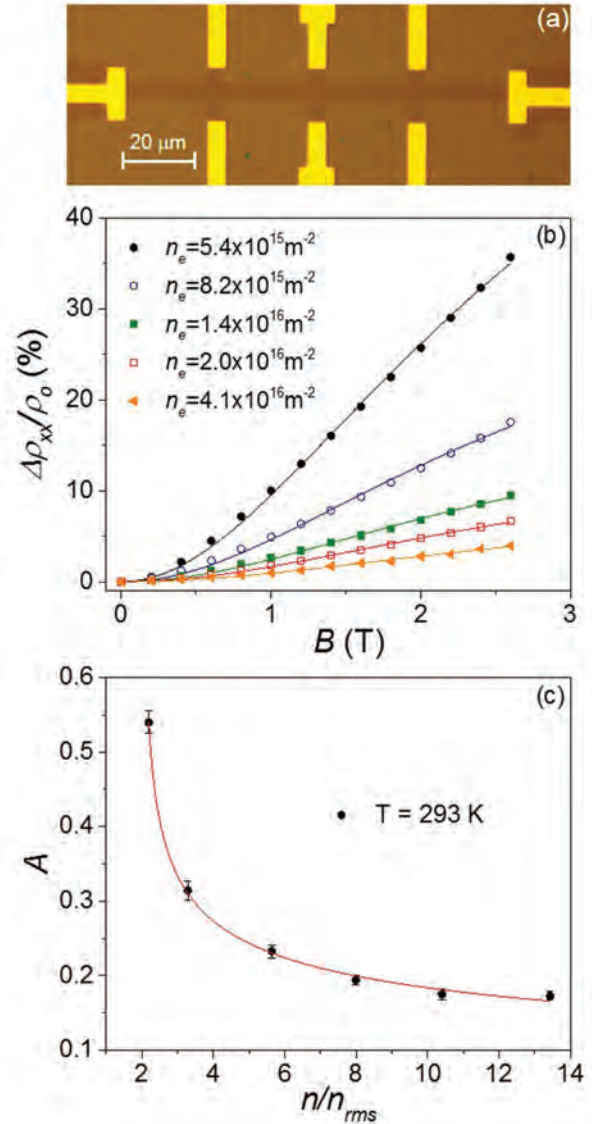


FIGURE 6 (a) Optical image of a graphene Hall bar. Light regions are Cr/Au contacts. The brown background is the SiO_2 substrate. (b) Percent change in the magnetoresistivity $\Delta\rho_{xx}/\rho_0$ as a function of magnetic field B at temperature $T = 293$ K for increasing electron concentration n_e . The solid lines are fits to Eq. (1). (c) Dimensionless magnetoresistive coefficient, A , as a function of the ratio between charge carrier density n and density fluctuations n_{rms} . The solid line is a fit to Eq. (2).

Disorder Through Inhomogeneous Charge Distributions: The strict two-dimensionality of atomically thin materials makes the transport in such materials highly susceptible to effects of the local environment. Previous studies in the literature have taken advantage of this susceptibility by using dielectric engineering as a way to favorably modify MoS_2 material quality and device performance within the metallic transport regime.^{3,4} Our studies demonstrate that such dielectric

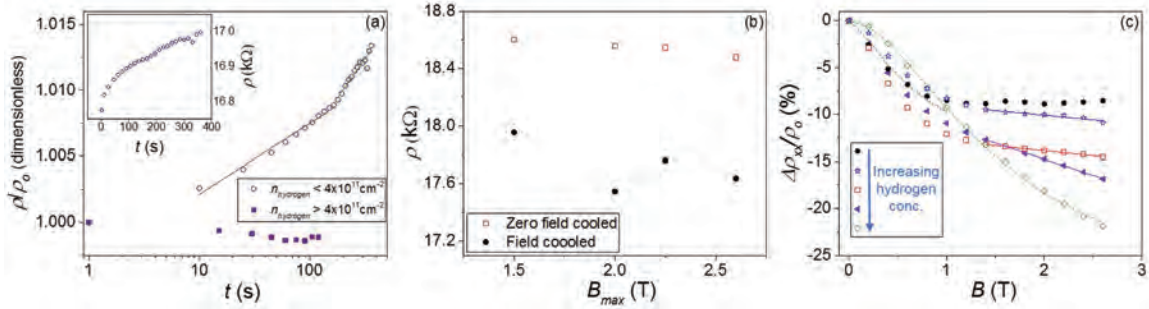


FIGURE 7
 (a) Normalized resistivity ρ/ρ_0 as a function of time t at temperature $T = 4.2$ K and at the Dirac point for two devices with different hydrogen concentrations n_{hydrogen} following a magnetic field B sweep from 2.6 T to 0 T. The solid lines are linear fits to the data. The inset shows the bare resistivity ρ as a function of time t for the device with a lower hydrogen concentration. (b) Measured resistivity ρ as a function of maximum set field B_{max} for the different cooling procedures for a separate hydrogenated device. (c) Percent change in the magnetoresistivity $\Delta\rho_{xx}/\rho_0$ versus B at the Dirac point and at $T = 4.2$ K for increasing hydrogen concentration. The dashed lines are fits to a localization theory for graphene for the lowest and highest hydrogen concentrations (solid black circles and open green diamonds, respectively). Solid lines are linear fits to the high- B data for intermediate hydrogen concentrations, where we measure spin glass behavior.

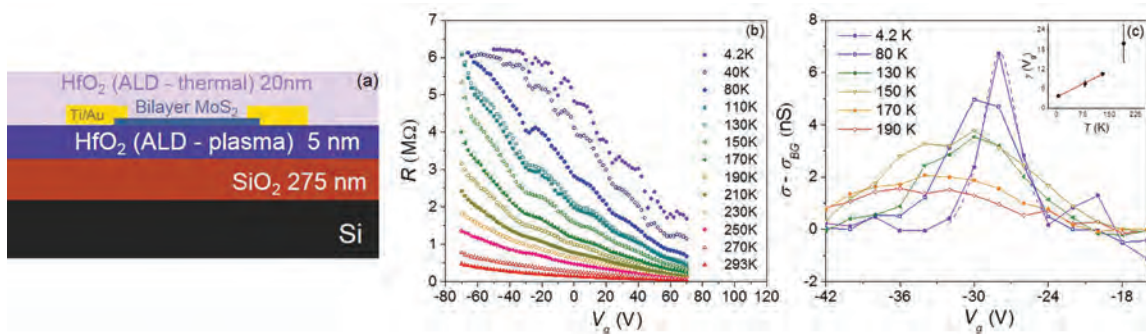


FIGURE 8
 (a) Schematic of a bilayer MoS_2 transistor encapsulated in ALD-grown HfO_2 . (b) Resistance R as a function of back-gate voltage V_g at varying temperature T determined by measuring the drain current I under an applied bias voltage $V_{SD} = 632$ μV AC. (c) Conductivity σ with a background conductivity σ_{BG} subtracted as a function of V_g at varying T for the most well isolated peak (lowest V_g) from (b). The dashed line is a fit of the $T = 4.2$ K data set to a Lorentzian lineshape (expected for resonant tunneling). Inset: experimentally observed full width at half maximum $\gamma(V_g)$ as a function of T . The solid red line is a linear fit to the data for $T \leq 130$ K.

engineering can also favorably modify material and device performance in the insulating regime where the transport occurs via tunneling through localized states formed from trapped charges residing in the nearby dielectric (which provides for the inhomogeneous charge distribution within the MoS_2).⁵

The device architecture used for our experiments is shown in Fig. 8(a), in which the high- κ dielectric HfO_2 ($\kappa = 25$) encapsulates a bilayer MoS_2 transistor. Measurements of device resistance R as a function of back-gate voltage V_g (and therefore charge carrier density n : $n \propto Vg$), shown in Fig. 8(b), demonstrate clear nonmonotonic behavior at low temperatures, which results from resonant tunneling through spatially isolated states. The temperature dependence of the most well isolated resonance, shown in Fig. 8(c), indicates that the tunneling processes are observable up to $T \sim 190$ K, which represents a factor of 6 increase in operating temperatures for resonant tunneling processes with respect to MoS_2 on the more commonly used SiO_2

substrate ($\kappa = 3.9$). The presence of the HfO_2 modifies the screening length of the charge carriers in the MoS_2 , which results in a more localized trapping potential across the charge distribution landscape and subsequent higher operating temperatures for resonant tunneling processes. Estimates of the tunneling time give $t \sim 1.2$ ps corresponding to a frequency $f \sim 0.84$ THz. Results of our studies suggest that interface engineering may be a macroscopic tool for controlling quantum transport in such materials and for increasing the operating temperatures for resonant-tunneling devices derived from such materials. Possible applications of these findings include high-frequency electronics and logic devices.

[Sponsored by ONR]

References

- 1 B.R. Matis, B.H. Houston, and J. W. Baldwin, "Influence of Spatial Inhomogeneity on Electronic and Magnetotransport in Graphene," *Phys. Rev. B* **91**, 205406 (2015).

- ² B.R. Matis, B.H. Houston, and J.W. Baldwin, “Evidence for Spin Glass Ordering near the Weak to Strong Localization Transition in Hydrogenated Graphene,” *ACS Nano* **10**, 4857–4862 (2016).
- ³ B. Radisavljevic and A. Kis, “Mobility Engineering and a Metal-Insulator Transition in Monolayer MoS₂,” *Nat. Mater.* **12**, 815–820 (2013).
- ⁴ X. Cui, G.-H. Lee, Y.D. Kim, G. Arefe, P.Y. Huang, C.-H. Lee, D.A. Chenet, X. Zhang, L. Wang, F. Ye, F. Pizzocchero, B.S. Jessen, K. Watanabe, T. Taniguchi, D.A. Muller, T. Low, P. Kim, and J. Hone, “Multi-Terminal Transport Measurements of MoS₂ Using a van der Waals Heterostructure Device Platform,” *Nat. Nanotechnol.* **10**, 534–540 (2015).
- ⁵ B.R. Matis, N.Y. Garces, E.R. Cleveland, B.H. Houston, and J.W. Baldwin, “Electronic Transport in Bilayer MoS₂ Encapsulated in HfO₂,” *ACS Appl. Mater. Interfaces* **9**, 27995–28001 (2017).



A Mixture Theory Based Approach to Poroacoustics

P.M. Jordan
Acoustics Division

Introduction: Poroacoustic, i.e., acoustic propagation in porous media, is one of the best known examples of a multi-phase flow. For decades, researchers have formulated and used continuum-based mathematical models, i.e., models involving partial differential equations, to describe this type of acoustic phenomena. The key feature that distinguishes these models from each other is the “drag law” that the modeler assumes. This term refers to the mathematical relation—what physicists call a constitutive relation—that describes the impact the solid phase (i.e., the porous matrix) has on the motion of the fluid which permeates it. One recent drag law that has been proposed is the so-called Jordan–Darcy–Cattaneo (JDC) law, namely,

$$\mu\chi K^{-1}(\tau D \mathbf{v}/Dt + \mathbf{v}) = -\text{grad}(P).$$

Here, the vector \mathbf{v} is the average velocity of the fluid; $\text{grad}(P)$ is the pressure gradient; t is time; μ is the fluid’s shear viscosity, K and χ are assumed constant and denote the porosity and permeability, respectively, of the porous solid; τ is the relaxation time parameter of the physical system; and the operator D/Dt represents a specific Lie derivative. The JDC law reduces to the classical drag law known as Darcy’s law on letting τ go to zero.

In 2013, Ciarletta et al.¹ investigated the behavior of poroacoustic acceleration waves, i.e., propagating surfaces across which the first derivatives of the acoustic field variables exhibit a jump discontinuity, using the JDC law as their drag law. Unfortunately, these authors were unable to recover the results generated by the

Darcy-based system, as they should have been able to do, because their solutions broke down when attempting to take the limit $\tau \rightarrow 0$.

Obtaining a Realistic Model: In 2016, Jordan et al.² revisited this problem. By basing their formulation on Mixture theory, as opposed to (incorrectly) treating the JDC law as the flow’s momentum equation, as was the case in Ciarletta et al.,¹ Jordan et al. obtained a physically realistic poroacoustic model that includes relaxation effects via its use of the JDC law. According to Mixture theory, the left-hand side of the JDC law is correctly regarded as an “interaction term” and is inserted on the right-hand side of the usual Euler momentum equation. Using this approach, Jordan et al. were able to formulate a (nonlinear) system of equations for the acoustic field whose solutions exhibit the required behavior when the limit $\tau \rightarrow 0$ is taken. Through their analysis, Jordan and his coauthors found that, because of the parameter, τ , their JDC-based system predicts that poroacoustic waves admit a slightly lower sound speed than (usual) sound waves propagating in unobstructed domains. They also determined (i) a critical amplitude value for poroacoustic acceleration waves; (ii) showed that certain poroacoustic traveling wave profiles develop a jump discontinuity under the JDC law as the speed at which the traveling wave propagates approaches the poroacoustic sound speed; and (iii) established that, because it includes the effects of relaxation (via τ), the traveling wave acceleration profile under the JDC law is always bounded.

Figure 9 illustrates the formation of a discontinuity in the traveling wave acceleration profile under the JDC-based model developed in Jordan et al.² As the speed at which the waveform propagates approaches the (above noted) poroacoustic sound speed, the red curves transform from being smooth (shown in (a)) to exhibiting a vertical step (i.e., jump discontinuity) (shown in (d)).

Conclusion: The means by which this work came to be performed highlights the need for the continuous re-examination and scrutiny of the scientific literature, both to correct errors and to extract new and deeper insight from existing works. Furthermore, this investigation not only provides researchers with a rigorously derived, relatively simple model, which captures the salient physics associated with nonlinear poroacoustic phenomena in a large class of technologically important media, but also hints at the potential benefits of applying new/generalized theories to acoustic modeling. Refinements to existing Navy models and unanticipated findings/applications are possibilities which could be realized.

[Sponsored by the NRL Base Program (CNR funded)]

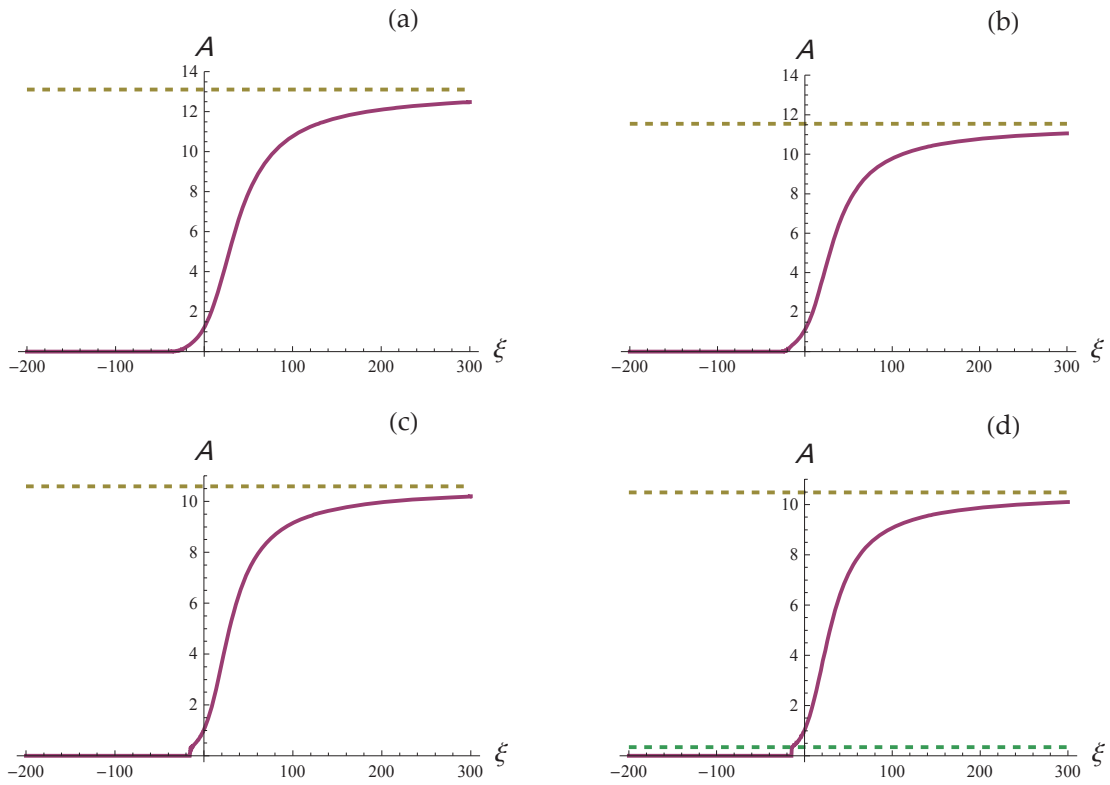


FIGURE 9
 Red curves: traveling wave acceleration profile; Gold line: upper bounding value (see (iii)) to which the acceleration profile tends to as $\xi \rightarrow \infty$; Green line: critical amplitude value noted in (ii). Here, A and ξ are the dependent (i.e., acceleration) and independent variables, respectively.

References

¹ M. Ciarletta, B. Straughan, and V. Zampoli, “Poroacoustic Acceleration Waves in a Jordan-Darcy-Cattaneo Material,” *Int. J. Non-Linear Mech.* **52**, 8–11 (2013).
² P. M. Jordan, F. Passarella, and V. Tibullo, “Poroacoustic Waves under a Mixture-Theoretic Based Reformulation of the Jordan-Darcy-Cattaneo Model,” *Wave Motion* (<http://dx.doi.org/10.1016/j.wavemoti.2016.07.014>).



- 116** Understanding Intense Pyroconvection and Its Impacts
- 118** Seeding the Wave Guide
- 120** Aerosol and Cloud Research in the South China Sea

Understanding Intense Pyroconvection and its Impacts

D.A. Peterson,¹ M.D. Fromm,² E.J. Hyer,¹
J.R. Campbell,¹ M.L. Surratt,¹ and J.E. Solbrig³

¹Marine Meteorology Division

²Remote Sensing Division

³Cooperative Institute for Research in the Atmosphere

Introduction and Motivation: Large smoke plumes from wildfires often become capped by cumulus clouds, which enhance the vertical lofting of smoke particles through heating and increased buoyancy. Under certain conditions, this moist “pyroconvection” mechanism allows these infant smoke clouds to mature into larger fire-triggered thunderstorms, known as pyrocumulonimbus (or pyroCb). The typical pyroCb life cycle involves initiation in mid-afternoon and termination a few hours after sunset. The deep convective column (Fig. 1) provides an efficient method for lofting smoke particles well into the upper troposphere, approaching or exceeding aircraft cruising altitudes. The large quantity of smoke within a pyroCb induces a shift toward smaller cloud droplets and ice particles, resulting from an overabundance of aerosol particles fighting for available water vapor. This suppresses precipitation and increases the lifetime of pyroCb outflow at the top of the troposphere, drastically enhancing downwind smoke transport.

Intense pyroCb activity can also inject a significant amount of aerosol mass into the lower stratosphere, occasionally exceeding 20 kilometers. At these altitudes, aerosol particles can persist for even longer durations, allowing for gradual spread over hemispheric scales. Studies of explosive volcanic eruptions highlight the effects of stratospheric aerosol particles on regional and global climate. However, several stratospheric aerosol



FIGURE 1
Intense pyrocumulonimbus cloud (smoke-induced thunderstorm; pyroCb) observed in Colorado during June 2013. Image available at: <http://www.ssec.wisc.edu/news/articles/4152>.

layers, previously presumed to be of volcanic origin, have recently been reclassified as originating from pyroCb activity. PyroCb events are also much more common than large volcanic events, and originate almost exclusively in the mid and upper-latitude forests of North America, Asia, and Australia during local summertime burning seasons. PyroCb are therefore highly relevant for understanding aerosol mass loading in the upper troposphere and lower stratosphere (UTLS), including potential impacts on global climate.

Detection and Inventory: The U.S. Naval Research Laboratory (NRL) was the first institution to identify pyroCb intrusions into the UTLS, and the first to conceptualize potential impacts. Nearly two decades of research has now culminated in a novel automated algorithm that systematically detects pyroCb in near-real-time based on geostationary weather satellites,¹ which provide coverage several times per hour over the majority of pyroCb-prone regions worldwide. The algorithm produces both imagery and statistical outputs. Additional research demonstrates potential for a fully automated alert system that detects and inventories extreme weather, including pyroCb, and issues warnings to Navy users, integrating near-real-time satellite data and model forecasts.

The NRL pyroCb algorithm first identifies deep convection (thunderstorms) near active fires, distinguishing between low-level and UTLS aerosol injections. During daytime, unique pyroCb plume microphysical properties are characterized by a medium-wave brightness temperature (4 μm) that is significantly larger than at longer wavelengths (11 μm), allowing pyroCb to be distinguished relative to other deep convective clouds. A cloud opacity test reduces potential false detections. The algorithm successfully captures individual intense pyroCb events, pyroCb embedded within traditional convection, and multiple, short-lived pulses of pyroCb activity. This algorithm therefore provides useful information for improved forecasting of smoke transport, visibility, and impacts on electro-optical (EO) propagation.

Application of the pyroCb detection algorithm to 88 intense wildfires observed in western North America during the 2013 fire season (June–August) provided an inventory of 26 pyroCb events. This inventory also includes 31 individual pulses of intense pyroCb activity, all of which were capable of injecting smoke into the UTLS. Figure 2 shows an example of an event with three distinct convective cloud outflow regions (anvil clouds) exhibiting pyroCb microphysical cloud properties downwind from the New Mexico Silver Fire on 28 June 2013. Red shading highlights the active pyroCb updraft region, while blue and green shading indicates earlier pyroCb pulses that were each detected in previous scenes.

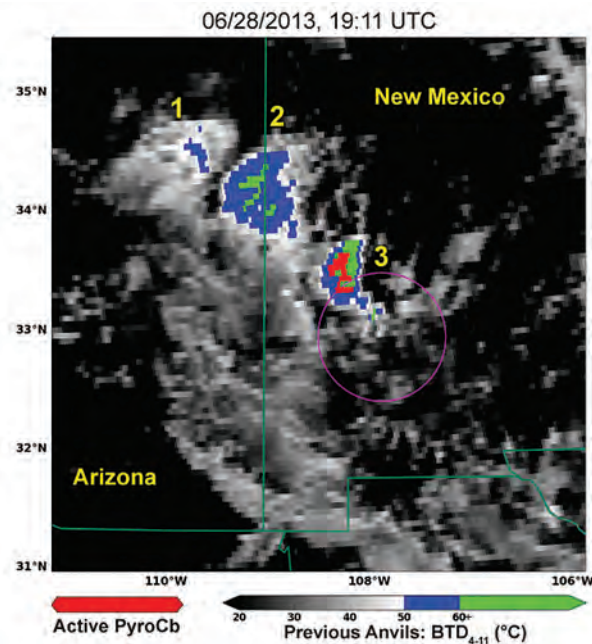


FIGURE 2
Multiple-pulse pyroCb event observed during the New Mexico Silver Fire on June 28, 2013. Red shading indicates active pyroCb pixels. Blue and green shading indicates the unique cloud microphysical properties of previous pyroCb anvils, highlighted by the 4 and 11 μm brightness temperature difference ($\text{BTD}_{4,11}$). Pink circle indicates a 60-kilometer quantitative detection radius.

Conceptual Model for Development: The 2013 pyroCb inventory was employed, in combination with meteorological reanalysis data, to construct the first conceptual model for pyroCb development (Fig. 3). One of the key components of this model is a deep, dry, and unstable near-surface mixed layer (allowing for hot, dry, and windy conditions that sustain large fires) surmounted by a moist and unstable mid-tropospheric layer, which is typical of relatively “dry” thunderstorms found over elevated terrain in semi-arid regions.^{2,3} Variation in topography and thermal buoyancy produced by intense fire activity are also key factors in pyroCb development. Periods of intense burning that fail to produce pyroCb activity usually lack a mid-tropospheric moisture source, which is the strongest selector for pyroCb development in the conceptual model.

Conditions driving pyroCb development were shown to be fundamentally different from other severe weather events, including supercell thunderstorms and associated tornado outbreaks. This suggests that the pyroCb conceptual model does not describe the most favorable environment for deep, overshooting convective cloud tops. However, it is the only meteorological environment that will support intense fire activity occurring at the same time as deep, moist convection. The pyroCb conceptual model therefore reconciles the most efficient mechanism for injecting large quantities

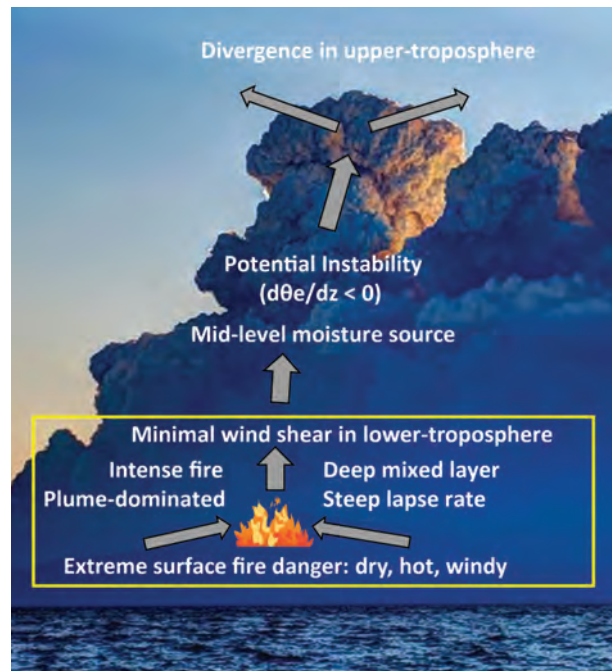


FIGURE 3
Schematic of a meteorology-based conceptual model for development of pyroCb activity. Yellow box indicates processes occurring at the surface and within the near-surface mixed layer. Background photo (via the National Weather Service in Sacramento, California) shows development of deep pyroconvection near Lake Tahoe during the 2014 King Fire (photo is available at <http://wildfiretoday.com/2014/09/14/california-king-fire-near-pollock-pines/>).

of aerosol particles into the UTLS, aside from volcanic eruptions.

Conclusions: Meteorological conditions favorable for pyroCb are often observed in several highly fire-prone regions worldwide. This implies that pyroCb, far from the niche phenomenon they initially appeared to be, are very likely significant features of regional summer climate. Annually recurring pyroCb events may therefore represent a new and potentially significant modulator of the lower stratospheric aerosol layer, with a potential impact on global climate and circulation.

Acknowledgements: This research was performed while David Peterson held a National Research Council Research Associateship Award at the NRL Marine Meteorology Division (Monterey, Calif.). Imagery products using the methods described in this article are posted in near-real-time at the NRL pyroCb website: <http://www.nrlmry.navy.mil/pyrocb-bin/pyrocb.cgi>. [Sponsored by the NRL Base Program (CNR funded)]

References

¹ D.A. Peterson, M.D. Fromm, J.E. Solbrig, E.J. Hyer, M.L. Surratt, and J.R. Campbell, “Detection and Inventory of Intense Pyro-

convection in Western North America Using GOES-15 Daytime Infrared Data,” *J. Appl. Meteorol. Clim.* **56**, 471–493 (2017).

² D.A. Peterson, E.J. Hyer, J.R. Campbell, M.D. Fromm, J.W. Hair, C.F. Butler, and M.A. Fenn, “THE 2013 RIM FIRE Implications for Predicting Extreme Fire Spread, Pyroconvection, and Smoke Emissions,” *Bull. Am. Meteor. Soc.* **96**, 229–247 (2015).

³ D.A. Peterson, E.J. Hyer, J.R. Campbell, J.E. Solbrig, and M.D. Fromm, “A Conceptual Model for Development of Intense Pyroconvection in Western North America,” *Mon. Weather Rev.* **45**, 2235–2255 (2017).



Seeding the Wave Guide

J.D. Doyle,¹ C.A. Reynolds,¹ and S.D. Eckermann²

¹*Marine Meteorology Division*

²*Space Science Division*

Introduction: The forecast skill of operational numerical weather prediction models has significantly improved over the past several decades. However, large errors still occur frequently in forecasts of high-impact weather (and related ocean surface waves) that can have a major influence on Navy operations (e.g., ship and aircraft routing, sea basing, resource protection, safety) and society in general (e.g., loss of life and property). The longstanding challenge to predicting these high-impact weather events is that they are often inherently linked to the jet stream or, more specifically, atmospheric waveguides associated with sharp boundaries between stratospheric and tropospheric air and characterized by regions of instability and rapid forecast error growth. The “seeds” for these poorly predicted high-impact weather events in the troposphere and stratosphere are closely related to the nature of the weather disturbances that act to perturb the waveguide. These waveguide seeds can amplify and propagate downstream, and associated growing errors can cause large forecast failures or “busts.” In this project, new observations and emerging modeling techniques are used in tandem—an approach used for the first time ever anywhere—to improve the prediction of these high-impact weather events.

Project Background: Emerging research from the U.S. Naval Research Laboratory’s base-funded program highlights the significance of diabatic processes (in which energy is added to or removed from the system due to such factors as radiation, latent heating due to phase changes, or turbulent mixing) that perturb the waveguide along sloping frontal regions.¹ The research also highlights the potential impact of the extratropical transition of tropical cyclones,² the part of the cyclone lifecycle that can lead to strong baroclinic develop-

ment in the waveguide and, in some conditions, launch deep propagating planetary and gravity waves into the stratosphere.³ In this project, we used state-of-the-science observations from the North Atlantic Waveguide and Downstream Impact Experiment (NAWDEX) and emerging NRL modeling techniques to quantify the factors that limit our ability to accurately predict high-impact events.

Methods: NAWDEX employed four different research aircraft (including the German High Altitude and Long Range Research Aircraft [HALO]) equipped with instruments to observe profiles of wind, temperature, moisture, and clouds. During NAWDEX, the Navy’s Coupled Ocean/Atmosphere Mesoscale Prediction System (COAMPS®) forecast and adjoint models^{1,2} were run in real time, and used to compute the forecast sensitivity to the initial state. These regions of high sensitivity were targeted for additional observations. The adjoint—which technically is the transpose of the forward tangent propagator of the forecast model—allows one to find the sensitivity of a particular forecast output to changes in the initial state in a mathematically rigorous and computationally feasible manner.^{1,2}

Observations: During NAWDEX Intensive Observing Period 5, strong transport of moisture was observed upstream of a high-impact weather event that caused heavy precipitation in southern Scandinavia, with accumulated precipitation of over 100 millimeters in a 72-hour period occurring in conjunction with a developing cyclone. Observations taken during this case are unique as the moist air masses that typically originate in the subtropics are difficult to reach even with a long-range aircraft. We applied the COAMPS adjoint in real time to provide forecast sensitivity products to guide the aircraft into key regions that may act as “seeds” for the waveguide.

In the example shown in Fig. 4, the COAMPS water vapor at the forecast initial time of 00Z 28 September 2016 is shown by the gray shading at 850 hPa (about 1.5 kilometers above mean sea level). A plume of water vapor is apparent traversing from the subtropical regions extending northeastward to just west of the United Kingdom. A response function region is shown by the blue box over Scandinavia in the region of observed heavy precipitation. The sensitivity of the 48-hour forecast rainfall in the blue box to the initial water vapor at 850 hPa is shown in Fig. 4 in the red and blue contours. A positive (negative) sensitivity region implies that an increase (decrease) of water vapor in these areas will increase the rainfall in the response function box. The HALO aircraft sampled this region of moisture sensitivity (its track is shown by the green line in Fig. 4). The HALO was equipped with the Water Vapor

850-hPa q_v (gray) 48-h q_v sensitivity

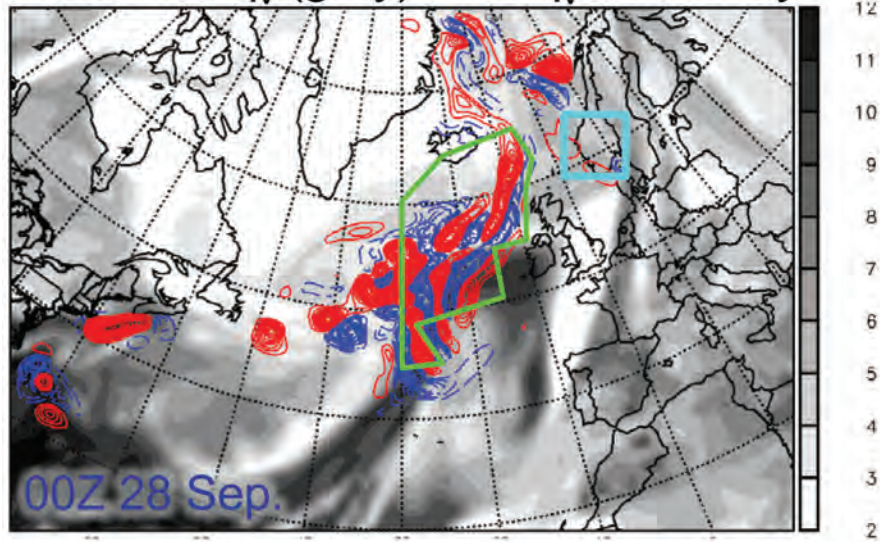


FIGURE 4
COAMPS forecast initial-time 850-hPa water vapor (gray shading) and the sensitivity of the 48-hour forecast rainfall in the blue box to the initial 850-hPa water vapor (red and blue contours), valid at 00Z 28 September 2016. The HALO aircraft track is shown by the green line.

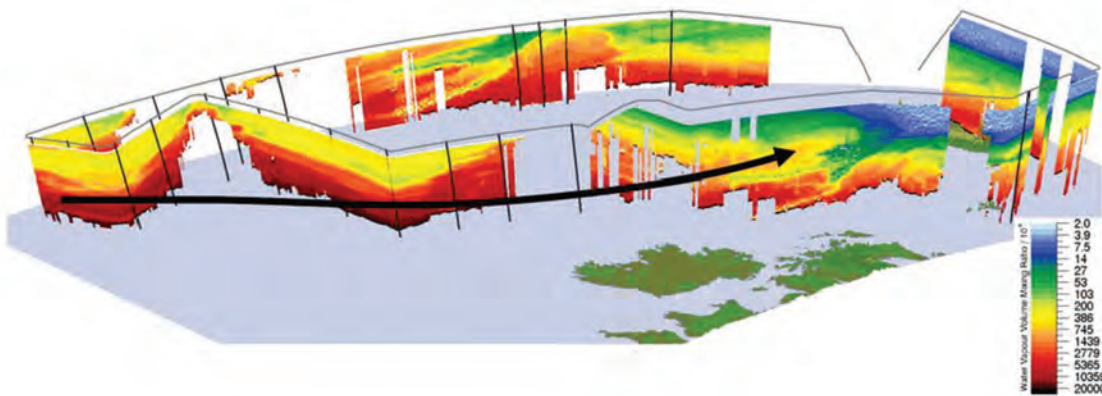


FIGURE 5
Water vapor volume mixing ratio (ppm) from WALES along the HALO flight path (courtesy of Martin Wirth, German Aerospace Center [DLR]) shown in Fig. 4.

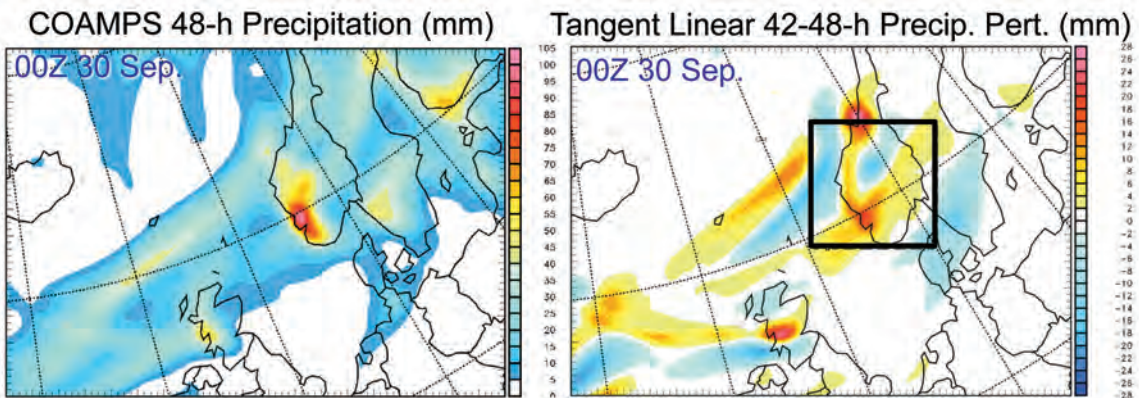


FIGURE 6
COAMPS 48-hour forecast precipitation (mm) valid at 00Z 30 September 2016 (left-hand panel). Precipitation differences (mm) in the 48-hour forecast obtained by adding small adjoint-based perturbations to the analysis (right-hand panel).

Lidar Experiment in Space (WALES) high spectral resolution and water vapor differential absorption lidar. Figure 5 shows the water vapor volume mixing ratio from WALES along the flight path in Fig. 4. Regions of large moisture sensitivity are coincident with the regions of high water vapor, particularly on the western and southern portion of the flight path.

The adjoint results illustrate how small changes in the water vapor in these sensitive regions will result in relatively large changes in the precipitation. For example, the total forecast precipitation after 48 hours (Fig. 6, left-hand panel) indicates over 100 millimeters of rainfall was forecast in southwestern Norway, similar to the observations. Adding small perturbations to the wind, moisture, and temperature sensitivity regions, with maximum moisture perturbations of 1 g kg^{-1} , results in an additional 30 millimeters of precipitation over southwestern Norway near the precipitation maximum.

Conclusion: The new observation of water vapor (such as shown in Fig. 5) in these sensitive regions will greatly help us understand what limits our forecast skill of high impact events, and ultimately will lead to improved short-term environmental forecasts of winds and precipitation in littoral regions to support Department of Defense missions. Studies are ongoing to better understand the fundamental nature of waveguide seeds and how they may influence predictability of high-impact weather using adjoint-based tools and these innovative observations.

Acknowledgments: The research is supported by the Chief of Naval Research through the NRL Base Program, PE 0601153N, and we also acknowledge the NRL Platform Support Program. We acknowledge the support and collaboration of the participants of the NAWDEX field program and Waves to Weather initiative. We also appreciate support for computational resources through a grant of Department of Defense High Performance Computing time from the DoD Supercomputing Resource Center at Stennis, Mississippi, and Vicksburg, Mississippi. COAMPS® is a registered trademark of the U.S. Naval Research Laboratory.
[Sponsored by the NRL Base Program (CNR funded)]

References

- ¹ J.D. Doyle, C. Amerault, C.A. Reynolds, and P. Alex Reinecke, "Initial Condition Sensitivity and Predictability of a Severe Extratropical Cyclone Using a Moist Adjoint," *Mon. Weather Rev.* **142**, 320–342 (2014).
- ² J.D. Doyle, C.A. Reynolds, and C. Amerault, "Diagnosing Tropical Cyclone Sensitivity," *Comp. Sci. Eng.* **13**, 31–39 (2011).
- ³ S.D. Eckermann and D.L. Wu, "Satellite Detection of Orographic Gravity-Wave Activity in the Winter Subtropical Stratosphere over Australia and Africa," *Geophys. Res. Lett.* **39**, L21807, doi:10.1029/2012GL053791 (2012).

Aerosol and Cloud Research in the South China Sea

J.S. Reid, E.J. Hyer, P. Xian, J.R. Campbell, E. Reid, A. Bucholtz, and A. Walker
Marine Meteorology Division

Introduction: In 2016, the Marine Meteorology Division (Monterey, Calif.) of the U.S. Naval Research Laboratory (NRL) completed a seven-year effort to perform the first comprehensive characterization of the aerosol and cloud environment of Southeast Asia and the South China Sea (SCS). From 2009 through 2016, in collaboration with Southeast Asia regional science partners (in Malaysia, the Philippines, Singapore, Taiwan, and Vietnam), NRL scientists helped lead a series of significant field observatory deployments as part of the 7 Southeast Asia Studies (7SEAS) program. The SCS in particular is economically important to the countries surrounding it and to the United States. For at least the past decade, and beginning long before geopolitical tensions had accelerated in the region over the SCS's Spratly Islands, NRL has been forging international research partnerships to better understand the region's atmospheric and oceanic environment.

Complex Environments, Interconnected Weather: Attention to the region is well warranted by Navy scientists, as peninsular Southeast Asia (e.g., Cambodia, Laos, Myanmar, Thailand, and Vietnam) and the Maritime Continent (East Timor, Indonesia, Malaysia, Philippines, and Singapore) include some of the world's most complex meteorological, oceanographic, and terrestrial environments, along with areas of very high population density. The weather of the United States is often connected to the global weather patterns of Southeast Asia. Moreover, the impact of biomass burning and pollution is of considerable concern to climate scientists, and data from the 7SEAS field studies will help NRL scientists understand more about the impact on the region's air quality, visibility, electro-optical (EO) propagation, cloud cover, precipitation, and meteorology.

The SCS can host both heavily polluted and near-pristine environments—and sometimes the two different kinds of environments can exist nearly side by side, as close as only a few hundred kilometers apart (Fig. 7).¹ But the complex meteorology and thick cirrus cloud coverage are challenges to environmental modeling and remote sensing systems. For applications ranging from EO propagation to climate change, the fundamentals of the SCS aerosol and cloud system before 7SEAS had only superficially been known.



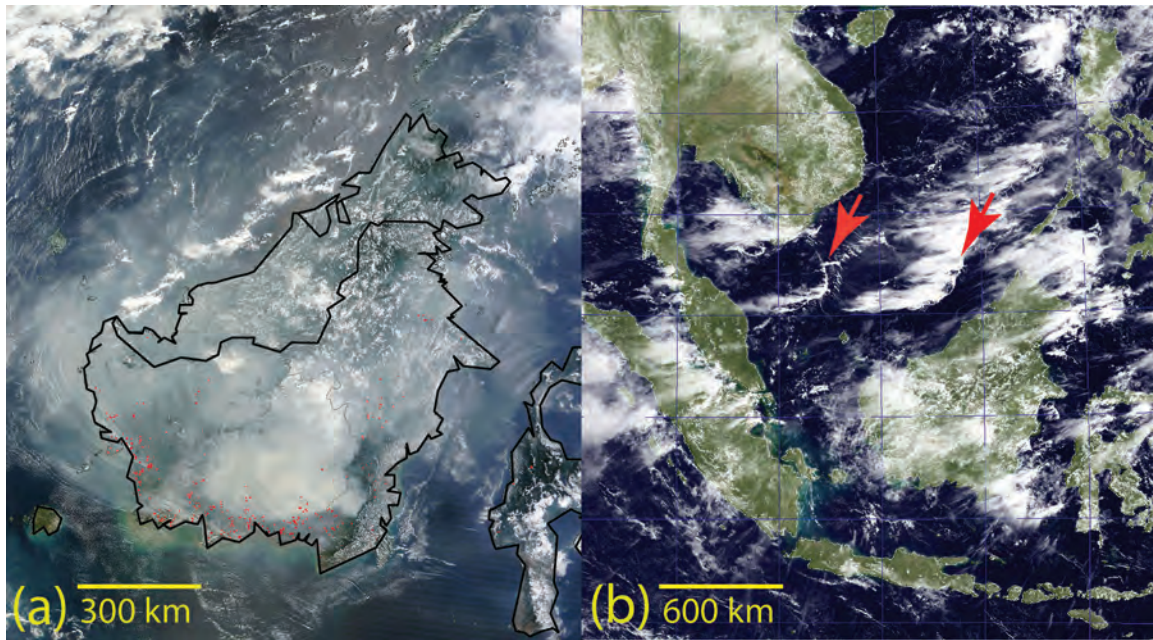


FIGURE 7
 (a) Terra MODIS RGB image of a severe biomass burning event on the island of Borneo (Sept. 10, 2015) that brought visibility to as low as 1 kilometer. (b) MTSAT false RGB image of squall lines 400 to 600 kilometers long but only 15 kilometers wide, propagating across the South China Sea (Sept. 18, 2011).

Field Studies on the Aerosol Lifecycle: Field studies under the 7SEAS program aimed to improve fundamental understanding of aerosol lifecycle in Southeast Asia and the SCS (e.g., emissions, transport, fate and ultimately meteorological impact). NRL initiated the 7SEAS program as a seven-year joint venture between NRL, NASA, Office of Naval Research Global (ONRG), and Taiwan, with researchers and students in seven Southeast Asia countries (Hong Kong/PRC, Indonesia, Malaysia, Philippines, Singapore, Thailand, and Vietnam). The 7SEAS field investigations helped researchers develop enhanced data collaboration in a region lacking fundamental data needed to monitor its dynamic aerosol and cloud environment. At the core of 7SEAS was the question, To what extent do aerosol particles influence weather and climate? To answer the question, NRL researchers coordinated the integration of seven areas of oceanographic and atmospheric investigation: (1) aerosol lifecycle and air quality, (2) tropical meteorology, (3) radiation and heat balance, (4) clouds and precipitation, (5) land processes and fire, (6) physical and biological oceanography, and (7) environmental characterization through satellite analyses, model predictions, and verification. These areas of investigation were explored between scientists at a grass roots level in an open and cooperative manner.

The work of NRL scientists engaged in 7SEAS field studies spanned a spectrum of interests, including hypotheses on relationships between aerosol particles, clouds, precipitation, and the overall meteorological

environment as well as practical technological development and assessments for improving space-based monitoring and prediction of aerosol lifecycle and effects. NRL led the integration of data into publically available data portals and followed this work with an assessment of the operability and performance of the region’s remote sensing capabilities and models as well as feedback on improving these systems. NRL formed lasting partnerships with both domestic and regional science institutions and supervised intensive data collection both on NRL-led campaigns and on sites managed by 7SEAS partners: four campaigns in Singapore, two in the Philippines, two in Vietnam, and one each in Malaysia and Thailand. As of this writing, two large field campaigns drawing on 7SEAS work are scheduled for 2018 by ONR and NASA.

Smoke, Modeling, and Big Storms: NRL work in the 7SEAS program addressed specific pollution and meteorological concerns. For one, NRL researchers were interested in one of the most significant and variable pollution sources in the region—smoke from land clearing. As part of 7SEAS, NRL scientists investigated the problem by creating the very first comprehensive “wiring diagram” of meteorological phenomena related to aerosol emissions and lifecycle across a range of scales in space and time;² elaborations on the findings were included in dozens of peer-reviewed journal articles by NRL authors and their collaborators. NRL scientists are now in turn using these measurements

to evaluate the region's modeling and remote sensing systems. For another, NRL researchers were interested in the region's small scale features, such as individual thunderstorms and sea breezes, which are notable for scaling up into a larger coupled system of tropical cyclones and monsoon enhancements that exert seasonal influence on aerosol emission and large scale transport. These relationships are then pasted on top of interannual phenomenon such as El Niño—Southern Oscillation (ENSO) variation and interseasonal oscillations such as the Madden Julian Oscillation (MJO).

Conclusion: NRL researchers demonstrated the importance of fine scale features in regulating the aerosol and cloud environment—features often neglected in analyses, such as the formation of squall lines, hundreds of kilometers long but only tens of kilometers wide, that regularly propagate across the SCS and bring instantaneous winds to as high as 80 miles per hour (Fig. 7(b)). These fine scale features dictate the effects of aerosol particles on the region's meteorology and climate.

[Sponsored by the NRL Base Program (CNR funded), NASA, and ONR Code 322]

References

- ¹ J.S. Reid, E.J. Hyer, R. Johnson, B.N. Holben, R.J. Yokelson, J. Zhang, J.R. Campbell, S.A. Christopher, L. Di Girolamo, L. Giglio, R.E. Holz, C. Kearney, J. Miettinen, E.A. Reid, F. Joseph Turk, J. Wang, P. Xian, G. Zhao, R. Balasubramanian, B.N. Chew, S. Janai, N. Lagrosas, P. Lestari, N.-H. Lin, M. Mahmud, X.A. Nguyen, B. Norris, T.K. Oahn, M. Oo, S.V. Salinas, E.J. Welton, and S.C. Liew, "Observing and Understanding the Southeast Asian Aerosol System by Remote Sensing: An Initial Review and Analysis for the Seven Southeast Asian Studies (7SEAS) Program," *Atmos. Res.* **122**, 403–468 (2013).
- ² J.S. Reid, P. Xian, E.J. Hyer, M.K. Flatau, E.M. Ramirez, F.J. Turk, C.R. Sampson, C. Zhang, E.M. Fukada, and E.M. Maloney, "Multi-Scale Meteorological Conceptual Analysis of Observed Active Fire Hotspot Activity and Smoke Optical Depth in the Maritime Continent," *Atmos. Chem. Phys.* **12**, 2117–2147, (2012). doi:10.5194/acp-12-2117-2012.



124 From the Depths of Marine Dark Biosphere

125 Shark Antibodies Make a Splash

From the Depths of the Marine Dark Biosphere

L. Fitzgerald,¹ D. Haridas,² Y. Maezato,² J. Biffinger,¹ T. Boyd,¹ L. Hamdan,³ J. Lee,⁴ and B. Little⁴

¹Chemistry Division

²American Society for Engineering Education
Postdoctoral Associate

³University of Southern Mississippi

⁴Oceanography Division

Introduction: The marine deep, dark biosphere is an environment permanently separated from light-driven energy production. Survival in the deep, dark biosphere defies the normal rules for life on the Earth's surface: there is no light, hydrostatic pressure is greatly increased, nutrient sources are limited, and, in some cases, carbon dioxide concentrations are high. Yet, microorganisms live in these extremes, having adapted mechanisms to generate cellular energy. Shipwrecks contain metal alloys, synthetic polymers and coatings, and even woody biomass, and provide sources of nutrients and other necessary materials for microorganisms that typically might not otherwise thrive in these habitats. The majority of microorganisms in the deep, dark biosphere historically have been “unculturable” with standard laboratory protocols. Given the enhanced biodiversity provided by shipwreck habitats, as has been observed for macrobiological communities and the metabolic substrate they provide, shipwrecks may harbor novel microbial populations and mechanisms for survival that have largely remained unexplored.

In 2014, we joined science partners aboard the R/V *Pelican* for research expeditions of shipwreck sites in the northern Gulf of Mexico as part of the Gulf of Mexico-Shipwreck Corrosion, Hydrocarbon Exposure, Microbiology, and Archaeology (GOM-SCHEMA) project (Fig. 1). With scientists from the Bureau of Ocean Energy Management, George Mason University, and other institutions, we collected water samples from areas around several metal and wooden shipwrecks (July 2014), metal-rich concretions from the wrecks (March 2014; July 2014), and in situ biofilm monitoring and corrosion platforms (March 2014; July 2014). The GOM-SCHEMA project was funded by the Bureau of Ocean Energy Management.

Microbiological Studies: One way to address culturing organisms that are resistant to traditional methods is through Biological Activity Reaction Test (BART) assays. These assays are a straightforward way to culture microbes when the ideal culture conditions outside of their native environment are not known. The eight assays target growth of different classes of microorganisms, such as sulfate- or nitrate-reducing or

iron-related bacteria. The assays were a necessary step in building our understanding of the growth conditions of microorganisms in water samples collected near historic shipwrecks in the marine dark biosphere.



FIGURE 1

A map of shipwrecks studied in 2014 during the Gulf of Mexico Shipwreck Corrosion, Hydrocarbon Exposure, Microbiology, and Archaeology (GOM-SCHEMA) project.

After cultivating natural microbial populations from waters around six Gulf of Mexico shipwreck sites (Fig. 1) in eight different BART assays, we identified several bacterial population groups. The water samples contained no viable fluorescent *Pseudomonas*, slime forming bacteria, or nitrifying bacteria. However, all samples contained culturable iron-related bacteria, heterotrophic aerobic bacteria, and acid-producing bacteria. Furthermore, all but one of the samples contained denitrifying (DN) bacteria. We evaluated nitrate reduction by using the DN consortium from two metal shipwrecks (*U-166* and *Halo*). The *U-166* DN microbial consortium performed denitrification at a much faster rate than the *Halo* DN microbial consortium (Fig. 2). Five of six shipwreck sites had at least one water sample that tested positive for sulfate-reducing bacteria. The data from the BART assays demonstrated that bacterial populations with different metabolic pathways collected from deep-sea shipwreck sites can be cultured when started from the defined nutrients provided with the BART assays. The novel microorganisms isolated from these cultures provide an opportunity to explore specific metabolic pathways with relevance to scientific and technological interests of the Navy.

Corrosion Studies: We used biofilm-monitoring platforms with wood and carbon steel coupons (Fig. 3(a)) to analyze samples for degradation. We documented surface morphology and the internal structure of intact samples with environmental scanning electron microscopy. We determined the mineralogy of accumulations associated with the wrecks through powder X-ray diffraction. We identified iron-encrusted stalks (indicative of iron-oxidizing bacteria) in iron-rich accumulations.

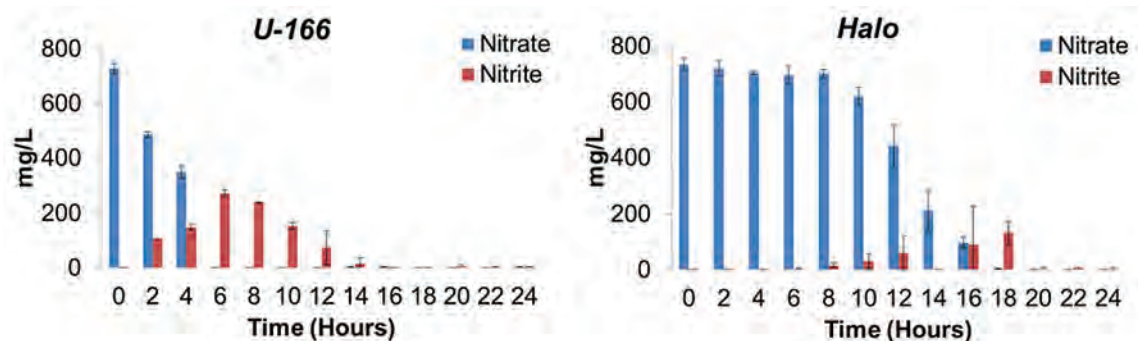


FIGURE 2
Ion chromatography results from denitrifying microbial consortium isolated from the *U-166* and *Halo* shipwreck sites in 2014 in the GOM-SCHEMA project.

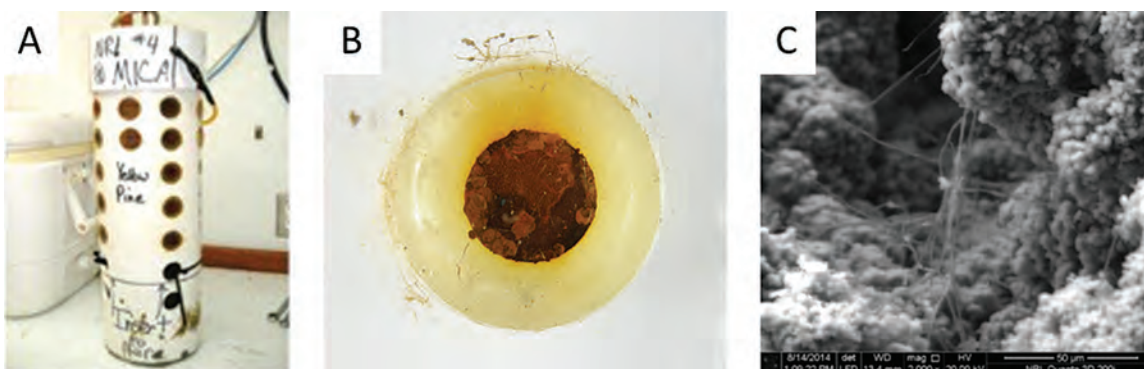


FIGURE 3
A) Corrosion monitoring platform deployed at the Mica shipwreck site immediately after recovery during a July 2014 GOM-SCHEMA project cruise, B) corrosion coupon from field experiment of water sample from a shipwreck site, C) microorganisms in interior of aluminum-rich accumulations from a water sample of the *U-166* shipwreck site.

Aluminum and iron accumulations collected from the *U-166* and *Anona*, respectively, were porous and fragile when dried (Fig. 3(b)). Rusticles and scales were layered with a centralized cavity. Four-month-old corrosion products on carbon steel coupons were similarly structured with distinct layers and fluid-filled cavities. The aluminum-rich accumulation from the *U-166* had an elongated shape, but did not have the structure and differentiation observed in the iron-rich structures. Microorganisms were associated with the exteriors and interiors of both aluminum and iron accumulations (Fig. 3(c)). In the aluminum products, the distribution of microorganisms appeared random, and cells were not encrusted. Our research in the GOM is leading to the development of novel techniques and to the identification of microorganisms adapted to life in the dark biosphere. Both endeavors will contribute to understanding mechanisms for the degradation of shipwrecks in the region.

Acknowledgments: We thank the captain, crew, and scientific party of the R/V *Pelican*. Funding was provided by the Office of Naval Research (ONR) through the Naval Research Laboratory (PE# 61153N),

Bureau of Ocean Energy Management (BOEM) No. M13PG00020 and the Navy Platform Support Program. [Sponsored by NRL (PE# 61153N), BOEM (M13PG00020), and Navy Platform Support]



Shark Antibodies Make a Splash

G. Anderson, D. Zabetakis, J. Liu, and E. Goldman
Center for Bio/Molecular Science and Engineering

Introduction: The shark is one of the oldest species on Earth, dating back more than 450 million years. Now, antibodies derived from the shark's ancient immune system are offering a new way to develop detection tools that protect the warfighter from biological threats. Antibodies are used in detection, diagnostic, and therapeutic applications. Typically, they are large proteins made from about 1,600 amino acids linked together in two heavy chains and two light chains that need to pair together to form their target binding

region. Sharks, like camelids, have unusual antibodies that contain only a pair of heavy chains. The binding region of these antibodies can be expressed recombinantly in yeast, plants, or bacteria, and are termed single-domain antibodies. Single-domain antibodies have a number of advantageous properties. For one, they are about 10 times smaller than traditional antibodies, comprising the smallest naturally occurring antigen binding domains, yet still retain the excellent binding ability and exquisite specificity that are hallmarks of antibodies. Because single-domain antibodies are comprised of only one domain, most refold after heat denaturation, recovering at least a portion of their three-dimensional structure, which enables them to retain their binding ability after exposure to extreme temperatures. Other advantages include the ability of single-domain antibodies to be rationally-selected, to be engineered to improve their properties and tailored to specific applications, and to be produced in mass quantity by standard fermentation technology.

Engineering of Shark Single-Domain Antibodies:

Our collaborators at the United Kingdom's Defence Science and Technology Laboratory previously identified a shark-derived single-domain antibody specific for the nucleoprotein of Ebola virus.¹ Further work confirmed the shark single-domain antibody's high affinity for the nucleoprotein, but also found a couple of limiting factors: (1) its melting temperature is low (52 °C) relative to most single-domain antibodies (60–70 °C), and (2) it recovered only about 68 percent of its structure following a single heat cycle. Using protein engineering approaches, we found a single-point mutation that increased the melting temperature of the shark antibody binding region by 11 °C without the antibody losing its high affinity and specificity. A double mutation increased the melting temperature by 14 °C (Fig. 4) with only a small loss or drop in affinity.² By increasing the single-domain antibody's melting temperature, thermal denaturation can be prevented, which facilitates long-term storage at elevated temperatures without loss of activity.

Our process for stabilizing the shark single-domain antibody followed the process we had delineated in previous work to raise the melting temperature of camelid derived single-domain antibodies.³ In that work, we demonstrated the ability to increase the melting temperature of camelid single-domain antibodies by up to 20 °C, and increased refolding to 100 percent. Stabilization was accomplished through a process that involves several techniques, including grafting antibody binding loops onto stable antibody frameworks and introducing point mutations.

Our work is the first demonstration of stabilizing a shark-derived single-domain antibody. In our investigation, we first grafted the binding loops of the

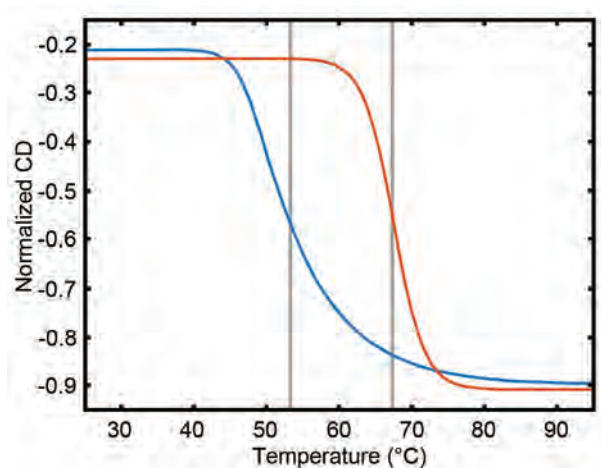


FIGURE 4

Evaluation of the melting temperature of the original shark single-domain antibody (blue) and the double mutant (orange) by circular dichroism.

single-domain antibody onto a highly stable shark-derived framework that we had previously identified. We next subjected the graft to a mutational study, in which we changed three positions in a segment of the shark single-domain antibody structure termed hyper variable region 2. Three single mutants and three double mutants were constructed, revealing that a single amino acid change in this graft resulted in a dramatic increase in temperature stability (Fig. 5). The melting temperature of the improved clone was 63 °C compared to 52 °C for the original. In addition, the improved clone demonstrated better structure recovery, regaining 78 percent of its three-dimensional structure after a single denaturing heat cycle versus 68 percent. As in the original, the stabilized clone maintained superb affinity for the Ebola virus nucleoprotein.

Conclusions: Ours is the first demonstration of molecular engineering to increase the thermal stability of a shark single-domain antibody. It also highlighted the importance of the hypervariable 2 region for both affinity and stability of shark-derived single-domain antibodies.

Compared to conventional antibodies, shark-derived single-domain antibodies offer a practical and cost-effective alternative for therapeutic, detection, and biotechnology applications. Recombinant production makes the shark antibodies a more uniform and consistent product, and, because they can be ruggedized, the shark antibodies require less refrigeration, thus making their shipping and storage easier and less expensive.

[Sponsored by the NRL Base Program (CNR funded) and the Defense Threat Reduction Agency (DTRA)]

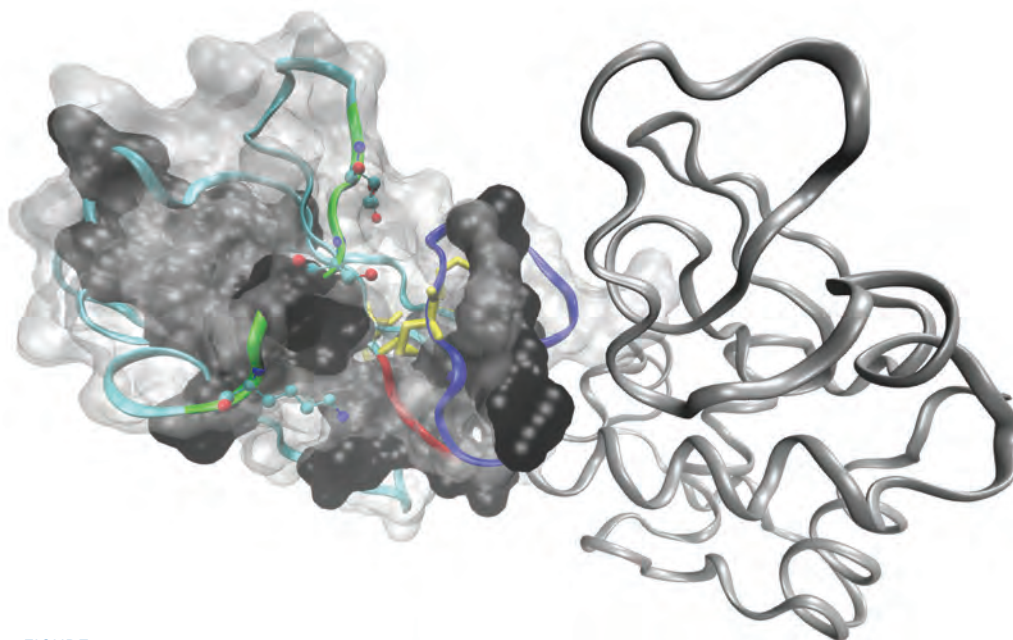


FIGURE 5

A shark single-domain antibody binds to its antigen. The protein structure of this antibody is rendered in various formats. The hydrophobic core is shown in black, while the protein backbone is rendered as a ribbon. The dark blue, red, and green sections of ribbon are the regions that determine the specific binding function of the antibody. The amino acids that were a particular focus of this work are shown as a ball-and-stick model on the green section of the ribbon. The antigen is represented as the grey backbone ribbon on the right-hand side of the figure.

References

- ¹ S.A. Goodchild, H. Dooley, R.J. Schoepp, M. Flajnik, and S.G. Lonsdale, "Isolation and Characterisation of Ebolavirus-Specific Recombinant Antibody Fragments from Murine and Shark Immune Libraries," *Mol. Immunol.* **48**, 2027–2037 (2011).
- ² G.P. Anderson, D.D. Teichler, D. Zabetakis, L.C. Shriver-Lake, J.L. Liu, S.G. Lonsdale, S.A. Goodchild, and E.R. Goldman, "Importance of Hypervariable Region 2 for Stability and Affinity of a Shark Single-Domain Antibody Specific for Ebola Virus Nucleoprotein," *Plos One* **11** (2016).
- ³ K.B. Turner, J.L. Liu, D. Zabetakis, A.B. Lee, G.P. Anderson, and E.R. Goldman, "Improving the Biophysical Properties of Anti-Ricin Single-Domain Antibodies," *Biotechnol. Rep.* **6**, 27–35 (2015).



- 130** Reshaping Antenna Patterns Using Metasurface Radomes
- 132** NRL Participates in NATO Electronic Warfare Trial
- 134** Magnetolectric Microbeam Resonators for Magnetic Field Sensing
- 137** Intense Laser-Driven Ion Accelerator
- 139** Normally-Off AlGaIn/GaN MOS-HEMTs with Record Performance
- 141** NexGen High Frequency Surface Wave Radar

Reshaping Antenna Patterns Using Metasurface Radomes

B. Raeker and S. Rudolph
Tactical Electronic Warfare Division

Introduction: The radiation pattern of an antenna is ultimately what determines its suitability for a specific application. However, generating complex radiation patterns from a single antenna requires significant expertise and substantial design effort. Researchers in the Offboard Countermeasures Branch of the Tactical Electronic Warfare Division at the U.S. Naval Research Laboratory have been interested in a method to directly design an antenna radiation pattern using a metasurface radome. A metasurface consists of subwavelength, two-dimensional unit cells which are designed to have a specific impedance. Such metasurfaces can be easily realized using printed circuit board fabrication techniques, making the production of these radomes widely available and inexpensive. In this article, we will first demonstrate this capability using a cylindrical radome, and then demonstrate the flexibility of the method by examining a spherical radome.

Such radomes would be beneficial to both the U.S. Navy and commercial applications. The metasurface radomes could be used to produce nulls in areas of interfering signals or reallocate power along different bearings without needing to redesign the enclosed antenna. Additionally, the radomes can be used to provide basic antennas with enhanced, mission-specific performance, allowing for the utility of a modular design while minimizing the amount of hardware that would need to be replaced. The next section outlines the method by which a radome can be designed to transform the radiation pattern of an existing antenna into any pattern that is desired.

Design Procedure: The first step in the design procedure is to calculate electromagnetic fields that must be produced on the surface of the radome. This is done by reverse propagating the desired field pattern. However, arbitrary radiation patterns cannot directly be propagated back and projected onto new surfaces; such operations can only be performed on solutions to the wave equation. Therefore, in our research project, we first decompose the desired radiation pattern into an infinite series of modes. This can be done in any separable coordinate system, but we provide examples here in two-dimensional cylindrical coordinates and three-dimensional spherical coordinates. This decomposition takes the form of a Fourier series in cylindrical coordinates and a Fourier-Legendre series in spherical coordinates. Once the desired field is separated into these orthogonal modes, they can be propagated

independently along the radial direction, i.e., inward or outward, such that the desired field on the image surface can be propagated inwards to produce the required fields on the surface of the radome.

The next step in the design is to find the necessary scattered field that must be produced by the radome to transform the incident field into the desired field. This is done by simply subtracting the incident field at the surface of the radome from the desired field which has been propagated back to the surface of the radome, such that $E^{\text{scattered}} = E^{\text{desired}} - E^{\text{incident}}$.

The subsequent step is to take the now-known scattered field and use it to design the metasurface that will actually transform the incident field into the desired field. By subdividing the surface of the radome into discrete subwavelength unit cells, we can use the Method of Moments to determine the current needed on each unit cell to produce the correct scattered field. Once the current is known, we can find the impedance of the unit cell by taking the ratio of the desired electric field and the current at any given location on the surface of the radome: $Z_i = E^{\text{desired}}/J_i$, where i indicates the unit cell number.

Once the impedance distribution across the metasurface has been calculated, we can then realize those impedances through printed circuit board methods, as can be seen in Fig. 1(b). This is typically done by solving for a few key points and then extrapolating to find the intermediate values.¹

Results: To prove the validity of our approach, we sought to transform the isotropic radiation pattern of an infinite filament of current into a binary radiation pattern such that radiation is permitted over a 180° sector and prohibited over the other 180° sector (see Fig. 1(a)).² The field patterns are remarkably consistent between the theoretical, simulated, and measured results, as shown in Fig. 1(c), with the measured field having a normalized RMS error of 0.034. Additionally, this proved to be a much more precise method of realizing our desired field distribution when compared with an alternative method for realizing the prescribed binary pattern, such as a conducting shield, as shown in Fig. 1(d).

Finally, to demonstrate the fully arbitrary nature of the radiation patterns that can be synthesized using this method, we sought to transform the radiation pattern of a small dipole into the shape of a nautical anchor, with the geometry shown in Fig. 2(a).³ The resulting simulated three-dimensional far-field pattern is presented in Fig. 2(b). A flattened version is compared to the ideal pattern we sought to achieve in Fig. 2(c). Fig. 2(d) presents individual linear cuts along the azimuthal angle of 180° and the elevation 90°.

[Sponsored by the NRL Base Program (CNR funded)]

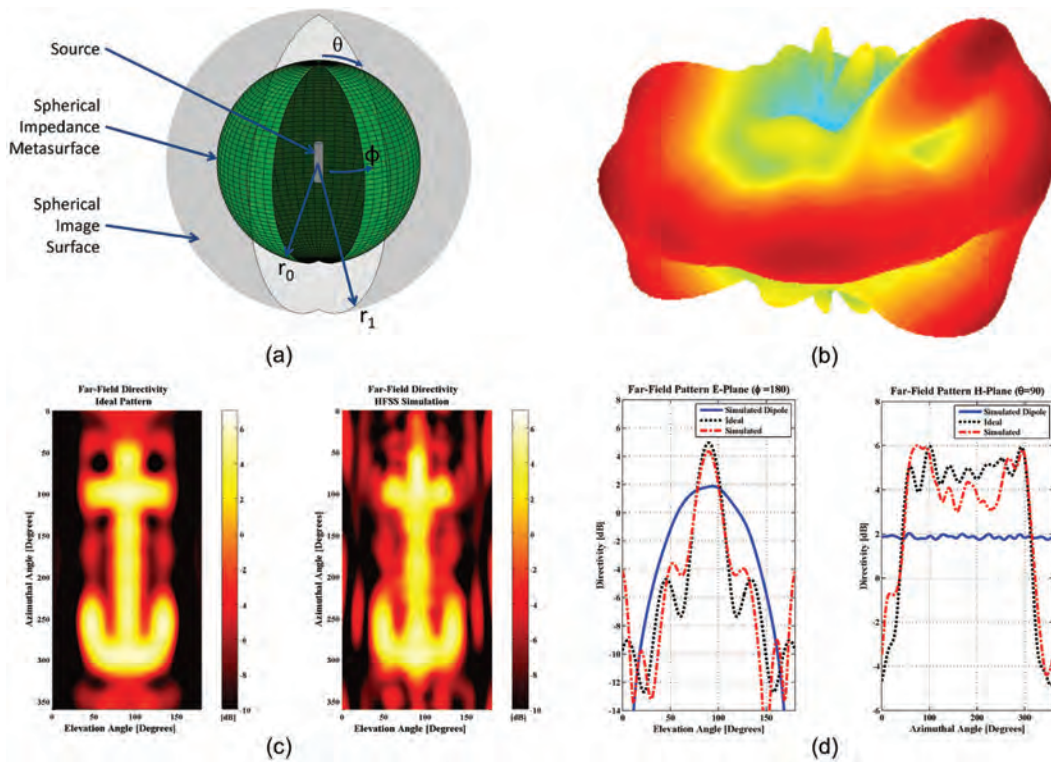


FIGURE 1 (a) Geometry of the cylindrical metasurface radome. (b) The fabricated metasurface radome, manufactured using printed circuit board techniques. (c) Plot of the theoretical, simulated, and measured radiation patterns. (d) Plot comparing the radiation patterns low-loss substrate radome, a radome with a conducting sector to block radiation over a 180° sector, and the metasurface radome.

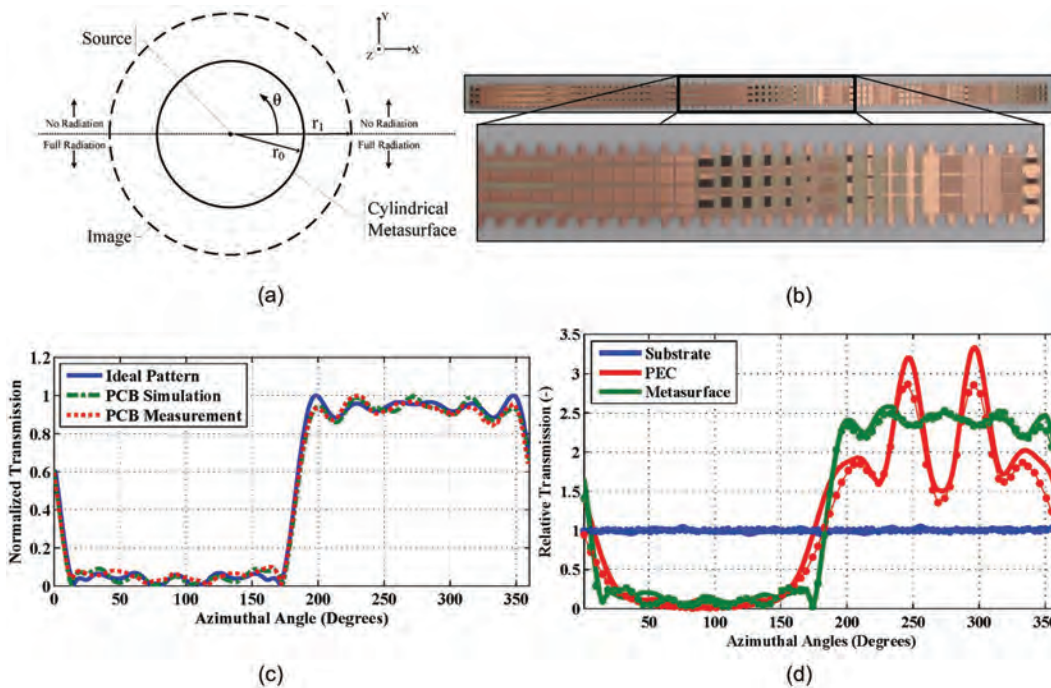


FIGURE 2 (a) Geometry of the spherical metasurface radome. (b) Simulated far-field pattern of the antenna enclosed in the metasurface radome displaying the shape of a nautical anchor on its side. (c) Comparison between the design radiation pattern (left) and the radiation pattern of the antenna enclosed in the radome (right). (d) Comparisons of the ideal and simulated far-field patterns along the E-plane ($\phi = 180^\circ$) and the H-plane ($\theta = 90^\circ$).

References

- ¹ B.O. Raeker and S.M. Rudolph, "Arbitrary Transformation of Antenna Radiation Using a Cylindrical Impedance Metasurface," *IEEE Antennas Wireless Propag. Lett.* **15**, 1101–1104 (2016).
- ² B.O. Raeker and S.M. Rudolph, "Verification of Arbitrary Radiation Pattern Control Using a Cylindrical Impedance Metasurface," *IEEE Antennas Wireless Propag. Lett.* **16**, 995–998 (2017).
- ³ B.O. Raeker and S.M. Rudolph, "Arbitrary Transformation of Radiation Patterns Using a Spherical Impedance Metasurface," *IEEE Trans. on Antennas and Propag. Lett.* **64**(12), 5243–5250 (2016).



NRL Participates in NATO Electronic Warfare Trial

A. Allegrezza and C. Maraviglia
Tactical Electronic Warfare Division

Introduction: During the week of June 6, 2016, the U.S. Naval Research Laboratory's (NRL) Tactical Electronic Warfare Division and the Royal Norwegian Navy cohosted the Naval Electromagnetic Operations (NEMO) Trials in Andøya, Norway. The trials, conducted by the NATO Above Water Warfare Capabilities Group, involved the participation of eight countries that provided 10 warships, four air assets, and several shore-based assets. The trials were conducted in the area of Andøya, Norway, about 200 miles north of the Arctic Circle. The Norwegian Air Force's 133rd Air Wing, based at Andøya Air Station, was the host location for the trials. Facilities and test support were provided by Andøya Air Station, the Andøya Space Launch Center, the Norwegian Navy Operational Logistics Unit, and associated Surface and Air Operations Areas.

Andøya Air Station is in Andenes, on the northern end of the island of Andøya. The area provided a protected fjord (Andfjorden) to the east and open ocean to the north and west. The air station provided ground sites for test and measurement stations as well as airfield and aircraft support.

U.S. Government objectives for the trials included collecting electro-optical and imaging infrared (EO/IIR) data for the various NATO warships, assessing the effectiveness of decoy deployment tactics against imaging seekers, evaluating detection ranges of various seeker platforms, and creating a multi-threat environment with the radiofrequency (RF) stimulator. To meet these objectives, the Tactical Electronic Warfare Division flew captive-carry IIR and EO seeker simulators on a Lear jet and set up shore sites at Andøya Air Station to support an IIR seeker simulator and an RF stimulator system (Fig. 3).



FIGURE 3

NRL used a Lear jet to fly sensors that captured electro-optical and imaging infrared data for the various NATO warships involved in the 2016 Naval Electromagnetic Operations (NEMO) Trials in Andøya, Norway.

NRL Objectives: NRL researchers focused on objectives established by a NATO capabilities group for both operational interoperability and scientific objectives. For the EO/IIR group, objectives included collection of EO/IIR imagery of various platforms, evaluating the effectiveness of decoys and tactics, and evaluating ship detection based on signature measurements. For RF researchers, the objective was to create a multi-threat environment using the Complex Arbitrary Waveform Synthesizer (CAWS) radar stimulator in conjunction with a German anti-ship cruise missile simulator.

Test Asset Descriptions: *Description of FOXTROT Anti-ship Missile (ASM) Simulator:* The FOXTROT simulator is a programmable, human-in-the-loop, real-time image tracking system designed to simulate IIR anti-ship missile threats. Developed as a research tool, the simulator can represent both modern and future classes of threats, with an imaging front end and sophisticated image processing capabilities. Video data from an imager can be processed in real time or saved as raw data that can be post-processed for target track evaluation and algorithm development. The FOXTROT simulator is composed mainly of off-the-shelf, commercially available components. The simulator is maintained under the U.S. Navy's Effectiveness of Naval Electronic Warfare Systems program. Control and integration software was developed by NRL's Tactical Electronic Warfare Division. Two versions of the simulator were fielded: (1) a flyable version, housed in a standard instrument pod (SIP) for captive-carry under the wing of the Learjet, and (2) a portable version, packaged in lightweight containers and located in a shelter at the ground operations IR test site. The FOXTROT simulators consist of several major subsystem components: commercially available infrared imager, wide field-of-view reference TV camera (visible band), video image processing and analysis computer, gyro-stabilized

gimbal with an electronic control loop, data recording devices, and standard PC for I/O control. The infrared imager and the reference camera are installed on the same gimbal. Both FOXTROT simulators (flyable and portable) were based on a NightConqueror II-256 IIR camera from L-3 Cincinnati Electronics (Mason, Ohio) as the primary tracker. The NightConqueror is a ruggedized, staring focal plane array-based, mid-wave infrared camera.

FOXTROT simulators also use a visual reference camera. The flyable system contains a Cohu Closed Circuit Television wide field-of-view visible band camera. The FOXTROT portable system uses a Photon Focus 14-bit monochrome visible band camera.

FOXTROT relies on manual acquisition by an experienced operator to select the target of interest, after which the target is auto-tracked. The tracking algorithm is based on a binary threshold, centroid track. The digital image is passed into the video processing PC, which determines a target pixel value threshold based on imagery inside several gates. Outer clutter gates adjust the threshold based on the amount of clutter in the scene/image. A background gate and track gate then determine the final threshold based on the image in their gates and clutter data from the clutter gates. The result is a binary color image of the target. This image is centroided, and new track gate dimensions are calculated for the next image. The resulting data is then passed back to the gimbal to maintain pointing accuracy.

Description of IOTA-MIKE Unmanned Aircraft System Simulator: The IOTA-MIKE system is a programmable simulator of a visible band optical unmanned aircraft system payload composed of off-the-shelf, commercially available components. The software is written and maintained by the Tactical Electronic Warfare Division, and the software load used for the NEMO 2016 Trials is unclassified. The system is housed in a SIP slightly modified to accommodate its gimbal and mounted to the wing of the Learjet for flight. The IOTA-MIKE simulator comprises several major subsystem components: commercially available CCD NTSC visible band imager, laptop computer for system control, gyro-stabilized gimbal with an electronic control loop, data recording devices, and an onboard PC/104 embedded computer for I/O control. The tracker works in the same way as the FOXTROT tracker (Fig. 4).

Description of the Complex Arbitrary Waveform: The Complex Arbitrary Waveform Synthesizer (CAWS) is a programmable radar stimulator (transmit only) developed and built by NRL. Each waveform parameter can be individually programmed to provide accurate signals for laboratory and operational testing. CAWS can be packaged in both portable (configuration used



FIGURE 4

The pod of the IOTA-MIKE system. The system's software is written and maintained by the NRL Tactical Electronic Warfare Division.

for NEMO 2016) and captive carry flyable configurations. CAWS requires a connection to an external RF amplifier and antenna. Amplifiers can vary in size to match the individual test requirements. The operational concept of CAWS is similar to Joint Electronic Warfare Countermeasure System ALQ-167 Stimulation Pods (Fig. 5).



FIGURE 5

The FOXTROT pod. The FOXTROT simulator is a programmable, human-in-the-loop, real-time image tracking system designed to simulate imaging-infrared anti-ship missile threats.

Summary: For NRL researchers, the primary objective of this trial was to take EO/IIR imagery of various platforms and evaluate the effectiveness of IIR decoys and deployment tactics against IIR seekers. The secondary objective was to support ESM operations by transmitting a radar signal with the CAWS system. All proposed U.S. test objectives were met. The flyable FOXTROT system collected over 776 files consisting of 314 megabytes of data. The flyable system collected both visible and mid-wave IR imagery and GPS tracking data for 86 ship runs. The portable FOXTROT system collected over 467 files consisting of 1.6 terabytes of data. The portable system collected both visible and mid wave IR imagery for 66 ship runs. The IOTA-MIKE system collected over 239 files consisting of 205 megabytes of data; the system collected visible band imagery and GPS tracking data for six ship runs. The CAWS stimulator operated for 22 runs, providing a multiple threat environment in conjunction with the German RF Simulator.

The collected data was post-processed by NRL researchers to evaluate decoy and inoperability tactics. The mission of NATO is to present a unified front. By working together in their trials and subsequent scientific research, a stronger alliance is formed. The size and scope of these types of exercises also offer an excellent venue for realistic data sets.

[Sponsored by OPNAV]

✦

Magnetolectric Microbeam Resonators for Magnetic Field Sensing

S.P. Bennett,¹ J.W. Baldwin,² M. Staruch,¹ B.R. Matis,² K. Bussmann,¹ D. Goldstein,² and P. Finkel¹

¹Materials Science and Technology Division

²Acoustics Division

Introduction: One of the great challenges of our time is to achieve maximum efficiency in the next generation of electronics. It is particularly crucial for self-sufficient platforms (e.g., autonomous vehicles and remote sensing) on which power requirements are a highly limiting factor towards performance. Of specific importance for the Navy is magnetic sensing technology, which has fallen far behind other technologies in power consumption and performance.

For many years there has been a growing need for a giant leap in the development of high sensitivity, cryogen-free, chip-based magnetic sensors that operate with ultra-low power consumption. To meet this need, a new generation of sensors must be realized based from a new set of physics for detection, and, if they are to outperform the current state of the art, they must operate at very low power consumption, ruling out the physics used by most of our current power hungry technologies (e.g., search-coil, Hall effect, flux gate, fiber optic, and the superconducting quantum interference device).

Very recent advances in materials physics have unveiled that micron scale Magnetolectric (ME) composite resonators could hold the answer. ME resonators basically consist of two strain-coupled materials; one magnetostrictive and another piezoelectric.¹ When the coupled structure is driven to mechanical resonance a peak in the piezoelectric signal is detected. If the resonating device is placed in a magnetic field the magnetoelastic layer responds by either stiffening, or loosening, the structure and in turn shifting this resonance signal. Similar devices have already shown remarkably high sensitivity and quality factors. Additionally, their direct coupling between magnetic and electric fields allows

for very low power consumption, or even completely passive, magnetic sensors.

The current state of the art for magnetolectric resonators is limited to very large sizes (>1cm) as well as their needs for op-amp detection, battery power, and a relatively high equivalent noise floor of $\sim 10^{-10}$ Tesla at frequencies away from the electromechanical resonance. The limitations are partly due to the size of the resonator structure. We expect that miniaturization chip-based micro-scale domain is expected to increase the signal-to-noise ratio and allow for broadband magnetic field detection with an equivalent noise floor of $\sim 10^{-12}$ Tesla at 1Hz. As an added perk such miniaturization allows for easy integration into silicon-based, low power, electronic systems.

Using advanced nanofabrication methods, we have demonstrated a fully suspended two-point connected thin film heterostructure where precisely engineered internal stresses hold the structure in a taut tensile stressed state, preserving the shape and allowing for a fundamental string mode resonance behavior at the first harmonic. The ME heterostructure demonstrated here consists of a Pt back electrode, an AlN piezoelectric signal layer and a magnetostrictive FeCo layer, which also serves as the top electrode. At the resonance mode, the time-variant strain signal is detected as a piezoelectric voltage from the AlN layer. When subjected to a magnetic field, magnetoelastic effects in the FeCo layer cause a shift in the resonance frequency, which is proportional to the field amplitude. This frequency shift is what allows for highly sensitive measurements of very low magnetic fields.

Fabrication: The fabrication process is outlined in the schematic diagrams given in Fig. 6(a). Double-side polished, 100-mm diameter, <100> orientation Si wafers were coated with 300nm of low stress LPCVD silicon nitride. The device side (top surface) was coated with a 10nm Ti adhesion layer followed by 150 nm of low stress Pt film deposited with DC magnetron sputtered. The AlN piezoelectric films were deposited by reactive sputtering to a thickness of 750 nm, with conditions optimized for low stress (~ 50 MPa.). Quality of the AlN films was verified through XRD having FWHM values for the (002) AlN diffraction peak less than 2 degrees. Using standard lithography techniques, the top FeCo film was defined by lift-off photolithography. The FeCo film films were co-sputtered by DC magnetron at a ratio of approximately (30%Fe, 70% Co) at room temperature to a total thickness of 500 nm. The AlN nitride layer was patterned using standard lithography techniques and subsequent wet etching using a PECVD a silicon nitride hard mask. The Ti/Pt bottom electrode was patterned with standard lithographic techniques followed by reactive ion etching using Cl₂/

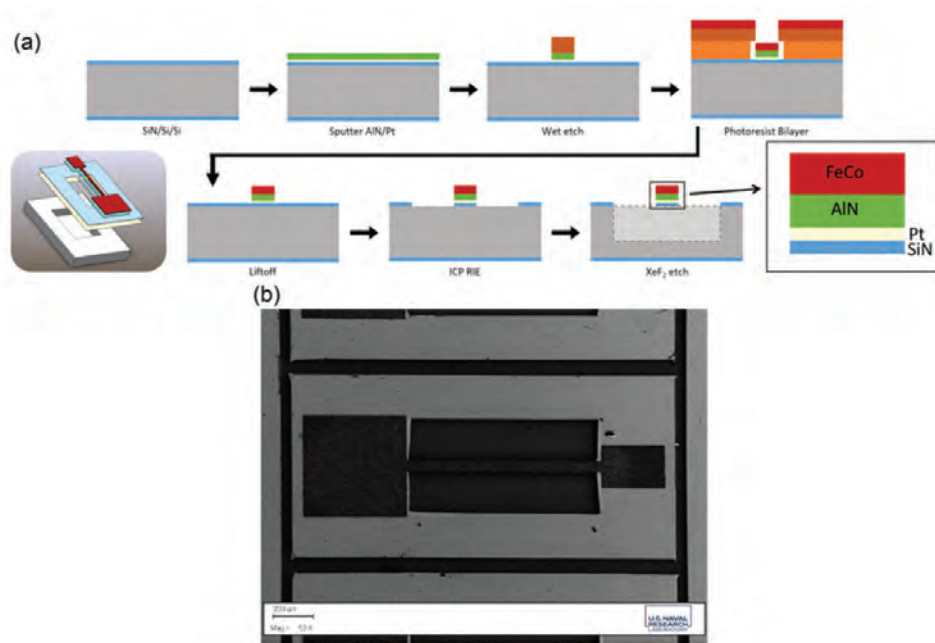


FIGURE 6
 (a) Nanofabrication steps shown schematically in flow diagram. (b) SEM image of fully fabricated microbeam device. The device is fully suspended over a XeF₂ etched cavity.

Ar chemistry. The beams were released using XeF₂ to etch a cavity from behind the device (Fig. 6(b)).

Measurements: To drive the beams to resonance, we tested four methods (see Fig. 7): (1) Lorentz force in a DC magnetic field (Fig. 7(a)), (2) magneto-repulsion in a coil driven AC magnetic field (Fig. 7(b)), (3) vibration using a piezoelectric crystal shaker (PMN-PT), and (4) direct AC voltage through the piezoelectric AlN layer (Fig. 7(d)). The lowest power consumption method is expected to be the AlN layer drive due to device size. By nature, this method will always drive the beam at its first fundamental as opposed to a piezoelectric crystal shaker

or the AC field drive coils which excite additional lower amplitude, higher order harmonics. As observed in the drive amplitude (measured by laser Doppler vibrometry) for the four different methods as shown in Fig. 7(e), the AC voltage applied to the AlN also demonstrated the largest amplitude of vibration, as well as the lowest noise. The other methods also introduced extra peaks in the frequency spectrum arising from internal resonances in the piezo crystal and substrate chip resonances. Though the amplitude from Lorentz force could be increased with a larger magnetic field, the need for a current flow through the FeCo top electrode eliminates it as a viable method for use in a sensing configuration.

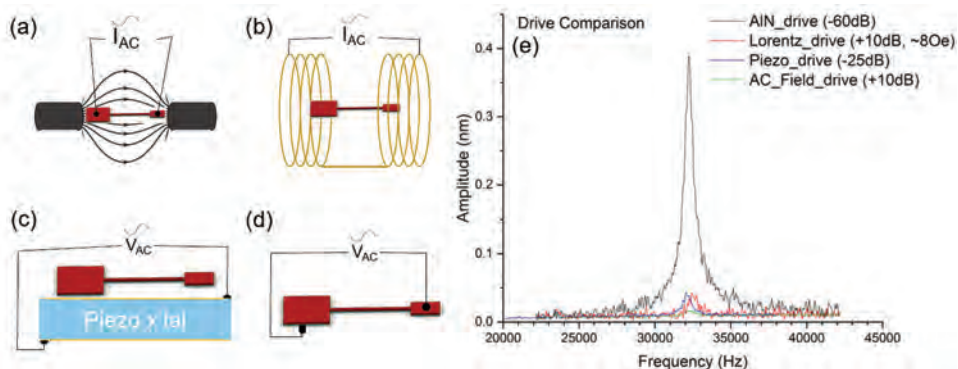


FIGURE 7
 Schematic diagrams of four different excitation methods. (a) Lorentz force method. (b) AC magnetic field drive method. (c) PMN-PT piezoelectric crystal drive (d) Direct drive using piezoelectric AlN layer by application of an AC time variant electric field. (e) Laser Doppler Vibrometer (LDV) measurements of beam displacements at structural resonance driven by four different excitation methods from (a), (b), (c), and (d).

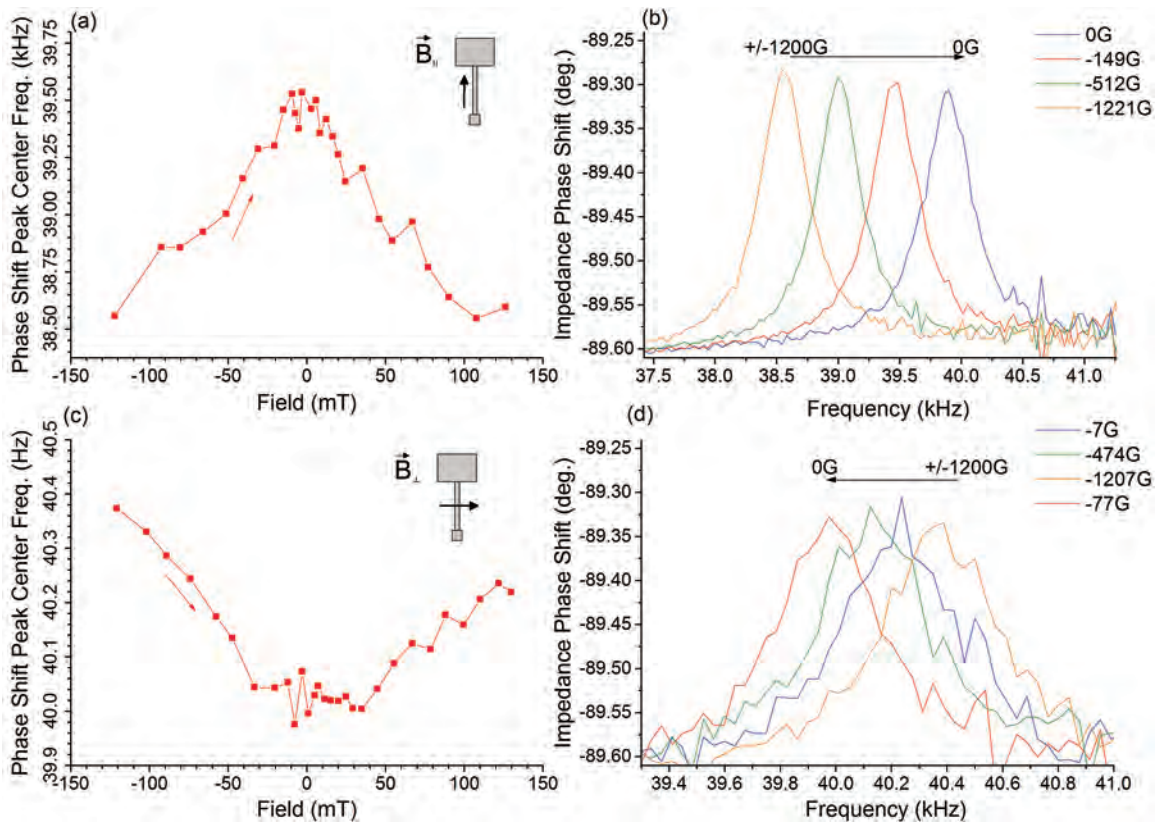


FIGURE 8 Diagrams showing impedance phase shift data collected using an impedance analyzer measuring the Piezo-electric AlN layer. Schematics show B-field orientation. (a) Measurement of field induced phase shift in parallel magnetic field. (b) Resonance peak shifting with field in parallel field arrangement shown in frequency space. (c) Measurement of field induced phase shift in perpendicular magnetic field. (d) Resonance peak shifting with field in perpendicular field arrangement shown in frequency space.

Based on these results, detection of the frequency shift with applied magnetic field was performed with measurements of the amplitude and phase of the impedance of the piezoelectric AlN film. Aside from increased noise, the impedance phase shift detection method demonstrated complete drive and detection using only the AlN film, eliminating both the need for an external drive method and piezoelectric signal voltage amplification. The shift in the impedance phase data in Fig. 8 showed a clear resonance shift as a function of magnetic field. This shift followed a trend which aligns to the expected magnetostrictive properties of the FeCo layer. When the material was magnetized, magnetostriction caused a stress to develop as magnetic field was changed since the length of the beam cannot be altered. Once the material started to lose spin alignment and demagnetized, the magnetostriction dropped off and the trend in frequency became noisy. This is known as the coercive field (H_c) region, which was measured for these films to be $H_c \sim 17$ mT using Magneto Optic Kerr Effect (MOKE) and vibrating sample magnetometry (VSM). The maximum magnetic field sensitivity, defined as the peak in derivative of the

data in Figure 3a and 3c, was revealed to be 33 Hz/mT ($0.083 \% f_r/\text{mT}$). Using this sensitivity of the resonance to magnetic fields, a low frequency ($\ll f_r$) AC field was detected with very high field sensitivity by extracting the modulation of the impedance phase shift from the AlN layer. In principle, this result would allow for the detection of low frequency magnetic signatures (e.g., electric motors). From the observed resonance frequency and magnetic field sensitivity, we predict a theoretical intrinsic magnetic noise floor of 34.8 pT/ $\sqrt{\text{Hz}}$ as calculated following previous works.^{5,6}

Conclusions: Our results reveal MEMS micro-beam magnetolectric resonators with a considerable strain induced resonance shift in a DC magnetic field when driven with the AlN piezoelectric film, which is revealed as the optimal mode of operation. Furthermore, we demonstrated how the use of a two ends clamped geometry fundamentally achieves an increased sensitivity to near-DC magnetic fields with relative insensitivity to the background (bias) field. This finding also presents a step forward in the stress engineering of thin film heterostructures to attain uniform free-

standing magnetoelectric thin film heterostructured devices whose mechanical integrity does not rely on the presence of a stiffening substrate. These devices open the door to silicon based on-chip fully integrated low power magnetic sensing technology.

[Sponsored by the NRL Base Program (CNR funded)]

References

- ¹ S.P. Bennett, A.T. Wong, A. Glavic, A. Herklotz, C. Urban, I. Valmianski, M.D. Biegalski, H.M. Christen, T.Z. Ward, and V. Lauter, *Sci. Rep.* **6**, 22708 (2016).
- ² Y. Wang, D. Gray, D. Berry, J. Gao, M. Li, J. Li, and D. Viehland, "An Extremely Low Equivalent Magnetic Noise Magnetoelastic Sensor," *Adv. Mater.* **23**(35), 4111 (2011).
- ³ T. Nan, Y. Hui, M. Rinaldi, and N.X. Sun, "Self-Biased 215HMz Magnetoelastic NEMS Resonator for Ultra-Sensitive DC Magnetic Field Detection," *Sci. Rep.* **3** (2013).
- ⁴ S. Marauska, R. Jahns, H. Greve, E. Quandt, R. Knöchel, and B. Wagner, "MEMS Magnetic Field Sensor Based on Magneto-electric Composites," *J. Micromech. Microengineer.* **22**(6), 65024 (2012).
- ⁵ J. Kiser, R. Lacombe, K. Bussmann, C.J. Hawley, J.E. Spanier, X. Zhuang, C. Dolabdjian, S. Lofland, and P. Finkel, "Magnetostrictive Stress Reconfigurable Thin Film Resonators for Near Direct Current Magnetoelastic Sensors," *Appl. Phys. Lett.* **104**, 072408 (2014).
- ⁶ M. Staruch, C. Kassner, S. Fackler, I. Takeuchi, K. Bussmann, S.E. Lofland, C. Dolabdjian, R. Lacombe, and P. Finkel, "Effects of Magnetic Field and Pressure in Magnetoelastic Stress Reconfigurable Thin Film Resonators," *Appl. Phys. Lett.* **107**, 032909 (2015).



Intense Laser-Driven Ion Accelerator

M.H. Helle,¹ D.F. Gordon,¹ D. Kaganovich,¹ Y.-H. Chen,² J.P. Palastro,¹ and A. Ting^{2,3}

¹Plasma Physics Division

²Research Support Instruments

³University of Maryland, College Park

Introduction: Since their invention nearly 100 hundred years ago, particle accelerators have become an important tool in modern society, employed by multi-billion dollar facilities like the European Organization for Nuclear Research (CERN) to expand our basic understanding of the universe, by hospitals to treat cancer patients, and by Silicon Valley technology firms to produce the next generation of electronics.¹ Unfortunately, the availability of particle accelerators has been limited due to their size and cost. Our development of a novel accelerator based on high power lasers and plasmas breaks new ground by introducing a way to make accelerators hundreds of times smaller. Our results are exciting not only because they establish a never-before-observed laser-acceleration mechanism

but also because they offer an energy efficient, high purity, compact source of ions with clear routes to high energies at high duty cycles (>10 kHz).² In addition to the other societal benefits mentioned above, such a source could enable applications relevant to interests of the Department of Defense, including flash radiography.³

Acceleration Process: Figure 9 illustrates the acceleration process we demonstrated. The accelerator starts by using an intense laser pulse to drive a plasma wave in a very thin (~100 microns) plasma sheet. Electrons from the ambient plasma are trapped and accelerated to high energies by this plasma wave, much the same way a surfer is accelerated by an ocean wave. The large magnetic field (~50 MG) generated by the electrons acts to compress and confine both the electrons and ions within the plasma (Fig. 9(a)). This type of process is considered a Z pinch. As the accelerated electrons exit the plasma region, a large electric field (~GV/m) is formed between the negatively charged electrons and the positive ions that acts to drag the ions out (Figure 9(b)). As the electron beam exits the plasma, the magnetic field also disperses and the compressed ions explode, forming an axial ion beam with a higher energy ion ring surrounding it (Fig. 9(c)).

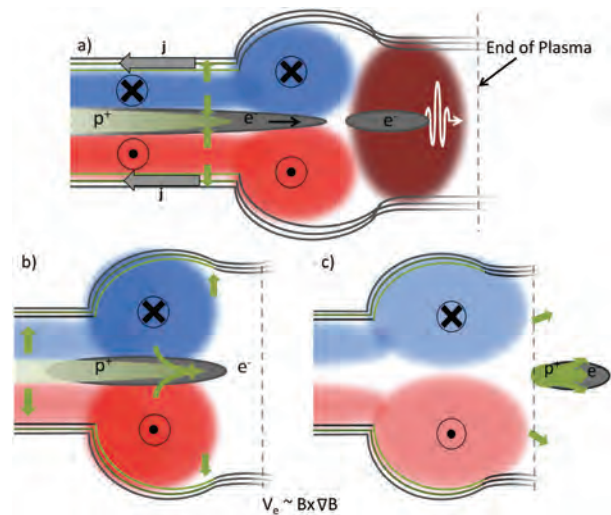


FIGURE 9 Illustration of the acceleration process: a) shows the acceleration of the electron beam and pinching process, b) shows forward acceleration of protons, and c) shows formation of a proton beam with a higher energy ring.

Building the Accelerator: The difficulty in building an ion accelerator is that ions are heavy and initially need a slow-moving wave to accelerate them. A laser pulse typically moves at the speed of light, much too fast to accelerate ions initially at rest. To slow down the laser pulse, we developed an accelerator structure

with an adjustable plasma density that allowed us to control the laser's velocity. The structure also needs to be thin, such that the laser can penetrate through the dense plasma. We achieved the prerequisite thinness by using two colliding shock waves to compress a gas jet in vacuum, as illustrated in Fig. 10. In this process, strong hydrodynamic shockwaves are ignited in a standard

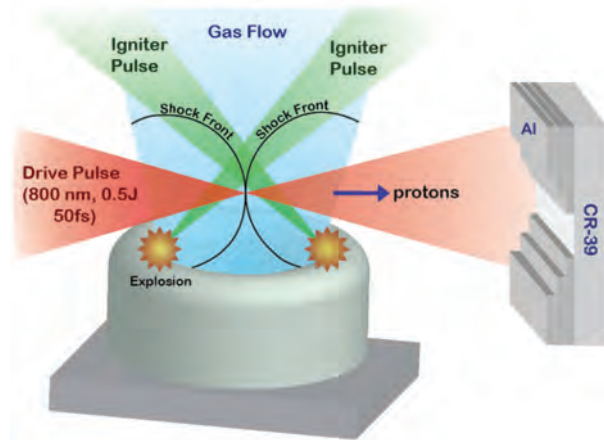


FIGURE 10
Illustration of experimental setup showing the accelerator structure, drive laser, and detector.

gas jet in vacuum using nanosecond frequency doubled Nd:YAG laser pulses. When the shocks collide, the shock fronts additively combine producing a thin gas region with a peak value that is ~ 10 higher than the initial gas density. For these acceleration experiments, we tailored a hydrogen gas flow into a $75 \mu\text{m}$ thick gas “foil” with $30 \mu\text{m}$ gradients and tunable peak densities from $2.5 - 5 \times 10^{20}$ molecules cm^{-3} . This approach provided a pure hydrogen target at densities and gradients previously unexplored. The accelerator was then driven by a 500 mJ, 800 nm, 50 fs laser pulse generated by the

TFL laser system at NRL. The pulse was focused to a vacuum radius of $2.6 \mu\text{m}$, reaching a peak intensity of $1 \times 10^{20} \text{ W cm}^{-2}$. The energy and spatial distribution of the ions was measured with a 1 mm thick CR-39 plate with aluminum filters of varying thickness.

Signature of Acceleration: We optimized the accelerator by performing a density scan over the operational range of our gas jet at intervals of 0.5×10^{20} molecules cm^{-3} . We observed that for densities above $\sim 3 \times 10^{20}$ molecules cm^{-3} a proton beam contained within the length of detector was accelerated in the forward direction. From the diagnostics, we measured the proton energies to be $< 200 \text{ keV}$. For densities below 3×10^{20} molecules cm^{-3} , we saw a vastly different situation: the forward accelerated protons were characterized by a low energy on-axis beam ($< 0.7 \text{ MeV}$) contained within the vacuum laser spot with a halo of high-energy protons ($< 2 \text{ MeV}$), indicating that we had reached the acceleration regime discussed above. We compared these results with simulations made using the NRL developed, fully three-dimensional, particle-in-cell code TurboWAVE. Comparisons between experiments and simulation show excellent agreement (Fig. 11).

Summary: Using a novel gas foil target, we observed the acceleration of ions from an intense laser plasma interaction. We also discovered a unique signature of the acceleration process, namely the formation of a high-energy halo. This acceleration mechanism is directly controlled by the laser and plasma parameters, and thus—by tailoring the plasma peak density, thickness, and gradients—even higher energy beams could be produced. This target and mechanism could provide a way to produce compact, high-repetition proton beams.

[Sponsored by the NRL Base Program (CNR funded) and DOE]

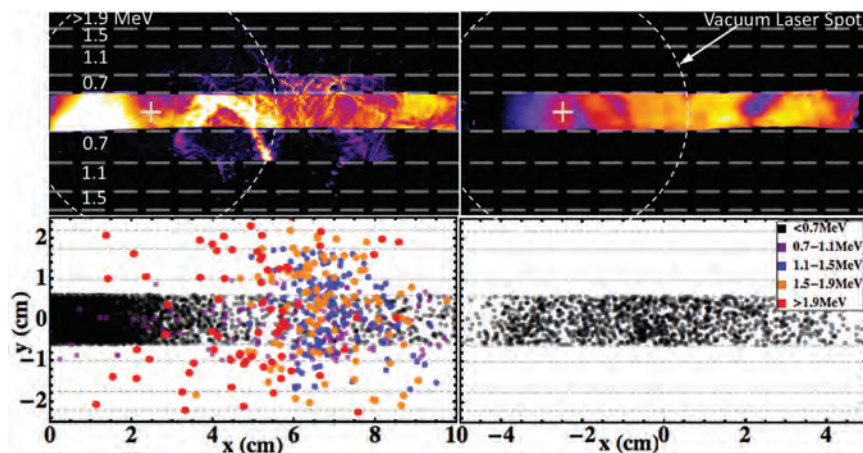


FIGURE 11
Detector images for optimized and un-optimized accelerator conditions (above) with comparisons to simulations (below).

References

- ¹ W. Henning and C. Shank (eds.), "Accelerators for America's Future," workshop report (2010).
- ² M. H. Helle, D. F. Gordon, D. Kaganovich, Y. Chen, J. P. Palastro, and A. Ting, "Laser Accelerated Ions from a Shock Compressed Gas Foil," *Phys. Rev. Lett.* **117** 165001 (2016).
- ³ T. A. Mehlhorn, "National Security Research in Plasma Physics and Pulsed Power: Past, Present, and Future," *IEEE Transactions on Plasma Science* **42**(5), 1088–1117 (2014).



Normally-Off AlGaIn/GaN MOS-HEMTs with Record Performance

T.J. Anderson, V.D. Wheeler, M.J. Tadjer, K.D. Hobart, and C.R. Eddy, Jr.
Electronics Science and Technology Division

Introduction: Gallium nitride (GaN) is an ideal material for power device applications due to its high breakdown field, high switching speed, and low switching losses. Devices based on this materials system are critical for next-generation Navy systems. However, insertion opportunities in power-switching applications are limited by the lack of a reliable normally-off (enhancement mode) device architecture, a critical attribute for fail-safe operation. Removing the AlGaIn barrier layer to eliminate the two-dimensional electron gas (2DEG) under the gate offers a way to achieve enhancement mode operation in high-electron mobility transistor (HEMT) device structures based on the aluminum gallium nitride (AlGaIn)/gallium nitride (GaN) heterostructure. This approach is possible by using either plasma etching or a novel etch stop structure developed by researchers in the High Power Electronics Branch (Code 6880) of the Electronics Science and Technology Division at the U.S. Naval Research Laboratory (NRL).¹ With the barrier layer removed from such a device, it is critical to implement a gate dielectric to suppress gate leakage and allow forward biasing of the gate to turn on the channel. Zirconium oxide (ZrO_2) is a particularly exciting potential gate dielectric for GaN-based electronics, because it offers a combination of high dielectric constant (25) and high breakdown field (15–20 MV/cm). Such films have been integrated with conventional depletion mode (normally-on) HEMT technology to realize reduced gate leakage current and improved reliability by mitigating diffusion of Ni-based Schottky metallization, but the trade-off is a negative shift in threshold (turn-on) voltage due to the increased effective barrier thickness. While acceptable for depletion mode devices, this trade-off is not desirable for enhancement mode devices, because the shift will push the value closer to zero or potentially even into depletion mode operation.

By introducing negative charge in the gate dielectric film, the threshold voltage can be stabilized or shifted positive, realizing reliable enhancement mode operation. The charge in gate dielectric films can be tuned by manipulating the precursors and growth conditions. In our study, by implementing this effect in a real device process and incorporating a barrier recess etch, we achieved record device performance, demonstrating the highest threshold voltage and current density for normally-off GaN transistors reported in the literature.

ZrO_2 Gate Dielectric: Gate dielectrics for wide bandgap devices are typically deposited by the atomic layer deposition technique, using a combination of metal organic and water or ozone precursors to achieve controlled layer-by-layer growth of the films. In the case of ZrO_2 , precursor options include the commonly used tetrakis(dimethylamino)zirconium (TDMA-Zr) and an alternative zirconium (IV) tert-butoxide (ZTB), which is expected to yield cleaner decomposition products but also contains oxygen in the precursor. While films deposited using the two different precursors exhibit similar surface morphology, the film composition and electrical characteristics are different. While the TDMA-Zr-derived film was stoichiometric, the ZTB-derived film contained excess oxygen. Electrically, the ZTB-derived film exhibited a positive shift in the capacitance-voltage curve, as shown in Fig. 12. This shift indicates the presence of substantial negative charge in the film or at the interface in the ZTB-derived film while the TDMA-Zr-derived film is consistent with theoretical values for the flat-band voltage. The

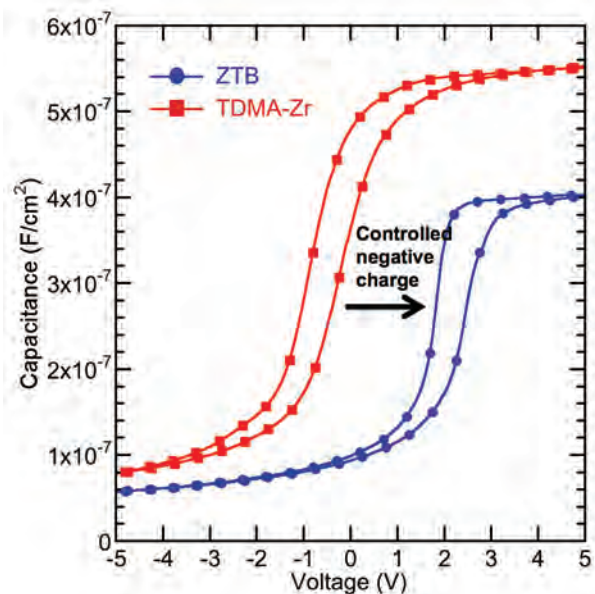


FIGURE 12
Capacitance-voltage characteristics of ZrO_2 films on GaN with varying precursors.

dielectric constant was similar for both films and consistent with expected values for ZrO_2 (~25).

Device Fabrication: For our study, we fabricated devices through standard compound semiconductor fabrication steps. We studied both TDMA-Zr and ZTB-derived films as gate dielectric layers and applied the barrier recess to achieve normally-off operation to select devices. We implemented high-performance passivation layers in all cases. Figure 13 shows a cross-section of the device structures. We also fabricated, in parallel, a conventional Schottky metal-gated HEMT device to serve as a reference.

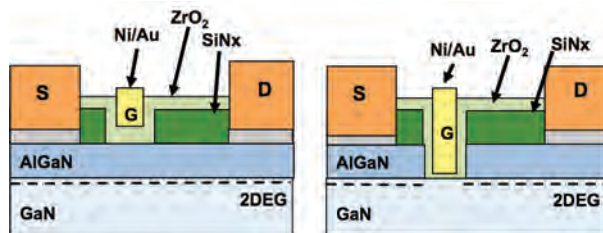


FIGURE 13
Schematic of non-recessed (left) and recessed gate (right) MOS-HEMTs.

Device Characterization and Testing: The non-recessed Schottky gated devices and MOS gated devices exhibited comparable DC characteristics (current density, transconductance, and ON-resistance). The threshold voltage was shifted positive for device structures incorporating the ZTB-derived ZrO_2 film, approaching enhancement mode even without the barrier recess and demonstrating an exceptionally high +4V with a barrier recess.² In contrast, the TDMA-Zr-derived ZrO_2 films exhibited a negative V_T shift due to the thicker effective barrier, just reaching enhancement mode operation even with a full barrier recess (Fig. 14). The ON-state current was degraded in the enhancement mode device; this was expected due to a reduction in electron mobility under the gate from a combination of plasma damage and barrier removal. As expected, the gate leakage was suppressed over five orders of magnitude compared to the reference Schottky gated HEMT. The breakdown voltage was comparable among all device structures both with and without recess and with and without gate dielectric, indicating no adverse effects from either process on OFF-state device performance.

Summary: We developed a gate dielectric process exhibiting high dielectric constant, high breakdown field, and high negative charge. We demonstrated application of this film to a device process, enhancement mode AlGaN/GaN MOS-HEMTs with a thin ALD- ZrO_2 gate oxide, and barrier recess. The integration of

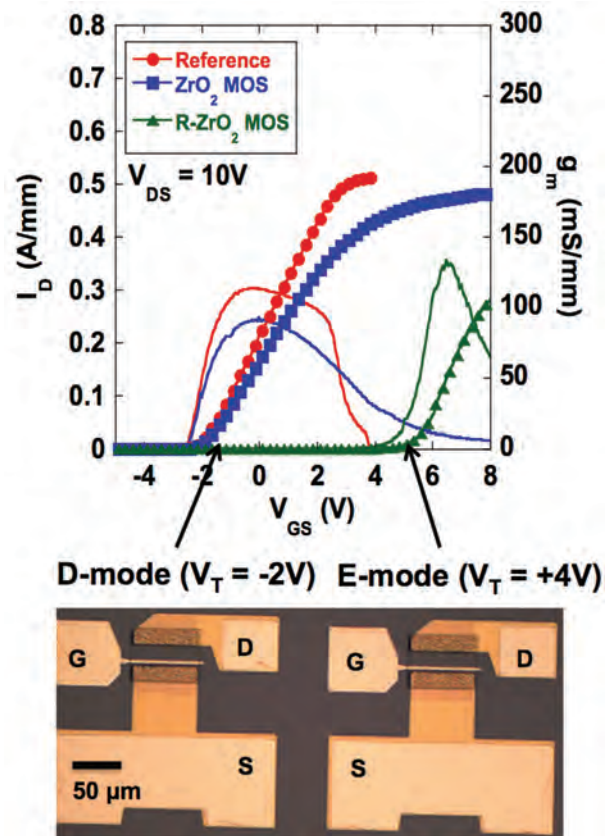


FIGURE 14
Current voltage characteristics for recess-gated MOS-HEMTs.

this particular high-k dielectric in the device structure resulted in a positive threshold voltage shift when using the ZTB precursor due to negative charge in the oxide film and at the interface, which when integrated with a barrier recess enables a $V_T \sim +4\text{V}$ while suppressing gate leakage by four orders of magnitude compared to a reference Schottky-gated HEMT. This result represents record device performance for normally-off AlGaN/GaN HEMTs.

Acknowledgments: The authors are sincerely grateful to the NRL Institute for Nanoscience for equipment use and support.

[Sponsored by the NRL Base Program (CNR funded)]

References

- ¹ T. J. Anderson, M. J. Tadjer, M. A. Mastro, J. K. Hite, K. D. Hobart, C. R. Eddy, and F. J. Kub, "An AlN/Ultrathin AlGaIn/GaN HEMT Structure for Enhancement-Mode Operation Using Selective Etching," *IEEE Electron Device Lett.* **30**(12), 1251–1253 (2009).
- ² T. J. Anderson, V. D. Wheeler, D. I. Shahin, M. J. Tadjer, A. D. Koehler, K. D. Hobart, A. Christou, F. J. Kub, and C. R. Eddy Jr., "Enhancement Mode AlGaIn/GaN MOS High-Electron-Mobility Transistors with ZrO_2 Gate Dielectric Deposited by Atomic Layer Deposition," *Appl. Phys. Express* **9**, 071003 (2016).



NexGen High Frequency Surface Wave Radar

G. San Antonio and T. Moskov
Radar Division

Introduction: The Radar Division of the U.S. Naval Research Laboratory (NRL) recently completed design and installation of a state-of-the-art high frequency surface wave radar (HFSWR) system. The experimental radar system implements the latest research and development ideas, such as two-dimensional receive and transmit arrays, fully digital arbitrary waveform generation, wideband direct digital multifunction receivers, spatial and temporal adaptive signal processing, multiple-input/multiple-output waveform techniques, and track-before-detect tracking. In this article, we provide a high-level description of NRL's NexGen high frequency surface wave radar (NG-HFSWR) system and demonstrate the enhanced capability afforded by its unique features through experimental data results collected so far. The NG-HFSWR system is an experimental prototype for potential U.S. operational systems.

Background: High frequency surface wave radar¹ is a well-established, wide-area, over-the-horizon surveillance technology. The surveillance technology typically operates in the lower half of the high frequency (HF) band (3–15 MHz) and uses a surface-attached, vertically polarized propagating wave field to detect targets over the visual horizon. Large high-power and high-sensitivity systems typically can detect targets to a range of 200 nautical miles. Current generation HFSWR systems can suffer performance degradation from a variety of noise and clutter sources. NRL has established a research and development effort to investigate ways to improve the detection and tracking performance of current-generation HFSWR systems.

Two-Dimensional Oversampled Receive Array: A key enabling technology of the present effort on NG-HFSWR is the concept of spatially oversampled two-dimensional receive arrays. Traditionally, all HF skywave and surface-wave radars have used one-dimensional receive apertures. Advances in adaptive signal processing, computing power, and receiver hardware design have enabled the consideration of more compact two-dimensional antenna layouts. A spatially oversampled antenna layout can occupy less linear space while producing higher directive gains than a one-dimensional array and with the same number of elements as in a one-dimensional array. A two-dimensional array can achieve higher gains through efficient sidelobe interference nulling and superdirectivity if oversampling is employed. Key theoretical and experimental results

published in the past few years indicate the potential benefit of this type of receive aperture.^{2–4}

Figure 15 illustrates a practical example of the types of antenna patterns that can be produced by two-dimensional, oversampled apertures. The figure shows several beamformer characteristics. Because the array is oversampled in both dimensions (depth and lateral), there are two distinct regions of K-space: (1) visible region (far-field directions of arrival) and (2) invisible region (non-physical steer solutions). This pattern shows that the receive mainbeam is pointed into the invisible region, which is a characteristic of a superdirective beamformer solution. The solution is lossy, as indicated by the 8-dB white noise gain, has areas of deep visible space nulls, and per other analysis, achieves higher signal-to-external noise ratio gains than more traditional conventional beamforming solutions.

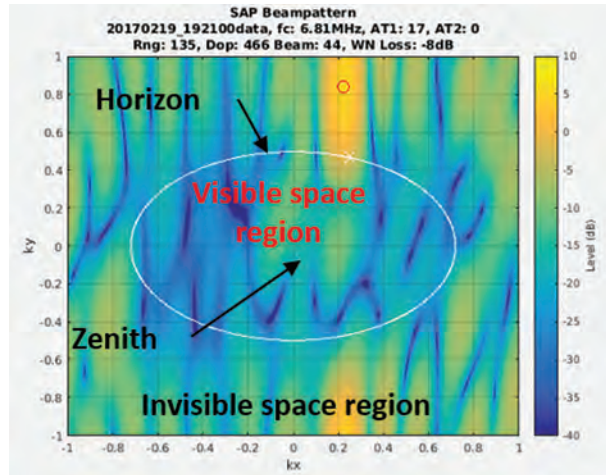


FIGURE 15 Example of a two-dimensional adaptive receive beampattern.

Experimental System: The NRL NG-HFSWR is installed on the East Coast of the United States. The system, configured as a bistatic radar system, provides a surveillance capability off the coasts of Maryland and Virginia. Figure 16 shows a modeled system coverage map.

The system uses two-dimensional phased arrays on both transmit and receive. The receive array is a 64-element, two-dimensional, quasi-hexagonal array arranged in four rows of 16 elements. Extensive electromagnetic modeling indicated that this configuration provides an excellent balance between sensitivity to array manifold errors and achievable optimum array beamforming gains.² The elements of the array are tubular aluminum vertical base-fed monopoles. The array is installed on the beach over a wire-mesh impedance-stabilizing ground screen (Fig. 17). The transmit system uses a 10-element, two-dimensional array arranged in two rows of five elements, in a hexagonal configuration.

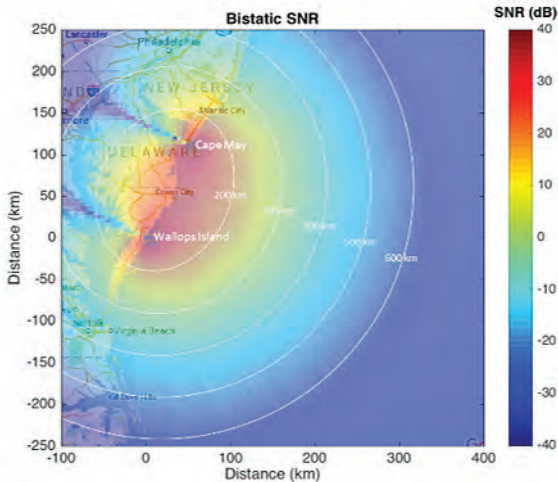


FIGURE 16
Estimated signal-to-noise ratio for $f_c=8\text{MHz}$.



FIGURE 17
Installed two-dimensional receive array.

A unique feature of the system is adaptive spatial and temporal processing combined with a per-element receiver hardware architecture. Advanced direct digital receiver technology provides precise, stable calibration to support advanced processing. Multiple digital down-converters in the receiver technology enable simultaneous multi-functionality.

The transmit system employs coherent independent high fidelity arbitrary waveform generators and power amplifiers per transmit element. This configuration permits flexibility in deciding how to beamform and transmit energy from the transmit site, e.g., transmitting on two frequencies simultaneously.

In addition to the adaptive range, azimuth, and Doppler processing, an advanced track-before-detect processing suite has been developed. The processing routines in this suite allow detection and tracking of threshold targets in heavy clutter inside, on top of, and outside the large first order ocean Bragg clutter. The tracking routines are unique, because they can accept multiple streams of processed data, e.g., from different beamformers or different frequencies.

Experimental Results: Experimental operation has shown that the NRL NG-HSFWR system performs successfully with probability of track versus probability of false track. We conducted a limited effort to confirm current system performance by performing track correlation studies between radar tracks and automatic identification system (AIS) tracks. Figure 18 presents an example track comparison; radar tracks are shown in red, and AIS tracks are shown in blue. The data covers an 8-hour period in which 182 radar tracks were generated. There are several instances of non-correlating high-quality radar tracks. Nearly all AIS tracks have a correlated radar track within the radar field of regard.

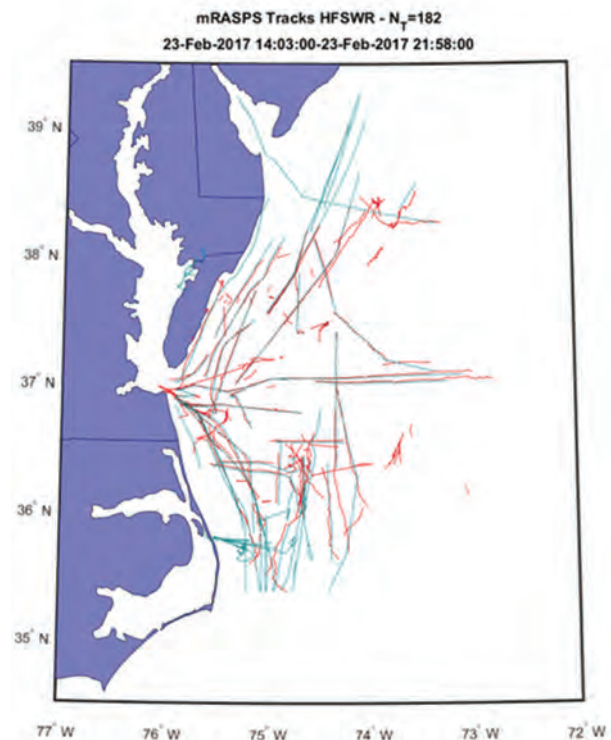


FIGURE 18
Wide area track comparison, high frequency surface wave radar tracks are shown in red; automatic identification system tracks are shown in blue.

In addition to radar track performance, there is an ancillary interest to better understand the nature of the HF noise and clutter conditions. Empirical measurements of two-dimensional noise and clutter spatial spectrums are beneficial in development of models for further radar design and performance assessment. Figure 19 shows an example of a two-dimensional noise spatial spectrum. The currently constructed two-dimensional receive array is the first HF receive system to produce such detailed, unambiguous, high-dynamic range, two-dimensional noise spatial spectrum estimates. Prior noise mapping results were produced with either one-dimensional apertures or sparse two-

dimensional apertures. The current results confirm that daytime low frequency HF noise is dominated by one-hop propagation and manmade noise is clearly the dominant noise generation source. The area of low noise (deep blue) between -40 and +10 degrees azimuth is in the direction of open ocean for more than 2,000 miles.

Summary: The NRL Radar Division has successfully designed, deployed, and operated a new NG-HFSWR system that has demonstrated the potential performance improvement of new technology concepts. Overall system performance can be characterized via tracker performance. Key enabling technologies include two-dimensional receive arrays and adaptive signal processing. Ongoing research includes collecting new environmental data for a better understanding of HFSWR performance, including its further refinement.

⁴ G.J. Frazer, C. Williams, Y.I. Abramovich, and G.S. San Antonio, "A Regular Two-Dimensional Over-Sampled Sparse Receiving Array for Over-The-Horizon Radar," IEEE Radar Conference, Washington, DC (2015).

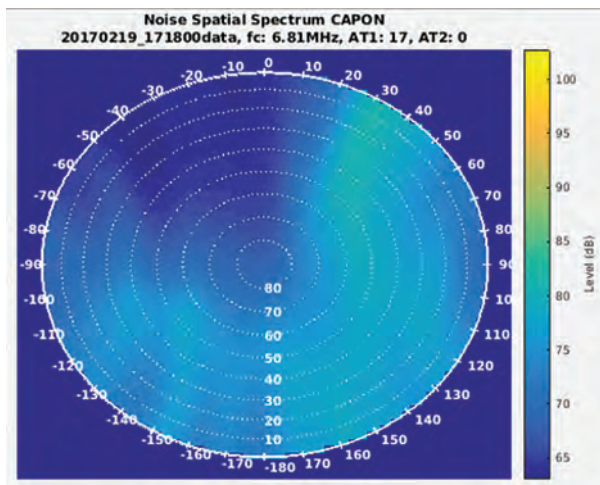


FIGURE 19 Two-dimensional high frequency noise spatial spectrum. Azimuth relative to receiver array boresite on circumference, radial dimension indicates elevation angle (zenith in center).

Acknowledgments: We thank the team from NRL; WR Systems, Ltd. (Fairfax, Virginia); and the Forces Surveillance Support Center, who made the experimental system a success. We also thank NASA and the U.S. Coast Guard for providing the support and infrastructure required to operate the NG-HFSWR system.

[Sponsored by the NRL Base Program (CNR funded)]

References

- ¹ J.M. Headrick and S.J. Anderson, "HF Over-the-Horizon Radar," in *Radar Handbook*, M.I. Skolnik, ed. (McGraw-Hill Education, New York, 2008). Ch. 20, 20.1–20.70.
- ² G.S. San Antonio and Y.I. Abramovich, "Two-Dimensional High Frequency Surface Wave Radar Receive Array Design," IEEE Radar Conference, Seattle, Wash., May 8–12, 2017.
- ³ G.S. San Antonio, Y.I. Abramovich, G.J. Frazer, and C. Williams, "Electromagnetic vs. Plane Wave Models for Superdirective 2D Adaptive HF Receive Antenna Performance Assessment," IEEE Radar Conference, Washington, DC (2015).

- 146** Goal Reasoning for AUV Control
- 147** The Application of Complex Network Analytics to Dynamic Wireless Network Systems
- 149** Navy Malware Catalog
- 151** Predicting Academic Attrition in Naval Air Traffic Control Training

Goal Reasoning for AUV Control

D.W. Aha,¹ M.A. Wilson,¹ J. McMahon,² B. Houston,² and A. Wolek³

¹Information Technology Division

²Acoustics Division

³ASEE Postdoctoral Fellow residing at NRL

Introduction: Goal reasoning is the ability of an artificial intelligence agent to respond to unexpected occurrences in uncertain, dynamic, or partially observable domains by reasoning about and altering its goals. Goal-Driven Autonomy (GDA) is a goal reasoning model that monitors plan execution for discrepancies between expectations and observations.¹ When a discrepancy is detected, a GDA agent constructs an explanation to reconcile its observation and action histories with the discrepancy, and thereby infers knowledge (i.e., the causes of the discrepancy) that the agent cannot directly observe. The agent then selects an appropriate goal based on its revised knowledge. We conducted initial at-sea tests of a GDA agent controlling an Iver2 autonomous underwater vehicle (AUV) as the AUV pursued a survey task (which typically occurs during, for example, mine countermeasure missions). We tested the agent's response to a simulated surface vessel that unexpectedly traverses the AUV's survey area.

AUV Control Architecture: In our system architecture (Fig. 1), the GDA Controller monitors the AUV and plans sensing and navigation tasks, delegating execution to other components. To control the AUV, we employ MOOS-IvP, an open-source autonomy architecture.²

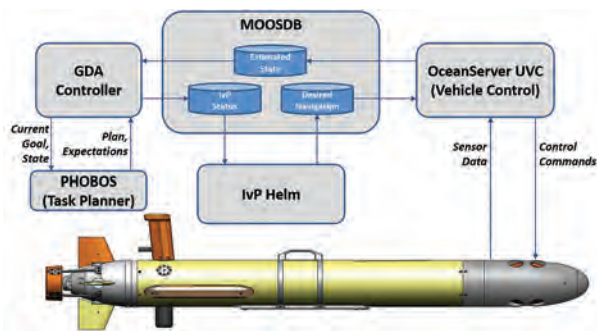


FIGURE 1
A diagram of our autonomy system architecture onboard an Iver2 autonomous underwater vehicle, illustrating the interaction of major system components.

IvP Helm is a reactive, behavior-based controller that produces decisions in the navigation space (heading, speed, and depth). The GDA Controller executes task plans by activating, deactivating, and configuring IvP Helm behaviors to perform task actions (e.g., driving to a waypoint).

Test Mission: The AUV starts at a launch point near the shoreline (Fig. 2) at the U.S. Naval Research Laboratory's (NRL's) Chesapeake Bay Detachment (CBD). The initial, user-provided goal of the AUV is to perform a simulated survey of the seafloor in a given region. The AUV also may pursue such goals as reaching the launch point, reaching an arbitrary waypoint, completing the survey of a given region, and waiting without action for the next observation.

A simulated surface vessel initially loiters in the center of the survey region, then transits to a randomly chosen destination in an endpoint region. The surface vessel is designated either "hostile" or "neutral." A hostile vessel emits active sonar pings such as it might use if searching for the AUV. A neutral vessel does not emit active sonar. In either case, the vessel emits engine noise.

When the surface vessel is within the AUV's sensor range, the simulator reports the engine noise to the GDA Controller. Since the agent does not know of the surface vessel's proximity in advance, the engine noise is a discrepancy. The agent will explain the discrepancy by assuming that a new contact is within sensor range. However, this knowledge does not affect goal selection, and the agent continues with the goal of surveying the region.

A similar sequence occurs if the surface vessel is hostile and its simulated pings are detected. However, in this case, the explanation indicates that a hostile contact is within range, and the agent formulates a new goal to return to a safe location.

When the surface vessel leaves the AUV's sensor range, the simulator stops reporting engine and ping noise to the agent. The agent resolves this discrepancy by assuming that the contact has exited sensor range and resuming the goal to survey the region. After the survey goal is complete, the agent formulates a new goal to return to its launch point.

Results: To demonstrate the agent's ability to react to discrepancies encountered by a real-world robotic platform, we conducted trials at the depicted NRL CBD location. The surface vessel and noise detection were simulated (on board the Iver2) to simplify operations.

We collected data from 25 simulated trials and six at-sea trials (two at the surface and four at a depth of 0.75 m). Ten simulated trials were conducted with a hostile surface vessel and 15 with a neutral vessel; three of each were conducted in at-sea trials. We confirmed that the agent can select goals and execute plans based on an initial user-defined mission, recognize when a goal is completed, detect discrepancies, and formulate new goals in response. In all cases, the agent correctly detected the vessel and, if hostile, its active pinging. In the case of a hostile vessel, the agent reacted by explain-

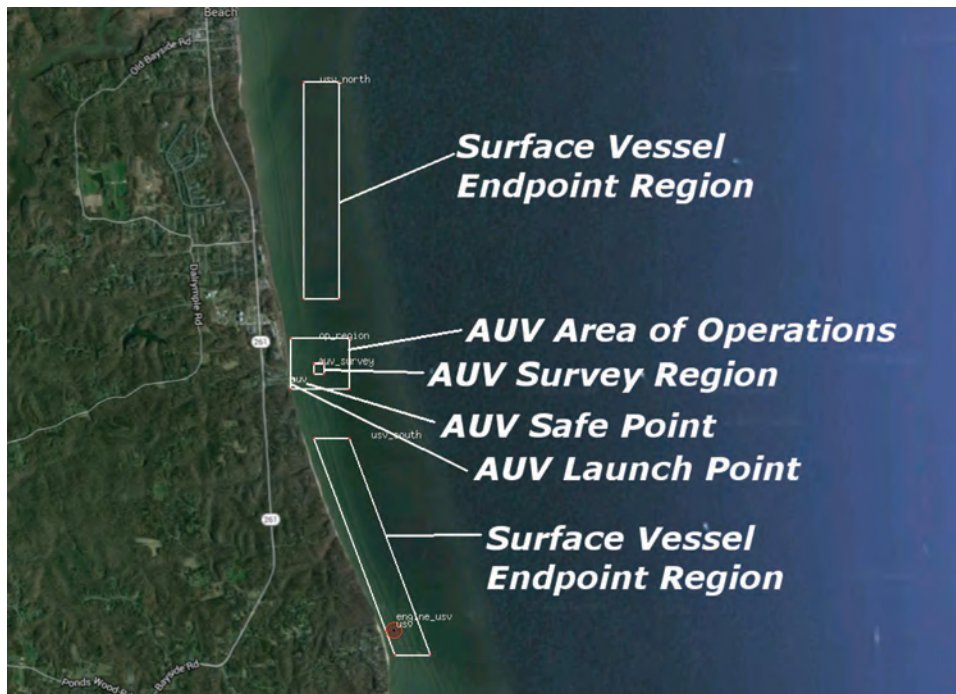


FIGURE 2
The configuration of the test survey mission at the U.S. Naval Research Laboratory's Chesapeake Bay Detachment.

ing the discrepancy and selecting the correct goal. The agent also detected and explained a discrepancy when it drifted too far before starting one at-sea trial.

In future work, we will employ motivator-based goal selection to reason about goal utility, introduce motion plans to reason about goal costs, and address more challenging mission elements such as noisy sensor models, marine sound sources, more advanced behaviors (e.g., following other vehicles), and the need to communicate events of interest to remote operators or gather information about specific environment features.

Acknowledgements: We thank Jeff Schindall of the Acoustic Signal Processing and Systems Branch (Code 7160) for his assistance with in-water exercises. [Sponsored by the NRL Base Program (CNR funded)]

References

- ¹ M. Klenk, M. Molineaux, and D.W. Aha, "Goal-Driven Autonomy for Responding to Unexpected Events in Strategy Simulations," *Computational Intelligence* **29**(2), 187–206 (2013).
- ² M.R. Benjamin, H. Schmidt, P.M. Newman, and J.J. Leonard, "Nested Autonomy for Unmanned Marine Vehicles with MOOS-IvP," *Journal of Field Robotics* **27**(6), 834–875 (2010).



The Application of Complex Network Analytics to Dynamic Wireless Network Systems

J. Macker, B. Adamson, J. Dean, and J. Weston
Information Technology Division

Overview: The ongoing proliferation and cost reduction of wireless computing, communications, and sensor systems is stimulating future plans for extreme interconnection of heterogeneous wireless systems at the tactical edge of the battle space. As these networked wireless systems become more complex, new methods of predictive analytics are needed to support the planning and optimization of tactical missions, and this capability can directly impact communications effectiveness, dynamic resource management, and cyber robustness. To address this gap, the U.S. Naval Research Laboratory (NRL) has been researching, developing, and adapting complex network theory models and metrics for use in the context of collaborative dynamic wireless network systems. A complex network is a graph-based model with nontrivial topological features that better represents an interaction model of a real-world network. Effective application of complex network theory and predictive analytics in mobile, wireless communication networks is challenged by extreme structural dynamics and commonplace disruptions. To address the modeling challenges, we applied tempo-

ral graph models to include metadata dynamics, such as fluctuating link quality and dynamic traffic loads, related to the underlying mobile and dynamic network structures under study. We also researched and extended graph-based structural metrics, such as centralities, including recent temporal variants emerging from basic research. We applied our modeling methods and related metrics to examine distributed computing optimization, traffic load and routing prediction, and dynamic communication workflow modeling.

A couple of examples illustrate the practical significance of research into this kind of predictive analytics. For one, future collaborative sensing or autonomous networked mission execution is challenged by the need for jointly optimizing communication and distributed computation over a wireless network. To research this problem, we formulated a working distributed computing model within a mobile ad hoc network (MANET) environment and measured the correlation between actual computing delay and a predictive model using complex network centrality metrics.¹ We showed that certain complex network metrics correlated strongly in predicting network locations of task controllers to achieve minimal computing delay. Such capability helps solve mission planning and optimization problems that require coordinated tasking over distributed wireless resources. Figure 3 shows an example graphic result from the predictive metric, illustrating a 100-node random geodesic network with 30 collaborative computing entities. The blue nodes represent the randomly chosen candidate worker nodes, and the green node represents the predicted task manager location to minimize delay.

As another example, much as in highway traffic planning, it is important to characterize and predict the paths and relative traffic loading likely to occur within



FIGURE 3
Controller location to minimized distributed computing delay.

a tactical network infrastructure. However, the structure of tactical wireless networks, unlike that of physical roadways, changes constantly, with related impacts on the overall network traffic loading. In recent work,² we demonstrated predictive analytics of actual traffic forwarding within a complex mobile ad hoc network using a temporal graph model of the structure and metrics relevant to the class of network being examined. Although prediction accuracy fluctuates in time, results demonstrated good correlation between predicted and actual measured routing load across several mobile network trials with multiple traffic profiles and routing classes. Such capability is beneficial in understanding and optimizing complex system resource usage, but it also has network cyber applications, as these temporal prediction models better identify and track critical communication nodes and edges within the system. Figures 4(a) and 4(b) illustrate recent results from correlating the predicted load rankings within an emulated mobile wireless network using a set of complex network prediction metric rankings. A perhaps surprising result is that the locally calculated metric (discussed below) performs well in predicting load ranking, and, there-

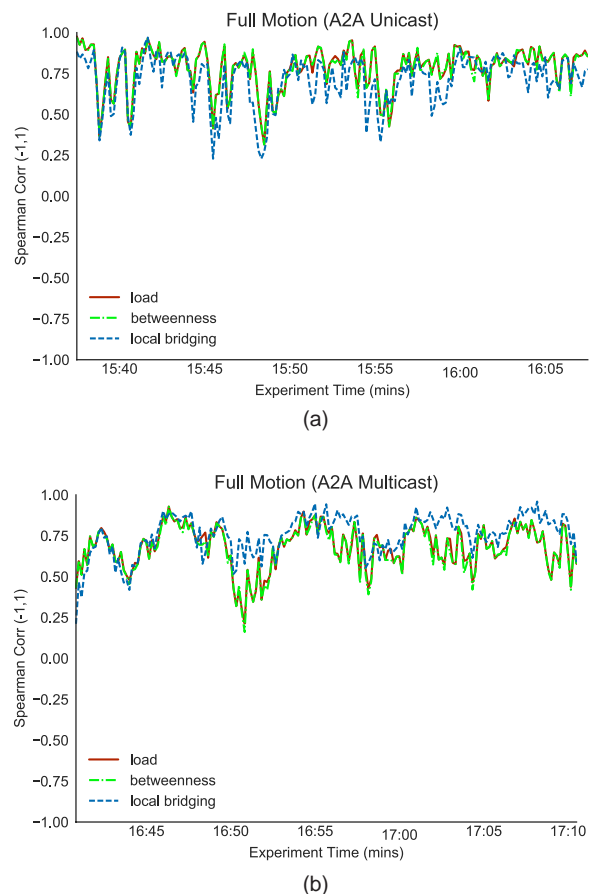


FIGURE 4
(a) Analytic prediction of unicast forwarding within a mobile network. (b) Analytic prediction of multicast forwarding within a mobile network.

fore, may lead to better ways of conducting distributed network management.

Most structural and predictive metrics from complex network theory (i.e., centralities) require global state to compute, and, when applied to distributed wireless systems, this requirement can be detrimental due to communication overhead and delay costs incurred in collecting global state. We carried out additional research³ that developed an improved localized centrality metric to identify bridging characteristics of a node within a communication network. To evaluate this algorithm's accuracy, we examined the ranking correlation to a known global state algorithm across a series of complex dynamic network scenarios. We demonstrated significant correlation improvement over past work, and the capability can be applied to improve localized decision-making of protocols or distributed management within networks. Figure 5 illustrates the correlation increase to the global results achieved by our Localized Bridging Centrality 2-hop (LBC2) algorithm when executed in a 600-second complex littoral mobile wireless network scenario.

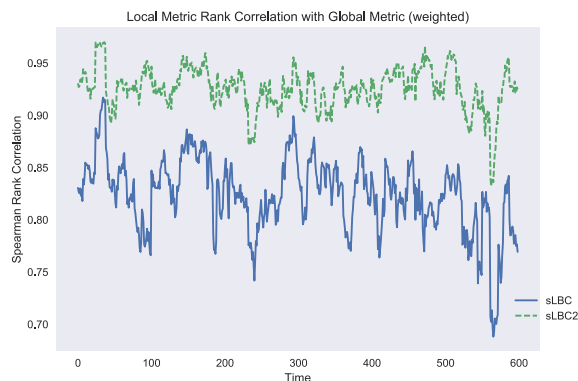


FIGURE 5 Performance enhancements to localized bridging centrality.

Future Work and Issues: This work demonstrates the application of complex systems theory to improve the modeling and prediction of dynamic tactical communication network performance. These analytic and predictive mechanisms provide new capabilities for designing, planning, and operating complex networked systems. Planned future work will address analytic applications to complex, autonomous networks across multiple heterogeneous system layers, including analyzing the dynamic flow of information at the mission layer.⁴⁻⁶

[Sponsored by the NRL Base Program (CNR funded)]

References

¹ J.P. Macker and I. Taylor, "Prediction and Planning of Distributed Task Management Using Network Centrality," in *IEEE MILCOM 2014 Proceedings* (2014).

² J.P. Macker and J. Weston, "An Examination of Forwarding Prediction Metrics in Dynamic Wireless Networks," in *IEEE MILCOM 2017 Proceedings* (2017).

³ J. Macker, "An Improved Local Bridging Centrality Model for Distributed Network Analytics," in *IEEE MILCOM 2016 Proceedings* (2016).

⁴ J. Macker, Workshop on Assured Autonomy, Design, Modeling, and Analysis of Dynamic Wireless Networks and Layered Autonomy, The University of Florida, April 3, 2017.

⁵ J.P. Macker and I. Taylor, "Orchestration and Analysis of Decentralized Workflows within Heterogeneous Networking Infrastructures," *Future Gener. Comput. Syst.* **75**, 388–401 (2017).

⁶ J. Macker, "Hamlet: A Metaphor for Modeling and Analyzing Network Conversational Adjacency Graphs," in *IEEE MILCOM 2016 Proceedings* (2016).



Navy Malware Catalog

J. Mathews

Information Technology Division

Introduction: Military doctrine for addressing malware cites key activities that share mission requirements to catalog digital artifacts suspected of being malicious, as well as metadata derived from those artifacts.¹ Recent studies underscore the role malware plays in facilitating cybersecurity breaches, note trends towards malware with targeted payloads motivated by economic gain, and provide evidence asserting the proliferation of Internet connected devices will catalyze the malware trade.^{2,3} The Department of Defense electronically exchanges information with federal agencies, academic research institutions, industry supply-chains, and multi-national forces, and, therefore, malware infections on military networks likely will be exacerbated by implicit trust relationships with the global Internet community. These factors highlight the importance of achieving efficiencies in the malware analysis mission.

Current mechanisms for acquiring, analyzing, and preserving malware are best characterized by their deficiencies. Analyses conducted on dirty networks are of limited utility when investigating malware designed only to display signs of nefarious behavior when in the target environment. Analysis results incorporating gleaned characteristics circulate as static content in technical reports that do not lend themselves well to timely, actionable, or automated responses by actuating defense mechanisms. Further, technical reports disseminated among a variety of classified channels require a knowledgeable person in the loop with the appropriate access to read, digest, and act upon information in the reports. Malware reports are niche, perishable content spread among disparate websites, forums, and email distribution lists, and, therefore, achieving a holistic understanding of how adversarial tradecraft evolves

over time is nearly impossible. There also exists limited unifying capability for sharing pertinent information between a broad array of activities incorporating a malware analysis component, and the analyst community is limited to a relatively small number of highly skilled specialists lacking the resources and critical mass to establish one. These dynamics constitute a significant challenge for those who might observe or respond to malware, particularly those conducting forensic intrusion investigations at the site of targeted activities and who need to rapidly triage suspicious artifacts.

Development of a Malware Cataloging System:

With these considerations in mind, we developed the Navy Malware Catalog (NMC), a system for collecting and analyzing cyber-intrusion artifacts on military networks. The NMC is an information repository for garnering deep insight into proliferating threats by providing a clear view into malware's de-obfuscated code, data, behavior, and reputation. It enables workflows for scrutinizing suspicious and potentially dangerous files of unknown provenance through automated mechanisms that safely execute, observe, and measure behavior. It further provides a tool to curate behavioral indicators, or characteristics of what the malware looks like in memory, how it communicates on the network, and other operating system artifacts. These indicators are critical to gauging the extent of compromise (i.e., knowing what other systems exhibit the same characteristics) and informing the creation of technical countermeasures (e.g., firewall rules, intrusion signatures, access control lists, and antivirus signatures) that limit collateral damage.

Traditionally an arduous process, malware analysis requires an exhaustive combination of software reverse engineering, source code debugging, runtime execution analysis, and network and memory forensics. Static analysis techniques identify surface characteristics such as cryptographic hash, size, type, header, embedded content, and the presence of a software packer. Dynamic analysis techniques identify runtime characteristics such as alterations to the file system, operating system, process listings, mutexes, and network touchpoints. Each submission to the NMC is subject to a gamut of iterative analysis techniques automating investigatory rote that conventionally demand a corpus of tools like those illustrated in Fig. 6.

The NMC orchestrates static and dynamic analysis in a scalable, distributed system, adopting technology from big-data ecosystems. Components execute through a containerized application infrastructure in which application-programming interfaces coordinate analysis mechanisms implemented as on-demand services. These mechanisms include antivirus engines, sandbox detonation chambers, and heuristic utilities that measure the reputation and behavior of files across a variety of target operating systems. Supported file types include common malware delivery vectors such as Microsoft's portable executable format, Adobe's portable document format, Java archives, rich text files, and Microsoft Office content including Word, Excel, and PowerPoint.

Conclusion: The NMC addresses the needs of a broad community of cybersecurity practitioners, including those who (1) provide the first line of response

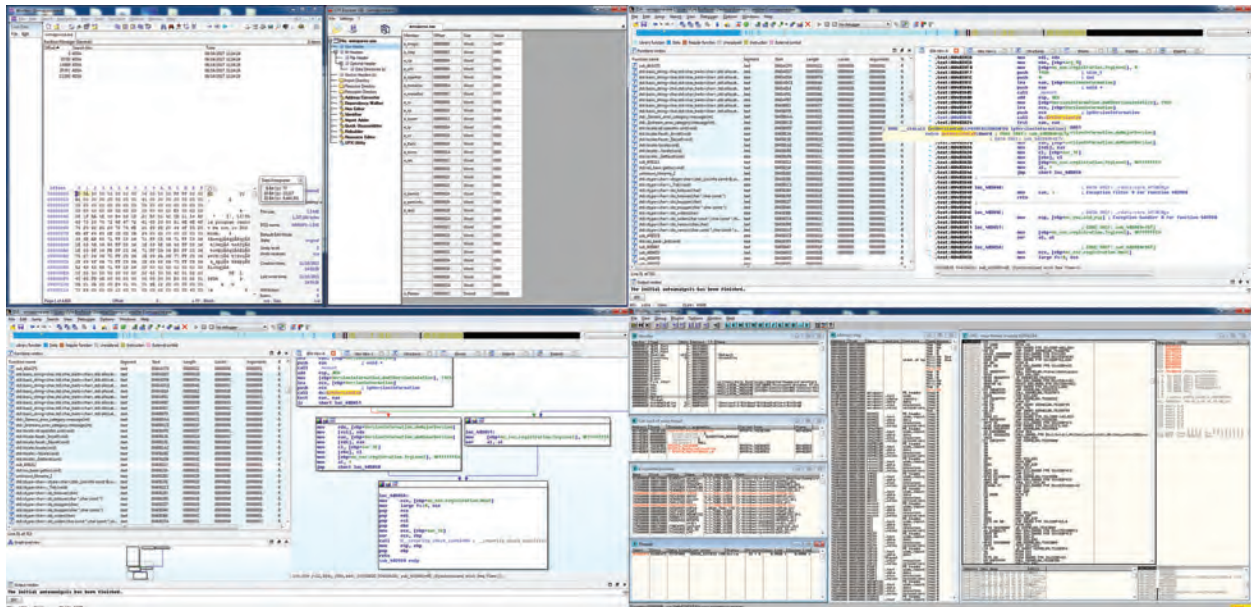


FIGURE 6
Example representation of malware investigatory methods.

to cyber-intrusions through continuous monitoring and incident response, (2) collect and distribute information on threats to DoD networks, (3) investigate and prosecute cyber-crime, (4) develop or maintain warfighting information technology, and (5) research information security vulnerabilities. Users access the NMC through a secure web browser and, once authenticated, are able to submit samples for analysis, view recent community submissions, and search for samples by any set of characteristic attributes. Users also may annotate samples with comments and information, thereby promoting collaboration across the community. The NMC affords its users a capability to understand the intent and pedigree of malware, while preserving empirical data on threats targeting military systems.

[Sponsored by the Navy Cyber Defense Operations Command]

References

¹ Chairman of the Joint Chiefs of Staff Manual 6510.01B, *Cyber Incident Handling Program*, 10 July 2012, published at <http://disa.mil/Services/DoD-Cloud-Broker/~media/Files/DISA/Services/Cloud-Broker/m651001.pdf>.

² Verizon, *2017 Data Breach Investigations Report*, 10th Edition, retrieved June 8, 2017, from http://www.verizonenterprise.com/resources/reports/rp_DBIR_2017_Report_en_xg.pdf.

³ MalwareBytes Labs, *2017 State of Malware Report*, retrieved June 8, 2017, from <https://www.malwarebytes.com/pdf/white-papers/stateofmalware.pdf>.



Predicting Academic Attrition in Naval Air Traffic Control Training

N.L. Brown,¹ D. Smith,² T. Olson,³ and C. Moclair³

¹*Marine Geosciences Division*

²*Formerly with the Marine Geosciences Division*

³*Naval Aerospace Medical Institute*

Introduction: The Center for Naval Aviation Technical Training (CNATT) Air Traffic Control (ATC) program experiences very high academic attrition rates. The Naval Aviation Technical Training Center (NATTC), which trains Navy and Marine Corps air traffic controllers, reported attrition rates of 31%, 19%, and 30% for fiscal years 2014, 2015, and 2016, respectively. The Armed Services Vocational Aptitude Battery (ASVAB) scores are used to help identify qualified candidates for the program, but, taken by themselves, the scores do not sufficiently differentiate between prospective students who will succeed and those who will struggle and ultimately fail ATC training. This finding is not surprising considering the ASVAB was designed

to identify qualified individuals for military enlistment and suitable occupational settings for them, and not to measure the specific cognitive aptitudes central to success in an ATC training program.¹

We expected performance in the ATC program to be influenced by cognitive functions, including spatial ability skills (the ability to mentally rotate objects and remember spatial locations) and working memory (the ability to actively process information in the face of new and competing information).² Based on a prior study (Held and Caretta),¹ we hypothesized that aptitudes in these areas would provide a better assessment of the skills required during ATC training than would the ASVAB alone. Thus, we expected that including additional assessments of working memory and spatial ability would improve the ability to identify individuals—before their training began—at risk of academic attrition, an improvement that, in turn, would reduce the academic failure rate during ATC training.

Human Subject Experiment: We offered prospective ATC students an opportunity to participate in our human subject experiment before the start of their ATC training. We assigned all participants a series of computer-based assessments designed to measure attention (the ability to selectively attend to relevant information), immediate memory (memory for recently presented information, specifically, information that was no more than 20 seconds old), working memory, and spatial ability. We then correlated the participants' assessment scores with their training performance (setbacks, retesting, and grades) and academic attrition as an approach to identifying the underlying causes of training successes and failures.

Participants. The results from the 107 ATC students who participated were reported. Seventy-six males and 31 females participated between the ages of 17 and 27 ($M = 20.9$, $SD = 2.4$); 32 were enlistees of the U.S. Marine Corps and 75 of the U.S. Navy. Officers and foreign nationals were excluded from our assessment.

Procedure. Participants volunteered for the assessment by reporting to the Naval Aerospace Medical Institute (NAMI) and providing consent, and then completed computerized versions of four tasks: (1) the Direction Orientation Task (DOT) simulation, (2) the n-back task,³ (3) the Automated Operation Span (Aospan)⁴ task, and (4) the Automated Symmetry Span (SymmSpan).⁴ Participants also completed a demographic questionnaire. The DOT simulation (Fig. 7(a)) and the SymmSpan (Fig. 7(b)) task measure spatial ability. Specifically, the DOT simulates the flight of an unmanned aerial vehicle (UAV) (a task akin to operating a drone) and assesses mental rotation and object tracking. The SymmSpan task measures memory for spatial location. The n-back (Fig. 7(c)) task measures attention, immediate

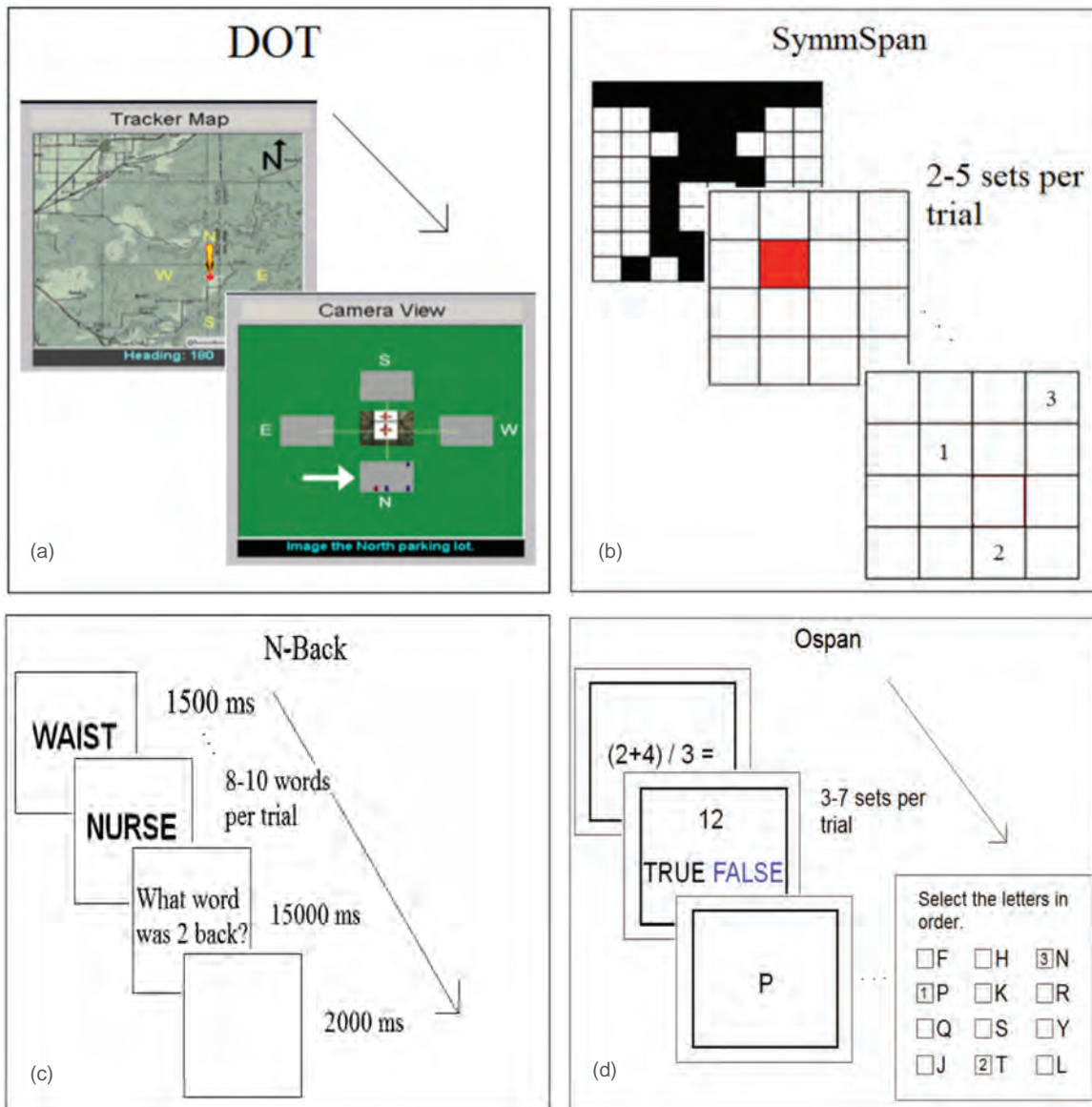


FIGURE 7
Examples of the tasks for assessing spatial ability and working memory among 107 air traffic control trainees: (a) the Direction Orientation Task (DOT) simulation, (b) the Automated Symmetry Span (SymmSpan) task, (c) the n-back task, and (d) the Automated Operation Span (Aospaspan) task.

memory, and working memory. The Aospaspan task (Fig. 7(d)) is a commonly used measure of working memory.

In the DOT simulation, participants watched an aerial view of an unmanned aerial vehicle (UAV) moving over a map. When the UAV came to a stop, the participants saw a parking lot from an aerial vantage under the UAV. The north direction, from the Camera View, varied depending on the direction the UAV faced, and participants had to determine the direction the UAV was facing.

In the n-back task, participants studied lists of words. Each word was presented one at a time. The lists varied in length to prevent participants from predicting the end of the list. At the end of each list, they had to

recall a word located one, two, or three words up from the end of the list.

In the Aospaspan task, participants were shown two-step math problems followed by a letter to remember. This sequence was repeated three to seven times per trial. At the end of the Aospaspan trial, participants were asked to indicate each letter in the order it was originally presented. Participants were encouraged to keep their math accuracy at or above 85% to prevent them from only attending to the memory portion of the task. Finally, the SymmSpan task required participants to judge whether a pattern was symmetrical along its vertical axis and then recall the location of darkened cell in a 4×4 matrix; this sequence was repeated two

to five times per trial. At the end of the SymmSpan trial, participants were required to indicate the locations of each cell in the order the cells were presented. Participants were encouraged to keep their symmetry accuracy at or above 85% to prevent them from focusing on the memory portion (i.e., recalling the location of the darkened cell) of the task.

NATTC provided four kinds of data on how the 107 participants fared in their ATC program training: (1) grades (test scores), (2) retests (number of tests re-taken due to poor conceptual knowledge), (3) setbacks (number of times participants were retained, or “held back,” for the next class due to poor academic performance), and (4) attrition (disenrollments for poor academic performance).

The NRL Institutional Review Board (IRB) reviewed and approved our research method and procedures prior to the start of our assessment. NAMI participated in the research under NRL’s IRB protocol. This partnership was further approved by the Department of Navy Human Research Protection Program. CNATT also reviewed the research in full and the CNATT Commanding Officer gave prior approval to participation of the ATC students in the study.

Results: The academic attrition rate of our sample was 32.7%, similar to the rates reported by NATTC over the past few fiscal years. Thus, it appeared this sample was representative of the general ATC population. The results are centered on the first of three training units because 88.6% of attrition occurred during this unit.

Preliminary Analyses. We ran bivariate correlations between the measures (accuracy and response latencies) from the cognitive assessments and academic status (passed or failed Unit 1 of ATC training). We used cognitive measures that held significant correlations with academic success to predict attrition. We considered a result significant whenever the likelihood that the outcome could be chance was less than 5% ($\alpha = .05$)

Ordinal Regression Predicting Graduate Status. We found three significant predictors of academic success in Unit 1 of the ATC training program: (1) working memory ability (assessed on the Aospan task), (2) attention (assessed on the n-back task), and (3) spatial ability (assessed on the DOT). We ran an ordinal regression model to classify participants as either passed or failed in Unit 1 (attrite). The model itself was a good fit ($\chi^2 = 18.56, p < .001$). The measures from the cognitive assessments were exceptionally good at predicting who would pass (94%, $n = 64$) but performed poorly at identifying who would fail Unit 1 (39%, $n = 31$) (see Fig. 8), i.e., participants who performed well on the cognitive assessments were likely to pass Unit 1. In comparison, the model could not accurately differentiate between success and failure in the training program when participants only did well on one or two of the measures. The model results indicated that performance on these three cognitive assessments identified about 25% of the variance in what may cause a student to drop out for academic reasons in Unit 1. Together, these results can be used to identify a pool of students who are most likely to be unsuccessful in Unit 1 before

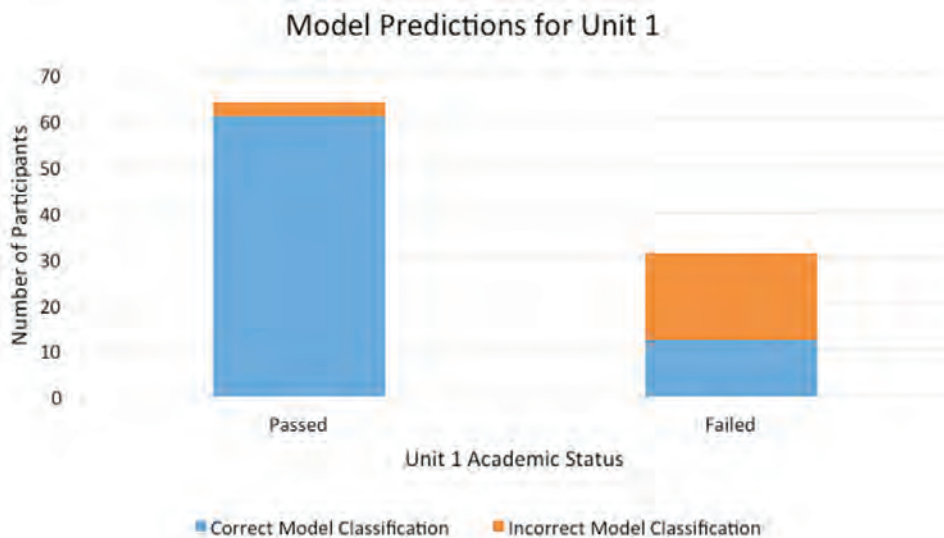


FIGURE 8 Model outputs predicting academic status (passed or failed) in a unit of study from an air traffic control training program for U.S. Navy and Marine Corps personnel. Data for 12 participants were missing on one or more of the cognitive assessments due to a computer error. Thus, their results were not included in the model.

they begin training and provide some insight into the areas where they may struggle (e.g., lower spatial ability skills).

Random Forest Predicting Graduate Status. We also included random forest machine learners in our evaluation of cognitive ability and ATC training performance. Although the current results do not represent “big data,” we expected the random forest to better select the most useful measures of cognitive ability for predicting graduate status, because we can include all of the more than 100 cognitive ability measures generated from the experiment. To reduce the influence of possible bias and error in the model, we included only the three measures in the regression model that shared a significant bivariate correlation with academic performance in Unit 1 and that were theoretically related to academic performance.

For the machine learning, we performed a supervised transformation on bite samples of the data, using a random forest to transform the samples into a high dimensional space. We then used a logistic regression classifier to classify the data in that space. We used a jackknife approach whereby a single participant’s data was removed as the test set and the remaining data were used as the training set. We used the Matthews Correlation Coefficient (MCC) to measure the quality of our model, because it takes into account both true and false positive and negative outcomes, thus providing a balanced measure of the model.

The results showed that the most important measures came from the n-back task, with the remaining measures providing lower and near equal levels of importance. Using this approach with the n-back task results only, we were able to obtain an MCC = .33, where 0 indicates a completely random result and 1 is a perfect prediction. This model correctly classified 86% of the students who passed and 49% of the students who failed. Using only the n-back task results, our machine learning approach was able to identify success and, importantly, those who were likely to fail Unit 1. Similar to the results of the ordinal regression, the model had difficulty correctly classifying students who were likely to fail but did outperform the ordinal regression. These results may indicate that results from the other cognitive assessments included in the ordinal regression may add to the model some noise that interferes with predicting academic failure in Unit 1.

Summary: Overall, the results suggest a connection between performance on the cognitive assessments and academic performance in the Navy’s ATC training program. Both models have similar outcomes, and can be used to identify the group of students who are most likely to have trouble in training before the program begins. NATTC can then use these results to provide

additional academic support for these students to help lower the attrition rate. Currently, the NATTC relies on the ASVAB to screen for students, but ASVAB has not been useful in identifying students who may be at risk of failing. Thus, including the cognitive assessments can provide a significant amount of value to NATTC. The high false positive rates (61% and 51%) observed in this study are considered low risk, because incorrectly identifying a student as likely to fail and offering more academic support is likely not harmful to the student and may even further benefit those students.

Our research provides insight into the causes of academic hardships in the Navy’s ATC training program. We can further improve the models by continuing to collect data. The sample size (N = 107) for our assessment is small for this type of research; a larger sample size would help reduce the error in our models. Our results also suggest the cognitive assessments alone may predict only a small amount of variance surrounding failures in ATC training. We might also find worthwhile the evaluation of additional factors (e.g., motivation, personality) that may influence training performance.

[Sponsored by the Center for Naval Aviation Technical Training]

References

- ¹J.D. Held and T.R. Carretta, “Evaluation of Tests of Processing Speed, Spatial Ability, and Working Memory for use in Military Occupational Classification,” *Navy Personnel Research, Studies, and Technology Research in Work Report* (2013).
- ²R.W. Engle, J.E. Laughlin, S.W. Tuholski, and A.R.A. Conway, “Working Memory, Short-Term Memory, and General Fluid Intelligence: A Latent Variable Approach,” *J. Exp. Psychol. Gen.* **128**, 309–331 (1999).
- ³J.T. Shelton, E.M. Elliott, B.D. Hill, M.R. Calamia, and D.W. Gouvier, “A Comparison of Laboratory and Clinical Working Memory Tests and Their Prediction of Fluid Intelligence,” *Intelligence* **37**, 283–293 (2009).
- ⁴N. Unsworth, R.P. Heitz, J.C. Schrock, and R.W. Engle, “An Automated Version of the Operation Span Task,” *Behav. Res. Methods* **37**, 498–505 (2005).



156 Modular Hydrogen Fuel Cells

157 Microstructures and Properties of As-Cast AlCrFeMnV, AlCrFeTiV, and AlCrMnTiV High Entropy Alloys

160 Non-Thermal X-ray Production from an Array of Non-Interacting, Magnetically-Imploded Wires

Modular Hydrogen Fuel Cells

B. Gould,¹ J. Rodgers,² R. Ramamurti,³

K. Swider-Lyons,¹ and M. Schuette,⁴

¹Chemistry Division

²Tactical Electronic Warfare Division

³Laboratory for Computational Physics and Fluid Dynamics

⁴Soltera Defense Solutions, Inc.

Introduction: Hydrogen fuel cells are gaining favor worldwide as electrochemical power sources for vehicle propulsion. Hydrogen fuel cells use catalytic membranes to convert hydrogen and oxygen in air to electricity, heat, and water. The U.S. Naval Research Laboratory (NRL) has been experimenting with hydrogen fuel cells in unmanned systems since 2003, but has relied on commercial vendors to provide fuel cells. Over the last 5 years, NRL has had the opportunity to build its own fuel cell in order to better understand the technology and incorporate specific features for application in unmanned air vehicles (UAVs). In its research and development of fuel cell technology, NRL has had numerous scientific and engineering successes, including a breakthrough methodology for making catalytic membranes, novel techniques for building a full fuel cell stack of 60 membranes in series, and the construction of a fully integrated operational fuel cell prototype. Here we describe our development of the fuel cell bipolar plates and our demonstration of their integration

into a fuel cell stack as part of an operational system onboard a UAV. Our research team used computational fluid dynamics (CFD) and fabrication tools, including additive manufacturing (AM), laser welding, and advanced metal forming techniques, to build a fuel cell stack that is modular in the range of 1,000 to 5,000 W.

Metal-Foil Bipolar Plates: The cornerstone of NRL's technology is the custom metal-foil bipolar plate, for which we created low-cost modular prototypes, using CFD in their design and custom fabrication tools in their construction. The bipolar plates are the backbone of our fuel cell, providing fluidic pathways for air, hydrogen, and coolant as well as conductive pathways for electrical current and for heat. In contrast to the graphite bipolar plates found in many small fuel cells, metal-foil bipolar plates are more robust (i.e., less susceptible to cracking and leaking because they are metal), and enabling stack designs of greater modularity.

Our prototype design relies heavily on CFD analysis of candidate bipolar plate variants to ensure that reactants and coolant are evenly distributed throughout the stack. Figure 1 shows the bipolar plate and a CFD simulation that illustrates the nearly uniform flow distribution of air through the plate's channels. From designs that showed promising attributes in CFD, we built our plates by taking advantage of the rapid prototyping capability of additive manufacturing, and we then experimentally evaluated each prototype plate.

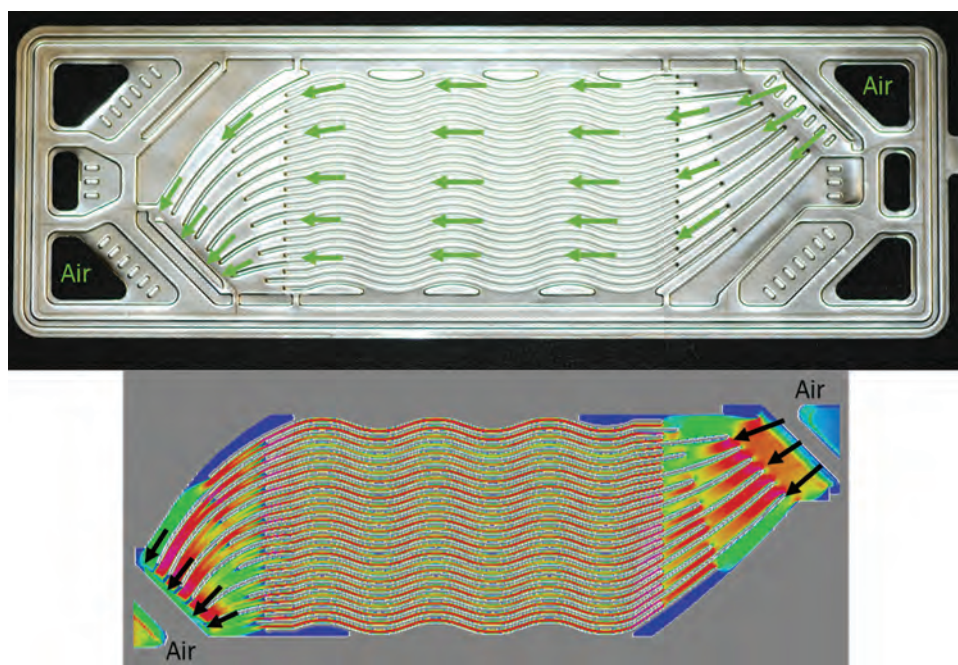


FIGURE 1

Top: Photograph of a stainless steel bipolar plate made by hydroforming. Bottom: Velocity gradients predicted by a computational fluid dynamic simulation. Evenly distributed flow is visible in the wavy portion of the bipolar plate.

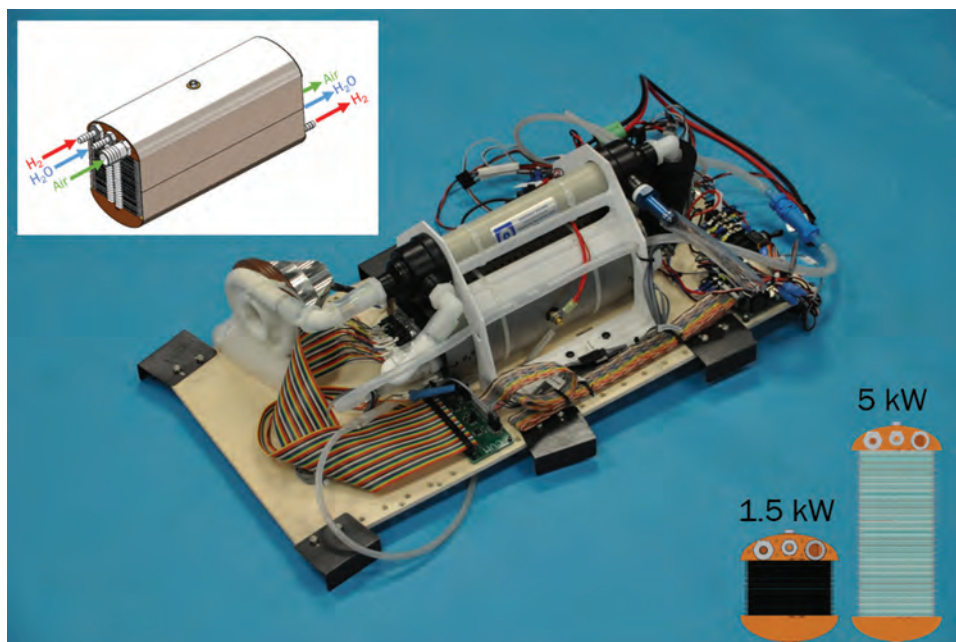


FIGURE 2
The NRL 1,500 W fuel cell system with metal-foil based stack. The NRL custom air compressor is visible in the top left corner of the system tray, with the fuel cell stack and humidifier in the middle, surrounded by sensors and control boards. The upper left-hand inset of the figure shows a CAD model of the fuel cell stack with the fluid inputs and outputs. The bottom right-hand inset shows how cells/bipolar plates can be added to a stack to increase its power from 1.5 to 5 kW in power.

When we compared simulations and the AM-built bipolar plate prototypes, we found that a fully viscous flow simulation was required to accurately model the flow of air through the bipolar plate. We constructed the bipolar plates shown in Fig. 1 by hydroforming two pieces of 75- μm -thick stainless steel foil to create the filigree features and then joining the resulting pieces together by laser welding. These bipolar plates have a custom coating that protects them from the corrosive environment of the fuel cell.

NRL's Modular Fuel Cell: We used the bipolar plates to assemble a fuel cell “stack” which is constructed of multiple metal-foil bipolar plates stacked in series with state-of-the-art electrode materials sandwiched between each plate (see inset in Fig. 2). In Fig. 2, multiple fuel cells are visible in the center region of the model between the two brown end plates. Unlike the heavy stack compression techniques often used for fuel cells, our innovative technique wraps the stack with a tensioned and spot-welded titanium strap that surrounds the bipolar plates (see illustration and model in Fig. 2). As illustrated in the bottom right-hand corner of Fig. 2, the stacks can be changed in voltage and power by simply adding more cells. We integrated the stack as part of an onboard operational system also consisting of NRL's unique air compressor and controls architecture, and then conducted a test-flight of the resulting 1,500 W system on the Ion Tiger UAV.

Summary: Founded by a fundamental understanding of fuel cell science, NRL research on fuel cell systems has produced the technology for small, lightweight, modular fuel cells. The Ion Tiger flight tests

validated our approach to designing and building a practical and lightweight fuel cell system. This fuel cell technology can deliver energy savings and increased capabilities across the operational spectrum, to ground, air, and undersea vehicles and for man-portable power generation.

[Sponsored by ONR]



Microstructures and Properties of As-Cast AlCrFeMnV, AlCrFeTiV, and AlCrMnTiV High Entropy Alloys

K.E. Knipling,¹ P.U. Narayana,² and L.T. Nguyen¹

¹Materials Science and Technology Division

²Thomas Jefferson High School for Science and Technology

Introduction: For millennia, new alloys have been developed by introducing various minor additions to a single principal element with the goal of improving an optimizing its properties. One example is steel, which primarily consists of iron with small additions of carbon, manganese, nickel, chromium, molybdenum, vanadium, silicon, boron, etc. Each element is added to enhance strength, toughness, corrosion resistance, etc. Developing alloys in this manner is extremely limiting, however, since the number of possible alloy systems is restricted to the available metals in the periodic table, and because the properties of a given family of alloys (e.g., aluminum, nickel, steel) are largely dictated by those of the primary element.

Researchers at the U.S. Naval Research Laboratory are taking a new approach to alloy design by developing high-entropy alloys (HEAs),^{1,2} which typically contain five or more principal elements in nearly equiatomic proportions. The virtually limitless combination of elements—simple combinatorial equations give billions of possible alloys—significantly expands the available composition space and hence the achievable properties of novel metallic materials.

Given this vast range of possible alloys, however, can one possibly hope to arrive at an optimum alloy composition? Using thermodynamic modeling, researchers at the Air Force Research Laboratory have recently developed a strategy for the accelerated discovery and optimization of possible HEA combinations, calculating the equilibrium phases and properties of thousands of three-, four-, five-, and six-component alloys.³ The present study is the first experimental verification of some of these predictions on three selected alloys—equimolar AlCrFeMnV, AlCrFeTiV, and AlCrMnTiV—which were chosen as potential replacements for titanium alloys in extreme and corrosive environments.

Physical Properties: The AlCrFeMnV, AlCrFeTiV, and AlCrMnTiV HEAs were made by arc-melting high-purity elemental constituents, producing finger-shaped ingots ~50 grams in mass. Figure 3 shows the measured densities, elastic moduli (stiffness), and hardness values

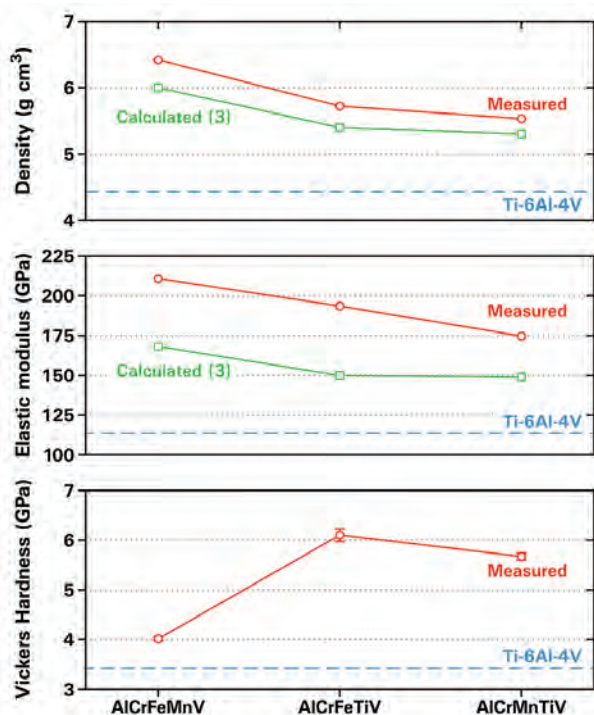


FIGURE 3 Measured densities, elastic moduli, and Vickers microhardness values of the alloys studied, compared with their predicted values and those of the titanium alloy Ti-6Al-4V.

of the alloys studied. The trends among the alloys' measured densities and elastic moduli match the predicted³ trends. Properties of the aerospace grade titanium alloy, Ti-6Al-4V, are also shown for comparison. While the AlCrFeMnV, AlCrFeTiV, and AlCrMnTiV alloys are 25–45% denser than Ti-6Al-4V, they are also 54–85% stiffer and 17–78% harder. The specific modulus and hardness (values normalized by the density) of these new alloys are thus ~30% greater than those of current state-of-the-art titanium alloys, enabling significant performance benefits and weight savings.

Alloy Microstructures: The microstructures of the alloys, examined by scanning electron microscopy (SEM), are displayed in Fig. 4. Back-scattered electron images of the ingot cross-sections, displayed at the top of Fig. 4, reveal a polycrystalline grain microstructure with equiaxed grains ~500 μm in diameter for each of the alloys. These grain morphologies and their crystallographic orientations are shown in more detail in the inverse pole figure (IPF) maps measured by electron backscattered diffraction (EBSD). In these images, the colors of the grains reflect their crystal structures and crystallographic orientations. The AlCrFeMnV and AlCrMnTiV alloys consist entirely of a body-centered cubic (BCC) crystal structure, while AlCrFeTiV is BCC with a minority hexagonal close-packed (HCP) phase. The morphology and distribution of this HCP phase is revealed more clearly in the enlarged EBSD maps displayed at the bottom of Fig. 4. The left-most map is colored according to phase identification, with red indexed as BCC and blue indexed as HCP. The HCP phase, which has an acicular morphology, forms both on the grain boundaries and within the grains themselves. The center image, an IPF map showing the crystallographic orientations of the BCC matrix, demonstrates that the HCP phase forms on multiple BCC grain boundaries. The IPF map on the far right shows that the HCP phase itself has multiple crystallographic orientations. The HCP phase observed in AlCrFeTiV is a Laves phase, which was predicted by thermodynamic predictions.³ This Laves phase is very hard, explaining the superior hardness of AlCrFeTiV in Fig. 3.

Energy dispersive spectroscopy (EDS), measured by SEM, maps the chemical segregation between the BCC and HCP phases in the AlCrFeTiV alloy. These maps, displayed in Fig. 5, demonstrate that the BCC phase in AlCrFeTiV is enriched in Fe, Ti, and (to a lesser extent) Al, while the HCP phase is enriched in Cr and V. More detailed compositional analysis is provided by atom probe tomography (APT), which pinpoints the locations of individual atoms in three dimensions. The atom probe reconstructions demonstrate that the BCC matrix is enriched in Ti, Fe, and Al, while the HCP Laves phase is predominantly V and Cr, matching the

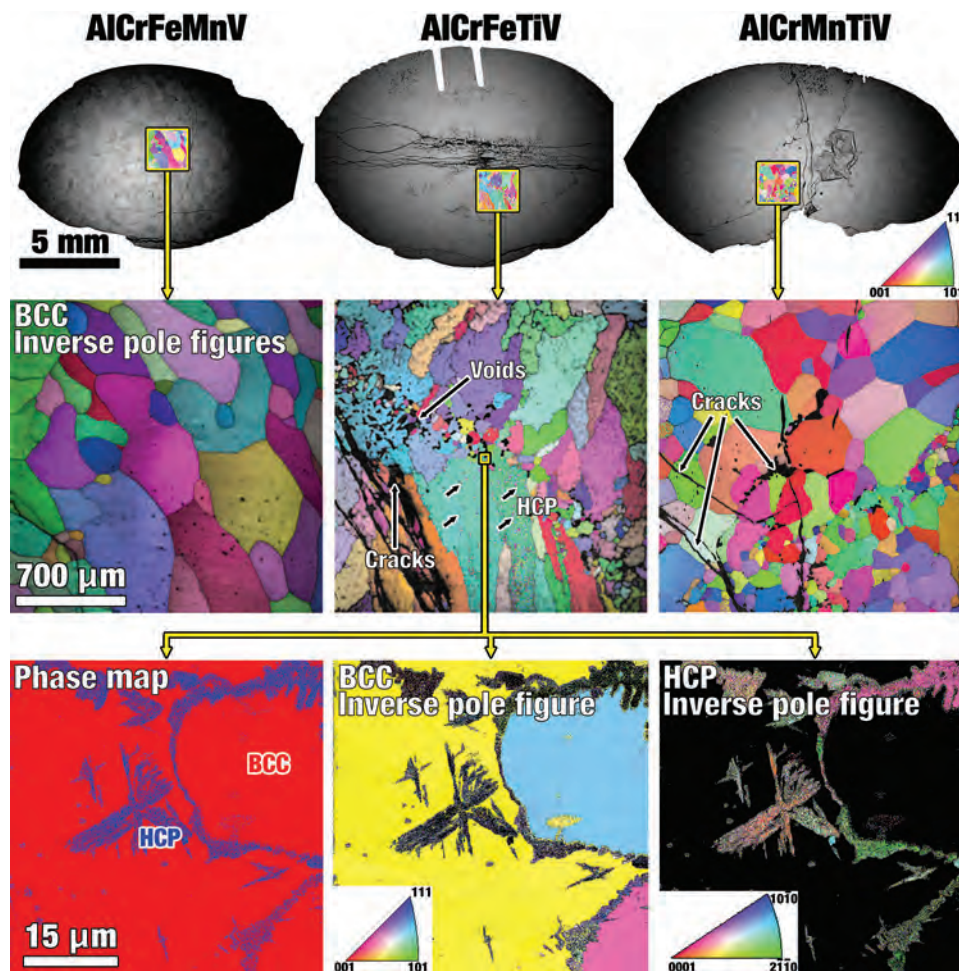


FIGURE 4 Backscattered electron micrographs of the ingot cross-sections, displaying a polycrystalline microstructure in each alloy. Inverse pole figure (IPF) maps measured by electron backscattered diffraction (EBSD) display the crystal structures and orientations of the individual grains, colored according to their crystallographic orientation as indicated by the inset legend. The AlCrFeMnV and AlCrMnTiV alloys consist entirely of a body-centered cubic (BCC) crystal structure, while AlCrFeTiV has a minority hexagonal close-packed (HCP) Laves phase, whose structure and crystallographic orientations is shown in more detail in the bottom EBSD maps.

EDS results. The bulk compositions of the two phases is shown in the reconstruction and the partitioning of atoms between these two phases is quantified, with sub-nanometer resolution, in the inset proximity histogram.

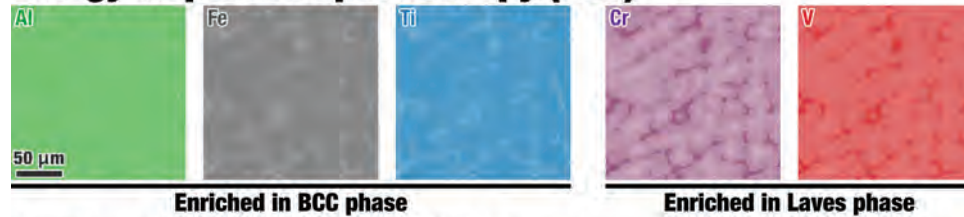
Summary: This study on equimolar AlCrFeMnV, AlCrFeTiV, and AlCrMnTiV HEAs is the first experimental verification of recent thermodynamic modeling predictions of the microstructures and properties of these alloys. We have measured the alloys' densities, elastic moduli, and Vickers microhardness values. These properties were correlated to the underlying microstructures, as measured by scanning electron microscopy and atom probe tomography. AlCrFeMnV and AlCrMnTiV are single-phase body-centered cubic (BCC) solid solutions, whereas AlCrFeTiV is BCC with a minority hexagonal close-packed (HCP) Laves phase

that is enriched in V and Cr, matching the thermodynamic predictions. The alloys are extraordinarily stiff and hard, exceeding the performance of the aerospace grade titanium alloy, Ti-6Al-4V. We are assessing the corrosion behavior of these high-strength alloys, as they could potentially replace titanium alloys in extreme and corrosive environments.

Acknowledgments: This work was funded by the U.S. Naval Research Laboratory under the auspices of the Office of Naval Research. Prithvi Narayana was a mentorship student from the Thomas Jefferson High School for Science and Technology. We thank Dan Miracle (Air Force Research Laboratory) for stimulating discussions.

[Sponsored by the NRL Base Program (CNR funded) and ONR]

Energy dispersive spectroscopy (EDS)



Atom probe tomography (APT)

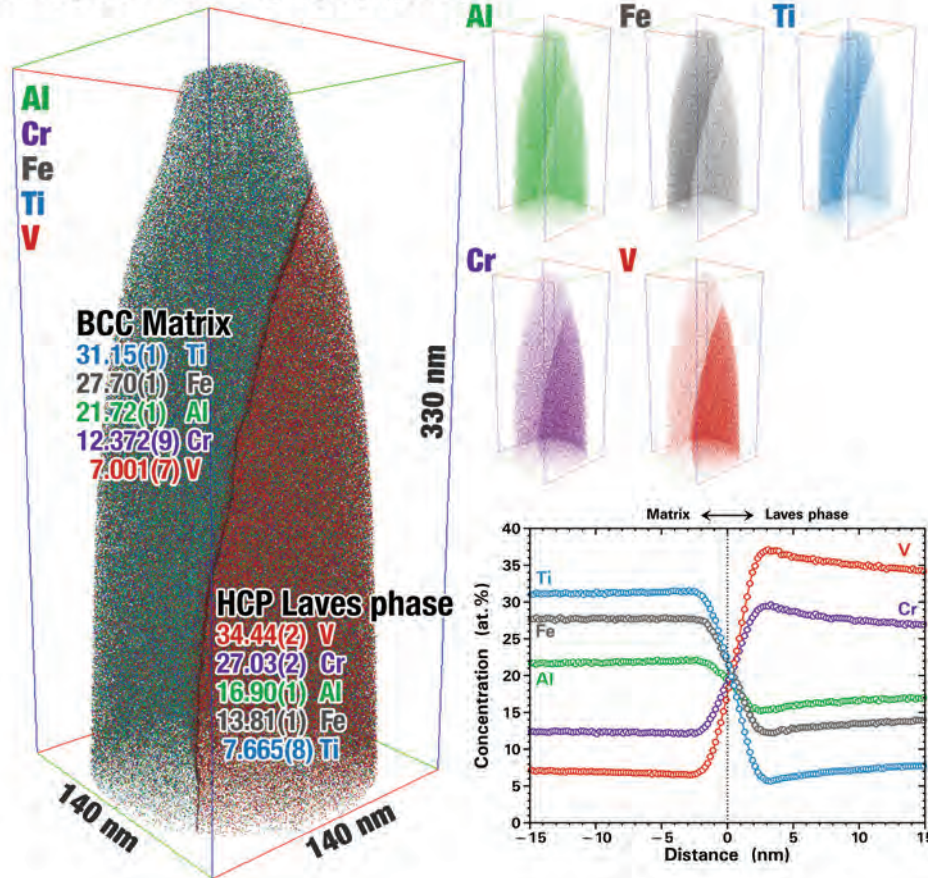


FIGURE 5 Energy dispersive spectroscopy (EDS) maps and atom probe tomography (APT) reconstructions displaying the chemical segregation between the BCC and HCP Laves phases in the AlCrFeTiV alloy.

References

- ¹M.H. Tsai and J.W. Yeh, "High-Entropy Alloys: A Critical Review," *Mat. Res. Lett.* 2(3), 107–123 (2014).
- ²D.B. Miracle and O.N. Senkov, "A Critical Review of High Entropy Alloys and Related Concepts," *Acta Mat.* 122, 448–511 (2017).
- ³O.N. Senkov, J.D. Miller, D.B. Miracle, and C. Woodward, "Accelerated Exploration of Multi-Principal Element Alloys for Structural Applications," *CALPHAD* 5, 32–48 (2015).



Non-Thermal X-ray Production from an Array of Non-Interacting, Magnetically-Imploded Wires

B.V. Weber,¹ J.T. Engelbrecht,¹ S.L. Jackson,¹ D. Mosher,¹ R.J. Comisso,¹ D.G. Phipps,² N. Qi,² and J. Levine²
¹Plasma Physics Division
²L-3 Applied Technologies, Inc.

Introduction: There is a desire for 10 keV to 100 keV X-ray sources with greater intensity than are presently available. One source with the potential to satisfy

this need is an array of isolated, imploded high-atomic-number wires driven by a pulsed-power generator. In single-wire radiator (SWR) experiments at the U.S. Naval Research Laboratory in the 1970s, the Gamble II pulsed-power generator drove a single wire, producing strong non-thermal X rays in the 10-keV to 100-keV range.^{1,2} The Gamble-II experiments recently revisited the SWR concept with encouraging results. To obtain more radiation than available from a single SWR, a configuration of SWRs, or an SWR array, needs to be developed that would allow each wire to act independently of the other wires while being driven in parallel by a single-pulsed power generator capable of delivering approximately 1 MA to each wire in the array. One such configuration was developed and successfully tested at NRL on Gamble II. Based on this work, an experiment on the Double-EAGLE generator was carried out at 5-MA with arrays of three and six SWRs.

Recent Gamble-II Experiments: The geometry for a single wire on Gamble II is illustrated in Fig. 6(a). Gamble II produced a peak current (900 kA) and a peak voltage (1.1 MV) in an electrical pulse width of 60 ns FWHM, generating an X-ray spectrum from the wire plasma similar to that of the 1970s experiments. The side-viewing, time-integrated pinhole camera image shown in Fig. 6(b), filtered to see ≥ 10 keV radiation, reveals a number (typically 15 to 20) of small ($< 600\text{-}\mu\text{m}$ FWHM, limited by pinhole resolution) relatively strongly-radiating spots from which the non-thermal radiation primarily emanates. In the heuristic model of the SWR, the wire explodes when the power pulse is first applied, and then, as a result of the very strong self-magnetic field, the wire implodes. Sausage-type instabilities develop along the imploded wire (enhanced by radiative collapse), and many small strongly-radiating regions of plasma, or spots, develop, separated by more weakly radiating neck regions (see Fig. 6(b)). Electrons accelerate between the spots to a fraction of the energy associated with the full voltage

across the entire wire and then interact with the spots to produce non-thermal bremsstrahlung and line radiation.³ Of the total energy radiated from the single wire, ~ 90 J (78%) lies between 10 and 200 keV. An order of magnitude more radiated energy, within a finite area, is required to be of interest for radiation-matter interaction studies. An array of wires configured so that the individual wires behave independently of their neighbors possibly could be used with a higher-current generator to obtain higher radiated energy.

Double-EAGLE Experiments: As an intermediate scaling point in current, we chose the $\sim 5\text{-MA}$, $\sim 1\text{-MV}$, $\sim 75\text{-ns}$ -FWHM electrical-pulse Double-EAGLE generator.⁴ The setup for multiple SWRs is illustrated in Fig. 7. Double-EAGLE has a triplate rather than coaxial front-end geometry. The negative high-voltage cathode is connected via posts to three concentric cylinders through holes in the bottom anode (see left-hand side of Fig. 7). The outer cylinder is grounded through an inductance, raising the anode voltage to positive high voltage, ensuring that electrons that may exist in vacuum do not hit the vacuum window. The anode is connected to one end of the wire via six posts through holes between the inner and middle cylindrical cathodes (see right-hand side of Fig. 7). The other end of the wire connects to the inner cathode cylinder. The transparent mesh allows two return current paths for the wire that can be inductively balanced so that the return current for each wire is equally divided between the inner and middle cylinders. This balances the magnetic forces above and below the wires, providing local azimuthal symmetry about each wire axis, as in the Gamble-II SWR experiments. The transparent mesh also allows the X rays generated from the wires to be transmitted out of the vacuum.

Figure 8 is a time-integrated pinhole camera image of a six-SWR azimuthal array on Double-EAGLE, filtered to see radiation ≥ 20 keV. The gross behavior of each wire is very much the same as observed on

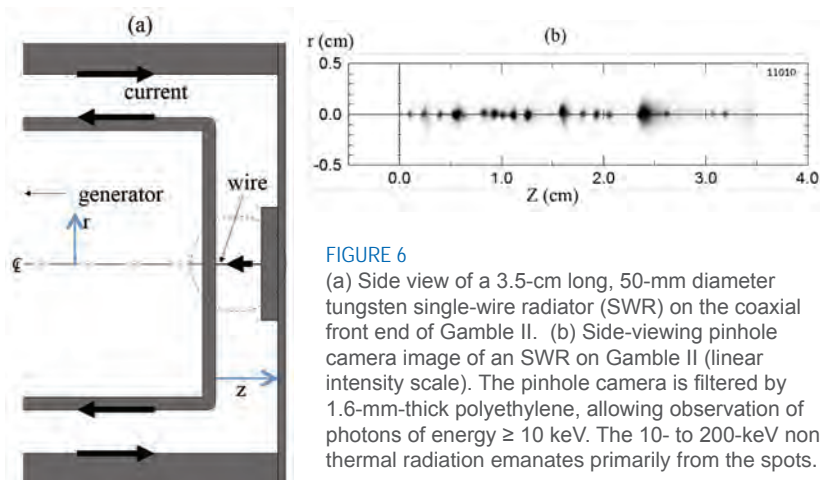


FIGURE 6 (a) Side view of a 3.5-cm long, 50-mm diameter tungsten single-wire radiator (SWR) on the coaxial front end of Gamble II. (b) Side-viewing pinhole camera image of an SWR on Gamble II (linear intensity scale). The pinhole camera is filtered by 1.6-mm-thick polyethylene, allowing observation of photons of energy ≥ 10 keV. The 10- to 200-keV non-thermal radiation emanates primarily from the spots.

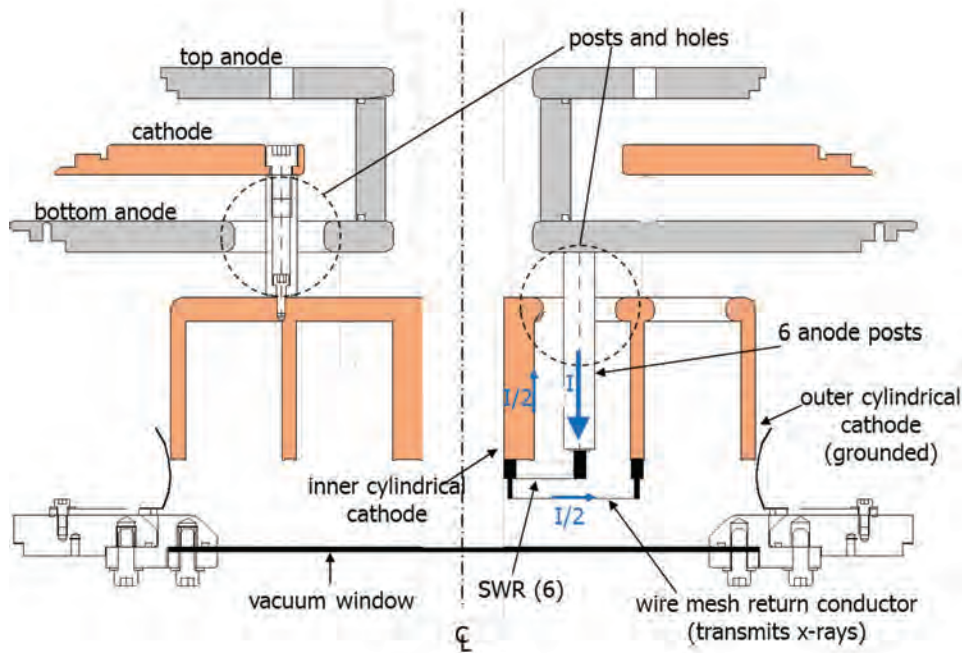


FIGURE 7 Section view of the multiple-wire load arrangement for Double-EAGLE. One of six wires is shown; each wire extends radially at a different azimuth between an anode post and the cathode. This arrangement is designed to produce no net magnetic force on the axis of the wire so that each wire implodes as an isolated wire onto its own axis.

Gamble II with a single wire, validating this approach for multiple wires and identifying a path for scaling to even higher-current generators.

Acknowledgments: The authors acknowledge the valuable technical assistance of E.C. Featherstone and B.J. Sobocinski in operating Gamble II, and M.L. Braun, M.C. Hansen, and P.L. Ramos, Jr. in operating Double-EAGLE.

[Sponsored by the Defense Threat Reduction Agency]

References

- ¹D. Mosher, S.J. Stephanakis, I.M. Vitkovitsky, C.M. Dozier, L.S. Levine, and D.J. Nagel, "X Radiation from High-Energy-Density Exploded-Wire Discharges," *Appl. Phys. Lett.* **23**(8), 429–430 (1973).
- ²D. Mosher, S.J. Stephanakis, K. Hain, C.M. Dozier, and F.C. Young, "Electrical Characteristics of High Energy-Density Exploded Wire Plasmas," *Ann. N. Y. Acad. Sci.* **251**(1), 632–648 (1975).
- ³D. Mosher and D. Colombant, "Pinch Spot Formation in High Atomic Number z Discharges," *Phys. Rev. Lett.* **68**, 2600–2603 (1992).
- ⁴G.B. Frazier, S.R. Ashby, L.J. Demeter, M. Di Capua, J. Douglas, S.C. Glidden, H.G. Hammon III, B. Huff, S.K. Lam, A. Rutherford, R. Ryan, P. Sincerny, and D.F. Strachan, "Eagle and Double-EAGLE," invited talk in *Digest of Technical Papers, Fourth IEEE Pulsed Power Conference*, Albuquerque, N.M., June 6–8, 1983 (1983).

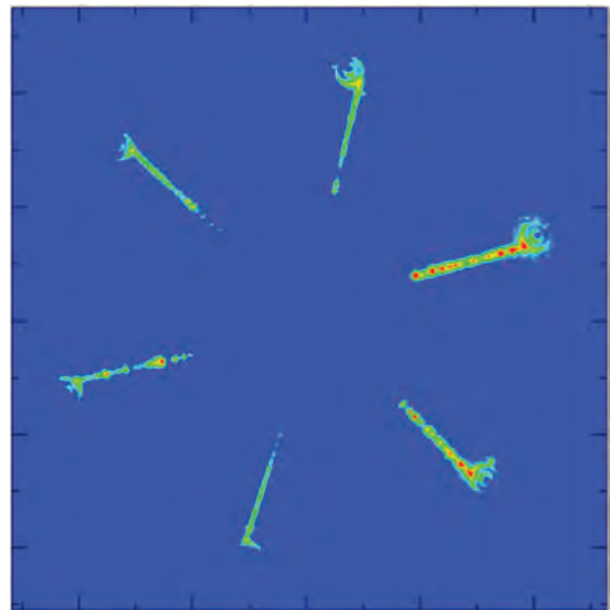


FIGURE 8 Time-integrated pinhole camera image of six SWRs driven by Double-EAGLE, viewed from the bottom of Fig. 7 looking up. Individual wire behavior is similar to a single wire driven by Gamble II.

164 Novel Active Tuning for Infrared Photonics

166 Opening a New Window into Nanoparticle Toxicity

Novel Active Tuning for Infrared Photonics

A.D. Dunkelberger,¹ C.T. Ellis,² D.C. Ratchford,¹ A.J. Giles,² M. Kim,⁴ C.S. Kim,³ B.T. Spann,⁵ I. Vurgaftman,³ J.G. Tischler,² J.C. Owrutsky,¹ and J.D. Caldwell⁶

¹*Chemistry Division*

²*Electronic Science and Technology Division*

³*Optical Sciences Division*

⁴*Sotera Defense Solutions, Inc.*

⁵*National Institute of Standards and Technology, Applied Physics*

⁶*Vanderbilt University*

Introduction: Infrared radiation has exciting potential for many fleet-relevant applications, like free-space communication, chemical agent sensing, and thermal camouflage. But infrared sources and detectors are often inefficient or impractical because of their power and cooling requirements. Attractive alternatives include new infrared photonic materials and devices that use nanotechnology to confine and enhance infrared electromagnetic fields. In the past few decades, approaches that rely on surface plasmon polaritons (collective oscillations of free electrons, typically in metals) have yielded promising results. For many applications, narrow, low-loss resonances are important, but surface plasmons rely on coherent electronic motion, and thus, decay on the femtosecond timescale of electron scattering. This rapid decay leads to broad, lossy resonances.

Our research is at the forefront of the development of a low-loss alternative to surface plasmon polaritons called surface-phonon polaritons (SPhP), which derive not from electron oscillations but from phonons, collective vibrations, in polar dielectrics. Because the scattering rates and relaxation times of phonons are much slower, by orders of magnitude, than for electrons, SPhPs have very narrow, high-quality resonances. These narrow resonances yield strong, subdiffraction field confinement and many other advantages for photonic applications, but one of their key disadvantages is the limited spectral coverage. The resonance position depends broadly on the material optical phonon frequencies and the geometry of the nanostructure, which cannot be modified after fabrication. We have recently demonstrated the ability to actively tune the SPhP resonances by exciting semiconductor nanostructures with laser light.^{1,2} Tuning the resonances can allow a nanostructured SPhP-based device to perform photonic functions at multiple infrared frequencies and can significantly extend the useful range of future devices.

Tuning the Optical Behavior of Polar Dielectric Semiconductors: We developed a tuning approach that relies on unique optical properties of polar dielectric

semiconductor materials like InP and SiC. Crystals of these materials exhibit transverse and longitudinal optical (TO and LO) phonons, readily observable through Raman spectroscopy, in the mid-infrared frequency regime. Between these two phonon frequencies, the materials have metal-like dielectric functions that lead to extremely high reflectivity. Figure 1 shows reflectance spectra of InP and 4H-SiC, centered on these reflective regions. It is within this metallic “Reststrahlen band” that the materials can support surface-phonon polariton resonances. Free carriers in semiconductors oscillate with a characteristic plasma frequency and interact with the surface optical modes, resulting in modified optical properties and altered Reststrahlen bands. We have shown that exciting carriers in 4H-SiC films with an ultraviolet laser pulse dynamically shifts the Reststrahlen band, transiently modifying the reflectivity of the films in the mid-infrared.³ The carrier tuned optical properties are the basis for active tuning of SPhPs.

Active Tuning of Surface-Phonon Polariton Resonances: Just as metal nanostructures can have surface plasmon resonances that depend on the dielectric function and nanostructure geometry, polar dielectric nanostructures can have surface-phonon polariton resonances. Our research is at the leading edge of the rapidly growing field of creating semiconductor nanostructures with SPhP resonances in the infrared. Figure 1 shows reflectance spectra of arrays of InP and 4H-SiC nanostructures, in which the low-loss resonances appear as sharp dips in the Reststrahlen band. We have shown that these resonances can achieve extremely strong confinement of infrared light for use in future applications.

Strong confinement is important for many photonic applications, but tuning resonances of a nanostructure array could enable devices with, for instance, thermal emission whose frequency can be rapidly modulated or chemical sensors that can be rapidly tuned to detect specific warfare agents. By exciting free carriers in InP and 4H-SiC nanostructure arrays, we have demonstrated this active tuning for the first time.¹

Carrier-induced changes in the dielectric function of the material that shift the Reststrahlen band also shift the SPhP resonances. Figure 2 shows resonance shifts for InP and 4H-SiC under laser illumination. For InP, we excited the nanostructures with continuous-wave green laser light and observe 2–3 cm^{-1} shifts of the strongest resonance. In 4H-SiC, we excited the structures with pulsed ultraviolet light and record up to 12 cm^{-1} shifts by time resolved infrared detection. To compare the performance of the tuning to the state of the art in plasmonics, we calculated a tuning figure of merit (FOM) by dividing the shift magnitude by the width of the resonance. Our highest FOM was 1.4, much larger than obtainable with nearly any plasmonics system, and

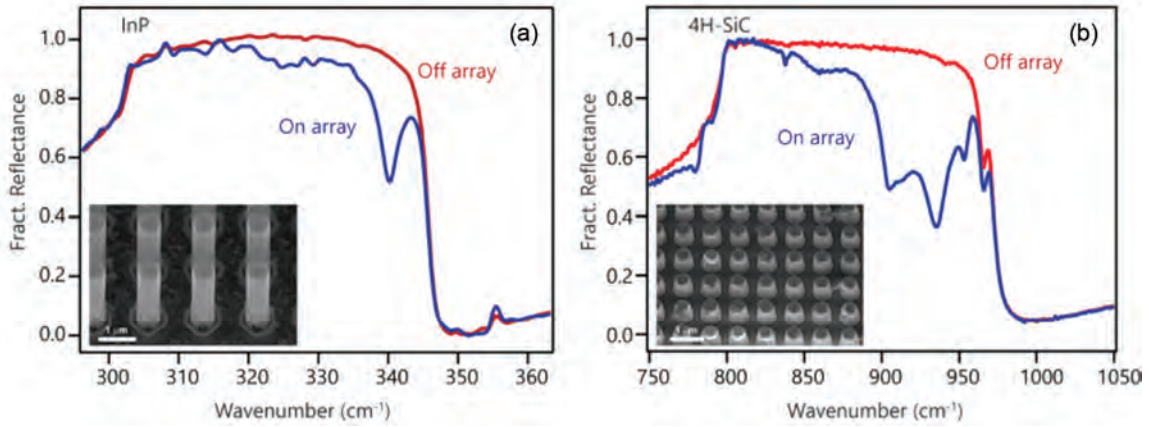


FIGURE 1

(a) Reflectance spectra of unpatterned InP substrate (red) and nanostructure array (blue, pictured in inset). The pillars are 1500 nm high, 500 nm across, and have a center-to-center pitch of 1500 nm. (b) Reflectance spectra of unpatterned 4H-SiC substrate (red) and nanostructure array (blue, pictured in inset). The pillars are 600 nm high, 300 nm across, and have a center-to-center pitch of 700 nm.

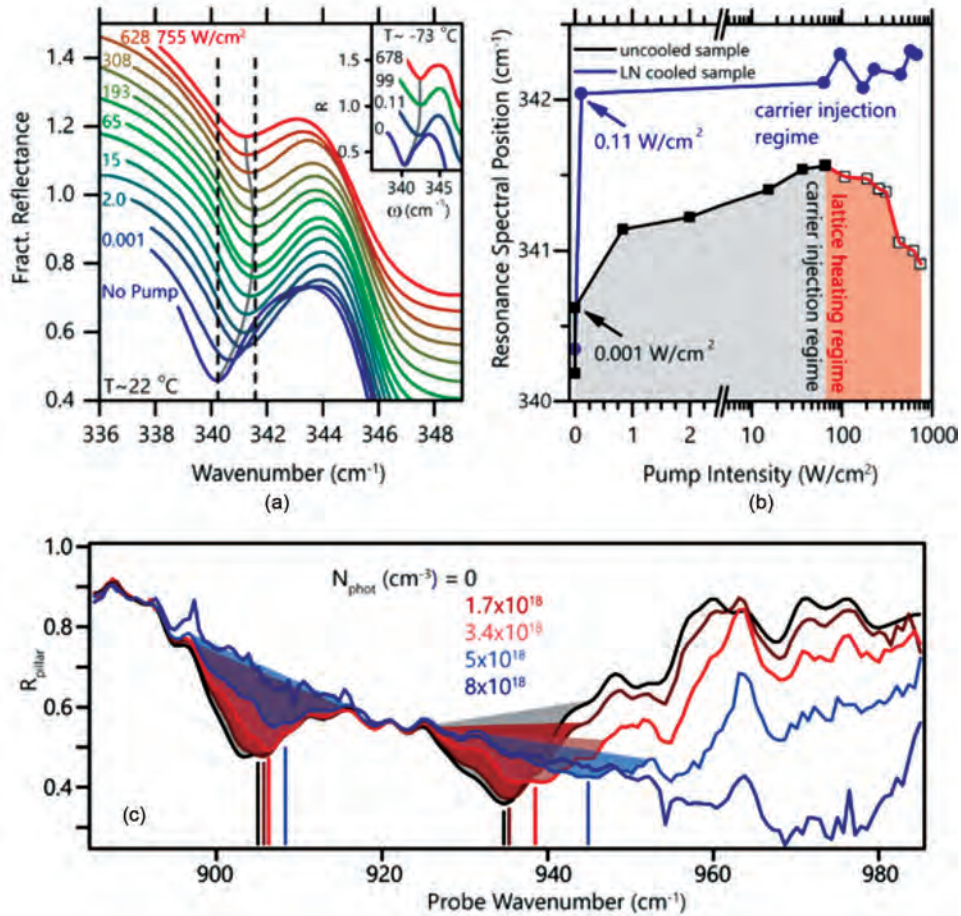


FIGURE 2

(a) Reflectance spectra of InP nanostructure array as 532 nm continuous-wave laser illumination increases from 0 (blue) to 755 W/cm² (red). Dashed lines indicate the maximum peak shift. Inset shows a subset of similar spectra obtained with sample cooled by liquid nitrogen. (b) Measured peak shift of InP resonance plotted against incident laser intensity. Without cooling, the shift saturates and reverses as lattice heating begins to dominate the behavior. (c) Transient reflection spectra of 4H-SiC nanostructure 5 ps after excitation with 266 nm laser pulses for increasing excitation intensity from an absorbed photon density of 0 (black) to 8x10¹⁸ photons/cm³ (dark blue). Vertical lines indicate peak position at each photon density.

with the added advantage of the narrow linewidth of the SPhP resonance.

The shift in the InP nanostructures was limited by substrate heating and carrier recombination pathways. Using ultrafast pulses, we observed that the resonances in 4H-SiC remain shifted for only 50 ps, at most, showing that extremely rapid modulation is possible. The results of these active tuning experiments point the way toward design improvements that can enable tunable photonic devices in the infrared.

[Sponsored by the NRL Base Program (CNR funded)]

References

- ¹ A.D. Dunkelberger, C.T. Ellis, D.C. Ratchford, A.J. Giles, M. Kim, C.S. Kim, B.T. Spann, I. Vurgaftman, J.G. Tischler, J.P. Long, O.J. Glembocki, J.C. Owrutsky, and J.D. Caldwell, "Active Tuning of Surface Phonon Polariton Resonances via Carrier Photoinjection," arXiv:1705.05980 (2017).
- ² J.P. Long, J.D. Caldwell, J.C. Owrutsky, and O.J. Glembocki, "Actively Tunable Polar-Dielectric Optical Devices," U.S. Patent No. 9,195,052 (2014).
- ³ B.T. Spann, R. Compton, D. Ratchford, J.P. Long, A.D. Dunkelberger, P.B. Klein, A.J. Giles, J.D. Caldwell, and J.C. Owrutsky, "Photoinduced Tunability of the Reststrahlen Band in 4H-SiC," *Phys. Rev. B* **93**, 085206 (2016).



Opening a New Window into Nanoparticle Toxicity

I.L. Medintz,¹ E. Oh,³ R. Liu,² M. Bilal,² and Y. Cohen,²

¹Center for Bio/Molecular Science and Engineering

²University of California

³Sotera Defense Solutions

Introduction: Bionanotechnology offers great opportunity for the development of new materials, and a large number of potential applications are now opening up in everything from biocomputing to theranostics. In this rapidly developing research field, nanoparticles (NPs) are one of the mainstay components frequently assembled with biological molecules, such as proteins and DNA, to create new composites with emergent properties. Typically synthesized from noble metals and semiconductors, NPs provide unique quantum confined properties like photoluminescence and plasmonic activity, while the biologicals contribute capabilities such as targeting along with structural and catalytic activity to the resulting hybrids. Since NPs and the resulting biohybrids are essentially new materials with unexplored properties, their toxicological potential is almost completely unknown. The challenge in engineering new nanomaterials for all manner of bioapplications is to make them safe by design, and this is predicated on a

full understanding of which NP physicochemical properties contribute to toxicity. This endeavor is, however, severely complicated by the number of different material variants available for each NP material (e.g., see Fig. 3), and by the lack of comprehensive, systematic, and parametric studies of their toxicity in relevant model systems. Indeed, the total body of published evidence on NP toxicity consists primarily of piecemeal studies typically focused on one material variant and using a limited range of experimental conditions and dosages.

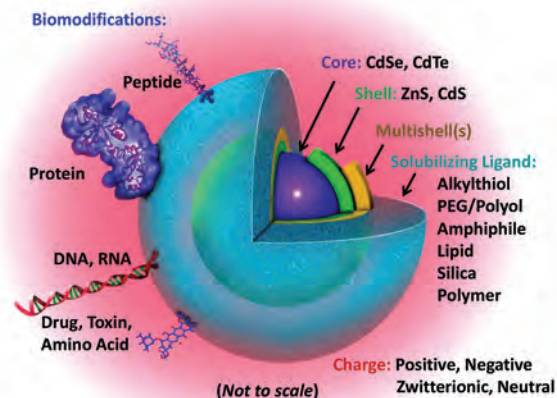


FIGURE 3

Schematic of a biocompatible quantum dot (QD) structure. The schematic highlights the many different physicochemical attributes that give rise to the many different QD material variants reported in the literature. This materials diversity includes types of core and shell materials, presence of other shell(s), type of solubilizing ligand and their charge along with presence and type of biomodification.

Collaborative Research Group: Researchers from the U.S. Naval Research Laboratory (NRL) collaborated with scientific partners in 2016 to learn more about NP toxicology. The researchers originated from the Center for Bio/Molecular Science and Engineering and the Optical Sciences Division at NRL, and from the University of California Center for the Environmental Implications of Nanotechnology. The group subsequently assembled the largest, most-detailed NP toxicity data set to date and subjected the data set to an intensive meta-analysis.¹

Methodology: The research group extracted and analyzed pertinent knowledge from published studies focusing on the cellular toxicity of cadmium-containing semiconductor quantum dots (QDs). The group initially screened more than 1,000 publications, of which more than 300 contained relevant toxicity information. For inclusion in the final data set and to provide a common thread amongst the data, only publications that met the following four criteria were included in

the analysis: (1) QDs were reported to contain Cd, (2) toxicity testing was performed on a eukaryotic cell line, (3) dosage information was reported; and (4) quantitative toxicity metrics were provided. This literature data mining approach yielded 1,741 QD cell viability-related data samples (the percentage of cells viable after a given QD dosage), each with 24 qualitative (e.g., core type, shell presence, biomodified) and quantitative attributes (e.g., exposure concentration, time) describing the material properties and experimental conditions. This set also included 514 distinct IC_{50} values (exposure concentration = 50 percent cell death or other toxicity metric) over a range of exposure concentrations.

Random forest (RF) regression models for cell viability and the IC_{50} data were developed to identify pertinent attributes that correlate with QD toxicity among these different published studies and the significance of given attributes (QD properties and experimental conditions). The models identified a combination of attributes as most significant for both models, including QD diameter, QD concentration ($mg\ l^{-1}$), surface ligand, presence of shell, exposure time, surface modification, and, surprisingly, even assay type (Fig. 4). Testing of the RF model accuracy showed good agreement between the predicted and observed responses, indicating the models were robust. A proximity matrix using the above identified attributes showed that the

data was quite heterogeneous, with sparse connections between the nodes. More important, these results opened the door for extraction of conditional dependencies using decision trees in which the association between QD data attributes and toxicity levels under certain experimental conditions could be identified. The primary example from the latter analysis revealed that more than 80 percent of the QDs in the IC_{50} data set with lipidic, amphiphilic polymer, or aminothiols surface functionalization chemistry are associated with high toxicity ($IC_{50} \leq 25\ mg\ l^{-1}$) but that those with alkylthiol as the ligand were not ($IC_{50} \geq 25\ mg\ l^{-1}$). However, if a QD diameter greater than 5 nm is considered in this equation, then more than 85 percent of the QD samples with this size and alkylthiol surface ligand are clearly nontoxic, while those with a diameter under 5 nm are significantly toxic (Fig. 5). This illustrated a complex underlying relationship between QD size and surface ligand chemistry.

Conclusions: The study provides both important data and key lessons to the burgeoning nanotoxicology research community. Prior to this study, it was thought that the initial literature data mining portion could be accomplished with only targeted software, but the complexity of the data required human participation at all levels of the data mining work and subsequent analysis.

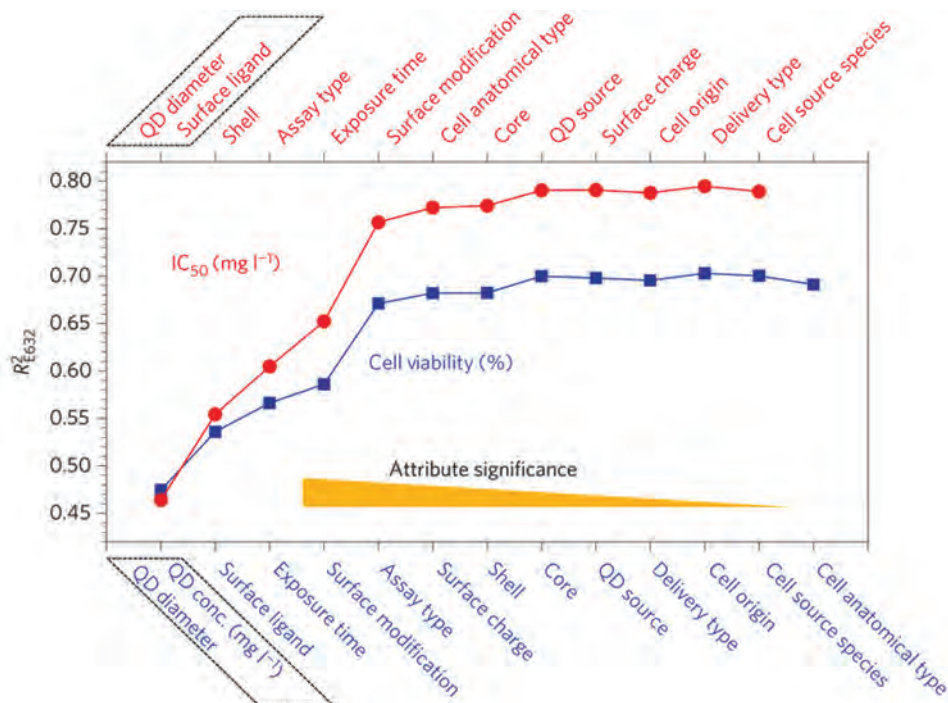


FIGURE 4 Random forest (RF) analysis and models. RF prediction accuracy for the most suitable set of attributes. Attributes were incrementally added to those previously selected by exhaustive search except those already contained in the dashed boxes. The order that a given descriptor was added also points to its importance when correlating with semiconductor QD bioactivity (cell viability or IC_{50}). The RF models for cell viability and IC_{50} demonstrated performance of $R^2 = 0.67$ and 0.75 , respectively, as assessed by the 0.632 estimator.

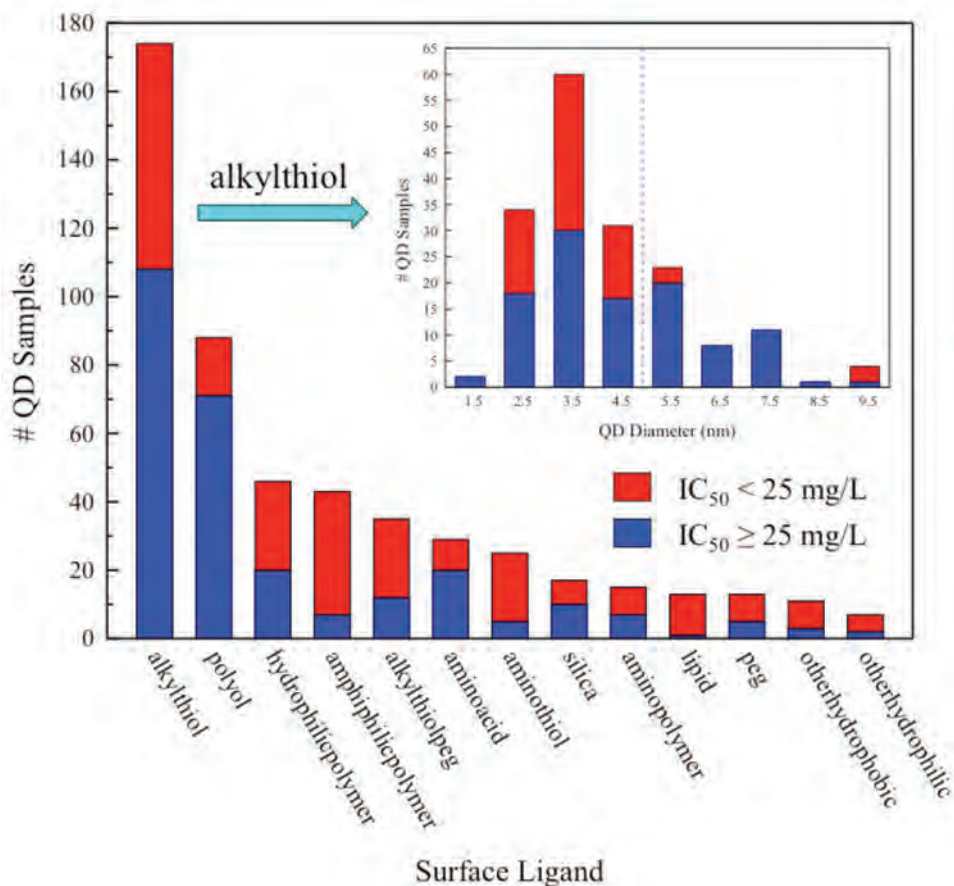


FIGURE 5 Conditional dependence of QD IC_{50} on *surface ligand* and/or *QD diameter*. The conditional dependence is illustrated via the distribution of the number (#) of QD samples with respect to *surface ligand* and the distribution of # QDs with *surface ligand* = alkylthiol with respect to *QD diameter*. For these purposes highly toxic is considered $IC_{50} \leq 25 \text{ mg l}^{-1}$ and less toxic is $IC_{50} \geq 25 \text{ mg l}^{-1}$. The combination of alkylthiol ligand and QD diameter of < 5 nm appears to conditionally correlate with significant toxicity.

IC_{50} data were found to be generally far more informative, because the data integrated the results over a range of sample concentrations as compared to single-point viability data, which are far more limited. The type of meta-analysis undertaken in this study should be useful in the study of many other types of nanomaterials, e.g., gold NPs. Moreover, the data sets resulting from such analysis do not need to remain static but rather are amenable to continual updating from the literature. While information derived from such meta-analysis data can provide important guidance for engineering of new nanomaterials, it should also be noted that the value of the published data and the models must be judiciously considered at all steps. This study also confirms that Department of Defense agencies and academic institutions can leverage their unique skill sets in collaborative efforts to address complex technological concerns in a mutually beneficial manner.

[Sponsored by the NRL Base Program (CNR funded)]

Reference

¹E. Oh, R. Liu, A. Nel, A., K. Boeneman Gemmill, M. Bilal, Y. Cohen, and I. L. Medintz, "Meta-Analysis of Cellular Toxicity for Cadmium Containing Quantum Dots," *Nat. Nanotech.* **11**, 479–486 (2016).



- 170 Parameterization of Whitecap Fraction Based on Satellite Observations
- 173 Successful Self-Embedment of a Large Benthic Microbial Fuel Cell Anode
- 175 What Is the Impact of Light on Ocean Primary Production and Hypoxia?

Parameterization of Whitecap Fraction Based on Satellite Observations

M.D. Anguelova,¹ M.F.M.A. Albert,² and G. de Leeuw³

¹Remote Sensing Division

²TNO, Utrecht, The Netherlands

³University of Helsinki, Helsinki, Finland

The Beauty and Significance of Oceanic Whitecaps: When out in the open sea, we all fancy the bright, fleeting sea foam capping the waves. In addition to their beauty, these whitecaps also play a critical role in the coupling between the ocean and the atmosphere. Oceanic whitecaps form at wind speeds of around 3 m s^{-1} and higher when waves break and entrain air in the water. The entrained air breaks up into bubbles, which then rise to the surface clustering into patches of sea foam. Whitecaps on the surface and bubbles in the water enhance the air-sea interaction (ASI) processes such as exchange of energy, heat, gases, and particles.¹ ASI processes are necessary to model the ocean-atmosphere coupling and the boundary conditions at the air-sea

interface in numerical weather prediction and climate models. In models of ASI processes, whitecap fraction W —defined as the fractional area of foam within a unit area of sea surface—quantifies the horizontal extent of whitecaps in the ocean. The whitecap fraction is suitable to represent ASI processes mathematically in models and is usually parameterized as a function of wind speed at 10 m reference height, $W(U_{10})$.

Most available $W(U_{10})$ parameterizations are based on whitecap fraction data collected from towers, ships, and airplanes.¹ These data, obtained from photographs and video images since early 1970s, show wide variation (see gray symbols in Fig. 1(a)), in part due to difficulties and differences in methods of extracting W from images. The spread of W data has narrowed recently as digital photography has increased the data volume while image processing algorithms have improved. Natural variability of whitecaps presumably explains the order-of-magnitude spread of W data that remains (see color symbols in Fig. 1(a)). Other factors, such as wave field, atmospheric stability (related to air-sea temperature differences), and seawater properties

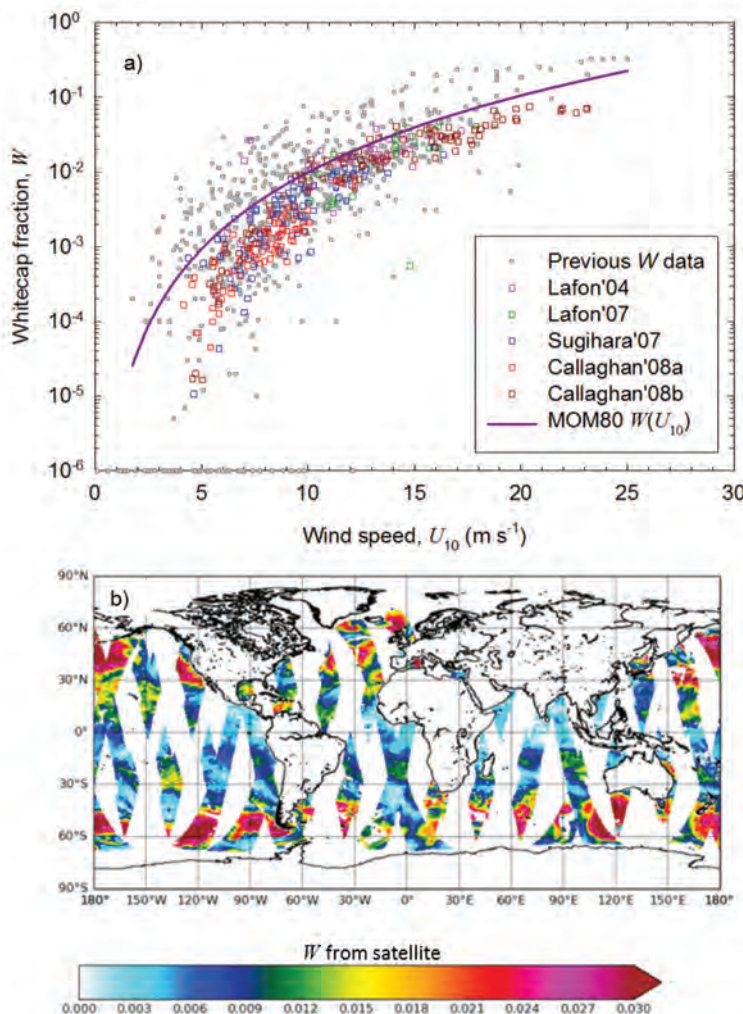


FIGURE 1
Whitecap fraction W as a function of wind speed at 10 m above the sea surface U_{10} : (a) In situ W data obtained from photographs. Gray symbols are for data collected before 2004³; color symbols are for new data sets¹; purple line is the $W(U_{10})$ parameterization based on photographic data². (b) Satellite-based estimates of W data at 37 GHz for 11 March 2006 for WindSat ascending and descending passes (map $0.5^\circ \times 0.5^\circ$).

(including sea surface temperature (SST), salinity, and surface-active materials) affect W also. This suggests that U_{10} alone cannot fully predict W variations because $W(U_{10})$ expressions represent only the trend of W with U_{10} , but not the spread of W . This is demonstrated with the purple line in Fig. 1(a), which depicts the most widely-used $W(U_{10})$ parametrization.² Thus, there is active research to model the natural spread of W data better by including secondary factors (in addition to U_{10}) in W parameterizations. To achieve this, a database of W data matched spatially and temporarily with U_{10} , SST (T), etc., is necessary. In situ collections of W data are sporadic and for limited oceanographic and meteorological conditions. A viable alternative to compile such a database is the use of satellite-based W data.

Seeing Whitecaps from Satellites: The brightness temperature of the ocean surface measured from satellite-based radiometers at microwave frequencies

(6 to 37 GHz) has been successfully used to obtain W data within the WindSat mission at the U.S. Naval Research Laboratory.^{3,4} This enabled compilation of a whitecap database, for the year 2006, of satellite-based W data accompanied with U_{10} and T . Figure 1(b) shows an example of W data from WindSat for a randomly chosen day. This whitecap database is used to develop a parametrization of W as a function of wind speed and SST, $W(U_{10}, T)$.

The Story that the Whitecap Data Tell: Our approach to obtaining $W(U_{10}, T)$ expression involved two steps.⁵ First, from a global scale assessment of the data, we developed a wind speed dependence $W(U_{10})$ in the form $W = a(U_{10} + b)^n$, where a and b are regression coefficients while n is the wind speed exponent, all freely adjusted as dictated by the whitecap database. The results show approximately quadratic correlation between W and U_{10} , which differs from the physically

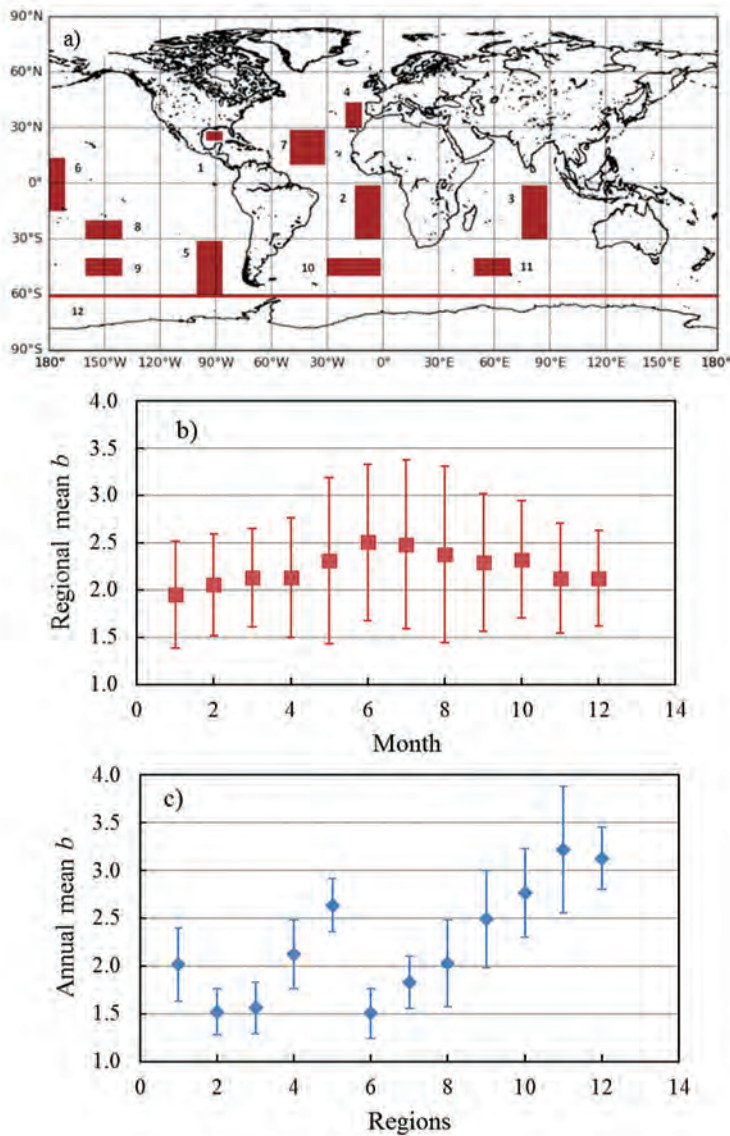


FIGURE 2
Regional analysis of satellite-based W data: (a) Selected regions to determine regional variations of the wind speed dependence $W(U_{10})$; (b) Regionally average b values for each month with error bars (\pm one standard deviation) representing regional variability of b ; (c) Annually averaged b values for each region with error bars representing the season variability of b .

expected cubic dependence $W \propto U_{10}^3$. The adjustment of the wind speed dependence from cubic to quadratic ($n = 2$) reflects the influence of globally averaged forcing parameters (i.e., U_{10} and all secondary factors) on W . In the second step, we analyzed the remaining variations of coefficients a and b on regional scale over the full year as follows. We extracted subsets of W data from the whitecap database for 12 regions and determined a and b for each region and each month. The chosen regions (Fig. 2(a)) cover the full range of global oceanic and meteorological conditions. Data analysis showed that the seasonal variations of a and b are not statistically significant, while the regional variations are. Figure 2 illustrates this with values for coefficient b . Figure 2(b) shows the seasonal cycle of b values; the error bars represent their regional variability. It is clear that the variations of b from month to month are statistically undistinguishable. Figure 2(c), conversely, shows that variations of b from region to region are significant and the geographical variations of b are not lost in the seasonal variability. Because SST is a distinct characteristic for different regions, we represented the regional variations of a and b in terms of SST and derived expressions $a(T)$ and $b(T)$. Combining these

with the quadratic wind speed dependence, the new parametrization of whitecap fraction has the form $W(U_{10}, T) = a(T)[U_{10} + b(T)]^2$.

Implications of the New Results: Figure 3(a) compares W from the new expressions to both in situ and satellite-based W data. Comparisons to the in situ W data (gray symbols) demonstrate order-of-magnitude consistency. The new $W(U_{10})$ parameterization (black symbols) follows the wind speed trend of the satellite-based W data (magenta symbols) well. The W values predicted with the new $W(U_{10}, T)$ parameterization (cyan symbols) are spread as the satellite-based W data are. We thus demonstrate that, accounting for at least one secondary factor, we are able to model both the trend and the spread of the W data. Figure 3(b) shows a difference map between the new $W(U_{10}, T)$ expression and the $W(U_{10})$ expression based on in situ data. The former predicts less latitudinal variations than the latter. Therefore, global distributions of sea spray production based on satellite data differ significantly from the conventional predictions. Such a difference affects the amount of sea salt aerosols in the atmosphere and thus their role in the heat transfer and formation of cloud

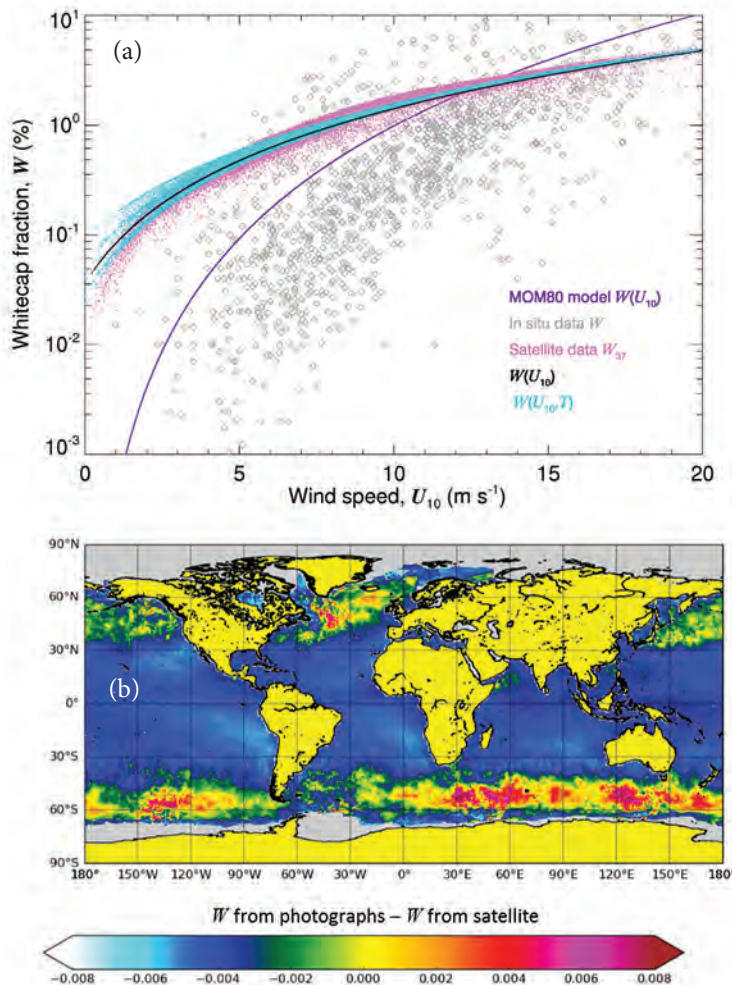


FIGURE 3
 (a) Comparison of W values obtained from the new parametrization $W(U_{10})$ (black symbols) and $W(U_{10}, T)$ (cyan symbols) to in situ W data (gray symbols, same as in Fig. 1(a)) and satellite-based W data at 37 GHz for 17 March 2007 (magenta symbols).
 (b) Difference map of annually averaged W distribution for 2006 calculated from the $W(U_{10})$ parametrization based on photographic data² minus the new $W(U_{10}, T)$ parametrization. The calculations use wind speed U_{10} and sea surface temperature T from the whitecap database.

droplets. The heat transfer plays an important role in tropical cyclones genesis. The formation of cloud droplets affects both the hydrological cycle by changing the precipitation pattern and the Earth radiation budget by altering the planetary albedo. To improve further whitecap parametrizations and the modeling of associated climate processes, we need to account for the influence of the wave field on the whitecap fraction.

[Sponsored by the NRL Base Program (CNR funded)]

References

- ¹ G. de Leeuw, E. L. Andreas, M.D. Anguelova, C.W. Fairall, E.R. Lewis, C.D. O'Dowd, M. Schulz, and S.E. Schwartz, "Production Flux of Sea-Spray Aerosol," *Rev. Geophys.* **49** (2011).
- ² E.C. Monahan and I. O'Muircheartaigh, "Optimal Power-Law Description of Oceanic Whitecap Coverage Dependence on Wind Speed," *J. Phys. Oceanogr.* **10**, 2094–2099 (1980).
- ³ M.D. Anguelova and F. Webster, "Whitecap Coverage from Satellite Measurements: A First Step Toward Modeling the Variability of Oceanic Whitecaps," *J. Geophys. Res.* **111**, C03017 (2006).
- ⁴ M.H. Bettenhausen, C.K. Smith, R.M. Bevilacqua, N.-Y. Wang, P.W. Gaiser, and S. Cox, "A Nonlinear Optimization Algorithm for Windsat Wind Vector Retrievals," *IEEE Trans. Geosci. Rem. Sens.* **44**, 597–610 (2006).
- ⁵ M.F.M.A. Albert, M.D. Anguelova, A.M.M. Manders, M. Schaap, and G. de Leeuw, "Parameterization of Oceanic Whitecap Fraction Based on Satellite Observations," *Atmos. Chem. Phys.* **16**, 13725–13751 (2016).



Successful Self-Embedment of a Large Benthic Microbial Fuel Cell Anode

J.W. Book,¹ L.M. Tender,² J.P. Golden,² J.R. Dale,³ A.J. Quaid,¹ I.R. Martens,¹ S. Barr Engel⁴

¹*Oceanography Division*

²*Center for Bio/Molecular Science and Engineering*

³*Marine Geosciences Division*

⁴*Cornell University*

Introduction: Benthic microbial fuel cells (BMFCs) are formed by connecting a noncorrosive anode embedded in anoxic ocean sediment to a noncorrosive cathode floating in oxygenated seawater. Electric potential results from oxidation of organic material in the sediment at the anode and reduction of oxygen at the cathode. If a power consuming device is inserted into this circuit, an electrical current will flow from the anode to the cathode. Theoretically, BMFCs should generate power indefinitely, due to their self-rejuvenating electrode catalysts, comprised of microbial biofilms that spontaneously grow on the electrode surfaces,^{1,2} and a continuous supply of organic material and oxygen in the marine environment. Most BMFC applications² have relied on divers and on remotely operated

vehicles to embed anodes large enough to generate appreciable power, which makes BMFC deployment expensive and cumbersome. In the Efficient Microbial Benthic Electrode Design program at the U.S. Naval Research Laboratory (NRL), we have investigated the possibility of incorporating BMFCs onto existing bottom moorings, thereby giving these moorings the benefits of BMFC power without significant modifications to deployment procedures.

BMFC Design and Mooring Integration: Numerous tests in the field and in NRL's Laboratory for Autonomous Systems Research showed that the simplest method of placing BMFC designs directly underneath bottom moorings failed to work, due to penetration of oxygenated water to the anode through imperfect seals between the mooring and the sediment along the outer edges of the mooring. Therefore, a new BMFC was designed to have a series of eight overlapping flukes around the anode's perimeter (Fig. 4) for a better seal and to prevent oxygen exposure to the anode. Flukes were made from 0.375-inch thick rubber for both strength and flexibility. The anode was made from 57 one-meter-long bottlebrush electrodes of carbon fiber which were formed into 19 rings and mounted on a fiberglass grating bolted onto a 1.2-m diameter fiberglass disk holding the rubber flukes (Fig. 4). The cathode was made from a linear array of seven of the meter-long carbon fiber bottlebrush electrodes (Fig. 5). To prevent the flukes from being folded under the mooring during deployment, the flukes are held up by rollers pinned against the mooring by a deployment cage (Fig. 4). After the mooring reaches the ocean bottom, the flukes are automatically deployed when this cage is acoustically released and brought back to the surface.

Results: We conducted the first field test of this new BMFC mooring in Maine's Damariscotta River estuary. The mooring was lowered to a bottom depth of 7 m and then the deployment cage was detached by acoustic command, releasing the rubber flukes and the floating cathode. Divers documented and verified the successful operation of the automatic deployment system (Fig. 5). A Scribner model 871 electronic load tester was used to control a variable resistor between the anode and cathode and to record the current passing through this circuit every hour. The 871 control system automatically varied the load resistance to attempt to maintain a 0.35 volt potential between the anode and cathode and thus measure the amount of sustained power that could be produced by this BMFC. Approximately 7 days after deployment, appreciable current began to flow through the BMFC, and power production rapidly increased over the next 4 days (Fig. 6). Then power production increased more gradually, reaching a maximum 24-hour-average power level of



FIGURE 4
 Benthic microbial fuel cell design and mooring integration. Top left-hand panel: the mounting of thick rubber flukes on the underside of the upside-down mooring body. Bottom left-hand panel: the 19 ring anode design on the underside of the mooring. Right-hand panel: the mooring with a deployment cage holding the flukes up as the mooring is lowered to the seafloor.

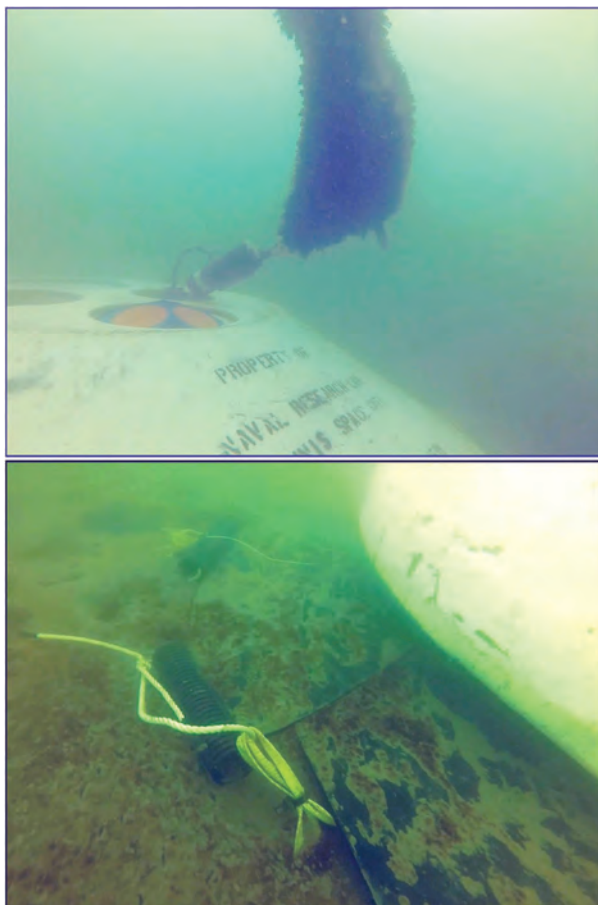


FIGURE 5
 The mooring as deployed on the seafloor. The top panel shows the floating cathode. The bottom panel shows the deployed rubber flukes extending from the mooring on the seafloor.

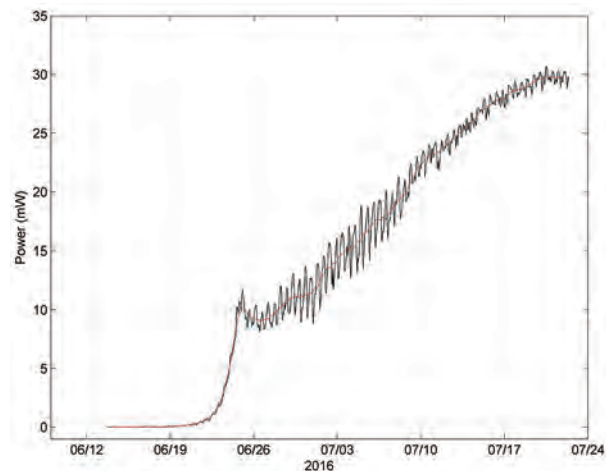


FIGURE 6
 Power produced by the benthic microbial fuel cell. Black is the measured current times the measured voltage. Red is a 24-hour running average of the black curve.

30 mW on day 38 after the deployment. The independent battery powering the 871 system failed on day 38, prematurely stopping the experiment 85 days early.

The BMFC was fully functioning up until the 871 system failure. Oxygen was being excluded from reaching the anode, as the median oxygen level at the anode was measured as 0.09 mg/l by an optode oxygen sensor, while the corresponding median oxygen level measured at the floating cathode was 9.74 mg/l. The BMFC produced a higher power per anode footprint surface area (26 mW/m^2) than a calibration plate BMFC anode system deployed nearby (17 mW/m^2).

Conclusions: This experiment showed that a large BMFC can be integrated into a bottom mooring and successfully deployed and operated without diver assistance. The results constitute a proof of concept demonstration of the potential for future practical BMFC mooring development.

Acknowledgments: We thank the staff of the Darling Marine Center of the University of Maine for their excellent support. Photos in Fig. 5 were taken by the Center's scientific dive team.

[Sponsored by ONR]

References

- ¹ C.E. Reimers, L.M. Tender, S. Fertig, and W. Wang, "Harvesting Energy from the Marine Sediment-Water Interface," *Environ. Sci. Technol.* **35**(1), 192–195 (2001).
- ² L.M. Tender, C.E. Reimers, H.A. Stecher III, D.E. Holmes, D.R. Bond, D.A. Lowy, K. Pilobello, S.J. Fertig, and D.R. Lovley, "Harnessing Microbially Generated Power on the Seafloor," *Nat. Biotechnol.* **20**, 821–825 (2002).



What is the Impact of Light on Ocean Primary Production and Hypoxia?

R.W. Gould, Jr.,¹ B. Penta,¹ D.S. Ko,¹ J.C. Lehrter,² L. Lowe,³ I. Shulman,¹ S.D. Ladner,¹ J.D. Hagy⁴

¹*Oceanography Division*

²*University of South Alabama*

³*CSRA, Inc.*

⁴*U.S. Environmental Protection Agency*

Introduction: The magnitude and distribution of solar radiation incident at the sea surface impacts the physics, chemistry, and biology of the ocean. From a physical perspective, it penetrates into the water column and heats the upper layer of the ocean, driving stratification and thermohaline circulation, and through ocean-atmosphere coupling and feedback mechanisms, influences air/sea heat exchange, winds, and climate. Biologically, a portion of the shortwave (SW) radiation, the photosynthetically available radiation (PAR), drives oceanic primary production.

In the northern Gulf of Mexico, nutrients from upstream agricultural fertilization and river runoff are delivered to the Louisiana Continental Shelf (LCS) via the Mississippi-Atchafalaya river basin. This increased nutrient loading stimulates a phytoplankton bloom; as the resulting phytoplankton biomass sinks to the seafloor and decays, oxygen levels in the water can be reduced to very low levels, causing hypoxia (dissolved oxygen levels below 2 mg/l). This "dead zone" develops seasonally every year from mid-April through Septem-

ber, and is the second largest hypoxic zone in the world (only the Baltic Sea hypoxic zone is larger). Hypoxia can impact local fisheries and benthic organisms, causing important ecological and economic consequences.

Our goal is to develop a modeling approach to better understand how interactions between biotic and abiotic factors affect primary production and oxygen dynamics on the LCS. Specifically, we are interested in how light variability (PAR) can impact the magnitude, distribution, and duration of hypoxia. Working together, the U.S. Naval Research Laboratory (NRL) and the U.S. Environmental Protection Agency (EPA) have developed a coupled hydrodynamic/ecosystem model. With our three-dimensional model, we can perform simulations with different, realistic input light conditions, such as those that might be expected to result from various climate change scenarios, and compare results to assess the impacts.

Model Development: The Navy Coastal Ocean Model-Louisiana Continental Shelf (NCOM-LCS) provides the hydrodynamic components of the coupled model system (horizontal and vertical transport and mixing, temperature, and salinity at 2-kilometer horizontal resolution for 20 equally-spaced sigma depth layers at a 5-minute time step). Land-sea forcing is through observed river discharges to the domain. The Coupled Ocean/Atmosphere Mesoscale Prediction System (COAMPS) and the Navy Operational Global Atmospheric Prediction System (NOGAPS) provide atmospheric forcing (air pressure, temperature, wind stress, and SW radiation). Open-ocean boundary conditions are from the 6-kilometer regional NCOM. The hydrodynamic forcing is supplied to the Coastal General Ecosystem Model (CGEM), which provides the ecosystem components of the coupled model system. CGEM¹ computes a suite of biogeochemical properties, such as phytoplankton and zooplankton biomass, nutrients, and oxygen concentration, at each model time step and grid location; it was applied to the LCS for a 1-year period (2006).

Estimating PAR Magnitude, Distribution, and Variability: Accurate estimates of sea-surface PAR (and its attenuation with depth) are required as input to the ecosystem model (CGEM), from which we then can derive accurate estimates of phytoplankton biomass and primary production. Such estimates are available from satellite ocean color imagery and atmospheric model predictions. Because the PAR values could come from either source, it is important to understand the variability and accuracies of each. We compare values derived from the imagery to those from the models, and to in situ measurements in the Gulf of Mexico, to assess PAR variability based on source. Spatial and

temporal analyses covering multiple years and seasons as well as clear/cloudy conditions indicate that PAR estimates can vary up to 10%, depending on the source.

In addition, changes in cloud coverage could impact the amount of PAR reaching the sea surface and its spatial distribution.² Furthermore, future river discharge patterns could change as a result of changing precipitation patterns,³ which would lead to associated regional increases or decreases in nutrients and colored dissolved organic matter (CDOM) in coastal areas, thereby impacting phytoplankton production and the horizontal and vertical distribution of PAR. Thus, the many interacting processes affecting water column and benthic light levels and primary production are difficult to separate, but coupled bio-physical ecological modeling provides an effective approach for doing so.

Impact of PAR on Primary Production and Hypoxia: Based on the PAR comparisons and a potential climate change scenario, we performed eight ecosystem (CGEM) sensitivity simulations using scaled PAR values, to assess the impact of PAR on oxygen production and hypoxia development. The NOGAPS-derived input PAR values were scaled by a constant factor (± 2 , 5, 10, 50% of original values) at each 3-hour time step for 1-year model runs (2006). Other parameters were held constant. The “baseline” run, for comparison to the scaled runs, used the original NOGAPS PAR values without any changes. Only results for a 10% increase in PAR are shown here (for a single day, 2 August 2006).

Based on the model results, PAR variability can impact the magnitude and distribution of simulated primary production and hypoxia. For example, a 10% increase in PAR can lead to higher water-column integrated primary production (IPP) over a large area (Fig. 7), with a 6–10% increase in IPP in offshore waters and

a smaller impact in coastal waters. For bottom water oxygen concentration, slightly smaller differences from the baseline run are observed (generally ~2 to 5%, but up to 20%). However, the differences can be observed over much of the model domain and can extend 5–35 meters into the water column from the bottom (depending on water depth and location on the LCS; Figs. 8 and 9). These increases in oxygen concentration can lead to decreases in daily bottom hypoxic area of 200–400 km² from June through September, and such decreases can be important locally.

Summary: Our research enables us to assess the impact of biotic factors, such as phytoplankton growth rate/mortality and zooplankton grazing, and abiotic factors, such as light and nutrients, on oceanic primary production and hypoxia development. We can separate the impacts of individual factors, as we did here, enabling us to focus on just the effect of light variability. The model simulations combine complex biogeochemical, ecological, and physical interactions, and this approach can be extended to examine a variety of applications, such as climate change scenarios, ocean acidification, and other processes that impact both navy and civilian operations. Model hindcasts and forecasts provide coastal managers with valuable analysis and predictive tools.

Acknowledgments: The authors are grateful to investigators at LUMCON and to Mr. C. MacDonald (Sonoma Technology, funded by the Bureau of Ocean Energy Management) for collection of in situ PAR data. This research was supported by the EPA and NRL. [Sponsored by the NRL Base Program (CNR funded) and the Environmental Protection Agency]

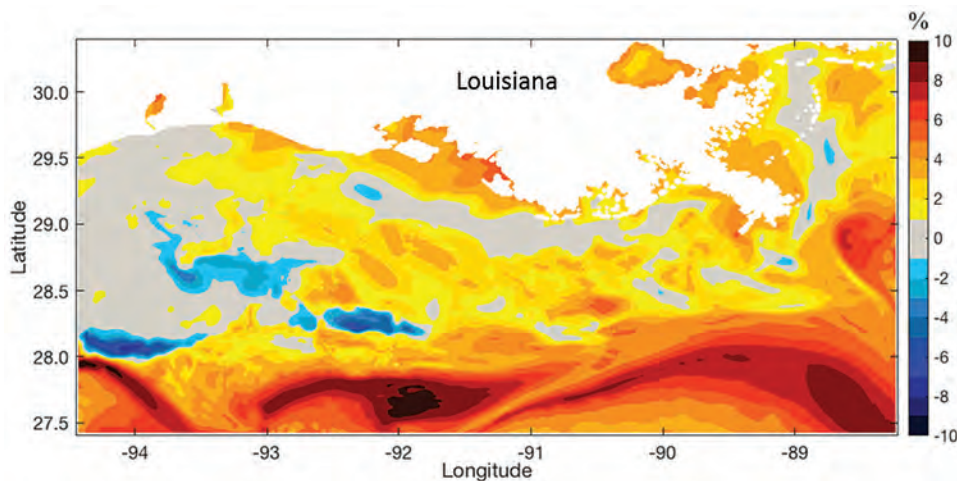


FIGURE 7 Simulation results showing the % difference between the “baseline” model run and the +10% PAR run, for integrated water column photosynthesis on 2 August 2006. Gray pixels indicate very little difference between the two model runs (see color scale).

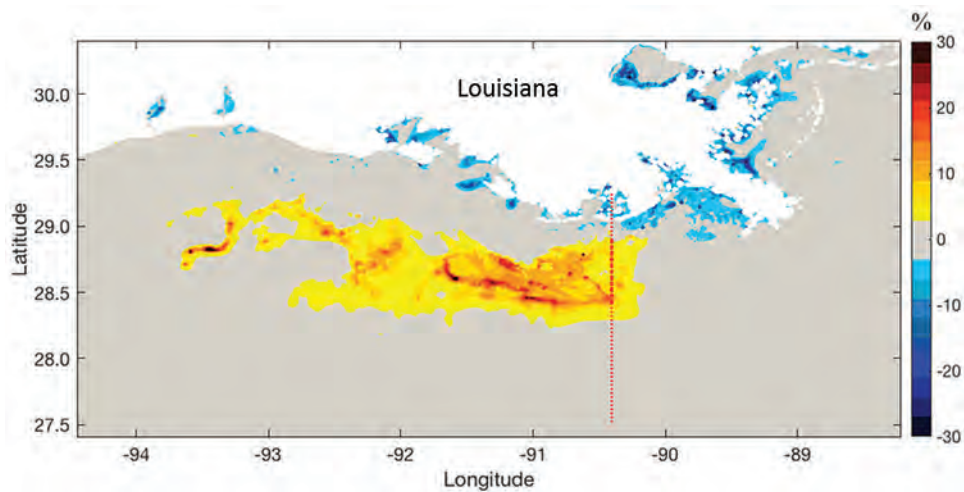


FIGURE 8 Simulation results showing the % difference between the “baseline” model run and the +10% PAR run, for bottom water oxygen concentration on 2 August 2006. Gray pixels indicate very little difference between the two model runs (see color scale).

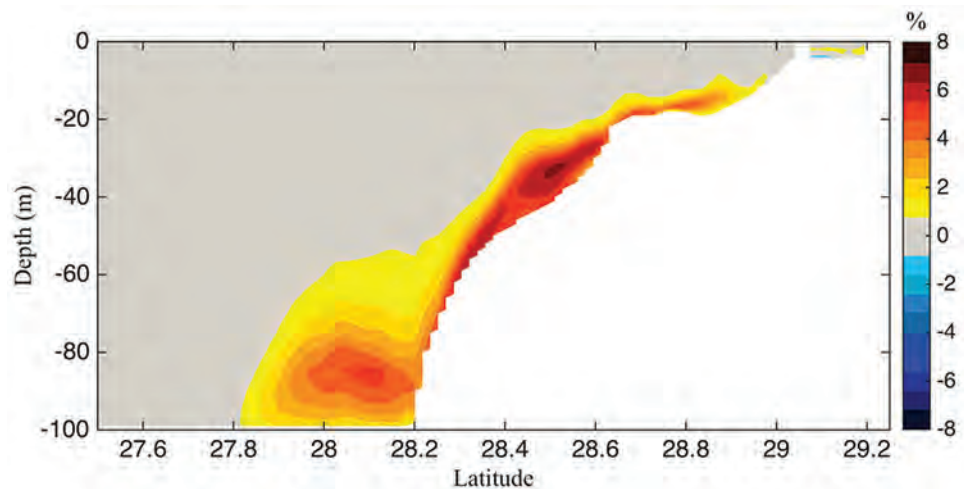


FIGURE 9 Simulation results showing the % difference between the “baseline” model run and the +10% PAR run, for water column oxygen concentration on 2 August 2006. North/South vertical transect through the water column, at the location indicated by the red dotted line in Figure 8. White pixels indicate the bottom and gray pixels indicate very little difference between the two model runs (see color scale).

References

- ¹P.M. Eldridge and D.L. Roelke, “Origins and Scales of Hypoxia on the Louisiana Shelf: Importance of Seasonal Plankton Dynamics and River Nutrients and Discharge,” *Ecol. Model.* **221**(7), 1028–1042 (2010).
- ²J.R. Norris, R. J. Allen, A.T. Evan, M.D. Zelinka, C.W. O’Dell, and S.A. Klein, “Evidence for Climate Change in the Satellite Cloud Record,” *Nature* **536**(7614), 72–75 (2016).
- ³F.C. Sperna Weiland, L.P.H. van Beek, J.C.J. Kwadijk, and M.F.P. Bierkens, “Global Patterns of Change in Discharge Regimes for 2100,” *Hydrol. Earth Syst. Sc.* **16**, 1047–1062 (2012).



- 180 Waveguides for Non-Mechanical Beam Steering in the Mid-Wave Infrared
- 182 Optical System Protection Using Pupil-Plane Phase Masks
- 183 Simultaneous Optical Beamforming for Phased-Array

Waveguides for Non-Mechanical Beam Steering in the Mid-Wave Infrared

J.D. Myers,¹ J.A. Frantz,¹ C.M. Spillmann,² R.Y. Bekele,⁴ L.B. Shaw,¹ J. Naciri,² J. Kolacz,² H. Gotjen,² M. Pauli,³ C. Dunay,³ D. Burchick,³ J. Auxier,³ J.S. Sanghera¹

¹Optical Sciences Division

²Center for Bio/Molecular Science and Engineering

³Tactical Electronic Warfare Division

⁴University Research Foundation

Introduction: The mid-wave infrared (MWIR) portion of the optical spectrum is of interest for a variety of military and civilian applications, including molecular fingerprint chemical sensing and thermal detection. Traditionally, in applications where an MWIR laser is used to illuminate a target of interest, the beam is steered mechanically using a gimbal. While mechanical gimbals have some positive attributes, including high efficiency, they are typically bulky and heavy, consume large amounts of power, have relatively slow slew rates, and, because they contain multiple motors and moving parts, require frequent maintenance. Combined, these attributes make mechanical gimbals unsuitable for new and emerging applications, including installation on small, unmanned vehicles that have constraints on the allowable size and weight of their components. New technologies are required that are free of the drawbacks associated with mechanical steering.

A New NRL Beam Steerer: In a combined effort between the Optical Sciences Division, the Center for Biomolecular Science and Engineering, and the Tactical Electronic Warfare Division, the U.S. Naval Research Laboratory (NRL) is developing an agile non-mechanical beam steerer suitable for advanced applications. The new

NRL beam steerer, called a Steerable Electro-Evanescent Optical Refractor (SEEOR), is based on a variable refractive index waveguide first developed by Vescent Photonics (Arvada, Colorado) (in the short-wave infrared) under U.S. Navy Small Business Innovation Research funding.¹ Development of the beam steerer has been fully transitioned to NRL for research into its possible usefulness in defense-related applications and exploration of its potential for expansion into other optical bands.²

Each SEEOR consists of three key regions, as shown in Fig. 1. First, polarized light must be efficiently coupled into the waveguide. This is accomplished via the use of an Ulrich coupler³ which relies on a faceted substrate, a precisely tapered subcladding, and a waveguide core. By illuminating the facet at a precise, wavelength-dependent angle, light is efficiently coupled through the substrate and confined within the waveguide core because of its high relative refractive index. The subcladding, which is tapered at angles that require microradian precision, is grown in the Optical Sciences Division using advanced deposition techniques.

Once in the waveguide core, light propagates until it enters the horizontal steering region. Here, the waveguide stack consists of the (now untapered) subcladding, the core, and an upper cladding of aligned liquid crystal. Liquid crystal is used because it has a variable, orientation-dependent refractive index due to its birefringent nature, which originates from the collective property of rod-shaped molecules possessing orientational order in a fluid-like state. In the absence of an applied electric field, the aligned liquid crystal molecules will orient in one preferred direction relative to the core with a certain refractive index. When a voltage is applied across the device, the molecules will reorient, controllably altering the refractive index. This effect is exploited to create steering.

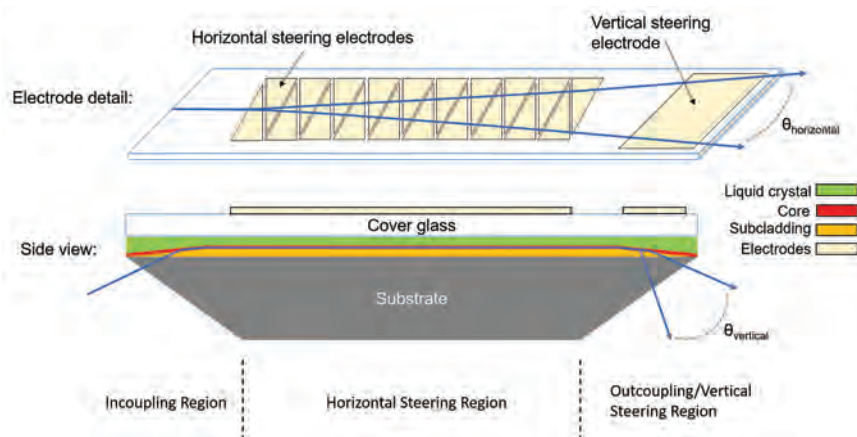


FIGURE 1

Schematic overview of a Steerable Electro-Evanescent Optical Refractor (SEEOR) non-mechanical beam steerer, denoting (top) the electrode detail required to achieve horizontal and vertical steering, and (bottom) a side-view cross-section of the waveguide, showing the different layers and steering regions (thicknesses not to scale).

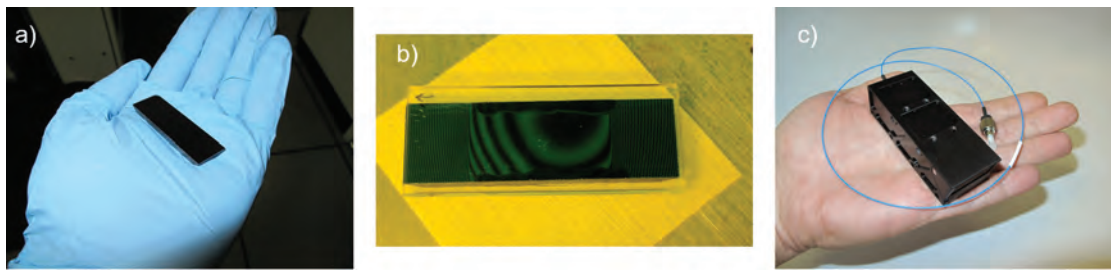


FIGURE 2

Examples of SEEOR devices at various stages of assembly. (a) Bare faceted substrate chip, prior to waveguide deposition. (b) Assembled mid-wave infrared SEEOR under crossed polarizers. Fine optical interference fringes show the tapering of the subcladding layer. (c) Fully assembled and packaged short-wave infrared SEEOR.

The waveguide in this region is designed to ensure that the optical mode is not strongly confined to the core and that part of the mode, the evanescent field, extends into the liquid crystal upper cladding. Because part of the mode is now interacting with the liquid crystal, any changes in the liquid crystal refractive index will change the overall effective refractive index of the mode propagating in the waveguide. Because the electrodes have been designed with a prismatic pattern, changing the refractive index of the liquid crystal with an applied voltage effectively creates a variable prism pattern that steers light to either the left or the right.

The final region of the waveguide is the outcoupling region, where the voltage-dependent refractive index of liquid crystal is used to create vertical steering. The outcoupling region is another Ulrich coupler with a tapered subcladding, but there is now an electrode present over the tapered region that is used to apply voltage and tune the liquid crystal index. As the index is varied, the exit angle of light from the waveguide also changes, resulting in vertical steering.

Technologies and Applications: These devices have been enabled by multiple key technologies. First, the subcladding and core layers utilize MWIR-transparent chalcogenide glasses (based on As-S and As-Se compounds) developed at NRL as part of the DARPA MGRIN program.⁴ These glasses exhibit robust processing as thin films via thermal evaporation and high transparency throughout the infrared.

Second, new liquid crystal mixtures have been developed with low absorption in the MWIR. Common commercial liquid crystal mixtures exhibit strong molecular absorption throughout the MWIR corresponding to resonant molecular vibrations of individual atomic bonds. By designing new liquid crystal blends based on halogenated compounds, the characteristic molecular absorptions are shifted away from the MWIR, making them suitable for use in our MWIR SEEORs.

These new, refractive beam steerers have numerous advantages over traditional gimbals—they are extreme-

ly light and very compact (Fig. 2), and the beam steerer itself consumes ~mW of power. In addition, because the steering mechanism utilizes liquid crystal reorientation rather than moving parts, steering can be incredibly fast, with point-to-point slew times of less than 1 ms. Further, the basic mechanism of operation is compatible across all bands from the visible to long-wave infrared, and we are actively developing steerers in numerous optical bands. With continued development, this technology shows immense potential for replacing mechanical steering in a wide range of applications, enabling new capabilities for applications relevant to both Department of Defense and civilian interests.

[Sponsored by the NRL Base Program (CNR funded)]

References

- ¹ M. Ziemkiewicz, S.R. Davis, S.D. Rommel, D. Gann, B. Luey, J. D. Gamble, and M. Anderson, "Laser-Based Satellite Communication Systems Stabilized by Non-Mechanical Electro-Optic Scanners," *Proc. SPIE 9828*, Airborne Intelligence, Surveillance, Reconnaissance (ISR) Systems and Applications XIII, 982808 (2016)
- ² J.A. Frantz, J.D. Myers, R.Y. Bekele, C.M. Spillmann, J. Naciri, J.S. Kolacz, H. Gotjen, L.B. Shaw, J.S. Sanghera, B. Sodergren, Y.-J. Wang, S.D. Rommel, M. Anderson, S.R. Davis, and M. Ziemkiewicz, "Non-Mechanical Beam Steering in the Mid-Wave Infrared," *Proc. SPIE 10181*, Advanced Optics for Defense Applications: UV through LWIR II, 101810X (2017).
- ³ R. Ulrich, "Optimum Excitation of Optical Surface Waves," *JOSA* **61**(11), 1467–1477 (1971).
- ⁴ D. Gibson, S. Bayya, J. Sanghera, V. Nguyen, D. Scribner, V. Maksimovic, J. Gill, A. Yi, J. Deegan, and B. Unger, "Layered Chalcogenide Glass Structures for IR Lenses," *Proc. SPIE 9070*, Infrared Technology and Applications XL, 90702I (2014).



Optical System Protection Using Pupil-Plane Phase Masks

A.T. Watnik,¹ K. Novak,² M. DePrenger,² J. Wirth,^{1,3} and G.A. Swartzlander, Jr.³

¹*Optical Sciences Division*

²*Tekla*

³*Rochester Institute of Technology*

Introduction: As directed energy weapons such as high energy lasers become more powerful, the threat to Department of Defense imaging assets can progress from degradation of the image quality to focal plane array damage. Focused laser light can be detrimental to the image quality due to the concentration of power in a few pixels on the array. The Applied Optics Branch of the Optical Sciences Division at the U.S. Naval Research Laboratory (NRL) develops novel robust intelligence, surveillance, reconnaissance, and tracking (ISRT) optical systems for the Navy, particularly systems with reduced susceptibility to disruption, damage, or destruction from high intensity laser sources.

Imaging with Passive and Active Illumination:

An interesting situation arises when a camera system captures both active, coherent illumination via lasers and passive illumination (indirect illumination via sunlight, room lights, etc.) from a scene. Lasers are often collimated, tightly focused beams that, when imaged, may saturate pixels in the imager. Using characteristics of the optics in the imaging system, it becomes possible to computationally subtract off the laser light from the rest of the image in post-processing, without any knowledge of the position of the laser or its intensity,

or of any information about the scene itself. However, if the laser saturates pixels in the scene, the underlying image in that region, which would have been formed without the laser present, cannot be recovered, even if we are able to identify and subtract off the laser light. To address the challenge of saturated pixels and its limit on image recovery, a new and very counterintuitive imaging system design and collection approach emerges, that of taking images that are blurry rather than sharp (Fig. 3). This approach exploits the very different properties of laser radiation compared to the rest of the light in the scene, and thereby prevents nuisance and adversarial lasers from degrading imaging systems critical to Navy operations.

Pupil-Plane Phase Masks: Central to our research in pursuit of the perfect blurry image is an optical system that, instead of focusing light on the imager's focal plane, requires a phase mask at the pupil-plane. The phase mask modifies the phase of the incoming light, changing the optical path and direction the light travels to the focal plane, which results in spreading the light across much of the focal plane. We have tested various phase mask designs, including cubic, vortex, axicon, random, and defocus as well as other Zernike phase functions.^{1,2} We use a spatial light modulator to create each phase mask (Fig. 4).

The properties and spatial characteristics of the phase mask introduce unique blur functions into the imaging system, affecting both the passive illumination from the background scene and the active illumination from the laser source. We are interested in understanding which phase masks introduce the kinds of blur functions that allow us to spread out the incoming light over the greatest number of pixels — an approach that

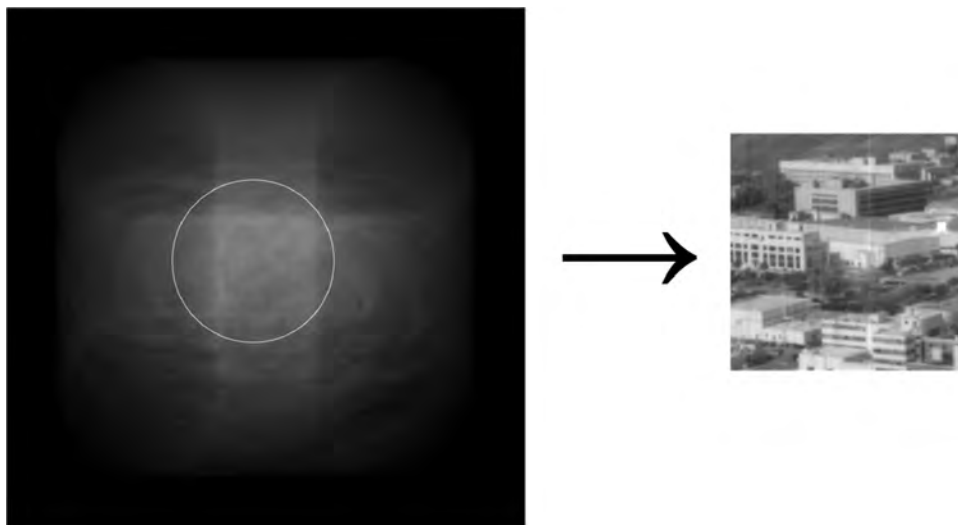


FIGURE 3

The recorded image is intentionally blurred beyond recognition. Using knowledge of the designed optical system, we can recover fine details from the scene. Here, only a small subset of the full recovered image is shown.

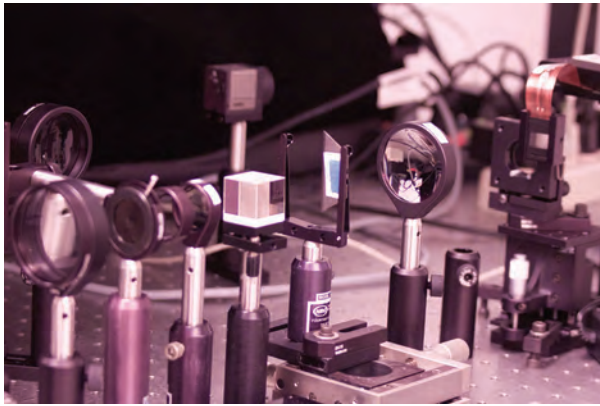


FIGURE 4
Hardware experiment for testing phase masks using a spatial light modulator.

helps limit regions of saturation caused by the laser light while simultaneously allowing for good reconstruction of the background image after the additional processing steps. These two goals oppose each other in the actual design of an optimum phase mask for a given imaging system; it is easy to spread out laser light to limit saturated pixels, but doing so makes it difficult to recover the underlying image, and vice versa.

Image Recovery: Our goal is to restore an image of the background scene that looks as if the laser source had never been present. To subtract off the laser light from the rest of the image, the specific type of blur function based on the phase masks is used in a deconvolution process. The knowledge of the blur function from the phase masks is then used to recover and restore the background scene as if that scene were the image taken with the camera. However, the process to remove the laser light from the image and recover the underlying background image is not perfect, and some artifacts are introduced, producing a slightly blurry image. Detecting scenes by purposefully upending the conventional approach of capturing a clear, sharp image opens new avenues for recovering scenes in the most challenging operational environments.

[Sponsored by the NRL Base Program (CNR funded), ONR, and Office of the Secretary of Defense]

References

- ¹ A.T. Watnik, G.J. Ruane, and G.A. Swartzlander, Jr. "Incoherent Imaging in the Presence of Unwanted Laser Radiation: Vortex and Axicon Wavefront Coding," *Opt. Eng.* **55**(12), 123102 (2016). <https://doi.org/10.1117/1.OE.55.12.123102>.
- ² G.J. Ruane, A.T. Watnik, and G.A. Swartzlander, "Reducing the Risk of Laser Damage in a Focal Plane Array Using Linear Pupil-Plane Phase Elements," *Appl. Opt.* **54**, 210–218 (2015), <https://doi.org/10.1364/AO.54.000210>.



Simultaneous Optical Beamforming for Phased-Array Applications

J.D. McKinney, M.R. Hyland, R.C. Duff, and K.J. Williams
Optical Sciences Division

Motivation: As platforms for electronic attack and electronic support become smaller, phased array-based apertures could offer improvements in effective isotropically-radiated power; reductions in size, weight, power, and cost (SWaP-C); and new capabilities, including direction-finding from a static aperture. A key component of phased-array apertures is the beam forming network that tailors the amplitude- and phase-response of each array element to form the desired beams. Radio frequency (RF) multi-beam beam formers (e.g., Rotman lenses) have been demonstrated,¹ but their size, determined by the RF wavelength, precludes their use on small platforms and across a wide frequency range. Our research in the Photonics Technology Branch of the Optical Sciences Division focuses on developing simultaneous optical beamformers for SWaP-C-constrained platforms. We have demonstrated four simultaneous beams, on both transmit and receive, with optical fiber-based implementations of a Rotman lens suitable for use from about 1 to 40 GHz. We are working on translating these architectures to photonic integrated circuit and planar lightwave circuit topologies. We are also running critical analysis of the performance of these topologies.

Wideband True-Time-Delay Optical Beamforming: Conventional RF beamformers, whether digital or analog, are inherently narrowband. In the case of electronically-steered arrays (digital beamforming), the required phase step between elements is determined modulo 2π leading to main beam directions which are frequency-dependent. The size of analog multi-beam beamformers (such as the Rotman lens) scales with the RF wavelength, limiting the achievable bandwidth to the order of about 4:1.¹ Optical beamformers, on the other hand, may be constructed using true time delays (TTD) to provide the appropriate phasing between array elements. Optical TTD lends itself to inherently broadband and squint-free operation when compared to traditional phased arrays or microstrip-based Rotman lenses. The delays required to form a particular beam are solely determined by the physical spacing of the elements in the antenna array. Therefore, arrays that use TTD beamformers exhibit a primary beam direction which is frequency-independent. This allows a given array to function over a wide frequency range for electromagnetic warfare (EW) applications in electronic support and electronic attack, without the need

to redesign the beamforming architecture. Additionally, the small size and weight afforded by photonic architectures allow formation of multiple wideband beams on platforms where use of conventional multi-beam RF beamformers would be intractable.

Figure 5 illustrates the most straightforward and flexible simultaneous optical beamforming architecture. As the figure shows, the output of a wideband phased-array antenna (N elements) feeds an optical antenna interface (an array of microwave photonic links)² where the RF output of each antenna is impressed onto a unique wavelength optical carrier with a Mach-Zehnder intensity modulator. These modulated optical carriers are then combined using an arrayed-waveguide grating (AWG) multiplexer. The output of the multiplexer is then distributed to M optical beamformers. Within each beamformer, the unique wavelengths are demultiplexed with an AWG and weighted in amplitude using variable optical attenuators. Subsequently, each path is given an incremental time delay using discrete changes in the optical fiber length. The time delay increment between paths is chosen such that a beam is formed in the desired direction. The modulated carriers are then recombined with a second AWG multiplexer, and the RF signal representing the desired beam is recovered through direct-detection of the modulated intensity with a high-speed photodiode. In this beamforming architecture, unique beams are formed in each beamformer, allowing the desired field of view (FOV) to be subdivided into multiple simultaneous beams. The wideband and simultaneous beamforming capability afforded by photonics would be prohibitive in both size and power consumption if implemented digitally.

To illustrate the potential of optical beamformers, an example beamformer is constructed to provide $M =$

4 beams across a 50° FOV for an $N = 8$ element array of wideband (18–42 GHz) spiral antennas. The time delay steps between elements in the array of 49.9 ps, 30.5 ps, 0, and -49.9 ps are chosen to produce beams in the -25° , -15° , 0° , and $+25^\circ$ directions from broadside (normal to the array). Figure 6 shows the relative delay between elements (left column) and the normalized measured antenna array pattern as a function of angle and frequency (right column) for each beam. The achieved delay steps of 49.83 ps, 30.6 ps, -0.08 ps, and -50.61 ps (as determined by linear fits to the measured element delays) show excellent agreement with the target values. As shown by the color of the delay data, the timing control between antenna elements is maintained to within ± 2.5 ps. This level of timing control is equivalent to an accuracy of ± 0.5 mm path length difference in optical fiber and represents the best one can generally achieve in controlling the length of bulk fiber. In the measured antenna patterns, the desired beams (filled) are formed in directions in excellent agreement with the desired angular locations, and, as expected, the main-beam direction does not change with frequency. The additional beams shown by the red contours are grating lobes which arise because the antenna elements are spaced by more than a wavelength in the 18–40 GHz frequency range these lobes change direction with of frequency).

The Push for Integration: Wideband antennas are becoming smaller. The decreased size allows use of arrays with element spacing that is about half of a wavelength at frequencies above 18 GHz; e.g., planar ultrawideband modular arrays³ may be spaced as close as 0.707 mm, which is half of a wavelength at about 21 GHz. The required delay increments are smaller than they would be for bulk fiber delays. Therefore, optical beamformers must be integrated at the chipscale

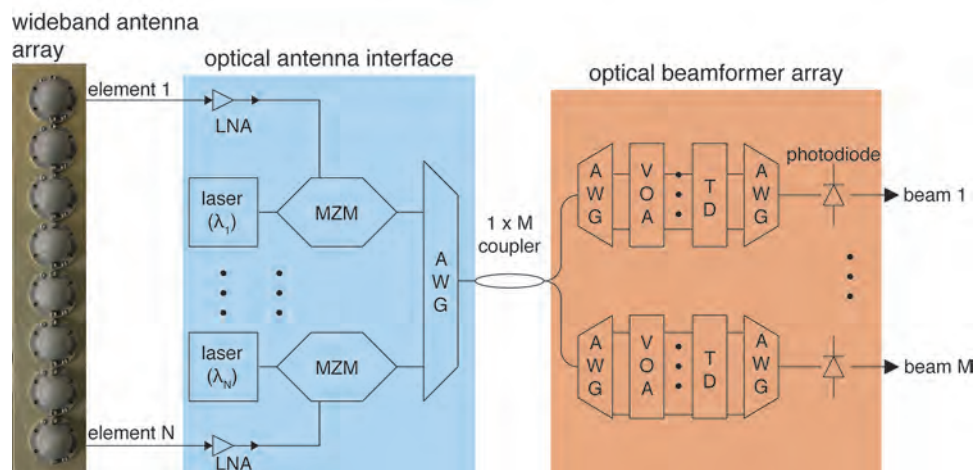


FIGURE 5 Schematic architecture of an optical beamformer architecture based on the RF propagation delay in optical fiber. Abbreviations: LNA = low-noise amplifier; MZM = Mach-Zehnder modulator; AWG = arrayed waveguide grating; VOA = variable optical attenuator; TD = time delay.

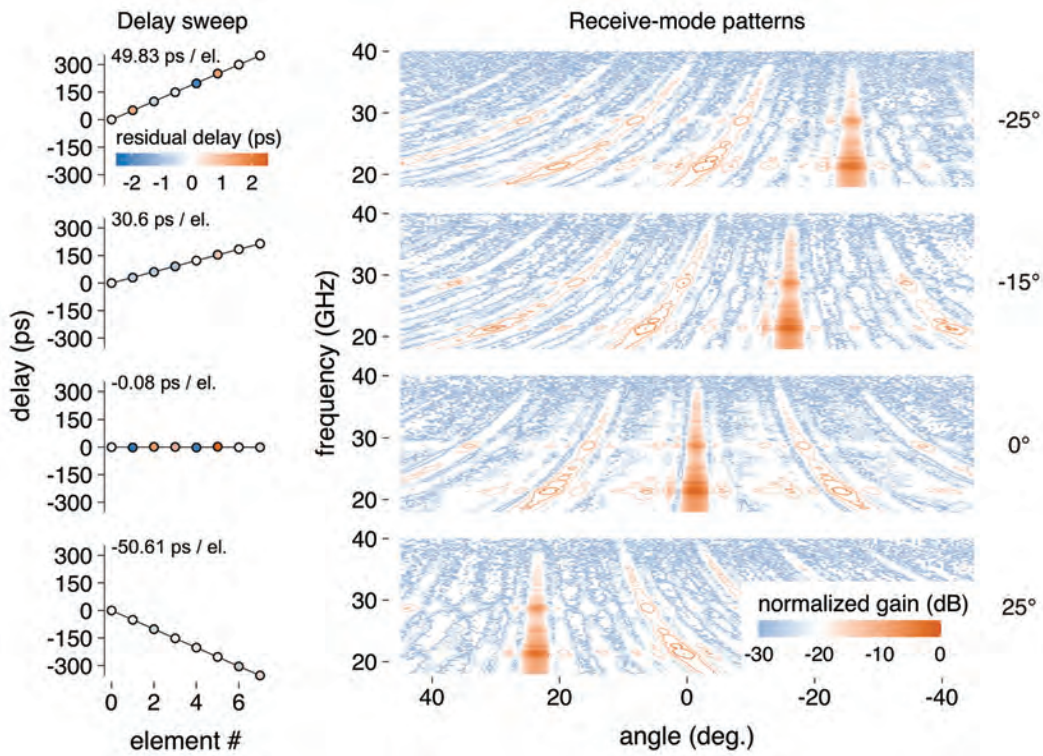


FIGURE 6 Time delay sweep across an 8-element antenna array (left) and measured receive-mode antenna array patterns (right) for simultaneous beams positioned at -25°, -15°, 0°, and +25° (top to bottom) relative to broadside. The main beams (filled) do not change angle with frequency—a unique capability of true time delay-based beamformer architectures.

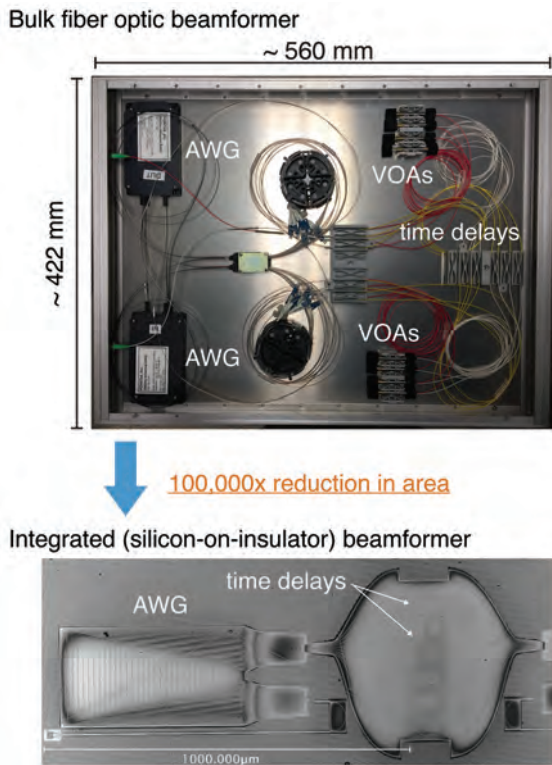


FIGURE 7 Comparison of a bulk fiber optic beamformer with an integrated realization using silicon-on-insulator fabrication technology.

if they are to be suitably applicable to such arrays. In our research, we are pursuing integrated beamformer architectures suitable for such high-frequency arrays. Figure 7 shows the comparison between a bulk fiber optic beamformer and silicon on insulator integrated beamformer. As is evident, a substantial reduction in size (more than 1×10^5 reduction in area) is achievable through integration. While size reduction has been touted as a primary driver for integrated beamformers in the microwave photonics community, little if any attention has been paid to whether integrated architectures can provide the capabilities required in modern EW systems. Our work is focused on critical evaluation of integrated beamformer performance and the design trades required to achieve practical devices.

Summary and Future Work: Several optical beamformer techniques suitable for phased-array applications are currently under development in the Photonics Technology Branch. The techniques could support the formation of multiple simultaneous staring beams over a wide field of view, and thereby could open new opportunities for advances in EW research and technology. We are translating and evaluating these techniques for integrated photonic architectures suitable to small SWaP-C-constrained platforms, such as unmanned aerial, surface, and underwater vehicles.

Acknowledgments: We thank W. Mark Dorsey and John Valenzi, both of the Analysis Branch of the Radar Division at the U.S. Naval Research Laboratory, for performing pattern measurements of the optical beamformers.

[Sponsored by ONR]

References

- ¹ P.S. Hall and S.J. Vetterlein, "Review of Radio Frequency Beamforming Techniques for Scanned and Multiple Beam Antennas," *IEEE Proc.* **137**(5), 293–303 (1990).
- ² V.J. Urick, J.D. McKinney, and K.J. Williams, *Fundamentals of Microwave Photonics*, John Wiley & Sons, 2015.
- ³ S.S. Holland and M.N. Vouvakis, "The Planar Ultrawideband Modular Antenna (PUMA) Array," *IEEE Trans. Antennas Propag.* **60**(1), 130–140 (2012).



- 188** Automatic Target Recognition of Small Crafts Using Multichannel Imaging Radar
- 190** Dust-Infused Baroclinic Cyclone Storm Clouds
- 192** A Multi-Channel Testbed for Next-Generation Maritime SAR

Automatic Target Recognition of Small Craft Using Multichannel Imaging Radar

R.G. Raj
Radar Division

Introduction: In maritime domain awareness (MDA) applications, U.S. Navy airborne radars are routinely tasked with surveilling vast areas of dynamic ocean surface for potential targets of interest. To accomplish this task, large amounts of data are generated, on the order of multiple terabytes per day. From this data, small craft identification information can be extracted for various applications. The entire set of computational methods that map the acquired radar data to class labels corresponding to the targets being sensed (e.g., fishing, pleasure, and military) is called automatic target recognition (ATR). In military radar systems, ATR is critical, because, for most MDA applications, the volume of data and the number of small craft render manual inspection impossible. Moreover, the importance of identifying types of craft in a given area, coupled with the inherent unreliability and time-consuming nature of manual inspection, make automated processes necessary for mapping raw data to object classes. In this paper, we describe recent accomplishments by the Radar and Remote Sensing divisions of the U.S. Naval Research Laboratory (NRL) in developing and validating ATR algorithms for radar systems.

Novel ATR Processing Structures: The Radar Division has developed advanced ATR algorithms for use with imaging radar systems. In these algorithms, a key step is the representation of the targets in terms of simpler, and well chosen, building blocks called basis functions. The chosen basis functions are critical to the quality of subsequent feature extraction and ultimately the classification performance. Of particular interest are basis functions that yield a robust sparse (compact) representation of targets that are not sensitive to target aspect angle. In our current implementation, we use basis functions that describe the textural characteristics (i.e., pattern of intensity arrangements) and shape of the target. Our ATR framework also features added flexibility with a customizable set of basis functions, known as a dictionary, that explicitly exploit the sparsity structure of targets. In particular, our approach incorporates novel statistical tools that allow tailoring the class-specific sparsity structure via the ATR learning process.

Previous approaches to ATR for classifying boats and ships have largely relied on exploiting geometrical features, such as ship length and mast location.¹

Our ATR framework can encapsulate such traditional structural features via our feature fusion methodology. In particular, we leverage recent advances in discriminative graph learning to explicitly capture dependencies between different competing sets of low-level features for the synthetic aperture radar (SAR) target ATR problem.

We have validated our ATR approach on a variety of different datasets. In this article, we focus on the application of our ATR methodology to multichannel SAR (MSAR) datasets.

Data Processing and Experimental Setup: MSAR systems are well suited for correcting distortions in imagery caused by the motion of objects in the maritime environment. A novel aspect of our approach is the development and validation of ATR techniques exploiting MSAR systems. In a collaborative effort between the Radar and Remote Sensing divisions, NRL researchers built the first MSAR system with a sufficiently high number of channels to enable automatic correction of motion-induced inverse SAR image distortions. The automatic correction process uses a variation of the velocity SAR imaging procedure.² The NRL MSAR team performed all aspects of system design, integration, calibration, and test execution. The resulting experimental system was installed on a Saab 340 aircraft in a belly-mounted radome, and served as the data collection asset for the ATR development described in this article (Fig. 1).

High-quality datasets are essential to the development of ATR algorithms. Using the MSAR system, in 2014–15, we systematically collected data on a diverse set of small boat classes in the mid-Atlantic region, obtaining data on over 30 boats ranging in size from 34 to 167 feet. Boats are broadly grouped into fishing, pleasure, tug boats, and military craft. Figure 2 shows examples of each vessel class. Figure 3 presents an outline of our data processing approach.

Experimental Results: Using a single channel of the MSAR data, we achieved a correct classification rate of over 96 percent when classifying over 30 boats and using moderate training. We performed the fusion of the multiple channels via NRL-developed novel MSAR imaging algorithms. We used the resulting MSAR images to train and classify the boats in a manner similar to the single-channel case. In our experiments, we achieved up to 3 percent improvement in classification performance due to incorporation of the multichannel information. This is the first time that anyone has quantified the classification performance improvements that result from incorporation of multichannel systems in ATR development.

This research and development at NRL promises to advance ATR development and delivers a wealth of information and a diverse set of computational tools that will enhance Naval and Department of Defense ATR capabilities.



FIGURE 1
NRL MSAR system mounted on a Saab 340 aircraft.



FIGURE 2
Sample boats from database of multichannel synthetic aperture radar (MSAR) automatic target recognition developed by researchers in the Radar and Remote Sensing divisions.

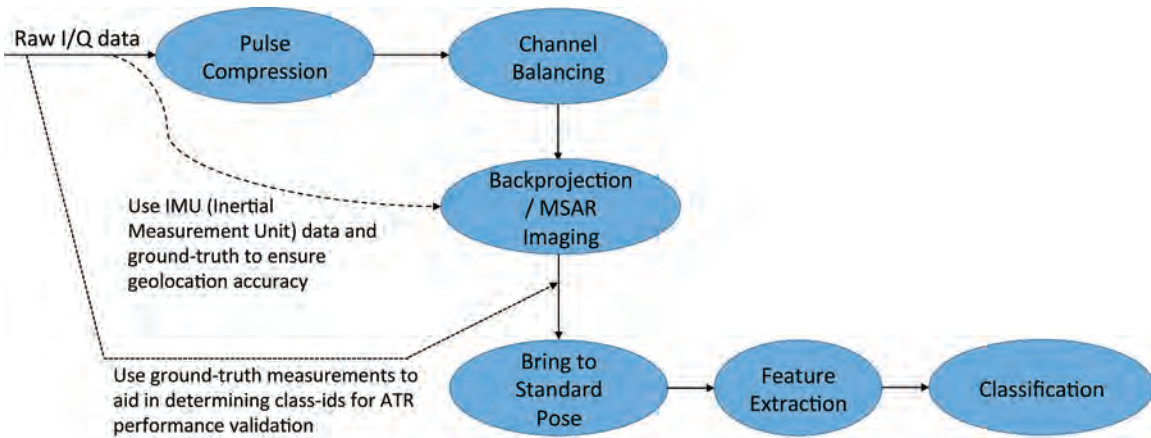


FIGURE 3
High-level ATR data processing flow.

Acknowledgement: This article is a summary of a larger NRL Technical Report to be published with the following co-authors: D.W. Baden, R.D. Lipps, R.W. Jansen, R. Madden, R.S. DeOcampo, M.A. Sletten, and D. Tahmoush.

[Sponsored by ONR]

References

¹ S. Musman, B. Rosenberg, and F. McFadden, “Automatic Recognition of Small Craft using ISAR,” *IMSI Technical Report* (2002).

² B. Friedlander and B. Porat, “VSAR: A High Resolution Radar System for Ocean Imaging,” *IEEE Trans. Aeros. Electron. Syst.* **34**(3), 755–776 (1998).



Dust-Infused Baroclinic Cyclone Storm Clouds

M. Fromm, G. P. Kablick III, and P. Caffrey
Remote Sensing Division

Introduction: Desert mineral dust is a ubiquitous yet still poorly understood component of weather and climate. Long-distance transport of dust is an important process and forecast challenge, yet uncertainty persists regarding its pathway from the desert floor to the upper troposphere: how might dust affect visibility, clouds, and precipitation while it is flowing through weather systems? Our research shows that a recurring—yet previously unappreciated—scenario for dust transport into the upper troposphere involves passage through a synoptic-scale baroclinic cyclonic storm. The evidence comes from a synergistic use of satellite-based, multispectral nadir-image data and lidar. Our so-called dust-infused baroclinic storm (DIBS) exhibits peculiar cirrus cloud-top reflected and emitted radiance from the ultra-violet through thermal infrared.¹ From the satellite perspective, the DIBS cloud appears unlike regular storm-scale cirrus, which are pure white with a fibrous texture. The DIBS has muted visible reflectivity (and even a dusty tinge), cellular texture, and systematically intense visible lidar backscatter on a storm scale. The DIBS is microphysically peculiar as well: standard multispectral infrared images indicate unusually small ice crystals on the broad cloud top. Our research indicates that desert dust, lofted from the surface by strong cyclone winds, routinely flows up into the synoptic-scale storm cloud, gets infused into the cloud from cloud-base to top, and remains in the upper troposphere after the storm lifecycle is complete. This finding raises many questions about how the storm’s precipitation, intensity, and lifetime might be altered by the dust infusion.

Satellite Views: The DIBS was discovered thanks to a suite of satellite-based platforms and measurement types. Our example is from a synoptic-scale baroclinic cyclone in northeast Siberia on April 9, 2010. The key satellite measurement leading to the discovery of the peculiar DIBS is the ultra-violet absorbing aerosol index (UVAI). “Colorful” particles such as dust, ash, and smoke elicit a positive UVAI whereas meteorological cloud particles—which are pure white—elicit no UVAI. We find that the DIBS cirrus have a tangible color or gray shading, the same properties that create the positive UVAI. Because the satellite UVAI instruments cannot see through opaque clouds, the unusual positive UVAI pixels in a cloud-filled scene mean unequivocally that detectable amounts of dust aerosol have arrived at the top of the cloud. The meteorological implication is that dust permeates the cloud, having traced its path along with the rising air that is part and parcel of the storm’s dynamics.

Another special satellite-based viewing technique and data item for DIBS research is NASA’s Cloud-Aerosol Lidar with Orthogonal Polarization (CALIOP). The Siberian DIBS was directly underneath CALIOP’s beam at several points in the storm’s lifetime. We find that the dust-polluted DIBS cirrus gives off a stunningly peculiar backscatter, much more intense than garden-variety synoptic-scale storm clouds. Not only is the cloud-top backscatter unusually intense but CALIOP’s lidar beam also completely attenuates in a very short distance (about 2 kilometers) below cloud top as compared to regular storm cirrus, because DIBS ice crystals are uniformly very small and highly concentrated vis-à-vis normal meteorological storm clouds. Hence, the dust particles have a microphysical impact on the storm. Figure 4 illustrates the above-discussed qualities of the Siberian DIBS example.

Another pattern that we see in DIBS views from space is a cellular texture that bears similarity to another cloud form, the low-altitude marine stratocumulus (Sc). The liquid-water Sc is well known and intensely studied. However, the DIBS cousin of this cumuliform cloud is new to our understanding; normal cyclone storm cirrus texture is streaky and fibrous. We now know that the DIBS cellular texture is a reliable marker of this peculiar dust-polluted storm throughout its lifetime. Figure 5 shows a comparison of a marine Sc, DIBS, and regular cyclone cirrus.

Modeling a Dust-Infused Baroclinic Storm:

To best understand the peculiar satellite signals, we employ the Weather Research and Forecasting model coupled with Chemistry (WRF-Chem) model. This regional grid-point model provides full meteorological rendering and coupling with erodible dust sources. Hence, we can follow the movement of desert dust for

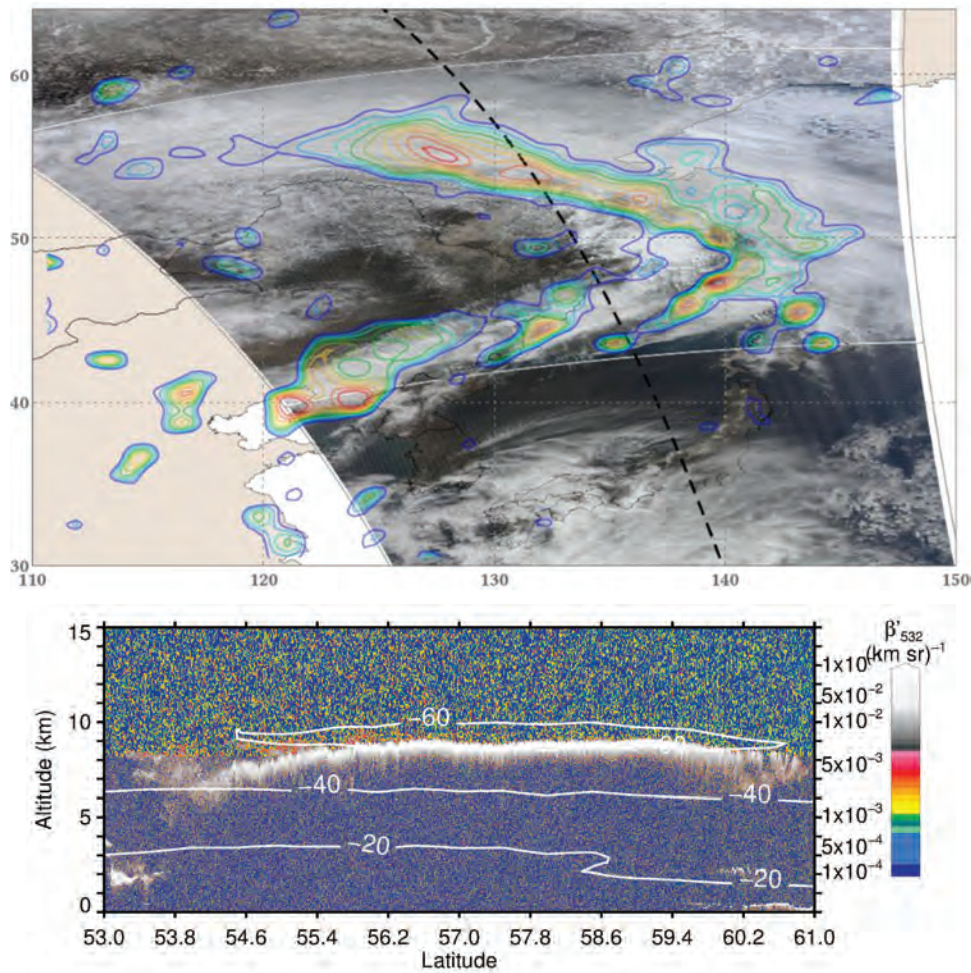


FIGURE 4
 Top: Moderate-resolution imaging spectroradiometer (MODIS) true-color image of dust-infused baroclinic storm (DIBS) cirrus with Global Ozone Monitoring Experiment-2 Absorbing Aerosol Index (colored contours), taken April 9, 2010. Dashed line shows overpass of NASA's Cloud-Aerosol Lidar with Orthogonal Polarization (CALIOP) through the storm at 04 UTC. Bottom: CALIOP backscatter profile through the DIBS showing intense backscatter at altitude of 9 kilometers.

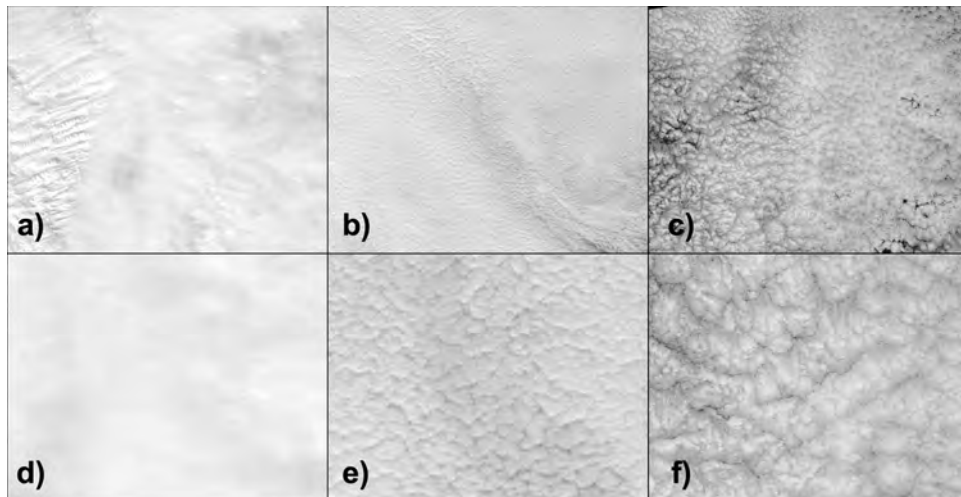


FIGURE 5
 Top row: MODIS images of (a) non-DIBS cirrus, (b) DIBS cirrus, and (c) marine stratocumulus (c). Each panel area is 550 x 425 km. The cellular texture in the presence of large amounts of desert dust (b) appears similar to marine stratocumulus formation in (c). Bottom row: zoomed to 138 x 106 km². The diameter of the DIBS cells (e) is estimated at ~10 km, while the marine stratocumulus (f) cell diameter is ~20 km. There is no cellular structure in the non-DIBS cirrus (a, d).

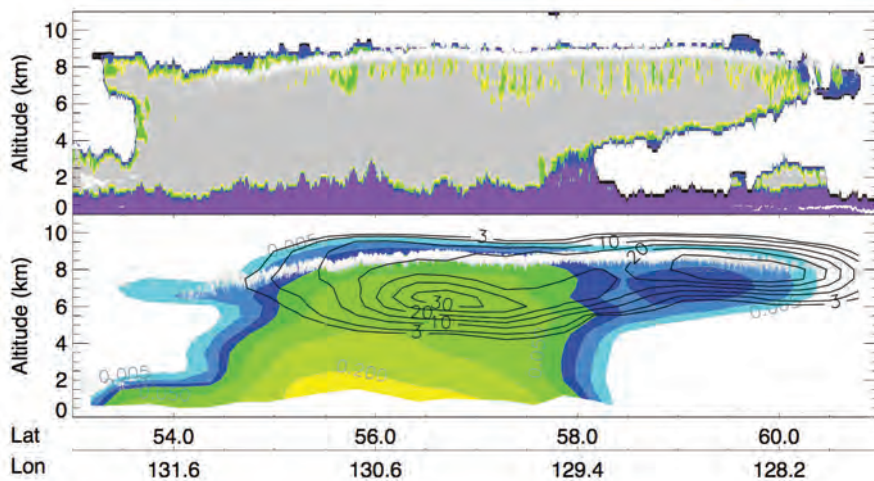


FIGURE 6
WRF-Chem simulation (bottom panel) of DIBS cloud water content (color shade), lidar backscatter (white layer), and dust concentration (black contours) along the slice shown in Fig. 4. Top: Corresponding satellite-based lidar backscatter (white) and radar-derived cloud type (color shade).

the weather conditions of the above-discussed Siberian DIBS. When the simulated storm formed on or about April 7, 2010, WRF-Chem showed that surface winds over erodible portions of the Gobi Desert were strong enough to generate a significant flux of dust, which was then lofted in a pattern conforming to the DIBS cloud, both horizontally and vertically. Figure 6 shows the WRF-Chem rendering of cloud content and dust concentration along the vertical slice of the DIBS observed by satellite-based radar and CALIOP on April 9, 2010 (Fig. 4). Hence, there is great consistency between what we infer from the incomplete satellite views of the DIBS cloud and a realistic four-dimensional simulation of the dust-polluted storm. In particular, we see considerable dust concentrations all the way to the cloud top, where satellites excel at capturing this new cloud formation.

[Sponsored by ONR]

Reference

¹M.D. Fromm, G.P. Kablick III, and P. Caffrey, "Dust-Infused Baroclinic Cyclone Storm Clouds: The Evidence, Meteorology, and Some Implications," *Geophys. Res. Lett.* **43**(24), 12,643–12,650 (2016). doi:10.1002/2016GL071801.



A Multi-Channel Testbed for Next-Generation Maritime SAR Systems

M.A. Sletten,¹ J. Jakabosky,² T. Higgins,² and R. Jansen¹

¹Remote Sensing Division

²Radar Division

Introduction: Researchers in the Remote Sensing and Radar divisions at the U.S. Naval Research Laboratory (NRL) have developed a multichannel synthetic aperture radar (MSAR) that serves as a unique testbed for next-generation maritime imaging systems. The MSAR's multiple phase centers (PHCs) provide the

ability to measure the complicated target and surface motions that characterize the maritime environment along with the means to correct, from first principles, the severe image distortions these motions can induce. The system supports multiple PHCs by using two simultaneous transmit channels and four simultaneous receive channels. The system antennas are also reconfigurable to support PHC displacement along the flight axis (the along-track direction), which provides the ability to measure scene motion, and perpendicular to the flight direction (the cross-track direction), which provides sensitivity to scene elevation. This paper describes the MSAR hardware and presents results that illustrate the system's capabilities, including distortion correction and measurement of ocean wave velocity and height.

Multichannel Synthetic Aperture Radar Hardware:

The NRL MSAR is an X-band system with a center frequency of 9.875 GHz and a bandwidth of 220 MHz. A two-channel Tektronix 70002 arbitrary waveform generator produces the desired transmit waveforms directly at X-band, which then drive separate 4 kW traveling wave tube amplifiers and horn antennas. On the receive side, the outputs from four receive channels are downconverted to an intermediate frequency of 1.375 GHz and then bandpass-sampled at 500 MHz by a 4-channel data recorder. The system also features a Litton LN200 Inertial Measurement Unit coupled with a GPS receiver for precise measurement of the antenna positions during flight. The entire system is deployed on a twin-engine Saab 340 aircraft outfitted with a custom belly-mounted radome.

Owing to a flexible mounting system in the radome, a number of different antenna configurations are available. In 2014 and 2015, an array of 16 printed circuit board antennas was used for receiving while two horn antennas were used for transmitting. Figure 7(a) shows this configuration, in which the receive ele-

ments are enclosed within the white boxes beneath the transmit horns. The white boxes also contain fast microwave switches that route the signals collected by the antennas to the receiver, four antennas at a time. Over the course of eight transmit pulses, the system uses all 32 combinations of transmit and receive antennas to collect data. Each combination of transmit and receive antennas produces an independent PHC, resulting in a linear array of 32 PHCs approximately 2 meters long. As described in Sletten et al. (2016),¹ this arrangement produces 32 SAR images from which detailed scene motion at each pixel can be extracted.

In 2016, data were collected using a combined along-track/cross-track configuration that consisted of two vertically-displaced transmit horns and a row of four receive horns (Fig. 7(b)). This configuration produces eight PHCs arranged in two rows of four, stacked vertically. While the along-track displacement again provides the ability to measure motion, the cross-track PHCs allow simultaneous measurement of wave height. The combination of these two measurements is particularly useful in the maritime environment.

Example Data: As first demonstrated in Sletten (2013),² data collected by SAR systems supporting

multiple along-track antennas can be manipulated to estimate detailed motion within the scene and correct image distortion induced by the motion itself. In essence, an MSAR of this type allows Doppler radar analysis at each and every pixel within the image. After estimation of the Doppler velocity spectrum, scene-motion-induced artefacts can be automatically removed from the imagery. This technique is referred to as velocity SAR (VSAR) and is particularly useful with maritime imagery, in which the entire scene is subject to the complicated motion of surface waves. Figure 8 illustrates VSAR-based distortion correction using a scene that features shoaling waves along the Atlantic coast of the United States. The data shown in Fig. 8 were collected in 2015 by using the 32-phase-center configuration of the NRL MSAR. In the figure, the shoaling wave signatures are the bright streaks near the shore, and are elongated in the along-track (or azimuth) direction in the standard SAR image (Fig. 8(a)) because of their significant velocity and acceleration towards the radar. The standard SAR processing used to generate this image cannot distinguish between this motion and the motion of the aircraft, resulting in the elongated smear. Figure 8(b) shows the image after VSAR-based correction for scene motion. VSAR

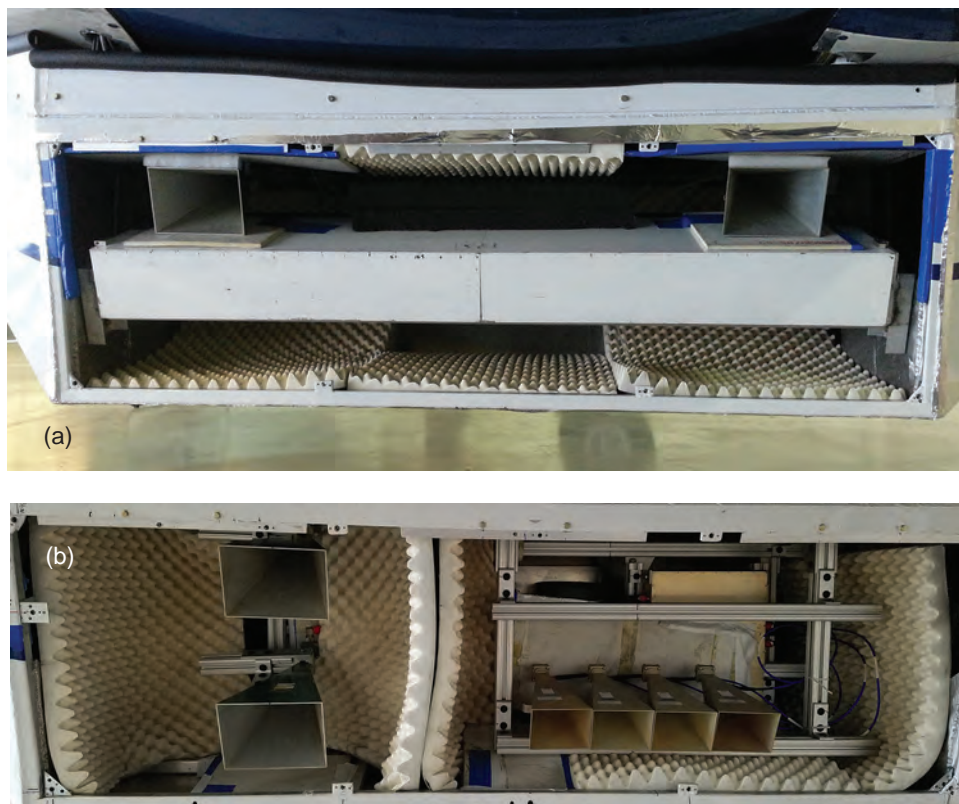


FIGURE 7 Radome interior of the U.S. Naval Research Laboratory multichannel synthetic aperture radar (MSAR) with antennas in the (a) 32 phase center (PHC) along-track configuration, and (b) 8 PHC combined along-track/cross-track configuration.

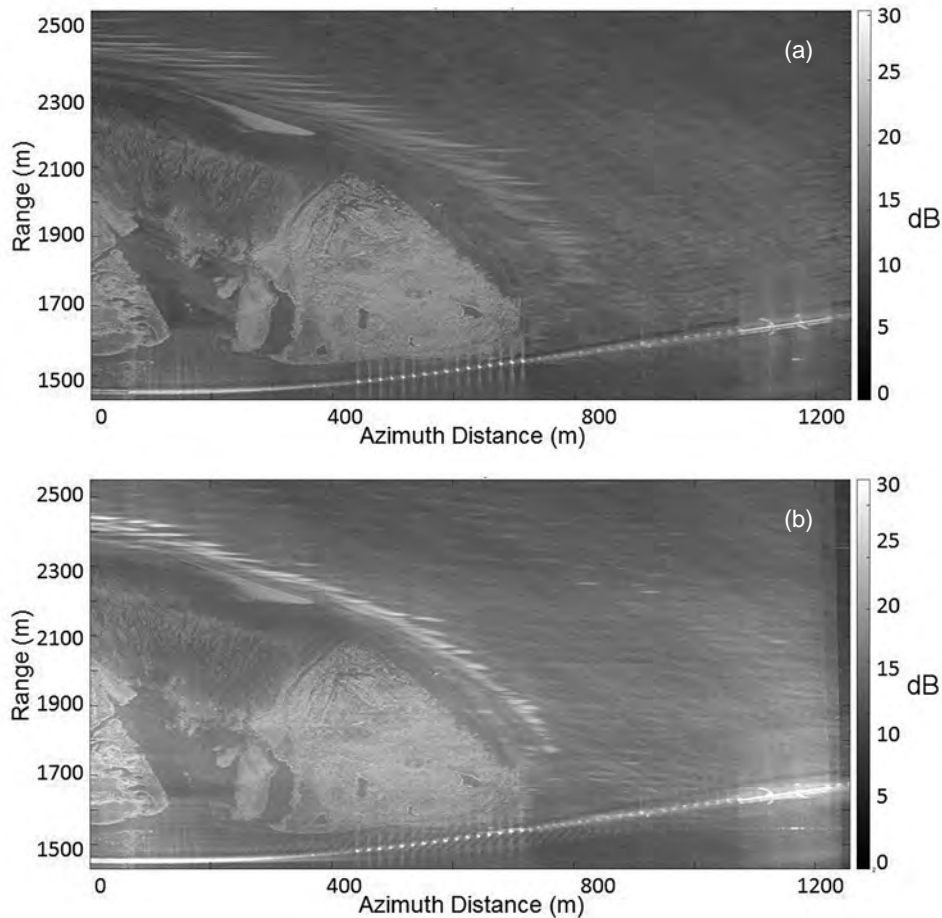


FIGURE 8
NRL MSAR images of shoaling waves along the North Carolina coast: a) standard synthetic aperture radar (SAR) image and b) Standard SAR image after correction using velocity SAR.

corrects the wave signatures by reversing the along-track distortion, thereby compressing the signatures to a size much more representative of the true size of the shoaling waves. VSAR has also been shown to correct the even more complicated distortion suffered by vessel signatures.^{1,2}

Figure 9 shows wave velocity and height maps generated from data collected using the combined along-track/cross-track antenna configuration (shown in Fig. 7(b)). Figure 9(a) displays the magnitude image; Figs. 9(b) and 9(c) show the corresponding velocity and height estimates, computed interferometrically.³ The scene is centered on a research pier on the Atlantic Coast, and waves propagating towards shore can be seen in the top half of the image. While the wave velocity and land topography measurements are within expected ranges, the wave height measurements in Fig. 9(c) are unrealistically high (mean value approximately 4 meters). Future work will investigate whether this error stems from the image distortion caused by the wave motion and, therefore, whether it can be reduced

through VSAR correction of the imagery before interferometric estimation of the wave height.

[Sponsored by the NRL Base Program (CNR funded)]

References

- ¹ M.A. Sletten, L. Rosenberg, S. Menk, J.V. Toporkov, and R. W. Jansen, "Maritime Signature Correction with the NRL Multichannel SAR," *IEEE Trans. Geosci. Rem. Sens.* **54**(11), 6783–6790 (2016).
- ² M.A. Sletten, "Demonstration of SAR Distortion Correction Using a Ground-Based Multichannel SAR Test Bed," *IEEE Trans. Geosci. Rem. Sens.* **51**(5), 3181–3190 (2013).
- ³ P.A. Rosen, S. Hensley, I.R. Joughin, F.K. Li, S.N. Madsen, E. Rodriguez, and R.M. Goldstein, "Synthetic Aperture Radar Interferometry," *Proc. IEEE* **88**(3), 333–382 (2000).

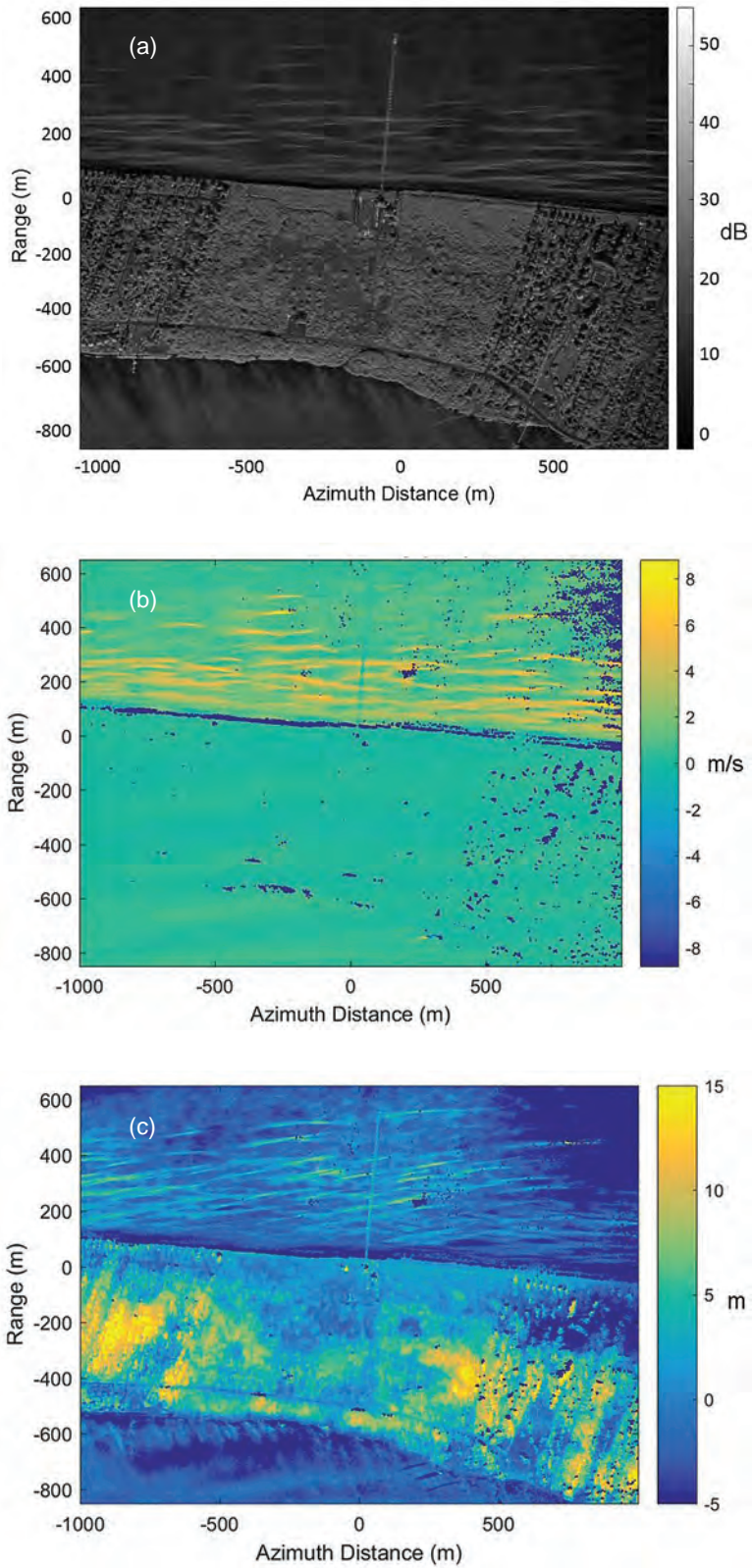


FIGURE 9 NRL MSAR images of shoaling waves near Duck, North Carolina, collected using the combined along-track/cross-track configuration: a) magnitude image, b) surface velocity image, and c) surface height image.



198 Advances in Simulation Technologies to Reduce Noise from Supersonic Military Aircraft Jets

201 Kr Plasmas on the Z and the National Ignition Facilities

203 Supporting Weather Forecasters in Predicting and Monitoring Saharan Air Layer Dust Events that Impact the Greater Caribbean

205 Reactive Flow Modeling for Hypersonic Flight

Advances in Simulation Technologies to Reduce Noise from Supersonic Military Aircraft Jets

K. Kailasanath, A. Corrigan, J. Liu, R. Ramamurti, K. Viswanath, and R. Johnson
Laboratories for Computational Physics and Fluid Dynamics

Background: The noise generated during take-off and landing on aircraft carriers has direct impact on shipboard health and safety issues. Also, noise complaints are increasing as communities move closer to military bases or when there are changes due to base closures and realignment. Therefore, there is a growing need to reduce significantly the noise generated by high performance, supersonic military aircraft. Thanks to environmental regulatory publications, there is a significant amount of literature dealing with noise reduction in civilian, subsonic aircrafts; published research on noise from supersonic military aircraft is less extensive.

The cost of field testing and evaluating various noise reduction concepts by a cut-and-try method is extremely time-consuming and expensive. Numerical simulations can significantly reduce the overall time and cost by evaluating various promising concepts and selecting a few for final field-testing, but for the results of these simulations to be credible, they first need to be compared and evaluated against relevant experimental data. These simulation conditions should include geometries and flow conditions representative of realistic engine configurations and operating conditions.

Over the past decade, the Laboratories for Computational Physics and Fluid Dynamics (LCP&FD) at the U.S. Naval Research Laboratory (NRL) has been developing numerous computational techniques and applying them to solve jet noise problems of increasing complexity. We succeeded in evaluating a noise reduction concept for the Navy's F/A-18 Aircraft, and we have turned our work now to simulating and understanding the flow field and noise from potential future jet exhaust nozzle configurations. In this article, we present progress to date on this research effort.

JENRE: The NRL Jet Noise Simulation Tool: Our primary research tool is the code JENRE (Jet Engine Noise Reduction), developed at NRL for the computational study of supersonic noise reduction. The JENRE code has been shown to be able to accurately and efficiently simulate the supersonic flows and noise representative of military aircraft jets in the context of realistic military engine geometry and operating conditions and with attention to complex and intricate flow features such as shocks, turbulence, and acoustics. The JENRE software can handle progressively complex sets

of jet noise problems, because it is capable of continual and systematic improvement and validation. With such capability, we can study noise generated by a range of sources, including conventional circular nozzles, military-style converging-diverging nozzles, nozzles with chevrons, fluidic nozzles, fluidically-enhanced chevrons, nozzles with pylons, multi-stream configurations, non-circular nozzles, and rectangular nozzles integrated to airframe surfaces. The flow conditions include not only the design condition with perfect or ideal expansion of the flow field but also non-ideal (under and over) expansion and jet exhaust temperatures ranging from room temperature (typical of laboratory experimental conditions) to representative afterburner conditions (practical ship-board operations).

JENRE implements a discretization of the compressible Navier-Stokes equations using the finite element method. The finite element method is implemented using linear elements, allowing for full second-order accuracy on unstructured tetrahedral grids. Tetrahedral grid generation is a mature technology, and this capability therefore alleviates the burden of generating semi-structured/hexahedral grids, as is often preferred by codes based on the finite volume method due to the limited accuracy of the finite volume method on unstructured grids. Shocks occur in the simulated flow at realistic operating conditions, and, therefore, JENRE implements the robust finite-element flux-corrected transport method in order to stably and accurately resolve such arduous flow features on fully unstructured grids. Time integration is performed on a second-order Taylor-Galerkin time discretization. JENRE is fast, achieving a five-fold increase in performance over its predecessor, FEFLO, which was used in early jet noise studies performed by NRL. JENRE is parallelized and scales well on standard distributed-memory parallel computing systems using message passing interface. JENRE is routinely run on thousands of cores, and scalability has been observed up to tens of thousands of central processing unit (CPU) cores. JENRE also supports shared-memory CPU and graphics processing unit (GPU) parallelism via such application programming interfaces as OpenMP (Open Multi-Processing), Thread Building Blocks, and CUDA. On GPU clusters, an additional two-fold increase in computational performance has been observed, giving us an order-of-magnitude in performance over our legacy code and meeting one of the key objectives of developing this code.

Simulations of Supersonic Jet Nozzle Flows: A key validation problem¹ was to simulate and compare with experimental data on the flow field and noise from a representative supersonic engine exhaust nozzle (Fig. 1). Sound pressure level (SPL) spectra at various locations in the exhaust flow were calculated and compared

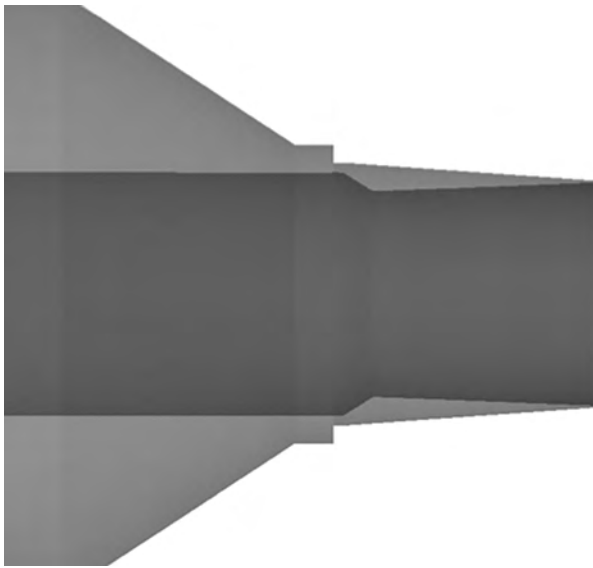


FIGURE 1
The basic nozzle geometry used in the simulations.

with the experimental measurements at the University of Cincinnati (Fig. 2); they showed very good agreement. Then attention was shifted to more complex configurations, since, in practice, the engine is attached to the aircraft using pylons, and this may interfere with the flow field and noise emanating from the jet exhaust. The geometry chosen for this validation study was from NASA-Glenn, which already had experimental data. Figure 3 shows a representative flow field simulation and comparison to experimental particle image velocimetry data. Further details of the comparative study have been published in an archival journal article.² After this successful work in flow field and noise, with excellent agreement between numerical simulations and experimental measurements, work on evaluating specific noise-reduction concepts was begun.

Simulations of Noise-Reduction Concepts: We first showed that mechanical chevrons (protuberances from the edge of the nozzle) are effective in reducing the noise generated by supersonic jets but have undesired effects at high frequencies. Fluidic injection is an alternative and complementary concept. Hence, it was logical to combine both these techniques together to get an optimal combination called fluidically-enhanced chevrons. This concept was simulated, and results were compared to experimental data from the University of Cincinnati, as shown in Fig. 4. Numerical simulations were also carried out on noise during carrier-deck operation.³

Simulation of Future Configurations: After this successful step in the computations of various current jet exhaust configurations, work now has begun on

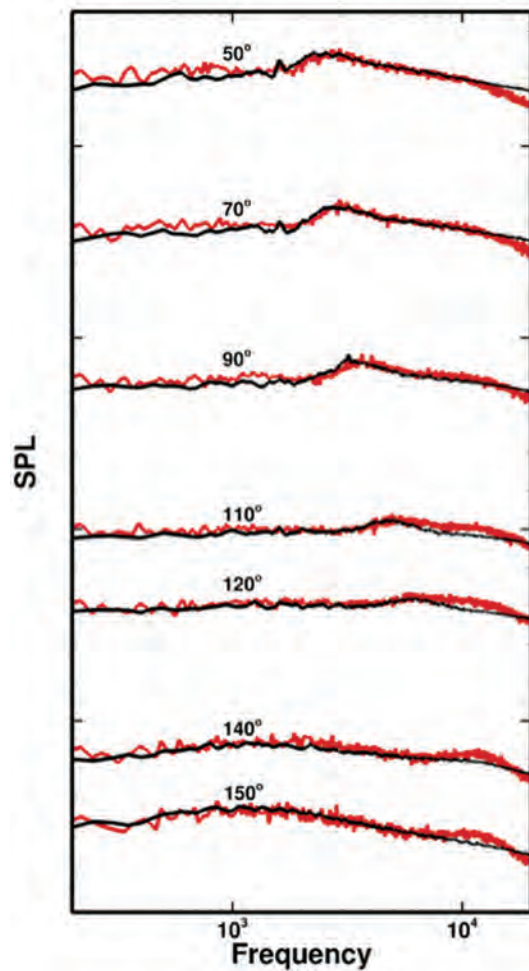


FIGURE 2
Comparison of the predicted far-field SPL with experimental data from the University of Cincinnati.

potential future configurations. Next generation military jets likely will have non-circular jet exhaust nozzle configurations. We are currently conducting simulations of rectangular jets with and without chevrons and comparing simulation results with experimental data.

Conclusions: Our simulations have described, accurately and efficiently, the flow field and noise from supersonic military aircraft jets. Speed and accuracy have enabled the effective use of the JENRE code to investigate potential noise reduction technologies in a cost-effective and timely manner. JENRE is key to our further research effort to develop and apply efficient and accurate computational tools to improve understanding of increasingly more complex jet noise physics. In current projects, we continue to build on these past accomplishments and ongoing work in the jet-noise scientific community to develop, demonstrate, and apply a general jet-noise-reduction Department of Navy simulation capability.

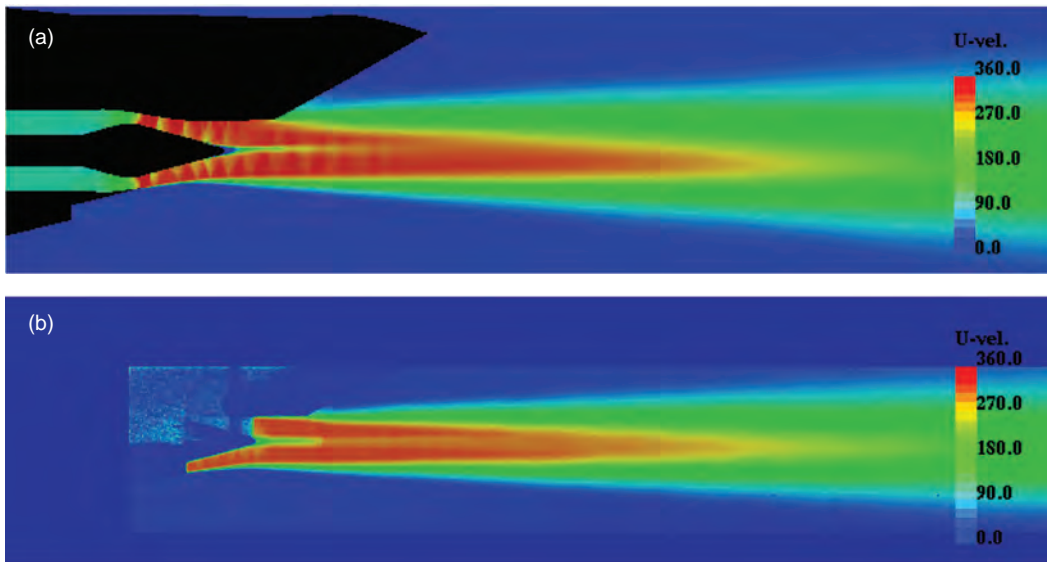


FIGURE 3 Time averaged velocity distribution along the plane of symmetry; (a) CFD and (b) PIV results.

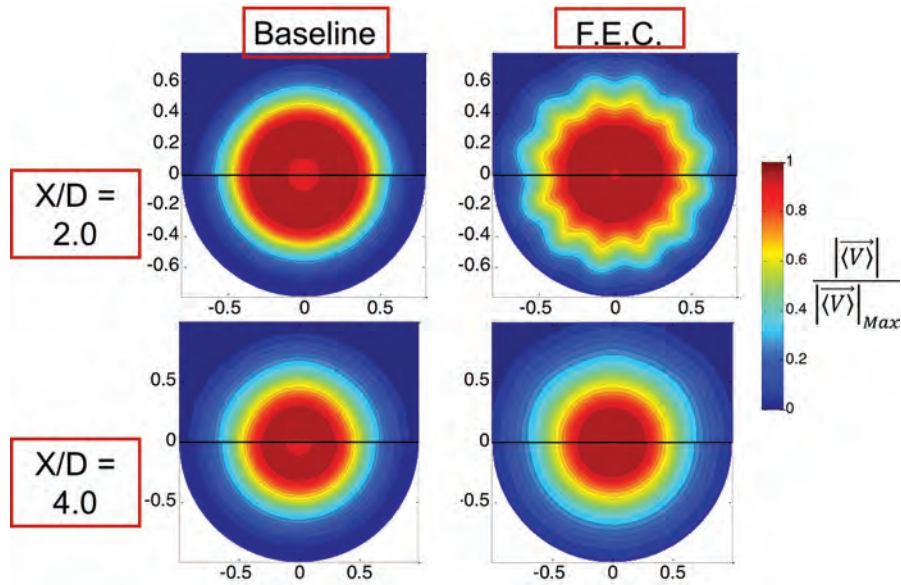


FIGURE 4 Comparison of computed data to PIV data for the case of an over-expanded supersonic jet. The upper half of each figure is computed data and the bottom half is experimental data from the University of Cincinnati.

Acknowledgments: Most of the experimental data used in the comparisons were obtained from the University of Cincinnati, and we gratefully acknowledge the efforts of N. Heeb and D. Munday under the leadership of E. Gutmark.

[Sponsored by the NRL Base Program (CNR funded) and ONR]

References

¹J. Liu, K. Kailasanath, R. Ramamurti, E. Munday, E. Gutmark, and R. Lohner, “Large-Eddy Simulation of a Supersonic Jet and Its Near-Field Acoustic Properties,” *AIAA J.* 47(8), 1849–1864 (2009).

²R. Ramamurti, A.T. Corrigan, J.H. Liu, K. Kailasanath, and B. Henderson, “Jet Noise Simulations of Complex Geometries,” *Inter. J. Aeroacoust.* 14(7), 947–975 (2015).

³J. Liu, A. Corrigan, K. Kailasanath, R. Ramamurti, N. Heeb, D. Munday, and E. Gutmark, “Impact of Deck and Jet Blast Deflector on the Flow and Acoustic Properties of an Imperfectly Expanded Supersonic Jet,” *Nav. Eng. J.* 127(3), 47–60 (2015).



Kr Plasmas on the Z and the National Ignition Facilities

A. Dasgupta,¹ R.W. Clark,² N.D. Ouart,¹ J.L. Giuliani¹

¹*Plasma Physics Division*

²*Berkeley Research Associates*

Introduction: High-energy X-ray radiation sources have a wide range of applications, from astrophysics and biomedical studies to research on thermonuclear fusion. These X-ray sources contribute to our basic understanding of radiation-matter interactions. In addition, tailored multi-keV high-flux X rays have useful applications for materials and component testing. Production of multi-keV photons with high radiative yield from various high-atomic-number elements is being pursued at many high energy density facilities, such as the Z machine at the Sandia National Laboratories and the flagship National Ignition Facility (NIF) at the Lawrence Livermore National Laboratory. On the Sandia National Laboratories Z machine, pulsed-power generated currents on wire arrays and gas puffs produce the X rays. On the NIF, X rays are generated by high-power laser using metallic foam, gas-filled pipe, and metal-lined cavity targets.

This article describes our work to understand the results of implosions and heating using krypton (Kr) as a plasma radiation source on both the Z machine and the NIF, respectively, and the probable causes that might explain the differences in X-ray conversion efficiencies (XRCE) of several radiation sources on the two facilities.

Kr Source Development: High fluence photon sources above 10 keV are a challenge for high energy density plasmas. This challenge has motivated radiation source development investigations of Kr with its K-shell energies around 13 keV. Recent pulsed power-driven gas-puff experiments on the Z machine have produced intense X rays in the multi-keV photon energy range. The radiative yield and XRCE fall off as the atomic number of the target species goes up, but the falloff for Kr on the Z accelerator is more severe than the reduction on the NIF, for which the drive, energy deposition process, and target dynamics are different. These differences are shown in Fig. 5. This figure compares both the yield (a) and the XRCE (b) for various species on Z at Sandia National Laboratories and on the NIF. Why is there such a rapid falloff in K-shell radiation for large atomic number in a z pinch compared to laser produced plasma? One of the reasons for the rapid falloff in z pinch K-shell radiation could be related to the electron heating mechanism, in which the ions become very hot through stagnation and eventually heat the electrons through equilibration. In a laser-heated

plasma as produced on the NIF, on the other hand, the electrons can be heated directly to a very high temperature by the various absorption processes.

Our theoretical investigation at the U.S. Naval Research Laboratory (NRL) focuses on the interpretation and analysis of X-ray emission from two contrasting high-temperature, high energy density laboratory plasmas: (a) the Sandia National Laboratories z pinch, which produces an imploded and stagnated plasma, and (b) the NIF, which produces a laser-heated target plasma. Understanding the atomic physics and radiative characteristics of these plasmas can lead to significant advances in their production and evolution.

Non-Local Thermodynamic Equilibrium

Kinetics Modeling: Our theoretical non-local thermodynamic equilibrium (non-LTE) model includes all atomic processes that significantly affect ionization balance and spectra of Kr plasmas at the temperatures and densities of concern. The model combines ionization physics, the radiation field, and one-dimensional radiation hydrodynamic. The model encompasses detailed atomic structure, including many singly and doubly excited levels and collisional and radiative coupling among all levels and a full multifrequency radiation transport method that resolves each emission line into about 20 frequencies for the simulations. Our hydrodynamic simulations using the 1-D radiation hydrodynamics code was developed primarily for the simulation of z-pinch implosions. We obtained detailed K- and L-shell spectra that match the experimental spectra from z pinch implosions fairly well, although, in this paper, we present only L-shell spectra for shot Z 2383 (Fig. 6). 1-D DZAPP simulation agrees much better with Z data than a snapshot spectrum, as shown in Fig. 6.

Experiments on the NIF were conducted to demonstrate 13 keV Kr K-shell X rays by using thin-walled epoxy pipes filled with Kr gas. We compared time-integrated data of the Kr K-shell on the NIF using the SuperSnoot II (SS II) spectrometer with our simulation of the K-shell region with simple density and temperature profiles. The NIF data indicates a hot core surrounded by cooler and denser plasma. We employed a full non-LTE collisional-radiative equilibrium method for the application of our atomic model, as described above. Our objective was to match the NIF data in energy position and intensity with the given plasma conditions and our analysis was carried out using bright-spot spectra from post-processing the data. Figure 7 (right-hand side) shows a comparison of our simulated spectra with the SS II data from the NIF.

Summary: Multi-keV X-ray sources are produced by pulsed powered driven z pinches at the Sandia National Laboratories Z machine and also by high power

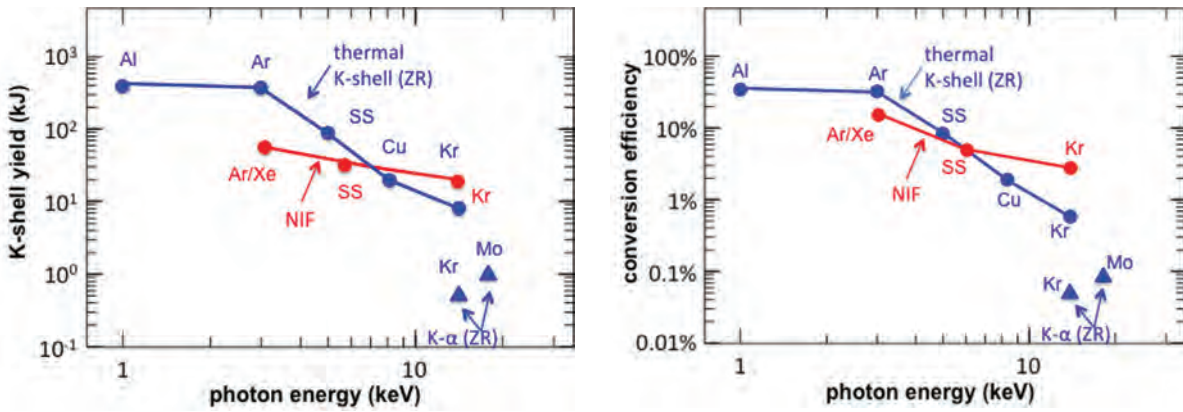


FIGURE 5 Left: K-shell yield for various elements on the Sandia National Laboratories Z machine (blue) and on National Ignitions Facility (red). Right: X-ray conversion efficiencies for various elements on the Sandia National Laboratories Z machine (blue) and on the National Ignitions Facility (red). The data marked with triangles on the lower right hand corners were electron beam generated.

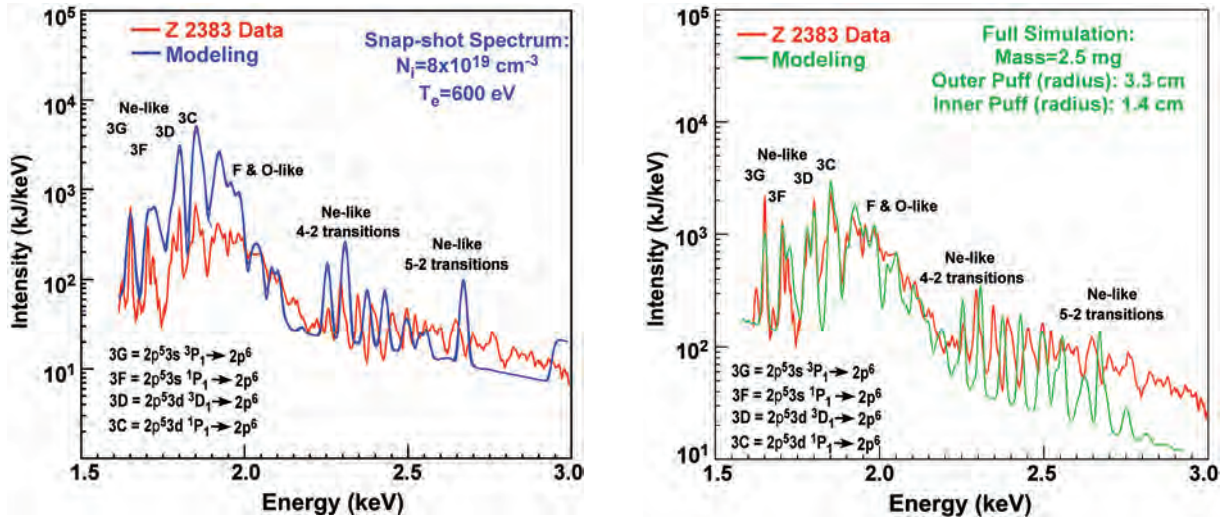


FIGURE 6 Left: Snapshot simulation of L-shell Kr spectra compared to Z-2383 data. Right: Time-integrated 1-D DZAPP simulation of Kr L-shell spectra compared to Z-2383 data. Only some of the strong lines are identified.

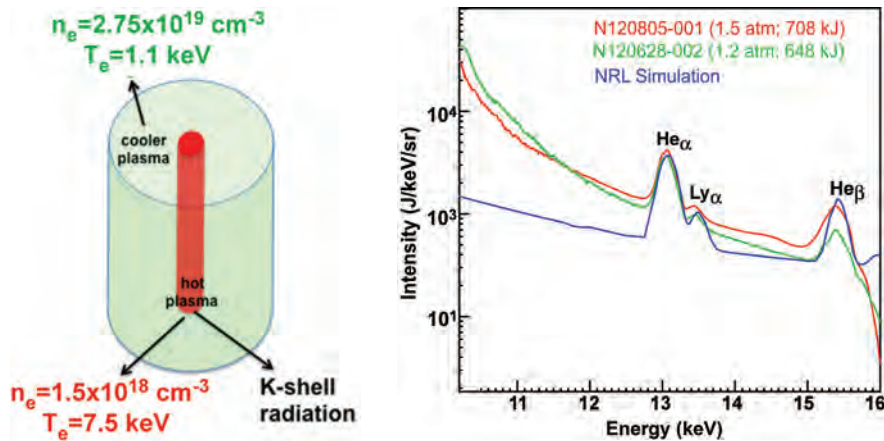


FIGURE 7 Left: Diagram of a hot plasma surrounded by a cooler plasma. These plasma parameters were used to generate the spectrum (NRL simulation) on the right. Right: Kr K-shell simulation compared to the National Ignitions Facility Super Snout spectra.

laser at the NIF. These radiation sources are used to test components and enhance the overall stewardship of the U.S. nuclear deterrent. This theoretical investigation by NRL contributes to improved understanding and performance of both z pinches and laser produced X-ray sources.

Acknowledgment: The work presented here is part of a larger program on plasma radiation source development involving many scientists from NRL, the Sandia National Laboratories, and the Lawrence Livermore National Laboratory.

[Sponsored by DOE/NNSA]

References

- ¹ A. Dasgupta, R.W. Clark, N. Ouart, J. Giuliani, A. Velikovich, D.J. Ampleford, S.B. Hansen, C. Jennings, A.J. Harvey-Thompson, B. Jones, T.M. Flanagan, K.S. Bell, J.P. Apruzese, K.B. Fournier, H.A. Scott, M.J. May, M.A. Barrios, J.D. Colvin, and G.E. Kemp, "A Non-LTE Analysis of High Energy Density Kr Plasmas on Z and NIF," *Phys. Plasmas, Special Issue* **23**, 101208 (2016).
- ² C.A. Jennings, D.J. Ampleford, D.C. Lamppa, S.B. Hansen, B. Jones, A.J. Harvey-Thompson, M. Jobe, T. Strizic, J. Reneker, G.A. Rochau, and M.E. Cuneo, "Computational Modeling of Krypton Gas Puffs with Tailored Mass Density Profiles on Z," *Phys. Plasmas* **22**, 056316 (2015).
- ³ K.B. Fournier, M.J. May, J.D. Colvin, M.A. Barrios, J.R. Patterson, and S.P. Regan, "Demonstration of a 13-keV Kr K-shell X-ray Source at the National Ignition Facility," *Phys. Rev. E* **88**, 033104 (2013).



Supporting Weather Forecasters in Predicting and Monitoring Saharan Air Layer Dust Events that Impact the Greater Caribbean

A.P. Kuciauskas,¹ P. Xian,¹ E.J. Hyer,¹ M.I. Oyola,² and J.R. Campbell¹

¹*Marine Meteorology Division*

²*American Society for Engineering Education*

The U.S. Naval Research Laboratory's Marine Meteorology Division (NRL-MMD) in Monterey, California, is in the final phase of a two-year project (funded by the National Oceanic and Atmospheric Administration) that provides environmental resources in monitoring and predicting African dust embedded in the Saharan Air Layer (SAL), an elevated air mass that passes across the greater Caribbean area. The primary consumer of these resources is the National Weather Service in San Juan, Puerto Rico (NWS-PR), and outreach also extends toward other local agencies, such as the Caribbean Institute for Meteorology and Hydrology, based in Barbados, West Indies. The overarching

goal is to protect the public from unhealthy respiratory conditions associated with the dust events; Puerto Rico currently suffers from historically high asthma rates.¹ Additional beneficiaries from this effort include global-wide human health services and maritime and airline operators who rely on accurate air quality and visibility reports.

Specifically, NRL-MMD provides NWS-PR with a publically accessible web-based platform (called SAL-WEB) that is designed to monitor these African dust events. SAL-WEB consists of satellite imagery, in situ air quality measurements, and model fields related to aerosol concentrations, covering the extent of dust from North African, westward across the Atlantic basin, and extending into Mexico. The products in SAL-WEB serve to augment the Advanced Weather Interactive Processing System-II (AWIPS-II) infrastructure currently in operation at the NWS-PR. A standard product suite available to NWS forecasters, AWIPS-II has not been optimized for SAL transport and regional observation.

Figure 8 presents a generalized two-dimensional isentropic depiction of SAL air mass transport characteristics. Viewing from right to left (East to West), the first panel depicts the initialization of the SAL over northeastern Africa (Sahel and Sahara regions t_{initial}) with strong intense desert heating at the surface that generates strong sensible heat, associated turbulent flux, and convection at the surface. Surface dust is often scoured by strong winds and then lifted upward to heights reaching 500 hPa. As the SAL eventually propagates westward across northwestern Africa and into the Atlantic basin, the SAL air mass follows the levels of constant air density (i.e., isentropic surfaces). Its base becomes decoupled from the surface; just offshore, the vertical layer extends between 850 and 500 hPa. The leading portion of the SAL layer typically takes 6–7 days to travel from the African coast to Barbados, where the water vapor mixing ratio is conserved at very dry values (~5–10%) and the descent rate of the layer is estimated at 7 hPa per day. The associated dust throughout the SAL airstream is maintained and well mixed in the vertical as a result of weak turbulent mixing. By the time the leading edge of the SAL layer reaches the Caribbean ($t_{+7 \text{ days}}$), the lower portion of the SAL layer often penetrates well into the marine boundary layer. At this time, much of the dust is impacting the surface.

Figures 9 and 10 present an overview of how the SAL-WEB can facilitate NWS-PR operations. Figure 9 is a series of image panels captured between June 23 and June 28, 2014; they track the leading edge of the SAL-related dust plume (yellow dashed lines) from its source in northwestern Africa (0623: 23 June) throughout the north tropical Atlantic basin and eventually into the Gulf of Mexico. Of operational interest are the

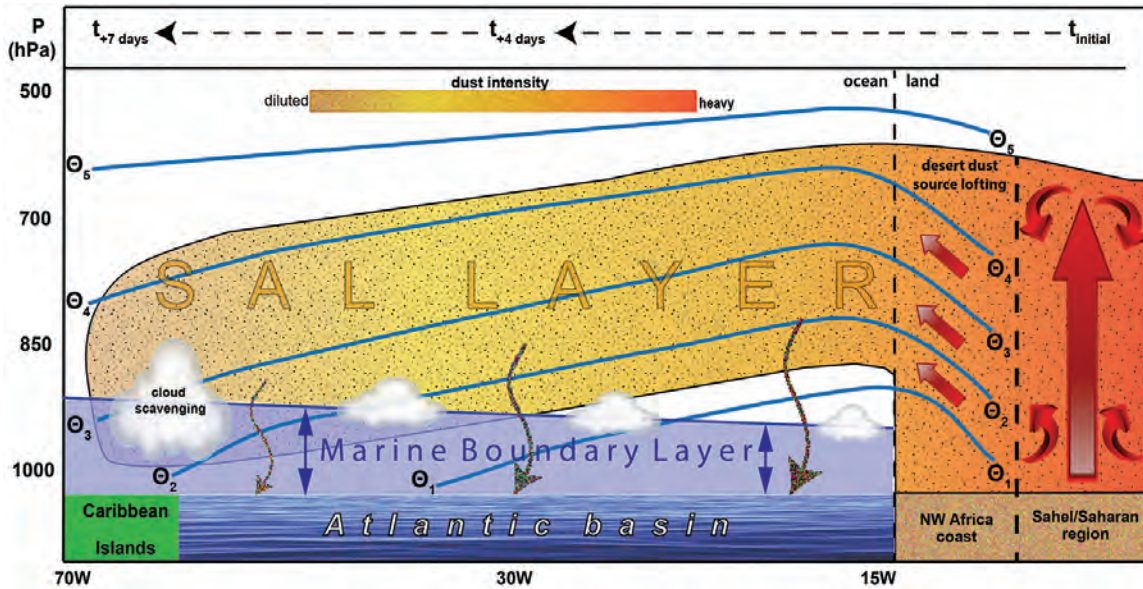


FIGURE 8 Vertical profile of the Saharan Air Layer (SAL) air mass as it is transported via convection and turbulent mixing from its hot desert source (right-hand side: Sahel/Saharan region) westward to the northwestern Africa coast, across the north tropical Atlantic basin, and finally through the Caribbean Islands. The color shading within the SAL layer represents the transition from coarse and large dust particles (red shades) to finer and more diffuse particles further west (yellow shades). The vertical brown curved arrows depict larger dust particles settling to the surface. Isentropic contours are annotated in blue, with associated theta labels. The marine boundary layer is shown sloping upwards from East to West.

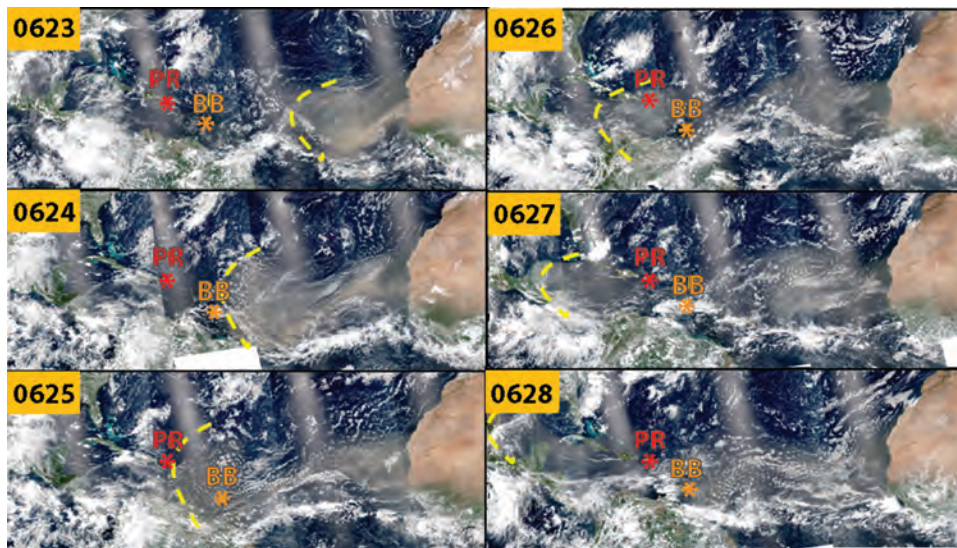


FIGURE 9 True-color products, derived from Visible Infrared Imaging Radiometer Suite, provide a daily sequential look (June 23–28, 2014) at the SAL event propagating from northwestern Africa westward to the greater Caribbean. The bold dashed yellow arcs depict the leading edge of the SAL. PR and BB locate the positions of Puerto Rico and Barbados, respectively. For each panel, the linear NNW/SSE oriented features of enhanced radiance across the open water represent sun glint.

approaching and passing of the leading dust edge over Barbados (BB: 0624) and Puerto Rico (PR: 0625). Figure 10 shows a model output comparison between the current operational version of the Navy Aerosol Analysis and Prediction System (NAAPS, upper left-hand panel) with a research testbed version (upper right-hand panel) that includes the addition of the data from

the Visible Infrared Imaging Radiometer Suite (VIIRS) on the Suomi National Polar-orbiting Partnership satellite. The ground-based aerosol measurements within the Aerosol Robotic Network radiometric profile of aerosol-induced solar transmission² at La Parguera, Puerto Rico (bottom panel), demonstrate how model results are improved by including the VIIRS data.

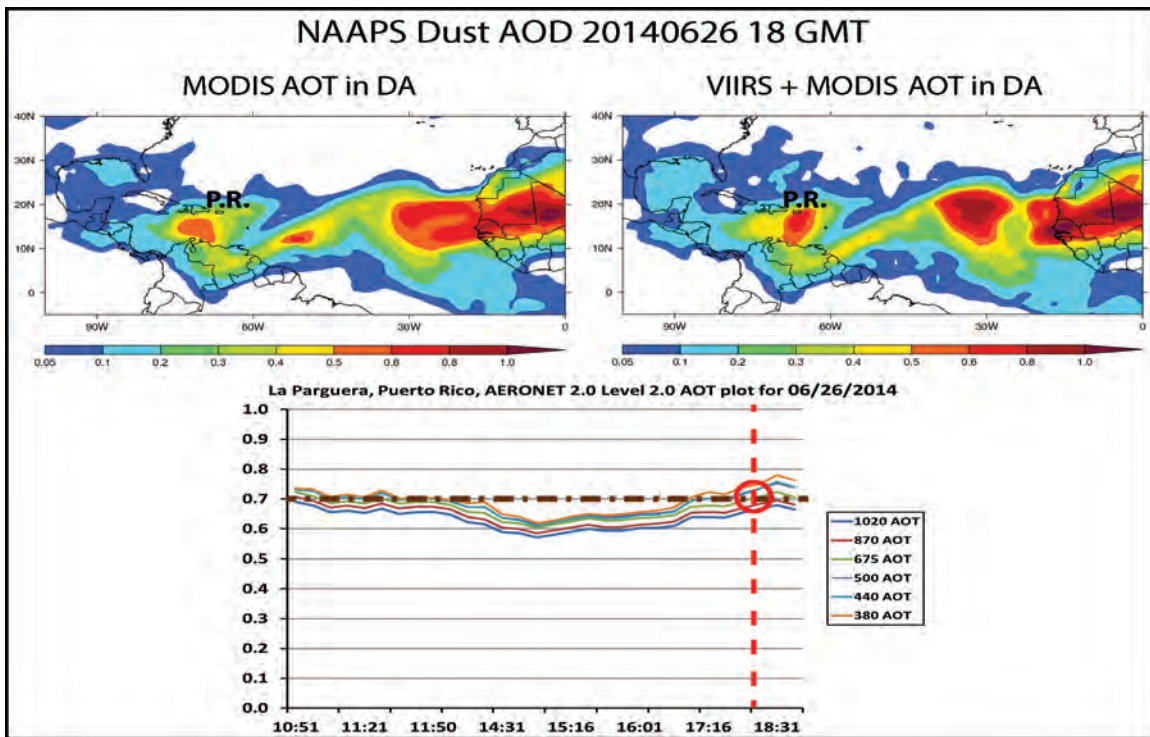


FIGURE 10

Comparing Navy Aerosol Analysis and Prediction System (NAAPS) with the data assimilation (DA) from the Moderate Resolution Imaging Spectroradiometer (MODIS) Aerosol Optical Thickness (AOT*) (upper left-hand) versus the NAAPS MODIS + VIIRS AOT (upper right-hand) on June 26, 2014, where P.R. represents Puerto Rico. The lower panel is the Aerosol Robotic Network (AERONET) AOT plot over La Parguera in southwestern Puerto Rico. The vertical red dashed line indicates the corresponding time (18 GMT) with the model outputs. (*Within the figure, aerosol optical depth (AOD) and aerosol optical thickness (AOT) are used interchangeably.)

This project was motivated in part during discussions at a symposium on airborne dust and its impacts on human health, May 19–21, 2015, in Miami,³ and on how both scientific and health communities can better combine and coordinate efforts in studying SAL impacts on human health. The overarching goal is to better educate and prepare the Caribbean populace in mitigating exposure to SAL's harmful dusty environment. Current and near-term plans for NRL-MMD include ongoing interactions with NWS-PR, the Caribbean Institute for Meteorology and Hydrology, and Caribbean Aerosol–Health Network agencies to share environmental resources, with the goal of hosting a more comprehensive set of SAL-related sensing products into SAL-WEB. The website is publically accessible; public feedback is encouraged via the SAL-WEB [<http://www.nrlmry.navy.mil/SAL.html>] feedback tab. [Sponsored by NOAA]

References

- ¹ L. Akinbami and J. E. Moorman, “Asthma Prevalence, Health Care Use, and Mortality: United States, 2005–2009,” *Natl. Health Stat. Rep.* **32**, 1–14 (2011).
- ² B.N. Holben, T.F. Eck, I. Slutsker, D. Tanrés, J.P. Buis, A. Setzer, E. Vermote, J.A. Reagan, Y.J. Kaufman, F. Lavenue, I. Jankowiak, and A. Smirnov, “AERONET—A Federated Instrument Network

and Data Archive for Aerosol Characterization,” *Remote Sens. Environ.* **66**(1), 1–16 (1998).

- ³ J. Prospero and H. Diaz, “The Impact of African Dust on Air Quality in the Caribbean Basin,” *Eos* **97** (2016).



Reactive Flow Modeling for Hypersonic Flight

G.B. Goodwin¹ and E.S. Oran²

¹*Space Engineering Department*

²*The University of Maryland*

Introduction: High-speed fluid dynamics is the study of fluid flow in the supersonic or hypersonic regimes, in which hypersonic typically refers to flow speeds of five times the speed of sound or greater. Reactive flows may consist of chemically reacting species undergoing processes such as combustion, molecular dissociation, or ionization. Examples of high-speed reactive flows in the context of defense applications include the combustion of fuel and air in supersonic combustion ramjet (scramjet) engines and detona-

tion of fuel-oxidizer mixtures in detonation engines. Airbreathing propulsion systems use oxygen from the atmosphere for combustion as opposed to rocket engines that must carry oxidizer onboard. Vehicles using airbreathing engines benefit from decreased fuel-mass and increased payload capacity. In the context of Department of Defense interests, airbreathing engines may be used to power extended range cruise missiles, deliver payload to low Earth orbit with single-stage-to-orbit vehicles, and rapidly deploy personnel and materiel across the globe via hypersonic transports.¹ Combustion stability in hypersonic airbreathing engines has been one of the predominant technical challenges in the design of a robust engine that is capable of operation across a wide range of altitudes and cruising speeds. For the Navy to develop these technologies for defense of the surface fleet, the ignition and combustion processes in the engines powering hypersonic vehicles must be fully understood.

In addition to experimentation in ground test facilities and flight tests of proof-of-concept vehicles, modeling and simulation are used to increase fundamental understanding of the high-speed reactive fluid dynamics encountered in hypersonic engines. Accurately simulating these flows is a challenge due to the small timescales of the macroscopic flow and the chemical reactions and the large length scales of engines. Simplified chemical models that effectively model the physical characteristics of the combustion and detonation processes are required to reduce the computational expense of the simulations to a threshold that is manageable using modern high performance computers. Despite these challenges, computational modeling allows researchers to resolve the physics of hypersonic propulsion systems at a high level of detail. This article presents results from a computational study of the acceleration of a turbulent flame and eventual transition of the flame to a detonation, in a thin chan-

nel filled with a highly reactive fuel-oxidizer mixture. The work was completed as part of a collaborative effort with the University of Maryland.

Shock-Focusing to Detonate Fuel-Oxidizer Mixtures: Pulse detonation engines and rotating detonation engines rely on the thrust generated by a detonation wave to propel a vehicle at supersonic and hypersonic speeds. To initiate the detonation wave, a spark is used to ignite a flame in a channel filled with a fuel-oxidizer mixture. Obstacles are placed in the igniter channel to perturb and accelerate the flame as it expands. The initially laminar flame accelerates to become a deflagration, or a turbulent flame traveling at a high subsonic speed. Eventually, the fuel-oxidizer mixture detonates. The deflagration-to-detonation transition (DDT) has been an active area of research for decades. In many cases, DDT must be prevented, such as in coal mines, but in others it must be controlled in time and space, such as in a detonation engine. The mechanism of DDT in a channel with obstacles, representative of the igniter in a detonation engine, was investigated computationally.^{2,3} The channel dimensions are 0.32 cm in height and 21 cm in length. Figure 11 shows temperature contour plots at six consecutive timesteps of the two-dimensional (2D) simulation, beginning with the initial condition of a laminar flame ignited by a weak spark. Expansion of the flame into the channel produces pressure waves that reflect from the obstacles and channel walls. The pressure waves act like a piston, pushing the unburned gas ahead of the flame over the obstacles. As the flame propagates into the channel, it interacts with the reflected pressure waves and vortices shed from the obstacles. These interactions cause the flame to become turbulent and accelerate. A Rayleigh-Taylor fluid instability is evident at the turbulent flame front, where the fingers of low-density burned gas extend into the high-density unburned gas. As the flame expands further

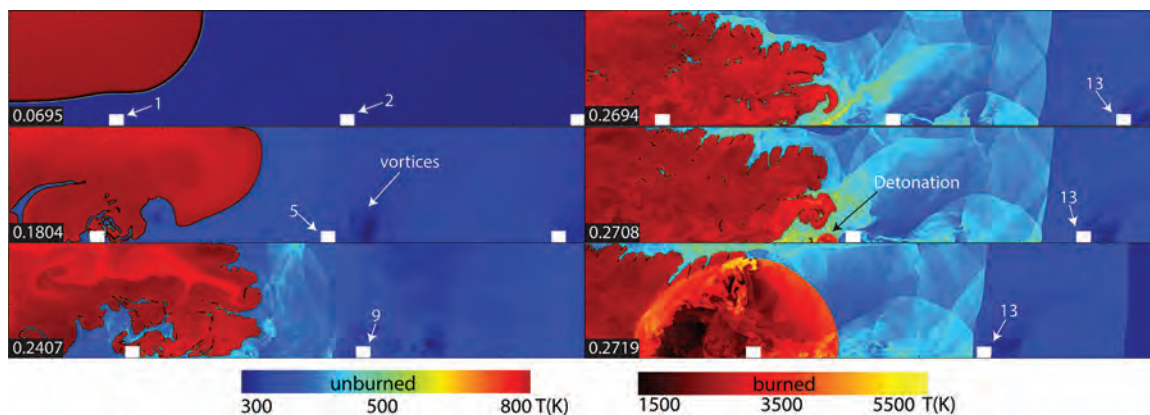


FIGURE 11 Two-dimensional simulation of flame acceleration and deflagration-to-detonation transition in a channel 0.32 cm in height. Obstacle height is 0.032 cm. Time is shown in milliseconds in frame corners. Frame length is 3.2 cm and total channel length is 21 cm. Flame front is traveling toward right side of frame. Obstacles are numbered.

into the channel, pressure waves in the unburned gas coalesce into shockwaves that compress and pre-heat the unburned gas prior to combustion, as one can see by the increased temperature in the region ahead of the flame. The shocks reflect against the channel surfaces and collide with one another, interacting with the flame front, burned gas, and unburned gas.

Shock collisions and reflections against channel surfaces deposit energy into the unburned gas at timescales much smaller than the acoustic timescale of the unburned gas. The rate of the energy deposition increases as the shocks become stronger. Eventually, this rapid increase in the rate of energy deposition is significant enough to detonate the unburned gas, as shown at 0.2708 milliseconds. To quantify the rate of energy deposition required for the detonation, a control volume analysis was performed on the volume of unburned gas where the detonation initiates, tracking the rate of internal and chemical energy deposition into the control volume during the shock collision and subse-

quent detonation. Figure 12 shows the energy rates plotted as a function of time. There is an increase in the rate of internal energy deposition into the control volume as the shocks collide, followed by a delay of 0.1 microseconds, then chemical and internal energy rates increase dramatically as the gas detonates. Thus, detonation occurs as the result of a shock collision focusing a tremendous amount of energy in a small volume of unburned gas.

Figure 13 shows a three-dimensional (3D) simulation that uses the same initial conditions as the 2D case, performed to verify that the shock-focusing DDT mechanism is independent of dimensionality. Although the time and distance into the channel at which DDT occurs differs slightly from the 2D case, detonation in the 3D case is initiated by the same mechanism. At 0.102 milliseconds, the unburned gas has detonated and the detonation wave begins to overtake the turbulent flame front. The detonation wave is fully formed at 0.113 milliseconds, and a 3D transverse wave structure is visible along the detonation front.

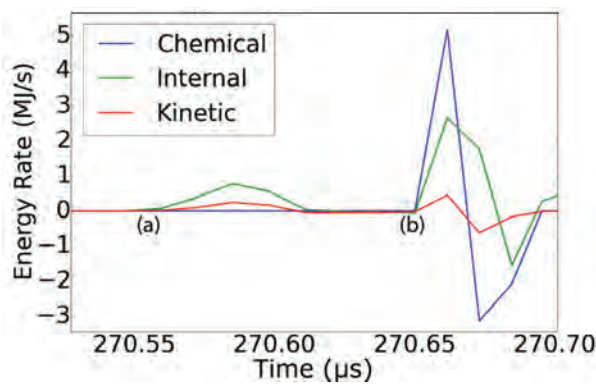


FIGURE 12 Rate of energy deposition in control volume. Compression of unburned gas by the shock collision begins at (a). Detonation occurs at (b).

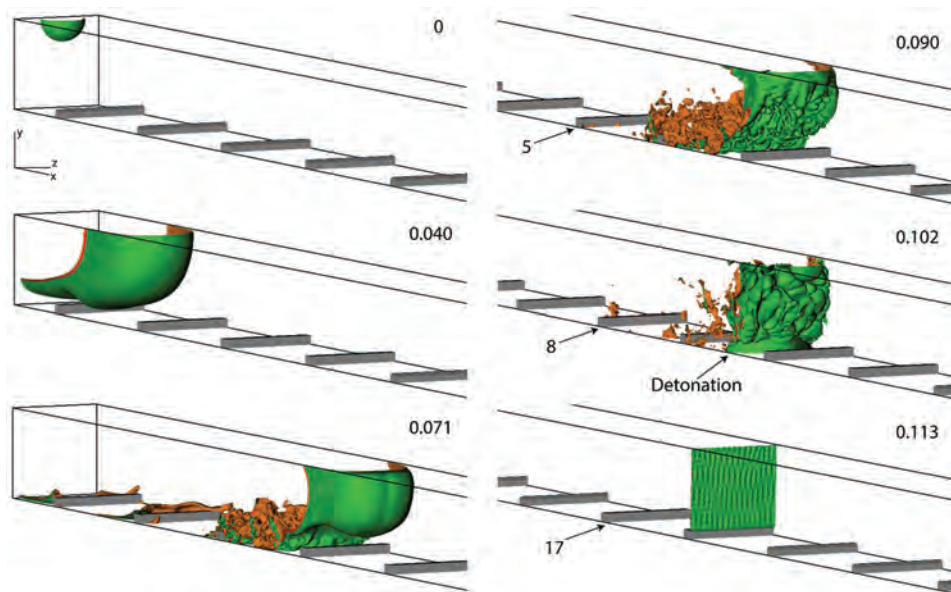


FIGURE 13 Isosurfaces of fuel-mass fractions of 0.2, 0.5, and 0.8 show flame acceleration and DDT in 3D channel. Time in milliseconds is shown in frame corners. Obstacles are numbered.

Significance: These calculations are used to examine the mechanism that causes DDT in a thin channel of a highly reactive fuel-oxidizer mixture. The interactions between the acoustic waves, shocks, boundary layers, and channel walls result in the rapid acceleration of the flame and initiation of a detonation due to a convergence of shocks on a small volume of unburned mixture. An understanding of the complex interactions in this system is essential to the design of stable and reliable detonation engines.

[Sponsored by the NRL Base Program (CNR funded) and ONR]

References

- ¹D. Szirczak and H. Smith, "A Review of Design Issues Specific to Hypersonic Flight Vehicles," *Prog. Aerosp. Sci.* **84**, 1–28 (2016).
- ²G.B. Goodwin, R.W. Houim, and E.S. Oran, "Effect of Decreasing Blockage Ratio on DDT in Small Channels with Obstacles," *Combust. Flame* **173**, 16–26 (2016).
- ³G.B. Goodwin, R.W. Houim, and E.S. Oran, "Shock Transition to Detonation in Channels with Obstacles," *Proc. Comb. Inst.* **36**(2), 2717–2724 (2017).



- 210** Mitigation of Spacecraft Communications Blackout via Microparticle Injection
- 211** LASCO: Pioneer of Space Weather
- 213** Slim-Edged Silicon Detectors: Advanced Nano-Fabrication Technology
- 215** Solar Coronal Power Spectra Modeling

Mitigation of Spacecraft Communications Blackout via Microparticle Injection

E.D. Gillman and W.E. Amatucci
Plasma Physics Division

Introduction and Motivation: Plasma discharges consist of positively charged ions, negatively charged electrons, and neutral gas particles. Complex, or “dusty,” plasmas contain a fourth species: charged microparticles or “dust grains.” When the dust grains interact with plasma particles, the dust grains become charged and thus subject to electrical and magnetic forces that lead to unique phenomena.

There are many examples of naturally occurring dusty plasmas. Saturn’s rings and comet tails are composed of microparticles suspended in plasma. Noctilucent clouds formed by ice crystals in the Earth’s polar ionosphere are dusty plasmas. Due to the constant bombardment by meteors and the presence of debris in low Earth orbit, many other regions of the ionosphere are also considered dusty plasmas. Dust grains can often form as unwanted species in manmade plasmas such as semiconductor processing reactors. The microparticles can collect on these devices after processing, resulting in contamination defects that limit feature size and result in poor quality control. Dust grains also cause significant inefficiencies in plasma fusion reactors.

Recent studies in the Plasma Physics Division of the U.S. Naval Research Laboratory (NRL) have focused on how the controlled release of dust grains

could mitigate the radio blackout that affects spacecraft reentering the Earth’s atmosphere.

The high velocity of spacecraft and frictional heating during atmospheric reentry causes a dense plasma layer to form around the vehicle. Electrons in the plasma layer block and attenuate electromagnetic (EM) radio waves, preventing the sending and receiving of telemetry, communications, and GPS navigation signals. Injecting microparticles to absorb a fraction of the plasma electron population may mitigate this problem (Fig. 1).

Technical Approach: EM waves interact with plasmas differently, depending on the wave frequency and plasma electron density. A critical frequency known as the cutoff frequency is dependent on the density of free electrons in the plasma. At frequencies below the cutoff frequency, the free electrons in the plasma are mobile enough to react and reflect the incident EM wave. However, at frequencies above the cutoff frequency, the EM wave passes through the plasma with minimal reflection or power loss. By inserting microparticles and transforming the plasma layer into a dusty plasma, a substantial portion of the electrons become strongly bound to the dust grains. With the reduced free electron density, the plasma cutoff frequency is lowered. The electrons bound to the microparticles can no longer react to low frequency EM signals, and the signal may be able to pass through the previously impenetrable layer.

While experiments have shown that dusty plasmas are depleted of electrons, theory has predicted that the interaction of electromagnetic signals with charged microparticles may also act as a source of signal scattering.¹⁻⁴

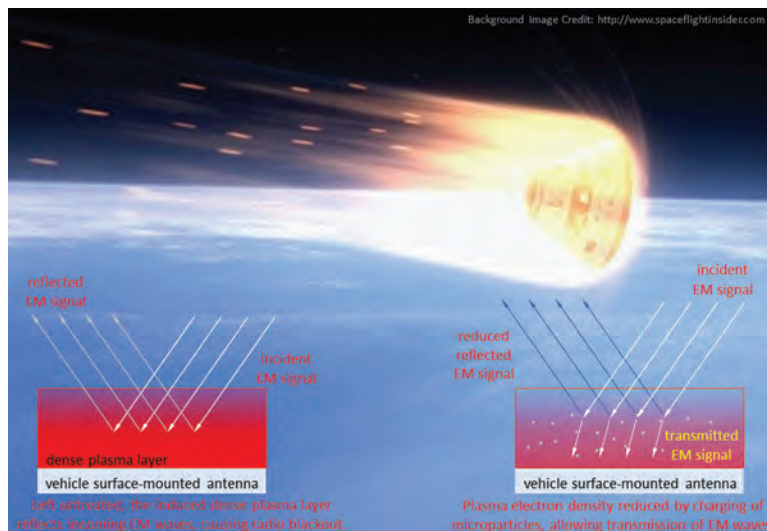


FIGURE 1 Microparticle injection into the plasma layer surrounding a reentering spacecraft can increase transmission of communications signals, mitigating the radio communications blackout effect.

Experiments and Results: Experiments at NRL were performed in the DUSty PLAsma EXperiments (DUPLEX, JR) vacuum facility. A linear hollow cathode plasma source and electromagnets were used to create a large area, dense, well collimated sheet of plasma. A transmitting and receiving horn were placed on each side of the plasma sheet, and the reception of signals near the GPS frequency band was monitored. Experiments were performed by creating a plasma layer dense enough to cutoff the transmission between the microwave horns. A dust shaker device then released microparticles as the transmission between the horns was monitored.

Two main effects were observed: (1) an initial increase in the scattering of the signal (reduced transmission) while the microparticles resided in the plasma layer and (2) a period during which transmission significantly increased immediately following, as the microparticles left the plasma. The reduction in transmission observed at early times is likely due to scattering of the EM signal caused by the charged microparticles. The later increase in transmission occurs as the charged microparticles leave the plasma layer, carrying with them the many free electrons bound to their surface and leaving behind an electron-depleted plasma layer.

It was discovered that by combining the release of microparticles in quick succession, the periods of transmission can build on the previous high transmission periods, resulting in a net increase in the total transmission over an extended period of time. Figure 2 shows the microparticle release periods (Fig. 2(a)) and the initial decrease in transmission, followed by the increase in transmission through the overly dense plasma layer (Fig 2(b)).

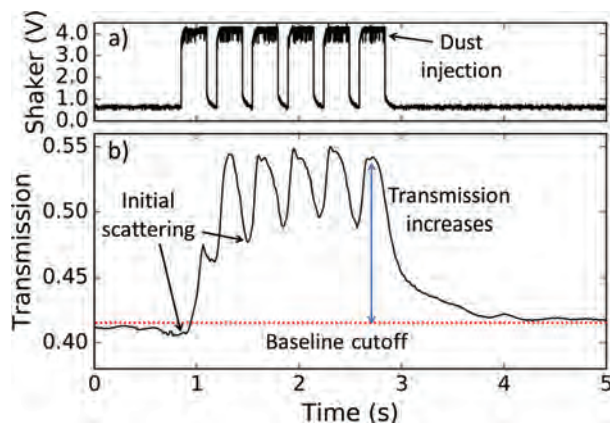


FIGURE 2 Injecting dust grains results in periods of increased transmission through an overly dense plasma layer. When dust grains are injected in rapid succession, transmission through the plasma layer can be extended for longer periods of time.

Conclusions: It is possible to increase the transmission of electromagnetic signals through a dense plasma layer with the addition of microparticles. However, these charged microparticles have also been shown to cause signal scattering in certain conditions for a short period of time. Regardless, the interaction of EM signals incident on a dense dusty plasma layer may be exploited for applications across many areas directly applicable to the Navy. This dusty plasma approach could help alleviate the problem of radio blackout experienced by spacecraft during atmospheric reentry, a critical time for spaceflight.

[Sponsored by the NRL Base Program (CNR funded)]

References

- ¹ Q.-Z. Luo and N. D'Angelo, "Observations of Dusty Plasmas with Magnetized Dust Grains," *J. Phys. D: Appl. Phys.* **33**(21), 2754 (2000).
- ² E.D. Gillman and J.E. Foster, "Electron Depletion via Cathode Spot Dispersion of Dielectric Powder into an Overhead Plasma," *J. Vac. Sci. and Technol. A* **31**, 061303 (2013).
- ³ R. Bingham, U. de Angelis, V.N. Tsytovich, and O. Havnes, "Electromagnetic Wave Scattering in Dusty Plasmas," *Phys. Fluids B* **3**, 811–817 (1991).
- ⁴ C. la Hoz, "Radar Scattering from Dusty Plasmas," *Phys. Scripta* **45**, 529 (1992).



LASCO: Pioneer of Space Weather

R. Colaninno, R. Howard, and S. Plunkett
Space Science Division

Introduction: Launched December 2, 1995, the Large Angle Spectrometric Coronagraph (LASCO)¹ experiment was designed and built by an NRL-led international consortium of four institutions from four countries (Fig. 3). As one of 12 instruments on the joint European Space Agency/NASA Solar and Heliospheric Observatory (SOHO) mission, LASCO has returned high cadence, nearly uninterrupted observations of the solar corona for more than two decades. A coronagraph is a specially designed telescope that blocks direct sunlight such that the atmosphere around the Sun, known as the corona, can be imaged. LASCO images the corona in the visible spectrum with a set of three telescopes with nested fields of view, providing data over a large spatial scale from a half a million to 14 million miles above the Sun's surface. Today, LASCO still provides data on a continuous duty cycle from SOHO at the L1 Lagrange point located between the Sun and the Earth. These near real-time images are made available on an NRL website to the general public and other

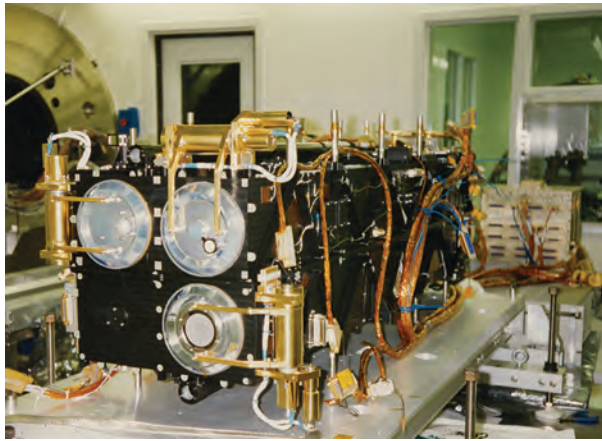


FIGURE 3
The three telescopes of the Large Angle Spectrometric Coronagraph (LASCO) at NRL's specialized facility, where LASCO was integrated and tested. NRL's Solar and Heliospheric Physics Branch in the Space Division is using these facilities to develop the next generation of space weather instrumentation.

government agencies. Of the six remote-sensing instruments onboard the SOHO spacecraft, it is the only one still in operation.

In the visible spectrum, the solar corona is observable because of sunlight scattering off fast-moving electrons, which, with other charged particles, make up the solar wind. In the corona, these charged particles are trapped along the magnetic field of the Sun, creating both quasi-static and dynamic features. These coronal features are the source of the solar wind and solar storms generated by coronal mass ejections (CMEs).

The plasma and magnetic fields from the corona propagate out and fill the interplanetary space environment to the edge of the solar system. The term “space weather” refers to the variable conditions caused by the Sun in interplanetary space near the Earth. The interaction of the Earth’s atmosphere and magnetic field with the surrounding space environment, especially CME driven solar storms, can negatively impact human activity and technology.

Solar Storms: The link between CMEs and terrestrial effects was inferred soon after CMEs were first detected by an NRL coronagraph in 1971. One of the most dramatic of these effects occurred on March 13, 1989, when the entire province of Quebec suffered a blackout caused by a geomagnetic storm produced by a CME. In addition to disrupting power grids, CME-driven space weather storms can interfere with GPS navigation systems, satellite operations, astronaut safety, radio communications, orbital tracking, and polar flight activities.

Because of their disruptive impact, CMEs have been the subject of intense study of their initiation mechanisms, their interaction with the corona and solar wind, and their association with other coronal phenomena such as flares and prominences. LASCO observations have proven fundamental to pursuing these fundamental questions about CME physics. We have observed that CMEs occur with and without visible solar flare activity on the solar disk,² and have determined the basic magnetic structure of the CMEs.³

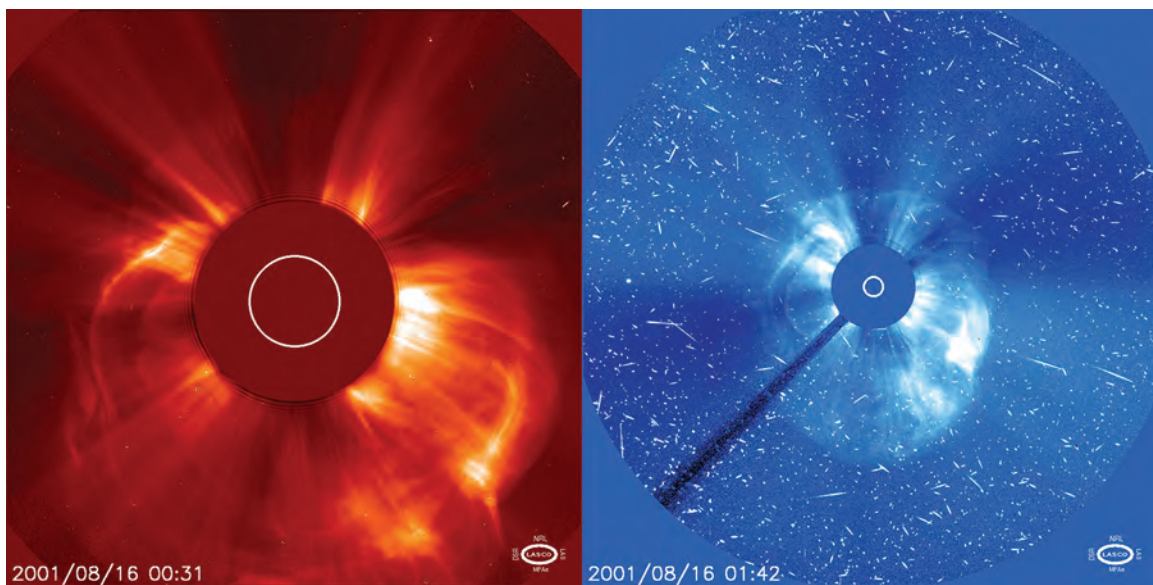


FIGURE 4
Observations from the two currently operating coronagraphs. *Left-hand panel:* LASCO C2 telescope image of a coronal mass ejection (CME) headed toward Earth. The white circle shows the size of the Sun behind the coronagraph’s occulter disks. *Right-hand panel:* The same CME imaged with LASCO C3. CMEs can accelerate particles in the corona, which appear as bright streaks or “snow” in the images. These highly energetic particles can also disrupt communications satellites and other essential technologies.

The combination of these fundamental discoveries has allowed us to determine the origin and propagation direction of CMEs in real-time from LASCO observations (Fig. 4).

Space Weather Forecasting: More than two decades' worth of LASCO observations provide the cornerstone of our understanding of the solar corona and its link with the geospace environment. In turn, this understanding has helped shape the development of the field of space weather forecasting, in which the goal of ongoing research is to mitigate the impacts of solar storms on human activities and technologies. Several research groups, including the National Oceanic and Atmospheric Administration's Space Weather Prediction Center, use real-time LASCO images to provide forecasts of the near-Earth space environment, including predictions of a solar storm's arrival time and severity. Space weather forecasts have become essential to the operations of many private, commercial, and international organizations as well as federal agencies and the military. NASA is even using LASCO data to forecast the space weather at their satellites and other assets throughout the solar system.

Conclusion: The remarkable dataset of observations from LASCO supports a diversity of scientific analyses that go beyond what was initially envisioned for the instrument. Furthermore, LASCO real-time images have introduced the space-weather forecasting capability and demonstrated the need for warnings about solar storms. LASCO is pioneering technology that helps set the course for the next generation of coronal research and observation, which will transition from science-based experimentation to development of operational instruments. Such operational coronagraphs will be essential for continued space weather forecasting that protects our technological infrastructure not only on Earth but also throughout the solar system.

[Sponsored by the NRL Base Program (CNR funded) and NASA]

References

- ¹G.E. Brueckner, R.A. Howard, M.J. Koomen, C.M. Korendyke, D.J. Michels, J.D. Moses, D.G. Socker, K.P. Dere, P.L. Lamy, A. Llebaria, M.V. Bout, R. Schwenn, G.M. Simnett, D.K. Bedford, and C.J. Eyles, "The Large Angle Spectroscopic Coronagraph (LASCO)," *Solar Phys.* **162**, 357–402 (1995).
- ²S.P. Plunkett, D.J. Michels, R.A. Howard, G.E. Brueckner, O.C. St. Cyr, B.J. Thompson, G.M. Simnett, R. Schwenn, and P. Lamy, "New Insights on The Onsets of Coronal Mass Ejections from SOHO," *Adv. Space Res.* **29**, 1473–1488 (2002).
- ³A.F.R. Thernisien, R.A. Howard, and A. Vourlidas, "Modeling of Flux Rope Coronal Mass Ejections," *Astrophys. J.* **652**(1), 763–773 (2006).

Slim-Edged Silicon Detectors: Advanced Nano-Fabrication Technology

M. Christophersen,¹ B.F. Phlips,¹ V. Fadeyev,² and H.F.-W. Sadrozinski²

¹Space Science Division

²University of California, Santa Cruz

Introduction: Patterned semiconductor sensors are vital components of many radiation detector systems. In the past 20 years, silicon sensors with either striped readout ("strips") or two-dimensional readout ("pixels") have been developed at an exponential pace, similar to other developments in the electronics industry commonly described by Moore's law.¹ A large-scale application of silicon strip detectors in space is the NASA-Department of Energy Fermi mission, which was based on sensors from 6-inch wafers instead of the 4-inch wafers used in earlier experiments, permitting the construction of larger assemblies with fewer interconnects and dead area (Fig. 5). Further minimization of the insensitive edge area is one of the key requirements for future space missions like ComPair and the Advanced Pair Telescope.

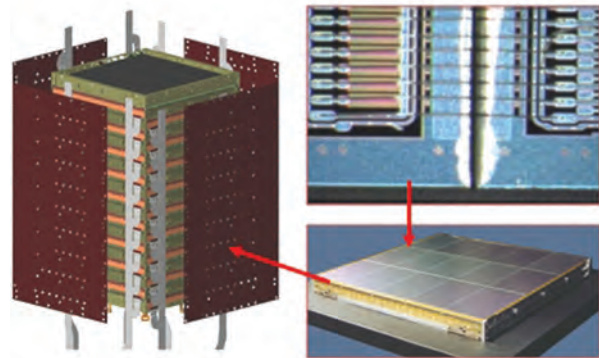


FIGURE 5 Schematic of the NASA Fermi tracker. Silicon sensors are tiled into sensor planes.

The requirements for high energy physics (HEP) experiments are similar with respect to the required silicon sensors. Silicon sensors normally have an inactive region along the perimeter of the sensor. This inactive area on the perimeter contains the guard rings that protect the active area from electrical currents and damage caused in the manufacturing of the device. These inactive areas can significantly degrade the performance of the closely arranged sensors for HEP instrumentation and need to be minimized.

Methods for Reducing Inactive Region of Silicon Detectors: Silicon detectors normally have a wide

inactive region (up to 1 millimeter) along the perimeter of the sensor for saw cut damage (chips and cracks) (Fig. 6). A reduction of this area would benefit the detector performance by reducing the amount of passive material, alleviating mechanical constraints in making a hermetic detector system, and allowing more device yield from a given size wafer. The edge termination in silicon radiation detectors is critical: It should shield the active area from any spurious current coming from the edges and improve the breakdown performance and long-term stability. In older generations of planar detectors, this was obtained by multiple guard-rings around the device, used to gradually drop the voltage toward the cut region and to drain parasitic currents coming from the edge. For high performance detectors with slim edges, two factors are required: (1) advanced dicing methods with minimal side wall damage, and (2) the exposed side-walls need to be passivated using atomic layer deposition, a modern nano-fabrication method, of alumina, Al_2O_3 for n-in-p sensors and of silicon oxide, SiO_2 for p-in-n types. This leads to a controlled drop of the potential along the side-wall.²

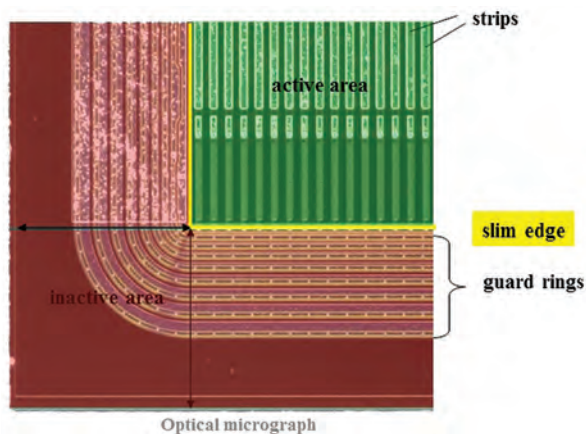


FIGURE 6
These sensors have an inactive area (green), reducing the overall performance of the tracker by introducing dead areas. Slim edges (yellow lines) will lead to sensors with minimal inactive areas.

Advanced dicing methods. One essential step is to replace regular blade dicing. Traditional blade dicing uses diamond-covered blades. This technique is well-established and has been used for decades. Blade cutting leads to micro-cracks and chipping at the die edge, leaving a damaged region approximately 100 μm wide. We used damage-free mechanical scribing and cleaving. This method has proven efficient for volume III-V-compound semiconductor laser manufacturing.³ Although silicon is more difficult to cleave than a III-V semiconductor, the cleaved silicon surface can be mirror-like with virtually no defects. Alternative dicing techniques with reduced edge damage are laser dicing and plasma dicing.²

Side-wall passivation. The edge termination in silicon radiation detectors is critical. The type of sidewall passivation depends on the substrate doping [see Christopherson et al. (2013) for details].² As a result, the optimal sidewall passivation leads to a controlled potential drop along the edge due to a fixed interface charge. We found that the use of atomic layer deposition alumina layers with a negative interface charge works best for p-type sensors. A plasma-enhanced chemical vapor deposition (PECVD) amorphous hydrogenated silicon nitride Si_3N_4 shows the lowest leakage currents for n-type sensors. A PECVD deposited H-SiXNy layer has a fixed positive interface charge. Similar passivations for p- and n-type silicon are used for solar cells to increase carrier lifetime and solar cell effectiveness.^{4,5}

Conclusion: Charge collection only happens in the active area of the devices; the border regions are non-active. Since the size of a single device is limited (maximum by the wafer size), larger detector arrays are formed using tiled semiconductor devices. The same approach could be used to tile large focal plane arrays, e.g., for space surveillance telescopes. This report describes the scribing-cleaving-passivation technique for slim-edge silicon sensors. Figure 7 shows a cross-section scanning electron microscope micrograph and IV curve of an n-type strip detector. The IV curve shows low leakage currents up to 1,000 V. Furthermore, we performed charge collections measurements for n- and p-type sensors.⁶ The technique presented works on full wafers or on a finished die scale.

Acknowledgments: This work has been performed within the framework of the European Organization for Nuclear Research (CERN) RD50 Collaboration. This research is supported by the Chief of Naval Research. Work at the Santa Cruz Institute for Particle Physics (University of California, Santa Cruz) was supported by the Department of Energy (Grant DEFG0204ER41286). [Sponsored by CNR and DOE]

References

- ¹ Moore's law. (2017). In Encyclopædia Britannica. Retrieved August 18, 2017, from *Encyclopædia Britannica Online*: <http://www.britannica.com/EBchecked/topic/Moores-law>.
- ² M. Christophersen, V. Fadeyev, B.F. Philips, H.F.-W. Sadrozinski, C. Parker, S. Ely, and J.G. Wright, "Alumina and Silicon Oxide/Nitride Sidewall Passivation for P- and N-Type Sensors," *Nuc. Instr. Meth. A.* **699**(21), 14–17 (2013).
- ³ K. Wasmer, C. Ballif, C. Pouvreau, D. Shulz, and J. Michler, "Dicing of Gallium Arsenide High Performance Laser Diodes for Industrial Applications: Part I. Scratching Operation," *J. Mat. Process. Tech.* **198**, 114 (2008).
- ⁴ B. Hoex, J. Schmidt, R. Bock, P.P. Altermatt, M.C.M van de Sanden, and W.M.M. Kessels, "Silicon Surface Passivation by Atomic Layer Deposited Al_2O_3 ," *Appl. Phys. Lett.* **91**, 112107–112110 (2007).

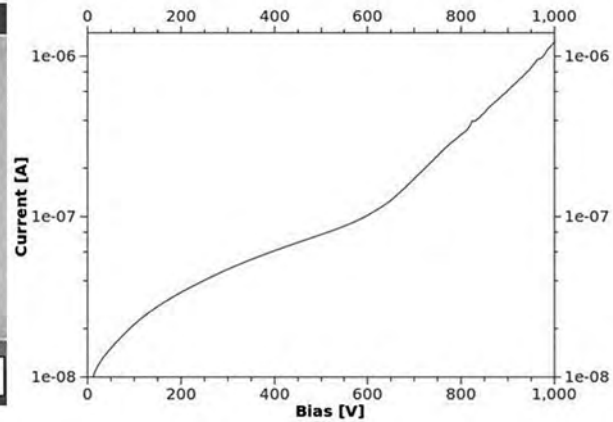
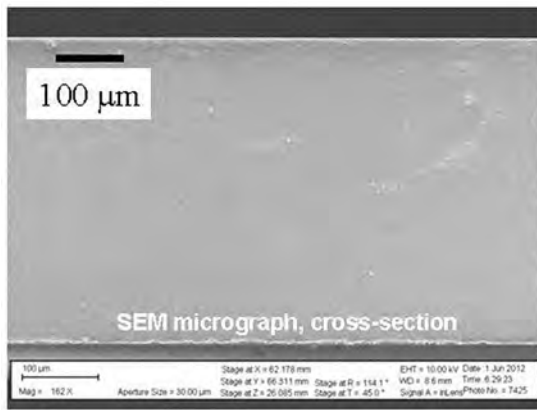


FIGURE 7 Scanning electron microscope micrograph (cross-section); the silicon sidewall shows no visible damage. The IV curve shows low leakage currents up to 1,000 V.

⁵ G. Dingemans, N.M. Terlinden, M.A. Verheijen, M.C.M. van de Snaden, and W.M.M. Kessels, “Controlling the Fixed Charge and Passivation Properties of Si(100)/Al₂O₃ Interfaces Using Ultrathin SiO₂ Interlayers Synthesized by Atomic Layer Deposition,” *J. Appl. Phys.* **110**, 093715 (2011).

⁶ R. Bates, A. Blue, M. Christophersen, L. Eklund, S. Ely, V. Fadeyev, E. Gimenez, V. Kachkanov, J. Kalliopuska, A. Macchiodo, D. Maneuski, B.F. Phelps, H.F.-W. Sadrozinski, G. Stewart, N. Tartoni, and R.M. Zahn, “Characterization of Edgeless Technologies for Pixelated and Strip Silicon Detectors with a Micro-Focused X-ray Beam,” *J. of Instrumentation*, P01018 (2013).



Solar Coronal Power Spectra Modeling

K. Battams,¹ B.M. Gallagher,² and R.S. Weigel²

¹Space Science Division

²George Mason University

Introduction: In 2010, NASA launched the Solar Dynamics Observatory (SDO) to study the Sun, providing extreme ultraviolet (EUV) observations of the Sun’s million-degree corona in unprecedented spatial and temporal resolution. Leveraging the capabilities of the SDO, we have developed a new technique to extract, model, and perform the first global surveys of solar coronal power spectra.¹ Many solar studies consider power spectra, primarily energy transfer, wave propagation, coronal heating, and solar wind turbulence. These processes are fundamental to many aspects of space weather research and of high importance for developing better prediction of geomagnetic storms that drive conditions in Earth’s space environment and upper atmosphere.

Methodology: Ours is the first technique capable of accurately determining fine-scale coronal power

spectral properties from direct solar observation over spatially large regions and across multiple wavelengths, enabling the parameterization of solar observations based on the properties of a multi-component power spectra model. This technique builds upon the work of Ireland (2014),² who demonstrated how 50 × 50 pixel regions of the solar corona could be broadly represented by a two- or three-component power law model.

The general outline of our procedure is as follows. A region of interest is selected from full temporal and spatial resolution solar EUV observations spanning several hours, and the corresponding data extracted (Figs. 8(a) and 8(b)) and co-aligned to account for solar rotation. Intensity profile time series are then extracted from each pixel (Fig. 8(c)) and converted to their power spectral equivalent via Fast Fourier Transform (FFT). We then fit models to each of the individual power spectra (Fig. 8(d)) and visualize the resulting model parameterizations.

Our M1 model consists of a power-law with a tail and contains parameters for the slope coefficient, the power-law index, and the tail constant. Our M2 model combines M1 with an additional Gaussian component described by its amplitude, location, and width. We then visualize the individual parameterizations as two-dimensional images mapped to the original observations.

Results: In our initial paper, we investigated the global spectral properties of a large (1600 × 1600 pixel) region in five wavelength channels from the SDO Atmospheric Imaging Assembly (AIA) obtained over a 12-hour period on June 26, 2013. We computed over 2.5-million spectral model fits to describe the observed power spectrum in each pixel of the region of interest and performed visualizations of individual model parameters. Our three-component M2 model produced an average data-to-model correlation coefficient of

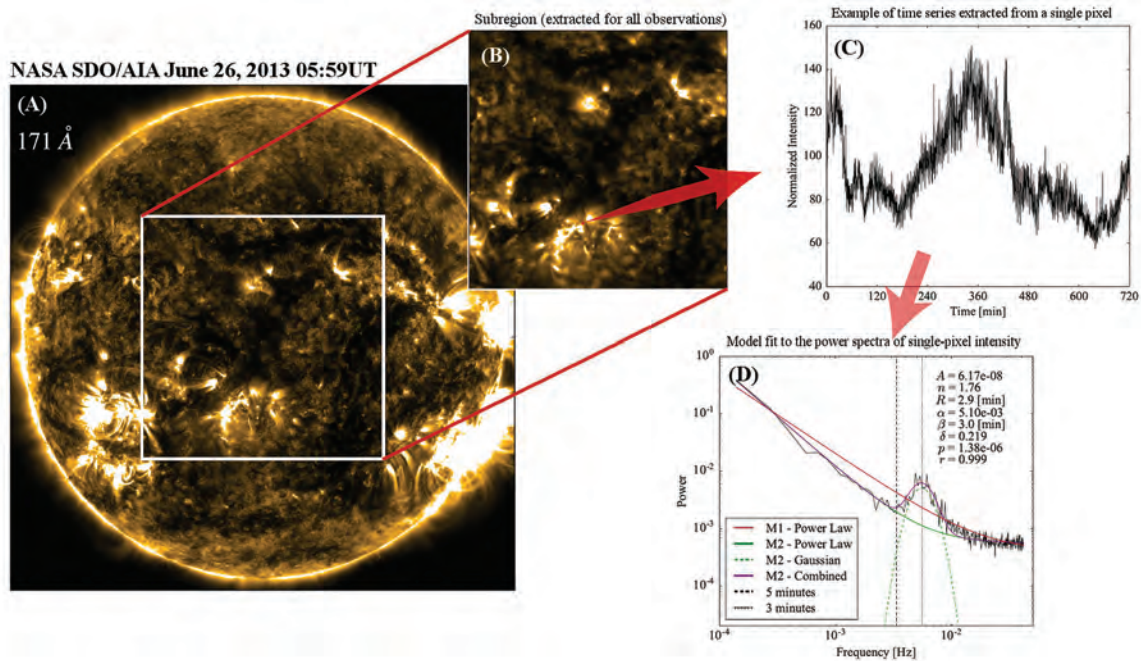


FIGURE 8

Panel A shows the full field of view for one 171Å image recorded by the NASA Solar Dynamics Observatory (SDO), with the white box indicating the region of interest (Panel B) for the study. Panel C shows an example of a 12-hour intensity time series extracted from a single pixel of the region of interest. Panel D shows the resulting power spectrum (solid black line) and power spectral model components as indicated in the figure legend. Such time series and model components were obtained for every pixel across the entire 1600 × 1600 pixel region of interest.

0.96, indicating a remarkably good representation of solar power spectra.

Figure 9 shows the regions of interest for the SDO/AIA 193, 171, 304, and 1600 Å wavelengths and indicates the primary features of interest, namely a large coronal hole, a filament, and an active region (seen as a sunspot in the 1600 Å observations). The top row of Fig. 10 visualizes the power law indices (n) representative of the slope of a power spectra, and relates to the transfer (cascade) of energy in the solar atmosphere. The bottom row of Fig. 10 visualizes the Gaussian location, representing the frequency (time) location of the center of the Gaussian component of the spectral model and highlighting oscillatory features in the solar atmosphere.

We made several key discoveries from our initial study. (1) All visible features in the solar atmosphere can be described by their unique spectral properties. (2) Direct observational evidence shows that high-power law indices relate to concentrated magnetic structures in the solar atmosphere (e.g., hot coronal loops, photospheric magnetic network). (3) Coronal holes (source regions for fast solar wind) exhibit very low power law indices as a consequence of their open magnetic fields. (4) Sunspots exhibit fast 3-minute oscillations at their core, with gradual radial damping of this periodicity. (5) Sunspot periodicities pervade the entire solar atmosphere, from the underlying

photosphere to the million-degree upper corona. (6) Sunspots observed near the photosphere all exhibit a circular “Gaussian Void” region in which no statistically significant periodicities are observed.

Impact and Future Work: Constituting essentially a new data product for the solar community, our spectral parameterizations are applicable to studies of a breadth of solar features and phenomena. This technique for the analysis of modern high-resolution solar data provides several new parameterizations of the Sun’s atmosphere, each of which is driven by specific unique physical mechanisms that relate directly to both energy transfer and wave propagation in the solar atmosphere. Our technique enables scientists to analyze the spectral properties of regions far larger than existing methods, at full resolution, and across the entire available power spectrum. It also now provides the first opportunity for theorists to compare high-resolution simulations (e.g., of coronal loops) with data-driven observation.

Acknowledgments: This work was supported by NASA and the NRL Edison Memorial Program. The work was a collaborative effort between NRL and George Mason University.

[Sponsored by the NRL Edison Program and NASA]

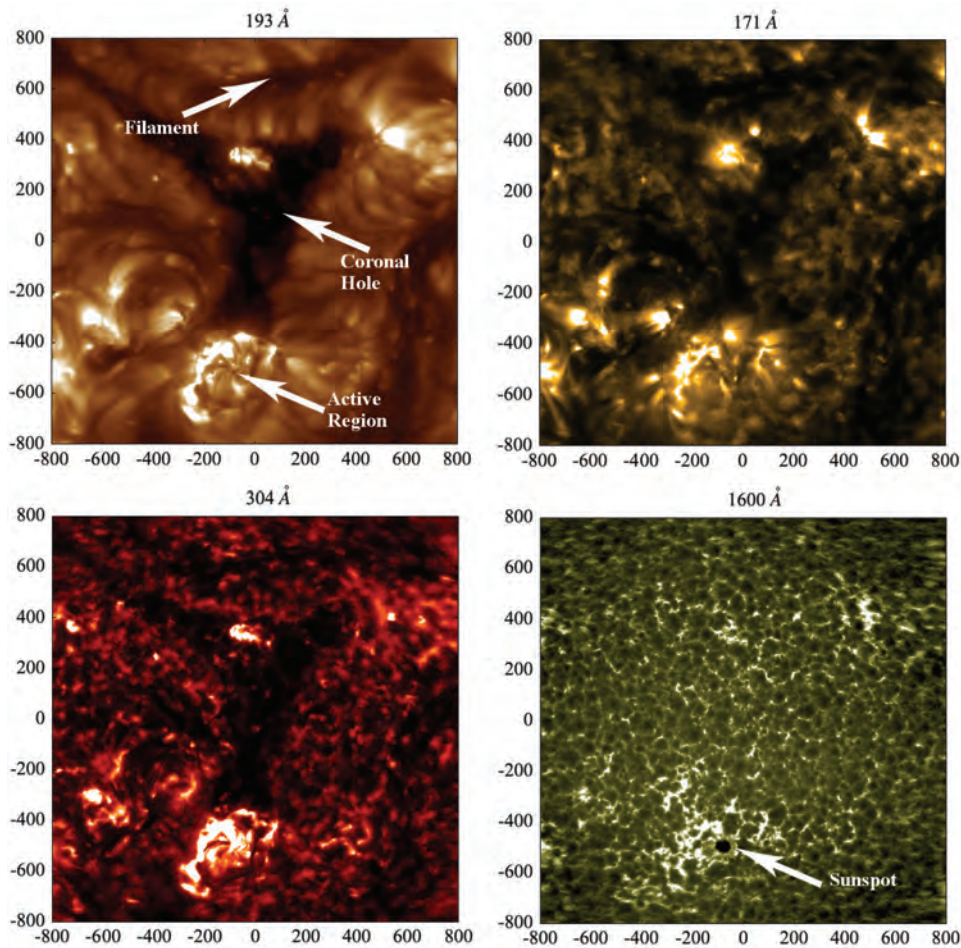


FIGURE 9
 Example SDO observations for the 193A, 171A, 304A, and 1600A Atmospheric Imaging Assembly (AIA) channels for our selected region of interest. The selected region contained a solar filament, coronal hole, and an active region with an underlying sunspot, as indicated in the figure panels.

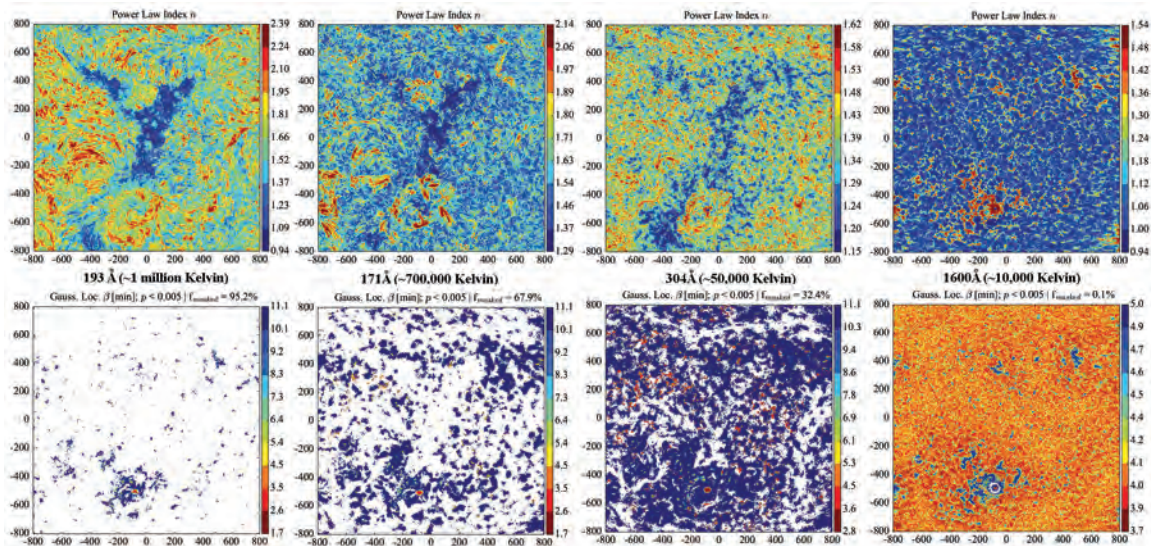


FIGURE 10
 Two model parameterizations of the four SDO/AIA channels presented in Fig. 9, showing the Power Law Index (*top row*) and Gaussian Location (*bottom row*) parameters of the model fitting process (Fig. 8(d)). The Power Law Index represents the slope of the power spectrum, and related to the cascade of energies in the solar corona. The Gaussian Location represents the peak (temporal [minutes]) location of the center of the Gaussian component of the model (Fig. 8(d)) and reveals oscillatory features in the solar atmosphere. Pixels in which no statistically significant Gaussian are observed are masked out of the visualizations, with the fractional percentage of the masked region indicated by the 'masked' value in the titles of the Gaussian Location panels.

References

- ¹K. Battams, B.M. Gallagher, and R.S. Weigel, “A Global Survey of EUV Coronal Power Spectra,” *Astrophys. J.* (Submitted: June 2017).
- ²J. Ireland, R.T.J. McAteer, and A.R. Inglis, “Coronal Fourier Power Spectra: Implications For Coronal Seismology and Coronal Heating,” *Astrophys. J.* **798**(1) (2014).



220 Special Awards and Recognition

229 Alan Berman Research Publication and NRL Edison (Patent) Awards

233 NRC/ASEE Postdoctoral Research Publication Awards

PRESIDENTIAL RANK AWARDS are granted by the U.S. government to career Senior Executive Service (SES) members and Senior Career Employees within the Office of Personnel Management-allocated Senior-Level (SL) or Scientific-Professional (ST) community. The awards have been given annually by the President of the United States since the establishment of the Senior Executive Service in 1978, except for a brief period of suspension from 2013 to 2014. The Awards honor high-performing senior career employees for “sustained extraordinary accomplishment.” Winners of these awards are deemed strong leaders, professionals, or scientists who achieve results and consistently demonstrate strength, integrity, industry, and a relentless commitment to excellence in public service.

2016 PRESIDENTIAL RANK AWARD OF MERITORIOUS EXECUTIVE

Dr. Banahalli Ratna

Superintendent, Center for Bio/Molecular Science and Engineering

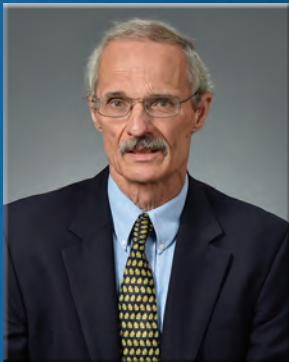


The Presidential Rank Award of Meritorious Executive is the second-highest annual award given to selected career SES members. Under Dr. Banahalli Ratna’s supervision, U.S. Naval Research Laboratory researchers developed an antibiotic resistance monitoring device that enables effective antibiotic prescription, demonstrated the variability of antimicrobial resistance genes across the globe, and validated performance of Next Generation Ebola Virus Diagnostic System during the height of the epidemic in Sierra Leone.

2016 PRESIDENTIAL RANK AWARD OF MERITORIOUS SENIOR PROFESSIONALS

Dr. Jerry Meyer

Optical Sciences Division



The Presidential Rank Award of Meritorious Senior Professional is awarded annually to selected SL/ST career professionals. Dr. Jerry Meyer is internationally recognized as an authority in semiconductor optoelectronic phenomena and the application of innovative quantum mechanical and optical engineering techniques to the invention of novel optoelectronic devices.

2016 PRESIDENTIAL RANK AWARD OF MERITORIOUS SENIOR PROFESSIONALS

Dr. David Stenger

Center for Bio/Molecular Science and Engineering

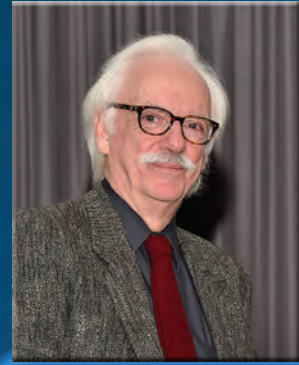


The Presidential Rank Award of Meritorious Senior Professional is awarded annually to selected SL/ST career professionals. Dr. David Stenger implemented international partnership programs to achieve global surveillance capability, established an overseas laboratory, and demonstrated Ebola virus detection and diagnosis that saved lives during the epidemic. He pioneered the concept of combining satellite imagery with ground-based data collection in unmapped areas of West Africa.

TRENT-CREDE MEDAL

Dr. Earl Williams
Acoustics Division

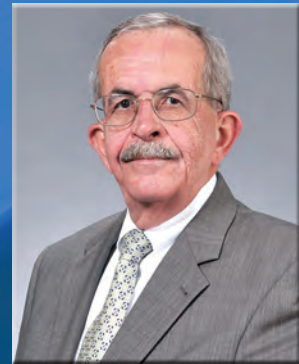
The Trent-Crede Medal is presented every two to six years to an individual who has made an outstanding contribution to the science of mechanical vibration and shock, as evidenced by publication of research results in professional journals or by other accomplishments in the field. Only 14 individuals have received the medal (not including Williams) since its inception in 1969. Dr. Williams was recognized for his 34 years of research, major contributions in the acoustics field, and development and application of near-field acoustical holography.



DEPARTMENT OF THE NAVY MERITORIOUS CIVILIAN SERVICE AWARD

Dr. Edward Franchi (retired)
Ocean and Atmospheric Science and Technology Directorate

Dr. Edward Franchi was recognized for exceptional meritorious service and significant contributions as the Associate Director of Research for the Ocean and Atmospheric Science and Technology Directorate at the U.S. Naval Research Laboratory (NRL) from April 2008 to June 2017. During this period, Dr. Franchi provided outstanding leadership and achievements, demonstrating unsurpassed professional knowledge and resourcefulness with unmatched work ethic in the performance of his duties. His long list of accomplishments and achievements includes successfully leading the NRL Undersea Warfare Program, service on the North Atlantic Treaty Organization (NATO) Science and Technology (S&T) Reform Implementation Team, and service as a member and chair of the NATO S&T Experts Committee. Dr. Franchi ably led the Laboratory as Acting Director of Research from August through December 2016, and in this capacity provided exceptional Navy leadership and expert testimony to the U.S. House Armed Services Committee's hearing on Department of Defense laboratories. He provided superb leadership over his directorate's six divisions and hundreds of scientists and engineers, effectively managing the constant change that occurs in a creative research-and-development organization that responds to changing Naval mission priorities. Dr. Franchi's many distinguished accomplishments reflect well on him and stand as testament to his unflinching dedication to NRL and to the security requirements of the United States.



2015 TOP NAVY SCIENTISTS AND ENGINEERS OF THE YEAR AWARD

The Honorable Dr. Delores Etter, Assistant Secretary of the Navy for Research, Development and Acquisition, established this award to recognize Navy civilian and military personnel for superior scientific and engineering achievements and to promote continued scientific and engineering excellence. Over 35,000 Navy scientists and engineers are eligible for this award. The honorees represented various commands across the Department of the Navy. Nominees must have demonstrated exceptional scientific and engineering achievement in their field during the preceding calendar year of the award. Achievements are considered significant when they establish a scientific basis for subsequent technical improvements of military importance, materially improve the Navy's technical capability, or materially contribute to national defense.

Top Scientists and Engineers:

Optical Sciences Division

Dr. Igor Vurgaftman

Chemistry Division

Dr. Jeffrey Long, Dr. Joseph Parker, and Dr. Debra Rolison



CAPTAIN ROBERT DEXTER CONRAD AWARD FOR SCIENTIFIC ACHIEVEMENT

Dr. Thomas Reinecke
Electronics Science and Technology Division

Captain Robert Dexter Conrad was a primary architect of the Navy's basic research program, and the head of the Planning Division of the Office of Naval Research at the time of its establishment. This award is designed to recognize and reward outstanding technical and scientific achievement in research and development for the Department of the Navy. Dr. Thomas Reinecke is engaged in research at the heart of nanoscience and nanotechnology. He contributes broadly and deeply to the understanding of the electronic, optical, and transport properties of semiconductors and nanosystems. He has a national and international reputation for seminal work in areas ranging from thermoelectrics and thermal transport to quantum information technologies, and he has initiated national and international efforts in these fields. His large numbers of publications (over 240) in refereed journals and the numbers of citations of his work (over 15,000) give clear evidence of his scientific productivity and wide technical leadership. His stature and leadership have resulted in his bringing together research and in building research capabilities in quantum information technologies at the Department of Defense service laboratories for the benefit of the Navy and the Department of Defense.



2016 SIGMA XI AWARD FOR PURE SCIENCE

Dr. Simon Cooke
Electronics Science and Technology Division

The Sigma Xi Pure Science Award is presented for distinguished contributions in pure science and to acknowledge exemplary technical success in scientific research at the U.S. Naval Research Laboratory. The award is based on unclassified articles in reviewed scientific publications or on classified reports. Dr. Cooke was recognized in the Pure Science category for his research in computational electromagnetics, charged particle beam simulation, and modeling techniques for vacuum electronic amplifiers.



2016 SIGMA XI AWARD FOR APPLIED SCIENCE

Dr. Andrew Guyette (former NRL employee)
Electronics Science and Technology Division

Winners of this award are selected for their distinguished contribution to pure and applied science during their research at the U.S. Naval Research Laboratory (NRL). The awards are given to encourage investigation in pure and applied science and promote the spirit of scientific research at NRL. Dr. Guyette was recognized for his research in the field of microwave filters and reconfigurable/adaptive circuits.

2016 SIGMA XI YOUNG INVESTIGATOR AWARD

Dr. Sarah Glaven
Center for Bio/Molecular Science and Engineering

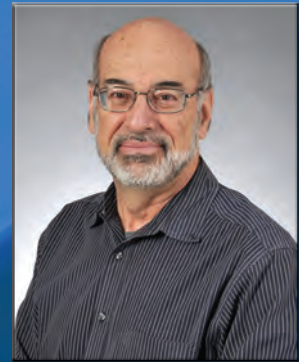
The Young Investigator Award recognizes researchers in the early stages of their careers whose outstanding contributions best exemplify the ideals of Sigma Xi. The award is given to young investigators for outstanding research performed within 10 years of earning their highest degree and for their ability to communicate that research to the public. Dr. Glaven was recognized for outstanding contributions to the field of microbial electrochemistry.



2017 SIGMA XI AWARD FOR PURE SCIENCE

Dr. Ira Schwartz
Plasma Physics Division

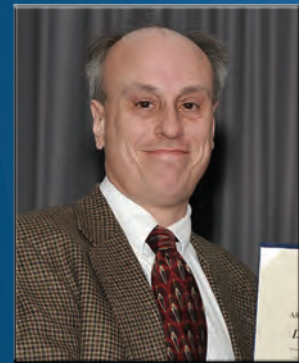
The Sigma Xi Pure Science Award is presented for distinguished contributions in pure science and to acknowledge exemplary technical success in scientific research at the U.S. Naval Research Laboratory. The award is based on unclassified articles in reviewed scientific publications or on classified reports. Dr. Schwartz was recognized in the Pure Science category for his extensive contributions to the theory of nonlinear dynamical systems and nonlinear science in general.



2017 SIGMA XI AWARD FOR APPLIED SCIENCE

Dr. William Rabinovich
Optical Sciences Division

Winners of this award are selected for their distinguished contribution to pure and applied science during their research at the U.S. Naval Research Laboratory (NRL). The awards are given to encourage investigation in pure and applied science and to promote the spirit of scientific research at NRL. Dr. Rabinovich was recognized for his innovations and discoveries that have greatly advanced the field of free space optical communication.



2017 SIGMA XI YOUNG INVESTIGATOR AWARD

Dr. Michael Stewart
Optical Sciences Division

The Young Investigator Award recognizes researchers in the early stages of their careers whose outstanding contributions best exemplify the ideals of Sigma Xi. The award is given to young investigators for outstanding research performed within 10 years of earning their highest degree and for their ability to communicate that research to the public. Dr. Stewart was recognized for his multifaceted research efforts in developing colloidal semiconductor quantum dot-based technologies for biological and solid-state optoelectronic applications.





APPLIED RESEARCH FOR THE ADVANCEMENT OF SCIENCE AND TECHNOLOGY PRIORITY (ARAP) AWARD

Dr. Linda Thomas
Space Systems Development Department

In 2017, the Department of Defense awarded a three-year, \$45 million grant to a tri-service project for a laser communications system. “This is basically fiber optic communications without the fiber,” said lead researcher Dr. Linda Thomas, whose U.S. Naval Research Laboratory team takes home about a third of the grant money. Their Tactical Line-of-sight Optical communications Network (TALON) device transmits messages via laser over distances comparable to current Marine Corps tactical radios, but because it is a narrow beam of light rather than a radio broadcast, it is much harder for an enemy to pick up the transmission, let alone interfere with it. While lasers cannot replace radios entirely, they provide a valuable alternative for vital battlefield communications. The modern U.S. military relies on wireless networks and other radiofrequency communications to transmit orders, intelligence, and targeting data, but it is increasingly anxious that advanced adversaries like Russia and China can detect those emissions, jam them, hack them, and triangulate their sources for bombardment, as the Ukrainian military learned with heavy losses in 2014. One solution to the problem is to make wireless networks more robust, but another option is to avoid using radiowaves entirely. That is where TALON comes in.

FEDERAL LABORATORIES CONSORTIUM (FLC) AWARD FOR EXCELLENCE IN TECHNOLOGY TRANSFER

The Federal Laboratories Consortium (FLC) was organized in 1974 and formally chartered by the Federal Technology Transfer Act of 1986 to promote and strengthen technology transfer nationwide. Today, more than 300 federal laboratories, facilities, and research centers and their parent agencies make up the FLC community. Members of the FLC community include world-renowned scientists, engineers, inventors, entrepreneurs, academia, laboratory personnel, and T2 professionals.



Mr. James Martin, Mr. Steven Marquis, Dr. Erick Iezzi, Mr. Paul Slebodnick, Mr. John Wegand, Mr. James Tagert, and Mr. Randy Terrill
Chemistry Division and Technology Transfer Office

The U.S. Naval Research Laboratory (NRL) received the FLC Award for Excellence in Technology Transfer for SiloxoGrip™: A Siloxane-Based Non-Skid Coating. NRL invented and transferred a coating to replace traditional epoxy resins with a siloxane-based material that marked a significant advancement in non-skid surface coating technology. The novel coating decreases environmental levels of volatile organic compounds, delivers greater durability, and improves direct adhesion to metals. Through a series of technology transfer efforts, NRL completed a non-exclusive patent license agreement with NCP Coatings, Inc., of Niles, Michigan. The new non-skid coating is commercially available under the company’s brand name, SiloxoGrip™, and NCP Coatings has achieved sales in both defense and commercial markets.



Top photo: Mr. James Martin, Mr. Steven Marquis, and Dr. Erick Iezzi.
Bottom photo: Mr. Paul Slebodnick, Mr. John Wegand, and Mr. James Tagert.

Ms. Amanda Horansky-McKinney, Ms. Kendra Flowers, Ms. Patricia Doutriaux, Mr. Adam Moses, Dr. Gopal Patnaik, Mr. Keith Obenschain, Mr. Cameron Childs, and Dr. John Dennis

Laboratories for Computational Physics and Fluid Dynamics and Technology Transfer Office

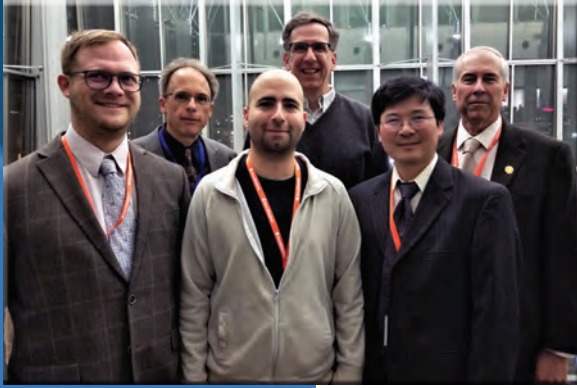
The U.S. Naval Research Laboratory (NRL) received the FLC Award for Excellence in Technology Transfer for the CT-Analyst® – Air Plume Contamination Crisis Management System, an instantaneous crisis management system that provides more timely and readily comprehensible information to emergency responders. This Navy-patented system, known as Contaminant Transfer Analyst (CT-Analyst®), uses detailed urban geometry and airflow data that can be computer-manipulated to predict the potential impact of urban air plume contamination more quickly than other similar modeling systems. Chemical, biological, or radiological (CBR) explosions can release toxic gas plumes, whether by accident or as a result of terrorism. Statistically, three-fourths of fatalities result from the direct exposure to CBR contaminants within the first 15 minutes of an event, making emergency response times critical. If an effective response begins within 3 to 5 minutes, an estimated 85 percent of those fatalities could be avoided. CT-Analyst® gives first responders a key advantage, allowing them to spend less time calculating response needs and more time saving lives. The system's database “imagines” every possible scenario, including where people are on the street, where emergency response vehicles are headed and, more importantly, where responders can set up a triage zone or whatever else is needed. It anticipates where the contaminant plume is likely to travel and what zones will be free of contaminants. Onsite demonstrations have consistently substantiated the Navy-patented technology's utility in urban settings. Two examples are the demonstrations during preparations for the 2006 Super Bowl in Detroit and the 2013 U.S. presidential inauguration, when the federal government's All-Hazards Center used CT-Analyst® to provide an initial assessment of airborne contaminant threats.

Mr. Christopher Vizas, Dr. Nicholas Lagakos, Mr. Vasilios Lagakos, and Mr. Cameron Childs
Acoustics Division and Technology Transfer Office

The U.S. Naval Research Laboratory (NRL) received the FLC Award for Excellence in Technology Transfer for Fiber Optic Amplitude Modulated Sensors (FOS). A suite of Navy-patented FOS, transferred to industry by NRL, is the up-and-coming game changer within the “smart grid” sector of the massive U.S. electrical power industry. The innovative sensors accurately measure pressure, strain, temperature, and other parameters relevant to monitoring and controlling electrical power generation, distribution, and storage. This Navy technology also has proven its superiority in industrial control systems, and is the basis of highly sensitive fiber optic microphones that can detect unmanned aerial vehicles or contribute to the acoustic design of buildings. Assembled in arrays, the high-performance microphones also can diagnose function problems in rotating machinery, computer hard drives, aircraft engines, and other multi-movement components.



First row: Ms. Amanda Horansky-McKinney, Ms. Kendra Flowers, and Ms. Patricia Doutriaux. Second row: Mr. Adam Moses, Dr. Gopal Patnaik, and Mr. Keith Obenschain.



Team members (from left): Jeremy E. Solbrig (Cooperative Institute for Research in the Atmosphere), F. Joseph Turk (NASA Jet Propulsion Laboratory), and Dr. Joshua Cossuth, Mr. Richard Bankert, Dr. Song Yang, and Mr. Jeffrey Hawkins (NRL).

AMERICAN METEOROLOGICAL SOCIETY (AMS) SPECIAL AWARD

Dr. Joshua Cossuth, Mr. Richard Bankert, Dr. Song Yang, and Mr. Jeffrey Hawkins
Marine Meteorology Division

The American Meteorological Society annual awards honor outstanding individuals and organizations of the weather, water, and climate community. Special Awards are presented to individuals, teams of individuals, or organizations not appropriately recognized by more specifically defined awards who have made important contributions to the science or practice of meteorology, related aspects of oceanography or hydrology, or to the Society. An inter-

disciplinary team of federal, private, and academic researchers, including scientists from the U.S. Naval Research Laboratory (NRL) Marine Meteorology Division, were bestowed the Special Award at the 98th Annual AMS Meeting. The team received the award for providing an innovative suite of satellite passive microwave products to the global tropical cyclone community via a tailored web site, enabling enhanced storm monitoring. Providing real-time storm monitoring since 1997, the NRL tropical cyclone [TC] satellite analysis team was an early adopter of storm-centric processing and Internet broadcast of satellite data through the creation of NRL TC Web. Using information provided by operational TC forecast centers via NRL's Automated Tropical Cyclone Forecast system, near real-time processing of value-added products from satellite imagery were created for TC centric analyses around the world. NRL TC Web has made these analyses of TC position, intensity, and structure an indispensable part of the forecasting toolbox at the Joint Typhoon Warning Center, National Hurricane Center, and Central Pacific Hurricane Center.



Left to right: Drs. John Steuben, John Michopoulos, and Athanasios Iliopoulos. Far right: Award presenter Monica Bordegoni, Chair of the ASME Computer and Information in Engineering Division.

AMERICAN SOCIETY OF MECHANICAL ENGINEERS (ASME) BEST OF CONFERENCE PAPER AWARD

Drs. John Steuben, John Michopoulos, and Athanasios Iliopoulos
Materials Science and Technology Division

The ASME Computer and Information in Engineering (CIE) Division Best Paper Awards recognize the best papers in each of the primary topics sponsored by the Technical Committees at the CIE annual conference, and the overall conference best paper. Primary topics include Advanced Modeling and Simulation; Computer-Aided Product and Process Development; Systems Engineering, Information and Knowledge Management; and Virtual Environments and Systems. Best of Conference Paper was awarded to Drs.

Athanasios Iliopoulos, John Michopoulos, and John Steuben at the 2016 conference for their paper on "Implicit Slicing for Functionally Tailored Additive Manufacturing." Additive manufacturing (AM), also known as layered manufacturing, rapid prototyping, or less formally as 3D printing, is an increasingly important family of fabrication techniques for the production of a wide variety of components. These fabrication techniques are characterized by successive additions of material to a domain, as opposed to the repeated subtractions [of excess material] employed by most traditional fabrication technologies. The primary focus of this research is to illustrate the many advantages of adopting an implicit slicing methodology that may significantly improve the state of the AM digital thread, reduce the deficiency of design data, and facilitate ongoing efforts to develop functionally imbued AM objects.

2016 STRATEGIC ENVIRONMENTAL RESEARCH AND DEVELOPMENT PROGRAM PROJECT OF THE YEAR AWARD FOR WEAPONS SYSTEMS AND PLATFORMS

Dr. Matthew Laskoski

Chemistry Division

Scientists from the U.S. Naval Research Laboratory (NRL) contributed valuable information to a project led by a team of scientists from the Naval Air Warfare Center Weapons Division, the results of which won the 2016 Strategic Environmental Research and Development Program (SERDP) Project of the Year Award for Weapons Systems and Platforms. The goal of the project was to find an alternative for the phenols used to synthesize thermosetting resins. Toxicity issues and cost inefficiency make these petroleum-based phenols a potentially hazardous piece of source material. The team explored the possibility of a replacement material based on biological feedstocks instead of the phenols previously used. Dr. Matthew Laskoski, a chemist in the NRL Advanced Materials Section, built upon this SERDP-funded project to synthesize a processable phthalonitrile (PN) resin that utilizes renewable starting materials. The PN resin functions as a substitute for PMR-15, a high temperature resin that contains a carcinogen called methylene dianiline. NRL's PN resins are a far less toxic alternative to PMR-15, yet equally effective because the renewable starting materials do not compromise the physical properties of the resulting polymer created. Dr. Laskoski's work in the project included incorporating input from NRL Pathways and Science and Engineering Apprenticeship Program student interns, who worked diligently with him to develop and test the resins.

NAVY MERITORIOUS CIVILIAN SERVICE AWARD

Mr. Joseph Peak (retired)

Tactical Electronic Warfare Division

The Navy Meritorious Civilian Service Award Medal is the third highest honorary award that the Navy can bestow upon a civilian employee. Mr. Peak was recognized for sustained performance, outstanding technical leadership, management, and research and development achievements that increased Navy, Marine Corps, Army, and Special Operations operational capabilities and survivability over the past 15 years. During this period, Mr. Peak served in multiple positions of great trust and responsibility, providing outstanding services and achievements, demonstrating unsurpassed professional knowledge and resourcefulness with unmatched work ethic in the performance of his duties. Directly supporting the maintenance of our national security, Mr. Peak significantly contributed to many projects in support of the global war on terrorism. His long list of accomplishments and achievements includes major advances in the state-of-the-art of signature control technologies and managing and transitioning these new capabilities to the field, resulting in significant improvements to the overall readiness and effectiveness in operational capabilities. His efforts increased military survivability and helped save the lives of our warfighters. Mr. Peak's distinctive accomplishments are a clear reflection of his unfailing dedication to the U.S. Naval Research Laboratory, the Department of the Navy, the Special Operations Command, and the Department of Defense.

NAVY MERITORIOUS CIVILIAN SERVICE AWARD

Dr. Teddy Keller

Chemistry Division

The Navy Meritorious Civilian Service Award Medal is the third highest honorary award that the Navy can bestow upon a civilian employee. Dr. Keller was recognized for his outstanding performance and scientific achievements accomplished throughout his 40-year career at the U.S. Naval Research Laboratory. During his tenure, Dr. Keller provided a significant service to the Navy and the Nation through development of an improved understanding of the synthesis and development of high temperature and nanostructural materials for marine and aerospace applications. He pioneered research on phthalonitrile- and carborane/siloxane-based polymers along with his recent work on the fabrication of unidirectional carbon nanotubes (CNT) and the novel polymeric synthesis of nanocrystalline refractory ceramics for use in hypersonic, armor, energy, and catalytic applications. Dr. Keller has received many awards and honors for his outstanding research innovations.





E.O. HULBURT ANNUAL SCIENCE AWARD

Dr. Alexander Efros
Materials Science and Technology Division

The E.O. Hulburt Science Award was established in December 1955, on the occasion of the retirement of American physicist Dr. Edward O. Hulburt, who was appointed the first Director of Research at the U.S. Naval Research Laboratory (NRL), January 28, 1949. The establishment of the award expresses, in part, the sincere and high esteem in which Hulburt was held at NRL as well as within the scientific community. The E.O. Hulburt Award is the highest award the NRL Commanding Officer can confer on an NRL civilian employee. Dr. Efros was recognized for his sustained superior performance over a number of years. His pioneering contributions to the theory of low-dimensional semiconductor nanostructures have established the basic theoretical concepts that are now used by all researchers in the field. These concepts include theories of the electronic and optical properties of nanocrystal quantum dots, nanorods, and nanowires. These concepts are also widely used for developing nanocrystal-based devices, such as lasers, light-emitting diodes, and photovoltaic cells. Dr. Efros maintains strong and rewarding connections with experimentalists, both inside and outside NRL.



Left to right: Dr. Edward Franchi, Jamie Baker, Gayle Fullerton, Beth Dalton, Kathy Parrish, Peggy Newman, Claire Peachey, Jonna Atkinson, James Marshall, CAPT Mark Bruington, and Dr. Bhakta Rath.

NRL EXCELLENCE IN MISSION SUPPORT AWARD

Technical Information Services Branch
Strategic Communication Office

The Technical Information Services (TIS) Branch at the U.S. Naval Research Laboratory (NRL) was presented the NRL Excellence in Mission Support Award in recognition of continued expert customer service and the production of professional, quality products and materials in support of NRL programs and mission. “Acknowledged for having a deep-seated corporate knowledge of NRL, the TIS staff possesses an enthusiastic spirit and attitude that ‘no task is too big a challenge.’” said Dr. Bhakta Rath, retired Associate Director of Research, Materials Science and

Component Technology Directorate. “The TIS team continues to exhibit an uncompromising dedication to their customers, coupled with a strong desire to produce quality products in support of the Office of Naval Research and NRL missions.” Offering a comprehensive fiscally sound and problem solving approach, the TIS team has won national and international awards in photography, videography, and publication design.



COMMANDING OFFICER'S AWARD FOR ACHIEVEMENT IN THE FIELD OF EQUAL EMPLOYMENT OPPORTUNITY (EEO)

Ms. Meredith Hutchinson
Optical Sciences Division

The Commanding Officers Award for Achievement in the Field of Equal Employment Opportunity (EEO) was established for bestowal by the Commanding Officer on U.S. Naval Research Laboratory (NRL) civilian employees in recognition of outstanding contributions to the EEO Program through excellence in their leadership skills, imagination, and accomplishments. Ms. Hutchinson was presented the award for providing outstanding leadership and vision in advancing the cause of the Women in Science and Engineering at NRL.

ALAN BERMAN RESEARCH PUBLICATION AND NRL EDISON (PATENT) AWARDS

The Annual Research Publication Awards Dinner (ARPAD) was established in 1968 to recognize the authors of the best U.S. Naval Research Laboratory (NRL) publications each year. These awards not only honor individuals for superior scientific accomplishments in the field of naval research, but also seek to promote continued excellence in research and in its documentation. In 1982, the name of this award was changed to the Alan Berman Research Publication Award in honor of its founder. Of the 202 papers nominated for the 2016 awards, 35 were selected for recognition. They represent 168 authors.

NRL also recognizes patents as part of its annual publication awards program. The NRL Edison (Patent) Awards were established in 1991 to recognize NRL employees for outstanding patents issued to NRL by the U.S. Patent and Trademark Office during the preceding calendar year. The awards recognize significant NRL contributions to science and engineering, as demonstrated by the patent process, that are perceived to have the greatest potential benefit to the country. Of the 106 patents considered for 2016, three were selected, representing 11 inventors and three patent attorneys.

PUBLICATION AWARDS

Radar Division

A New Class of Planar Ultrawideband Modular Antenna (PUMA) Arrays
with Improved Bandwidth

Dr. John Logan, Dr. Rick Kindt, Dr. Michael Lee, and Dr. Marinos Vouvakis

Wind Turbine Bistatic Scattering Measurements in the High Frequency Band (3–30 MHz)

Mr. Serafin Rodriquez, Dr. William Lee, Dr. Jennifer Eisenman, and Dr. Scott Coultts

Information Technology Division

Decision Forests for Machine Learning Classification of Large, Noisy Seafloor Feature Sets

Dr. Wallace Lawson, Dr. Donald Sofge, Dr. Denson Smith,

Dr. Paul Elmore, and Dr. Frederick Petry

Assessing Situation Awareness in an Unmanned Vehicle Control Task:

A Case for Eye Tracking Based Metrics

Dr. Joseph Coyne, Mrs. Ciara Sibley, and Mr. Samuel Monfort

Optical Sciences Division

Machine Learning Approach to OAM Beam Demultiplexing via
Convolutional Neural Networks

Dr. Timothy Doster and Dr. Abbie Watnik

Surface Enhanced Raman Spectroscopy of Individual Suspended Aerosol Particles

Dr. Vasanthi Sivaprakasam, Dr. Matthew Hart, and Dr. Jay Eversole

Tactical Electronic Warfare Division

Time-Frequency Synthetic Aperture Radar: A Technique for Adaptive Imaging of Regions
Containing Weak and Intermittent Transmitters

Dr. James Given and Dr. Margaret Cheney

Design of 45 to 110 GHz Components for Use in a Rotman Lens Transmitter Assembly
Dr. Mark Patrick and Dr. Jaikrishna Venkatesan

Laboratories for Computational Physics and Fluid Dynamics

Development of an Unmanned Hybrid Vehicle Using Artificial Pectoral Fins
*Mr. Jason Geder, Dr. Ravi Ramamurti, Dr. Daniel Edwards,
Dr. Trenton Young, and Mr. Marius Pruessner*

Chemistry Division

Quantification of Efficient Plasmonic Hot-Electron Injection in
Gold Nanoparticle-TiO₂ Films
*Dr. Daniel Ratchford, Dr. Adam Dunkelberger, Dr. Jeffrey Owrutsky,
Dr. Pehr Pehrsson, and Dr. Igor Vurgaftman*

Trace Explosives Sensor Testbed (TESTbed)
*Dr. Greg Collins, Dr. Cy Tamanaha, Mr. Mark Hammond, Dr. Braden Giordano,
Dr. Christopher Field, Dr. Duane Rogers, Dr. Richard Colton, Dr. Susan Rose-Pehrsson,
Dr. Michael Malito, Dr. Adam Lubrano, and Mr. Russell Jeffries*

Materials Science and Technology Division

Understanding Variations in Circularly Polarized Photoluminescence
in Monolayer Transition Metal Dichalcogenides
*Dr. Kathleen McCreary, Dr. Aubrey Hanbicki, Dr. Berend Jonker,
Dr. Marc Currie, and Dr. Hsun-Jen Chuang*

Microstructure-Sensitive Modeling of Pitting Corrosion:
Effect of the Crystallographic Orientation
*Dr. Patrick Brewick, Dr. Virginia DeGiorgi, Dr. Andrew Geltmacher,
Dr. Nithya Kota, Dr. Alexis Lewis, and Dr. Siddiq Qidwai*

Plasma Physics Division

Bayesian Spectral Analysis of Chorus Subelements from the Van Allen Probes
*Dr. Chris Crabtree, Dr. Erik Tejero, Dr. Gurudas Ganguli,
Dr. George Hospodarsky, and Dr. Craig Kletzing*

Effective NO_x Remediation from a Surrogate Flue Gas Using the
U.S. NRL Electra Electron Beam Facility
*Dr. Tzvetelina Petrova, Dr. George Petrov, Dr. Matthew Wolford, Dr. John Giuliani,
Dr. Frank Hegeler, Mr. Matthew Myers, Dr. John Sethian, and Dr. Harold Ladouceur*

Electronics Science and Technology Division

Nonlinear Thermoelastoelectroelastic Analysis of III-N Semiconductor Devices
Dr. Mario Ancona

Modeling Vacuum Electronic Devices Using Generalized Impedance Matrices
*Dr. Igor Chernyavskiy, Dr. John Rodgers, Dr. Alexander Vlasov,
Dr. Baruch Levush, Dr. Thomas Antonsen, and Dr. David Chernin*

Center for Bio/Molecular Science and Engineering

Nanoparticle Cellular Uptake by Dendritic Wedge Peptides: Achieving Single Peptide Facilitated Delivery

*Dr. Joyce Breger, Dr. James Delehanty, Dr. Jeffrey Deschamps, Dr. George Anderson,
Dr. Scott Walper, Dr. Igor Medintz, Dr. Eunkeu Oh, Dr. Kimihiro Susumu,
Dr. Markus Muttenhaler, Dr. Darren Thompson, Dr. Lauren Field, and Dr. Philip Dawson*

Quantum Dot–Peptide–Fullerene Bioconjugates for Visualization of In Vitro and In Vivo Cellular Membrane Potential

*Dr. Okhil Nag, Dr. Jeffrey Deschamps, Dr. Igor Medintz, Dr. James Delehanty,
Dr. Michael Stewart, Dr. Alan Huston, Dr. Alexander Efros, Dr. YungChia Chen,
Dr. Thomas O’Shaughnessy, Dr. Eunkeu Oh, Dr. Kimihiro Susumu, Dr. Vassiliy Tsytsarev,
Dr. Qinggong Tang, Dr. Lauren Field, Dr. Yu Chen, Dr. Roman Vaxenburg, Dr. Bryan Black,
Dr. Joseph Pancrazio, Dr. Stella North, Dr. Philip Dawson, and Dr. Reha Erzurumlu*

Acoustics Division

Mesh-Type Acoustic Vector Sensor

*Dr. Maxim Zalalutdinov, Dr. Douglas Photiadis, Dr. William Szymczak,
Dr. James McMahon, Dr. Brian Houston, and Dr. Joseph Bucaro*

Demonstration of Acoustic Source Localization in Air Using Single Pixel Compressive Imaging

*Dr. Jeffrey Rogers, Dr. Charles Rohde, Dr. Matthew Guild, Dr. Theodore Martin,
Dr. Gregory Orris, and Dr. Christina Naify*

Remote Sensing Division

Autonomous Coral Reef Survey in Support of Remote Sensing

*Dr. Steven Ackleson, Dr. Wesley Moses, Dr. Joseph Smith,
Mr. Luis Rodriguez, and Dr. Brandon Russell*

Application of Mixture Regression for Improved Polarimetric SAR Speckle Filtering

Dr. Yanting Wang, Dr. Thomas Ainsworth, and Dr. Jong-Sen Lee

Oceanography Division

The Impact of Ocean Surface Currents on Sverdrup Transport in the Midlatitude North Pacific via the Wind Stress Formulation

Dr. Zhitao Yu, Dr. E. Joseph Metzger, and Dr. Yalin Fan

Turbulent Large-Eddy Momentum Flux Divergence During High-Wind Events

*Dr. Hemantha Wijesekera, Dr. David Wang, Dr. Ewa Jarosz,
Dr. William Teague, Dr. W. Scott Pegau, and Dr. James Moum*

Marine Geosciences Division

Modeling and Observation

Dr. Allison Penko, Dr. Joseph Calantoni, and Dr. Brian Hefner

Tile Prediction Schemes for Wide Area Motion Imagery Maps in GIS

Dr. Chris Michael and Dr. Bruce Lin

Marine Meteorology Division

The Local Ensemble Tangent Linear Model: An Enabler for Coupled Model 4D-Var
Dr. Craig Bishop, Dr. Sergey Frolov, Dr. Douglas Allen, Dr. David Kuhl, and Dr. Karl Hoppel

Evidence for a Nimbostratus Uncinus in a Convectively Generated
Mixed-Phase Stratiform Cloud Shield
Dr. Jerome Schmidt, Dr. Paul Harasti, and Dr. Piotr Flatau

Space Science Division

Michelson Interferometer for Global High-Resolution Thermospheric Imaging (MIGHTI):
Instrument Design and Calibration

*Dr. Christoph Englert, Dr. Charles Brown, Dr. Kenneth Marr, Dr. Michael Stevens,
Dr. John Harlander, Dr. Ian Miller, Ms. J. Eloise Stump, Dr. Jed Hancock,
Dr. James Peterson, Dr. Jay Kumler, Dr. William Morrow, Dr. Thomas Mooney,
Dr. Scott Ellis, Dr. Stephen Mende, Dr. Stewart Harris, Dr. Thomas Immel,
Dr. Jonathan Makela, and Dr. Brian Harding*

Neutron-Decay Protons from Solar Flares as Seed Particles for
CME-Shock Acceleration in the Inner Heliosphere
Dr. Ronald Murphy and Dr. Yuan-Kuen Ko

Space Systems Development Department

The Next Generation GPS Time
Dr. Ken Senior and Dr. Michael Coleman

Comparing Double Difference Global Navigation Satellite Systems at Mid Latitude
Ms. Krysta Lemm and Mr. Gregory Carbott

Spacecraft Engineering Department

Performance Analysis of a Hypersonic Scramjet Engine with a Morphable Waverider Inlet
Mr. Gabriel Goodwin and Mr. Jesse Maxwell

Performance Impacts of Geometry and Operating Conditions on a
Low Reynolds Number Micro-Nozzle Flow
Mr. Logan Williams and Mr. Michael Osborn

NRL EDISON (PATENT) AWARDS

Multi-Ply Heterogeneous Armor with Viscoelastic Layers
Dr. Charles Roland, Dr. Daniel Fragiadakis, Dr. Raymond Gamache, and Mr. Scott Bell

Microwave Initiation for Deposition of Porous Organosilicate Materials on Fabrics
Dr. Brandy White, Dr. Brian Melde, and Dr. Roy Roberts

Chemical Mapping using Thermal Microscopy at the Micro and Nano Scales
*Dr. Robert Furstenberg, Dr. Chris Kendziora, Dr. Andrew McGill,
Mr. Viet Nguyen, and Ms. Rebecca Forman*

Nanosplasmonic Imaging Technique for the Spatio-Temporal Mapping of Single Cell
Secretions in Real Time
*Dr. Marc Raphael, Dr. Joseph Christodoulides, Dr. Jeff Byers,
Dr. James Delehanty, and Ms. Rebecca Forman*

Paired Laser and Electrokinetic Separation, Manipulation, and Analysis Device
Dr. Alexander Terray, Dr. Sean Hart, Dr. Greg Collins, Dr. Sarah Staton, and Dr. Roy Roberts

NRC/ASEE POSTDOCTORAL RESEARCH PUBLICATION AWARDS

Information Technology Division

Pupil Size as a Measure of Within-Task Learning
Cyrus K. Foroughi, Ciara M. Sibley, and Joseph T. Coyne

Chemistry Division

First-Principles-Based Method for Electron Localization: Application to
Monolayer Hexagonal Boron Nitride
Chinedu E. Ekuma, Vladimir Dobrosavljević, and Lennart D. Gunlycke

Multifunctional PolyHIPE Wound Dressings for the Treatment of Severe Limb
Trauma
*Christopher L. McGann, Benjamin C. Streifel, Jeffrey G. Lundin,
and James H. Wynne*

Electronics Science and Technology Division

Controlling the H to T Structural Phase Transition via Chalcogen Substitution
in MoTe₂ Monolayers
Joshua Young and Thomas L. Reinecke

Center for Bio/Molecular Science and Engineering

Utilizing HomoFRET to Extend DNA-Scaffolded Photonic Networks and
Increase Light-Harvesting Capability
*William P. Klein, Sebastian A. Diaz, Susan Buckhout-White, Joseph S. Melinger,
Paul D. Cunningham, Ellen R. Goldman, Mario G. Ancona, Wan Kuang,
and Igor L. Medintz*

Space Science Division

Seasonal Dependence of Northern High-Latitude Upper Thermospheric Winds: A Quiet Time
Climatological Study Based on Ground-Based and Space-Based Measurements
*Manbharat S. Dhadly, John T. Emmert, Douglas P. Drob, Mark Conde, Eelco Doornbos,
Gordon Shepherd, Jonathan Makela, Qian Wu, Rick Niciejewski, and Aaron Ridley*

- 236** Programs for NRL Employees — Graduate Programs, Continuing Education, Professional Development, Equal Employment Opportunity (EEO) Programs, and Other Activities
- 238** Programs for Non-NRL Employees — Postdoctoral Research Associateships, Faculty Member Programs, Professional Appointments, and Student Programs
- 241** NRL Employment Opportunities

PROGRAMS FOR NRL EMPLOYEES

The NRL Human Resources Office (HRO) supports and provides traditional and alternative methods of training for employees. NRL employees are encouraged to develop their skills and enhance their job performance so they can meet the current and future needs of NRL and enhance their own personal development.

Long-Term Training and Developmental Programs

The **Advanced Graduate Research Program** enables selected professional employees to pursue collaborative research in their own field or a related field on a full-time basis for up to one year at an institution or research facility of their choice. Participants receive full pay and benefits. NRL pays all travel and moving expenses for the employee. Criteria for eligibility include professional stature consistent with the applicant's opportunities and experience, the ability and special aptitude for advanced training, and acceptance by the facility selected by the applicant. The program is open to employees who have completed six years of Federal service, four of which have been at NRL by the commencement of the program.

The **Edison Memorial Graduate Training Program** enables employees to pursue graduate-level work that may lead to a graduate degree at a local university. Participants in this program normally work 24 hours per week at the work site, while carrying an appropriate academic load of either graded, credited classes or dissertation research credits. The criteria for eligibility include a minimum of one year of Federal service at NRL by program commencement, a bachelor's degree in an appropriate field, professional stature consistent with the applicant's opportunities and experience, and the ability and special aptitude for advanced training.

The **Select Graduate Training Program** develops employees of exceptional talent by assisting them in full-time graduate study that may lead to the acquisition of a graduate degree at a facility of their choice within the continental United States. To be eligible for this program, employees must possess at least a bachelor's degree in an appropriate field, have completed at least one full year of Federal service at NRL by program commencement, and have demonstrated ability and aptitude for advanced training. Students accepted into this program receive one-half of their salary and one-half of their benefits. NRL pays for tuition and travel expenses.

The **Naval Postgraduate School (NPS)**, located in Monterey, California, provides graduate programs to enhance the technical preparation of Naval officers

and civilian employees who serve the Navy in the fields of science, engineering, operations analysis, and management. This program enables employees to pursue full-time graduate studies that may lead to the completion of a graduate degree. Thesis work will be accomplished at NRL. To be eligible for this program, employees must possess at least a bachelor's degree in an appropriate field and must have maintained at least a 3.0 GPA in undergraduate course work or previous graduate studies. Employees must also have completed at least two full years of Federal service at NRL, have demonstrated the ability and aptitude for advanced training, and have professional stature consistent with the applicant's opportunities and experience. Participants in the NPS program will continue to receive full pay and benefits during their periods of study. NRL also pays for tuition and travel expenses.

In addition to NRL and university offerings, applications may be submitted for a number of noteworthy Navy developmental programs. These and other fellowship programs are grade-specific, and the courses vary in length. A few examples of these opportunities are the **Aspiring Leader Program (ALP)**, **Defense Civilian Emerging Leader Program (DCELP)**, **Executive Leadership Development Program (ELDP)**, and the **Defense Senior Leader Development Program (DSLDP)**. Announcements for these programs are posted on the HRO web page as schedules are published.

Continuing Education

Undergraduate and graduate courses offered at local colleges and universities may be subsidized by NRL for employees interested in improving their skills and keeping abreast of current developments in their fields.

NRL offers **short courses** to all employees in a number of fields of interest, including administrative subjects and supervisory and management techniques. Laboratory employees may also attend these courses at nongovernment facilities. HRO advertises training opportunities on Pipeline, the HRO website, and in the email newsletter *HRO Highlights*.

For further information on any of the Long-Term Training, Leadership Development, and Continuing Education programs, contact the Employee Development and Management Branch (Code 1840) at (202) 767-8306 or via email at Training@hro.nrl.navy.mil.

The **Scientist-to-Sea Program (STSP)** provides opportunities for Navy R&D laboratory/center personnel to go to sea to gain firsthand insight into opera-

tional factors affecting system design, performance, and operations on a variety of ships. NRL is a participant in the program. When these opportunities become available from ONR, NRL divisions are informed to nominate candidates. For further information, call (202) 404-2701.

Professional Development

NRL has several programs, professional society chapters, and informal clubs that enhance the professional growth of employees. Some of these are listed below.

The NRL chapter of **Women In Science and Engineering (WISE)** was established to address current issues concerning the scientific community of women at NRL, such as networking, funding, work-life satisfaction, and effective use of our resources. We address these issues by empowering members through the establishment of a supportive and constructive network that serves as a sounding board to develop solutions that address said issues, and then serve as a platform in which members work together to implement solutions. Recently, WISE hosted Dr. Stephanie Tompkins of DARPA, Dr. Wen Masters of ONR, and a summer career panel with guest lecturer Dr. Brenda Little. The NRL WISE organization also provided feedback that led to an official NRL lactation policy and NRL's first-ever lactation room as well as support for adding more spaces and other improvements. Membership in WISE is open to all employees. For more information call (202) 767-9549.

Sigma Xi, The Scientific Research Society, encourages and acknowledges original investigation in pure and applied science. It is an honor society for research scientists. Individuals who have demonstrated the ability to perform outstanding research are elected to membership in local chapters. The NRL Edison Chapter, comprising approximately 200 members, recognizes exceptional research by presenting annual awards in pure and applied science to two outstanding NRL staff members per year. In addition, an award seeking to reward rising stars at NRL is presented annually through the Young Investigator Award. The chapter also sponsors several lectures per year at NRL on a wide range of topics of general interest to the scientific and DoD community. These lectures are delivered by scientists from all over the world. The highlight of the Sigma Xi Lecture Series is the Edison Memorial Lecture, which traditionally is given by an internationally distinguished scientist. Call (202) 767-0351.

The **NRL Mentor Program** was established to provide an innovative approach to professional and career training and an environment for personal and professional growth. It is open to permanent NRL

employees in all job series and at all sites. Mentees are matched with successful, experienced colleagues who have more technical or managerial experience and who can provide mentees with the knowledge and skills needed to maximize their contribution to their immediate organization, to NRL, the Navy, and their chosen career fields. The ultimate goal of the program is to increase job productivity, creativity, and satisfaction through better communication, understanding, and training. NRL Instruction 12400.1B provides policy and procedures for the program. For more information, please email mentor@hro.nrl.navy.mil or call (202) 767-8324.

Employees interested in developing effective self-expression, listening, thinking, and leadership potential are invited to join the NRL Forum Toastmasters Club, a chapter of **Toastmasters International**. Members of this club possess diverse career backgrounds and talents and learn to communicate not by rules but by practice in an atmosphere of understanding and helpful fellowship. NRL's Commanding Officer and Director of Research endorse Toastmasters. Call (202) 404-4670.

The **Department of the Navy Civilian Employee Assistance Program (DONCEAP)** provides confidential assessment, referral, and short-term counseling for employees (or their eligible family members) to help resolve personal concerns that otherwise might adversely affect job performance, such as challenging relationships (at work or home); dealing with stress, anxiety, or depression; grief and loss; or substance abuse. The DONCEAP also provides work/life referral services, such as "live" or on-demand webinars; discussion groups; and advice on parenting, wellness, financial and legal issues, education, and much more. Call (844) 366-2327, or visit <http://donceap.foh.hhs.gov>.

Equal Employment Opportunity (EEO) Programs

NRL provides equal employment opportunity (EEO) for all employees regardless of race, color, national origin, sex, religion, age, physical or mental disability, or genetic information. The NRL EEO Office is a service organization responsible for counseling employees to resolve employee/management conflicts, processing formal discrimination complaints and requests for reasonable accommodation, providing EEO training, and managing NRL's MD-715 and affirmative employment recruitment programs. The NRL EEO Office is also responsible for sponsoring special-emphasis programs to promote awareness and increase sensitivity and appreciation of the issues or the history relating to females, individuals with disabilities, and minorities. Contact the NRL Deputy EEO Officer at (202) 767-8390 for additional information on programs and services.

Other Activities

NRL's **Community Outreach Program** emphasizes STEM education. Managed by the Public Affairs Section of the Strategic Communication Office, the program is designed to inspire, engage, educate, and employ the next generation of scientists and educators. The robust program originated in response to our nation placing a high priority on STEM education and workforce development.

The NRL Community Outreach Program continues to grow many STEM initiatives aimed at K–12 and its primary audience of undergraduate, graduate, and post-doctoral students. At the K–12 level, the program partners with researchers to create STEM-inspired presentations that fit education lesson plans for hands-on activities. The program also reaches out to students in institutions of higher learning who are considering STEM careers, and fosters collaboration between colleges and universities and NRL researchers. Lecture series, STEM demonstrations, Q&As, digital engagements, and STEM competitions focused on the needs of the Navy are primary program drivers.

NRL volunteer mentors actively engage in judging science fairs, guiding science projects, and employing interns, and vigorously support STEM competitions. At the end of each year, an annual holiday party is held for DC-neighborhood schoolchildren. Through the Community Outreach Program, NRL has built active partnerships with several District of Columbia public schools. To find out how you can get involved, contact the STEM Outreach Coordinator at (202) 767-2541.

Other programs that enhance the development of NRL employees include sports groups and the **Amateur Radio Club**. The **NRL Fitness Center** at NRL-DC, managed by Naval Support Activity Washington Morale, Welfare and Recreation (NSAW-MWR), houses a fitness room with treadmills, bikes, ellipticals, step mills, and a full strength circuit; a gymnasium for basketball, volleyball, and other activities; and full locker rooms. The Fitness Center is free to NRL employees and contractors. NRL employees are also eligible to participate in all NSAW-MWR activities on Joint Base Anacostia–Bolling and Washington Navy Yard, less than five miles down the road from the NRL D.C. campus.

PROGRAMS FOR NON-NRL EMPLOYEES

Several programs have been established for non-NRL professionals. These programs encourage and support the participation of visiting scientists and engineers in research of interest to the Laboratory. Some of the programs may serve as stepping-stones to Federal careers in science and technology. Their two-fold objective is to enhance the quality of the Laboratory's research activities through working associations and interchanges with highly capable scientists and engineers and provide opportunities for outside scientists and engineers to work in the Navy laboratory environment. Along with enhancing the Laboratory's research, these programs acquaint participants with Navy capabilities and concerns, and may provide a path to full-time employment at NRL.

Postdoctoral Research Associateships

Every year, NRL hosts several postdoctoral research associates through the National Research Council (NRC) and American Society for Engineering Education (ASEE) postdoctoral associateship and fellowship programs. These competitive positions provide postdoctoral scientists and engineers with the opportunity to pursue research at NRL in collaboration with NRL scientists and engineers. Research associates are guest investigators, not employees of NRL.

NRL/NRC Cooperative Research Associateship Program: The National Research Council conducts a national competition to recommend and make awards to outstanding scientists and engineers at recent postdoctoral levels for tenure as guest researchers at participating laboratories. The objectives of the NRC program are (1) to provide postdoctoral scientists and engineers of unusual promise and ability opportunities for research on problems, largely of their own choice, that are compatible with the interests of the sponsoring laboratories and (2) to contribute thereby to the overall efforts of the Federal laboratories. The program provides an opportunity for concentrated research in association with selected members of the permanent professional laboratory staff, often as a climax to formal career preparation.

NRL/NRC Postdoctoral Associateships are awarded to individuals who have held a doctorate less than five years at the time of application. The awards are made initially for one year, renewable for a second and possible third year. Information and applications may be found at <http://www.national-academies.org/rap>. To contact NRL's program coordinator, call (202) 767-8323 or email nrc@hro.nrl.navy.mil.

NRL/ASEE Postdoctoral Fellowship Program: The ASEE program is designed to significantly increase

the involvement of creative and highly trained scientists and engineers from academia and industry in scientific and technical areas of interest and relevance to the Navy. Fellowship awards are based upon the technical quality and relevance of the proposed research, recommendations by the Navy laboratory, academic qualifications, reference reports, and availability of funds.

NRL/ASEE Fellowship awards are made to individuals who have held a doctorate for less than five years at the time of application. The awards are made for one year, renewable for a second and possible third year. Information and applications may be found at <http://www.asee.org/nrl/>. To contact NRL's program coordinator, call (202) 767-8323 or email asee@hro.nrl.navy.mil.

Faculty Member Programs

The **Office of Naval Research Summer Faculty Research and Sabbatical Leave Program** provides opportunities for university faculty members to work for 10 weeks (or longer, for those eligible for sabbatical leave) with professional peers in participating Navy laboratories on research of mutual interest. Applicants must hold a teaching or research position at a U.S. college or university. Contact NRL's program coordinator at sfrp@hro.nrl.navy.mil.

The **NRL/United States Naval Academy Cooperative Program for Scientific Interchange** allows faculty members of the U.S. Naval Academy (USNA) to participate in NRL research. This collaboration benefits the Academy by providing the opportunity for USNA faculty members to work on research of a more practical or applied nature. In turn, NRL's research program is strengthened by the available scientific and engineering expertise of the USNA faculty. Contact NRL's program coordinator at usna@hro.nrl.navy.mil.

Professional Appointments

Faculty Member Appointments use the special skills and abilities of faculty members for short periods to fill positions of a scientific, engineering, professional, or analytical nature at NRL.

Consultants and experts are employed because they are outstanding in their fields of specialization or because they possess ability of a rare nature and could not normally be employed as regular civil servants.

Intergovernmental Personnel Act Appointments temporarily assign personnel from state or local governments or educational institutions to the Federal government (or vice versa) to improve public services rendered by all levels of government.

Student Programs

The student programs are tailored to high school, undergraduate, and graduate students to provide employment opportunities and work experience in naval research.

The **Naval Research Enterprise Intern Program (NREIP)** is a 10-week summer research opportunity for undergraduate sophomores, juniors, and seniors, and graduate students. The Office of Naval Research (ONR) offers summer appointments at Navy laboratories to current college sophomores, juniors, seniors, and graduate students from participating schools. Application is online at www.asee.org/nreip through the American Society for Engineering Education. Electronic applications are sent for evaluation to the point of contact at the Navy laboratory identified by the applicant. Contact NRL's program coordinator at nreip@nrl.navy.mil.

The **National Defense Science and Engineering Graduate Fellowship Program** helps U.S. citizens obtain advanced training in disciplines of science and engineering critical to the U.S. Navy. The three-year program awards fellowships to recent outstanding graduates to support their study and research leading to doctoral degrees in specified disciplines such as electrical engineering, computer sciences, material sciences, applied physics, and ocean engineering. Award recipients are encouraged to continue their study and research in a Navy laboratory during the summer. Contact NRL's program coordinator at (202) 404-7450 or ndseg@hro.nrl.navy.mil.

The **Pathways Intern Program** (formerly STEP and SCEP) provides students enrolled in a wide variety of educational institutions, from high school to graduate level, with opportunities to work at NRL and explore Federal careers while still in school and while getting paid for the work performed. Students can work full-time or part-time on a temporary or non-temporary appointment. Students must be continuously enrolled on at least a half-time basis at a qualifying educational institution and be at least 16 years of age. The primary focus of our **Non-temporary** intern appointment is to attract students enrolled in undergraduate and graduate programs in engineering, computer science, or the physical sciences. Students on non-temporary appointments are eligible to remain on their appointment until graduation and may be noncompetitively converted to a permanent appointment within 120 days after completion of degree requirements. Conversion is not guaranteed. Conversion is dependent on work performance, completion of at least 640 hours of work under the intern appointment before completion of degree requirements, and meeting the qualifications for the position. The **Temporary** intern appointment is initially a one-year appointment. This program enables students to earn a salary while continuing their studies and offers them valuable work experience. NRL's Pathways Intern Program opportunities are announced on USAJOBS four times per year. Visit USA-

JOBS at <https://www.usajobs.gov/> to create an account, search for jobs, set up an email notification alert of when positions of interest are posted (see “Saved Searches”), and apply for our intern opportunities when they are posted. For additional information on NRL’s Intern Program, visit http://hroffice.nrl.navy.mil/student/student_only.asp or call (202) 767-8313.

The **STEM Student Employment Program (SSEP)** provides paid employment opportunities for undergraduate and graduate degree-seeking students enrolled in scientific, technical, engineering, or mathematics majors. Appointments are made to Science and Engineering Professional (NP) or Science and Engineering Technical (NR) career track positions in the competitive service. Appointments can be temporary (NTE 1 year), term (no more than 4 years), or flexible length appointments that expire 120 days after completion of the academic course of study. Upon completion of the degree program, SSEP participants may be noncompetitively converted to permanent NP career track positions, provided the OPM science and engineering qualification requirements are met and the candidate is otherwise eligible. Applicants for NP career track positions must have at least a 3.0 GPA, and applicants for NR career track positions must have at least a 2.5 GPA. Applications are accepted year-round. For additional information, visit https://hroffice.nrl.navy.mil/student/pdf/STEM_StudentDirectHire.pdf.

The **Department of Defense Science and Engineering Apprenticeship Program (SEAP)** provides an opportunity for high school students, who have completed at least grade 9 and are at least 15 years of age, to serve as junior research associates. Under the direction of a mentor, for eight weeks in the summer, students gain a better understanding of research — its challenges and its opportunities — through participation in scientific, engineering, and mathematics programs. Criteria for eligibility are based on science and mathematics courses completed and grades achieved; scientific motivation, curiosity, and the capacity for sustained hard work; a desire for a technical career; teacher recommendations; and exceptional test scores. The NRL program is the largest in the Department of Defense. For detailed information, visit <https://seap.asee.org/>, email seap@hro.nrl.navy.mil, or call (202) 767-8324.

The **Summer Research Program for Historically Black College or University (HBCU) or Minority Institution (MI)** is a 10-week summer internship program that provides opportunities for undergraduate and graduate students to participate in research under the guidance of a mentor at NRL. Preference is given to students planning careers in science, technology, engineering, and mathematics (STEM) disciplines. Applicants must be U.S. citizens or have permanent residency and be enrolled at an HBCU, MI, or Tribal College or University. Participating students receive a stipend. Information and application materials are available online at the TWCIAAS-NRL

HBCU Information Page. Online applications can be found at <http://nrl.e.twc.edu/>.

Volunteer Opportunities

The **Student Volunteer Program** helps students gain valuable experience by allowing them to voluntarily perform educationally related work at NRL. It provides exposure to the work environment and also provides an opportunity for students to make realistic decisions regarding their future careers. Applications are accepted year-round. For additional information, visit http://hroffice.nrl.navy.mil/student/student_only.asp or call (202) 767-8313.

NRL EMPLOYMENT OPPORTUNITIES

for Highly Innovative, Motivated, and Creative Professionals

NRL offers a wide variety of challenging S&T positions that involve skills from basic and applied research to equipment development. The nature of the research and development conducted at NRL requires professionals with experience. Typically there is a continuing need for electronics, mechanical, aerospace, and materials engineers, metallurgists, computer scientists, and oceanographers with bachelor's and/or advanced degrees and physical and computer scientists with Ph.D. degrees.

■ **Biologists.** Biologists conduct research in areas that include biosensor development, tissue engineering, molecular biology, genetic engineering, proteomics, and environmental monitoring.

■ **Chemists.** Chemists are recruited to work in the areas of combustion, polymer science, bioengineering and molecular engineering, surface science, materials synthesis, nanostructures, corrosion, fiber optics, electro-optics, microelectronics, electron device technology, and laser physics.

■ **Electronics Engineers and Computer Scientists.** These employees may work in the areas of communications systems, electromagnetic scattering, electronics instrumentation, electronic warfare systems, radio frequency/microwave/millimeter-wave/infrared technology, radar systems, laser physics technology, radio-wave propagation, electron device technology, spacecraft design, artificial intelligence, information processing, signal processing, plasma physics, vacuum science, microelectronics, electro-optics, fiber optics, solid-state physics, software engineering, computer design/architecture, ocean acoustics, stress analysis, and expert systems.

■ **Materials Scientists/Engineers.** These employees are recruited to work on materials, microstructure characterization, electronic ceramics, solid-state physics, fiber optics, electro-optics, microelectronics, fracture mechanics, vacuum science, laser physics and joining technology, and radio frequency/microwave/millimeter-wave/infrared technology.



■ **Mechanical and Aerospace Engineers.** These employees may work in areas of spacecraft design, remote sensing, propulsion, experimental and computational fluid mechanics, experimental structural mechanics, solid mechanics, elastic/plastic fracture mechanics, materials, finite-element methods, nondestructive evaluation, characterization of fracture resistance of structural alloys, combustion, CAD/CAM, and multifunctional material response.

■ **Oceanographers, Meteorologists, and Marine Geophysicists.** These employees work in the areas of ocean and atmospheric dynamics, air-sea interaction, upper-ocean dynamics, oceanographic bio-optical modeling, oceanic and atmospheric numerical modeling and prediction, data assimilation and data fusion, retrieval and application of remote sensing data, benthic processes, aerogeophysics, marine sedimentary processes, advanced mapping techniques, atmospheric physics, and remote sensing. Oceanographers and marine geophysicists are located in Washington, DC, and at the Stennis Space Center, Bay St. Louis, Mississippi. Meteorologists are located in Washington, DC, and Monterey, California.

■ **Physicists.** Physics graduates may concentrate on such fields as materials, solid-state physics, fiber optics, electro-optics, microelectronics, vacuum science, plasma physics, fluid mechanics, signal processing, ocean acoustics, information processing, artificial intelligence, electron device technology, radio-wave propagation, laser physics, ultraviolet/X-ray/gamma-ray technology, electronic warfare, electromagnetic interaction, communications systems, radio frequency/microwave/millimeter-wave/infrared technology, computational physics, radio and high-energy astronomy, solar physics, and space physics.

For more information and current vacancy listings,
visit <http://www.nrl.navy.mil/careers>.

- 244** Technical Output
- 245** Key Personnel
- 246** Contributions by Divisions, Laboratories, and Departments
- 249** Subject Index
- 251** Author Index
- 252** Map/Quick Reference Telephone Numbers

TECHNICAL OUTPUT

The Navy continues to be a leader in initiating new developments and applying these advancements to military requirements. The primary method of informing the scientific and engineering community of the advances made at NRL is through the Laboratory's technical output — reports, articles in scientific journals, contributions to books, papers presented to scientific societies and topical conferences, patents, and inventions.

The figures for calendar year 2017 presented below represent the output of NRL facilities in Washington, D.C.; Bay St. Louis, Mississippi; and Monterey, California.

In addition to the output listed, NRL scientists made 1484 oral presentations during 2017.

<u>Type of Contribution</u>	<u>Unclassified</u>	<u>Classified</u>	<u>Total</u>
Articles in periodicals, chapters in books, and papers in published proceedings	1236*	0	1236*
NRL Formal Reports	3	3	6
NRL Memorandum Reports	42	2	44
Books	2	0	2
U.S. patents granted	115	1	116
Foreign patents granted	14		14
U.S. Trademark Registrations	1		1

*This is a provisional total based on information available to the Ruth H. Hooker Research Library on February 13, 2018. Additional publications carrying a 2017 calendar year publication date are anticipated. Total includes refereed and nonrefereed publications.

KEY PERSONNEL

Area Code (202) unless otherwise listed
 Personnel Locator - 767-3200
 DSN-297 or 754

Code	Office	Phone Number
EXECUTIVE DIRECTORATE		
1000	Commanding Officer	767-3403
1000.1	Inspector General	404-3309
1000.2	Deputy EEO Officer	767-5264
1001	Director of Research	767-3301
1001.1	Executive Assistant for the Director of Research	767-2445
1002	Executive Officer	767-3621
1004	Head, Technology Transfer Office	767-3083
1006	Head, Office of Program Administration and Policy Development	767-3091
1008	Office of Counsel	767-2244
1030	Head, Strategic Communication Office	404-3322
1100	Director, Institute for Nanoscience	767-3261
1200	Head, Command Support Division	404-1004
1220	Head, Information Assurance and Communications Security	767-0213
1400	Head, Military Support Division	767-2273
1600	Commander, Scientific Development Squadron One	301-342-3751
1700	Director, Laboratory for Autonomous Systems Research	767-2684
1800	Director, Human Resources Office	767-3421
1900	Head, Office of the Command Information Officer	767-9225
3005	Deputy for Small Business	767-6263
3540	Head, Safety Branch	767-2232
BUSINESS OPERATIONS DIRECTORATE		
3000	Associate Director of Research	767-2371
3200	Head, Contracting Division	767-5227
3300	Head, Financial Management Division (Comptroller)	767-3405
3400	Head, Supply and Administration Services Division	767-3446
3500	Director, Research and Development Services Division	404-4054
SYSTEMS DIRECTORATE		
5000	Associate Director of Research	767-3425
5300	Superintendent, Radar Division	404-2700
5500	Superintendent, Information Technology Division/NRL Command Information Officer*	767-2903
5600	Superintendent, Optical Sciences Division	767-7375
5700	Superintendent, Tactical Electronic Warfare Division	767-6278
MATERIALS SCIENCE AND COMPONENT TECHNOLOGY DIRECTORATE		
6000	Associate Director of Research	767-3566
6040	Director, Laboratories for Computational Physics and Fluid Dynamics	767-2402
6100	Superintendent, Chemistry Division	767-3026
6300	Superintendent, Materials Science and Technology Division	767-2926
6700	Superintendent, Plasma Physics Division	767-2723
6800	Superintendent, Electronics Science and Technology Division	767-3693
6900	Director, Center for Bio/Molecular Science and Engineering	404-6000
OCEAN AND ATMOSPHERIC SCIENCE AND TECHNOLOGY DIRECTORATE		
7000	Associate Director of Research	404-8690
7100	Superintendent, Acoustics Division	767-3482
7200	Superintendent, Remote Sensing Division	767-3391
7300	Superintendent, Oceanography Division	228-688-4670
7400	Superintendent, Marine Geosciences Division	228-688-4650
7500	Superintendent, Marine Meteorology Division	831-656-4721
7600	Superintendent, Space Science Division	767-6343
NAVAL CENTER FOR SPACE TECHNOLOGY		
8000	Director	767-6547
8100	Superintendent, Space Systems Development Department	767-0410
8200	Superintendent, Spacecraft Engineering Department	404-3727

*Additional Duty

CONTRIBUTIONS BY DIVISIONS, LABORATORIES, AND DEPARTMENTS

Radar Division

- 141 NexGen High Frequency Surface Wave Radar (NG-HFSWR)
G. San Antonio and T. Moskov
- 188 Automatic Target Recognition of Small Craft using Multichannel Imaging Radar
R.G. Raj, D.W. Baden, R.D. Lipps, R.W. Jansen, R. Madden, R.S. DeOcampo, M.A. Sletten, and D. Tahmoush
- 192 A Multi-Channel Testbed for Next-Generation Maritime SAR Systems
M.A. Sletten, J. Jakobosky, T. Higgins, and R. Jansen

Information Technology Division

- 78 Safely Measuring Tor
R. Jansen and A. Johnson
- 146 Goal Reasoning for AUV Control
D.W. Aha, M.A. Wilson, J. McMahon, A. Wolek, and B. Houston
- 147 The Application of Complex Network Analytics to Dynamic Wireless Network Systems
J. Macker, B. Abamson, J. Dean, and J. Weston
- 149 Navy Malware Catalog
J. Mathews

Optical Sciences Division

- 84 Quantum Memories Based on Optically Trapped Neutral Atoms
M. Bashkansky, A. Black, T. Akin, M. Piotrowicz, A. Kuzmich, and J. Reintjes
- 180 Waveguides for Non-Mechanical Beam Steering in the Mid-Wave Infrared
J.D. Myers, J.A. Frantz, C.M. Spillman, R.Y. Bekele, L.B. Shaw, J. Naciri, J.S. Kolacz, H. Gotjen, M. Pauli, C. Dunay, D. Burchick, J. Auxier, and J.S. Sanghera
- 182 Optical System Protection Using Pupil-Plane Phase Masks
A.T. Watnik, K. Novak, M. DePrenger, J. Wirth, and G.A. Swartzlander, Jr.

- 183 Simultaneous Optical Beamforming for Phased-Array Applications
J.D. McKinney, M.R. Hyland, R.C. Duff, and K.J. Williams

- 164 Novel Active Tuning for Infrared Photonics
A.D. Dunkelberger, C.T. Ellis, D.C. Ratchford, A.J. Giles, M. Kim, C.S. Kim, B.T. Spann, I. Vurgaftman, J.G. Tischler, J.C. Owrutsky, and J.D. Caldwell

Tactical Electronic Warfare Division

- 130 Reshaping Antenna Patterns Using Metasurface Radomes
B. Raeker and S. Rudolph
- 132 NRL Participates in NATO Electronic Warfare Trial
A. Allegrezza and C. Maraviglia
- 156 Modular Hydrogen Fuel Cells
B. Gould, J. Rodgers, M. Schuette, R. Ramamurti, and K. Swider-Lyons

Chemistry Division

- 164 Novel Active Tuning for Infrared Photonics
A.D. Dunkelberger, C.T. Ellis, D.C. Ratchford, A.J. Giles, M. Kim, C.S. Kim, B.T. Spann, I. Vurgaftman, J.G. Tischler, J.C. Owrutsky, and J.D. Caldwell
- 124 From the Depths of the Marine Dark Biosphere
L. Fitzgerald, D. Harodas, Y. Maezato, J. Biffinger, T. Boyd, L. Hamdan, J. Lee, and B. Little
- 156 Modular Hydrogen Fuel Cells
B. Gould, J. Rodgers, M. Schuette, R. Ramamurti, and K. Swider-Lyons

Laboratories for Computational Physics and Fluid Dynamics

- 198 Advances in Simulation Technologies to Reduce Noise from Supersonic Military Aircraft Jets
K. Kailasanath, A. Corrigan, J. Liu, R. Ramamurti, K. Viswanath, and R. Johnson

Materials Science and Technology Division

- 156 Modular Hydrogen Fuel Cells
B. Gould, J. Rodgers, M. Schuette, R. Ramamurti, and K. Swider-Lyons
- 157 Microstructures and Properties of As-Cast AlCrFeMnV, AlCrFeTiV, and AlCrMnTiV High Entropy Alloys
K.E. Knipling, P. Narayana, and L.T. Nguyen
- 134 Magnetoelectric Microbeam Resonators for Magnetic Field Sensing
S.P. Bennett, M. Staruch, B.R. Matis, J.W. Baldwin, K. Bussmann, D. Goldstein, and P. Finkel
- 139 Normally-Off AlGaIn/GaN MOS-HEMTs with Record Performance
T.J. Anderson, V.D. Wheeler, M.J. Tadjer, K.D. Hobart, and C.R. Eddy, Jr.

Plasma Physics Division

- 137 Intense Laser Driven Ion Accelerator
M.H. Helle, D.F. Gordon, D. Kaganovich, Y. Chen, J.P. Palaastro, and A. Ting
- 201 Kr Plasmas on the Z and NIF Facilities
A. Dasgupta, R.W. Clark, N.D. Quart, and J.L. Giuliani
- 160 Non-Thermal X-ray Production from an Array of Non-Interacting, Magnetically-Imploded Wires
B.V. Weber, J.T. Engelbrecht, S.L. Jackson, D. Mosher, R.J. Comisso, D.G. Phipps, N. Qi, and J. Levine
- 210 Mitigation of Spacecraft Communications Blackout via Microparticle Injection
E.D. Gillman and W.E. Amatucci

Electronics Science and Technology Division

- 91 3D Printing and Electroforming for Millimeter-Wave Vacuum Electronics
A.M. Cook, C.D. Joye, J.P. Calame, and F.K. Perkins
- 164 Novel Active Tuning for Infrared Photonics
A.D. Dunkelberger, C.T. Ellis, D.C. Ratchford, A.J. Giles, M. Kim, C.S. Kim, B.T. Spann, I. Vurgaftman, J.G. Tischler, J.C. Owrutsky, and J.D. Caldwell

Center for Bio/Molecular Science and Engineering

- 125 Shark Antibodies Make a Splash
G. Anderson, D. Zabetakis, J. Liu, and E. Goldman
- 166 Opening a New Window into Nanoparticle Toxicity
E. Oh, R. Liu, M. Bilal, Y. Cohen, and I.L. Medintz
- 173 Successful Self-Embedment of a Large Benthic Microbial Fuel Cell Anode
J.W. Book, L.M. Tender, J.P. Golden, J.R. Dale, A.J. Quaid, I.R. Martens, and S.B. Engel

Acoustics Division

- 146 Goal Reasoning for AUV Control
D.W. Aha, M.A. Wilson, J. McMahon, A. Wolek, and B.H. Houston
- 134 Magnetoelectric Micro-beam Resonators for Magnetic Field Sensing
S.P. Bennett, M. Staruch, B.R. Matis, J.W. Baldwin, K. Bussmann, D. Goldstein, and P. Finkel
- 108 Impulsive Noise Mitigation of Fire Suppression Systems
P.C. Herdic, W.G. Szymczak, B.H. Houston, and J. Vignola
- 110 Understanding the Influence of Disorder in Atomically Thin Materials
B.R. Matis, B.H. Houston, and J.W. Baldwin
- 113 A Mixture Theory Based Approach to Poroacoustics
P.M. Jordan

Remote Sensing Division

- 188 Automatic Target Recognition of Small Craft using Multichannel Imaging Radar
R.G. Raj, D.W. Baden, R.D. Lipps, R.W. Jansen, R. Madden, R.S. DeOcampo, M.A. Sletten, and D. Tahmouh
- 190 Dust-Infused Baroclinic Cyclone Storm Clouds
M. Fromm, G.P. Kablick, III, and P. Caffrey
- 192 A Multi-Channel Testbed for Next-Generation Maritime SAR Systems
M.A. Sletten, J. Jakabosky, T. Higgins, and R. Jansen
- 170 Parameterization of Whitecap Fraction Based on Satellite Observations
M.D. Anguelova, M.F.M.A. Albert, and G. de Leeuw

- 116 Understanding Intense Pyroconvection and its Impacts
D.A. Peterson, M.D. Fromm, E.J. Hyer, J.R. Campbell, M.L. Surratt, and J.E. Solbrig

Oceanography Division

- 124 From the Depths of the Marine Dark Biosphere
L. Fitzgerald, D. Harodas, Y. Maezato, J. Biffinger, T. Boyd, L. Hamdan, J. Lee, and B. Little
- 173 Successful Self-Embedment of a Large Benthic Microbial Fuel Cell Anode
J.W. Book, L.M. Tender, J.P. Golden, J.R. Dale, A.J. Quaid, I.R. Martens, and S.B. Engel
- 175 What is the Impact of Light on Ocean Primary Production and Hypoxia?
R. W. Gould, Jr., B. Penta, D.S. Ko., J.C. Lehrter, L. Lowe, I. Schulman, S.D. Ladner, and J.D. Hagy

Marine Geosciences Division

- 173 Successful Self-Embedment of a Large Benthic Microbial Fuel Cell Anode
J.W. Book, L.M. Tender, J.P. Golden, J.R. Dale, A.J. Quaid, I.R. Martens, and S.B. Engel
- 151 Predicting Academic Attrition in Naval Air Traffic Control Training
N.L. Bowen, D. Smith, T. Olson, and C. Moclair

Marine Meteorology Division

- 116 Understanding Intense Pyroconvection and its Impacts
D.A. Peterson, M.D. Fromm, E.J. Hyer, J.R. Campbell, M.L. Surratt, and J.E. Solbrig
- 118 Seeding the Wave Guide
J.D. Doyle, C.A. Reynolds, and S.D. Eckermann
- 203 Supporting Weather Forecasters in Predicting and Monitoring Saharan Air Layer Dust Events as They Impact the Greater Caribbean
A.P. Kuciauskas, P. Xian, E.J. Hyer, M.I. Oyola, and J.R. Campbell
- 120 Aerosol and Cloud Research in the South China Sea
J.S. Reid, E.J. Hyer, P. Xian, J.R. Campbell, E.A. Reid, A. Bucholtz, and A.L. Walker

Space Science Division

- 99 From Sensor Idea to Satellite Instrument
C.R. Englert, C.M. Brown, K.D. Marr, and J.M. Harlander
- 118 Seeding the Wave Guide
J.D. Doyle, C.A. Reynolds, and S.D. Eckermann
- 211 LASCO: Pioneer of Space Weather
R. Colaninno, R. Howard, and S. Plunkett
- 213 Slim-Edged Silicon Detectors: Advanced Nano-Fabrication Technology
M. Christophersen, B.F. Philips, V. Fadeyev, and H.F.W. Sadrozinski
- 215 Solar Coronal Power Spectra Modeling
K. Battams, R.S. Weigel, and B.M. Gallagher

Spacecraft Engineering Department

- 205 Reactive Flow Modeling for Hypersonic Flight
G.B. Goodwin and E.S. Oran

SUBJECT INDEX

- 3D printing, 91
- 3D X-ray Computed Microtomography facility, 45
- Accelerator Mass Spectrometry Facility, 45
- Acoustic modeling, 113
- Acoustic Reverberation Simulation Facility, 67
- Acoustics Division, 52
- Acoustics, 198
- Active tuning, 164
- Adaptive beamforming, 141
- Administrative Services, 69
- Advanced Graduate Research Program, 236
- Advanced Thin Films Laboratory, 36
- Advanced Two Phase Heat Transfer Facility, 67
- Aerosol indirect effect, 190
- Aerosol, 116, 120
- Air quality, 203
- Air-sea fluxes, 170
- ALD dielectrics, 139
- Amateur Radio Club, 238
- Anechoic chamber, 38
- Antenna, 130
- Antibody engineering, 125
- Artificial intelligence, 146
- Atom probe tomography, 157
- Atomic Target Recognition (ATR), 188
- Atomically thin materials, 110
- Autonomous underwater vehicle (AUV), 146
- Battery Laboratory, 67
- Benthic microbial fuel cell, 173
- Bio-aerosol containment chamber, 37
- Biothreat detection, 125
- Bipolar plates, 156
- Blossom Point Tracking Facility, 65, 74
- Bulk Materials Fabrication Facility, 45
- Cameca atom probe, 44
- Center for Bio/Molecular Science and Engineering, 50
- Central Target Simulation Facility, 39
- Chemistry Division, 42
- Chesapeake Bay Detachment (CBD), 61
- Chesapeake Bay Detachment LaserComm Test Facility (LCTF), 65
- Climate, 116, 120
- Cloud, 190
- Cognitive aptitude, 151
- Cold atoms, 84
- Combustion, 205
- Communications blackout, 210
- Community Outreach Program, 238
- Complex networks, 147
- Complex plasma, 210
- Compound Semiconductor Processing Facility (CSPF), 48
- Computing, 198
- Contracting Division, 68
- Coronal mass ejections, 211
- Coronagraph, 211
- Corrosion, 124
- Coupled Ocean-Atmosphere Mesoscale Prediction System (COAMPS), 61
- CT-Analyst, 14, 40
- CyberSecurity, 149
- Dark biosphere, 124
- Data analysis, 215
- Department of Defense Science and Engineering Apprenticeship Program (SEAP), 240
- Department of the Navy Civilian Employee Assistance Program (DONCEAP), 237
- Diabatic processes, 118
- Differential privacy, 78
- Digital forensics, 149
- Directed energy, 182
- Disorder, 110
- Dust storms, 203
- Dynamic Spectrum Access Laboratory, 34
- Ebola virus, 125
- Ecological modeling, 175
- Edison Memorial Graduate Training Program, 236
- Electrical, Magnetic, and Optical Measurement Facility, 45
- Electromagnetic Maneuver Warfare Testbed, 32
- Electron backscattered diffraction, 157
- Electronic Attack Technique Evaluation System (EATES), 39
- Electronics Science and Technology Division, 48
- Embedment, 173
- Epicenter, 48
- Financial Management Division, 68
- Fire, 116
- Fluid dynamics, 205
- Focal plane arrays, 213
- Free Surface Hydrodynamics Laboratory (FSHL), 55
- Fuel cells, 156
- GaN, 139
- Goal reasoning, 146
- Goal-driven autonomy, 146
- Gravity Offset Table (GOT), 67
- Haas VM-3 Vertical Machining Center, 42
- HBCU/MI Program, 20
- HICO/RAIDS Experiment Payload (HREP), 54
- High entropy alloys, 157
- High frequency surface wave radar, 141
- High intensity laser-plasma interactions, 137
- Hypersonics, 205
- Hypoxia, 175
- Image processing, 182
- Impulsive fire suppression, 108
- Information Technology Division, 34
- Infrared photonics, 164
- Infrared, 180
- Institute for Nanoscience, 28
- Joint Maritime Test Facility (JMTF), 75
- Laboratories for Computational Physics and Fluid Dynamics, 40
- Laboratory for Advanced Materials Synthesis, 48
- Laboratory for Autonomous Systems Research, 30
- Laminar Flow Clean Room, 67
- Large Angle Spectrometric and Coronagraph Telescope (LASCO), 63
- Laser-driven ion acceleration, 137
- Laser-induced magnetic fields in plumes, 137
- Laser, 182
- Lidar, 58
- Liquid crystal, 180
- Magnetic field sensor, 134
- Magnetolectric, 134
- Malware, 149
- Marine Corrosion Facility, 75
- Marine Geosciences Division, 58
- Marine Meteorology Division, 60
- Mass transport, 203
- Material Science and Technology Division, 44
- MEMS resonator, 134
- Meta analysis, 166
- Metasurface, 130
- Meteorology, 116, 120
- Micro/Nanostructure Characterization Facility, 45
- Microbes, 124
- Microfabrication, 91
- Microwave Atmospheric Spectroscopy Laboratory (MASL), 55
- Microwave photonics, 183
- Mid-wave Infrared (MWIR), 180
- Midway Research Center (MRC), 65, 73
- Millimeterwave, 91
- Mineral dust, 190
- Model of attrition, 151
- Molecular beam epitaxy system, 37
- Monterey (NRL-MRY), 71
- Mooring, 173
- Multi-keV X-rays, 201
- Multichannel SAR (MSAR), 188
- Multiferroic, 134
- Nanoparticle, 166
- Nanoscience, 166
- Nanotechnology, 166

National Defense Science and Engineering Graduate Fellowship Program, 239
 NATO Electronic Warfare Trial, 132
 Naval Electromagnetic Operations Trial (NEMO), 132
 Naval Postgraduate School (NPS), 236
 Naval Research Enterprise Intern Program (NREIP), 239
 Navy Cyber Defense Research Laboratory, 35
 Navy Global Environmental Model (NAVGEM), 60
 Navy Technology Center for Safety and Survivability, 61
 Network security, 149
 Nike target chamber, 47
 Noise mitigation, 108
 Noise, 198
 Non-LTE kinetics, 201
 Non-mechanical beam steering, 180
 Non-thermal radiation, 160
 Nonlinear waves, 113
 NRL Fitness Center, 238
 NRL Mentor Program, 237
 NRL/ASEE Postdoctoral Fellowship Program, 239
 NRL/NRC Cooperative Research Associateship Program, 238
 NRL/United States Naval Academy Cooperative Program for Scientific Interchange, 239
 Numerical simulation, 198
 Numerical weather prediction, 118
 Ocean Dynamics and Prediction Computational Network Facility, 56
 Ocean imaging, 192
 Ocean primary production, 175
 Ocean-atmosphere coupling, 170
 Oceanography Division, 56
 Octavia, 35
 Office of Naval Research Summer Faculty Research and Sabbatical Leave Program, 239
 Onion routing, 78
 Operational forecasting, 203
 Optical beamforming, 183
 Optical Sciences Division, 36
 Optical vortex, 182
 Oversampled arrays, 141
 Pathways Intern Program, 239
 Phased arrays, 183
 Plasma Physics Division, 46
 Plasma radiation sources, 201
 Plasma-beam interactions, 137
 Plasma, 210
 Pomonkey Facility, 74
 Poroacoustics, 113
 Power switches, 139
 Precision Clock Evaluation Facility (PCEF), 65
 Predictability, 118
 Predictive analytics, 147
 Private data publishing, 78
 Proximity Operations Testbed (POT), 67
 Pyroconvection, 116
 Quantum dot, 166
 Quantum memory, 84
 Radar Division, 32
 Radar Range facility, 61
 Radiation pattern synthesis, 130
 Random forest, 166
 Remote Sensing Division, 54
 Remote sensing, 116
 Renewable energy, 173
 Research and Development Services Division, 68
 Ruth H. Hooker Research Laboratory, 69
 S-band Waveform Development Testbed, 33
 Satellite instruments, 99
 Scene Exploitation and Analysis Laboratory (SEALAB), 55
 Scientific Development Squadron ONE (VXS-1), 72
 Scientist-to-Sea Program (STSP), 236
 Secure communication, 84
 Secure computation, 78
 Select Graduate Training Program, 236
 Selection and screening, 151
 Semiconductor radiation detectors, 213
 SEPTR, 56
 Shark technology, 125
 Shipboard Lidar Optical Profiler, 57
 Shipwrecks, 124
 Sigma Xi, 237
 Single domain antibody, 125
 Single wire, 160
 Slim edges, 213
 Solar corona, 215
 Solar Coronagraph Optical Test Chamber (SCOTCH), 62
 Solar physics, 215
 South China Sea, 120
 Space Physics Simulation Chamber, 46
 Space Science Division, 62
 Space Systems Development Department, 64
 Space weather, 211
 Spacecraft Engineering Department, 66
 Spacecraft Robotics Engineering and Controls Laboratory, 66
 Spectroscopy, 99
 Spin Test Facility, 67
 Static Loads Test Facility, 67
 STEM Program, 240
 STEM Student Employment Program (SSEP), 240
 Stennis Space Center (NRL-SSC), 71
 Student Volunteer Program, 240
 Summer Research Program for Historically Black College or University (HBCU) or Minority Institution (MI), 240
 Sun-Earth Connection Coronal Heliospheric Investigation (SECCHI), 63
 Supersonic jets, 198
 Surface-phonon polariton, 164
 Synthetic aperture radar, 192
 Tactical Electronic Warfare Division, 38
 Tactical wireless communications, 147
 Technical Information Services, 68
 Technology Transfer Office, 68
 Thermal Fabrication and Test Facility, 67
 Thermal Vacuum Test Facility, 67
 Thin film heterostructure, 134
 Thin-Film Materials Synthesis and Processing Facility, 45
 Toastmasters International, 237
 Toxicity, 166
 Trace Explosives Sensor Testbed, 43
 Trace Vapor Generator for Explosives and Narcotics, 43
 Track-before-detect, 141
 Transparent Armor, 16
 Transport, 110
 Two-dimensional arrays, 141
 Underwater autonomous vehicles (UAVs), 156
 Upper atmosphere wind, 99
 Vacuum electronics, 91
 Vacuum Ultraviolet Solar Instrument Test (SIT) facility, 62
 Vibration Test Facility, 67
 VXS-1, 16
 Waveguide, 180
 Whitecap fraction, 170
 Whitecaps, 170
 Women in Science and Engineering (WISE), 237
 ZrO₂, 139

AUTHOR INDEX

- Adamson, B., 147
Aha, D.W., 146
Akin, T.G., 84
Albert, M.F.M.A., 170
Allegrezza, A., 132
Amatucci, W.E., 210
Anderson, G.P., 125
Anderson, T.J., 139
Anguelova, M.D., 170
Auxier, J., 180
Baden, D.W., 188
Baldwin, J.W., 110, 134
Bashkansky, M., 84
Battams, K., 215
Bekele, R.Y., 180
Bennett, S.P., 134
Biffinger, J., 124
Bilal, M., 166
Black, A.T., 84
Book, J.W., 173
Boyd, T., 124
Brown, C.M., 99
Brown, N.L., 151
Bucholtz, A., 120
Burchick, D., 180
Busmann, K., 134
Caffrey, P., 190
Calame, J.P., 91
Caldwell, J.D., 164
Campbell, J.R., 116, 120, 203
Chen, Y., 137
Christophersen, M., 213
Clark, R.W., 201
Cohen, Y., 166
Colaninno, R., 211
Commisso, R.J., 160
Cook, A.M., 91
Corrigan, A., 198
Dale, J.R., 173
Dasgupta, A., 201
de Leeuw, G., 170
Dean, J., 147
DeOcampo, R.S., 188
DePreger, M., 182
Doyle, J.D., 118
Duff, R.C., 183
Dunay, C., 180
Dunkelberger, A.D., 164
Eckermann, S.D., 118
Eddy, Jr., C.R., 139
Ellis, C.T., 164
Engel, S.B., 173
Engelbrecht, J.T., 160
Englert, C.R., 99
Fadeyev, V., 213
Finkel, P., 134
Fitzgerald, L., 124
Frantz, J.A., 180
Fromm, M.D., 116, 190
Gallagher, B.M., 215
Giles, A.J., 164
Gillman, E.D., 210
Giuliani, J.L., 201
Golden, J.P., 173
Goldman, E., 125
Goldstein, D., 134
Goodwin, G.B., 205
Gordon, D.F., 137
Gotjen, H., 180
Gould, B., 156
Gould, Jr., R.W., 175
Hagy, J.D., 175
Hamdan, L., 124
Harlander, J.M., 99
Harodas, D., 124
Helle, M.H., 137
Herdic, P.C., 108
Higgins, T., 192
Hobart, K.D., 139
Houston, B.H., 108, 110, 146
Howard, R., 211
Hyer, E.J., 116, 120, 203
Hyland, M.R., 183
Jackson, S.L., 160
Jakabosky, J., 192
Jansen, R.W., 78, 188, 192
Johnson, A., 78
Johnson, R., 198
Jordan, P.M., 113
Joye, C.D., 91
Kablick, III, G.P., 190
Kaganovich, D., 137
Kailasanath, K., 198
Kim, C.S., 164
Kim, M., 164
Knipling, K.E., 157
Ko, D.S., 175
Kolacz, J., 180
Kuciauskas, A.P., 203
Kuzmich, A., 84
Ladner, S.D., 175
Lee, J., 124
Lehrter, J.C., 175
Levine, J., 160
Lipps, R.D., 188
Little, B., 124
Liu, J., 125, 198
Liu, R., 166
Lowe, L., 175
Macker, J., 147
Madden, R., 188
Maezato, Y., 124
Maraviglia, C., 132
Marr, K.D., 99
Martens, I.R., 173
Mathews, J., 149
Matis, B.R., 110, 134
McKinney, J.D., 183
McMahon, J., 146
Medintz, I.L., 166
Moclair, C., 151
Mosher, D., 160
Moskov, T., 141
Myers, J.D., 180
Naciri, J., 180
Narayana, P., 157
Nguyen, L.T., 157
Novak, K., 182
Oh, E., 166
Olson, T., 151
Oran, E.S., 205
Ouart, N.D., 201
Owrutsky, J.C., 164
Oyola, M.I., 203
Palastro, J.P., 137
Pauli, M., 180
Penta, B., 175
Perkins, F.K., 91
Peterson, D.A., 116
Phipps, D.G., 160
Philips, B.F., 213
Piotrowicz, M., 84
Plunkett, S., 211
Qi, N., 160
Quaid, A.J., 173
Raeker, B., 130
Raj, R.G., 188
Ramamurti, R., 156, 198
Ratchford, D.C., 164
Reid, E.A., 120
Reid, J.S., 120
Reintjes, J.F., 84
Reynolds, C.A., 118
Rodgers, J., 156
Rudolph, S., 130
Sadrozinski, H.F.W., 213
San Antonio, G., 141
Sanghera, J.S., 180
Schuette, M., 156
Schulman, I., 175
Shaw, L.B., 180
Sletten, M.A., 188, 192
Smith, D., 151
Solbrig, J.E., 116
Spann, B.T., 164
Spillmann, C.M., 180
Staruch, M., 134
Surratt, M.L., 116
Swartzlander, Jr., G.A., 182
Swider-Lyons, K., 156
Szymczak, W.G., 108
Tadger, M.J., 139
Tahmouh, D., 188
Tender, L.M., 173
Ting, A., 137
Tischler, J.G., 164
Vignola, J., 108
Viswanath, K., 198
Vurgafman, I., 164
Walker, A.L., 120
Watnik, A.T., 182
Weber, B.V., 160
Weigel, R.S., 215
Weston, J., 147
Wheeler, V.D., 139
Williams, K.J., 183
Wilson, M.A., 146
Wirth, J., 182
Wolek, A., 146
Xian, P., 120, 203
Zabetakis, D., 125

NAVAL RESEARCH LABORATORY

4555 Overlook Ave., SW • Washington, DC 20375-5320

LOCATION OF NRL IN THE CAPITAL AREA



Quick Reference Telephone Numbers

	NRL Washington	NRL- SSC	NRL- Monterey	NRL CBD	NRL VXS-1 Patuxent River
Hotline	(202) 767-6543	(202) 767-6543	(202) 767-6543	(202) 767-6543	(202) 767-6543
Personnel Locator	(202) 767-3200	(228) 688-3390	(831) 656-4763	(410) 257-4000	(301) 342-3751
DSN	297- or 754-	828	878	—	342
Direct-in-Dialing	767- or 404-	688	656	257	342
Strategic Comm.	(202) 767-2541	(228) 688-5328	(202) 767-2541	—	(202) 767-2541

Additional telephone numbers are listed on page 245

General information on the research described in this *NRL Review* can be obtained from the Strategic Communications Office, Code 1030, (202) 767-2541. Information concerning Technology Transfer is available from the Technology Transfer Office, Code 1004, (202) 767-7230. Sources of information on the various educational programs at NRL are listed in the *NRL Review* chapter titled “Programs for Professional Development.”

For additional information about NRL, the *NRL Fact Book* lists the organizations and key personnel for each division. It contains information about Laboratory funding, programs, and field sites. The Fact Book can be obtained from the Technical Information Services Branch, Code 3430, (202) 404-4963. The web-based *NRL Major Facilities* publication, which describes each NRL facility in detail, can be accessed at <http://www.nrl.navy.mil/media/publications>.

2017 NRL REVIEW



www.nrl.navy.mil